ISSN 1007-9327 (print)
ISSN 2219-2840 (online)

World Journal of *Gastroenterology*

World J Gastroenterol 2018 August 14; 24(30): 3313-3468

Published by Baishideng Publishing Group Inc

World Journal of Gastroenterology

Contents

Weekly Volume 24 Number 30 August 14, 2018

REVIEW

MINIREVIEWS

ORIGINAL ARTICLE

Basic Study

Retrospective Study

World Journal of Gastroenterology

Contents

Weekly Volume 24 Number 30 August 14, 2018

ABOUT COVER

Editorial board member of *World Journal of Gastroenterology*, Herwig Cerwenka, MD, Professor, Department of Surgery, Medical University of Graz, Graz A-8036, Austria

AIMS AND SCOPE

World Journal of Gastroenterology (*World J Gastroenterol*, *WJG*, print ISSN 1007-9327, online ISSN 2219-2840, DOI: 10.3748) is a peer-reviewed open access journal. *WJG* was established on October 1, 1995. It is published weekly on the 7th, 14th, 21st, and 28th each month. The *WJG* Editorial Board consists of 642 experts in gastroenterology and hepatology from 59 countries.

The primary task of *WJG* is to rapidly publish high-quality original articles, reviews, and commentaries in the fields of gastroenterology, hepatology, gastrointestinal endoscopy, gastrointestinal surgery, hepatobiliary surgery, gastrointestinal oncology, gastrointestinal radiation oncology, gastrointestinal imaging, gastrointestinal interventional therapy, gastrointestinal infectious diseases, gastrointestinal pharmacology, gastrointestinal pathophysiology, gastrointestinal pathology, evidence-based medicine in gastroenterology, pancreatology, gastrointestinal laboratory medicine, gastrointestinal molecular biology, gastrointestinal immunology, gastrointestinal microbiology, gastrointestinal genetics, gastrointestinal translational medicine, gastrointestinal diagnostics, and gastrointestinal therapeutics. *WJG* is dedicated to become an influential and prestigious journal in gastroenterology and hepatology, to promote the development of above disciplines, and to improve the diagnostic and therapeutic skill and expertise of clinicians.

INDEXING/ABSTRACTING

World Journal of Gastroenterology (*WJG*) is now indexed in Current Contents®/Clinical Medicine, Science Citation Index Expanded (also known as SciSearch®), Journal Citation Reports®, Index Medicus, MEDLINE, PubMed, PubMed Central and Directory of Open Access Journals. The 2018 edition of Journal Citation Reports® cites the 2017 impact factor for *WJG* as 3.300 (5-year impact factor: 3.387), ranking *WJG* as 35th among 80 journals in gastroenterology and hepatology (quartile in category Q2).

NAME OF JOURNAL
World Journal of Gastroenterology

ISSN
ISSN 1007-9327 (print)
ISSN 2219-2840 (online)

LAUNCH DATE
October 1, 1995

FREQUENCY
Weekly

EDITORIAL OFFICE
Ze-Mao Gong, Director
World Journal of Gastroenterology
Baishideng Publishing Group Inc
7901 Stoneridge Drive, Suite 501,
Pleasanton, CA 94588, USA
Telephone: +1-925-2238242
Fax: +1-925-2238243
E-mail: editorialoffice@wjgnet.com
Help Desk: http://www.f6publishing.com/helpdesk
http://www.wjgnet.com

PUBLISHER
Baishideng Publishing Group Inc
7901 Stoneridge Drive, Suite 501,
Pleasanton, CA 94588, USA
Telephone: +1-925-2238242
Fax: +1-925-2238243
E-mail: bpgoffice@wjgnet.com
Help Desk: http://www.f6publishing.com/helpdesk
http://www.wjgnet.com

PUBLICATION DATE
August 14, 2018

INSTRUCTIONS TO AUTHORS
Full instructions are available online at http://www.wjgnet.com/bpg/gerinfo/204

ONLINE SUBMISSION
http://www.f6publishing.com

World Journal of Gastroenterology

Submit a Manuscript: http://www.f6publishing.com

World J Gastroenterol 2018 August 14; 24(30): 3313-3329

DOI: 10.3748/wjg.v24.i30.3313

ISSN 1007-9327 (print) ISSN 2219-2840 (online)

REVIEW

MicroRNAs as non-invasive diagnostic biomarkers for gastric cancer: Current insights and future perspectives

Alexander Link, Juozas Kupcinskas

Alexander Link, Department of Gastroenterology, Hepatology and Infectious Diseases, Otto-von-Guericke University, Magdeburg 39120, Germany

Juozas Kupcinskas, Institute for Digestive Research and Department of Gastroenterology, Lithuanian University of Health Sciences, Kaunas LT-44307, Lithuania

ORCID number: Alexander Link (0000-0002-9514-4562); Juozas Kupcinskas (0000-0002-8760-7416).

Author contributions: Link A contributed to conception and design of the study, literature review and analysis, drafting, critical revision, editing and final approval of the final version, guarantor of the study; Kupcinskas J contributed to literature review, analysis, drafting, editing and approval of the final version.

Conflict-of-interest statement: No potential conflicts of interest. No financial support.

Manuscript source: Invited manuscript

Correspondence to: Alexander Link, MD, PhD, Academic Research, Associate Professor, Department of Gastroenterology, Hepatology and Infectious Diseases, Otto-von-Guericke University, Leipziger str. 44, Magdeburg 39120, Germany. alexander.link@med.ovgu.de
Telephone: +49-391-6713745
Fax: +49-391-6713105

Received: April 4, 2018
Peer-review started: April 4, 2018
First decision: May 30, 2018
Revised: June 10, 2018
Accepted: June 28, 2018
Article in press: June 28, 2018
Published online: August 14, 2018

Abstract

Non-invasive diagnostic biomarkers may contribute to an early identification of gastric cancer (GC) and improve the clinical management. Unfortunately, no sensitive and specific screening biomarkers are available yet and the currently available approaches are limited by the nature of the disease. GC is a heterogenic disease with various distinct genetic and epigenetic events that occur during the multifactorial cascade of carcinogenesis. MicroRNAs (miRNAs) are commonly deregulated in gastric mucosa during the *Helicobacter pylori* infection and in stepwise manner from chronic gastritis, through preneoplastic conditions such as atrophic gastritis and intestinal metaplasia, to early dysplasia and invasive cancer. Identification of miRNAs in blood in 2008 led to a great interest on miRNA-based diagnostic, prognostic biomarkers in GC. In this review, we provide the most recent systematic review on the existing studies related to miRNAs as diagnostic biomarkers for GC. Here, we systematically evaluate 75 studies related to differential expression of circulating miRNAs in GC patients and provide novel view on various heterogenic aspects of the existing data and summarize the methodological differences. Finally, we highlight several important aspects crucial to improve the future translational and clinical research in the field.

Key words: MicroRNA; Biomarkers; Screening; Stomach; Gastric cancer; Systematic review; Blood; Serum; Plasma

Core tip: Over the past years, large amount of data to microRNAs (miRNAs) in gastric cancer (GC) has been

published. We aimed to provide the critical, first of its kind in depth overview of existing studies to the miRNAs diagnostic biomarkers in GC. For this, we systematically reviewed published literature and identified 75 studies related specifically to microRNAs as blood-related non-invasive diagnostic biomarker in GC. This work provides a critical compendium to 106 studied microRNAs and summarizes the technical and methodological differences in reported studies. Furthermore, we highlight several aspects that need careful attention in future studies.

Link A, Kupcinskas J. MicroRNAs as non-invasive diagnostic biomarkers for gastric cancer: Current insights and future perspectives. *World J Gastroenterol* 2018; 24(30): 3313-3329 Available from: URL: http://www.wjgnet.com/1007-9327/full/v24/i30/3313.htm DOI: http://dx.doi.org/10.3748/wjg.v24.i30.3313

INTRODUCTION

Gastric cancer (GC) is a deadly disease with a great challenge in clinical management despite of a steady decline of the cancer incidence[1,2]. Despite of increasing understanding of genetic and epigenetic cancer events, the absence of non-invasive methods or biomarkers for early identification of GC is one of the biggest difficulties in GC. With an ongoing technical revolution, there is a great hope to find an appropriate way to solve this limitation. Non-coding RNAs (ncRNAs) and specifically microRNAs (miRNAs) have entered the "cancer-arena" for now more than 10 years ago[3] and much research has been done over the past decade. For several years we performed systematic analysis and reviewed the role of miRNAs in GC and potential of miRNAs as a biomarker in gastrointestinal cancers[4,5]. Since then, huge amount of data has been gained, making impossible to keep an overview of existing research. In this work, we performed a systematic search and reviewed published papers related to miRNAs as non-invasive biomarkers in GC. Because of the overwhelming amount of published data, we focused solely on miRNAs as non-invasive diagnostic biomarkers in GC and excluded the data to functional alterations, prognostic and predictive role. In the first part, we will briefly review the specific and unique issues related to GC crucial for understanding the disease, provide the compiling data showing the current stand of the research and highlight the need for the future development and new directions in the field.

GC - HETEROGENIC DISEASE

GC is a multifactorial heterogenic disease with unique cascade of genetic and epigenetic events leading to the cancer. There are multiple factors that, in more or less fashion, responsible for the clinical and biologically-relevant tumor heterogeneity, which may substantially impact an identification of potential diagnostic biomarkers. Those factors include geographical differences in prevalence of the risk factors, genetic background of the population, environmental factors and probably nutrition. For instance, the prevalence of GC in Asian countries and Russia is higher than in United States, Canada and northern Europe. Interestingly, geographical differences correlate with anatomical localization of primary gastric tumors. Tumors in corpus-distal subtype are predominant in Asian countries and junctional-proximal subtype in Europe. Among the most important etiological factors that may influence the tumor biology at least during the process of carcinogenesis is the *Helicobacter pylori* (*H. pylori)* infection, which is now acknowledged as an infectious disease with all the consequences of prevention and treatment[6]. For in depth review of the role of *H. pylori* in GC development, we refer to several recent publications[7,8]. Briefly, *H. pylori* is a chronic infectious diseases that causes almost always an active chronic inflammation of the gastric mucosa[6]. The persistent chronic inflammation of gastric mucosa causes different range of molecular alterations with increasing loss and accumulation of changes that leads to the phase of atrophic gastritis (AG) with intestinal metaplasie (IM) and dysplasia, which may further progress to GC and is known as Correa's cascade[9]. AG and IM are well acknowledged preneoplastic stages of GC with an increased GC risk[10]. Close endoscopic follow up of patients with preneoplastic conditions and lesions is recommended[11]. The risk of *H. pylori*-related GC development may be associated with severity of mucosal inflammation and be partially dependent on bacterial virulence factors such as cytotoxin-associated gene A (CagA) and vacuolating cytotoxin A (VacA)[12]. We and others have recently shown that VacA is probably one of the most important bacterial factors that correlate with mucosa inflammation[13] and is strongly associated with anti-CagA-IgG production[14]. *H. pylori* eradication is suggested as the most effective way in GC reduction in high-prevalence regions[15]; however, its value is beneficial mainly for primary and secondary GC prevention without strong diagnostic value in GC screening.

Historically, GC is divided based on the Lauren's classification into 2 histologic subtypes: intestinal and diffuse[16]. Lauren's classification is of the remarkable value in treatment decisions and has prognostic and predictive value. With an advance of high throughput technologies, the value of Lauren's classification has been questioned. The landmark work from The Cancer Genome Atlas (TCGA) has provided a new molecular classification subdividing GC in chromosomal instable (CIN), genomically stable (GS), microsatellite instable (MSI) and Epstein-Barr-Virus positive (EBV) tumor groups[17]. GS group shows relatively strong overlap with Lauren's diffuse type tumors. Hence, one of the main advantages of TCGA molecular classification may be in further subdivision of intestinal subtype of GC tumors in CIN, MSI and EBV. Those tumor subtypes carry not only unique molecular patterns relevant for understanding

the etiology but have potential predictive value for implementation of individualized novel therapeutic strategies.

CURRENTLY AVAILABLE BIOMARKERS FOR GC

To date, different molecules have been analyzed as potential biomarkers in patients with GC; however, as of 2018, there are no single blood-based biomarker that have sufficient sensitivity or specificity for implementation in GC screening routinely[8]. Several well-known antigens including carcinoembryonic antigen (CEA), cancer antigen 19-9 (CA19-9) and cancer antigen 72-4 (CA72-4) have been investigated in relation to GC[18]. Although the concentration of those antigens may be increased in some GC patients, the overall sensitivity of individual or combined CEA, CA19-9 and CA72-4 levels remains of insufficient discriminative power necessary for GC screening[18]. Besides typical "tumor-based" biomarkers, an effort has been made to establish a "functional" test for gastric mucosa also called "serological biopsy"[15]. Pepsinogen Ⅰ and Ⅱ (PGⅠ and PGⅡ) concentration correlate with AG, which is the preneoplastic condition of intestinal type of GC is intestinal type of GC, and is frequently used in Asian countries. In Europe the PGI and PGⅡ panels is expanded by the use of Gastrin-17 (G17). G17 is produced by the G-cells and stimulates the hydrochloric acid and pepsinogen production and therefore is part of the same physiological cascade as PGI. Unfortunately, the use of G17 is hampered by the stability of the peptide and the net benefit in addition to PGI and Ⅱ is a matter of ongoing research[19]. According to the recent systemic reviews and meta-analysis the sensitivity for AG identification is up to 70%[20,21]. Thus, PGI and PGⅡ may be helpful for serological identification of patients with probability of AG in regions with limited resources and availability of endoscopy. However, upper GI endoscopy with careful assessment of the gastric mucosa and targeted biopsies remains the gold-standard for GC screening and identification of patients at risk. One's upper GI endoscopy is performed, there is no additional diagnostic benefit of PGI/PGⅡ/G17 for instance in GC screening or risk assessment[22].

MiRNAs have gathered a lot of scientific attention during the past 10 years. As we have mentioned above, miRNAs are unique subgroup of ncRNAs with crucial role in multiple biological processes. MiRNAs are involved in regulation of different molecular pathways including cell differentiation, cell cycle progression or apoptosis through post-transcriptional regulation of gene expression[23]. Deregulation of miRNAs can influence carcinogenesis through mRNA targets encoding tumor suppressor genes or oncogenes[24]. Due to its unique biogenesis, miRNAs have several features that make them an attractive group of molecules in biomarker research field. MiRNAs are very stable and are easily and reproducibly retrieved from different biological material including tissues, blood, feces, saliva, ascites and even paraffin embedded blocks[25-32]. Due to those properties, miRNAs carry a huge potential as biomarkers and have been recently extensively explored in GC. For detailed information we kindly refer to our recent reviews[4,5].

MIRNA ALTERATIONS IN GC AND FUNCTIONAL ROLE

Multiple studies have demonstrated the differential expression of miRNAs in GC tissues and its functional role in GC has been suggested[4]. It is believed that miRNA alterations appear early in the cascade of the preneoplastic events. For instance, differential expression of miRNAs is identified in subjects with *H. pylori* infection and expression of miR-155 and miR-223 showed gradual increase in correlation to Correa's cascade both in antrum and corpus mucosa[25]. TCGA group has shown that different molecular subtypes of GC have unique miRNA expression profiles[17], which is in support of several other profiling studies[26,33]. Understanding of the mechanisms of miRNA expression such as CpG island promoter methylation, provides valuable information for biomarker research. For example, miR-137 was implicated in GI cancers showing differential methylation in colorectal cancer (CRC) and GC patients, although the magnitude of changes was superior in CRC[34]. MiR-29c expression is reduced early in gastric carcinogenesis and has been suggested as a diagnostic and therapeutic biomarker for patients with GC[35]. The interplay of the two transcription factors HNF4γ and NR2F2 and their coordinated regulation by miR-30 and miR-194, respectively, may represent a miRNA related network responsible for expression regulation of intestinal transcripts in the development of intestinal metaplasia[36].

Another growing field of miRNA research in GC is related to the analysis of single nucleotide polymorphisms (SNPs) in miRNA genes. Variation in miRNA-sequences may lead to the expression differences and modify regulatory function of miRNAs[37,38]. To date, both gene sequences encoding precursor miRNAs[39,40] as well as variations in miRNA binding regions of target genes[41] have been extensively explored in cancer studies. The most investigated SNPs in GC are related to miR-27a, miR-146a, miR-421, miR-449a; miR-196a-2, miR-492 and miR-608[42]. Although some associations between the risk of GC development and miRNA-related SNPs have been suggested, none of the identified associations is ready to be applied in clinical settings in particular in GC screening.

MIRNAS AS BIOMARKERS

Having shown the miRNA changes in tumor tissues, multiple research groups simultaneously evaluated the potential of miRNAs as non-invasive biomarkers in various specimens. Three publications related to large B-cell lymphoma, prostate and lung cancer appeared in 2008

strongly suggesting miRNAs as potential biomarkers for cancer[43–45]. This knowledge has been further extended to systematic analysis in feces in CRC[28], pancreatic cancer[29], and other diseases and specimens. Recently, it has been shown that miRNAs can be reproducibly measured in peritoneal fluid and ascites from cancer patients with peritoneal carcinomatosis and ascites[31,46]. It seems that basically any kind of body fluids (breast milk, urine, synovial fluids *etc*.) have measurable expression of miRNAs, which may potentially reflect a normal condition or be associated with pathophysiological alterations and therefore used as a biomarkers[5]. With existence of the overwhelming data to miRNAs in GC, we provide in the next chapter the most comprehensive summary of the exiting published data to miRNAs as non-invasive diagnostic biomarkers in GC.

METHODS AND LITERATURE SEARCH

To identify all available papers, we performed a systematic search with following steps: (1) Identify papers in MEDLINE/PUBMED using following criteria: gastric cancer, stomach cancer, microRNA, miRNA, biomarkers, plasma, serum, blood (until 30th November 2017); (2) We further screened all available abstracts manually one by one and excluded following papers: reviews, duplicates, retracted work, paper primarily related to miRNAs in tissues, *in vitro* or as prognostic or predictive biomarkers, papers without confirmed GC at the time point of the analysis or missing control group for direct comparison; (3) in January 2018 we updated the list including the papers published in December 2017 by applying more stringed criteria: diagnostic biomarkers, GC, plasma, serum. Overall, we obtained 75 original papers analyzing the expression of miRNAs in blood/serum/plasma between GC patients and controls. Among those, 18 papers refer to profiling of circulating miRNAs in GC compared to controls. Seventy-four full text papers and 1 abstract were systematically reviewed and the data were entered into the database. GraphPad Prism 7 (La Jolla, CA, United States) was used to create the figures.

MIRNA AS DIAGNOSTIC BIOMARKERS IN GC: TIMELINE AND PUBLICATION TRENDS

The first data to potential of miRNAs as diagnostic biomarkers in GC appeared in 2010 only two years after the first reports to detection of circulating miRNAs. We identified 75 publications from 2010 to 2017 where miRNA expression was studied in blood of GC patients and controls independently to the primary aim of the study. Over the period of 8 years, as shown in the Figure 1, we observed an increasing number of publication per year with maximum of 21 papers published in 2015 suggesting an increasing interest to the topic during the last years. To access the regional differences, we evaluated the origin of the used specimens as a surrogate. Majority of GC specimens and according published papers originate from China (55/75 or 73.3%) followed by Japan, Taiwan, Korea and others, further suggesting the regional difference in priority of the research topic and potential clinical relevance (Figure 1B).

SCIENTIFIC EVIDENCE AND REPORTING QUALITY

As next, we aimed to systematically assess the reporting quality and translational potential of the published work. For this, we created 4 internal quality measures: (1) how many samples from GC patients was used; (2) is TNM-Stage reported; (3) is Lauren's classification reported; and (4) proportion of patients with TNM Ⅰ/Ⅱ in total amount of GC tumors. Figure 1C shows the number of GC samples used among the 75 published papers. The median number included in the study was 57 (range 3-285) and total 5699 specimens were analyzed. Among those, 5 reports included over 200 samples each with highest number of included samples published by Qiu *et al*[47].

As we have shown in the introduction part, the Lauren's classification is among the most valuable tools to assess the histological subtype, which further correlates with molecular subtype[17]. Unfortunately, the data to Lauren's classification were available only for 16% (12/74) of the studies. TNM staging was used as another reporting quality surrogate as it correlated with prognosis and potential biomarkers need to be able to identify early cancers. Interestingly, TNM staging was reported only in 69% (51/74) of studies, which may substantially limit the quality assessment of the published work (Figure 1D). Among the studies with reported TNM staging, the proportion of GC with relatively early stages (TNM Ⅰ/Ⅱ) was quite heterogenic between the studies (Figure 1E). Only two studies focused solely on samples from GC patients with TNM stage Ⅰ and Ⅱ, while 68.8% (35/51) of studies had more than 50% of samples from patients with metastatic GC (lymph node or distant metastases).

TECHNICAL DIFFERENCES AMONG THE STUDIES

Among the identified papers, 38 papers studied the expression of miRNAs in plasma, 32 studies in serum, 3 studies in blood and only 2 reports for peripheral blood mononuclear cell (PBMC) (Figure 2). For miRNA extraction, the mirVana, Trizol and miRNeasy were the most frequently used kits. There were substantial differences between the methods for detection/analysis. SYBR Green-based method was applied in 57% (42/74) more frequently used as TaqMan-based method (Figure 2C).

As next, we focused on the data to internal normalization of circulating miRNAs (Figure 2D). In several previous publications, RNU6b has been clearly criticized for unsuitability for normalization of blood samples as it shows different biogenesis, stability and may not reflect biogenesis of miRNAs[5]. Nevertheless, almost

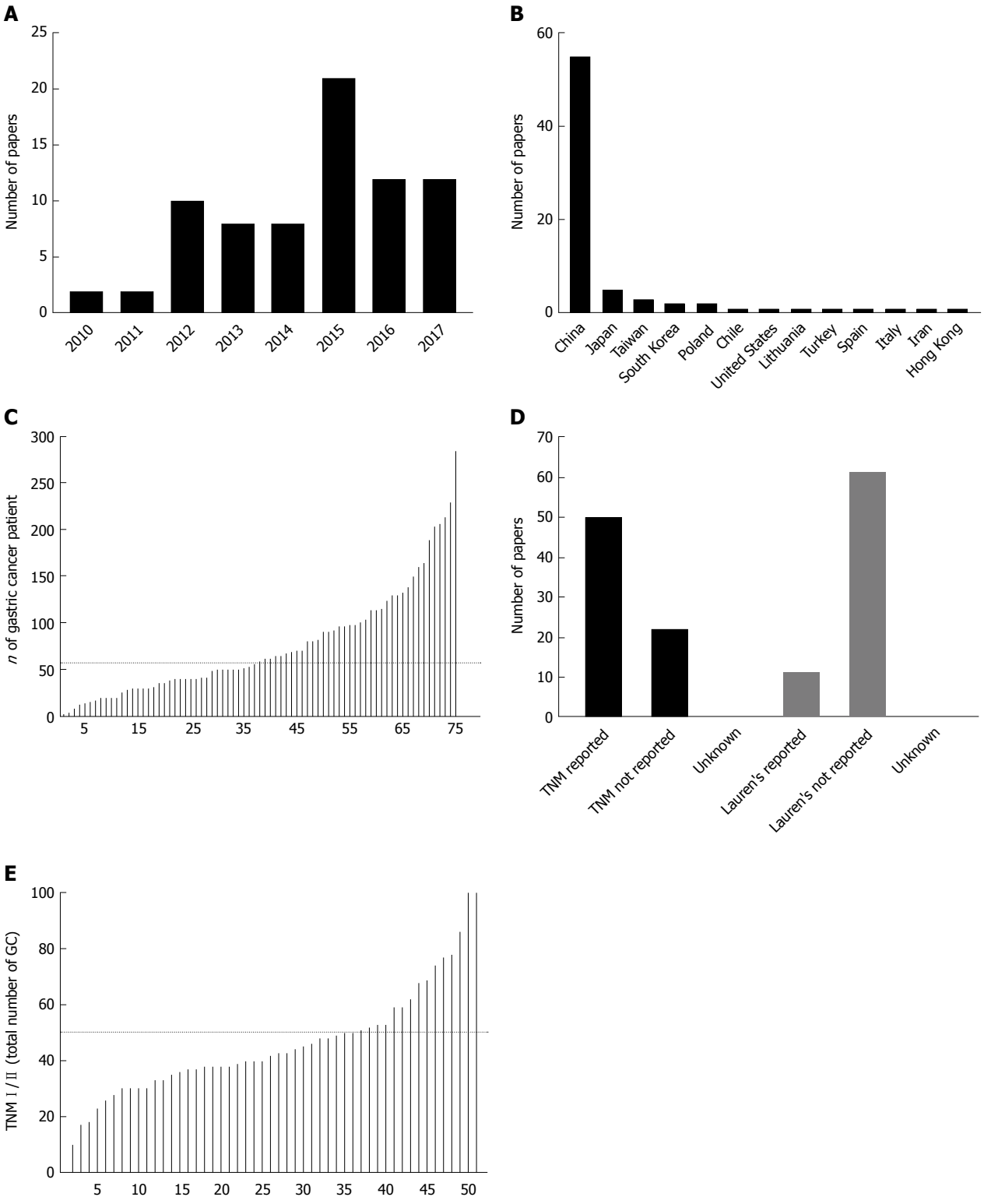

Figure 1 Characteristics of the studies to microRNAs as diagnostic biomarkers in gastric cancer. In total we have identified 75 studies. A: Time trends in number of published papers starting 2010 to 2017. B: Number of papers dependent on the origin of GC tumor specimens studied. C: Total number of specimens per publication/analysis from GC patients studied. D: Number of papers reporting or not reporting TNM staging or Lauren´s classification. E: Proportion of patients with early (TNM stage Ⅰ and Ⅱ) to total number of GC specimen's studied. GC: Gastric cancer.

60% of studies used the RNU6b-method for internal normalization of blood specimens. In similar fashion, 15% of papers applied miR-16-based method (alone or in combination with other methods), although an increasing evidence suggests that miR-16-based method may not be the best way for normalization of circulating miRNAs. Spiked-in-based method (most frequently cel-miR-39) is still considered as the most appropriate currently available methods for miRNAs normalization in blood and was used in up to 26% of studies, even though, it may

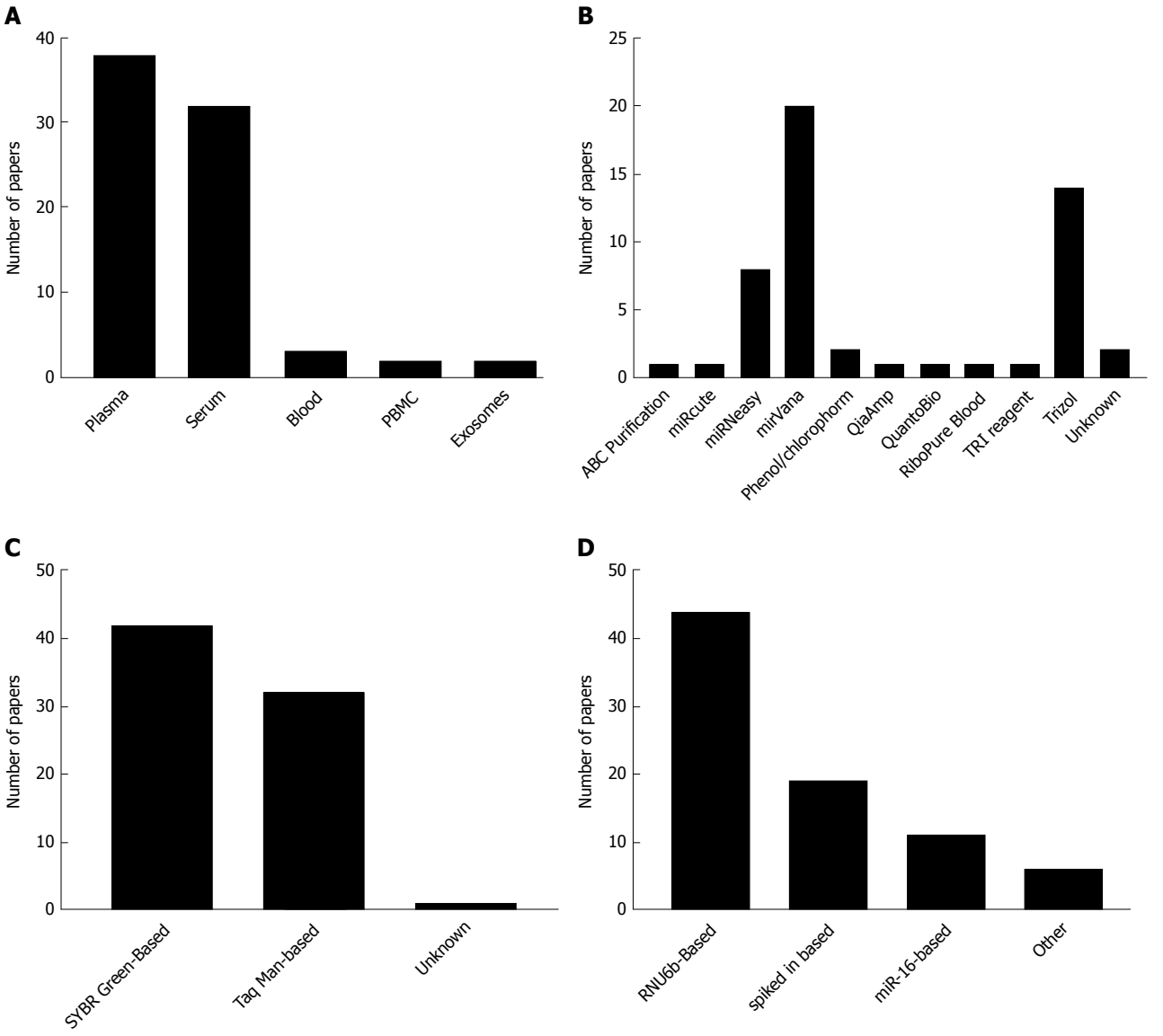

Figure 2 Characteristics of the studies to microRNAs as non-invasive diagnostic biomarkers in gastric cancer based on technical characteristics. A: Number of studies based on the used blood specimens. B: Number of papers using various extraction kits. C: Number of papers with various method for miRNA analysis. D: Number of studies using different normalization methods for miRNA analysis. Since several studies used one or several methods, the total number may exceed 75.

probably not be the perfect long-term solution for miRNA normalization.

Challenges with normalization of circulating miRNAs may probably be the most disappointing issue related to this topic. Several papers deal with the normalization issues and compare several methods, most frequently miR-16 and RNU6b. For instance, Song *et al*[48] studied the expression of several miRNAs in blood and showed that there is quite a large degree of variation among miRNAs. In particular, the expression of miR-21 was higher in stage Ⅳ GC patients; however, only if the samples were normalized to miR-16, miR-93 or miR-16 and miR-93 together. This was not the case if normalization was done based on the volume[48]. Interestingly, both miR-16 and miR-93 showed substantial variation and lower expression in healthy controls arguing against it usefulness as a normalizer. Peng *et al*[49] studied the expression of miR-191 and miR-425 in serum of 57 GC patients. No difference was found if the authors used RNU6b, while miR-16-based normalization led to significantly higher values of miR-191. In another study, Shiotani *et al*[50] also compared different normalization methods in GC samples from GC patients after endoscopic submucosal dissection. The authors conclude that only normalization to miR-16, but not RNU6b, led to the higher expression of miR-106b and let-7. According to our search (Table 1)[26,47,48,51-120], there are 3 reports to differential expression of miR-16 in GC with 399 studies samples[51-53]. Two reports show up- and one report downregulation of miR-16 in plasma and sera samples, further questioning the usefulness of miR-16 for normalization of circulating miRNAs.

The approach of miR-16-based normalization may be also called as a "proportional normalization" as rather the proportion between certain miRNAs (in comparison to miR-16) and not the absolute value of studied

Table 1 Differentially expressed circulating microRNAs in gastric cancer

microRNA	Changes in GC	Changes in GC tissue	Controls (*n*)	GC (*n*)	TNM reported	ROC	Validation	Source (PI/BI/Se)	qPCR	Normalization (qPCR)	Ref.
let-7a	↓	↓	30	69	Yes		Yes	Plasma	TaqMan	RNU6b	[56]
	↓	↓	45	80	Yes			Serum	SYBR	RNU6b	[57]
	↔		30	30	Yes			Plasma	TaqMan	RNU6b	[58]
let-7c	↔		202	214	No			Serum	SYBR	standard curve	[59]
let-7e	↑		82	82	No	0.7	Yes	Serum	TaqMan	cel-miR-39	[60]
let-7f	↔		30	30	Yes			Plasma	TaqMan	RNU6b	[58]
	↑		202	214	No			Serum	SYBR	standard curve	[59]
let-7g	↔		30	30	No			Serum	SYBR	miR-16	[61]
let-7i	↑		202	214	No			Serum	SYBR	standard curve	[59]
miR-1	↑		127	164	Yes			Serum	TaqMan	volume	[62]
	↔		30	30	No			Plasma	SYBR	cel-miR-39	[63]
miR-100	↑		47	50	Yes	0.71		Serum	TaqMan	RNU6b	[52]
miR-103	↑		14	17	No			Plasma	SYBR	Sp6	[64]
	↔		50	50	No	0.548		Plasma	SYBR	cel-miR-39	[65]
miR-106a	↑		30	69	Yes		Yes	Plasma	TaqMan	RNU6b	[56]
	↑		27	41	No	0.684		PBMC	SYBR	RNU6b	[66]
	↔		30	30	No			Plasma	SYBR	cel-miR-39	[63]
	↑	↑	22	48	NA			Serum	NA	NA	[67]
	↑	↑	20	20	Yes		Yes	Serum	TaqMan	cel-miR-39 miR-191-5p	[68]
	↑		130	130	No	0.786	Yes	Serum+ Exosomes	TaqMan	cel-miR-39	[69]
miR-106b	↑	↑	30	69	Yes	0.721	Yes	Plasma	TaqMan	RNU6b	[56]
	↑		90	90	Yes	0.773	Yes	Plasma	SYBR	cel-miR-39	[63]
	↑		15	31	Yes			Serum	TaqMan	cel-miR-39	[70]
	↑	↑	20	20	Yes			Plasma	TaqMan	cel-miR-39 RNU6b	[71]
	↓		36	40	Yes	0.856		Serum	SYBR	QuantoEC	[72]
	↑		65	65	Yes	0.898		Plasma	TaqMan	RNU6b	[73]
miR-107	↑	↑	36	36	No	0.63		Serum	SYBR	5srRNA	[74]
	↑		14	14	Yes			Serum	TaqMan	RNU6b	[75]
	↔		50	50	No	0.563		Plasma	SYBR	cel-miR-39	[65]
miR-10b-5p	↑	↑	167	203	Yes	0.627	Yes	Serum+ Exosomes	SYBR	cel-miR-39 miR-16	[76]
miR-122	↔		36	96	Yes			Plasma	SYBR	ath-miR-159a	[77]
miR-1233	↓		3	3	No			Plasma	SYBR	RNU6b	[78]
miR-130a	↑	↑	41	41	No	0.905		Serum	SYBR	RNU6B	[79]
	↑	↑	20	20	Yes		Yes	Serum	TaqMan	cel-miR-39 miR-191-5p	[68]
miR-132-3p	↑	↑	167	203	Yes	0.652	Yes	Serum+ Exosomes	SYBR	cel-miR-39 miR-16	[76]
miR-139	↓	↑	18	25	No	0.940		Plasma	SYBR	RNU6b	[80]
miR-140-5p	↑		50	50	Yes			Plasma	SYBR	RNU6B	[81]
miR-141	↓		3	3	No			Plasma	SYBR	RNU6b	[78]
	↓		14	17	No			Plasma	SYBR	Sp6	[64]
miR-142-3p	↓		285	285	Yes	0.839	Yes	Plasma	TaqMan	cel-miR-39	[47]
miR-143-3p	↔		73	206	Yes		Yes	Serum	SYBR	RNU6b	[82]
miR-144	↓	↓	40	96	Yes	0.821		Serum	SYBR	RNU6b	[83]
miR-146a	↔		15	31	Yes			Serum	TaqMan	cel-miR-39	[70]
	↔		73	206	Yes		Yes	Serum	SYBR	RNU6b	[82]
	↑	↔	20	20	Yes		Yes	Serum	TaqMan	cel-miR-39 miR-191-5p	[68]
miR-146b	↑	↔	20	20	Yes		Yes	Serum	TaqMan	cel-miR-39 miR-191-5p	[68]
miR-148a	↔		15	31	Yes			Serum	TaqMan	cel-miR-39	[70]
	↓		285	285	Yes	0.842	Yes	Plasma	TaqMan	cel-miR-39	[47]
	↓	↓	39	38	Yes	0.349		Plasma	TaqMan	miR-16-5p	[26]
miR-151-5p	↑		130	230	Yes	0.625	Yes	Plasma	TaqMan	RNU6b	[58]
miR-155	↑		20	30	No		Yes	Plasma	TaqMan	RNU6b	[84]
	↔		15	15	No			Plasma	TaqMan	RNU6b	[85]
miR-15b-5p	↑	↑	100	100	No			Plasma	SYBR	RNU6b	[86]
miR-16	↑		106	160	Yes	0.768-0.925	Yes	Plasma	TaqMan	cel-miR-39	[51]
	↑		47	50	Yes	0.90		Serum	TaqMan	RNU6b	[52]
	↓		129	189	Yes	0.772	Yes	Plasma	TaqMan	cel-miR-39 miR-16-5p	[53]

miR-17	↑		27	41	No	0.743		PBMC	SYBR	RNU6b	[66]
	↓		36	40	Yes	0.879		Serum	SYBR	QuantoEC	[72]
	↑		30	69	Yes		Yes	Plasma	TaqMan	RNU6b	[56]
	↔		30	30	No			Plasma	SYBR	cel-miR-39	[63]
	↔		20	20	No			Serum+ Exosomes	TaqMan	cel-miR-39	[69]
miR-181a	↑	↑	18	25	No	0.882		Plasma	SYBR	RNU6b	[80]
miR-181b	↓		89	92	Yes		Yes	Serum	SYBR	miR-16	[61]
miR-181c	↑	↑	60	30	No			Plasma	SYBR	RNU6b	[87]
miR-185	↑	↑	109	133	Yes	0.65	Yes	Plasma	SYBR	cel-miR-39 RNU6b	[88]
	↑	↔	167	203	Yes	0.637	Yes	Serum+ Exosomes	SYBR	cel-miR-39 miR-16	[76]
miR-187-3p	↑		61	61	Yes		Yes	Serum	SYBR	RNU6b	[89]
miR-18a	↑		50	50	Yes			Plasma	SYBR	RNU6B	[81]
	↑	↑	65	104	Yes	0.805		Plasma	TaqMan	RNU6b	[90]
miR-191	↑		82	82	No	0.63	Yes	Serum	TaqMan	cel-miR-39	[60]
	↑		58	57	Yes	0.849		Serum	TaqMan	miR-16	[49]
miR-192	↔		36	96	Yes			Plasma	SYBR	ath-miR-159a	[77]
miR-194	↑		3	3	No			Plasma	SYBR	RNU6b	[78]
	↔		50	50	No	0.512		Plasma	SYBR	cel-miR-39	[65]
miR-195	↓		285	285	Yes	0.765	Yes	Plasma	TaqMan	cel-miR-39	[47]
	↓	↓	36	62	Yes		Yes	Serum	SYBR	RNU6b	[91]
	↓		190	20	No			Plasma	(TaqMan)	global mean	[92]
	↑	↔	167	203	Yes	0.683	Yes	Serum+ Exosomes	SYBR	cel-miR-39 miR-16	[76]
mir-196a	↓	↑	14	17	No			Plasma	SYBR	Sp6	[64]
	↑	↑	126	98	Yes	0.864		Plasma	SYBR	miR-16	[93]
miR-196b	↑	↑	126	98	Yes	0.811		Plasma	SYBR	miR-16	[93]
miR-198	↔		30	30	Yes			Plasma	TaqMan	RNU6b	[58]
miR-199a-3p	↑		70	80	Yes	0.818	Yes	Plasma	TaqMan	RNU6b	[94]
	↑		130	230	Yes	0.837	Yes	Plasma	TaqMan	RNU6b	[58]
	↑		50	50	Yes			Plasma	SYBR	RNU6B	[81]
miR-19a	↑	↑	20	20	Yes		Yes	Serum	TaqMan	cel-miR-39 miR-191-5p	[68]
miR-19b	↑	↔	20	20	Yes		Yes	Serum	TaqMan	cel-miR-39 miR-191-5p	[68]
	↑		3	3	No			Plasma	SYBR	RNU6b	[78]
	↓		129	189	Yes	0.749	Yes	Plasma	TaqMan	cel-miR-39, miR-16-5p	[53]
	↑		130	130	No	0.769	Yes	Serum+ Exosomes	TaqMan	cel-miR-39	[69]
miR-200b	↓		14	17	no			Plasma	SYBR	Sp6	[64]
miR-200c	↑		15	52	Yes	0.715		Blood	SYBR	RNU6b 5SrRNA	[95]
	↑		100	98	Yes			Serum	SYBR	RNU6b	[96]
miR-203	↓		89	92	Yes		Yes	Serum	SYBR	miR-16	[61]
	↓		22	130	Yes	0.707	Yes	Serum	TaqMan	cel-miR-39	[97]
miR-204	↓		40	115	Yes		Yes	Serum	SYBR	RNU6b	[98]
miR-206	↓		150	150	Yes	0.89		Serum	TaqMan	cel-miR-39	[99]
miR-20a	↑		127	164	Yes			Serum	TaqMan	volume	[62]
	↑		90	90	Yes	0.859	Yes	Plasma	SYBR	cel-miR-39	[63]
	↑	↑	30	30	No			Plasma	SYBR	RNU6b	[100]
	↑	↑	109	133	Yes	0.67	Yes	Plasma	SYBR	cel-miR-39 RNU6b	[88]
	↑	↑	28	28	No			Plasma	SYBR	RNU6b	[101]
	↑	↔	167	203	Yes	0.637	Yes	Serum+ Exosomes	SYBR	cel-miR-39 miR-16	[76]
	↑		12	12	No			Serum	SYBR	cel-miR-39	[102]
miR-21	↑		30	69	Yes		Yes	Plasma	TaqMan	RNU6b	[56]
	↑		20	53	Yes	0.853		Blood	SYBR	RNU6b	[103]
	↑		70	70	Yes	0.794	Yes	Plasma	TaqMan	cel-miR-39	[104]
	↑		39	30	Yes	0.81		Serum	SYBR	miR-16	[105]
	↑		20	40	Yes			Serum	All-in-one	Volume miR-16, miR-93	[48]
	↔		90	90	Yes			Plasma	SYBR	cel-miR-39	[63]
	↔		15	31	Yes			Serum	TaqMan	cel-miR-39	[70]
	↔		15	15	No			Plasma	TaqMan	RNU6b	[85]
	↑		50	50	Yes	0.912		Serum	SYBR	RNU6b	[106]
	↑		50	50	Yes	0.898		PBMC	SYBR	RNU6b	[106]
	↑	↑	14	17	No			Plasma	SYBR	Sp6	[64]
	↑		89	92	Yes		Yes	Serum	SYBR	miR-16	[61]
	↑	↑	20	20	Yes		Yes	Serum	TaqMan	cel-miR-39 miR-191-5p	[68]

miR-210	↑	↑	109	133	Yes	0.75	Yes	Plasma	SYBR	cel-miR-39 RNU6b	[88]
miR-212	↑	↔	20	20	Yes		Yes	Serum	TaqMan	cel-miR-39 miR-191-5p	[68]
miR-218	↓		70	70	Yes	0.743	Yes	Plasma	TaqMan	cel-miR-39	[104]
	↓		56	68	Yes			Serum	SYBR	cel-miR-39	[107]
miR-220	↑	↔	20	20	Yes		Yes	Serum	TaqMan	cel-miR-39 miR-191-5p	[68]
miR-221	↑		82	82	No	0.7	Yes	Serum	TaqMan	cel-miR-39	[60]
	↑		90	90	Yes	0.796	Yes	Plasma	SYBR	cel-miR-39	[63]
	↑		14	17	No			Plasma	SYBR	Sp6	[64]
miR-222	↑		82	82	No	0.65	Yes	Serum	TaqMan	cel-miR-39	[60]
	↑		56	114	Yes	0.85		Plasma	TaqMan	RNU6b	[108]
miR-223	↑		70	70	Yes	0.91	Yes	Plasma	TaqMan	cel-miR-39	[104]
	↑		15	31	Yes			Serum	TaqMan	cel-miR-39	[70]
	↑		47	50	Yes	0.85		Serum	TaqMan	RNU6b	[52]
	↑	↑	50	50	Yes	0.81		Plasma	SYBR	RNU6b	[109]
	↑		3	3	No			Plasma	SYBR	RNU6b	[78]
	↑	↑	20	20	Yes		Yes	Serum	TaqMan	cel-miR-39 miR-191-5p	[68]
	↑	↑	20	15	Yes			Plasma	NCode	cel-miR-39/-54/-238; miR-16	[110]
	↑	↑	39	38	Yes	0.671		Plasma	TaqMan	miR-16-5p	[26]
miR-23a	↑		14	17	No			Plasma	SYBR	Sp6	[64]
miR-23b	↑		50	138	Yes	0.80		Plasma	SYBR	RNU6b	[111]
miR-25	↔		10	10	No			Plasma	TaqMan	cel-miR-39	[104]
	↑		106	160	Yes	0.694-0.925	Yes	Plasma	TaqMan	cel-miR-39	[51]
	↑	↑	20	20	Yes			Plasma	TaqMan	cel-miR-39; RNU6b	[71]
	↑	↑	109	133	Yes	0.65	Yes	Plasma	SYBR	cel-miR-39; RNU6b	[88]
	↔	↑	70	70	Yes			Plasma	TaqMan	RNU6B	[112]
	↑		14	14	Yes			Serum	TaqMan	RNU6b	[75]
	↑		65	65	Yes	0.817		Plasma	TaqMan	RNU6b	[73]
miR-26a	↓		285	285	Yes	0.882	Yes	Plasma	TaqMan	cel-miR-39	[47]
miR-26b	↔		30	30	Yes			Plasma	TaqMan	RNU6b	[58]
miR-27a	↑		127	164	Yes			Serum	TaqMan	volume	[62]
	↑		82	82	No	0.67	Yes	Serum	TaqMan	cel-miR-39	[60]
	↔		30	30	No			Plasma	SYBR	cel-miR-39	[63]
	↔		15	31	Yes			Serum	TaqMan	cel-miR-39	[70]
	↑	↑	35	35	Yes	0.70	Yes	Plasma	TaqMan	RNU6b	[85]
miR-27b	↑		82	82	No	0.66	Yes	Serum	TaqMan	cel-miR-39	[60]
miR-296	↑	↔	20	20	Yes		Yes	Serum	TaqMan	cel-miR-39; miR-191-5p	[68]
	↑	↑	167	203	Yes	0.652	Yes	Serum+ Exosomes	SYBR	cel-miR-39 miR-16	[76]
miR-30a-5p	↔		20	20	No			Serum+ Exosomes	TaqMan	cel-miR-39	[69]
miR-30c	↑	↔	20	20	Yes		Yes	Serum	TaqMan	cel-miR-39; miR-191-5p	[68]
miR-31	↓		89	92	Yes		Yes	Serum	SYBR	miR-16	[61]
miR-32	↑	↑	40	40	No			Plasma	SYBR	RNU6b	[113]
miR-323-3p	↑	↔	20	20	Yes		Yes	Serum	TaqMan	cel-miR-39; miR-191-5p	[68]
miR-331	↑	↑	20	20	Yes		Yes	Serum	TaqMan	cel-miR-39; miR-191-5p	[68]
miR-335	↓	↓	7	4	No			Plasma	TaqMan	RNU6b	[114]
miR-34	↔		30	30	No			Plasma	SYBR	cel-miR-39	[63]
miR-346	↓		14	17	No			Plasma	SYBR	Sp6	[64]
miR-34a	↑		127	164	Yes			Serum	TaqMan	volume	[62]
miR-365	↑	↔	20	20	Yes		Yes	Serum	TaqMan	cel-miR-39; miR-191-5p	[68]
miR-370	↑	↑	12	40	Yes	0.79		Plasma	TaqMan	miR-16	[115]
miR-371-5p	↑		61	61	Yes		Yes	Serum	SYBR	RNU6b	[89]
miR-374	↑	↑	20	20	Yes		Yes	Serum	TaqMan	cel-miR-39; miR-191-5p	[68]
miR-375	↓	↓	20	20	No	0.835		serum	TaqMan	RNU6b	[116]
	↓	↓	39	38	Yes	0.32		Plasma	TaqMan	miR-16-5p	[26]
miR-376a	↔	↑	108	65	Yes			Plasma	TaqMan	RNU6B	[117]
miR-376c	↑		82	82	No	0.71	Yes	Serum	TaqMan	cel-miR-39	[60]
	↔		30	30	No			Plasma	SYBR	cel-miR-39	[63]
	↑	↑	108	65	Yes	0.77		Plasma	TaqMan	RNU6B	[117]

miR-378	↑	↓	61	61	Yes	0.861	Yes	Serum	SYBR	RNU6b	[89]
	↔		30	30	No			plasma	SYBR	cel-miR-39	[63]
	↓		14	17	No			Plasma	SYBR	Sp6	[64]
miR-421	↑		17	40	Yes	0.773		PBMC	SYBR	RNU6b	[118]
	↑		50	50	No		Yes	Serum (?)	SYBR	RNU6b	[119]
	↑		90	90	No	0.779		Serum	SYBR	RNU6b	[120]
	↑		90	90	No	0.821		PBMC	SYBR	RNU6b	[120]
miR-423-5p	↑		127	164	Yes			Serum	TaqMan	volume	[62]
	↔		30	30	No			Plasma	SYBR	cel-miR-39	[63]
miR-425	↔		58	57	Yes			Serum	TaqMan	miR-16	[49]
miR-433	↔		15	31	Yes			Serum	TaqMan	cel-miR-39	[70]
	↑	↔	20	20	Yes		Yes	Serum	TaqMan	cel-miR-39; miR-191-5p	[68]
miR-451	↑	↓	30	56	Yes	0.96	Yes	Plasma	TaqMan	RNU6b	[54]
	↔		90	90	Yes			Plasma	SYBR	cel-miR-39	[63]
	↑	↔	20	20	Yes		Yes	Serum	TaqMan	cel-miR-39; miR-191-5p	[68]
	↑		106	160	Yes	0.790-0.850	Yes	Plasma	TaqMan	cel-miR-39	[51]
	↔		73	206	Yes		Yes	Serum	SYBR	RNU6b	[82]
miR-484	↓	↓	14	17	No			Plasma	SYBR	Sp6	[64]
miR-486	↑	↓	30	56	Yes	0.92	Yes	Plasma	TaqMan	RNU6b	[54]
	↔		30	30	No			Plasma	SYBR	cel-miR-39	[63]
	↑		106	160	Yes	0.779-0.863	Yes	Plasma	TaqMan	cel-miR-39	[51]
	↓		14	17	No			Plasma	SYBR	Sp6	[64]
miR-501-3p	↔		73	206	Yes		Yes	Serum	SYBR	RNU6b	[82]
miR-518d	↑	↔	20	20	Yes		Yes	Serum	TaqMan	cel-miR-39; miR-191-5p	[68]
miR-518f	↑	↔	20	20	Yes		Yes	Serum	TaqMan	cel-miR-39; miR-191-5p	[68]
miR-627	↑	↑	111	123	Yes	0.937	Yes	Plasma	SYBR	RNU6B	[81]
miR-629	↑	↑	111	123	Yes	0.912	Yes	Plasma	SYBR	RNU6B	[81]
miR-652	↑	↑	111	123	Yes	0.918	Yes	Plasma	SYBR	RNU6B	[81]
miR-720	↔		30	30	Yes			Plasma	TaqMan	RNU6b	[58]
miR-744	↑		82	82	No	0.74	Yes	Serum	TaqMan	cel-miR-39	[60]
	↔		30	30	No			Plasma	SYBR	cel-miR-39	[63]
miR-92a	↑		106	160	Yes	0.732-0.913	Yes	Plasma	TaqMan	cel-miR-39	[51]
	↓		89	92	Yes		Yes	Serum	SYBR	miR-16	[61]
miR-92b	↑	↑	109	133	Yes	0.69	Yes	Plasma	SYBR	cel-miR-39; RNU6b	[88]
miR-93	↑	↑	20	20	Yes			Plasma	TaqMan	cel-miR-39; RNU6b	[71]
	↑		65	65	Yes	0.756		Plasma	TaqMan	RNU6b	[73]
miR-940	↓	↓	105	115	Yes	0.96	Yes	Plasma	SYBR	miR-16	[55]

GC: Gastric cancer; phen/chlor: Phenol-chloroform method; SYBR: SYBR Green; NA: Non available.

miRNAs is used. This has been implemented by multiple studies and has been shown of potential diagnostic benefit independently to its scientific objectivity and validity. For instance, we analyzed miRNAs expression in ascites and showed that miR-21 was upregulated in patients with peritoneal carcinomatosis compared to control group[31]. However, also patients with peritonitis demonstrated similar increase as patients with peritoneal carcinomatosis. To overcome this limitation, we used the proportion of miR-21 (cancer-associated) and miR-223 (inflammation-associated) to differentiate the groups[31]. For miR-16, the very high values of miR-16 in erythrocytes strongly suggest that other factors such as tumor anemia or hemolysis may have an additional impact on the results. Nevertheless, this does not necessarily mean that miR-16 is not suitable, but rather that we need to know the influential factors and to know exact biogenesis of miR-16 in circulation. Further studies are needed to provide the comprehensive view on patients-related factors.

An alternative normalization way has been proposed where multiple miRNAs can be used simultaneously. For instance, miRCURY LNA Universal RT microRNA PCR System offers internal standard including miR-103a-3p, miR-191-5p, miR-423-3p and -5p and miR-451. However, we strongly doubt the usefulness of this method, as every single of those selected miRNAs have been reported as deregulated in cancer and in particular GC (Table 1). Furthermore, miR-451 is highly dependent on hemolysis and may provide some unexpected bias in analysis. Thus, in similar way as addressed for miR-16, additional studies are needed to confirm the usefulness, biological suitability and stability of the methods.

DIFFERENTIALLY EXPRESSED CIRCULATING MIRNAS IN GC PATIENTS

In the Table 1, we have summarized the miRNAs that have been analyzed for the differential expression between GC patients and controls. According to our search, we identified 106 miRNAs that were studied in different studies. Among those, 13 miRNAs such as let-

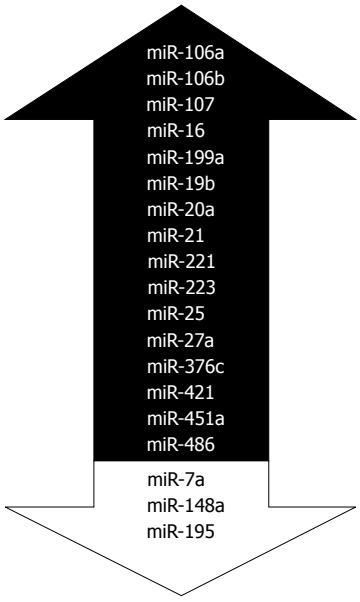

Figure 3 Schematic presentation of most frequently deregulated microRNAs in gastric cancer. Selection was made using following criteria: at least 3 reports with at least 2 reports with either up or downregulation.

7c, let-7g, miR-143-3p, miR-122, miR-192, miR-198 etc. showed no significant changes. As shown in in Table 1, multiple miRNAs have conflicting results showing differential expression in one cohort while no changes found in another. In the Figure 3 we summarize the most frequently deregulated miRNAs. Those were selected using two criteria: (1) at least 3 publications and (2) at least two with reproducible report on increased or decreased expression. Among the most consistent miRNAs are the miR-20a, miR-223 and miR-421. Among the most studied is the miR-21 with total 13 reports. Summarizing the data to miR-21 expression, three reports showed no differences while 10 reports show an upregulation of miR-21 both in sera and in plasma of GC patients. As shown in the Table 1, multiple groups used samples from independent cohorts to confirm the results, which substantially contributes to the quality of the reports.

To estimate the diagnostic potential of miRNAs as biomarkers in GC, multiple studies provided receiver operator curves (ROC) values. For instance, Konishi *et al*[54] reported the diagnostic accuracy for miR-451 reaching 0.96 with calculated sensitivity of 96% and specificity of 100%. Liu *et al*[55] studied miR-940 and reported the ROC value of 0.96 although with slightly lower sensitivity 81.2% and specificity 98.6%. Although those results are striking, we need to keep in mind that validation of the results from independent groups or cohorts in prospective studies are still to come. We believe that the data from our summary table will be helpful for the future search, validation and discussion of the results.

PROFILING OF CIRCULATING MIRNAS IN GC PATIENTS

It is well known that the most promising way to identify the potential biomarkers is the unbiased profiling of the samples. This approach was applied in the pivotal work by Chen *et al*[45] in 2008 in lung cancers, where the authors used multiple pooled samples for profiling and performed independent validation using qPCR. As shown in the Table 2[47,51,53-55,58,60,62,64,68,76,78,81,82,88,92,121], this approach was very intensively used for miRNA-profiling in GC patients. Among the total eighteen miRNA-profiling studies, 50% (9/18) reported the use of the pooled samples. Majority of studies used single technical pooled profiling from 5-40 samples for GC and controls. Although, this may be an appropriate way for proof-of-principle studies, it has several limitations where inappropriate changes of miRNAs in few subjects may create very strong deviation and bias and therefore independent validation is mandatory. Among the 18 profiling studies (Table 2), 11 reports studied miRNA in plasma, 6 in sera and 1 in blood samples. From the technical perspective there was substantial variation in use of extraction kits and profiling platforms used for analysis. Similar to the overall data in total cohort (Table 1), researches from China with 12 profiling studies provided the most overwhelming data. Remaining work comes from Poland, Japan, Turkey, Hong-Kong and United States. The first studies tend to use relatively small number of samples while more recent studies provide increasing number of samples and include an impressive number of samples for validation analysis as well[68,76].

FUTURE PERSPECTIVES AND CONCLUDING REMARKS

In this review, we systematically summarized and analyzed the existing data to miRNAs as non-invasive biomarkers for GC. There is no doubt that further studies with an improved study design will follow and it is a matter of time until the miRNA-based biomarkers will enter the clinical studies either in oncologic patients or patients with other diseases. However, following our critical review of the existing papers we would like to provide several cautionary notes for improvement.

Quality of reports

The era of proof-of-principle studies in GC has passed and with 75 published data it is time to improve the quality of the work. There are several ways that may be considered: (1) description of patient's cohort including Lauren's Classification, TNM staging and precise number of patients is necessary; (2) reporting of the methodological steps (extraction kits, measurements, reproducibility, validation *etc*.) need to be carefully reviewed and reported; (3) for primary research an independent cohort of samples need to be included; and (4) reporting of ROC/AUC values, sensitivity and specificity are currently used in quite biased way in proportion of GC patients to controls mostly in 1:1; however, in real-life settings the proportion will be at least 100-1000:1. Unless the prospective study is done it is clear that the real-life settings are not possible to achieve and additional effort is needed to increase the number of

Table 2 Profiling of circulating microRNAs in gastric cancer

Ref.	Year	Source	Extraction Kit	Platform	Sample Origin	GC (number of technical runs)	Controls (number of technical runs)	pooled samples	GC (number of pooled samples)	Controls (number of pooled samples)
Liu *et al*[62]	2011	Serum	phen/chlor	Solexa	China	1	1	Yes	20	20
Song *et al*[60]	2012	Serum	miRNeasy	qPCR-array	China	1	1	Yes	14	14
Liu *et al*[89]	2012	Serum	mirVana	Agilent	China	7	10	No		
Konishi *et al*[54]	2012	Plasma	mirVana	microarray	Japan	3	3	No		
Gorur *et al*[92]	2013	Plasma	high-pure miRNA Isolation	TaqMan Array	Turkey	1	1	Yes	20	190
Shah *et al*[121]	2013	Blood	miRNeasy	Geniom Biochip	Poland	1	1	Yes	8	19
Li *et al*[58]	2013	Plasma	mirVana	Agilent	China	20	20	No		
Zhu *et al*[51]	2014	Plasma	miRNeasy	TaqMan Array	China	1	1	Yes	40	40
Zhang *et al*[53]	2015	Plasma	mirVana	Agilent	China	16	18	No		
Zhou *et al*[88]	2015	Plasma	mirVana	Exiqon	China	3	1	Yes	30	10
Shin *et al*[81]	2015	Plasma	Trizol miRNeasy	miRCURY LNA	China	5	5	No		
Zhang *et al*[78]	2015	Plasma	mirVana	Agilent	China	3	3	No		
Liu *et al*[55]	2016	Plasma	miRNeasy	miRCURY LNA	Hong-Kong	5	5	No		
Qiu *et al*[47]	2016	Plasma	miRNeasy	Agilent	China	1	1	Yes	5	5
Treece *et al*[64]	2016	Plasma	miRCURY	GastroGenus miR Panel	United States	17	14	No		
Jiang *et al*[82]	2017	Serum	unknown	miSeq	China	2	1	Yes	20	10
Huang *et al*[76]	2017	Serum	mirVana	Exiqon	China	3	1	Yes	30	10
Sierzega *et al*[68]	2017	Serum	miRNA ABC Purification	TaqMan Array	Poland	20	20	No		

GC: Gastric cancer; phen/chlor: Phenol-chloroform method.

control sample.

Technical comparison between the studies

In the present review of the studies, there is a substantial technical heterogeneity among the studies: various extraction kits, qPCR methods and most importantly normalization. We have just recently published our data showing the differences between various extraction kits and miRNA expression in ascites[31]. Those results need to be taking to account and an independent validation of the primary samples will be needed. As we have recently reviewed[5], use of serum and plasma will probably have an independent effect on recovery and stability of miRNAs. Besides, contamination with various parts of circulating cells (erythrocytes, thrombocytes) may also provide an additional bias and caution in interpreting of miRNA data is necessary. As reviewed above, one of the larges differences among the studies is related to the choice of reference genes for normalization of miRNAs. Here we would like to caution the use of RNU6b for normalization of miRNAs and also probably reduce the use of miR-16 for normalization of circulating miRNAs unless additional studies provide the evidence for the objectivity of measurements.

High-risk patients

Taking to account the unique biology of GC, further focus should be made to identify the high-risk patients with the highest risk of GC development. For instance, patients with moderate to severe AG or IM are at increased risk for development of intestinal type of GC. Here, much more effort needs to be done to characterize the miRNA changes not only in GC but also in patients with preneoplastic conditions or lesions. It would be extremely interesting to know the cascade of changes in miRNA expression in subjects with hereditary diffuse GC.

GC-heterogenic disease

In currently available studies, all GC subtypes are pooled together and most effort is made to identify "all fits one" biomarkers for GC. This is definitely the most desirable way, where all GC patients could be diagnosed with the same biomarkers; however, we need also keep in mind that GC is a heterogenic disease with unique molecular alterations[17]. Since GC shows subtype-unique miRNA alterations, it may be very likely that circulating miRNAs, at least partly, may behave differently between intestinal and diffuse types of GC. With the knowledge of TCGA molecular classification, it would also very exciting to see if different molecular subtypes have characteristic circulating miRNA expression pattern.

Beyond miRNAs: Value of isomiR's in GC

High throughput genomic data sequencing showed that conventional miRNAs may differ both in length of the molecule and its' sequence[122,123]. These variant miRNA-sequences are now being referred to as isoforms of miRNAs or isomiR's. Up to date, the role of these molecules in GC remains largely unexplored. Nevertheless, increasing number of studies point out important deregulation patterns of isomiR's in cancer. For instance, in a recent study, we identified 219 deregulated isomiR'

s between gastrointestinal stromal tissue and tumor adjacent tissues[124]. To our knowledge, the only study that investigated isomiR's in GC found that certain isomiR-types preferentially occur in normal gastric tissue but other types prefer GC tissue[122]. Although these data may be available, no published data is available to isomiR's changes in blood samples of GC patients and may be focus of future studies.

Circulating tumor cells and miRNA analysis

As discussed in above, multiple studies have shown that circulating miRNAs may serve as diagnostic biomarkers for GC; however, the origin of these molecules is not fully clear. Using profiling data from sera and tumor tissues, Sierzega *et al*[68] identified differences in expression pattern in GC patients; however, miRNA expression data analysis did not support the conclusion that circulating miRNA originate primarily from the tumor tissue. Hence, it remain open if exosomal miRNAs or even certain blood-cells-related miRNAs may be more promising to study[27]. Furthermore, flow-cytometry or microfluidic-based single-cell or cell-type specific sequencing analysis may provide more specific transcription patterns with higher diagnostic and prognostic value[125]. Therefore, additional studies employing single-cell based analysis from blood samples of GC patients are needed in order to identify more sensitive and specific biomarkers.

CONCLUSION

During the past 7 years, large amount of data has been gathered to support the need for intensive research on miRNA-based biomarkers in GC. In this review, we systematically summarized the data to miRNAs as non-invasive diagnostic biomarkers in GC. Meticulous analysis of the published work revealed relatively high level of heterogeneity not only in methodological and technical aspects, but also in reporting quality of the studies. At present, no miRNA-based biomarkers are ready to be implemented for GC-screening other than in research studies; however, the provided data clearly highlight the potential of miRNAs as diagnostic biomarkers and also highlight the need for the further improvement. We hope that this first of its kind comprehensive review with critical points may lead to a "next wave" of "second generation" comprehensive studies that take into account not only technical aspects of miRNA research but also unique aspects of GC biology.

REFERENCES

1 **Chen W**, Zheng R, Baade PD, Zhang S, Zeng H, Bray F, Jemal A, Yu XQ, He J. Cancer statistics in China, 2015. *CA Cancer J Clin* 2016; **66**: 115-132 [PMID: 26808342 DOI: 10.3322/caac.21338]

2 **Siegel RL**, Miller KD, Jemal A. Cancer statistics, 2018. *CA Cancer J Clin* 2018; **68**: 7-30 [PMID: 29313949 DOI: 10.3322/caac.21442]

3 **Lu J**, Getz G, Miska EA, Alvarez-Saavedra E, Lamb J, Peck D, Sweet-Cordero A, Ebert BL, Mak RH, Ferrando AA, Downing JR, Jacks T, Horvitz HR, Golub TR. MicroRNA expression profiles classify human cancers. *Nature* 2005; **435**: 834-838 [PMID: 15944708 DOI: 10.1038/nature03702]

4 **Link A**, Kupcinskas J, Wex T, Malfertheiner P. Macro-role of microRNA in gastric cancer. *Dig Dis* 2012; **30**: 255-267 [PMID: 22722550 DOI: 10.1159/000336919]

5 **Link A**, Goel A. MicroRNA in gastrointestinal cancer: a step closer to reality. *Adv Clin Chem* 2013; **62**: 221-268 [PMID: 24772669 DOI: 10.1016/B978-0-12-800096-0.00006-8]

6 **Sugano K**, Tack J, Kuipers EJ, Graham DY, El-Omar EM, Miura S, Haruma K, Asaka M, Uemura N, Malfertheiner P; faculty members of Kyoto Global Consensus Conference. Kyoto global consensus report on Helicobacter pylori gastritis. *Gut* 2015; **64**: 1353-1367 [PMID: 26187502 DOI: 10.1136/gutjnl-2015-309252]

7 **Malfertheiner P**, Link A, Selgrad M. Helicobacter pylori: perspectives and time trends. *Nat Rev Gastroenterol Hepatol* 2014; **11**: 628-638 [PMID: 25001975 DOI: 10.1038/nrgastro.2014.99]

8 **Bornschein J**, Leja M, Kupcinskas J, Link A, Weaver J, Rugge M, Malfertheiner P. Molecular diagnostics in gastric cancer. *Front Biosci (Landmark Ed)* 2014; **19**: 312-338 [PMID: 24389187 DOI: 10.2741/4210]

9 **Chiba T**, Marusawa H, Ushijima T. Inflammation-associated cancer development in digestive organs: mechanisms and roles for genetic and epigenetic modulation. *Gastroenterology* 2012; **143**: 550-563 [PMID: 22796521 DOI: 10.1053/j.gastro.2012.07.009]

10 **Song H**, Ekheden IG, Zheng Z, Ericsson J, Nyrén O, Ye W. Incidence of gastric cancer among patients with gastric precancerous lesions: observational cohort study in a low risk Western population. *BMJ* 2015; **351**: h3867 [PMID: 26215280 DOI: 10.1136/bmj.h3867]

11 **Beardwell I**, Holden L, Claydon T. Human resource management: a contemporary approach [Internet]. 2004

12 **Atherton JC**. The pathogenesis of Helicobacter pylori-induced gastro-duodenal diseases. *Annu Rev Pathol* 2006; **1**: 63-96 [PMID: 18039108 DOI: 10.1146/annurev.pathol.1.110304.100125]

13 **Basso D**, Zambon CF, Letley DP, Stranges A, Marchet A, Rhead JL, Schiavon S, Guariso G, Ceroti M, Nitti D, Rugge M, Plebani M, Atherton JC. Clinical relevance of Helicobacter pylori cagA and vacA gene polymorphisms. *Gastroenterology* 2008; **135**: 91-99 [PMID: 18474244 DOI: 10.1053/j.gastro.2008.03.041]

14 **Link A**, Langner C, Schirrmeister W, Habendorf W, Weigt J, Venerito M, Tammer I, Schlüter D, Schlaermann P, Meyer TF, Wex T, Malfertheiner P. *Helicobacter pylori* vacA genotype is a predominant determinant of immune response to *Helicobacter pylori* CagA. *World J Gastroenterol* 2017; **23**: 4712-4723 [PMID: 28765692 DOI: 10.3748/wjg.v23.i26.4712]

15 **Malfertheiner P**, Megraud F, O'Morain CA, Gisbert JP, Kuipers EJ, Axon AT, Bazzoli F, Gasbarrini A, Atherton J, Graham DY, Hunt R, Moayyedi P, Rokkas T, Rugge M, Selgrad M, Suerbaum S, Sugano K, El-Omar EM; European Helicobacter and Microbiota Study Group and Consensus panel. Management of Helicobacter pylori infection-the Maastricht V/Florence Consensus Report. *Gut* 2017; **66**: 6-30 [PMID: 27707777 DOI: 10.1136/gutjnl-2016-312288]

16 **Lauren P**. The two histological main types of gastric carcinoma: diffuse and so-called intestinal-type carcinoma. An attempt at a histo-clinical classification. *Acta Pathol Microbiol Scand* 1965; **64**: 31-49 [PMID: 14320675 DOI: 10.1111/apm.1965.64.1.31]

17 **Cancer Genome Atlas Research Network**. Comprehensive molecular characterization of gastric adenocarcinoma. *Nature* 2014; **513**: 202-209 [PMID: 25079317 DOI: 10.1038/nature13480]

18 **Shimada H**, Noie T, Ohashi M, Oba K, Takahashi Y. Clinical significance of serum tumor markers for gastric cancer: a systematic review of literature by the Task Force of the Japanese Gastric Cancer Association. *Gastric Cancer* 2014; **17**: 26-33 [PMID: 23572188 DOI: 10.1007/s10120-013-0259-5]

19 **Goni E**, Venerito M, Schulz C, Weigt J, Langner C, Link A, Malfertheiner P. Influence of laboratory-related and endoscopy-related factors on the assessment of serum pepsinogens and gastrin-17. *Eur J Gastroenterol Hepatol* 2017; **29**: 1340-1345 [PMID: 28984679 DOI: 10.1097/MEG.0000000000000952]

20 **Zagari RM**, Rabitti S, Greenwood DC, Eusebi LH, Vestito A, Bazzoli F. Systematic review with meta-analysis: diagnostic performance of the combination of pepsinogen, gastrin-17 and

anti-Helicobacter pylori antibodies serum assays for the diagnosis of atrophic gastritis. *Aliment Pharmacol Ther* 2017; **46**: 657-667 [PMID: 28782119 DOI: 10.1111/apt.14248]
21 **Huang YK**, Yu JC, Kang WM, Ma ZQ, Ye X, Tian SB, Yan C. Significance of Serum Pepsinogens as a Biomarker for Gastric Cancer and Atrophic Gastritis Screening: A Systematic Review and Meta-Analysis. *PLoS One* 2015; **10**: e0142080 [PMID: 26556485 DOI: 10.1371/journal.pone.0142080]
22 **Bornschein J**, Selgrad M, Wex T, Kuester D, Malfertheiner P. Serological assessment of gastric mucosal atrophy in gastric cancer. *BMC Gastroenterol* 2012; **12**: 10 [PMID: 22289789 DOI: 10.1186/1471-230X-12-10]
23 **Lujambio A**, Lowe SW. The microcosmos of cancer. *Nature* 2012; **482**: 347-355 [PMID: 22337054 DOI: 10.1038/nature10888]
24 **McLean MH**, El-Omar EM. Genetics of gastric cancer. *Nat Rev Gastroenterol Hepatol* 2014; **11**: 664-674 [PMID: 25134511 DOI: 10.1038/nrgastro.2014.143]
25 **Link A**, Schirrmeister W, Langner C, Varbanova M, Bornschein J, Wex T, Malfertheiner P. Differential expression of microRNAs in preneoplastic gastric mucosa. *Sci Rep* 2015; **5**: 8270 [PMID: 25652892 DOI: 10.1038/srep08270]
26 **Juzėnas S**, Saltenienė V, Kupcinskas J, Link A, Kiudelis G, Jonaitis L, Jarmalaite S, Kupcinskas L, Malfertheiner P, Skieceviciene J. Analysis of Deregulated microRNAs and Their Target Genes in Gastric Cancer. *PLoS One* 2015; **10**: e0132327 [PMID: 26172537 DOI: 10.1371/journal.pone.0132327]
27 **Juzenas S**, Venkatesh G, Hübenthal M, Hoeppner MP, Du ZG, Paulsen M, Rosenstiel P, Senger P, Hofmann-Apitius M, Keller A, Kupcinskas L, Franke A, Hemmrich-Stanisak G. A comprehensive, cell specific microRNA catalogue of human peripheral blood. *Nucleic Acids Res* 2017; **45**: 9290-9301 [PMID: 28934507 DOI: 10.1093/nar/gkx706]
28 **Link A**, Balaguer F, Shen Y, Nagasaka T, Lozano JJ, Boland CR, Goel A. Fecal MicroRNAs as novel biomarkers for colon cancer screening. *Cancer Epidemiol Biomarkers Prev* 2010; **19**: 1766-1774 [PMID: 20551304 DOI: 10.1158/1055-9965.EPI-10-0027]
29 **Link A**, Becker V, Goel A, Wex T, Malfertheiner P. Feasibility of fecal microRNAs as novel biomarkers for pancreatic cancer. *PLoS One* 2012; **7**: e42933 [PMID: 22905187 DOI: 10.1371/journal.pone.0042933]
30 **Yu L**, Todd NW, Xing L, Xie Y, Zhang H, Liu Z, Fang H, Zhang J, Katz RL, Jiang F. Early detection of lung adenocarcinoma in sputum by a panel of microRNA markers. *Int J Cancer* 2010; **127**: 2870-2878 [PMID: 21351266 DOI: 10.1002/ijc.25289]
31 **Schindler P**, Kupcinskas J, Juzenas S, Skieceviciene J, Salteniene V, Schulz C, Weigt J, Malfertheiner P, Link A. Expression of microRNAs in the ascites of patients with peritoneal carcinomatosis and peritonitis. *Cancer Cytopathol* 2018; **126**: 353-363 [PMID: 29360196 DOI: 10.1002/cncy.21966]
32 **Weber JA**, Baxter DH, Zhang S, Huang DY, Huang KH, Lee MJ, Galas DJ, Wang K. The microRNA spectrum in 12 body fluids. *Clin Chem* 2010; **56**: 1733-1741 [PMID: 20847327 DOI: 10.1373/clinchem.2010.147405]
33 **Ueda T**, Volinia S, Okumura H, Shimizu M, Taccioli C, Rossi S, Alder H, Liu CG, Oue N, Yasui W, Yoshida K, Sasaki H, Nomura S, Seto Y, Kaminishi M, Calin GA, Croce CM. Relation between microRNA expression and progression and prognosis of gastric cancer: a microRNA expression analysis. *Lancet Oncol* 2010; **11**: 136-146 [PMID: 20022810 DOI: 10.1016/S1470-2045(09)70343-2]
34 **Steponaitiene R**, Kupcinskas J, Langner C, Balaguer F, Venclauskas L, Pauzas H, Tamelis A, Skieceviciene J, Kupcinskas L, Malfertheiner P, Link A. Epigenetic silencing of miR-137 is a frequent event in gastric carcinogenesis. *Mol Carcinog* 2016; **55**: 376-386 [PMID: 25663388 DOI: 10.1002/mc.22287]
35 **Han TS**, Hur K, Xu G, Choi B, Okugawa Y, Toiyama Y, Oshima H, Oshima M, Lee HJ, Kim VN, Chang AN, Goel A, Yang HK. MicroRNA-29c mediates initiation of gastric carcinogenesis by directly targeting ITGB1. *Gut* 2015; **64**: 203-214 [PMID: 24870620 DOI: 10.1136/gutjnl-2013-306640]
36 **Sousa JF**, Nam KT, Petersen CP, Lee HJ, Yang HK, Kim WH, Goldenring JR. miR-30-HNF4γ and miR-194-NR2F2 regulatory networks contribute to the upregulation of metaplasia markers in the stomach. *Gut* 2016; **65**: 914-924 [PMID: 25800782 DOI: 10.1136/gutjnl-2014-308759]
37 **Mishra PJ**, Bertino JR. MicroRNA polymorphisms: the future of pharmacogenomics, molecular epidemiology and individualized medicine. *Pharmacogenomics* 2009; **10**: 399-416 [PMID: 19290790 DOI: 10.2217/14622416.10.3.399]
38 **Liu C**, Rennie WA, Carmack CS, Kanoria S, Cheng J, Lu J, Ding Y. Effects of genetic variations on microRNA: target interactions. *Nucleic Acids Res* 2014; **42**: 9543-9552 [PMID: 25081214 DOI: 10.1093/nar/gku675]
39 **Kupcinskas J**, Bruzaite I, Juzenas S, Gyvyte U, Jonaitis L, Kiudelis G, Skieceviciene J, Leja M, Pauzas H, Tamelis A, Pavalkis D, Kupcinskas L. Lack of association between miR-27a, miR-146a, miR-196a-2, miR-492 and miR-608 gene polymorphisms and colorectal cancer. *Sci Rep* 2014; **4**: 5993 [PMID: 25103961 DOI: 10.1038/srep05993]
40 **Kupcinskas J**, Wex T, Link A, Leja M, Bruzaite I, Steponaitiene R, Juzenas S, Gyvyte U, Ivanauskas A, Ancans G, Petrenkiene V, Skieceviciene J, Kupcinskas L, Malfertheiner P. Gene polymorphisms of micrornas in Helicobacter pylori-induced high risk atrophic gastritis and gastric cancer. *PLoS One* 2014; **9**: e87467 [PMID: 24475294 DOI: 10.1371/journal.pone.0087467]
41 **Petkevicius V**, Salteniene V, Juzenas S, Wex T, Link A, Leja M, Steponaitiene R, Skieceviciene J, Kupcinskas L, Jonaitis L, Kiudelis G, Malfertheiner P, Kupcinskas J. Polymorphisms of microRNA target genes *IL12B*, *INSR*, *CCND1* and *IL10* in gastric cancer. *World J Gastroenterol* 2017; **23**: 3480-3487 [PMID: 28596683 DOI: 10.3748/wjg.v23.i19.3480]
42 **Fu B**, Song P, Lu M, Wang B, Zhao Q. The association between miR-146a gene rs2910164 polymorphism and gastric cancer risk: a meta-analysis. *Biomed Pharmacother* 2014; **68**: 923-928 [PMID: 25455160 DOI: 10.1016/j.biopha.2014.10.002]
43 **Lawrie CH**, Gal S, Dunlop HM, Pushkaran B, Liggins AP, Pulford K, Banham AH, Pezzella F, Boultwood J, Wainscoat JS, Hatton CS, Harris AL. Detection of elevated levels of tumour-associated microRNAs in serum of patients with diffuse large B-cell lymphoma. *Br J Haematol* 2008; **141**: 672-675 [PMID: 18318758 DOI: 10.1111/j.1365-2141.2008.07077.x]
44 **Mitchell PS**, Parkin RK, Kroh EM, Fritz BR, Wyman SK, Pogosova-Agadjanyan EL, Peterson A, Noteboom J, O'Briant KC, Allen A, Lin DW, Urban N, Drescher CW, Knudsen BS, Stirewalt DL, Gentleman R, Vessella RL, Nelson PS, Martin DB, Tewari M. Circulating microRNAs as stable blood-based markers for cancer detection. *Proc Natl Acad Sci U S A* 2008; **105**: 10513-10518 [PMID: 18663219 DOI: 10.1073/pnas.0804549105]
45 **Chen X**, Ba Y, Ma L, Cai X, Yin Y, Wang K, Guo J, Zhang Y, Chen J, Guo X, Li Q, Li X, Wang W, Zhang Y, Wang J, Jiang X, Xiang Y, Xu C, Zheng P, Zhang J, Li R, Zhang H, Shang X, Gong T, Ning G, Wang J, Zen K, Zhang J, Zhang CY. Characterization of microRNAs in serum: a novel class of biomarkers for diagnosis of cancer and other diseases. *Cell Res* 2008; **18**: 997-1006 [PMID: 18766170 DOI: 10.1038/cr.2008.282]
46 **Tokuhisa M**, Ichikawa Y, Kosaka N, Ochiya T, Yashiro M, Hirakawa K, Kosaka T, Makino H, Akiyama H, Kunisaki C, Endo I. Exosomal miRNAs from Peritoneum Lavage Fluid as Potential Prognostic Biomarkers of Peritoneal Metastasis in Gastric Cancer. *PLoS One* 2015; **10**: e0130472 [PMID: 26208314 DOI: 10.1371/journal.pone.0130472]
47 **Qiu X**, Zhang J, Shi W, Liu S, Kang M, Chu H, Wu D, Tong N, Gong W, Tao G, Zhao Q, Qiang F, Zhu H, Wu Q, Wang M, Zhang Z. Circulating MicroRNA-26a in Plasma and Its Potential Diagnostic Value in Gastric Cancer. *PLoS One* 2016; **11**: e0151345 [PMID: 27010210 DOI: 10.1371/journal.pone.0151345]
48 **Song J**, Bai Z, Han W, Zhang J, Meng H, Bi J, Ma X, Han S, Zhang Z. Identification of suitable reference genes for qPCR analysis of serum microRNA in gastric cancer patients. *Dig Dis Sci* 2012; **57**: 897-904 [PMID: 22198701 DOI: 10.1007/s10620-011-1981-7]
49 **Peng WZ**, Ma R, Wang F, Yu J, Liu ZB. Role of miR-191/425

cluster in tumorigenesis and diagnosis of gastric cancer. *Int J Mol Sci* 2014; **15**: 4031-4048 [PMID: 24603541 DOI: 10.3390/ijms15034031]

50 **Shiotani A**, Murao T, Kimura Y, Matsumoto H, Kamada T, Kusunoki H, Inoue K, Uedo N, Iishi H, Haruma K. Identification of serum miRNAs as novel non-invasive biomarkers for detection of high risk for early gastric cancer. *Br J Cancer* 2013; **109**: 2323-2330 [PMID: 24104965 DOI: 10.1038/bjc.2013.596]

51 **Zhu C**, Ren C, Han J, Ding Y, Du J, Dai N, Dai J, Ma H, Hu Z, Shen H, Xu Y, Jin G. A five-microRNA panel in plasma was identified as potential biomarker for early detection of gastric cancer. *Br J Cancer* 2014; **110**: 2291-2299 [PMID: 24595006 DOI: 10.1038/bjc.2014.119]

52 **Wang H**, Wang L, Wu Z, Sun R, Jin H, Ma J, Liu L, Ling R, Yi J, Wang L, Bian J, Chen J, Li N, Yuan S, Yun J. Three dysregulated microRNAs in serum as novel biomarkers for gastric cancer screening. *Med Oncol* 2014; **31**: 298 [PMID: 25367852 DOI: 10.1007/s12032-014-0298-8]

53 **Zhang J**, Song Y, Zhang C, Zhi X, Fu H, Ma Y, Chen Y, Pan F, Wang K, Ni J, Jin W, He X, Su H, Cui D. Circulating MiR-16-5p and MiR-19b-3p as Two Novel Potential Biomarkers to Indicate Progression of Gastric Cancer. *Theranostics* 2015; **5**: 733-745 [PMID: 25897338 DOI: 10.7150/thno.10305]

54 **Konishi H**, Ichikawa D, Komatsu S, Shiozaki A, Tsujiura M, Takeshita H, Morimura R, Nagata H, Arita T, Kawaguchi T, Hirashima S, Fujiwara H, Okamoto K, Otsuji E. Detection of gastric cancer-associated microRNAs on microRNA microarray comparing pre- and post-operative plasma. *Br J Cancer* 2012; **106**: 740-747 [PMID: 22262318 DOI: 10.1038/bjc.2011.588]

55 **Liu X**, Kwong A, Sihoe A, Chu KM. Plasma miR-940 may serve as a novel biomarker for gastric cancer. *Tumour Biol* 2016; **37**: 3589-3597 [PMID: 26456959 DOI: 10.1007/s13277-015-4019-5]

56 **Tsujiura M**, Ichikawa D, Komatsu S, Shiozaki A, Takeshita H, Kosuga T, Konishi H, Morimura R, Deguchi K, Fujiwara H, Okamoto K, Otsuji E. Circulating microRNAs in plasma of patients with gastric cancers. *Br J Cancer* 2010; **102**: 1174-1179 [PMID: 20234369 DOI: 10.1038/sj.bjc.6605608]

57 **Wang WN**, Chen Y, Zhang YD, Hu TH. The regulatory mechanism of CCR7 gene expression and its involvement in the metastasis and progression of gastric cancer. *Tumour Biol* 2013; **34**: 1865-1871 [PMID: 23519840 DOI: 10.1007/s13277-013-0728-9]

58 **Li C**, Li JF, Cai Q, Qiu QQ, Yan M, Liu BY, Zhu ZG. miRNA-199a-3p in plasma as a potential diagnostic biomarker for gastric cancer. *Ann Surg Oncol* 2013; **20** Suppl 3: S397-S405 [PMID: 22956063 DOI: 10.1245/s10434-012-2600-3]

59 **Liu WJ**, Xu Q, Sun LP, Dong QG, He CY, Yuan Y. Expression of serum let-7c, let-7i, and let-7f microRNA with its target gene, pepsinogen C, in gastric cancer and precancerous disease. *Tumour Biol* 2015; **36**: 3337-3343 [PMID: 25549793 DOI: 10.1007/s13277-014-2967-9]

60 **Song MY**, Pan KF, Su HJ, Zhang L, Ma JL, Li JY, Yuasa Y, Kang D, Kim YS, You WC. Identification of serum microRNAs as novel non-invasive biomarkers for early detection of gastric cancer. *PLoS One* 2012; **7**: e33608 [PMID: 22432036 DOI: 10.1371/journal.pone.0033608]

61 **Huang S**, Wang J, Li J, Luo Q, Zhao M, Zheng L, Dong X, Chen C, Che Y, Liu P, Qi J, Huang C. Serum microRNA expression profile as a diagnostic panel for gastric cancer. *Jpn J Clin Oncol* 2016; **46**: 811-818 [PMID: 27380811 DOI: 10.1093/jjco/hyw085]

62 **Liu R**, Zhang C, Hu Z, Li G, Wang C, Yang C, Huang D, Chen X, Zhang H, Zhuang R, Deng T, Liu H, Yin J, Wang S, Zen K, Ba Y, Zhang CY. A five-microRNA signature identified from genome-wide serum microRNA expression profiling serves as a fingerprint for gastric cancer diagnosis. *Eur J Cancer* 2011; **47**: 784-791 [PMID: 21112772 DOI: 10.1016/j.ejca.2010.10.025]

63 **Cai H**, Yuan Y, Hao YF, Guo TK, Wei X, Zhang YM. Plasma microRNAs serve as novel potential biomarkers for early detection of gastric cancer. *Med Oncol* 2013; **30**: 452 [PMID: 23307259 DOI: 10.1007/s12032-012-0452-0]

64 **Treece AL**, Duncan DL, Tang W, Elmore S, Morgan DR, Dominguez RL, Speck O, Meyers MO, Gulley ML. Gastric adenocarcinoma microRNA profiles in fixed tissue and in plasma reveal cancer-associated and Epstein-Barr virus-related expression patterns. *Lab Invest* 2016; **96**: 661-671 [PMID: 26950485 DOI: 10.1038/labinvest.2016.33]

65 **Oze I**, Shimada S, Nagasaki H, Akiyama Y, Watanabe M, Yatabe Y, Matsuo K, Yuasa Y. Plasma microRNA-103, microRNA-107, and microRNA-194 levels are not biomarkers for human diffuse gastric cancer. *J Cancer Res Clin Oncol* 2017; **143**: 551-554 [PMID: 27909811 DOI: 10.1007/s00432-016-2316-z]

66 **Zhou H**, Guo JM, Lou YR, Zhang XJ, Zhong FD, Jiang Z, Cheng J, Xiao BX. Detection of circulating tumor cells in peripheral blood from patients with gastric cancer using microRNA as a marker. *J Mol Med (Berl)* 2010; **88**: 709-717 [PMID: 20349219 DOI: 10.1007/s00109-010-0617-2]

67 **Yuan R**, Wang G, Xu Z, Zhao H, Chen H, Han Y, Wang B, Zhou J, Hu H, Guo Z, Shen H, Xue X. Up-regulated Circulating miR-106a by DNA Methylation Promised a Potential Diagnostic and Prognostic Marker for Gastric Cancer. *Anticancer Agents Med Chem* 2016; **16**: 1093-1100 [PMID: 26179261 DOI: 10.2174/1871520615666150716110657]

68 **Sierzega M**, Kaczor M, Kolodziejczyk P, Kulig J, Sanak M, Richter P. Evaluation of serum microRNA biomarkers for gastric cancer based on blood and tissue pools profiling: the importance of miR-21 and miR-331. *Br J Cancer* 2017; **117**: 266-273 [PMID: 28641313 DOI: 10.1038/bjc.2017.190]

69 **Wang N**, Wang L, Yang Y, Gong L, Xiao B, Liu X. A serum exosomal microRNA panel as a potential biomarker test for gastric cancer. *Biochem Biophys Res Commun* 2017; **493**: 1322-1328 [PMID: 28986250 DOI: 10.1016/j.bbrc.2017.10.003]

70 **Kim SY**, Jeon TY, Choi CI, Kim DH, Kim DH, Kim GH, Ryu DY, Lee BE, Kim HH. Validation of circulating miRNA biomarkers for predicting lymph node metastasis in gastric cancer. *J Mol Diagn* 2013; **15**: 661-669 [PMID: 23806809 DOI: 10.1016/j.jmoldx.2013.04.004]

71 **Zhang R**, Wang W, Li F, Zhang H, Liu J. MicroRNA-106b~25 expressions in tumor tissues and plasma of patients with gastric cancers. *Med Oncol* 2014; **31**: 243 [PMID: 25218271 DOI: 10.1007/s12032-014-0243-x]

72 **Zeng Q**, Jin C, Chen W, Xia F, Wang Q, Fan F, Du J, Guo Y, Lin C, Yang K, Li J, Peng X, Li X, Cao K. Downregulation of serum miR-17 and miR-106b levels in gastric cancer and benign gastric diseases. *Chin J Cancer Res* 2014; **26**: 711-716 [PMID: 25561770 DOI: 10.3978/j.issn.1000-9604.2014.12.03]

73 **Li F**, Guo Y, Liu J, Zhang R. The significance of elevated plasma expression of microRNA 106b~25 clusters in gastric cancer. *PLoS One* 2017; **12**: e0178427 [PMID: 28562634 DOI: 10.1371/journal.pone.0178427]

74 **Ayremlou N**, Mozdarani H, Mowla SJ, Delavari A. Increased levels of serum and tissue miR-107 in human gastric cancer: Correlation with tumor hypoxia. *Cancer Biomark* 2015; **15**: 851-860 [PMID: 26406411 DOI: 10.3233/CBM-150529]

75 **Zhang M**, Wang X, Li W, Cui Y. miR-107 and miR-25 simultaneously target LATS2 and regulate proliferation and invasion of gastric adenocarcinoma (GAC) cells. *Biochem Biophys Res Commun* 2015; **460**: 806-812 [PMID: 25824045 DOI: 10.1016/j.bbrc.2015.03.110]

76 **Huang Z**, Zhu D, Wu L, He M, Zhou X, Zhang L, Zhang H, Wang W, Zhu J, Cheng W, Chen Y, Fan Y, Qi L, Yin Y, Zhu W, Shu Y, Liu P. Six Serum-Based miRNAs as Potential Diagnostic Biomarkers for Gastric Cancer. *Cancer Epidemiol Biomarkers Prev* 2017; **26**: 188-196 [PMID: 27756776 DOI: 10.1158/1055-9965.EPI-16-0607]

77 **Chen Q**, Ge X, Zhang Y, Xia H, Yuan D, Tang Q, Chen L, Pang X, Leng W, Bi F. Plasma miR-122 and miR-192 as potential novel biomarkers for the early detection of distant metastasis of gastric cancer. *Oncol Rep* 2014; **31**: 1863-1870 [PMID: 24481716 DOI: 10.3892/or.2014.3004]

78 **Zhang ZZ**, Wang CJ, Niu L, Xu J, Wang M, Cao H, Hu B. Analysis of plasma MicroRNAs to identifying early diagnostic molecule for gastric cancer. *Int J Clin Exp Med* 2015; **8**: 3700-3706 [PMID: 26064265]

79 **Jiang H**, Yu WW, Wang LL, Peng Y. miR-130a acts as a potential diagnostic biomarker and promotes gastric cancer migration, invasion and proliferation by targeting RUNX3. *Oncol Rep* 2015; **34**: 1153-1161 [PMID: 26134263 DOI: 10.3892/or.2015.4099]

80 **Chen S**, Zhu J, Yu F, Tian Y, Ma S, Liu X. Combination of miRNA and RNA functions as potential biomarkers for gastric cancer. *Tumour Biol* 2015; **36**: 9909-9918 [PMID: 26168960 DOI: 10.1007/s13277-015-3756-9]

81 **Shin VY**, Ng EK, Chan VW, Kwong A, Chu KM. A three-miRNA signature as promising non-invasive diagnostic marker for gastric cancer. *Mol Cancer* 2015; **14**: 202 [PMID: 26607322 DOI: 10.1186/s12943-015-0473-3]

82 **Jiang X,** Wang W, Yang Y, Du L, Yang X, Wang L, Zheng G, Duan W, Wang R, Zhang X, Wang L, Chen X, Wang C. Identification of circulating microRNA signatures as potential noninvasive biomarkers for prediction and prognosis of lymph node metastasis in gastric cancer. *Oncotarget* 2017;724:65132-65142 [DOI: 10.18632/oncotarget.17789]

83 **Liu S**, Suo J, Wang C, Sun X, Wang D, He L, Zhang Y, Li W. Prognostic significance of low miR-144 expression in gastric cancer. *Cancer Biomark* 2017; **20**: 547-552 [PMID: 28800316 DOI: 10.3233/CBM-170351]

84 **Tang G**, Shen X, Lv K, Wu Y, Bi J, Shen Q. Different normalization strategies might cause inconsistent variation in circulating microRNAs in patients with hepatocellular carcinoma. *Med Sci Monit* 2015; **21**: 617-624 [PMID: 25719241 DOI: 10.12659/MSM.891028]

85 **Park JL**, Kim M, Song KS, Kim SY, Kim YS. Cell-Free miR-27a, a Potential Diagnostic and Prognostic Biomarker for Gastric Cancer. *Genomics Inform* 2015; **13**: 70-75 [PMID: 26523130 DOI: 10.5808/GI.2015.13.3.70]

86 **Zhao C**, Li Y, Chen G, Wang F, Shen Z, Zhou R. Overexpression of miR-15b-5p promotes gastric cancer metastasis by regulating PAQR3. *Oncol Rep* 2017; **38**: 352-358 [PMID: 28560431 DOI: 10.3892/or.2017.5673]

87 **Cui MH**, Hou XL, Lei XY, Mu FH, Yang GB, Yue L, Fu Y, Yi GX. Upregulation of microRNA 181c expression in gastric cancer tissues and plasma. *Asian Pac J Cancer Prev* 2013; **14**: 3063-3066 [PMID: 23803080 DOI: 10.7314/APJCP.2013.14.5.3063]

88 **Zhou X**, Zhu W, Li H, Wen W, Cheng W, Wang F, Wu Y, Qi L, Fan Y, Chen Y, Ding Y, Xu J, Qian J, Huang Z, Wang T, Zhu D, Shu Y, Liu P. Diagnostic value of a plasma microRNA signature in gastric cancer: a microRNA expression analysis. *Sci Rep* 2015; **5**: 11251 [PMID: 26059512 DOI: 10.1038/srep11251]

89 **Liu H**, Zhu L, Liu B, Yang L, Meng X, Zhang W, Ma Y, Xiao H. Genome-wide microRNA profiles identify miR-378 as a serum biomarker for early detection of gastric cancer. *Cancer Lett* 2012; **316**: 196-203 [PMID: 22169097 DOI: 10.1016/j.canlet.2011.10.034]

90 **Tsujiura M**, Komatsu S, Ichikawa D, Shiozaki A, Konishi H, Takeshita H, Moriumura R, Nagata H, Kawaguchi T, Hirajima S, Arita T, Fujiwara H, Okamoto K, Otsuji E. Circulating miR-18a in plasma contributes to cancer detection and monitoring in patients with gastric cancer. *Gastric Cancer* 2015; **18**: 271-279 [PMID: 24626859 DOI: 10.1007/s10120-014-0363-1]

91 **Shen YH**, Xie ZB, Yue AM, Wei QD, Zhao HF, Yin HD, Mai W, Zhong XG, Huang SR. Expression level of microRNA-195 in the serum of patients with gastric cancer and its relationship with the clinicopathological staging of the cancer. *Eur Rev Med Pharmacol Sci* 2016; **20**: 1283-1287 [PMID: 27097947]

92 **Gorur A**, Balci Fidanci S, Dogruer Unal N, Ayaz L, Akbayir S, Yildirim Yaroglu H, Dirlik M, Serin MS, Tamer L. Determination of plasma microRNA for early detection of gastric cancer. *Mol Biol Rep* 2013; **40**: 2091-2096 [PMID: 23212612 DOI: 10.1007/s11033-012-2267-7]

93 **Tsai MM**, Wang CS, Tsai CY, Huang CG, Lee KF, Huang HW, Lin YH, Chi HC, Kuo LM, Lu PH, Lin KH. Circulating microRNA-196a/b are novel biomarkers associated with metastatic gastric cancer. *Eur J Cancer* 2016; **64**: 137-148 [PMID: 27420607 DOI: 10.1016/j.ejca.2016.05.007]

94 **Li C**, Li JF, Cai Q, Qiu QQ, Yan M, Liu BY, Zhu ZG. MiRNA-199a-3p: A potential circulating diagnostic biomarker for early gastric cancer. *J Surg Oncol* 2013; **108**: 89-92 [PMID: 23733518 DOI: 10.1002/jso.23358]

95 **Valladares-Ayerbes M**, Reboredo M, Medina-Villaamil V, Iglesias-Díaz P, Lorenzo-Patiño MJ, Haz M, Santamarina I, Blanco M, Fernández-Tajes J, Quindós M, Carral A, Figueroa A, Antón-Aparicio LM, Calvo L. Circulating miR-200c as a diagnostic and prognostic biomarker for gastric cancer. *J Transl Med* 2012; **10**: 186 [PMID: 22954417 DOI: 10.1186/1479-5876-10-186]

96 **Zhang HP**, Sun FB, Li SJ. Serum miR-200c expression level as a prognostic biomarker for gastric cancer. *Genet Mol Res* 2015; **14**: 15913-15920 [PMID: 26662382 DOI: 10.4238/2015.December.7.2]

97 **Imaoka H**, Toiyama Y, Okigami M, Yasuda H, Saigusa S, Ohi M, Tanaka K, Inoue Y, Mohri Y, Kusunoki M. Circulating microRNA-203 predicts metastases, early recurrence, and poor prognosis in human gastric cancer. *Gastric Cancer* 2016; **19**: 744-753 [PMID: 26233325 DOI: 10.1007/s10120-015-0521-0]

98 **Chen X**, Liu XS, Liu HY, Lu YY, Li Y. Reduced expression of serum miR-204 predicts poor prognosis of gastric cancer. *Genet Mol Res* 2016; **15**: [PMID: 27173244 DOI: 10.4238/gmr.15027702]

99 **Hou CG**, Luo XY, Li G. Diagnostic and Prognostic Value of Serum MicroRNA-206 in Patients with Gastric Cancer. *Cell Physiol Biochem* 2016; **39**: 1512-1520 [PMID: 27614739 DOI: 10.1159/000447854]

100 **Du Y**, Zhu M, Zhou X, Huang Z, Zhu J, Xu J, Cheng G, Shu Y, Liu P, Zhu W, Wang T. miR-20a enhances cisplatin resistance of human gastric cancer cell line by targeting NFKBIB. *Tumour Biol* 2016; **37**: 1261-1269 [PMID: 26286834 DOI: 10.1007/s13277-015-3921-1]

101 **Zhu M**, Zhou X, Du Y, Huang Z, Zhu J, Xu J, Cheng G, Shu Y, Liu P, Zhu W, Wang T. miR-20a induces cisplatin resistance of a human gastric cancer cell line via targeting CYLD. *Mol Med Rep* 2016; **14**: 1742-1750 [PMID: 27357419 DOI: 10.3892/mmr.2016.5413]

102 **Yang R**, Fu Y, Zeng Y, Xiang M, Yin Y, Li L, Xu H, Zhong J, Zeng X. Serum miR-20a is a promising biomarker for gastric cancer. *Biomed Rep* 2017; **6**: 429-434 [PMID: 28413641 DOI: 10.3892/br.2017.862]

103 **Zheng Y**, Cui L, Sun W, Zhou H, Yuan X, Huo M, Chen J, Lou Y, Guo J. MicroRNA-21 is a new marker of circulating tumor cells in gastric cancer patients. *Cancer Biomark* 2011; **10**: 71-77 [PMID: 22430134 DOI: 10.3233/CBM-2011-0231]

104 **Li BS**, Zhao YL, Guo G, Li W, Zhu ED, Luo X, Mao XH, Zou QM, Yu PW, Zuo QF, Li N, Tang B, Liu KY, Xiao B. Plasma microRNAs, miR-223, miR-21 and miR-218, as novel potential biomarkers for gastric cancer detection. *PLoS One* 2012; **7**: e41629 [PMID: 22860003 DOI: 10.1371/journal.pone.0041629]

105 **Wang B**, Zhang Q. The expression and clinical significance of circulating microRNA-21 in serum of five solid tumors. *J Cancer Res Clin Oncol* 2012; **138**: 1659-1666 [PMID: 22638884 DOI: 10.1007/s00432-012-1244-9]

106 **Wu J**, Li G, Wang Z, Yao Y, Chen R, Pu X, Wang J. Circulating MicroRNA-21 Is a Potential Diagnostic Biomarker in Gastric Cancer. *Dis Markers* 2015; **2015**: 435656 [PMID: 26063956 DOI: 10.1155/2015/435656]

107 **Xin SY**, Feng XS, Zhou LQ, Sun JJ, Gao XL, Yao GL. Reduced expression of circulating microRNA-218 in gastric cancer and correlation with tumor invasion and prognosis. *World J Gastroenterol* 2014; **20**: 6906-6911 [PMID: 24944481 DOI: 10.3748/wjg.v20.i22.6906]

108 **Fu Z**, Qian F, Yang X, Jiang H, Chen Y, Liu S. Circulating miR-222 in plasma and its potential diagnostic and prognostic value in gastric cancer. *Med Oncol* 2014; **31**: 164 [PMID: 25129310 DOI: 10.1007/s12032-014-0164-8]

109 **Zhou X**, Ji G, Chen H, Jin W, Yin C, Zhang G. Clinical role of circulating miR-223 as a novel biomarker in early diagnosis of cancer patients. *Int J Clin Exp Med* 2015; **8**: 16890-16898 [PMID: 26629240]

110 **Fassan M**, Saraggi D, Balsamo L, Realdon S, Scarpa M, Castoro C, Coati I, Salmaso R, Farinati F, Guzzardo V, Arcidiacono D, Munari G, Gasparini P, Veronese N, Luchini C, Valeri N, Rugge M. Early miR-223 Upregulation in Gastroesophageal Carcinogenesis. *Am J Clin Pathol* 2017; **147**: 301-308 [PMID: 28395057 DOI: 10.1093/ajcp/aqx004]

111 **Zhuang K**, Han K, Tang H, Yin X, Zhang J, Zhang X, Zhang L. Up-Regulation of Plasma miR-23b is Associated with Poor Prognosis of Gastric Cancer. *Med Sci Monit* 2016; **22**: 356-361 [PMID: 26835790 DOI: 10.12659/MSM.895428]

112 **Li BS**, Zuo QF, Zhao YL, Xiao B, Zhuang Y, Mao XH, Wu C, Yang SM, Zeng H, Zou QM, Guo G. MicroRNA-25 promotes gastric cancer migration, invasion and proliferation by directly targeting transducer of ERBB2, 1 and correlates with poor survival. *Oncogene* 2015; **34**: 2556-2565 [PMID: 25043310 DOI: 10.1038/onc.2014.214]

113 **Yan C**, Yu J, Liu Y, Kang W, Ma Z, Zhou L. MiR-32 promotes gastric carcinoma tumorigenesis by targeting Kruppel-like factor 4. *Biochem Biophys Res Commun* 2015; **467**: 913-920 [PMID: 26471298 DOI: 10.1016/j.bbrc.2015.10.044]

114 **Sandoval-Bórquez A**, Polakovicova I, Carrasco-Véliz N, Lobos-González L, Riquelme I, Carrasco-Avino G, Bizama C, Norero E, Owen GI, Roa JC, Corvalán AH. MicroRNA-335-5p is a potential suppressor of metastasis and invasion in gastric cancer. *Clin Epigenetics* 2017; **9**: 114 [PMID: 29075357 DOI: 10.1186/s13148-017-0413-8]

115 **Lo SS**, Hung PS, Chen JH, Tu HF, Fang WL, Chen CY, Chen WT, Gong NR, Wu CW. Overexpression of miR-370 and downregulation of its novel target TGFβ-R Ⅱ contribute to the progression of gastric carcinoma. *Oncogene* 2012; **31**: 226-237 [PMID: 21666718 DOI: 10.1038/onc.2011.226]

116 **Zhang WH**, Gui JH, Wang CZ, Chang Q, Xu SP, Cai CH, Li YN, Tian YP, Yan L, Wu B. The identification of miR-375 as a potential biomarker in distal gastric adenocarcinoma. *Oncol Res* 2012; **20**: 139-147 [PMID: 23461060 DOI: 10.3727/096504012X13522227232156]

117 **Hung PS**, Chen CY, Chen WT, Kuo CY, Fang WL, Huang KH, Chiu PC, Lo SS. miR-376c promotes carcinogenesis and serves as a plasma marker for gastric carcinoma. *PLoS One* 2017; **12**: e0177346 [PMID: 28486502 DOI: 10.1371/journal.pone.0177346]

118 **Zhou H**, Xiao B, Zhou F, Deng H, Zhang X, Lou Y, Gong Z, Du C, Guo J. MiR-421 is a functional marker of circulating tumor cells in gastric cancer patients. *Biomarkers* 2012; **17**: 104-110 [PMID: 22263628 DOI: 10.3109/1354750X.2011.614961]

119 **Zhao G**, Xu L, Hui L, Zhao J. Level of circulated microRNA-421 in gastric carcinoma and related mechanisms. *Int J Clin Exp Pathol* 2015; **8**: 14252-14256 [PMID: 26823741]

120 **Wu J**, Li G, Yao Y, Wang Z, Sun W, Wang J. MicroRNA-421 is a new potential diagnosis biomarker with higher sensitivity and specificity than carcinoembryonic antigen and cancer antigen 125 in gastric cancer. *Biomarkers* 2015; **20**: 58-63 [PMID: 25510566 DOI: 10.3109/1354750X.2014.992812]

121 **Shah AA**, Leidinger P, Backes C, Keller A, Karpinski P, Sasiadek MM, Blin N, Meese E. A set of specific miRNAs is connected with murine and human gastric cancer. *Genes Chromosomes Cancer* 2013; **52**: 237-249 [PMID: 23124995 DOI: 10.1002/gcc.22024]

122 **Li SC**, Liao YL, Ho MR, Tsai KW, Lai CH, Lin WC. miRNA arm selection and isomiR distribution in gastric cancer. *BMC Genomics* 2012; **13** Suppl 1: S13 [PMID: 22369582 DOI: 10.1186/1471-2164-13-S1-S13]

123 **Telonis AG**, Rigoutsos I. Race Disparities in the Contribution of miRNA Isoforms and tRNA-Derived Fragments to Triple-Negative Breast Cancer. *Cancer Res* 2018; **78**: 1140-1154 [PMID: 29229607 DOI: 10.1158/0008-5472.CAN-17-1947]

124 **Gyvyte U**, Juzenas S, Salteniene V, Kupcinskas J, Poskiene L, Kucinskas L, Jarmalaite S, Stuopelyte K, Steponaitiene R, Hemmrich-Stanisak G, Hübenthal M, Link A, Franke S, Franke A, Pangonyte D, Lesauskaite V, Kupcinskas L, Skieceviciene J. MiRNA profiling of gastrointestinal stromal tumors by next-generation sequencing. *Oncotarget* 2017; **8**: 37225-37238 [PMID: 28402935 DOI: 10.18632/oncotarget.16664]

125 **Lawson DA**, Bhakta NR, Kessenbrock K, Prummel KD, Yu Y, Takai K, Zhou A, Eyob H, Balakrishnan S, Wang CY, Yaswen P, Goga A, Werb Z. Single-cell analysis reveals a stem-cell program in human metastatic breast cancer cells. *Nature* 2015; **526**: 131-135 [PMID: 26416748 DOI: 10.1038/nature15260]

P- Reviewer: Aurello P, Gurkan A, Kim GH, Lin JY, Yoshiyama H
S- Editor: Gong ZM **L- Editor**: A **E- Editor**: Yin SY

World Journal of Gastroenterology

Submit a Manuscript: http://www.f6publishing.com

World J Gastroenterol 2018 August 14; 24(30): 3330-3346

DOI: 10.3748/wjg.v24.i30.3330

ISSN 1007-9327 (print) ISSN 2219-2840 (online)

REVIEW

Nutritional issues in patients with obesity and cirrhosis

Luigi Schiavo, Luca Busetto, Manuela Cesaretti, Shira Zelber-Sagi, Liat Deutsch, Antonio Iannelli

Luigi Schiavo, Department of Translational Medical Science, University of Campania "Luigi Vanvitelli", Naples 80131, Italy

Luigi Schiavo, IX Division of General Surgery, Vascular Surgery and Applied Biotechnology, Naples University Policlinic, Naples 80131, Italy

Luca Busetto, Department of Medicine, University of Padua, Padua 35128, Italy

Luca Busetto, Center for the Study and the Integrated Management of Obesity, University Hospital of Padua, Padua 35128, Italy

Manuela Cesaretti, Department of HPB Surgery and Liver Transplantation, Hôpital Beaujon, AP-HP, Clichy 92110, France

Manuela Cesaretti, Department of Nanophysics, Italian Institute of Technology, Genova 16163, Italy

Shira Zelber-Sagi, School of Public Health, University of Haifa, Haifa 3498838, Israel

Shira Zelber-Sagi, Liat Deutsch, Department of Gastroenterology and Liver disease, Tel Aviv Medical Center, 62431, Tel-Aviv 62431, Israel

Liat Deutsch, The Sackler Faculty of Medicine, Tel-Aviv University, Tel-Aviv 62431, Israel

Antonio Iannelli, Digestive Unit, Archet 2 Hospital, University Hospital of Nice, F-06202, Nice, France; Inserm, U1065, Team 8 "Hepatic complications of obesity", Nice F-06204, France

Antonio Iannelli, University of Nice Sophia-Antipolis, Nice F-06107, France

ORCID number: Luigi Schiavo (0000-0003-3639-6847); Luca Busetto (0000-0003-4883-8980); Manuela Cesaretti (0000-0001-6419-1481); Shira Zelber-Sagi (0000-0002-1324-7497); Liat Deutsch (0000-0001-5022-4318); Antonio Iannelli (0000-0002-1611-071X).

Author contributions: All authors equally contributed to this paper with conception and design of the study, literature review and analysis, drafting and critical revision and editing, and final approval of the final version.

Conflict-of-interest statement: No potential conflicts of interest. No financial support.

Manuscript source: Invited manuscript

Correspondence to: Antonio Iannelli, MD, PhD, Professor, Digestive Unit, Archet 2 Hospital, University Hospital of Nice, 151 route Saint Antoine de Ginestiere, Nice F-06202, France. iannelli.a@chu-nice.fr
Telephone: +33-310-2678771
Fax: +33-310-2678772

Received: April 3, 2018
Peer-review started: April 4, 2018
First decision: May 30, 2018
Revised: June 15, 2018
Accepted: June 25, 2018
Article in press: June 25, 2018
Published online: August 14, 2018

Abstract

Obesity and metabolic syndrome are considered as responsible for a condition known as the non-alcoholic fatty liver disease that goes from simple accumulation of triglycerides to hepatic inflammation and may progress to cirrhosis. Patients with obesity also have an increased risk of primary liver malignancies and increased body mass index is a predictor of decompensation of liver cirrhosis. Sarcopenic obesity confers a risk of physical impairment and disability that is significantly higher than the risk induced by each of the two conditions alone as it has been shown to be an independent risk factor for chronic

liver disease in patients with obesity and a prognostic negative marker for the evolution of liver cirrhosis and the results of liver transplantation. Cirrhotic patients with obesity are at high risk for depletion of various fat-soluble, water-soluble vitamins and trace elements and should be supplemented appropriately. Diet, physical activity and protein intake should be carefully monitored in these fragile patients according to recent recommendations. Bariatric surgery is sporadically used in patients with morbid obesity and cirrhosis also in the setting of liver transplantation. The risk of sarcopenia, micronutrient status, and the recommended supplementation in patients with obesity and cirrhosis are discussed in this review. Furthermore, the indications and contraindications of bariatric surgery-induced weight loss in the cirrhotic patient with obesity are discussed.

Key words: Obesity; Cirrhosis; Sarcopenia; Malnutrition; Bariatric surgery

Core tip: Obesity is a frequent cause of chronic liver disease that can progress to cirrhosis. Cirrhotic patients with obesity frequently have alterations in specific aspects of nutritional status, such as poor protein intake and micronutrient deficiencies. Diet, physical activity and protein intake should be carefully monitored. Bariatric surgery may be an option in the management of patients with morbid obesity and cirrhosis also in the setting of liver transplantation but scientific evidence is still scarce.

Schiavo L, Busetto L, Cesaretti M, Zelber-Sagi S, Deutsch L, Iannelli A. Nutritional issues in patients with obesity and cirrhosis. *World J Gastroenterol* 2018; 24(30): 3330-3346 Available from: URL: http://www.wjgnet.com/1007-9327/full/v24/i30/3330.htm DOI: http://dx.doi.org/10.3748/wjg.v24.i30.3330

INTRODUCTION

Liver cirrhosis and obesity: Definitions and epidemiology

Obesity is associated with many adverse consequences for health and is closely related to insulin resistance, dyslipidemia, and hypertension. Non-alcoholic fatty liver disease (NAFLD) represents the hepatic manifestation of metabolic syndrome and is intimately related to the chronic intrahepatic inflammation that, in turn, is linked to adiposity and insulin resistance. Defined as a fatty infiltration of the liver exceeding 5% at histology in the absence of previous or ongoing significant alcohol consumption[1] and/or drug and/or virus infection, NAFLD includes a wide spectrum of histopathological alterations ranging from simple steatosis (Figure 1A) to non-alcoholic steatohepatitis (NASH) (Figure 1B) and cirrhosis (Figure 1C) with end-stage liver disease. Furthermore, NAFLD has been also shown to increase the risk of primary liver malignancies such as hepatocellular carcinoma (HCC)[2-4]. However, the vast majority of patients with NAFLD will not progress as only a minority of those with NASH (3%-5%)[5] are at a high risk of developing chronic liver disease complications. In patients with NASH, 11% develop cirrhosis and approximately 40% of patients die within 15 years from any cause (of which 7.3% are due to liver-related complications, especially in those with advanced fibrosis or cirrhosis)[6]. Obesity and the chronic inflammation associated with it also have a negative effect on health. Excessive adipose tissue leads to an increased production of adipokines (such as IL-6, TNFa, monocyte chemoattracting protein-1, and plasminogen activator inhibitor-1) with proinflammatory, pro-fibrogenic, pro-angiogenic, and pro-oxidant effects on several tissues. Few data exist regarding the epidemiological and clinical impact of obesity in patients with pre-existent liver disease, however, obesity is considered an independent risk factor for the presence of severe fibrosis, fibrosis progression, and cirrhosis[7,8]. Several population-based studies have identified obesity as an independent risk factor for alcohol-induced liver damage. Indeed, ethanol influences the adipose tissue production of hormones and cytokines, and excess adiposity induces an exacerbation of the proinflammatory state. However, it is still unclear whether the hepatotoxic consequences of obesity and ethanol ingestion are additive or synergistic. The DIONYSOS study clearly showed a synergistic effect between alcohol consumption and elevated body mass index (BMI) on hepatic steatosis in a large cohort of subjects in Northern Italy[9]. The prevalence of hepatic steatosis determined by ultrasonography was increased to 46% in subjects with a daily intake of > 60 g of alcohol and to 76% in patients with obesity compared to lean controls who only revealed hepatic steatosis in 16% of cases. Moreover, in individuals with obesity drinking > 60 g of alcohol per day, steatosis was found at an even higher level of 95% and the relative risk of cirrhosis increased more than six-fold in women with obesity and alcohol consumption (> 150 g/wk) *vs* normal weight and drinking < 70 g/wk women. Ekstedt *et al*[10] found an accelerated progression of fibrosis in patients with NAFLD who drank moderate amounts of alcohol (up to 140 g/wk). Liu *et al*[11] analyzed more than 1 million middle-aged women in the UK and reported that in women with obesity who drank > 150 g of alcohol/week, the relative risk of cirrhosis increased more than six fold.

In patients with chronic hepatitis C virus (HCV)-related liver disease and severe liver fibrosis or compensated cirrhosis, up to 43% had obesity, and 32% were overweight. Each quartile increase in BMI is associated with a 14% increase in the risk of clinical events in the follow-up (worsening of liver fibrosis or decompensation of cirrhosis over 3.5 years of follow-up)[12]. Among obesity-related variables, the severity of insulin resistance and the histological grade of steatosis appeared as the factors more tightly associated with the progression of liver disease. Contrarily, weight loss is indeed beneficial in patients with advanced chronic liver disease, reducing the progression of fibrosis and cirrhosis[13,14].

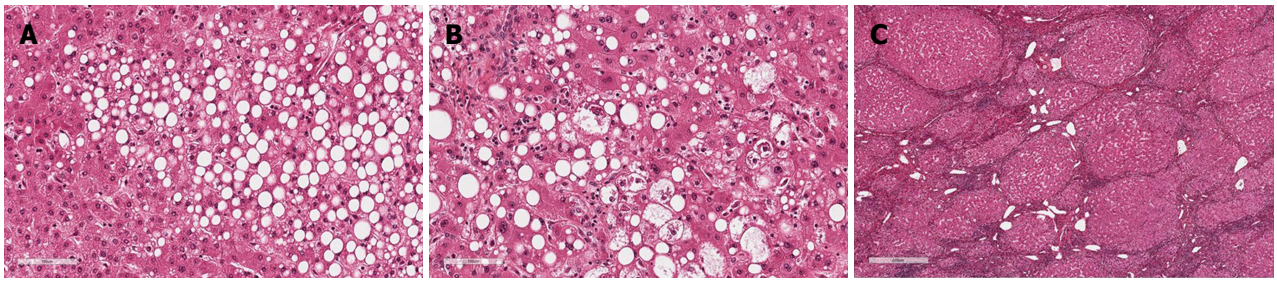

Figure 1 Non-alcoholic fatty liver disease and hepatic histopathological alterations. NAFLD includes a wide spectrum of histopathological alterations ranging from simple steatosis (A) to non-alcoholic steatohepatitis (B) and cirrhosis (C). NAFLD: Non-alcoholic fatty liver disease.

Berzigotti *et al*[13,14] demonstrate that increased BMI is a strong predictor of decompensation in patients with compensated cirrhosis of various etiologies, independent of other previously described predictors such as albumin and portal hypertension. More specifically, clinical decompensation of cirrhosis (ascites, encephalopathy, or jaundice) developed in 14% of patients with normal weight, in 31% of overweight patients, and in 43% of patients with obesity. Obesity also negatively impacts portal hypertension. Indeed, when comparing the results after a 1-year course of timolol or a placebo, portal hypertension was reduced only in patients who were of normal weight or overweight, whereas patients with obesity showed a significant increase.

Even in patients with end-stage liver disease and, therefore, awaiting liver transplantation (LT), obesity could worsen the prognosis. Recent data suggest that in these patients, obesity increases substantially (HR = 13.1), independently and significantly (P = 0.016) the risk of portal vein thrombosis[15], which may render the transplantation technically more difficult and increase the risk of portal thrombosis recurrence. Indeed, obesity is considered as a risk factor for venous thromboembolism as well as thrombosis of the hepatic artery[16]. The proinflammatory, prothrombotic, and hypofibrinolytic milieu patients with obesity may be responsible for the local thrombophilia that favors portal vein thrombosis. Concerning perioperative LT complications, operative time, blood product usage, length of stay in the intensive care unit, infectious complications, and biliary complications requiring intervention have been shown to be higher in recipients with obesity[17]. Despite the increased technical operative challenges and medical complexities associated with recipients with obesity, morbid obesity in itself should not be an absolute contraindication to LT as these patients have reasonable long-term outcomes. Although the complex interplay between obesity and cirrhosis is far from elucidated, undoubtedly alcohol, viral hepatitis, and obesity appear to be a dangerous combination. General impact of obesity on liver pathophysiology are summarized in Table 1.

RISK OF SARCOPENIA IN PATIENTS WITH OBESITY AND CIRRHOSIS

Sarcopenia is a syndrome characterized by progressive and generalized loss of skeletal muscle mass and strength with a risk of adverse outcomes such as physical disability, poor quality of life, and death[18]. The profound negative clinical impact of low skeletal muscle mass and function was originally described in the elderly, but its role is now unequivocally emerging in many chronic progressive diseases, such as chronic kidney disease, chronic heart failure, chronic pulmonary insufficiency, and type 2 diabetes[18]. Recent evidence suggests that low muscle mass and function may have a similar negative impact in obesity despite the potential difficulties in identifying and defining muscle changes within the obese phenotype[19]. Whatever the definition, the coexistence of sarcopenia and obesity in the same patient, now indicated as "sarcopenic obesity", confers a risk of physical impairment and disability that is significantly higher than the risk induced by each of the two conditions alone[19-21]. The precise determination of body muscle and body mass fat requires the use of dual energy X-ray absorptiometry (DXA), but an estimation can be obtained at the clinical level with the use of bioimpedance analysis (BIA) or anthropometric measurements[18]. In this section, the role of sarcopenic obesity as a prognostic factor in patients with liver chronic disease will be briefly elucidated. The problem will be analyzed according to two different perspectives. First, the possible role played by sarcopenia as an independent risk factor for the occurrence of liver diseases in patients with obesity will be discussed and, second, the significance of sarcopenia as a negative prognostic marker for disease progression and death in patients with obesity and advanced liver disease will be addressed.

Sarcopenia as an independent risk factor for chronic liver disease in patients with obesity

As already mentioned above, NAFLD is today the most common liver disorder in Western countries and it is becoming the leading cause of chronic liver disease and cirrhosis[22]. Visceral obesity and related metabolic disorders, insulin resistance, in particular, are considered the most relevant risk factors for NAFLD occurrence and progression[22]. Recent evidence suggests, however, that the prevalence of NAFLD and its severity could be independently and negatively affected also by the coexistence of sarcopenia in the clinical picture, with sarcopenic obesity being both an independent risk factor for NAFLD and a marker for its progression to the more

Table 1 Impact of obesity on liver pathophysiology

Pathologies	Obesity
Hepatic steatosis[9]	Increased[1]
Cirrhosis[11]	Increased[1]
Hepatoxicity[9]	Increased[1]
Liver primary tumors (as hepatocarcinoma)[2-4]	Increased[2]
Chronic hepatitis C progression[12]	Increased
Decompensation of cirrhotic patients[13,14]	Increased
Portal hypertension[13,14]	Increased
[3]Risk of post-operative complications after LT[15-17]	Increased

[1]Mostly if associated to alcohol ingestion; [2]Mostly if associated to non-alcoholic fatty liver disease (NAFLD); [3]Thromboembolism, infectious and biliary complications. LT: Liver transplantation.

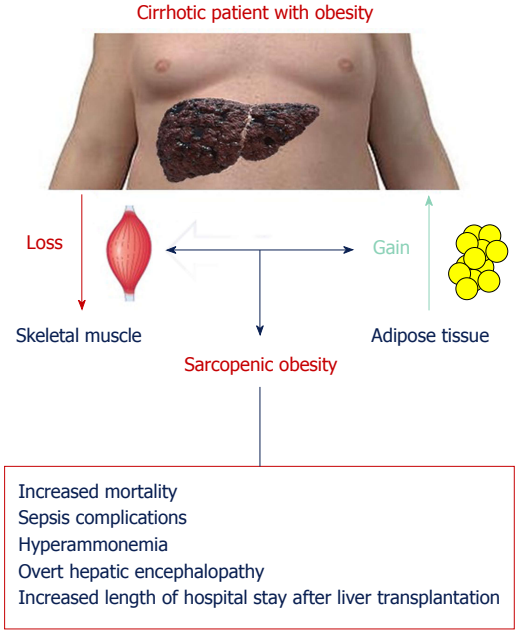

Figure 2 Sarcopenia as a prognostic negative marker in the cirrhotic patient with obesity. Cirrhotic patients with obesity frequently have a combined loss of skeletal muscle and gain of adipose tissue, culminating in the condition known as "*sarcopenic obesity*". Sarcopenia in cirrhotic patients has been associated with increased mortality, sepsis complications, hyperammonemia, overt hepatic encephalopathy, and an increased length of hospital stay after liver transplantation.

advanced stages and cirrhosis[23].

Significant information about the role of sarcopenia in chronic liver disease was produced in an analysis of data from the Korea National Health and Nutrition Examination Survey (KNHANES). KNHANES includes a nationwide cross-sectional cohort with a representative sample of the Korean population and is conducted annually to assess health and nutritional status. Hong *et al*[24], by analyzing 452 apparently healthy adults in the Korean Obesity Sarcopenic Study, demonstrated a higher risk of NAFLD in individuals with lower muscle mass compared to a control group. Individuals with sarcopenia had more body fat mass, more components of the metabolic syndrome, and higher levels of low-grade systemic inflammation compared with those of people with normal muscle mass. Moreover, the association between sarcopenia retained its significance also after adjustment for all these potential confounding factors[24]. More recently, Lee *et al*[25] tested the association between sarcopenia and progression of NALFD by analyzing the degree of liver fibrosis in the KNHANES population. NAFLD was identified in 2761 (28.5%) of 9676 subjects and sarcopenia was identified in 337 of the subjects with NAFLD (12.2%). In subjects with NAFLD, sarcopenia was significantly and independently associated with a higher level of liver fibrosis. The authors concluded that sarcopenia was associated with significant liver fibrosis in subjects with NAFLD, and this association was independent of obesity and insulin resistance[25].

The independent and additive role of reduced skeletal muscle mass and increased visceral fat mass in increasing the risk of the onset of NAFLD, and in serving as important factors involved in the progression from simple steatosis to liver fibrosis, has been recently confirmed in an independent Japanese sample[26]. Taking into consideration the limitation of these studies and the caveats in extrapolating these data to the Caucasian population, the association of sarcopenia with visceral obesity and insulin resistance is now considered an important risk factor for NAFLD, which further accelerates its progression to more advanced life-threatening stages.

Sarcopenia as a prognostic negative marker in the cirrhotic patient with obesity

As shown in Figure 2, cirrhotic patients with obesity frequently have a combined loss of skeletal muscle and gain of adipose tissue, culminating in the condition known as "*sarcopenic obesity*." Sarcopenia in cirrhotic patients has been associated with increased mortality, sepsis complications, hyperammonemia, overt hepatic encephalopathy (HE), and an increased length of hospital stay after LT[27]. The prognostic impact of the coexistence of sarcopenia and obesity in patients with chronic liver disease has been analyzed recently in a few studies. Montano-Loza *et al*[28] evaluated the frequencies of sarcopenia and sarcopenic obesity in a cohort of 457 cirrhotic patients evaluated for LT, aiming to establish the impact of these muscular abnormalities on the prognosis of cirrhotic patients. In this sample, sarcopenia was present in 43% and sarcopenic obesity in 20% of patients. Both patients with sarcopenia and with sarcopenic obesity had worse median survival than patients without muscular abnormalities[28]. Hara *et al*[29] evaluated the independent prognostic impact of skeletal muscle mass and visceral fat accumulation in 161 patients with cirrhosis. Patients with sarcopenia or sarcopenic obesity both had a poor prognosis, and this difference was pronounced in the subset of patients classified as Child-Pugh class A. However, the group with the worst prognosis was represented by patients having sarcopenic obesity[29]. This latter observation seems to confirm that the coexistence of visceral obesity and sarcopenia could be considered the worst clinical

situation for a patient with cirrhosis. Muscle wasting and fatty muscle infiltration in cirrhotic patients are part of the frailty complex present in these patients, characterized as decreased reserve and resistance to stressors, resulting from cumulative declines across multiple physiologic systems and predisposition to poor outcomes[28].

The prognostic negative role of sarcopenia and obesity could have an impact also in LT. Sarcopenia and sarcopenic obesity are seen in a significant number of patients with cirrhosis undergoing liver transplant evaluation, particularly in patients with NASH[30]. Pre-transplant sarcopenia is widely recognized as associated with short-term survival after living donor LT[31]. The question of whether the coexistence of obesity and sarcopenia could impose additional risk after LT over that imposed by sarcopenia alone is still debated. Hammad *et al*[32] evaluated 200 patients undergoing adult-to-adult living donor LT and classified them into four subgroups: sarcopenic overweight, sarcopenic non-overweight, non-sarcopenic overweight, and non-sarcopenic non-overweight. Sarcopenic patients had a higher incidence of postoperative bacteremia and major postoperative complications, and poorer overall post-transplant survival than non-sarcopenic patients. Overweight recipients had a significantly higher overall survival rate than non-overweight patients. In contrast, sarcopenic non-overweight subjects had a higher incidence of postoperative bacteremia, and major postoperative complications compared with the sarcopenic overweight subgroup and possessed the poorest overall survival among the four recipient subgroups. Thus, this study indicates that a preoperative sarcopenic overweight status does not confer additional significant morbidity or mortality risks than the stand-alone sarcopenia in living donor LT. The study was however mostly confined to patients who were overweight and does not address specifically the impact of obesity itself[32]. On the other hand, obesity presents important medical and surgical challenges during and after a liver transplant. Specifically, obesity is associated with an increased incidence of wound infections, wound dehiscence, biliary complications, and overall infection[33].

Sarcopenic obesity could represent an important clinical problem also for long-term survival after LT. Sarcopenia tends to persist after transplantation[30,31], possibly as the consequence of insufficient physical exercise or use of immunosuppressive agents that impair skeletal muscle growth and protein accretion[30], whereas body fat normally increased as a result of better nutrition and the regression of the hypermetabolic state related to the pre-transplant chronic disease state[34]. This double phenomenon paves the way to sarcopenic obesity. Schütz *et al*[35] analyzed body composition in patients after liver and kidney transplantation and patients with liver cirrhosis or on chronic hemodialysis and demonstrated that, despite excellent graft function, many long-term liver or kidney transplant survivors exhibit a phenotype of sarcopenic obesity with increased fat but low muscle mass[35]. Choudhary *et al*[36] evaluated 82 living donor liver transplant recipients with at least 12 mo of follow-up. Post-transplant sarcopenic obesity was present in 88%, and metabolic syndrome was present in 52% of recipients with no significant difference among liver failure etiologies. Patients with sarcopenic obesity had a significantly higher BMI and significantly higher prevalence of metabolic syndrome when compared to patients without sarcopenic obesity[36]. Thus, the weight gain frequently observed after LT could contribute to the creation of a novel group of patients with sarcopenic obesity and associated metabolic derangements.

MICRONUTRIENT STATUS AND RECOMMENDED SUPPLEMENTATION IN PATIENTS WITH OBESITY AND CIRRHOSIS

Micronutrient deficiencies of fat-soluble and water-soluble vitamins as well as minerals are highly common in end-stage liver disease. Therefore, a periodical nutritional and clinical assessment should be performed to test micronutrient serum levels, estimating adequate nutritional intake and paying attention to clinical signs of vitamins and minerals deficiencies. Fat-soluble vitamin (A, D, E, and K) deficiencies and other free radical scavengers, such as carotenoids are likely to develop in liver disease due to reduced oral intake, malabsorption, and/or hepatic effects involving the reduced synthesis of carrier and transfer proteins, cholestasis and bacterial overgrowth[37,38].

Deficiencies in water-soluble vitamins, leading to neuropsychiatric symptoms, may stem from diminished hepatic storage, inadequate diet, alcoholism, medications, and chronic renal failure[37]. The most prevalent and significant deficiencies are discussed below, beginning with vitamin D deficiency, which is almost universal and also related with obesity.

Vitamin D deficiency (VDD, < 50 nmol/L; < 20 ng/mL) is a worldwide pandemic, reported in more than half of the general adult population[39-42]. Specifically, VDD is widespread among patients with chronic liver disease, with prevalence described between 70%-90%[40,43-49], while the prevalence of vitamin D insufficiency (< 75 nmol/L; < 30 ng/mL) is almost universal[49]. For example, among 202 adults before LT, 84% were 25(OH)D deficient and 77% had low 1,25(OH)2D, whereas 3 mo following transplantation, both increased significantly but to a lesser extent for 1,25(OH)2D[50]. Moreover, the severity of VDD is positively correlated with the severity of liver disease[44-47]. In cirrhotic patients, significant correlations were found between vitamin D levels and the degree of liver dysfunction, whether expressed as Child-Pugh stages A-C, MELD score, or liver stiffness evaluated by transient elastography[44,45]. In epidemiologic studies, VDD has been demonstrated to be a predictor of liver disease morbidity and mortality. In a Danish population-based sample of over 2500 middle-

aged subjects followed prospectively for a median follow-up period of 16.5 years, lower serum 25(OH)D levels were independently associated with higher incidence of fatal and non-fatal liver disease[51]. Similarly, in another prospective study with 22 years follow-up[52], those with a higher serum 25(OH) vitamin D had lower chronic liver disease mortality. Among cirrhotic patients, VDD was found to be an independent risk factor for mortality[43,45]. With the increasing prevalence of obesity and NAFLD-related cirrhosis, attention should be paid to the cirrhotic patient with obesity. An association between VDD and obesity has also been suggested. Since vitamin D is a lipophilic molecule it is selectively deposited in subcutaneous and visceral adipose tissue. This sequestration leads to a reduction of its availability for hydroxylation[40,41,53,54]. In addition, an independent association was also observed between VDD and insulin resistance[55,56], the metabolic syndrome as a whole[57], and type 2 diabetes or prediabetes, after adjusting for multiple confounders including BMI[55,56,58,59]. In contrast, some studies failed to show such associations once adiposity is adjusted for[60,61] or any significant association between markers of insulin resistance and 25(OH)D serum levels[62,63]. NAFLD by itself has been suggested to be associated with VDD, but the independence of this association from body fat mass is controversial. The association between a diagnosis of NAFLD and lower serum 25(OH)D levels compared to healthy controls was demonstrated in several studies[64-67], however, NAFLD was biopsy-proven in only two of the studies[64,65]. In addition, significantly higher levels of 25(OH)D were observed among patients with steatosis compared to patients with NASH[64,65]. In partial agreement, another study, describing a sub-analysis of the NASH Clinical Research Network (CRN) cohort, found that VDD was independently associated with NASH and the presence of fibrosis, but not with the degree of steatosis[68]. However, while most studies adjusted for BMI or waist circumference, a study carefully adjusting for adiposity (evaluated by dual-energy X-ray absorptiometry), suggests that there is no relationship between vitamin D levels and the amount of liver fat (by Magnetic Resonance Spectroscopy and liver biopsy) or the severity of NASH[69].

To summarize, a few possible mechanisms could explain VDD among cirrhotic patients with obesity: (1) NAFLD as the undelaying cause of cirrhosis; (2) Sedentary lifestyle or long standing chronic illness leading to reduced exposure to sunlight; (3) Consumption of high-caloric "empty" foods, low in mineral and vitamin content; (4) Increased fat mass which enables sequestration of vitamin D in the adipose tissue compartment thus lowering plasma concentration; and (5) Hepatocellular dysfunction in chronic liver disease which may disturb the formation of the active metabolite of vitamin D as well as vitamin D-binding proteins.

Due to the high prevalence of VDD among cirrhotic patients, especially those with advanced disease, NAFLD, or cholestatic liver diseases[70], it is reasonable to assess serum 25(OH)D levels[71]. The main sources of vitamin D are sunlight exposure, food naturally enriched or artificially fortified with vitamin D, and oral supplements. The adequate sunlight exposure is 5-15 min during the daytime (10:00 AM-15:00 PM) on a daily basis[40]. However, after exposing healthy individuals with obesity (BMI > 30 kg/m^2) and matched lean control subjects (BMI < 25 kg/m^2) to whole-body ultraviolet radiation, the subjects with obesity showed a 57% lower increase in circulating concentrations of vitamin D3, 24 h after irradiation[53]. Vitamin D3 can be found abundantly in egg yolk and oily fish (e.g. salmon, mackerel, tuna, sardines) and vitamin D2 mainly in mushrooms[40,49]. Industrial products such as bread, margarine, cereals, or milk may be fortified with either vitamin D2 or vitamin D3. Oral supplements may contain vitamin D2 or D3 depending on the manufacturer and brand[40,49]. However, most studies that have evaluated NAFLD and high-dose vitamin D supplementation, failed to show improvement in liver fat, NASH histology, or liver enzymes[72,73]. Oral high-dose vitamin D supplementation administrated to subjects with NAFLD and type-2 diabetes for 24 wk, did not lead to significant change in hepatic steatosis, HOMA-IR, or liver enzymes[74]. Similarly, in a pilot prospective study, administration of high-dose oral vitamin D3 supplementation (25000 IU/wk) for 24 wk to 12 non-cirrhotic patients with biopsy-proven NASH resulted in no significant impact on liver histology, liver enzymes, insulin resistance, or adipocytokine profile[73]. Conversely, some studies, not specific for NAFLD but mostly pre-diabetic patients, demonstrated improvement in insulin sensitivity with vitamin D supplementation[75-77]. Findings are also conflicting with regard to the effect of vitamin D supplementation in the case of advanced liver disease. In a cohort of advanced decompensated cirrhotic patients (Child-Pugh C, score of $\geqslant$ 10) randomly assigned to vitamin D treatment or a control receiving standard care and followed for 6 mo, the survival, as well as Child-Pugh and MELD scores, were comparable between the groups[48]. Nevertheless, supplementation of high-dose oral vitamin D resulted in several clinical improvements such as an anti-depressant effect among patients with chronic liver disease (mainly women)[78], and 60% risk reduction for acute rejection among patients after LT[79]. In a Cochrane review of vitamin D supplementation for chronic liver diseases in adults, including 15 randomized clinical trials (RCT) with 1034 participants[80], vitamin D supplementation had no beneficial or harmful effects on all-cause mortality (OR = 0.69; 95%CI: 0.09 to 5.40), and the authors concluded that there is no convincing evidence that vitamin D supplementation has a therapeutic impact in chronic liver disease.

There are no guidelines or clear recommendations regarding vitamin D supplementation for cirrhotic patients with obesity. One authoritative paper[49] recommended vitamin D status assessment in all patients with chronic liver disease and initiation of supplementation with 1000-4000 IU/d of vitamin D3 when 25(OH)D levels are under < 50 nmol/L or < 20 ng/mL. The

guidelines of a consensus workshop supported by the British Association for the Study of the Liver and the British Liver Trust, recommends supplementation of 1 g calcium and 800 IU/D vitamin D to patients with chronic liver disease (especially patients with cirrhosis or severe cholestasis) as a general preventive treatment for osteoporosis along with adequate nutrition monitoring[81]. The European Association for the Study of the Liver (EASL) recommendation includes supplementation with calcium (1000-1200 mg/d) and vitamin D (400-800 IU/d) in all patients with cholestatic liver disease for bone loss reduction, although the evidence to support this is low[70]. Interestingly, in a small study of NAFLD patients, daily supplementation with 2000 IU cholecalciferol for 6 mo did not correct hypovitaminosis D in the majority of patients with NASH compared to those with steatosis, thus a higher dose may be needed in NASH or NASH-cirrhosis patients but this finding needs further confirmation[82].

Vitamin E (tocopherol) is an inexpensive and well-tolerated molecule with antioxidant properties. In vitro and animal studies have shown that vitamin E ameliorates liver necrosis and fibrosis[83], and prevents hepatic stellate cell activation[84]. Relevantly for patients with obesity and liver disease, high-dose (800 IU/d) long-term (24 mo) vitamin E treatment among nondiabetic NASH patients led to improvement in NASH versus placebo but not fibrosis. However, cirrhotic patients were excluded from this RCT[85], and thus vitamin E cannot be recommended for NASH-cirrhosis or cryptogenic cirrhosis patients[86]. Vitamin E status, expressed as serum vitamin E/total serum cholesterol ratio, is lower among patients with primary biliary cholangitis and primary sclerosing cholangitis compared to patients with either cryptogenic or alcoholic cirrhosis, probably due to reduced gastrointestinal absorption[87]. Indeed, a reduced concentration of vitamin E and low vitamin E/total cholesterol ratio has been demonstrated in 44% and 64% of patients with primary biliary cholangitis and 32% and 43% of patients with other chronic cholestatic liver diseases, respectively. Serum vitamin E concentration and vitamin E/total cholesterol ratio were restored to normal by oral or intramuscular supplements of the vitamin, but not in patients with severe deficiency of vitamin E (less than 5 μmol/L and less than 1 μmol/mmol total cholesterol)[88]. Generally, carotenoids, as well as tocopherols, are major natural protective agents against free radical-mediated liver damage. Interestingly, it has been demonstrated that patients with cirrhosis (of mixed etiologies) have extremely low hepatic levels of carotenoids and tocopherols, compared with controls, even in the presence of normal serum levels[89]. Similarly, retinol, a-tocopherol, and carotenoid plasma levels in patients with chronic cholestatic liver disease (primary biliary cholangitis and primary sclerosing cholangitis) were demonstrated to be significantly lower compared to the general population, despite comparable nutritional intake, suggesting a role for the malabsorption of fat-soluble vitamins[38]. Clinical manifestations of vitamin E deficiency may include increased platelet aggregation, decreased red blood cell survival, hemolytic anemia, decreased serum creatinine with creatinuria, and neuronal degeneration[37], but these are not common[38,87,88].

Zinc is the second most prevalent trace element in the body, playing a central role in several metabolic, anti-inflammatory and immune response pathways, with more than 300 enzymes having zinc ions within their catalytic domains[90]. Dietary zinc is prevalent in foods which are rich in protein (*i.e*. red meat, lamb, pork, oysters, *etc*.) and its absorption can be inhibited by high consumption of foods rich in phytate, certain dietary fibers, and calcium[91,92]. The recommended dietary allowance (RDA) of zinc is 8 mg/d for women and 13 mg/d for men over 19 years old[93]. The liver is the main organ of zinc metabolism, however, in chronic liver disease, metabolism is altered by inadequate dietary intake, protein and amino acid metabolism alterations, diminished hepatic extraction, portosystemic shunts, impaired absorption (mostly in advanced liver disease), and an increase in various inflammatory cytokines[90,94]. Moreover, cirrhosis is a catabolic state resulting in muscle catabolism leading to increased zinc loss in the urine. This urinary loss of zinc is aggravated by the prevalent use of diuretics in order to treat edema and ascites[95]. Zinc deficiency has many clinical implications in cirrhotic patients. One of the major complications in cirrhotic patients is HE, presented in 30%-40% of the patients as overt encephalopathy (OHE) and in 60%-80% as mild cognitive dysfunction (minimal hepatic encephalopathy, MHE)[96]. Zinc deficiency results in impaired nitrogen metabolism due to the reduced enzymatic activity of urea cycle enzymes and decreased muscle glutamine synthesis. Furthermore, zinc levels were found to be negatively correlated with ammonia serum levels[97,98]. These impaired metabolic pathways can be corrected by supplementing zinc. In a small preliminary double-blind, placebo-controlled trial among patients with cirrhosis, hyperammonemia, and hypozincemia, zinc acetate preparation at a dose of 150 mg/d for 3 mo decreased blood ammonia levels[99]. Indeed, Marchesini *et al*[100] demonstrated in patients with advanced cirrhosis, that long-term treatment with zinc supplementation accelerated and improved hepatic conversion of amino acids to urea compared with matched controls receiving standard treatment. This biochemical improvement was associated with a clinical improvement measured by the performance in psychometric tests and Child-Pugh score. Similar results were observed in an RCT comparing zinc supplementation on top of standard treatment *vs*. standard treatment alone (protein-restricted diet, branched-chain amino acids, and lactulose) for 6 mo. Zinc supplementation improved the physical component scale and neuropsychological tests and decreased HE grade, Child-Pugh score and blood ammonia levels[101]. A significant improvement in neuropsychological tests and Child-Pugh score along with ammonia was also reported in patients with only MHE after 3 mo of lactulose, antioxidant and zinc therapy *vs* lactulose therapy

alone[102]. Additionally, zinc is a crucial co-factor in the process of wound healing since it activates the synthesis of collagen and metabolism of nucleic acids. Thus, zinc is an essential factor in the restoration of liver parenchyma after liver injury or resection and is required in large amounts over a short period of time[90,103]. In terms of clinical signs for zinc deficiency, skin lesions are very prominent, usually an erythematous rash or scaly plaques. A unique manifestation is necrolytic acral erythema (NAE), associated with zinc deficiency in patients with HCV infection[104], expressed on the dorsal aspects of the feet and extending to the toes. The treatment of NAE must combine oral zinc supplementation and HCV eradication. For more than 70 years, hypozincemia has also been associated with impaired night vision, initially in alcoholic cirrhosis and later on in various liver cirrhosis etiologies[103]. Importantly, one of the disturbing manifestations of zinc deficiency is an alteration in taste and smell. This may further exacerbate malnutrition due to reduced intake in the cirrhotic patient[37,105,106]. According to expert opinion, zinc supplementation can be administrated as a long-term treatment or at least until zinc blood level is within normal range with a recommended dose of 50 mg elemental zinc (220 mg zinc sulfate) once daily, in order to avoid copper malabsorption[37,103].

Magnesium is one of the most prevalent intracellular cations, secondary only to potassium. It has been demonstrated that chronic alcohol consumption impairs magnesium homeostasis affecting the brain, skeletal muscles, heart, and liver[107]. In addition, alcohol abuse can decrease nutritional intake and increase excretion of magnesium by an indirect effect on renal tubules[107]. Other factors that might lead to hypomagnesemia in cirrhotic patients are the poor absorption of magnesium in the distal jejunum, exacerbation of magnesium urinary excretion due to elevated aldosterone, growth hormone, and glucagon blood levels, and chronic administration of loop diuretics[108]. The association between magnesium serum levels and the presence of cirrhosis or its severity is questionable. Two studies have found that magnesium concentration was not significantly different between patients with and without liver cirrhosis and no significant correlation was found with the Child-Pugh score[109,110]. One study found magnesium levels were significantly lower in cirrhotic patients compared to controls, but there was no difference between compensated and decompensated patients[111]. Conversely, another study demonstrated a negative correlation between serum magnesium and Child-Pugh score, and lower levels of magnesium among patients with cirrhosis compared to controls[112]. This disagreement can result from the different disparity of etiologies for the liver disease. Nangliya *et al*[112] reported that the prevalence of alcoholic liver disease was over 40%, however, Agarwal *et al*[110] excluded chronic alcohol abuse. Another explanation is that magnesium is a cellular cation and perhaps its serum level does not reflect its true concentration. Koivisto *et al*[113] argued that serum magnesium concentrations may be normal despite intracellular depletion and that a true estimation of magnesium depletion is through a magnesium loading test, since magnesium uptake is increased in the condition of magnesium depletion. In their study, 10 cirrhotic patients were compared to six healthy controls. No difference was found between pre-loading magnesium levels, but the uptake of magnesium (calculated as the delta between the IV administered dose and the amount excreted in 24-h urine) was more than four-fold higher among cirrhotics compared to controls[113]. Due to scarce data and conflicting evidence, there are no clear clinical practice recommendations regarding magnesium supplementation in cirrhotic patients.

While all patients with chronic liver disease are at risk for depletion of various fat-soluble, water-soluble vitamins and trace elements, the most well-recognized micronutrient deficiencies related to alcohol overuse are vitamin B12 (cyanocobalamin), vitamin A, vitamin D, thiamine (B1), folate (B9), pyridoxine (B6), and zinc[114,115]. Following supplementation, when needed, an annual check-up once stable levels are achieved may be recommended[116]. Administration of B-complex vitamins such as thiamine, folate, and pyridoxine is needed to prevent Wernicke encephalopathy[114], Korsakoff's syndrome, megaloblastic anaemia and neuropathies[116]. Moreover, and regardless of the etiology of cirrhosis, a consensus paper by the International Society for Hepatic Encephalopathy and Nitrogen Metabolism stated that since vitamin status is not easily assessed and since multivitamin supplementation is cheap and generally safe, use of short-term (2-wk course) oral vitamin supplements could be justified in patients with decompensated cirrhosis or at risk of malnutrition, and clinically apparent vitamin deficiencies should be treated specifically[117].

PROTEIN AND CALORIE INTAKE IN PATIENTS WITH OBESITY AND CIRRHOSIS

Decreased muscle mass and function are more prevalent among cirrhotic patients with either MHE or OHE compared to no HE, and protein malnutrition is an independent risk factor for both OHE (OR = 3.4; 95%CI: 1.4-6.9; $P < 0.001$) and MHE (OR = 2.15; 95%CI: 1.1-4.1; $P = 0.002$)[118]. In the late 90s, the recommendations for caloric intake were near-normal for patients with well-compensated liver cirrhosis [25-35 kcal/(kg•d)] and up to 30-40 kcal/(kg•d) in malnourished or critically ill cirrhotic patients[119]. The ESEPEN currently recommends a daily caloric intake of 35-40 kcal/(kg•d) for all cirrhotic patients regardless of their liver disease etiology or degree of liver function compensation[120], without a specific reference for cirrhotic patients with obesity, which may still be malnourished. However, weight loss should be encouraged in patients with obesity and well-compensated cirrhosis,

Table 2 Nutritional recommendations for cirrhotic patients with obesity

Nutrient	Recommendation
[1]Daily energy intake[117]	25-35 kcal/(kg•d) in patients with BMI 30-40 kg/m^2 20-25 kcal/(kg•d) in patients with BMI > 40 kg/m^2
[2]Protein intake[119]	1.2-1.5 g/(kg•d)
[3]Micronutrients	Identify and correct micronutrient deficiencies
Fiber	25-45 g/d

[1]The recommended dietary pattern is for small, frequent meals evenly distributed throughout the day (every 3-6 h) with a late evening snack containing at least 50 g of complex carbohydrate. [2]Vegetable-protein based diets can also be beneficial in terms of caloric and fiber intake among overweight patients with cirrhosis who are attempting to lose weight. In addition, plant-based proteins are rich in branched-chain amino acids (BCAA)[117,127,128]. [3]Cirrhotic patients with obesity are at high risk for depletion of various fat-soluble, water-soluble vitamins and trace elements and should be supplemented appropriately. BMI: Body mass index.

nevertheless, over-restriction will result in endogenous muscle breakdown. Indeed, in later guidelines, Amodio *et al*[117] recommend careful monitoring alongside increased physical activity and caloric intake of 25-35 kcal/(kg•d) in patients with obesity (30-40 kg/m^2) and not less than 20-25 kcal/(kg•d) in patients with morbid obesity (> 40 kg/m^2). The recommended dietary pattern is for small, frequent meals evenly distributed throughout the day (every 3-6 h) with a late evening snack containing at least 50 g of complex carbohydrate[117].

The attitude toward daily protein intake has also changed. In the past, the daily protein intake of cirrhotic patients was tightly restricted to less than 0.8 g/(kg•d) due to concerns about the increased risk for HE. However, the tolerance of proteins in cirrhotic patients has been shown to be higher than previously believed[117,121], and the importance of substantial daily protein intake for sustaining adequate muscle mass is becoming more and more clear[117]. Córdoba *et al*[121] showed that administration of a low-protein diet [0.5 g/(kg•d)] worsened HE and exacerbated protein breakdown compared to a daily protein intake of 1.2 g/(kg•d).

Currently, the recommended daily protein intake is 1.2-1.5 g/(kg•d)[120]. For cirrhotic patients with obesity, a moderately hypocaloric diet must include an adequate amount of proteins [1.2-1.5 g/(kg•d)] in order to accomplish weight loss without muscle or lean mass depletion[117]. In cirrhotic patients, there is variable tolerance to different dietary proteins according to their source. Some uncontrolled studies have shown a better tolerance to vegetable proteins over meat proteins and to dairy proteins over mixed source proteins[122-124]. Interestingly, a 14-d casein-vegetable, high-protein, high-calorie diet was shown to improve mental performance and to decrease ammonia levels in 150 patients with overt HE[125]. The advantages of vegetable proteins may stem from the fact that they are rich in dietary fiber with prebiotic properties, which result in decreased transit time and intraluminal pH leading to increased fecal ammonia excretion. Moreover, vegetable proteins are rich in ornithine and arginine, that can facilitate clearance of ammonia through the urea cycle[126,127]. Vegetable-protein based diets can also be beneficial in terms of caloric and fiber intake among overweight patients with cirrhosis who are attempting to lose weight. In addition, plant-based proteins are rich in branched-chain amino acids (BCAA)[117,128,129]. In hepatic decompensation, there is a shift toward aromatic amino acids (AAA) (phenylalanine, tyrosine, and tryptophan) rather than BCAAs (isoleucine, leucine, and valine), however, AAA are assumed to cross the blood-brain barrier, act as false neurotransmitters, and induce HE[130,131]. BCAA supplementation can induce tolerability to meat protein and enable adequate protein intake[132]. Moreover, substituting meat with dairy or vegetable proteins along with BCAA supplements is better than reducing total proteins intake[117]. In a meta-analysis of 16 RCTs, BCAAs were found to have a beneficial effect on HE compared to placebo or best supportive care (diet, lactulose, or neomycin), however, no conclusions could be drawn regarding nutritional effects[133]. General nutritional recommendations in the cirrhotic patients with obesity are summarized in Table 2.

BARIATRIC SURGERY-INDUCED WEIGHT LOSS IN PATIENTS WITH OBESITY AND CIRRHOSIS: INDICATIONS AND CONTRAINDICATIONS

In recent years, parallel to the rapid and sharp increase in the prevalence of obesity[134], bariatric surgery has reached a rapid and deep penetration, as it is the only therapeutic means leading to long-term weight loss with consequent improvement of obesity-related comorbidities and patients' quality of life[135]. NAFLD has become an extremely frequent condition in recent years due to the obesity epidemic[136]. While NAFLD includes a spectrum of histologic features ranging from simple liver steatosis to steatohepatitis (NASH), liver fibrosis has been shown to be the main determinant of mortality linked to NASH in the long-term[137,138]. Obesity has been shown to be associated with an increased risk of primary liver cancer in several large epidemiological studies. Potential mechanisms responsible for this increased risk include the occurrence of NAFLD and type 2 diabetes[139]. Furthermore, there is evidence that the probability of clinical decompensation of liver cirrhosis is significantly

increased in the presence of obesity compared to overweight and lean subjects[140].

As a consequence, LT surgeons are faced more and more frequently with candidates for LT with morbid obesity[141]. Traditionally obesity has been considered a main risk factor for postoperative morbidity and mortality in the context of major and complex surgical procedures[142,143]. However, obesity is a heterogeneous disease including different conditions sharing a common denominator represented by an increased BMI. Indeed, there is clear epidemiological evidence that the presence of obesity has a protective effect against postoperative mortality and morbidity in the range of BMI below 35 kg/m^2. This phenomenon, known as the obesity paradox, has been attributed to the increased reserve of energy due to obesity that may confer an advantage in a condition of stress such as that after a major surgical procedure[144]. Furthermore, the presence of metabolic syndrome, which is associated with obesity but not obesity alone, is significantly associated with an increased risk of postoperative morbidity and mortality after major abdominal surgery. In spite of this, in many LT centers the presence of obesity, defined only on the basis of a BMI above 35 or 40 kg/m^2, is considered as a contraindication to LT[145]. Interestingly, the use of simple diagnostic tools such as anthropometric measures that include the psoas muscle diameter and visceral fat measure coupled with the presence of metabolic comorbidities may help to identify suitable candidates for LT among individuals with obesity without the need for massive weight loss[146,147].

Losing weight before LT remains an important goal but there is no consensus on how best to achieve it, especially in patients with obesity and cirrhosis. Many non-surgical methods can be used to allow patients to reach the desired BMI and be finally listed for LT, including increased physical activity, diet, and behavioral therapy as well as intragastric balloon[33]. Spengler *et al*[33] recently suggested the use of diet and lifestyle modifications in patients with compensated cirrhosis. For patients with compensated cirrhosis, bariatric surgery has also been proposed in preparation for LT[145-147]. Although this strategy may seem legitimate, bariatric surgery may lead to severe postoperative complications that a patient with a compromised liver function may not tolerate. Indeed, only patients with compensated cirrhosis are potential candidates for bariatric surgery as mortality in patients with decompensated cirrhosis would be inacceptable[148]. There is also evidence that bariatric surgery is associated with a significantly lower morbidity and mortality if an LT program is also present in the same hospital. This underlines the complexity of the patients that need multidisciplinary care from specialists in both hepatology and bariatrics.

The timing of surgery

The timing of bariatric surgery in LT candidates is imperative. While it has been suggested that bariatric surgery-induced weight loss may increase the candidacy for LT, only patients with compensated liver cirrhosis are potential candidates to bariatric surgery because the risk of mortality is too high in the setting of decompensated cirrhosis[148]. The primary indication for LT in patients with a conserved liver function is represented by HCC. While international guidelines for access to bariatric surgery include a disease-free interval of at least five years after the radical treatment of any malignancy, a different strategy to access a curative treatment such as LT for this specific category of patients seems to be legitimate. Only patients with the best chances of long-term survival should then be selected for this ambitious therapeutic strategy, which includes bariatric surgery to lose weight and control metabolic comorbidities followed by LT. Endovascular and/or percutaneous interventional radiology techniques should be concomitantly used to obtain temporary local control of HCC. Several preoperative scores such as the alpha-fetoprotein score[149], the Milan criteria, and Metroticket 2.0 may be useful tools to guide the selection of patients in order to obtain long-term survival rates after LT comparable to those obtained for patients with non-tumoral disease[150].

The option of performing bariatric surgery after LT offers several advantages including normal liver function with normal prothrombin time, the restoration of normal portal pressure, the possibility to optimize the nutritional status and the choice of procedure in relation to the presence or absence of metabolic syndrome. The presence of adhesions linked to transplantation is not a formal contraindication to the laparoscopic approach nor is the use of immunosuppressive drugs[151].

As obesity recurs often after LT, affecting the graft with NASH recurrence and patient survival with metabolic comorbidities, some authors evoked the seducing possibility of performing a bariatric procedure, namely sleeve gastrectomy (SG), at the same time as the LT[152]. However, a panel of argument still stands against this policy, these include: the potentially disastrous consequences of the most feared complication of SG, a leak at the top of the staple line in the setting of immunosuppressive treatment in a freshly transplanted patient; the reduced amount of calories that the transplanted patient would be able to assume with the diet spontaneously for several months after surgery; the impact of the two procedures on the body composition with the risk of excessive fatty free mass loss.

The choice of procedure

The presence of portal hypertension may render any bariatric procedure difficult and lead to life-threatening bleeding. The choice of the procedure should then take into account the risk of bleeding. A transjugular intrahepatic portosystemic shunt (TIPS) may be considered in patients with signs of portal hypertension such as platelets below 100000, a large spleen on CT scan, the presence of collateral circulation on the abdomen or on CT scan and esophageal varices. In case of doubt,

Table 3 Main factors involved in the choice of the bariatric procedure in the setting of liver transplantation

Factors to consider	SG	RYGB
Bleeding risk of bleeding[1]	Increased	Low
Endoscopic access to the biliary tree	Conserved	Impossible
Risk of portal vein thrombosis	Increased	Not affected
Risk of bariatric surgery induced liver failure	Absent	Low
Absorption of immunosuppressive drugs	Poorly affected	Decreased
Etiology of liver cirrhosis (NASH *vs* others)	Effective	Very Effective

[1]Consider measuring of portal pressure and use of transjugular intrahepatic portosystemic shunt in case of bariatric surgery before liver transplantation. SG: Sleeve gastrectomy; RYGP: Roux-en-Y gastric bypass; NASH: Non-alcoholic steato hepatitis.

a direct measure of the portal pressure should be obtained. It should be considered that in the case of large spontaneous portosystemic shunts (larger than 1 cm), the TIPS might be inefficacious. The possibility to access the biliary tree endoscopically after LT should also be considered. Procedures with an intestinal bypass definitely limit the endoscopic access to the bile duct. Furthermore, some patients may need a biliodigestive reconstruction on a Roux-en-Y loop that should be then fashioned in addition to the intestinal bypass of the bariatric procedure. There is a risk of portal vein thrombosis in any abdominal procedure and bariatric surgery has been shown to increase this risk. The potential risk of liver complications due to the intestinal bypass is another point that needs attention. It is well recognized that bariatric procedures including an intestinal bypass may lead to liver failure. Although the mechanisms underlying this complication have not been completely elucidated, the abnormal intestinal microbiota derived from bacterial overgrowth may cause intestinal permeability defects that expose hosts to noxious gut-derived factors such as bacterial lipopolysaccharide, other toll-like receptor ligands, and toxic bile acids[153]. Interestingly, most, if not all, cases of liver failure reported in the literature include patients with a biliopancreatic diversion, in which the length of the bypassed intestine is very long, and the jejuno-ileal bypass, whereas only a few cases of liver failure in patients with Roux-en-Y gastric bypass (RYGP) have been reported[154]. The jejuno-ileal bypass was proscribed several decades ago and nowadays the Scopinaro's procedure is rarely performed. This is in line with the hypothesis that an altered microbiota may be a major determinant of increased intestinal permeability as the more distal is the bypass the more altered is the intestinal flora.

The absorption of immunosuppressive drugs should also be considered when choosing the most appropriate bariatric procedure. The absorption of drugs may not only be altered by the presence of an intestinal bypass but also by the changes in the intestinal pH linked to the suppression of hydrochloric acid secretion[155]. Finally, the etiology of liver disease (namely NASH *vs* viral infections and alcohol abuse), the presence of metabolic syndrome, and NASH recurrence on the graft in cases of patients that have already been transplanted are key factors to consider when choosing the type of bariatric procedure.

The three most common bariatric procedures currently performed worldwide are laparoscopic adjustable gastric banding (LAGB), the SG, and RYGP. Several factors are involved in the choice of the bariatric procedure in the setting of LT (Table 3). Although the LAGB has the advantage of being the easiest procedure with the lowest risk of bleeding, it also has the worse results in terms of weight loss with the highest rate of failure. Furthermore, the presence of foreign material around the mesogastric junction, especially in patients with esophageal varices, may cause problems. The SG is currently the most performed procedure[156,157] that offers several advantages, including the fact that no intestinal bypass is done, leaving the whole digestive tract accessible to endoscopic exploration, avoiding intestinal bypass related interference with the absorption of immunosuppressive drugs, and leaving the possibility to fashion a Roux-en-Y loop in the event of biliary complications after LT or in cases where a biliodigestive reconstruction is indicated such as in primary biliary cholangitis. However, in cases of portal hypertension, the division of the greater curvature vessels may expose to the risk of bleeding especially if portal pressure is increased and no TIPS has been put in place. Bleeding may be then difficult to control and should be feared as a life-threatening complication. The use of buttressing material for the division of the stomach may reduce significantly the risk of bleeding in these patients and should be used[158].

Of note is also the fact that the SG is followed by an extreme decrease in hydrochloric acid secretion, resulting in an altered pH, which may consequently interfere with immunosuppressive drug absorption[155]. Although short and medium-term results of SG on weight loss and control of metabolic syndrome indicate equivalent efficacy between the SG and the RYGP[159], long-term results of SG are still too scarce to drive definite conclusions on the equivalence of efficacy between the two procedures, especially in a NASH setting[160].

The RYGP has the advantage of a reduced risk of bleeding, as only the lesser curvature of the stomach, where bleeding may occur, needs to be dissected before gastric division. It is also more effective against metabolic complications of obesity that may be either present before or after LT[161]. Strong evidence in support of the preventive effect of RYGP against the occurrence of type

2 diabetes has come from several studies[162,163]. Recently Safwan *et al*[164] reported a series of 11 patients with a previous history of bariatric surgery that underwent LT and showed that biliary complications could be successfully addressed with a second Roux-en-Y loop in patients with an RYGP. One additional technical point concerns the use of the endoluminal tube to guide the shaping of the gastric pouch or sleeve. If the preoperative endoscopy has shown the presence of esophageal varices, in spite of appropriate endoscopic eradication, the orogastric tube may eventually injure the varices causing bleeding. For this reason, it should be better avoided as far as possible especially in patients with a low prothrombin time and platelet count. SG is also associated with an increased risk of portal thrombosis compared to RYGP in non-cirrhotic patients[165]. This may be a further concern, as liver cirrhosis is a risk factor for portal thrombosis in itself. The occurrence of portal thrombosis may further complicate the access to LT. The risk of dumping syndrome and hyperinsulinemic hypoglycemia may be further concerns of the RYGP.

In conclusion, with all of the potential that bariatric surgery has candidates to LT with morbid obesity, well-designed studies are still necessary to gain widespread acceptance from clinicians. Several points need to be clarified, including the most appropriate methods for accurate patient evaluation and selection, the optimal surgical procedure and its timing to maximize the efficiency of bariatric surgery in liver recipients with obesity. Only when this research is furthered to the point where the effectiveness of bariatric surgery is no longer in doubt, the latter will be included in the care of liver recipients with obesity for mainstream use. In the meantime, the policy of a case-by-case discussion involving a multidisciplinary team, including hepatologists and both LT and bariatric surgeons, seems to be justified.

CONCLUSION

With the recent epidemic of obesity, the coexistence of liver cirrhosis and obesity has become very frequent. The complex interplay between obesity and the liver especially in the setting of liver cirrhosis is a formidable challenge for current medicine that goes from the prevention of liver complications of obesity, screening for these complications in patients at risk to the management of patients with sarcopenia and end-stage liver disease. Bariatric surgery has shown promising results although evidence is still scarce.

REFERENCES

1 **Kleiner DE**, Brunt EM, Van Natta M, Behling C, Contos MJ, Cummings OW, Ferrell LD, Liu YC, Torbenson MS, Unalp-Arida A, Yeh M, McCullough AJ, Sanyal AJ; Nonalcoholic Steatohepatitis Clinical Research Network. Design and validation of a histological scoring system for nonalcoholic fatty liver disease. *Hepatology* 2005; **41**: 1313-1321 [PMID: 15915461 DOI: 10.1002/hep.20701]

2 **Welzel TM**, Graubard BI, Zeuzem S, El-Serag HB, Davila JA, McGlynn KA. Metabolic syndrome increases the risk of primary liver cancer in the United States: a study in the SEER-Medicare database. *Hepatology* 2011; **54**: 463-471 [PMID: 21538440 DOI: 10.1002/hep.24397]

3 **Starley BQ**, Calcagno CJ, Harrison SA. Nonalcoholic fatty liver disease and hepatocellular carcinoma: a weighty connection. *Hepatology* 2010; **51**: 1820-1832 [PMID: 20432259 DOI: 10.1002/hep.23594]

4 **Ascha MS**, Hanouneh IA, Lopez R, Tamimi TA, Feldstein AF, Zein NN. The incidence and risk factors of hepatocellular carcinoma in patients with nonalcoholic steatohepatitis. *Hepatology* 2010; **51**: 1972-1978 [PMID: 20209604 DOI: 10.1002/hep.23527]

5 **Chalasani N**, Younossi Z, Lavine JE, Diehl AM, Brunt EM, Cusi K, Charlton M, Sanyal AJ. The diagnosis and management of non-alcoholic fatty liver disease: practice Guideline by the American Association for the Study of Liver Diseases, American College of Gastroenterology, and the American Gastroenterological Association. *Hepatology* 2012; **55**: 2005-2023 [PMID: 22488764 DOI: 10.1002/hep.25762]

6 **Angulo P**. Long-term mortality in nonalcoholic fatty liver disease: is liver histology of any prognostic significance? *Hepatology* 2010; **51**: 373-375 [PMID: 20101746 DOI: 10.1002/hep.23521]

7 **Raynard B**, Balian A, Fallik D, Capron F, Bedossa P, Chaput JC, Naveau S. Risk factors of fibrosis in alcohol-induced liver disease. *Hepatology* 2002; **35**: 635-638 [PMID: 11870378 DOI: 10.1053/jhep.2002.31782]

8 **Ortiz V**, Berenguer M, Rayón JM, Carrasco D, Berenguer J. Contribution of obesity to hepatitis C-related fibrosis progression. *Am J Gastroenterol* 2002; **97**: 2408-2414 [PMID: 12358265 DOI: 10.1111/j.1572-0241.2002.05995.x]

9 **Bellentani S**, Saccoccio G, Masutti F, Crocè LS, Brandi G, Sasso F, Cristanini G, Tiribelli C. Prevalence of and risk factors for hepatic steatosis in Northern Italy. *Ann Intern Med* 2000; **132**: 112-117 [PMID: 10644271 DOI: 10.7326/0003-4819-132-2-200001180-00029]

10 **Ekstedt M**, Franzén LE, Holmqvist M, Bendtsen P, Mathiesen UL, Bodemar G, Kechagias S. Alcohol consumption is associated with progression of hepatic fibrosis in non-alcoholic fatty liver disease. *Scand J Gastroenterol* 2009; **44**: 366-374 [PMID: 19016382 DOI: 10.1080/00365520802555991]

11 **Liu B**, Balkwill A, Reeves G, Beral V; Million Women Study Collaborators. Body mass index and risk of liver cirrhosis in middle aged UK women: prospective study. *BMJ* 2010; **340**: c912 [PMID: 20223875 DOI: 10.1136/bmj.c912]

12 **Everhart JE**, Lok AS, Kim HY, Morgan TR, Lindsay KL, Chung RT, Bonkovsky HL, Ghany MG; HALT-C Trial Group. Weight-related effects on disease progression in the hepatitis C antiviral long-term treatment against cirrhosis trial. *Gastroenterology* 2009; **137**: 549-557 [PMID: 19445938 DOI: 10.1053/j.gastro.2009.05.007]

13 **Berzigotti A**, Abraldes JG. Impact of obesity and insulin-resistance on cirrhosis and portal hypertension. *Gastroenterol Hepatol* 2013; **36**: 527-533 [PMID: 23731977 DOI: 10.1016/j.gastrohep.2013.03.005]

14 **Berzigotti A**, Albillos A, Villanueva C, Genescá J, Ardevol A, Augustín S, Calleja JL, Bañares R, García-Pagán JC, Mesonero F, Bosch J; Ciberehd SportDiet Collaborative Group. Effects of an intensive lifestyle intervention program on portal hypertension in patients with cirrhosis and obesity: The SportDiet study. *Hepatology* 2017; **65**: 1293-1305 [PMID: 27997989 DOI: 10.1002/hep.28992]

15 **Ayala R**, Grande S, Bustelos R, Ribera C, García-Sesma A, Jimenez C, Moreno E, Martínez-López J. Obesity is an independent risk factor for pre-transplant portal vein thrombosis in liver recipients. *BMC Gastroenterol* 2012; **12**: 114 [PMID: 22909075 DOI: 10.1186/1471-230X-12-114]

16 **Allman-Farinelli MA**. Obesity and venous thrombosis: a review. *Semin Thromb Hemost* 2011; **37**: 903-907 [PMID: 22198855 DOI: 10.1055/s-0031-1297369]

17 **LaMattina JC**, Foley DP, Fernandez LA, Pirsch JD, Musat AI, D'Alessandro AM, Mezrich JD. Complications associated with liver transplantation in the obese recipient. *Clin Transplant* 2012; **26**: 910-918 [PMID: 22694047 DOI: 10.1111/j.1399-0012.2012.01669.x]

18 **Cruz-Jentoft AJ**, Baeyens JP, Bauer JM, Boirie Y, Cederholm T,

Landi F, Martin FC, Michel JP, Rolland Y, Schneider SM, Topinková E, Vandewoude M, Zamboni M; European Working Group on Sarcopenia in Older People. Sarcopenia: European consensus on definition and diagnosis: Report of the European Working Group on Sarcopenia in Older People. *Age Ageing* 2010; **39**: 412-423 [PMID: 20392703 DOI: 10.1093/ageing/afq034]

19 **Rolland Y**, Lauwers-Cances V, Cristini C, Abellan van Kan G, Janssen I, Morley JE, Vellas B. Difficulties with physical function associated with obesity, sarcopenia, and sarcopenic-obesity in community-dwelling elderly women: the EPIDOS (EPIDemiologie de l'OSteoporose) Study. *Am J Clin Nutr* 2009; **89**: 1895-1900 [PMID: 19369381 DOI: 10.3945/ajcn.2008.26950]

20 **Koster A**, Ding J, Stenholm S, Caserotti P, Houston DK, Nicklas BJ, You T, Lee JS, Visser M, Newman AB, Schwartz AV, Cauley JA, Tylavsky FA, Goodpaster BH, Kritchevsky SB, Harris TB; Health ABC study. Does the amount of fat mass predict age-related loss of lean mass, muscle strength, and muscle quality in older adults? *J Gerontol A Biol Sci Med Sci* 2011; **66**: 888-895 [PMID: 21572082 DOI: 10.1093/gerona/glr070]

21 **Beavers KM**, Hsu FC, Houston DK, Beavers DP, Harris TB, Hue TF, Kim LJ, Koster A, Penninx BW, Simonsick EM, Strotmeyer ES, Kritchevsky SB, Nicklas BJ; Health ABC Study. The role of metabolic syndrome, adiposity, and inflammation in physical performance in the Health ABC Study. *J Gerontol A Biol Sci Med Sci* 2013; **68**: 617-623 [PMID: 23109678 DOI: 10.1093/gerona/gls213]

22 **European Association for the Study of the Liver (EASL)**, European Association for the Study of Diabetes (EASD), European Association for the Study of Obesity (EASO). EASL-EASD-EASO Clinical Practice Guidelines for the Management of Non-Alcoholic Fatty Liver Disease. *Obes Facts* 2016; **9**: 65-90 [PMID: 27055256 DOI: 10.1159/000443344]

23 **Tovo CV**, Fernandes SA, Buss C, de Mattos AA. Sarcopenia and non-alcoholic fatty liver disease: Is there a relationship? A systematic review. *World J Hepatol* 2017; **9**: 326-332 [PMID: 28293382 DOI: 10.4254/wjh.v9.i6.326]

24 **Hong HC**, Hwang SY, Choi HY, Yoo HJ, Seo JA, Kim SG, Kim NH, Baik SH, Choi DS, Choi KM. Relationship between sarcopenia and nonalcoholic fatty liver disease: the Korean Sarcopenic Obesity Study. *Hepatology* 2014; **59**: 1772-1778 [PMID: 23996808 DOI: 10.1002/hep.26716]

25 **Lee YH**, Kim SU, Song K, Park JY, Kim DY, Ahn SH, Lee BW, Kang ES, Cha BS, Han KH. Sarcopenia is associated with significant liver fibrosis independently of obesity and insulin resistance in nonalcoholic fatty liver disease: Nationwide surveys (KNHANES 2008-2011). *Hepatology* 2016; **63**: 776-786 [PMID: 26638128 DOI: 10.1002/hep.28376]

26 **Shida T**, Akiyama K, Oh S, Sawai A, Isobe T, Okamoto Y, Ishige K, Mizokami Y, Yamagata K, Onizawa K, Tanaka H, Iijima H, Shoda J. Skeletal muscle mass to visceral fat area ratio is an important determinant affecting hepatic conditions of non-alcoholic fatty liver disease. *J Gastroenterol* 2018; **53**: 535-547 [PMID: 28791501 DOI: 10.1007/s00535-017-1377-3]

27 **Anand AC**. Nutrition and Muscle in Cirrhosis. *J Clin Exp Hepatol* 2017; **7**: 340-357 [PMID: 29234200 DOI: 10.1016/j.jceh.2017.11.001]

28 **Montano-Loza AJ**, Angulo P, Meza-Junco J, Prado CM, Sawyer MB, Beaumont C, Esfandiari N, Ma M, Baracos VE. Sarcopenic obesity and myosteatosis are associated with higher mortality in patients with cirrhosis. *J Cachexia Sarcopenia Muscle* 2016; **7**: 126-135 [PMID: 27493866 DOI: 10.1002/jcsm.12039]

29 **Hara N**, Iwasa M, Sugimoto R, Mifuji-Moroka R, Yoshikawa K, Terasaka E, Hattori A, Ishidome M, Kobayashi Y, Hasegawa H, Iwata K, Takei Y. Sarcopenia and Sarcopenic Obesity Are Prognostic Factors for Overall Survival in Patients with Cirrhosis. *Intern Med* 2016; **55**: 863-870 [PMID: 27086797 DOI: 10.2169/internalmedicine.55.5676]

30 **Carias S**, Castellanos AL, Vilchez V, Nair R, Dela Cruz AC, Watkins J, Barrett T, Trushar P, Esser K, Gedaly R. Nonalcoholic steatohepatitis is strongly associated with sarcopenic obesity in patients with cirrhosis undergoing liver transplant evaluation. *J Gastroenterol Hepatol* 2016; **31**: 628-633 [PMID: 26399838 DOI: 10.1111/jgh.13166]

31 **Kaido T**, Tamai Y, Hamaguchi Y, Okumura S, Kobayashi A, Shirai H, Yagi S, Kamo N, Hammad A, Inagaki N, Uemoto S. Effects of pretransplant sarcopenia and sequential changes in sarcopenic parameters after living donor liver transplantation. *Nutrition* 2017; **33**: 195-198 [PMID: 27649861 DOI: 10.1016/j.nut.2016.07.002]

32 **Hammad A**, Kaido T, Hamaguchi Y, Okumura S, Kobayashi A, Shirai H, Kamo N, Yagi S, Uemoto S. Impact of sarcopenic overweight on the outcomes after living donor liver transplantation. *Hepatobiliary Surg Nutr* 2017; **6**: 367-378 [PMID: 29312971 DOI: 10.21037/hbsn.2017.02.02]

33 **Spengler EK**, O'Leary JG, Te HS, Rogal S, Pillai AA, Al-Osaimi A, Desai A, Fleming JN, Ganger D, Seetharam A, Tsoulfas G, Montenovo M, Lai JC. Liver Transplantation in the Obese Cirrhotic Patient. *Transplantation* 2017; **101**: 2288-2296 [PMID: 28930104 DOI: 10.1097/TP.0000000000001794]

34 **Richards J**, Gunson B, Johnson J, Neuberger J. Weight gain and obesity after liver transplantation. *Transpl Int* 2005; **18**: 461-466 [PMID: 15773968 DOI: 10.1111/j.1432-2277.2004.00067.x]

35 **Schütz T**, Hudjetz H, Roske AE, Katzorke C, Kreymann G, Budde K, Fritsche L, Neumayer HH, Lochs H, Plauth M. Weight gain in long-term survivors of kidney or liver transplantation--another paradigm of sarcopenic obesity? *Nutrition* 2012; **28**: 378-383 [PMID: 22304858 DOI: 10.1016/j.nut.2011.07.019]

36 **Choudhary NS**, Saigal S, Saraf N, Mohanka R, Rastogi A, Goja S, Menon PB, Mishra S, Mittal A, Soin AS. Sarcopenic obesity with metabolic syndrome: a newly recognized entity following living donor liver transplantation. *Clin Transplant* 2015; **29**: 211-215 [PMID: 25594826 DOI: 10.1111/ctr.12505]

37 **Johnson TM**, Overgard EB, Cohen AE, DiBaise JK. Nutrition assessment and management in advanced liver disease. *Nutr Clin Pract* 2013; **28**: 15-29 [PMID: 23319353 DOI: 10.1177/0884533612469027]

38 **Floreani A**, Baragiotta A, Martines D, Naccarato R, D'odorico A. Plasma antioxidant levels in chronic cholestatic liver diseases. *Aliment Pharmacol Ther* 2000; **14**: 353-358 [PMID: 10735930 DOI: 10.1046/j.1365-2036.2000.00729.x]

39 **Hansen KE**, Johnson MG. An update on vitamin D for clinicians. *Curr Opin Endocrinol Diabetes Obes* 2016; **23**: 440-444 [PMID: 27653000 DOI: 10.1097/MED.0000000000000288]

40 **Stokes CS**, Volmer DA, Grünhage F, Lammert F. Vitamin D in chronic liver disease. *Liver Int* 2013; **33**: 338-352 [PMID: 23402606 DOI: 10.1111/liv.12106]

41 **Lim LY**, Chalasani N. Vitamin d deficiency in patients with chronic liver disease and cirrhosis. *Curr Gastroenterol Rep* 2012; **14**: 67-73 [PMID: 22113744 DOI: 10.1007/s11894-011-0231-7]

42 **Targher G**, Byrne CD. Lower 25-hydroxyvitamin D3 levels and increased risk of liver diseases: is there a causal link? *Endocrine* 2014; **47**: 3-4 [PMID: 24595898 DOI: 10.1007/s12020-014-0220-3]

43 **Stokes CS**, Krawczyk M, Reichel C, Lammert F, Grünhage F. Vitamin D deficiency is associated with mortality in patients with advanced liver cirrhosis. *Eur J Clin Invest* 2014; **44**: 176-183 [PMID: 24236541 DOI: 10.1111/eci.12205]

44 **Paternostro R**, Wagner D, Reiberger T, Mandorfer M, Schwarzer R, Ferlitsch M, Trauner M, Peck-Radosavljevic M, Ferlitsch A. Low 25-OH-vitamin D levels reflect hepatic dysfunction and are associated with mortality in patients with liver cirrhosis. *Wien Klin Wochenschr* 2017; **129**: 8-15 [PMID: 27888359 DOI: 10.1007/s00508-016-1127-1]

45 **Putz-Bankuti C**, Pilz S, Stojakovic T, Scharnagl H, Pieber TR, Trauner M, Obermayer-Pietsch B, Stauber RE. Association of 25-hydroxyvitamin D levels with liver dysfunction and mortality in chronic liver disease. *Liver Int* 2012; **32**: 845-851 [PMID: 22222013 DOI: 10.1111/j.1478-3231.2011.02735.x]

46 **Arteh J**, Narra S, Nair S. Prevalence of vitamin D deficiency in chronic liver disease. *Dig Dis Sci* 2010; **55**: 2624-2628 [PMID: 19960254 DOI: 10.1007/s10620-009-1069-9]

47 **Fisher L**, Fisher A. Vitamin D and parathyroid hormone in outpatients with noncholestatic chronic liver disease. *Clin Gastroenterol Hepatol*

2007; **5**: 513-520 [PMID: 17222588 DOI: 10.1016/j.cgh.2006.10.015]
48 **Jha AK**, Jha SK, Kumar A, Dayal VM, Jha SK. Effect of replenishment of vitamin D on survival in patients with decompensated liver cirrhosis: A prospective study. *World J Gastrointest Pathophysiol* 2017; **8**: 133-141 [PMID: 28868183 DOI: 10.4291/wjgp.v8.i3.133]
49 **Kitson MT**, Roberts SK. D-livering the message: the importance of vitamin D status in chronic liver disease. *J Hepatol* 2012; **57**: 897-909 [PMID: 22634121 DOI: 10.1016/j.jhep.2012.04.033]
50 **Reese PP**, Bloom RD, Feldman HI, Huverserian A, Thomasson A, Shults J, Hamano T, Goral S, Shaked A, Olthoff K, Rickels MR, Bleicher M, Leonard MB. Changes in vitamin D binding protein and vitamin D concentrations associated with liver transplantation. *Liver Int* 2012; **32**: 287-296 [PMID: 22098635 DOI: 10.1111/j.1478-3231.2011.02638.x]
51 **Skaaby T**, Husemoen LL, Borglykke A, Jørgensen T, Thuesen BH, Pisinger C, Schmidt LE, Linneberg A. Vitamin D status, liver enzymes, and incident liver disease and mortality: a general population study. *Endocrine* 2014; **47**: 213-220 [PMID: 24272594 DOI: 10.1007/s12020-013-0107-8]
52 **Wang JB**, Abnet CC, Chen W, Dawsey SM, Fan JH, Yin LY, Yin J, Major JM, Taylor PR, Qiao YL, Freedman ND. Association between serum 25(OH) vitamin D, incident liver cancer and chronic liver disease mortality in the Linxian Nutrition Intervention Trials: a nested case-control study. *Br J Cancer* 2013; **109**: 1997-2004 [PMID: 24008664 DOI: 10.1038/bjc.2013.546]
53 **Wortsman J**, Matsuoka LY, Chen TC, Lu Z, Holick MF. Decreased bioavailability of vitamin D in obesity. *Am J Clin Nutr* 2000; **72**: 690-693 [PMID: 10966885 DOI: 10.1093/ajcn/72.3.690]
54 **Stein EM**, Strain G, Sinha N, Ortiz D, Pomp A, Dakin G, McMahon DJ, Bockman R, Silverberg SJ. Vitamin D insufficiency prior to bariatric surgery: risk factors and a pilot treatment study. *Clin Endocrinol (Oxf)* 2009; **71**: 176-183 [PMID: 19018785 DOI: 10.1111/j.1365-2265.2008.03470.x]
55 **Chiu KC**, Chu A, Go VL, Saad MF. Hypovitaminosis D is associated with insulin resistance and beta cell dysfunction. *Am J Clin Nutr* 2004; **79**: 820-825 [PMID: 15113720 DOI: 10.1093/ajcn/79.5.820]
56 **Ganji V**, Zhang X, Shaikh N, Tangpricha V. Serum 25-hydroxyvitamin D concentrations are associated with prevalence of metabolic syndrome and various cardiometabolic risk factors in US children and adolescents based on assay-adjusted serum 25-hydroxyvitamin D data from NHANES 2001-2006. *Am J Clin Nutr* 2011; **94**: 225-233 [PMID: 21613551 DOI: 10.3945/ajcn.111.013516]
57 **Barchetta I**, De Bernardinis M, Capoccia D, Baroni MG, Fontana M, Fraioli A, Morini S, Leonetti F, Cavallo MG. Hypovitaminosis D is independently associated with metabolic syndrome in obese patients. *PLoS One* 2013; **8**: e68689 [PMID: 23935881 DOI: 10.1371/journal.pone.0068689]
58 **Shankar A**, Sabanayagam C, Kalidindi S. Serum 25-hydroxyvitamin d levels and prediabetes among subjects free of diabetes. *Diabetes Care* 2011; **34**: 1114-1119 [PMID: 21430085 DOI: 10.2337/dc10-1203]
59 **Knekt P**, Laaksonen M, Mattila C, Härkänen T, Marniemi J, Heliövaara M, Rissanen H, Montonen J, Reunanen A. Serum vitamin D and subsequent occurrence of type 2 diabetes. *Epidemiology* 2008; **19**: 666-671 [PMID: 18496468 DOI: 10.1097/EDE.0b013e318176b8ad]
60 **Kayaniyil S**, Retnakaran R, Harris SB, Vieth R, Knight JA, Gerstein HC, Perkins BA, Zinman B, Hanley AJ. Prospective associations of vitamin D with β-cell function and glycemia: the PROspective Metabolism and ISlet cell Evaluation (PROMISE) cohort study. *Diabetes* 2011; **60**: 2947-2953 [PMID: 21911752 DOI: 10.2337/db11-0465]
61 **Grimnes G**, Emaus N, Joakimsen RM, Figenschau Y, Jenssen T, Njølstad I, Schirmer H, Jorde R. Baseline serum 25-hydroxyvitamin D concentrations in the Tromsø Study 1994-95 and risk of developing type 2 diabetes mellitus during 11 years of follow-up. *Diabet Med* 2010; **27**: 1107-1115 [PMID: 20854377 DOI: 10.1111/j.1464-5491.2010.03092.x]
62 **Lamendola CA**, Ariel D, Feldman D, Reaven GM. Relations between obesity, insulin resistance, and 25-hydroxyvitamin D. *Am J Clin Nutr* 2012; **95**: 1055-1059 [PMID: 22440850 DOI: 10.3945/ajcn.111.032060]
63 **Rajakumar K**, de las Heras J, Lee S, Holick MF, Arslanian SA. 25-hydroxyvitamin D concentrations and in vivo insulin sensitivity and β-cell function relative to insulin sensitivity in black and white youth. *Diabetes Care* 2012; **35**: 627-633 [PMID: 22238280 DOI: 10.2337/dc11-1825]
64 **Targher G**, Bertolini L, Scala L, Cigolini M, Zenari L, Falezza G, Arcaro G. Associations between serum 25-hydroxyvitamin D3 concentrations and liver histology in patients with non-alcoholic fatty liver disease. *Nutr Metab Cardiovasc Dis* 2007; **17**: 517-524 [PMID: 16928437 DOI: 10.1016/j.numecd.2006.04.002]
65 **Dasarathy J**, Periyalwar P, Allampati S, Bhinder V, Hawkins C, Brandt P, Khiyami A, McCullough AJ, Dasarathy S. Hypovitaminosis D is associated with increased whole body fat mass and greater severity of non-alcoholic fatty liver disease. *Liver Int* 2014; **34**: e118-e127 [PMID: 24118743 DOI: 10.1111/liv.12312]
66 **Jablonski KL**, Jovanovich A, Holmen J, Targher G, McFann K, Kendrick J, Chonchol M. Low 25-hydroxyvitamin D level is independently associated with non-alcoholic fatty liver disease. *Nutr Metab Cardiovasc Dis* 2013; **23**: 792-798 [PMID: 23415456 DOI: 10.1016/j.numecd.2012.12.006]
67 **Barchetta I**, Angelico F, Del Ben M, Baroni MG, Pozzilli P, Morini S, Cavallo MG. Strong association between non alcoholic fatty liver disease (NAFLD) and low 25(OH) vitamin D levels in an adult population with normal serum liver enzymes. *BMC Med* 2011; **9**: 85 [PMID: 21749681 DOI: 10.1186/1741-7015-9-85]
68 **Nelson JE**, Roth CL, Wilson LA, Yates KP, Aouizerat B, Morgan-Stevenson V, Whalen E, Hoofnagle A, Mason M, Gersuk V, Yeh MM, Kowdley KV. Vitamin D Deficiency Is Associated With Increased Risk of Non-alcoholic Steatohepatitis in Adults With Non-alcoholic Fatty Liver Disease: Possible Role for MAPK and NF-κB? *Am J Gastroenterol* 2016; **111**: 852-863 [PMID: 27002799 DOI: 10.1038/ajg.2016.51]
69 **Bril F**, Maximos M, Portillo-Sanchez P, Biernacki D, Lomonaco R, Subbarayan S, Correa M, Lo M, Suman A, Cusi K. Relationship of vitamin D with insulin resistance and disease severity in non-alcoholic steatohepatitis. *J Hepatol* 2015; **62**: 405-411 [PMID: 25195551 DOI: 10.1016/j.jhep.2014.08.040]
70 **European Association for the Study of the Liver**. EASL Clinical Practice Guidelines: management of cholestatic liver diseases. *J Hepatol* 2009; **51**: 237-267 [PMID: 19501929 DOI: 10.1016/j.jhep.2009.04.009]
71 **Leslie WD**, Bernstein CN, Leboff MS; American Gastroenterological Association Clinical Practice Commitee. AGA technical review on osteoporosis in hepatic disorders. *Gastroenterology* 2003; **125**: 941-966 [PMID: 12949738 DOI: 10.1016/S0016-5085(03)01062-X]
72 **Barchetta I**, Cimini FA, Cavallo MG. Vitamin D Supplementation and Non-Alcoholic Fatty Liver Disease: Present and Future. *Nutrients* 2017; **9**: [PMID: 28906453 DOI: 10.3390/nu9091015]
73 **Kitson MT**, Pham A, Gordon A, Kemp W, Roberts SK. High-dose vitamin D supplementation and liver histology in NASH. *Gut* 2016; **65**: 717-718 [PMID: 26294696 DOI: 10.1136/gutjnl-2015-310417]
74 **Barchetta I**, Del Ben M, Angelico F, Di Martino M, Fraioli A, La Torre G, Saulle R, Perri L, Morini S, Tiberti C, Bertoccini L, Cimini FA, Panimolle F, Catalano C, Baroni MG, Cavallo MG. No effects of oral vitamin D supplementation on non-alcoholic fatty liver disease in patients with type 2 diabetes: a randomized, double-blind, placebo-controlled trial. *BMC Med* 2016; **14**: 92 [PMID: 27353492 DOI: 10.1186/s12916-016-0638-y]
75 **Nagpal J**, Pande JN, Bhartia A. A double-blind, randomized, placebo-controlled trial of the short-term effect of vitamin D3 supplementation on insulin sensitivity in apparently healthy, middle-aged, centrally obese men. *Diabet Med* 2009; **26**: 19-27 [PMID: 19125756 DOI: 10.1111/j.1464-5491.2008.02636.x]
76 **von Hurst PR**, Stonehouse W, Coad J. Vitamin D supplementation reduces insulin resistance in South Asian women living in New Zealand who are insulin resistant and vitamin D deficient - a randomised, placebo-controlled trial. *Br J Nutr* 2010; **103**: 549-555

[PMID: 19781131 DOI: 10.1017/S0007114509992017]
77 **Pittas AG**, Dawson-Hughes B, Li T, Van Dam RM, Willett WC, Manson JE, Hu FB. Vitamin D and calcium intake in relation to type 2 diabetes in women. *Diabetes Care* 2006; **29**: 650-656 [PMID: 16505521 DOI: 10.2337/diacare.29.03.06.dc05-1961]
78 **Stokes CS**, Grünhage F, Baus C, Volmer DA, Wagenpfeil S, Riemenschneider M, Lammert F. Vitamin D supplementation reduces depressive symptoms in patients with chronic liver disease. *Clin Nutr* 2016; **35**: 950-957 [PMID: 26212170 DOI: 10.1016/j.clnu.2015.07.004]
79 **Bitetto D**, Fabris C, Falleti E, Fornasiere E, Fumolo E, Fontanini E, Cussigh A, Occhino G, Baccarani U, Pirisi M, Toniutto P. Vitamin D and the risk of acute allograft rejection following human liver transplantation. *Liver Int* 2010; **30**: 417-444 [PMID: 19849776 DOI: 10.1111/j.1478-3231.2009.02154.x]
80 **Bjelakovic G**, Nikolova D, Bjelakovic M, Gluud C. Vitamin D supplementation for chronic liver diseases in adults. *Cochrane Database Syst Rev* 2017; **11**: CD011564 [PMID: 29099543 DOI: 10.1002/14651858.CD011564.pub2]
81 **Collier JD**, Ninkovic M, Compston JE. Guidelines on the management of osteoporosis associated with chronic liver disease. *Gut* 2002; **50 Suppl 1**: i1-i9 [PMID: 11788576 DOI: 10.1136/gut.50.suppl_1.i1]
82 **Dasarathy J**, Varghese R, Feldman A, Khiyami A, McCullough AJ, Dasarathy S. Patients with Nonalcoholic Fatty Liver Disease Have a Low Response Rate to Vitamin D Supplementation. *J Nutr* 2017; **147**: 1938-1946 [PMID: 28814531 DOI: 10.3945/jn.117.254292]
83 **Parola M**, Leonarduzzi G, Biasi F, Albano E, Biocca ME, Poli G, Dianzani MU. Vitamin E dietary supplementation protects against carbon tetrachloride-induced chronic liver damage and cirrhosis. *Hepatology* 1992; **16**: 1014-1021 [PMID: 1398481 DOI: 10.1002/hep.1840160426]
84 **Houglum K**, Venkataramani A, Lyche K, Chojkier M. A pilot study of the effects of d-alpha-tocopherol on hepatic stellate cell activation in chronic hepatitis C. *Gastroenterology* 1997; **113**: 1069-1073 [PMID: 9322499 DOI: 10.1053/gast.1997.v113.pm9322499]
85 **Sanyal AJ**, Chalasani N, Kowdley KV, McCullough A, Diehl AM, Bass NM, Neuschwander-Tetri BA, Lavine JE, Tonascia J, Unalp A, Van Natta M, Clark J, Brunt EM, Kleiner DE, Hoofnagle JH, Robuck PR; NASH CRN. Pioglitazone, vitamin E, or placebo for nonalcoholic steatohepatitis. *N Engl J Med* 2010; **362**: 1675-1685 [PMID: 20427778 DOI: 10.1056/NEJMoa0907929]
86 **Chalasani N**, Younossi Z, Lavine JE, Charlton M, Cusi K, Rinella M, Harrison SA, Brunt EM, Sanyal AJ. The diagnosis and management of nonalcoholic fatty liver disease: Practice guidance from the American Association for the Study of Liver Diseases. *Hepatology* 2018; **67**: 328-357 [PMID: 28714183 DOI: 10.1002/hep.29367]
87 **Muñoz SJ**, Heubi JE, Balistreri WF, Maddrey WC. Vitamin E deficiency in primary biliary cirrhosis: gastrointestinal malabsorption, frequency and relationship to other lipid-soluble vitamins. *Hepatology* 1989; **9**: 525-531 [PMID: 2925155 DOI: 10.1002/hep.1840090403]
88 **Jeffrey GP**, Muller DP, Burroughs AK, Matthews S, Kemp C, Epstein O, Metcalfe TA, Southam E, Tazir-Melboucy M, Thomas PK. Vitamin E deficiency and its clinical significance in adults with primary biliary cirrhosis and other forms of chronic liver disease. *J Hepatol* 1987; **4**: 307-317 [PMID: 3036938 DOI: 10.1016/S0168-8278(87)80539-1]
89 **Leo MA**, Rosman AS, Lieber CS. Differential depletion of carotenoids and tocopherol in liver disease. *Hepatology* 1993; **17**: 977-986 [PMID: 8514270 DOI: 10.1002/hep.1840170606]
90 **Grüngreiff K**, Reinhold D, Wedemeyer H. The role of zinc in liver cirrhosis. *Ann Hepatol* 2016; **15**: 7-16 [PMID: 26626635 DOI: 10.5604/16652681.1184191]
91 **Ma J**, Betts NM. Zinc and copper intakes and their major food sources for older adults in the 1994-96 continuing survey of food intakes by individuals (CSFII). *J Nutr* 2000; **130**: 2838-2843 [PMID: 11053529 DOI: 10.1093/jn/130.11.2838]
92 **Huskisson E**, Maggini S, Ruf M. The role of vitamins and minerals in energy metabolism and well-being. *J Int Med Res* 2007; **35**: 277-289 [PMID: 17593855 DOI: 10.1177/147323000703500301]
93 **Gibson RS**, King JC, Lowe N. A Review of Dietary Zinc Recommendations. *Food Nutr Bull* 2016; **37**: 443-460 [PMID: 27312357 DOI: 10.1177/0379572116652252]
94 **Himoto T**, Masaki T. Associations between Zinc Deficiency and Metabolic Abnormalities in Patients with Chronic Liver Disease. *Nutrients* 2018; **10**: [PMID: 29342898 DOI: 10.3390/nu10010088]
95 **Chiba M**, Katayama K, Takeda R, Morita R, Iwahashi K, Onishi Y, Kita H, Nishio A, Kanno T, Saito T, Maeda K, Naito M, Michida T, Ito T. Diuretics aggravate zinc deficiency in patients with liver cirrhosis by increasing zinc excretion in urine. *Hepatol Res* 2013; **43**: 365-373 [PMID: 22994500 DOI: 10.1111/j.1872-034X.2012.01093.x]
96 **Nusrat S**, Khan MS, Fazili J, Madhoun MF. Cirrhosis and its complications: evidence based treatment. *World J Gastroenterol* 2014; **20**: 5442-5460 [PMID: 24833875 DOI: 10.3748/wjg.v20.i18.5442]
97 **Van der Rijt CC**, Schalm SW, Schat H, Foeken K, De Jong G. Overt hepatic encephalopathy precipitated by zinc deficiency. *Gastroenterology* 1991; **100**: 1114-1118 [PMID: 2001810 DOI: 10.1016/0016-5085(91)90290-2]
98 **Rabbani P**, Prasad AS. Plasma ammonia and liver ornithine transcarbamoylase activity in zinc-deficient rats. *Am J Physiol* 1978; **235**: E203-E206 [PMID: 686166 DOI: 10.1152/ajpendo.1978.235.2.E203]
99 **Katayama K**, Saito M, Kawaguchi T, Endo R, Sawara K, Nishiguchi S, Kato A, Kohgo H, Suzuki K, Sakaida I, Ueno Y, Habu D, Ito T, Moriwaki H, Suzuki K. Effect of zinc on liver cirrhosis with hyperammonemia: a preliminary randomized, placebo-controlled double-blind trial. *Nutrition* 2014; **30**: 1409-1414 [PMID: 25280421 DOI: 10.1016/j.nut.2014.04.018]
100 **Marchesini G**, Fabbri A, Bianchi G, Brizi M, Zoli M. Zinc supplementation and amino acid-nitrogen metabolism in patients with advanced cirrhosis. *Hepatology* 1996; **23**: 1084-1092 [PMID: 8621138 DOI: 10.1053/jhep.1996.v23.pm0008621138]
101 **Takuma Y**, Nouso K, Makino Y, Hayashi M, Takahashi H. Clinical trial: oral zinc in hepatic encephalopathy. *Aliment Pharmacol Ther* 2010; **32**: 1080-1090 [PMID: 20822500 DOI: 10.1111/j.1365-2036.2010.04448.x]
102 **Mousa N**, Abdel-Razik A, Zaher A, Hamed M, Shiha G, Effat N, Elbaz S, Elhelaly R, Hafez M, El-Wakeel N, Eldars W. The role of antioxidants and zinc in minimal hepatic encephalopathy: a randomized trial. *Therap Adv Gastroenterol* 2016; **9**: 684-691 [PMID: 27582881 DOI: 10.1177/1756283X16645049]
103 **Mohammad MK**, Zhou Z, Cave M, Barve A, McClain CJ. Zinc and liver disease. *Nutr Clin Pract* 2012; **27**: 8-20 [PMID: 22307488 DOI: 10.1177/0884533611433534]
104 **Tabibian JH**, Gerstenblith MR, Tedford RJ, Junkins-Hopkins JM, Abuav R. Necrolytic acral erythema as a cutaneous marker of hepatitis C: report of two cases and review. *Dig Dis Sci* 2010; **55**: 2735-2743 [PMID: 20499177 DOI: 10.1007/s10620-010-1273-7]
105 **Pimentel CF**, Lai M. Nutrition Interventions for Chronic Liver Diseases and Nonalcoholic Fatty Liver Disease. *Med Clin North Am* 2016; **100**: 1303-1327 [PMID: 27745596 DOI: 10.1016/j.mcna.2016.06.010]
106 **Tandon P**, Raman M, Mourtzakis M, Merli M. A practical approach to nutritional screening and assessment in cirrhosis. *Hepatology* 2017; **65**: 1044-1057 [PMID: 28027577 DOI: 10.1002/hep.29003]
107 **Romani AM**. Magnesium homeostasis and alcohol consumption. *Magnes Res* 2008; **21**: 197-204 [PMID: 19271417]
108 **Cohen L**. Magnesium and liver cirrhosis: a hypothesis. *Magnesium* 1985; **4**: 1-4 [PMID: 4033201]
109 **Rahelić D**, Kujundzić M, Romić Z, Brkić K, Petrovecki M. Serum concentration of zinc, copper, manganese and magnesium in patients with liver cirrhosis. *Coll Antropol* 2006; **30**: 523-528 [PMID: 17058518]
110 **Agarwal A**, Avarebeel S, Choudhary NS, Goudar M, Tejaswini CJ. Correlation of Trace Elements in Patients of Chronic Liver Disease with Respect to Child- Turcotte- Pugh Scoring System. *J Clin Diagn Res* 2017; **11**: OC25-OC28 [PMID: 29207755 DOI: 10.7860/

JCDR/2017/26519.10655]
111 **Kar K**, Dasgupta A, Vijaya Bhaskar M, Sudhakar K. Alteration of micronutrient status in compensated and decompensated liver cirrhosis. *Indian J Clin Biochem* 2014; **29**: 232-237 [PMID: 24757308 DOI: 10.1007/s12291-013-0349-5]
112 **Nangliya V**, Sharma A, Yadav D, Sunder S, Nijhawan S, Mishra S. Study of trace elements in liver cirrhosis patients and their role in prognosis of disease. *Biol Trace Elem Res* 2015; **165**: 35-40 [PMID: 25613584 DOI: 10.1007/s12011-015-0237-3]
113 **Koivisto M**, Valta P, Höckerstedt K, Lindgren L. Magnesium depletion in chronic terminal liver cirrhosis. *Clin Transplant* 2002; **16**: 325-328 [PMID: 12225427 DOI: 10.1034/j.1399-0012.2002.01141.x]
114 **Chao A**, Waitzberg D, de Jesus RP, Bueno AA, Kha V, Allen K, Kappus M, Medici V. Malnutrition and Nutritional Support in Alcoholic Liver Disease: a Review. *Curr Gastroenterol Rep* 2016; **18**: 65 [PMID: 27787787 DOI: 10.1007/s11894-016-0539-4]
115 **O'Shea RS**, Dasarathy S, McCullough AJ; Practice Guideline Committee of the American Association for the Study of Liver Diseases; Practice Parameters Committee of the American College of Gastroenterology. Alcoholic liver disease. *Hepatology* 2010; **51**: 307-328 [PMID: 20034030 DOI: 10.1002/hep.23258]
116 **Rossi RE**, Conte D, Massironi S. Diagnosis and treatment of nutritional deficiencies in alcoholic liver disease: Overview of available evidence and open issues. *Dig Liver Dis* 2015; **47**: 819-825 [PMID: 26164399 DOI: 10.1016/j.dld.2015.05.021]
117 **Amodio P**, Bemeur C, Butterworth R, Cordoba J, Kato A, Montagnese S, Uribe M, Vilstrup H, Morgan MY. The nutritional management of hepatic encephalopathy in patients with cirrhosis: International Society for Hepatic Encephalopathy and Nitrogen Metabolism Consensus. *Hepatology* 2013; **58**: 325-336 [PMID: 23471642 DOI: 10.1002/hep.26370]
118 **Merli M**, Giusto M, Lucidi C, Giannelli V, Pentassuglio I, Di Gregorio V, Lattanzi B, Riggio O. Muscle depletion increases the risk of overt and minimal hepatic encephalopathy: results of a prospective study. *Metab Brain Dis* 2013; 28: 281-284 [PMID: 23224378 DOI: 10.1007/s11011-012-9365-z]
119 **Plauth M**, Merli M, Kondrup J, Weimann A, Ferenci P, Müller MJ; ESPEN Consensus Group. ESPEN guidelines for nutrition in liver disease and transplantation. *Clin Nutr* 1997; **16**: 43-55 [PMID: 16844569 DOI: 10.1016/S0261-5614(97)80022-2]
120 **Plauth M**, Cabré E, Riggio O, Assis-Camilo M, Pirlich M, Kondrup J; DGEM (German Society for Nutritional Medicine), Ferenci P, Holm E, Vom Dahl S, Müller MJ, Nolte W; ESPEN (European Society for Parenteral and Enteral Nutrition). ESPEN Guidelines on Enteral Nutrition: Liver disease. *Clin Nutr* 2006; **25**: 285-294 [PMID: 16707194 DOI: 10.1016/j.clnu.2006.01.018]
121 **Córdoba J**, López-Hellín J, Planas M, Sabín P, Sanpedro F, Castro F, Esteban R, Guardia J. Normal protein diet for episodic hepatic encephalopathy: results of a randomized study. *J Hepatol* 2004; **41**: 38-43 [PMID: 15246205 DOI: 10.1016/j.jhep.2004.03.023]
122 **BESSMAN AN**, MIRICK GS. Blood ammonia levels following the ingestion of casein and whole blood. *J Clin Invest* 1958; **37**: 990-998 [PMID: 13563627 DOI: 10.1172/JCI103695]
123 **Fenton JC**, Knight EJ, Humpherson PL. Milk-and-cheese diet in portal-systemic encephalopathy. *Lancet* 1966; **1**: 164-166 [PMID: 4159095 DOI: 10.1016/S0140-6736(66)90696-9]
124 **Greenberger NJ**, Carley J, Schenker S, Bettinger I, Stamnes C, Beyer P. Effect of vegetable and animal protein diets in chronic hepatic encephalopathy. *Am J Dig Dis* 1977; **22**: 845-855 [PMID: 335882 DOI: 10.1007/BF01076158]
125 **Gheorghe L**, Iacob R, Vădan R, Iacob S, Gheorghe C. Improvement of hepatic encephalopathy using a modified high-calorie high-protein diet. *Rom J Gastroenterol* 2005; **14**: 231-238 [PMID: 16200232]
126 **Uribe M**, Dibildox M, Malpica S, Guillermo E, Villallobos A, Nieto L, Vargas F, Garcia Ramos G. Beneficial effect of vegetable protein diet supplemented with psyllium plantago in patients with hepatic encephalopathy and diabetes mellitus. *Gastroenterology* 1985; **88**: 901-907 [PMID: 2982694 DOI: 10.1016/S0016-5085(85)80006-8]
127 **Weber FL Jr**, Minco D, Fresard KM, Banwell JG. Effects of vegetable diets on nitrogen metabolism in cirrhotic subjects. *Gastroenterology* 1985; **89**: 538-544 [PMID: 2991068 DOI: 10.1016/0016-5085(85)90448-2]
128 **Uribe M**, Márquez MA, Garcia Ramos G, Ramos-Uribe MH, Vargas F, Villalobos A, Ramos C. Treatment of chronic portal--systemic encephalopathy with vegetable and animal protein diets. A controlled crossover study. *Dig Dis Sci* 1982; **27**: 1109-1116 [PMID: 6756833 DOI: 10.1007/BF01391449]
129 **Shekib LA**, Zoueil ME, Youssef MM, Mohamed SW. Amino acid composition and In Vitro digestibility of lentil and rice proteins and their mixture (Koshary). *Food Chem* 1986; **20**: 61-67 [DOI: 10.1016/0308-8146(86)90167-6]
130 **Silk DB**. Branched chain amino acids in liver disease: fact or fantasy? *Gut* 1986; **27** Suppl 1: 103-110 [PMID: 3098636 DOI: 10.1136/gut.27.Suppl_1.103]
131 **Fischer JE**, Baldessarini RJ. False neurotransmitters and hepatic failure. *Lancet* 1971; **2**: 75-80 [PMID: 4103986 DOI: 10.1016/S0140-6736(71)92048-4]
132 **Dam G**, Ott P, Aagaard NK, Vilstrup H. Branched-chain amino acids and muscle ammonia detoxification in cirrhosis. *Metab Brain Dis* 2013; **28**: 217-220 [PMID: 23315357 DOI: 10.1007/s11011-013-9377-3]
133 **Gluud LL**, Dam G, Les I, Marchesini G, Borre M, Aagaard NK, Vilstrup H. Branched-chain amino acids for people with hepatic encephalopathy. *Cochrane Database Syst Rev* 2017; **5**: CD001939 [PMID: 28518283 DOI: 10.1002/14651858.CD001939.pub4]
134 **NCD Risk Factor Collaboration (NCD-RisC)**. Trends in adult body-mass index in 200 countries from 1975 to 2014: a pooled analysis of 1698 population-based measurement studies with 19·2 million participants. *Lancet* 2016; **387**: 1377-1396 [PMID: 27115820 DOI: 10.1016/S0140-6736(16)30054-X]
135 **Angrisani L**, Santonicola A, Iovino P, Formisano G, Buchwald H, Scopinaro N. Bariatric Surgery Worldwide 2013. *Obes Surg* 2015; **25**: 1822-1832 [PMID: 25835983 DOI: 10.1007/s11695-015-1657-z]
136 **Diehl AM**, Day C. Cause, Pathogenesis, and Treatment of Nonalcoholic Steatohepatitis. *N Engl J Med* 2017; **377**: 2063-2072 [PMID: 29166236 DOI: 10.1056/NEJMra1503519]
137 **Angulo P**, Kleiner DE, Dam-Larsen S, Adams LA, Bjornsson ES, Charatcharoenwitthaya P, Mills PR, Keach JC, Lafferty HD, Stahler A, Haflidadottir S, Bendtsen F. Liver Fibrosis, but No Other Histologic Features, Is Associated With Long-term Outcomes of Patients With Nonalcoholic Fatty Liver Disease. *Gastroenterology* 2015; **149**: 389-97.e10 [PMID: 25935633 DOI: 10.1053/j.gastro.2015.04.043]
138 **Ekstedt M**, Hagström H, Nasr P, Fredrikson M, Stål P, Kechagias S, Hultcrantz R. Fibrosis stage is the strongest predictor for disease-specific mortality in NAFLD after up to 33 years of follow-up. *Hepatology* 2015; **61**: 1547-1554 [PMID: 25125077 DOI: 10.1002/hep.27368]
139 **Bhaskaran K**, Douglas I, Forbes H, dos-Santos-Silva I, Leon DA, Smeeth L. Body-mass index and risk of 22 specific cancers: a population-based cohort study of 5·24 million UK adults. *Lancet* 2014; **384**: 755-765 [PMID: 25129328 DOI: 10.1016/S0140-6736(14)60892-8]
140 **Watt KD**. Reducing the load: the evolution and management of obesity and nonalcoholic steatohepatitis before liver transplantation. *Liver Transpl* 2012; **18** Suppl 2: S52-S58 [PMID: 22821716 DOI: 10.1002/lt.23515]
141 **Iannelli A**. Bariatric surgery and liver transplant. *Liver Transpl* 2017; **23**: 1369-1370 [PMID: 28945954 DOI: 10.1002/lt.24948]
142 **Saab S**, Lalezari D, Pruthi P, Alper T, Tong MJ. The impact of obesity on patient survival in liver transplant recipients: a meta-analysis. *Liver Int* 2015; **35**: 164-170 [PMID: 24313970 DOI: 10.1111/liv.12431]
143 **Perez-Protto SE**, Quintini C, Reynolds LF, You J, Cywinski JB, Sessler DI, Miller C. Comparable graft and patient survival in lean and obese liver transplant recipients. *Liver Transpl* 2013; **19**: 907-915 [PMID: 23744721 DOI: 10.1002/lt.23680]
144 **Karagozian R**, Bhardwaj G, Wakefield DB, Baffy G. Obesity paradox in advanced liver disease: obesity is associated with lower mortality in hospitalized patients with cirrhosis. *Liver Int* 2016; **36**: 1450-1456 [PMID: 27037497 DOI: 10.1111/liv.13137]

145 **Terjimanian MN**, Harbaugh CM, Hussain A, Olugbade KO Jr, Waits SA, Wang SC, Sonnenday CJ, Englesbe MJ. Abdominal adiposity, body composition and survival after liver transplantation. *Clin Transplant* 2016; **30**: 289-294 [PMID: 26717257 DOI: 10.1111/ctr.12688]

146 **Hamaguchi Y**, Kaido T, Okumura S, Kobayashi A, Shirai H, Yagi S, Kamo N, Okajima H, Uemoto S. Impact of Skeletal Muscle Mass Index, Intramuscular Adipose Tissue Content, and Visceral to Subcutaneous Adipose Tissue Area Ratio on Early Mortality of Living Donor Liver Transplantation. *Transplantation* 2017; **101**: 565-574 [PMID: 27926595 DOI: 10.1097/TP.0000000000001587]

147 **Lazzati A**, Iannelli A, Schneck AS, Nelson AC, Katsahian S, Gugenheim J, Azoulay D. Bariatric surgery and liver transplantation: a systematic review a new frontier for bariatric surgery. *Obes Surg* 2015; **25**: 134-142 [PMID: 25337867 DOI: 10.1007/s11695-014-1430-8]

148 **Mosko JD**, Nguyen GC. Increased perioperative mortality following bariatric surgery among patients with cirrhosis. *Clin Gastroenterol Hepatol* 2011; **9**: 897-901 [PMID: 21782772 DOI: 10.1016/j.cgh.2011.07.007]

149 **Duvoux C**, Roudot-Thoraval F, Decaens T, Pessione F, Badran H, Piardi T, Francoz C, Compagnon P, Vanlemmens C, Dumortier J, Dharancy S, Gugenheim J, Bernard PH, Adam R, Radenne S, Muscari F, Conti F, Hardwigsen J, Pageaux GP, Chazouillères O, Salame E, Hilleret MN, Lebray P, Abergel A, Debette-Gratien M, Kluger MD, Mallat A, Azoulay D, Cherqui D; Liver Transplantation French Study Group. Liver transplantation for hepatocellular carcinoma: a model including α-fetoprotein improves the performance of Milan criteria. *Gastroenterology* 2012; **143**: 986-94.e3; quiz e14-145 [PMID: 22750200 DOI: 10.1053/j.gastro.2012.05.052]

150 **Mazzaferro V**, Sposito C, Zhou J, Pinna AD, De Carlis L, Fan J, Cescon M, Di Sandro S, Yi-Feng H, Lauterio A, Bongini M, Cucchetti A. Metroticket 2.0 Model for Analysis of Competing Risks of Death After Liver Transplantation for Hepatocellular Carcinoma. *Gastroenterology* 2018; **154**: 128-139 [PMID: 28989060 DOI: 10.1053/j.gastro.2017.09.025]

151 **Al-Nowaylati AR**, Al-Haddad BJ, Dorman RB, Alsaied OA, Lake JR, Chinnakotla S, Slusarek BM, Sampson BK, Ikramuddin S, Buchwald H, Leslie DB. Gastric bypass after liver transplantation. *Liver Transpl* 2013; **19**: 1324-1329 [PMID: 24039124 DOI: 10.1002/lt.23734]

152 **Heimbach JK**, Watt KD, Poterucha JJ, Ziller NF, Cecco SD, Charlton MR, Hay JE, Wiesner RH, Sanchez W, Rosen CB, Swain JM. Combined liver transplantation and gastric sleeve resection for patients with medically complicated obesity and end-stage liver disease. *Am J Transplant* 2013; **13**: 363-368 [PMID: 23137119 DOI: 10.1111/j.1600-6143.2012.04318.x]

153 **Prakash G**, Drenick EJ, Wexler H, DeLucia L, Finegold SM. Microbial flora in the bypassed jejunum of patients with biliopancreatic bypass for obesity. *Am J Clin Nutr* 1987; **46**: 273-276 [PMID: 3618530 DOI: 10.1093/ajcn/46.2.273]

154 **D'Albuquerque LA**, Gonzalez AM, Wahle RC, de Oliveira Souza E, Mancero JM, de Oliveira e Silva A. Liver transplantation for subacute hepatocellular failure due to massive steatohepatitis after bariatric surgery. *Liver Transpl* 2008; **14**: 881-885 [PMID: 18508357 DOI: 10.1002/lt.21472]

155 **Rogers CC**, Alloway RR, Alexander JW, Cardi M, Trofe J, Vinks AA. Pharmacokinetics of mycophenolic acid, tacrolimus and sirolimus after gastric bypass surgery in end-stage renal disease and transplant patients: a pilot study. *Clin Transplant* 2008; **22**: 281-291 [PMID: 18482049 DOI: 10.1111/j.1399-0012.2007.00783.x]

156 **Clapp B**, Wynn M, Martyn C, Foster C, O'Dell M, Tyroch A. Long term (7 or more years) outcomes of the sleeve gastrectomy: a meta-analysis. *Surg Obes Relat Dis* 2018; **14**: 741-747 [PMID: 29625744 DOI: 10.1016/j.soard.2018.02.027]

157 **Noel P**, Nedelcu M, Eddbali I, Manos T, Gagner M. What are the long-term results 8 years after sleeve gastrectomy? *Surg Obes Relat Dis* 2017; **13**: 1110-1115 [PMID: 28755888 DOI: 10.1016/j.soard.2017.03.007]

158 **Berger ER**, Clements RH, Morton JM, Huffman KM, Wolfe BM, Nguyen NT, Ko CY, Hutter MM. The Impact of Different Surgical Techniques on Outcomes in Laparoscopic Sleeve Gastrectomies: The First Report from the Metabolic and Bariatric Surgery Accreditation and Quality Improvement Program (MBSAQIP). *Ann Surg* 2016; **264**: 464-473 [PMID: 27433904 DOI: 10.1097/SLA.0000000000001851]

159 **Peterli R**, Wölnerhanssen BK, Vetter D, Nett P, Gass M, Borbély Y, Peters T, Schiesser M, Schultes B, Beglinger C, Drewe J, Bueter M. Laparoscopic Sleeve Gastrectomy Versus Roux-Y-Gastric Bypass for Morbid Obesity-3-Year Outcomes of the Prospective Randomized Swiss Multicenter Bypass Or Sleeve Study (SM-BOSS). *Ann Surg* 2017; **265**: 466-473 [PMID: 28170356 DOI: 10.1097/SLA.0000000000001929]

160 **Schneck AS**, Anty R, Patouraux S, Bonnafous S, Rousseau D, Lebeaupin C, Bailly-Maitre B, Sans A, Tran A, Gugenheim J, Iannelli A, Gual P. Roux-En Y Gastric Bypass Results in Long-Term Remission of Hepatocyte Apoptosis and Hepatic Histological Features of Non-alcoholic Steatohepatitis. *Front Physiol* 2016; **7**: 344 [PMID: 27594839 DOI: 10.3389/fphys.2016.00344]

161 **Geerts A**, Darius T, Chapelle T, Roeyen G, Francque S, Libbrecht L, Nevens F, Pirenne J, Troisi R. The multicenter Belgian survey on liver transplantation for hepatocellular failure after bariatric surgery. *Transplant Proc* 2010; **42**: 4395-4398 [PMID: 21168706 DOI: 10.1016/j.transproceed.2010.07.010]

162 **Sjöström L**. Review of the key results from the Swedish Obese Subjects (SOS) trial - a prospective controlled intervention study of bariatric surgery. *J Intern Med* 2013; **273**: 219-234 [PMID: 23163728 DOI: 10.1111/joim.12012]

163 **Adams TD**, Davidson LE, Litwin SE, Kim J, Kolotkin RL, Nanjee MN, Gutierrez JM, Frogley SJ, Ibele AR, Brinton EA, Hopkins PN, McKinlay R, Simper SC, Hunt SC. Weight and Metabolic Outcomes 12 Years after Gastric Bypass. *N Engl J Med* 2017; **377**: 1143-1155 [PMID: 28930514 DOI: 10.1056/NEJMoa1700459]

164 **Safwan M**, Collins KM, Abouljoud MS, Salgia R. Outcome of liver transplantation in patients with prior bariatric surgery. *Liver Transpl* 2017; **23**: 1415-1421 [PMID: 28752920 DOI: 10.1002/lt.24832]

165 **Shaheen O**, Siejka J, Thatigotla B, Pham DT. A systematic review of portomesenteric vein thrombosis after sleeve gastrectomy. *Surg Obes Relat Dis* 2017; **13**: 1422-1431 [PMID: 28526434 DOI: 10.1016/j.soard.2017.03.015]

P- Reviewer: Giorgio A, Grassi A, Karatapanis S, Manesis EK, McMillin MA, Ocker M, Romanelli RG
S- Editor: Gong ZM **L- Editor**: A **E- Editor**: Yin SY

World Journal of Gastroenterology

Submit a Manuscript: http://www.f6publishing.com

World J Gastroenterol 2018 August 14; 24(30): 3347-3360

DOI: 10.3748/wjg.v24.i30.3347

ISSN 1007-9327 (print) ISSN 2219-2840 (online)

REVIEW

Host genetic factors affecting hepatitis B infection outcomes: Insights from genome-wide association studies

Izzet Mehmet Akcay, Seyma Katrinli, Kamil Ozdil, Gizem Dinler Doganay, Levent Doganay

Izzet Mehmet Akcay, Seyma Katrinli, Gizem Dinler Doganay, Department of Molecular Biology and Genetics, Istanbul Technical University, Istanbul 34469, Turkey

Kamil Ozdil, Levent Doganay, Department of Gastroenterology and Hepatology, Umraniye Teaching and Research Hospital, Istanbul 34764, Turkey

ORCID number: Izzet Mehmet Akcay (0000-0001-6364-0062); Seyma Katrinli (0000-0003-1575-8642); Kamil Ozdil (0000-0003-2556-3064); Gizem Dinler Doganay (0000-0002-3586-1287); Levent Doganay (0000-0002-2263-6689).

Author contributions: Akcay IM and Katrinli S researched the literature and wrote the article; Akcay IM, Katrinli S, Ozdil K, Doganay GD and Doganay L discussed the content; Akcay IM, Katrinli S, Doganay GD and Doganay L reviewed and edited the manuscript before submission; all authors approved the final version of the manuscript to be published.

Conflict-of-interest statement: We declare no potential conflict of interests.

Manuscript source: Unsolicited manuscript

Correspondence to: Levent Doganay, MD, Associate Professor, Doctor, Department of Gastroenterology and Hepatology, Umraniye Teaching and Research Hospital, Umraniye, Istanbul 34764, Turkey.
levent.doganay@saglik.gov.tr
Telephone: +90-216-6321818/1846
Fax: +90-216-6327124

Received: April 9, 2018
Peer-review started: April 10, 2018
First decision: May 16, 2018
Revised: May 29, 2018
Accepted: June 25, 2018
Article in press: June 25, 2018
Published online: August 14, 2018

Abstract

The clinical outcome of Hepatitis B Virus (HBV) infection depends on the success or failure of the immune responses to HBV, and varies widely among individuals, ranging from asymptomatic self-limited infection, inactive carrier state, chronic hepatitis, cirrhosis, hepatocellular carcinoma, to liver failure. Genome-wide association studies (GWAS) identified key genetic factors influencing the pathogenesis of HBV-related traits. In this review, we discuss GWAS for persistence of HBV infection, antibody response to hepatitis B vaccine, and HBV-related advanced liver diseases. HBV persistence is associated with multiple genes with diverse roles in immune mechanisms. The strongest associations are found within the classical human leukocyte antigen (HLA) genes, highlighting the central role of antigen presentation in the immune response to HBV. Associated variants affect both epitope binding specificities and expression levels of HLA molecules. Several other susceptibility genes regulate the magnitude of adaptive immune responses, determining immunity *vs* tolerance. HBV persistence and nonresponse to vaccine share the same risk variants, implying overlapping genetic bases. On the other hand, the risk variants for HBV-related advanced liver diseases are largely different, suggesting different host-virus dynamics in acute *vs* chronic HBV infections. The findings of these GWAS are likely to pave the way for developing more effective preventive and therapeutic interventions by personalizing the management of HBV infection.

Key words: Genome-wide association studies; Hepatitis B infection; Hepatocellular carcinoma; Cirrhosis; Antigen

presentation; Immune response to hepatitis B virus

Core tip: Genome-wide association studies (GWAS) have proven to be very useful in uncovering the host genetic factors that influence the clinical outcomes of hepatitis B virus (HBV) infection. Both class Ⅰ and class Ⅱ human leukocyte antigen (HLA) genes were implicated in persistence of HBV infection; associated variants affected antigen-binding specificities and expression levels of HLA molecules. HBV persistence and vaccine nonresponse were associated with the same HLA-DP allotypes, suggesting a critical role for the surface antigen in HBV pathogenesis. These findings might be exploited for development of potent vaccines based on alternative epitopes. GWAS for HBV-related pathologies identified many other immune-related genes, and provided genetic markers to detect the individuals at high risk for HBV-related diseases.

Akcay IM, Katrinli S, Ozdil K, Dinler Doganay G, Doganay L. Host genetic factors affecting hepatitis B infection outcomes: Insights from genome-wide association studies. *World J Gastroenterol* 2018; 24(30): 3347-3360 Available from: URL: http://www.wjgnet.com/1007-9327/full/v24/i30/3347.htm DOI: http://dx.doi.org/10.3748/wjg.v24.i30.3347

INTRODUCTION

Hepatitis B virus (HBV) is the most common viral pathogen of the human liver, and is a prominent cause of acute and chronic hepatitis, liver failure, cirrhosis and hepatocellular carcinoma (HCC). Around 257 million people, or 3.5% of the global population, are estimated to have chronic HBV infection[1], and more than 800 thousands people lose their life annually due to HBV-related complications[2]. Perinatal and childhood infections are very common in regions with high endemicity, and mostly result in life-long persistence, whereas infections at adulthood are mostly self-limited[3]. Chronic HBV carriers are at a high risk of developing end-stage liver diseases, such as cirrhosis and HCC[4]. Indeed, HBV infection is responsible for 27% of cirrhosis and 53% of HCC cases worldwide[5]. Hepatitis B vaccine effectively prevents new infections, while antiviral medicines suppress progression of HBV-related liver damage. However, vaccination, safe healthcare practices, and access to treatment do not have full population coverage, and HBV infection still remains a major public health problem[6].

HBV is generally considered to be non-cytopathic *per se*; the liver injury associated with HBV infection is immune-driven. The clinical outcome of HBV infection varies greatly among individuals, ranging from asymptomatic self-limited infection, inactive carrier state, chronic hepatitis to end-stage liver diseases with life-threatening complications[3,7-9]. Viral, host and environmental factors affect these outcomes. Viral core/pre-core mutations, certain viral genotypes (*e.g.*, genotype C in comparison to genotype B), high viral load, early-life (perinatal and childhood) infections, male sex, host genetic factors (*e.g.*, HLA class Ⅱ homozygosity), suppressed immune status, co-existing metabolic diseases, and exposure to hepatotoxic substances (*e.g.*, aflatoxin, alcohol) are associated with worse prognosis[7,10]. A complete understanding of these factors is crucial for developing more tailored and effective preventive and therapeutic interventions to reduce the burden of HBV-related complications.

The contribution of host genetic factors to the variation in HBV infection outcomes was most notably evidenced by twin studies[11], which reported higher concordance rates in monozygotic twins than in same-sex dizygotic twins for HBV carrier status[12] and for antibody titers in response to hepatitis B vaccine[13,14]. The host genetic factors were investigated in association studies whereby the frequencies of genetic variants were compared between case and control groups, using candidate gene and whole genome approaches[15-18]. Candidate gene studies focused on polymorphisms in immunologically relevant genes, especially the classical human leukocyte antigen (HLA) genes[19-21]. HLA genes encode the molecules that present antigens to T lymphocytes, and polymorphisms in these genes may alter the specificity and strength of antigen binding, affecting the T cell-mediated immune responses. In accordance with this paradigm, HLA typing studies found an ample amount of HLA allelic variations associated with the clinical outcomes of HBV infection[15]. However, the associations reported in these studies were largely inconsistent, even within the same ethnicity, with few exceptions. The validity of these studies were undermined by inappropriately small sample sizes, lack of replication in an independent cohort, ambiguous allele assignments, genotyping confined to only one or two exons that show the highest genetic variability, low population coverage, and weak statistical evidences[11,15].

The development of high-throughput genotyping technologies (*e.g.*, microarrays) and the construction of a detailed map of common genetic polymorphisms in humans enabled genome-wide investigation of genetic variants for association to complex traits and diseases. In contrast to candidate gene-based studies, genome-wide association studies (GWAS) test hundreds of thousands to millions of common SNPs across the genome, providing an unbiased method to investigate genetic risk loci, and allowing the discovery of novel disease-relevant genes. Several GWAS were conducted to identify the risk loci that predisposes to persistence of HBV infection, non-response to hepatitis B vaccine, and progression of liver disease in chronic HBV infections. In this review, we discuss the findings of these GWAS, and we emphasize how GWAS has driven the research on the genetic basis of variability in HBV-related pathologies.

GWAS FOR HBV INFECTION PERSISTENCE

The first GWAS to identify the genetic risk factors for

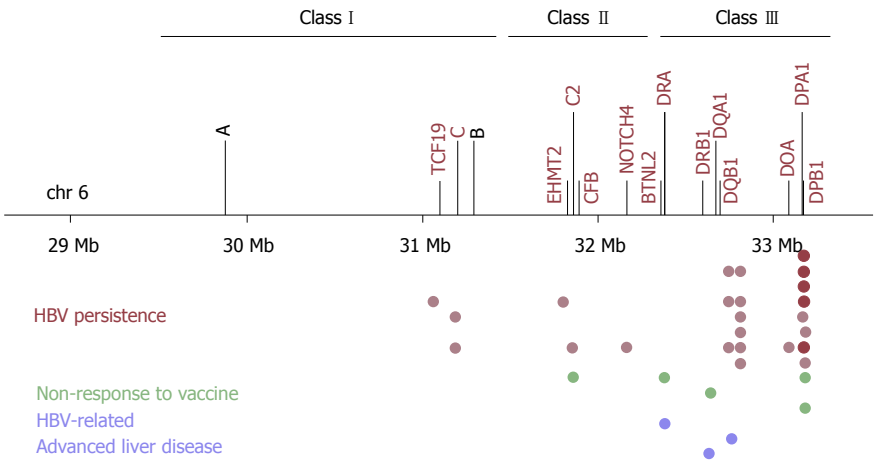

Figure 1 Associations within the human leukocyte antigen locus identified by genome-wide association studies for hepatitis B virus-related traits. GWAS hits for HBV-related pathologies are concentrated on the HLA region. Top SNPs in each GWAS are demonstrated in rows in the chronological order of publication; red for HBV persistence, green for Hepatitis B vaccine non-response, and blue for advanced HBV-related liver diseases. The nearest genes for the identified SNPs are colored in red; *HLA-A* and *HLA-B* are also marked. GWAS: Genome-wide association studies; HLA: Human leukocyte antigen; HBV: Hepatitis B virus; SNPs: Single nucleotide polymorphisms.

susceptibility to HBV infection persistence was performed in a Japanese population, and published in 2009[22]. Seven hundred and eighty-six chronic hepatitis B (CHB) cases and 2201 HBsAg seronegative controls were used in the discovery phase. This GWAS detected significantly associated SNPs within the *HLA-DP* locus. rs3077 in *HLA-DPA1* 3'UTR and rs9277535 in *HLA-DPB1* 3'UTR were selected, and further replicated in independent Japanese and Thai samples[22]. The same group employed a second GWAS using additional Japanese case-control samples where they confirmed the associations of *HLA-DP* variants, and, additionally, detected significant associations around the *HLA-DQ* locus[23]. The *HLA-DQ* SNPs, rs2856718 and rs7453920, were not in LD with the *HLA-DP* SNPs, and their associations remained significant after adjusting for the effect of rs9277535. These findings revealed that *HLA-DP* and *HLA-DQ* variants were independently associated with chronic HBV infection. rs2856718 tagged an LD block comprising *HLA-DQA1* and *HLA-DQB1*, which produce the functional HLA-DQ molecules. rs7453920 was located in *HLA-DQB2*, which, along with *HLA-DQA2*, is thought to be nonfunctional. The association of rs7453920 with functional *HLA-DQ* alleles was shown later[24].

Additional GWAS for HBV persistence were performed in Japanese[25], Korean[26], Han Taiwanese[27], and Han Chinese populations[28-30] (Table 1, Figure 1). These GWAS repeatedly mapped the strongest signals within the *HLA-DP* and/or *HLA-DQ* loci, replicating the associations of rs3077, rs9277535, rs7453920 and rs2856718. Furthermore, independent studies genotyping the same SNPs validated these associations with high consistency in diverse Asian populations, including Chinese[31-39], Japanese[40], Thai[41], Indonesians[42], Tibetans and Uygurs (Asian-Caucasian mix)[43]. A meta-analysis of 62050 subjects from 29 case-control studies, mostly from Asian populations, further validated the associations of rs3077 and rs9277535[44]. Replication studies were also conducted in non-Asian populations, including Caucasians in Germany[45], European Americans, African Americans[46], Saudi Arabians population[47], and multiethnic Argentine populations (Native American-European Caucasian mix)[48]. With few exceptions and inconsistencies, probably due to different allele frequencies and LD structures in these populations, the associations of *HLA-DP* (rs3077 and rs9277535) and *HLA-DQ* (rs7453920 and rs2856718) SNPs were validated in these populations, too.

Most of the subsequent GWAS also revealed additional susceptibility loci for HBV persistence. To begin with, a GWAS in Korean chronic HBV carriers and non-infected healthy individuals identified two novel loci within the HLA region[26]. These two loci, marked by rs652888 in *EHMT2* and rs1419881 in *TCF19*, had independent effects on HBV persistence. EHMT2 is a histone lysine methyltransferase involved in gene expression regulation, and plays roles in immune cell development and differentiation[49]. TCF19 is a transcription factor necessary for cell survival and proliferation[50]. A previous GWAS associated a non-synonymous SNP in *TCF19* with blood cell counts, including lymphocyte and monocyte (macrophage precursor) cell counts[51], suggesting a potential mechanism by which *TCF19* variants affected immune mechanisms. However, the associations of rs652888 (*EHMT2*) and rs1419881 (*TCF19*) were not replicated in Chinese and Thai populations, probably due to different genetic structures[24,30,41]. Additional replication studies are, therefore, necessary for both loci.

Another GWAS in Han Chinese used chronic HBV carriers as cases and individuals who naturally cleared HBV infection as controls, and revealed two additional loci[28]. The first locus was marked by the lead SNP rs3130542, located near *HLA-C* within the HLA region. Conditional analysis showed that the effect of rs3130542 was independent of *HLA-DP* and *HLA-DQ* variants. Therefore, both class Ⅰ and class Ⅱ variants were detected by GWAS for HBV persistence. The second

Table 1 Results of genome-wide association studies for persistence of hepatitis B virus infection

Ref.	Study population	SNP ID	Minor/major alleles	Risk allele	*P*	OR	Location	Nearest gene	Functional class
Kamatani *et al*[22]	Japanese, Thai (n = 6387)[1]	rs3077	A/G	G	2.31×10^{-38}	0.56	6p21.32	*HLA-DPA1*	3'UTR
		rs9277535	A/G	G	6.34×10^{-39}	0.57	6p21.32	*HLA-DPB1*	3'UTR
Mbarek *et al*[23]	Japanese (n = 9163)[1]	rs3077	A/G	G	1.57×10^{-61}	1.87	6p21.32	*HLA-DPA1*	3'UTR
		rs9277535	A/G	G	2.55×10^{-54}	1.77	6p21.32	*HLA-DPB1*	3'UTR
		rs2856718	A/G	A	3.99×10^{-37}	1.56	6p21.32	*HLA-DQB1, HLA-DQA2*	Intergenic
		rs7453920	A/G	G	5.98×10^{-28}	1.81	6p21.32	*HLA-DQB2*	Intron
Nishida *et al*[25]	Japanese (n = 1793)[2]	rs3077	A/G	G	4.40×10^{-19}	0.46	6p21.32	*HLA-DPA1*	3'UTR
		rs9277542	A/G	G	1.28×10^{-15}	0.5	6p21.32	*HLA-DPB1*	Exon
Kim *et al*[26]	Korean (n = 4309)[2]	rs3077	A/G	G	3.74×10^{-40}	0.53	6p21.32	*HLA-DPA1*	3'UTR
		rs9277535	A/G	G	5.25×10^{-39}	0.53	6p21.32	*HLA-DPB1*	3'UTR
		rs2856718	A/G	A	1.78×10^{-24}	1.6	6p21.32	*HLA-DQB1, HLA-DQA2*	Intergenic
		rs7453920	A/G	G	6.71×10^{-26}	0.5	6p21.32	*HLA-DQB2*	Intron
		rs652888	G/A	G	7.07×10^{-13}	1.38	6p21.33	*EHMT2*	Intron
		rs1419881	G/A	A	1.26×10^{-18}	0.73	6p21.33	*TCF19*	3'UTR
Hu *et al*[28]	Chinese (n = 11791)[3]	rs7453920	A/G	G	4.93×10^{-37}	0.53	6p21.32	*HLA-DQB2*	Intron
		rs3130542	A/G	A	9.49×10^{-14}	1.33	6p21.33	*HLA-C*	Intergenic
		rs4821116	A/G	G	1.71×10^{-12}	0.82	22q11.21	*UBE2L3*	Intron
		rs3077	A/G	G	6.50×10^{-14}	0.75	6p21.32	*HLA-DPA1*	3'UTR
Chang *et al*[27]	Han Taiwanese (n = 2688)[2]	rs9277535	A/G	G	4.87×10^{-14}	1.59	6p21.32	*HLA-DPB1*	3'UTR
		rs7453920	A/G	G	6.66×10^{-15}	2.31	6p21.32	*HLA-DQB2*	Intron
Jiang *et al*[29]	Chinese (n = 18371)[1]	rs12614	T/C	C	1.28×10^{-34}	1.89	6p21.33	*CFB*	Exon
		rs422951	G/A	A	5.33×10^{-16}	1.27	6p21.32	*NOTCH4*	Exon
		rs378352	T/C	T	1.04×10^{-23}	1.26	6p21.32	*HLA-DOA*	Exon
		rs2853953	A/G	G	5.06×10^{-20}	1.47	6p21.33	*HLA-C*	Intergenic
		rs1883832	T/C	T	2.95×10^{-15}	1.19	20q13.12	*CD40*	5'UTR
		rs2856718	G/A	A	7.35×10^{-28}	1.28	6p21.32	*HLA-DQB1, HLA-DQA2*	Intergenic
		rs7453920	A/G	G	1.28×10^{-60}	2	6p21.32	*HLA-DQB2*	Intron
		rs9277535	A/G	G	9.84×10^{-71}	1.52	6p21.32	*HLA-DPB1*	3'UTR
		rs3077	A/G	G	1.15×10^{-53}	1.45	6p21.32	*HLA-DPA1*	3'UTR
Li *et al*[30]	Chinese (n = 9569)[3]	rs7000921	C/T	T	3.20×10^{-12}	0.78	8p21.3	*INTS10*	Intergenic
		rs7453920	A/G	G			6p21.32	*HLA-DQB2*	Intron
		rs9277535	A/G	G			6p21.32	*HLA-DPB1*	3'UTR

Participant phenotypes: [1]CHB *vs* Non-infected; [2]Chronic HBV carriers *vs* Non-infected; [3]Chronic HBV carriers *vs* Spontaneously recovered. OR: Odds ratio.

locus was marked by the lead SNP rs4821116, located in *UBE2L3* on chromosome 22. *UBE2L3* encodes an ubiquitin-conjugating enzyme, which enhances NFκB activation upon CD40 stimulation in B cells and TNF stimulation in monocytes[52]. The protective variant of rs4821116 was associated with higher *UBE2L3* mRNA levels in peripheral blood monocytes[53]. Moreover, *UBE2L3* was implicated in multiple autoimmune diseases; the risk variants correlated with higher *UBE2L3* expression in B cells and monocytes, enhanced NFκB activation, enhanced B cell proliferation and activation[52]. Thus, hyperactivity of UBE2L3-related immune mechanisms conferred protection from infections on the one hand, but predisposed to autoimmunity on the other hand.

The GWAS with the largest sample size (2514 chronic HBV carriers and 1130 healthy controls of Chinese ethnicity in the discovery phase) was published in 2015, revealing five new SNPs independently associated with HBV persistence[29]. Four of these SNPs, rs12614 in *CFB*, rs422951 in *NOTCH4*, rs2853953 near *HLA-C*, and rs378352 in *HLA-DO* were located within the HLA region, whereas the other SNP, rs1883832, was located in *CD40* on chromosome 20. rs12614_T/C in *CFB* represents a non-synonymous amino acid polymorphism (R32W) in complement factor B. The complement system is part of the innate immune response against viral infections, and is also involved in enhancing adaptive immune responses[54]. Chronic HBV carriers and individuals with the risk genotype CC for rs12614 had significantly lower plasma CFB protein levels[29]. rs422951 in *NOTCH4* also causes a non-synonymous amino acid change (T320A). Notch signaling regulates immune cell development and T-cell mediated immune responses[55]. rs2853953 tagged *HLA-C* gene; however it was not in LD with the previously reported *HLA-C* tagging SNP rs3130542. Indeed, these two SNPs marked different *HLA-C* alleles; rs2853953 marked *HLA-C*06:02*, whereas rs3130542 marked *HLA-C*07:02*. rs378352 is located in exon 4 of *HLA-DOA*, causing a synonymous codon change. *HLA-DOA* encodes the α chain of the HLA-DO molecule, which, along with HLA-DM, regulates peptide loading to class Ⅱ molecules. Whether or how this polymorphism affects HLA-DO function is currently unknown. Lastly, rs1883832_T/C is located in the Kozak sequence of

Table 2 Human leukocyte antigen classical alleles associated with hepatitis B virus persistence in more than one study

HLA gene	Associated alleles	Effect on HBV persistence	Study population	Ref.
HLA-C	*07:02	Protective	Chinese	[24,28,29]
HLA-DPA1	*01:03	Protective	Japanese, Korean, Chinese, Thai	[22,24,58]
	*02:02	Susceptible	Japanese, Korean, Chinese	[22,24,58]
HLA-DPB1	*04:01	Protective	Japanese, Chinese	[22,28,58]
	*04:02	Protective	Japanese, Korean	[22,58]
	*02:01	Protective	Chinese, Japanese	[28,58]
	*05:01	Susceptible	Japanese, Korean, Chinese	[22,24,58,59]
	*09:01	Susceptible	Japanese, Chinese	[22,24,58,59]
HLA-DQA1	*06:01	Susceptible	Chinese	[24,28,30]
HLA-DQB1	*03:02	Protective	Japanese, Chinese	[24,28,30,59]
	*03:01	Susceptible	African American, Chinese	[18,28,30]
	*06:01	Susceptible	Japanese	[23,59]
HLA-DRB1	*13:02	Protective	Japanese, Chinese, Gambian, Korean, Germany, European Americans	[24,59,68]

CD40, and was previously shown to affect its translational efficiency[56]. The risk genotype TT for rs1883832 correlated with lower CD40 levels in the serum in both cases and controls[29]. CD40 is a co-stimulatory receptor protein found on antigen-presenting cells. Its engagement with CD40 ligand (CD40L) on T cells initiates and promotes humoral and cellular adaptive immune responses[57]. Intriguingly, rs1883832_T was previously associated with protection against multiple autoimmune diseases[56]. Thus, CD40 plays an important role in regulating the magnitude of immune responses, and determining immunity *vs* tolerance. So far, the associations of rs12614 (*CFB*) and rs1883832 (*CD40*) were validated by independent studies in Han Chinese[24,30]. Additional validation and functional studies are required to establish the roles of other genes and genetic variants in HBV persistence.

The most recent GWAS identified another novel locus (tagged by rs7000921) on chromosome 8 using persistently infected cases and spontaneously recovered controls in a Chinese population[30]. rs7000921 was an eQTL for the nearby *INTS10* gene; the protective allele was associated with elevated *INTS10* expression in liver. *INTS10* encodes a subunit of the Integrator complex, which has multiple roles in transcriptional regulation. Subsequent analysis showed that INTS10 was involved in suppressing HBV replication in hepatocyte cell lines, likely through an interferon-dependent mechanism[30].

To sum up, GWAS for HBV infection persistence revealed many candidate genes with diverse functions in immune responses, improving our understanding of the molecular mechanisms leading to the success or failure of HBV clearance.

CLASSICAL HLA GENE VARIANTS AT THE INTERFACE OF HBV CLEARANCE AND PERSISTENCE

GWAS association signals within the *HLA-DP*, *HLA-DQ* and *HLA-C* loci implicated variable efficiencies in presenting immunodominant HBV epitopes to T cells. Thus, in the next step after GWAS, the respective HLA genes were typed by direct sequencing or imputation (on the basis of typed SNPs from the study populations and haplotypes from the genetic reference populations), and classical HLA alleles with significant effects on HBV persistence were determined (Table 2). *HLA-DP* susceptible alleles (*DPA1*02:02*; *DPB1*05:01*, **09:01*) and protective alleles (*DPA1*01:03*; *DPB1*02:01*, **04:01*, **04:02*) were identified with a high degree of consistency in multiple Japanese, Korean and Chinese populations[22,24,28,30,58,59]. Moreover, *DPB1*01:01* and *DPB1*04:01* were identified as the most susceptible and the most protective *DPB1* allele, respectively, in European Americans and African Americans[46]. Alleles with consistent effects in more than one population were also found for *HLA-DQ* and *HLA-C* genes; *DQB1*03:02* was revealed as a protective allele[24,28,30,59], whereas *DQA1*06:01*, *DQB1*03:01*, *DQB1*06:01*, and *HLA-C*07:02* were revealed as susceptible alleles[23,24,28-30,59]. Systematic epitope discovery studies are warranted to identify the HBV-derived peptides efficiently presented by protective allotypes, but not by susceptible allotypes. The results of such studies might form the basis for epitope-specific therapeutic interventions.

A major distinction between *DPB1* protective alleles (**02:01*, **04:01*, **04:02*) and *DPB1* susceptible alleles (**01:01*, **05:01*, **09:01*) was in their amino acid residues at positions 84-87. Protective alleles encoded Gly/Gly/Pro/Met (GGPM), while susceptible alleles encoded Asn/Glu/Ala/Val (DEAV) at 84-87. These residues corresponded to the pocket-1 of the antigen-binding groove, an anchor region that determines the binding specificity of DP molecules[60,61]. Epitope binding studies revealed that DP molecules with 84GGPM87 strongly bound aromatic and hydrophobic residues in their hydrophobic pocket-1, whereas DP molecules with 84DEAV87 also preferred positively charged residues, owing to the acidic residues at 84 and 85[61,62]. These distinct binding motifs of DP allotypes likely form the basis of HBV chronicity as multiple risk-associated DP allotypes ineffectively present a common epitope motif

and lead to the failure of viral elimination. The identities of HBV peptides with this motif and their immunogenic properties remain to be determined by further functional assays.

It should be noted that the contribution of HLA-DP allotypes to HBV chronicity might also involve previously unprecedented mechanisms. It was recently shown that Gly-84 residue in DP molecules prevents the binding of the invariant chain *via* its CLIP region on the antigen-binding groove[63]. CLIP binding is necessary to block endogenous peptide binding to class Ⅱ molecules till they reach the MIIC compartment where exogenous peptide loading takes place. Therefore, DP^{84Gly} molecules are able to present both intracellular and extracellular peptides[63]. Whether or how this contributes to immunity against HBV needs to be examined in functional studies.

The HLA locus is characterized by high gene density, high genetic diversity and extensive LD structure, limiting the ability to pinpoint the causal variants[64]. Some class Ⅱ associations might not reflect primary effects given the strong LD between *DQ* and *DR* loci, and the weak LD between *DQ*-*DR* and *DP* loci. Hence, uncovering the LD patterns between the *DP*, *DQ* and *DR* alleles in the study population, rather than examining the alleles at a single locus, would help detecting the alleles with primary effects[59]. Fine mapping studies in which associated loci are interrogated with many more variants than in GWAS prove to be useful in pinpointing the causal variants and revealing potential mechanisms. An interrogation of the entire HLA locus with 5375 variants, including 4356 SNPs, 849 amino acid polymorphisms and 170 classical alleles, in 1888 Chinese case-control individuals (from a previous HBV-persistence GWAS[28]) identified four independently associated loci by stepwise conditional analysis[24]. HLA-DPβ1 amino acid polymorphisms at positions 84-87 were the strongest association, whereas HLA-C Leu-15 was the second strongest association, conferring the effect of *HLA-C*07:02*. The two other associated loci were novel; *HLA-DRB*13* allele and rs400488. *HLA-DRB*13* was associated with protection against HBV chronicity, and was in partial LD with the *CFB*-tagging SNP rs12614. *HLA-DRB*13* allele is distinct from other *DRB1* alleles by the presence of Glu-71 in pocket-4, an anchor region for epitope binding of DR molecules, implying a specific binding motif. Remarkably, *HLA-DRB*13* was one of the few classical HLA alleles identified in the pre-GWAS era with highly reproducible associations across different ethnicities[65-68]. On the other hand, the biological relevance of rs400488, an eQTL for the pseudogene *HLA-J*, is currently unknown[24].

The effects of associated SNPs on HLA gene expression were also investigated. An eQTL analysis showed that the risk alleles of rs3077 and rs9277535 were associated with lower *HLA-DPA1* and *HLA-DPB1* mRNA levels, respectively, in normal liver tissues[69]. Furthermore, allelic expression imbalance assays for both SNPs confirmed that the risk alleles were expressed less abundantly than the protective alleles in liver and blood monocyte samples from heterozygous individuals[69]. Two separate genome-wide gene expression association studies previously found similar trends for the *HLA-DQ* SNP rs7453920 and the *HLA-C* SNP rs3130542. The risk variant of rs7453920 was associated with lower *HLA-DQ* mRNA levels in peripheral blood monocytes[53], while the risk variant of rs3130542 was associated with lower *HLA-C* mRNA in lymphoblastoid cell lines derived from European subjects[70]. Moreover, the susceptible *HLA-C*07:02* allele, tagged by rs3130542, have an intact mir-148a binding site, and a low expression due to RNA interference[71]. These results suggested that reduced expression of HLA-DP and HLA-DQ molecules in antigen-presenting cells, and reduced expression of HLA-C molecule in hepatocytes might result in ineffective antigen presentation to T cells, leading to inability to clear HBV infection, and thus, HBV persistence. However, a discrepant result was noted for rs9277534_A/G, the most significant *HLA-DPB1* SNP in European Americans and African Americans[46]. The risk allele rs9277534_G correlated with higher HLA-DPB1 surface protein levels in lymphoid cell lines and higher *HLA-DPB1* mRNA levels in B lymphocytes isolated from healthy donors. This conflicting result can be reconciled with the previous findings by taking into account that rs9277534_G was also in strong LD with the most susceptible *HLA-DPB1* allele (**01:01*) in these populations. Thus, the risk-conferring effect of *HLA-DPB1*01:01* probably prevailed over the protective effect of its increased expression.

To sum up, polymorphisms marking the classical HLA genes influence immune responses by altering the antigen-binding properties of HLA molecules and the expression levels thereof. The relative contributions of these effects to susceptibility to HBV persistence vary among populations depending on the allele frequencies of variants and LD relationships among them.

GWAS FOR IMMUNE RESPONSE TO HEPATITIS B VACCINE

The standard 3 doses of hepatitis B vaccine (based on recombinant HBs antigen) have been implemented as part of the routine infantile vaccination program in more than 160 countries, as a result of which substantial declines in the prevalence of chronic HBV carriers and in the incidence of childhood HBV-related liver diseases have been observed[6,72]. However, there is a large natural variation in the antibody response to hepatitis B vaccine. Post-vaccination antibody titers range from undetectable levels to higher than 2000 mIU/mL[73]. Anti-HBs titers above 100 mIU/mL are referred to as successful vaccination, whereas anti-HBs titers below 10 mIU/mL as non-protective. Individuals that mount an antibody response below this threshold, *i.e.*, non-responders, are at a high risk of HBV infection. Booster vaccination can trigger an antibody response at protective levels in a subset of non-responders[74].

Three GWAS were implemented to date to identify the genetic factors that underlie the variation in the

Table 3 Results of genome-wide association studies for non-response to hepatitis B vaccine

Ref.	Study population	SNP ID	Minor/major alleles	Risk allele	*P*	OR	Location	Nearest gene	Functional class
Png *et al*[73]	Indonesian (n = 3614)[1]	rs3135363	C/T	C	6.53×10^{-22}	1.53	6p21.32	*BTNL2, HLA-DRA*	Intergenic
		rs9277535	A/G	G	2.91×10^{-12}	0.72	6p21.32	*HLA-DPB1*	3'UTR
		rs9267665	T/C	T	1.24×10^{-17}	2.05	6p21.33	*STK19*	Intron
Pan *et al*[76]	Chinese (n = 1944)[2]	rs477515	T/C	T	2.63×10^{-19}	2.05	6p21.32	*HLA-DRB1*	Intergenic
Wu *et al*[81]	Taiwanese (n = 285)[3]	rs7770370	A/G	G	1.20×10^{-08}	0.33	6p21.32	*HLA-DPB1*	Intergenic

Participant phenotypes: [1]Low, intermediate and high responders to primary vaccine (ordinal groups); [2]High responders to primary vaccine *vs* non-responders to booster vaccine; [3]Non-responders *vs* responders to booster vaccine.

immune response to hepatitis B vaccine (Figure 1, Table 3). The first GWAS was conducted in Indonesians by grouping vaccine recipients into three classes (*i.e.*, low, intermediate and high) on the basis of their post-vaccination antibody titers[73]. Stepwise conditional analysis revealed three independently associated haplotype blocks within the HLA region. The first haplotype block, tagged by rs3135363, encompassed *HLA-DRA* and *BTNL2*. *HLA-DRA* encodes the sole α chain for HLA-DR molecules, and *BTNL2* encodes a transmembrane protein involved in the negative regulation of T cell activation. *BTNL2* was previously associated with autoimmune diseases[75]. The second haplotype block, tagged by rs9277535, encompassed *HLA-DPA1* and *HLA-DPB1* genes, suggesting that *HLA-DP* variants contribute to both HBV persistence and non-response to vaccine. A shared genetic basis for these traits is conceivable given that anti-HBs antibody production is a marker for both successful immune response to vaccine and clearance of HBV infection[3]. Lastly, the third haplotype block, tagged by rs9267665, was located within the class Ⅲ region, consisting of many genes found in strong LD. Therefore, further research is needed to pinpoint the causal genes[73].

The second GWAS for vaccine nonresponse used Chinese adults with marginal phenotypes: non-responders (< 10 mIU/mL) after booster vaccination *vs* high-responders (> 1000 mIU/mL) after primary vaccination[76]. The strongest associations (led by rs477515) were detected within the *HLA-DR* locus, and *HLA-DRB1*07:01* was significantly associated with nonresponse to hepatitis B vaccination[76]. Numerous studies previously associated *DRB1*07:01* with both vaccine non-response and persistent HBV infection in multiple ethnic populations[77-79]. Furthermore, *DRB1*07* was also associated with decreased risk of HBV-related cirrhosis in a Turkish population[80], implicating a *DRB1*07*-associated hypo-immune profile against HBV.

The third GWAS used subjects with detectable and undetectable (> or < 1 mIU/mL, respectively) post-booster antibody titers from a cohort of booster vaccine recipient Taiwanese adolescents who had not responded to primary vaccination as infants[81]. Significant associations were mapped to the *HLA-DP* locus. The lead SNP rs7770370 was in strong LD with rs9277535. *HLA-DPB1* alleles **02:01*, **02:02*, **03:01*, **04:01* and **14:01* (encoding 84GGPM87) were associated with vaccine response, whereas **05:01* and **09:01* (encoding 84DEAV87) were associated with vaccine nonresponse[74,81]. These associations were further confirmed in a Japanese population[82]. Hence, *HLA-DPB1* alleles influenced the outcome of vaccine response in the same manner as of HBV persistence, corroborating further that the ability to present the same HBs epitopes is critical in both traits. In line with this, *HLA-DP* SNPs (*e.g.*, rs7770370, rs9277535 and rs3077) were also associated with vaccine nonresponse in independent replication studies in Korean infants[83] and Japanese medical students[84]; and vaccine nonresponse-associated rs477515 (*HLA-DRB1*) also correlated with HBV persistence in a Chinese population[30]. However, *HLA-DQ* SNPs (rs2856718 and rs7453920) were not associated with vaccine responsiveness[84]. Therefore, the genetic bases of HBV persistence and nonresponse to hepatitis B vaccine overlap considerably, but not completely.

GWAS FOR HBV-RELATED ADVANCED LIVER DISEASES

Host genetic variation underlying the clinical heterogeneity of chronic HBV infections has been the topic of GWAS, too (Figure 1, Table 4). A GWAS used 648 HBV-infected Saudi Arabian subjects, comprising 343 inactive carriers, 249 patients with CHB, and 76 patients with end-stage liver diseases (*i.e.*, cirrhosis and HCC), to study liver disease progression in chronic HBV infection[85]. The strongest association, rs2724432, was obtained using cases with end-stage liver diseases and controls with inactive HBV infection. rs2724432 was located upstream of *FDX1*, the product of which is involved in electron transfer from NADH to cytochrome P450. FDX1 plays a role in steroid and vitamin D synthesis in the adrenals, and bile acid synthesis in the liver[85]. Further functional assays are necessary to confirm the association of rs2724432 and the underlying molecular mechanisms. Some of the GWAS for HBV persistence contained in their case groups chronic HBV carriers with and without

Table 4 Results of genome-wide association studies for hepatitis B virus-related advanced liver diseases

Ref.	Study population	Participant phenotypes	SNP ID	Minor/ major alleles	Risk allele	*P*	OR	Location	Nearest gene	Functional class
Al-Qahtani *et al*[85]	Saudi Arabian (n = 693)	LC/HCC *vs* Inactive[1]	rs2724432	T/C	T	4.29×10^{-08}	3.01	11q22.3	*FDX1*	Intergenic
Zhang *et al*[88]	Chinese (n = 4107)	HCC *vs* Non-HCC[2]	rs17401966	G/A	A	3.40×10^{-19}	0.62	1p36.22	*KIF1B*	Intron
Chan *et al*[91]	Chinese (n = 1420)	HCC *vs* Non-HCC[2]	rs12682266	A/G	G	3.76×10^{-05}	1.38	8p12	Expressed sequenced tag	Intergenic
Li *et al*[89]	Chinese (n = 12159)	HCC *vs* Non-HCC[2]	rs9272105	A/G	A	5.24×10^{-22}	1.28	6p21.32	*HLA-DQA1, HLA-DRB1*	Intergenic
			rs455804	A/C	C	5.24×10^{-10}	0.84	21q21.3	*GRIK1*	Intron
Jiang *et al*[90]	Chinese (n = 11799)	HCC *vs* Non-HCC[2]	rs7574865	T/G	G	2.48×10^{-10}	1.21	2q32.2-2q32.3	*STAT4*	Intron
			rs9275319	G/A	A	2.72×10^{-17}	1.49	6p21.32	*HLA-DQB1, HLA-DQA2*	Intergenic
Tan *et al*[86]	Chinese (n = 3387)	ACLF *vs* Inactive[3]	rs3129859	C/G	C	2.64×10^{-20}	1.83	6p21.32	*HLA-DQB1, HLA-DRA*	Intergenic

[1]HBV carriers with LC or HCC *vs* inactive chronic carriers; [2]Chronic HBV carriers with HCC *vs* chronic HBV carriers without HCC; [3]Acute-on-chronic liver failure *vs* inactive chronic HBV carriers. LC: Liver cirrhosis; HCC: Hepatocellular carcinoma; HBV: Hepatitis B virus.

end-stage liver diseases. At least one GWAS employed a secondary genome-wide analysis using these subgroups[25]; however, failed to identify any significant association, possibly due to small sample size.

A GWAS in Han Chinese investigated the risk loci for acute-on-chronic liver failure (ACLF) in chronic HBV carriers, a life-threatening condition that develops as a result of sudden acute exacerbation of chronic infection[86]. rs3129859 within the *HLA-DR* locus was associated with HBV-related ACLF. Subsequent in silico genotyping of *HLA* alleles and conditional association analysis showed that the effect of rs3129859 was dependent on the *HLA-DRB1*12:02* allele[86]. Concordant with this finding, *HLA-DRB1*12* was previously associated with the development of HBV-related cirrhosis and HCC in Han Chinese[87].

To find the genetic risk loci for HBV-related HCC, several GWAS were implemented using HBV carriers with HCC as cases and HCC-free HBV carriers as controls[88-92] (Table 4). All of these GWAS used Chinese cohorts, exploiting the facts that more than half of HCC cases were found in China, and 80% of HCC incidences were attributable to HBV[93]. The first GWAS identified rs17401966, located in *KIF1B* on chromosome 1[88]. *KIF1B* encodes a kinesin protein involved in organelle and vesicle transport, and is a putative tumor suppressor[94]. The protective variant of rs17401966 significantly correlated with higher KIF1B protein levels in tumor-adjacent tissues, but not in HCC tissues[88]. The haplotype block tagged by rs17401966 also encompassed the entire *PGD* gene and the 3' end of *UBE4B* gene. The products of these genes are involved in pentose phosphate metabolism and multiubiquitin chain assembly, respectively. Additional studies are necessary to identify the causal gene in this locus. Another GWAS identified rs9272105 within the HLA region and rs455804 on chromosome 21[89]. rs9272105 was located in the intergenic region between *HLA-DQA1* and *HLA-DRB1*. *HLA-DRB1* alleles **04:05* and **09:01* only partially accounted for the association of rs9272105, implying additional risk variants in LD with this SNP. rs455804 was located in intron 1 of *GRIK1*, which encodes an ionotropic glutamate receptor, suggesting involvement of glutamate signaling in hepatocarcinogenesis. Two additional risk loci were revealed in another GWAS: rs7574865 and rs9275319[90]. rs7574865 tagged *STAT4* on chromosome 2. STAT4 is a transcription factor with important roles in the regulation of antiviral immune responses; it induces IFN-γ production in response to stimulation by interleukin-12 and type Ⅰ interferons (IFN-α and IFN-β)[95]. HCC risk-associated variant of rs7574865 correlated with lower *STAT4* mRNA expression in both HCC and non-tumor tissues[90]. rs9275319 tagged *HLA-DQB1* and *HLA-DQA2*, and its effect on HCC risk was only partially accounted for by *DQB1*04:01* and *DQA1*03:03* alleles, indicating other risk variants in the associated locus.

SNPs identified in GWAS for HBV-related HCC were further investigated in replication studies. Intriguingly, no evidence was found for the association of rs17401966 (*KIF1B*) with HCC risk in chronic HBV carriers in subsequent GWAS and other replication studies in Chinese[36,96], Japanese[97], Korean[97], and Thai populations[98]. Moreover, rs17401966 was also not associated with HBV infection persistence in Chinese[99], Japanese[23] and Saudi Arabian populations[100]. Comparable allele frequencies were detected between different subgroups of chronic carriers (namely, inactive carriers, active carriers, cirrhosis and HCC) in Saudi Arabian and Chinese populations[100,101]. These results indicated that rs17401966 was a risk factor neither for HBV infection persistence nor for advancement of liver disease.

Replication studies for rs7574865 (*STAT4*) produced inconsistent results. The association of rs7574865 with HBV-related HCC was validated in Vietnamese[102] and Korean[103] populations, but not in two separate Chinese populations[38,96]. The effect of rs7574865_T/G on susceptibility to persistent HBV infection was also examined. HCC risk allele rs7574865_G was significantly associated with chronic HBV infection in Koreans[103] and Chinese[104]. However, this association was not reproduced in another Chinese population[38]. Lastly, rs7574865_G was also significantly associated with the risk of HBV-related cirrhosis in a Chinese population[101]. Overall, these results supported a role for *STAT4* polymorphisms in HBV infection outcomes in a population specific manner.

The associations of the two HBV-related HCC risk SNPs within the *HLA-DQ/DR* locus (rs9275319 and rs9272105) were validated by an independent replication study in Chinese subjects[105], whereas two separate studies in Koreans[103] and in Chinese[106] failed to replicate the association of rs9275319. rs9275319 was also associated with susceptibility to HBV persistence in the original GWAS[90], and in other replication studies performed in Korean[103] and Chinese populations[30,106]. Moreover, rs9275319 was associated with increased risk of cirrhosis in Chinese HBV carriers[101]. Therefore, it might be speculated that rs9275319 was associated with an ineffective immune profile against HBV that is too weak to clear HBV infection, yet strong enough to maintain a state of basal liver necroinflammation leading to advanced liver diseases. On the other hand, the effect of rs9272105 on HBV persistence is not yet clear. HCC risk-associated variant of rs9272105 conferred susceptibility to chronic HBV infection in one Chinese population[30], and protection against chronic HBV infection in another Chinese population[89]. These conflicting results indicated that rs9272105 did not have a primary effect on HBV persistence.

To fully explore whether the genetic bases of HBV persistence and HBV-related liver diseases overlap, SNPs identified in GWAS for HBV persistence were also examined for possible effects on the development of advanced liver diseases. Most studies showed that *HLA-DP* variants (rs3077 and rs9277535) were associated neither with progression from inactive carrier state to disease-active states[35,37,39,45], nor with development of end-stage liver diseases[31,35,38,39,47]. Similar results were found for *HLA-DQ* variants (rs2856718 and rs7453920) regarding the development of end-stage liver diseases[38,39,47]. Only few studies reported significant associations of these SNPs with HBV-related HCC risk[36,89,107]. A meta-analysis with 4864 HBV-positive HCC cases and 29790 HBV-infected controls also failed to associate rs3077 and rs9277535 with HCC risk[44]. Lastly, none of the 13 HBV persistence risk SNPs that were identified hitherto in GWAS were found to be associated with HBV-related HCC in a population of 1161 cases and 1353 controls[29]. Therefore, SNPs that were associated with HBV persistence/clearance had minimal, if any, effects on progression of liver disease in chronic carriers. These results implied that distinct immune mechanisms might be critical at different stages of HBV infection, probably reflecting the evolving dynamics between HBV and the host immune system during chronic infections.

CONCLUSION

It is important to have a comprehensive understanding of the mechanisms of failure to clear HBV infection, and translate this knowledge into effective therapies to prevent the development of chronicity and other adverse outcomes. With this motive, many GWAS were performed to dissect the genetic basis of HBV-related traits. These GWAS provided novel insights into the pathogenesis of HBV persistence and non-response to hepatitis B vaccine. For instance, the association of *HLA-DPB1* with HBV persistence was unknown before GWAS. *DPB1* gene was neglected in previous candidate gene-based association studies, mainly because it was less polymorphic than *DQB1* and *DRB* genes[46]. In addition to the classical HLA genes *HLA-DP*, *HLA-DQ* and *HLA-C*, GWAS for HBV persistence provided candidate genes including non-classical HLA genes (*EHMT2*, *TCF19*, *CFB*, *NOTCH4*) and non-HLA genes (*UBE2L3*, *CD40*, *INTS10*), indicating that genetic susceptibility to HBV persistence is determined by regulation of immune responses at multiple levels. Many of these candidate genes had known roles in immune responses, whereas some were novel. Besides improving our understanding of the molecular mechanisms underlying HBV-related pathologies, GWAS findings are likely to have other immediate and long-running clinical implications. For instance, genetic markers provided by GWAS can be used to predict the individuals that are at a higher risk for worse prognosis, demanding a closer medical surveillance. Furthermore, identification of novel protective HLA allotypes might be exploited for the development of more effective vaccines based on alternative epitopes.

Despite their initial success, some of these GWAS also had certain limitations, including small sample sizes, lack of information on age at first infection, transmission route, maternal status and HBV genotype, unknown infection history of controls, unknown infection status for HCV and HIV, and imperfect match of age, gender and genetic background among some case-control groups. GWAS for HBV-related advanced liver diseases additionally suffered from the stochasticity of disease pathogenesis. For instance, the randomness of HBV DNA integration events in the host genome adds to the heterogeneity of HBV-related HCC[108]. Cirrhosis and HCC typically occur more than 20 years after the initial infection[109]. Smoking, alcohol consumption, aflatoxin exposure, obesity, diabetes, and treatment interventions during this period are strong confounders that also lead to clinical heterogeneity[110]. The lack of consistent associations in GWAS for HBV-related advanced liver diseases might be due to these confounders. Hence, these GWAS must be designed in a better way to ac-

count for each of these factors[111,112].

Interestingly, the susceptible alleles in the *HLA-DP/DQ* locus are more frequent in Asian populations than in Caucasians, which might be one of the causes for higher prevalence of chronic HBV infections in Asia[22,113]. However, most of these susceptible alleles are not frequent in Africa, too, even though chronic hepatitis B is as prevalent in Africa as in Asia. Given that the predominant mode of transmission and HBV genotypes are different in Asia and Africa (vertical *vs* horizontal; B, C *vs* A, D, E; respectively), the genetic architecture for predisposition to chronic HBV infection also varies among these populations[7,113]. Hence, allele frequency distributions across human populations might give important insights into human-HBV co-evolution.

GWAS for HBV-related traits have almost exclusively been implemented in Asian populations. So far, there is no GWAS in Africans, and only one GWAS in Saudi Arabians, where the dominant HBV genotype is D[7]. Populations with different ancestries harbor different haplotype structures and allele frequencies; therefore, implementing GWAS in other populations might also help narrow down the associated loci. This is especially desirable for fine mapping studies. Fine mapping studies on the HLA locus, where extensive LD structure hampers the detection of causal variants, are of utmost importance since immune-related genes are concentrated in this region. The findings of such studies would reveal novel insights into the pathogenesis of HBV-related traits. Therefore, additional GWAS and fine mapping studies, implemented with more refined case-control designs, larger samples, and in other ethnic populations, would further improve our understanding of HBV infection pathophysiology.

REFERENCES

1 **Schweitzer A**, Horn J, Mikolajczyk RT, Krause G, Ott JJ. Estimations of worldwide prevalence of chronic hepatitis B virus infection: a systematic review of data published between 1965 and 2013. *Lancet* 2015; **386**: 1546-1555 [PMID: 26231459 DOI: 10.1016/S0140-6736(15)61412-X]

2 **Lozano R**, Naghavi M, Foreman K, Lim S, Shibuya K, Aboyans V, Abraham J, Adair T, Aggarwal R, Ahn SY, Alvarado M, Anderson HR, Anderson LM, Andrews KG, Atkinson C, Baddour LM, Barker-Collo S, Bartels DH, Bell ML, Benjamin EJ, Bennett D, Bhalla K, Bikbov B, Bin Abdulhak A, Birbeck G, Blyth F, Bolliger I, Boufous S, Bucello C, Burch M, Burney P, Carapetis J, Chen H, Chou D, Chugh SS, Coffeng LE, Colan SD, Colquhoun S, Colson KE, Condon J, Connor MD, Cooper LT, Corriere M, Cortinovis M, de Vaccaro KC, Couser W, Cowie BC, Criqui MH, Cross M, Dabhadkar KC, Dahodwala N, De Leo D, Degenhardt L, Delossantos A, Denenberg J, Des Jarlais DC, Dharmaratne SD, Dorsey ER, Driscoll T, Duber H, Ebel B, Erwin PJ, Espindola P, Ezzati M, Feigin V, Flaxman AD, Forouzanfar MH, Fowkes FG, Franklin R, Fransen M, Freeman MK, Gabriel SE, Gakidou E, Gaspari F, Gillum RF, Gonzalez-Medina D, Halasa YA, Haring D, Harrison JE, Havmoeller R, Hay RJ, Hoen B, Hotez PJ, Hoy D, Jacobsen KH, James SL, Jasrasaria R, Jayaraman S, Johns N, Karthikeyan G, Kassebaum N, Keren A, Khoo JP, Knowlton LM, Kobusingye O, Koranteng A, Krishnamurthi R, Lipnick M, Lipshultz SE, Ohno SL, Mabweijano J, MacIntyre MF, Mallinger L, March L, Marks GB, Marks R, Matsumori A, Matzopoulos R, Mayosi BM, McAnulty JH, McDermott MM, McGrath J, Mensah GA, Merriman TR, Michaud C, Miller M, Miller TR, Mock C, Mocumbi AO, Mokdad AA, Moran A, Mulholland K, Nair MN, Naldi L, Narayan KM, Nasseri K, Norman P, O'Donnell M, Omer SB, Ortblad K, Osborne R, Ozgediz D, Pahari B, Pandian JD, Rivero AP, Padilla RP, Perez-Ruiz F, Perico N, Phillips D, Pierce K, Pope CA 3rd, Porrini E, Pourmalek F, Raju M, Ranganathan D, Rehm JT, Rein DB, Remuzzi G, Rivara FP, Roberts T, De León FR, Rosenfeld LC, Rushton L, Sacco RL, Salomon JA, Sampson U, Sanman E, Schwebel DC, Segui-Gomez M, Shepard DS, Singh D, Singleton J, Sliwa K, Smith E, Steer A, Taylor JA, Thomas B, Tleyjeh IM, Towbin JA, Truelsen T, Undurraga EA, Venketasubramanian N, Vijayakumar L, Vos T, Wagner GR, Wang M, Wang W, Watt K, Weinstock MA, Weintraub R, Wilkinson JD, Woolf AD, Wulf S, Yeh PH, Yip P, Zabetian A, Zheng ZJ, Lopez AD, Murray CJ, AlMazroa MA, Memish ZA. Global and regional mortality from 235 causes of death for 20 age groups in 1990 and 2010: a systematic analysis for the Global Burden of Disease Study 2010. *Lancet* 2012; **380**: 2095-2128 [PMID: 23245604 DOI: 10.1016/S0140-6736(12)61728-0]

3 **Trépo C**, Chan HL, Lok A. Hepatitis B virus infection. *Lancet* 2014; **384**: 2053-2063 [PMID: 24954675 DOI: 10.1016/S0140-6736(14)60220-8]

4 **Beasley RP**, Hwang LY, Lin CC, Chien CS. Hepatocellular carcinoma and hepatitis B virus. A prospective study of 22 707 men in Taiwan. *Lancet* 1981; **2**: 1129-1133 [PMID: 6118576 DOI: 10.1016/S0140-6736(81)90585-7]

5 **Perz JF**, Armstrong GL, Farrington LA, Hutin YJ, Bell BP. The contributions of hepatitis B virus and hepatitis C virus infections to cirrhosis and primary liver cancer worldwide. *J Hepatol* 2006; **45**: 529-538 [PMID: 16879891 DOI: 10.1016/j.jhep.2006.05.013]

6 **World Health Organization**. Global Hepatitis Report 2017. Accessed October 2017. [ISBN: 978-92-4-156545-5]. Available from: URL: http://www.who.int/hepatitis/publications/global-hepatitis-report2017/en/

7 **McMahon BJ**. The natural history of chronic hepatitis B virus infection. *Hepatology* 2009; **49**: S45-S55 [PMID: 19399792 DOI: 10.1002/hep.22898]

8 **Liang TJ**. Hepatitis B: the virus and disease. *Hepatology* 2009; **49**: S13-S21 [PMID: 19399811 DOI: 10.1002/hep.22881]

9 **Hoofnagle JH**, Doo E, Liang TJ, Fleischer R, Lok AS. Management of hepatitis B: summary of a clinical research workshop. *Hepatology* 2007; **45**: 1056-1075 [PMID: 17393513 DOI: 10.1002/hep.21627]

10 **Nguyen VT**, Law MG, Dore GJ. Hepatitis B-related hepatocellular carcinoma: epidemiological characteristics and disease burden. *J Viral Hepat* 2009; **16**: 453-463 [PMID: 19302335 DOI: 10.1111/j.1365-2893.2009.01117.x]

11 **He YL**, Zhao YR, Zhang SL, Lin SM. Host susceptibility to persistent hepatitis B virus infection. *World J Gastroenterol* 2006; **12**: 4788-4793 [PMID: 16937459 DOI: 10.3748/WJG.V12.I30.4788]

12 **Lin TM**, Chen CJ, Wu MM, Yang CS, Chen JS, Lin CC, Kwang TY, Hsu ST, Lin SY, Hsu LC. Hepatitis B virus markers in Chinese twins. *Anticancer Res* 1989; **9**: 737-741 [PMID: 2764519]

13 **Höhler T**, Reuss E, Evers N, Dietrich E, Rittner C, Freitag CM, Vollmar J, Schneider PM, Fimmers R. Differential genetic determination of immune responsiveness to hepatitis B surface antigen and to hepatitis A virus: a vaccination study in twins. *Lancet* 2002; **360**: 991-995 [PMID: 12383669 DOI: 10.1016/S0140-6736(02)11083-X]

14 **Newport MJ**, Goetghebuer T, Weiss HA, Whittle H, Siegrist CA, Marchant A; MRC Gambia Twin Study Group. Genetic regulation of immune responses to vaccines in early life. *Genes Immun* 2004; **5**: 122-129 [PMID: 14737096 DOI: 10.1038/sj.gene.6364051]

15 **Singh R**, Kaul R, Kaul A, Khan K. A comparative review of HLA associations with hepatitis B and C viral infections across global populations. *World J Gastroenterol* 2007; **13**: 1770-1787 [PMID: 17465466 DOI: 10.3748/wjg.v13.i12.1770]

16 **Wang L**, Zou ZQ, Wang K. Clinical Relevance of HLA Gene Variants in HBV Infection. *J Immunol Res* 2016; **2016**: 9069375 [PMID: 27243039 DOI: 10.1155/2016/9069375]

17 **Matsuura K**, Isogawa M, Tanaka Y. Host genetic variants influencing the clinical course of hepatitis B virus infection. *J Med Virol* 2016; **88**: 371-379 [PMID: 26255971 DOI: 10.1002/jmv.24350]

18 **Tong Hv**, Bock CT, Velavan TP. Genetic insights on host and hepatitis B virus in liver diseases. *Mutat Res Rev Mutat Res* 2014; **762**: 65-75 [PMID: 25475418 DOI: 10.1016/j.mrrev.2014.06.001]

19 **Katrinli S**, Nigdelioglu A, Ozdil K, Dinler-Doganay G, Doganay L. The association of variations in TLR genes and spontaneous immune control of hepatitis B virus. *Clin Res Hepatol Gastroenterol* 2018; **42**: 139-144 [PMID: 29276096 DOI: 10.1016/j.clinre.2017.10.002]

20 **Katrinli S**, Enc FY, Ozdil K, Ozturk O, Tuncer I, Doganay GD, Doganay L. Effect of HLA-DPA1 alleles on chronic hepatitis B prognosis and treatment response. *North Clin Istanb* 2017; **3**: 168-174 [PMID: 28275747 DOI: 10.14744/nci.2016.27870]

21 **Doganay L**, Tuncer I, Katrinli S, Enc FY, Ozturk O, Colak Y, Ulasoglu C, Dinler G. The effect of HLA-DQB1 alleles on virologic breakthroughs during chronic hepatitis B treatment with genetically low barrier drugs. *Clin Res Hepatol Gastroenterol* 2013; **37**: 359-364 [PMID: 23273495 DOI: 10.1016/j.clinre.2012.10.013]

22 **Kamatani Y**, Wattanapokayakit S, Ochi H, Kawaguchi T, Takahashi A, Hosono N, Kubo M, Tsunoda T, Kamatani N, Kumada H, Puseenam A, Sura T, Daigo Y, Chayama K, Chantratita W, Nakamura Y, Matsuda K. A genome-wide association study identifies variants in the HLA-DP locus associated with chronic hepatitis B in Asians. *Nat Genet* 2009; **41**: 591-595 [PMID: 19349983 DOI: 10.1038/ng.348]

23 **Mbarek H**, Ochi H, Urabe Y, Kumar V, Kubo M, Hosono N, Takahashi A, Kamatani Y, Miki D, Abe H, Tsunoda T, Kamatani N, Chayama K, Nakamura Y, Matsuda K. A genome-wide association study of chronic hepatitis B identified novel risk locus in a Japanese population. *Hum Mol Genet* 2011; **20**: 3884-3892 [PMID: 21750111 DOI: 10.1093/hmg/ddr301]

24 **Zhu M**, Dai J, Wang C, Wang Y, Qin N, Ma H, Song C, Zhai X, Yang Y, Liu J, Liu L, Li S, Liu J, Yang H, Zhu F, Shi Y, Shen H, Jin G, Zhou W, Hu Z. Fine mapping the MHC region identified four independent variants modifying susceptibility to chronic hepatitis B in Han Chinese. *Hum Mol Genet* 2016; **25**: 1225-1232 [PMID: 26769676 DOI: 10.1093/hmg/ddw003]

25 **Nishida N**, Sawai H, Matsuura K, Sugiyama M, Ahn SH, Park JY, Hige S, Kang JH, Suzuki K, Kurosaki M, Asahina Y, Mochida S, Watanabe M, Tanaka E, Honda M, Kaneko S, Orito E, Itoh Y, Mita E, Tamori A, Murawaki Y, Hiasa Y, Sakaida I, Korenaga M, Hino K, Ide T, Kawashima M, Mawatari Y, Sageshima M, Ogasawara Y, Koike A, Izumi N, Han KH, Tanaka Y, Tokunaga K, Mizokami M. Genome-wide association study confirming association of HLA-DP with protection against chronic hepatitis B and viral clearance in Japanese and Korean. *PLoS One* 2012; **7**: e39175 [PMID: 22737229 DOI: 10.1371/journal.pone.0039175]

26 **Kim YJ**, Kim HY, Lee JH, Yu SJ, Yoon JH, Lee HS, Kim CY, Cheong JY, Cho SW, Park NH, Park BL, Namgoong S, Kim LH, Cheong HS, Shin HD. A genome-wide association study identified new variants associated with the risk of chronic hepatitis B. *Hum Mol Genet* 2013; **22**: 4233-4238 [PMID: 23760081 DOI: 10.1093/hmg/ddt266]

27 **Chang SW**, Fann CS, Su WH, Wang YC, Weng CC, Yu CJ, Hsu CL, Hsieh AR, Chien RN, Chu CM, Tai DI. A genome-wide association study on chronic HBV infection and its clinical progression in male Han-Taiwanese. *PLoS One* 2014; **9**: e99724 [PMID: 24940741 DOI: 10.1371/journal.pone.0099724]

28 **Hu Z**, Liu Y, Zhai X, Dai J, Jin G, Wang L, Zhu L, Yang Y, Liu J, Chu M, Wen J, Xie K, Du G, Wang Q, Zhou Y, Cao M, Liu L, He Y, Wang Y, Zhou G, Jia W, Lu J, Li S, Liu J, Yang H, Shi Y, Zhou W, Shen H. New loci associated with chronic hepatitis B virus infection in Han Chinese. *Nat Genet* 2013; **45**: 1499-1503 [PMID: 24162738 DOI: 10.1038/ng.2809]

29 **Jiang DK**, Ma XP, Yu H, Cao G, Ding DL, Chen H, Huang HX, Gao YZ, Wu XP, Long XD, Zhang H, Zhang Y, Gao Y, Chen TY, Ren WH, Zhang P, Shi Z, Jiang W, Wan B, Saiyin H, Yin J, Zhou YF, Zhai Y, Lu PX, Zhang H, Gu X, Tan A, Wang JB, Zuo XB, Sun LD, Liu JO, Yi Q, Mo Z, Zhou G, Liu Y, Sun J, Shugart YY, Zheng SL, Zhang XJ, Xu J, Yu L. Genetic variants in five novel loci including CFB and CD40 predispose to chronic hepatitis B. *Hepatology* 2015; **62**: 118-128 [PMID: 25802187 DOI: 10.1002/hep.27794]

30 **Li Y**, Si L, Zhai Y, Hu Y, Hu Z, Bei JX, Xie B, Ren Q, Cao P, Yang F, Song Q, Bao Z, Zhang H, Han Y, Wang Z, Chen X, Xia X, Yan H, Wang R, Zhang Y, Gao C, Meng J, Tu X, Liang X, Cui Y, Liu Y, Wu X, Li Z, Wang H, Li Z, Hu B, He M, Gao Z, Xu X, Ji H, Yu C, Sun Y, Xing B, Yang X, Zhang H, Tan A, Wu C, Jia W, Li S, Zeng YX, Shen H, He F, Mo Z, Zhang H, Zhou G. Genome-wide association study identifies 8p21.3 associated with persistent hepatitis B virus infection among Chinese. *Nat Commun* 2016; **7**: 11664 [PMID: 27244555 DOI: 10.1038/ncomms11664]

31 **An P**, Winkler C, Guan L, O'Brien SJ, Zeng Z; HBV Study Consortium. A common HLA-DPA1 variant is a major determinant of hepatitis B virus clearance in Han Chinese. *J Infect Dis* 2011; **203**: 943-947 [PMID: 21402545 DOI: 10.1093/infdis/jiq154]

32 **Lau KC**, Lam CW, Law CY, Lai ST, Tsang TY, Siu CW, To WK, Leung KF, Mak CM, Poon WT, Chan PK, Chan YW. Non-invasive screening of HLA-DPA1 and HLA-DPB1 alleles for persistent hepatitis B virus infection: susceptibility for vertical transmission and toward a personalized approach for vaccination and treatment. *Clin Chim Acta* 2011; **412**: 952-957 [PMID: 21310144 DOI: 10.1016/j.cca.2011.01.030]

33 **Wang L**, Wu XP, Zhang W, Zhu DH, Wang Y, Li YP, Tian Y, Li RC, Li Z, Zhu X, Li JH, Cai J, Liu L, Miao XP, Liu Y, Li H. Evaluation of genetic susceptibility loci for chronic hepatitis B in Chinese: two independent case-control studies. *PLoS One* 2011; **6**: e17608 [PMID: 21408128 DOI: 10.1371/journal.pone.0017608]

34 **Guo X**, Zhang Y, Li J, Ma J, Wei Z, Tan W, O'Brien SJ. Strong influence of human leukocyte antigen (HLA)-DP gene variants on development of persistent chronic hepatitis B virus carriers in the Han Chinese population. *Hepatology* 2011; **53**: 422-428 [PMID: 21274863 DOI: 10.1002/hep.24048]

35 **Li J**, Yang D, He Y, Wang M, Wen Z, Liu L, Yao J, Matsuda K, Nakamura Y, Yu J, Jiang X, Sun S, Liu Q, Jiang X, Song Q, Chen M, Yang H, Tang F, Hu X, Wang J, Chang Y, He X, Chen Y, Lin J. Associations of HLA-DP variants with hepatitis B virus infection in southern and northern Han Chinese populations: a multicenter case-control study. *PLoS One* 2011; **6**: e24221 [PMID: 21904616 DOI: 10.1371/journal.pone.0024221]

36 **Hu L**, Zhai X, Liu J, Chu M, Pan S, Jiang J, Zhang Y, Wang H, Chen J, Shen H, Hu Z. Genetic variants in human leukocyte antigen/DP-DQ influence both hepatitis B virus clearance and hepatocellular carcinoma development. *Hepatology* 2012; **55**: 1426-1431 [PMID: 22105689 DOI: 10.1002/hep.24799]

37 **Wong DK**, Watanabe T, Tanaka Y, Seto WK, Lee CK, Fung J, Lin CK, Huang FY, Lai CL, Yuen MF. Role of HLA-DP polymorphisms on chronicity and disease activity of hepatitis B infection in Southern Chinese. *PLoS One* 2013; **8**: e66920 [PMID: 23825586 DOI: 10.1371/journal.pone.0066920]

38 **Liao Y**, Cai B, Li Y, Chen J, Tao C, Huang H, Wang L. Association of HLA-DP/DQ and STAT4 polymorphisms with HBV infection outcomes and a mini meta-analysis. *PLoS One* 2014; **9**: e111677 [PMID: 25365208 DOI: 10.1371/journal.pone.0111677]

39 **Tao J**, Su K, Yu C, Liu X, Wu W, Xu W, Jiang B, Luo R, Yao J, Zhou J, Zhan Y, Ye C, Yuan W, Jiang X, Cui W, Li MD, Li L. Fine mapping analysis of HLA-DP/DQ gene clusters on chromosome 6 reveals multiple susceptibility loci for HBV infection. *Amino Acids* 2015; **47**: 2623-2634 [PMID: 26197724 DOI: 10.1007/s00726-015-2054-6]

40 **Zhang X**, Jia J, Dong J, Yu F, Ma N, Li M, Liu X, Liu W, Li T, Liu D. HLA-DQ polymorphisms with HBV infection: different outcomes upon infection and prognosis to lamivudine therapy. *J Viral Hepat* 2014; **21**: 491-498 [PMID: 24750255 DOI: 10.1111/jvh.12159]

41 **Posuwan N**, Payungporn S, Tangkijvanich P, Ogawa S, Murakami S, Iijima S, Matsuura K, Shinkai N, Watanabe T, Poovorawan Y, Tanaka Y. Genetic association of human leukocyte antigens with chronicity or resolution of hepatitis B infection in thai population. *PLoS One* 2014; **9**: e86007 [PMID: 24465836 DOI: 10.1371/journal.pone.0086007]

42 **Wasityastuti W**, Yano Y, Ratnasari N, Triyono T, Triwikatmani C, Indrarti F, Heriyanto DS, Yamani LN, Liang Y, Utsumi T, Hayashi Y. Protective effects of HLA-DPA1/DPB1 variants against Hepatitis B virus infection in an Indonesian population. *Infect Genet Evol* 2016; **41**: 177-184 [PMID: 27051043 DOI: 10.1016/j.meegid.2016.03.034]

43 **Liao Y**, Cai B, Li Y, Chen J, Ying B, Tao C, Zhao M, Ba Z, Zhang Z, Wang L. Association of HLA-DP/DQ, STAT4 and IL-28B variants with HBV viral clearance in Tibetans and Uygurs in China. *Liver Int* 2015; **35**: 886-896 [PMID: 25041342 DOI: 10.1111/liv.12643]

44 **Yu L**, Cheng YJ, Cheng ML, Yao YM, Zhang Q, Zhao XK, Liu HJ, Hu YX, Mu M, Wang B, Yang GZ, Zhu LL, Zhang S. Quantitative assessment of common genetic variations in HLA-DP with hepatitis B virus infection, clearance and hepatocellular carcinoma development. *Sci Rep* 2015; **5**: 14933 [PMID: 26462556 DOI: 10.1038/srep14933]

45 **Vermehren J**, Lötsch J, Susser S, Wicker S, Berger A, Zeuzem S, Sarrazin C, Doehring A. A common HLA-DPA1 variant is associated with hepatitis B virus infection but fails to distinguish active from inactive Caucasian carriers. *PLoS One* 2012; **7**: e32605 [PMID: 22448225 DOI: 10.1371/journal.pone.0032605]

46 **Thomas R**, Thio CL, Apps R, Qi Y, Gao X, Marti D, Stein JL, Soderberg KA, Moody MA, Goedert JJ, Kirk GD, Hoots WK, Wolinsky S, Carrington M. A novel variant marking HLA-DP expression levels predicts recovery from hepatitis B virus infection. *J Virol* 2012; **86**: 6979-6985 [PMID: 22496224 DOI: 10.1128/JVI.00406-12]

47 **Al-Qahtani AA**, Al-Anazi MR, Abdo AA, Sanai FM, Al-Hamoudi W, Alswat KA, Al-Ashgar HI, Khalaf NZ, Eldali AM, Viswan NA, Al-Ahdal MN. Association between HLA variations and chronic hepatitis B virus infection in Saudi Arabian patients. *PLoS One* 2014; **9**: e80445 [PMID: 24465366 DOI: 10.1371/journal.pone.0080445]

48 **Trinks J**, Nishida N, Hulaniuk ML, Caputo M, Tsuchiura T, Marciano S, Haddad L, Blejer J, Bartoli S, Ameigeiras B, Frías SE, Vistarini C, Heinrich F, Remondegui C, Ceballos S, Echenique G, Charre Samman M, D'Amico C, Rojas A, Martínez A, Ridruejo E, Fernández RJ, Burgos Pratx L, Salamone H, Nuñez F, Galdame O, Gadano A, Corach D, Sugiyama M, Flichman D, Tokunaga K, Mizokami M. Role of HLA-DP and HLA-DQ on the clearance of hepatitis B virus and the risk of chronic infection in a multiethnic population. *Liver Int* 2017; **37**: 1476-1487 [PMID: 28267888 DOI: 10.1111/liv.13405]

49 **Scheer S**, Zaph C. The Lysine Methyltransferase G9a in Immune Cell Differentiation and Function. *Front Immunol* 2017; **8**: 429 [PMID: 28443098 DOI: 10.3389/fimmu.2017.00429]

50 **Krautkramer KA**, Linnemann AK, Fontaine DA, Whillock AL, Harris TW, Schleis GJ, Truchan NA, Marty-Santos L, Lavine JA, Cleaver O, Kimple ME, Davis DB. Tcf19 is a novel islet factor necessary for proliferation and survival in the INS-1 β-cell line. *Am J Physiol Endocrinol Metab* 2013; **305**: E600-E610 [PMID: 23860123 DOI: 10.1152/ajpendo.00147.2013]

51 **Ferreira MA**, Hottenga JJ, Warrington NM, Medland SE, Willemsen G, Lawrence RW, Gordon S, de Geus EJ, Henders AK, Smit JH, Campbell MJ, Wallace L, Evans DM, Wright MJ, Nyholt DR, James AL, Beilby JP, Penninx BW, Palmer LJ, Frazer IH, Montgomery GW, Martin NG, Boomsma DI. Sequence variants in three loci influence monocyte counts and erythrocyte volume. *Am J Hum Genet* 2009; **85**: 745-749 [PMID: 19853236 DOI: 10.1016/j.ajhg.2009.10.005]

52 **Lewis MJ**, Vyse S, Shields AM, Boeltz S, Gordon PA, Spector TD, Lehner PJ, Walczak H, Vyse TJ. UBE2L3 polymorphism amplifies NF-κB activation and promotes plasma cell development, linking linear ubiquitination to multiple autoimmune diseases. *Am J Hum Genet* 2015; **96**: 221-234 [PMID: 25640675 DOI: 10.1016/j.ajhg.2014.12.024]

53 **Zeller T**, Wild P, Szymczak S, Rotival M, Schillert A, Castagne R, Maouche S, Germain M, Lackner K, Rossmann H, Eleftheriadis M, Sinning CR, Schnabel RB, Lubos E, Mennerich D, Rust W, Perret C, Proust C, Nicaud V, Loscalzo J, Hübner N, Tregouet D, Münzel T, Ziegler A, Tiret L, Blankenberg S, Cambien F. Genetics and beyond--the transcriptome of human monocytes and disease susceptibility. *PLoS One* 2010; **5**: e10693 [PMID: 20502693 DOI: 10.1371/journal.pone.0010693]

54 **Stoermer KA**, Morrison TE. Complement and viral pathogenesis. *Virology* 2011; **411**: 362-373 [PMID: 21292294 DOI: 10.1016/j.virol.2010.12.045]

55 **Radtke F**, Fasnacht N, Macdonald HR. Notch signaling in the immune system. *Immunity* 2010; **32**: 14-27 [PMID: 20152168 DOI: 10.1016/j.immuni.2010.01.004]

56 **Jacobson EM**, Concepcion E, Oashi T, Tomer Y. A Graves' disease-associated Kozak sequence single-nucleotide polymorphism enhances the efficiency of CD40 gene translation: a case for translational pathophysiology. *Endocrinology* 2005; **146**: 2684-2691 [PMID: 15731360 DOI: 10.1210/en.2004-1617]

57 **Elgueta R**, Benson MJ, de Vries VC, Wasiuk A, Guo Y, Noelle RJ. Molecular mechanism and function of CD40/CD40L engagement in the immune system. *Immunol Rev* 2009; **229**: 152-172 [PMID: 19426221 DOI: 10.1111/j.1600-065X.2009.00782.x]

58 **Nishida N**, Sawai H, Kashiwase K, Minami M, Sugiyama M, Seto WK, Yuen MF, Posuwan N, Poovorawan Y, Ahn SH, Han KH, Matsuura K, Tanaka Y, Kurosaki M, Asahina Y, Izumi N, Kang JH, Hige S, Ide T, Yamamoto K, Sakaida I, Murawaki Y, Itoh Y, Tamori A, Orito E, Hiasa Y, Honda M, Kaneko S, Mita E, Suzuki K, Hino K, Tanaka E, Mochida S, Watanabe M, Eguchi Y, Masaki N, Murata K, Korenaga M, Mawatari Y, Ohashi J, Kawashima M, Tokunaga K, Mizokami M. New susceptibility and resistance HLA-DP alleles to HBV-related diseases identified by a trans-ethnic association study in Asia. *PLoS One* 2014; **9**: e86449 [PMID: 24520320 DOI: 10.1371/journal.pone.0086449]

59 **Nishida N**, Ohashi J, Khor SS, Sugiyama M, Tsuchiura T, Sawai H, Hino K, Honda M, Kaneko S, Yatsuhashi H, Yokosuka O, Koike K, Kurosaki M, Izumi N, Korenaga M, Kang JH, Tanaka E, Taketomi A, Eguchi Y, Sakamoto N, Yamamoto K, Tamori A, Sakaida I, Hige S, Itoh Y, Mochida S, Mita E, Takikawa Y, Ide T, Hiasa Y, Kojima H, Yamamoto K, Nakamura M, Saji H, Sasazuki T, Kanto T, Tokunaga K, Mizokami M. Understanding of HLA-conferred susceptibility to chronic hepatitis B infection requires HLA genotyping-based association analysis. *Sci Rep* 2016; **6**: 24767 [PMID: 27091392 DOI: 10.1038/srep24767]

60 **Díaz G**, Amicosante M, Jaraquemada D, Butler RH, Guillén MV, Sánchez M, Nombela C, Arroyo J. Functional analysis of HLA-DP polymorphism: a crucial role for DPbeta residues 9, 11, 35, 55, 56, 69 and 84-87 in T cell allorecognition and peptide binding. *Int Immunol* 2003; **15**: 565-576 [PMID: 12697658 DOI: 10.1093/intimm/dxg057]

61 **Sidney J**, Steen A, Moore C, Ngo S, Chung J, Peters B, Sette A. Five HLA-DP molecules frequently expressed in the worldwide human population share a common HLA supertypic binding specificity. *J Immunol* 2010; **184**: 2492-2503 [PMID: 20139279 DOI: 10.4049/jimmunol.0903655]

62 **Andreatta M**, Nielsen M. Characterizing the binding motifs of 11 common human HLA-DP and HLA-DQ molecules using NNAlign. *Immunology* 2012; **136**: 306-311 [PMID: 22352343 DOI: 10.1111/j.1365-2567.2012.03579.x]

63 **Yamashita Y**, Anczurowski M, Nakatsugawa M, Tanaka M, Kagoya Y, Sinha A, Chamoto K, Ochi T, Guo T, Saso K, Butler MO, Minden MD, Kislinger T, Hirano N. HLA-DP^{84Gly} constitutively presents endogenous peptides generated by the class I antigen processing pathway. *Nat Commun* 2017; **8**: 15244 [PMID: 28489076 DOI: 10.1038/ncomms15244]

64 **de Bakker PI**, Raychaudhuri S. Interrogating the major histocompatibility complex with high-throughput genomics. *Hum Mol Genet* 2012; **21**: R29-R36 [PMID: 22976473 DOI: 10.1093/hmg/dds384]

65 **Thursz MR**, Kwiatkowski D, Allsopp CE, Greenwood BM, Thomas HC, Hill AV. Association between an MHC class Ⅱ allele and clearance of hepatitis B virus in the Gambia. *N Engl J Med* 1995; **332**: 1065-1069 [PMID: 7898524 DOI: 10.1056/NEJM199504203321604]

66 **Höhler T**, Gerken G, Notghi A, Lubjuhn R, Taheri H, Protzer U, Löhr HF, Schneider PM, Meyer zum Büschenfelde KH, Rittner C.

HLA-DRB1*1301 and *1302 protect against chronic hepatitis B. *J Hepatol* 1997; **26**: 503-507 [PMID: 9075656 DOI: 10.1016/S0168-8278(97)80414-X]

67 **Ahn SH**, Han KH, Park JY, Lee CK, Kang SW, Chon CY, Kim YS, Park K, Kim DK, Moon YM. Association between hepatitis B virus infection and HLA-DR type in Korea. *Hepatology* 2000; **31**: 1371-1373 [PMID: 10827165 DOI: 10.1053/jhep.2000.7988]

68 **Thio CL**, Thomas DL, Karacki P, Gao X, Marti D, Kaslow RA, Goedert JJ, Hilgartner M, Strathdee SA, Duggal P, O'Brien SJ, Astemborski J, Carrington M. Comprehensive analysis of class I and class Ⅱ HLA antigens and chronic hepatitis B virus infection. *J Virol* 2003; **77**: 12083-12087 [PMID: 14581545 DOI: 10.1128/jvi.77.22.12083-12087.2003]

69 **O'Brien TR**, Kohaar I, Pfeiffer RM, Maeder D, Yeager M, Schadt EE, Prokunina-Olsson L. Risk alleles for chronic hepatitis B are associated with decreased mRNA expression of HLA-DPA1 and HLA-DPB1 in normal human liver. *Genes Immun* 2011; **12**: 428-433 [PMID: 21346778 DOI: 10.1038/gene.2011.11]

70 **Montgomery SB**, Sammeth M, Gutierrez-Arcelus M, Lach RP, Ingle C, Nisbett J, Guigo R, Dermitzakis ET. Transcriptome genetics using second generation sequencing in a Caucasian population. *Nature* 2010; **464**: 773-777 [PMID: 20220756 DOI: 10.1038/nature08903]

71 **Kaur G**, Gras S, Mobbs JI, Vivian JP, Cortes A, Barber T, Kuttikkatte SB, Jensen LT, Attfield KE, Dendrou CA, Carrington M, McVean G, Purcell AW, Rossjohn J, Fugger L. Structural and regulatory diversity shape HLA-C protein expression levels. *Nat Commun* 2017; **8**: 15924 [PMID: 28649982 DOI: 10.1038/ncomms15924]

72 **Zanetti AR**, Van Damme P, Shouval D. The global impact of vaccination against hepatitis B: a historical overview. *Vaccine* 2008; **26**: 6266-6273 [PMID: 18848855 DOI: 10.1016/j.vaccine.2008.09.056]

73 **Png E**, Thalamuthu A, Ong RT, Snippe H, Boland GJ, Seielstad M. A genome-wide association study of hepatitis B vaccine response in an Indonesian population reveals multiple independent risk variants in the HLA region. *Hum Mol Genet* 2011; **20**: 3893-3898 [PMID: 21764829 DOI: 10.1093/hmg/ddr302]

74 **Wu TW**, Chu CC, Ho TY, Chang Liao HW, Lin SK, Lin M, Lin HH, Wang LY. Responses to booster hepatitis B vaccination are significantly correlated with genotypes of human leukocyte antigen (HLA)-DPB1 in neonatally vaccinated adolescents. *Hum Genet* 2013; **132**: 1131-1139 [PMID: 23739870 DOI: 10.1007/s00439-013-1320-5]

75 **Nguyen T**, Liu XK, Zhang Y, Dong C. BTNL2, a butyrophilin-like molecule that functions to inhibit T cell activation. *J Immunol* 2006; **176**: 7354-7360 [PMID: 16751379 DOI: 10.4049/jimmunol.176.12.7354]

76 **Pan L**, Zhang L, Zhang W, Wu X, Li Y, Yan B, Zhu X, Liu X, Yang C, Xu J, Zhou G, Xu A, Li H, Liu Y. A genome-wide association study identifies polymorphisms in the HLA-DR region associated with non-response to hepatitis B vaccination in Chinese Han populations. *Hum Mol Genet* 2014; **23**: 2210-2219 [PMID: 24282030 DOI: 10.1093/hmg/ddt586]

77 **Li Y**, Ni R, Song W, Shao W, Shrestha S, Ahmad S, Cunningham CK, Flynn PM, Kapogiannis BG, Wilson CM, Tang J. Clear and independent associations of several HLA-DRB1 alleles with differential antibody responses to hepatitis B vaccination in youth. *Hum Genet* 2009; **126**: 685-696 [PMID: 19597844 DOI: 10.1007/s00439-009-0720-z]

78 **Li ZK**, Nie JJ, Li J, Zhuang H. The effect of HLA on immunological response to hepatitis B vaccine in healthy people: a meta-analysis. *Vaccine* 2013; **31**: 4355-4361 [PMID: 23887040 DOI: 10.1016/j.vaccine.2013.06.108]

79 **Yan ZH**, Fan Y, Wang XH, Mao Q, Deng GH, Wang YM. Relationship between HLA-DR gene polymorphisms and outcomes of hepatitis B viral infections: a meta-analysis. *World J Gastroenterol* 2012; **18**: 3119-3128 [PMID: 22791948 DOI: 10.3748/wjg.v18.i24.3119]

80 **Doganay L**, Fejzullahu A, Katrinli S, Yilmaz Enc F, Ozturk O, Colak Y, Ulasoglu C, Tuncer I, Dinler Doganay G. Association of human leukocyte antigen DQB1 and DRB1 alleles with chronic hepatitis B. *World J Gastroenterol* 2014; **20**: 8179-8186 [PMID: 25009391 DOI: 10.3748/wjg.v20.i25.8179]

81 **Wu TW**, Chen CF, Lai SK, Lin HH, Chu CC, Wang LY. SNP rs7770370 in HLA-DPB1 loci as a major genetic determinant of response to booster hepatitis B vaccination: results of a genome-wide association study. *J Gastroenterol Hepatol* 2015; **30**: 891-899 [PMID: 25389088 DOI: 10.1111/jgh.12845]

82 **Sakai A**, Noguchi E, Fukushima T, Tagawa M, Iwabuchi A, Kita M, Kakisaka K, Miyasaka A, Takikawa Y, Sumazaki R. Identification of amino acids in antigen-binding site of class Ⅱ HLA proteins independently associated with hepatitis B vaccine response. *Vaccine* 2017; **35**: 703-710 [PMID: 28043736 DOI: 10.1016/j.vaccine.2016.08.068]

83 **Roh EY**, Yoon JH, In JW, Lee N, Shin S, Song EY. Association of HLA-DP variants with the responsiveness to Hepatitis B virus vaccination in Korean Infants. *Vaccine* 2016; **34**: 2602-2607 [PMID: 27083422 DOI: 10.1016/j.vaccine.2016.03.090]

84 **Okada Y**, Uno N, Sato S, Mori S, Sasaki D, Kaku N, Kosai K, Morinaga Y, Hasegawa H, Yanagihara K. Strong influence of human leukocyte antigen-DP variants on response to hepatitis B vaccine in a Japanese population. *Vaccine* 2017; **35**: 5662-5665 [PMID: 28882445 DOI: 10.1016/j.vaccine.2017.08.045]

85 **Al-Qahtani A**, Khalak HG, Alkuraya FS, Al-hamoudi W, Alswat K, Al Balwi MA, Al Abdulkareem I, Sanai FM, Abdo AA. Genome-wide association study of chronic hepatitis B virus infection reveals a novel candidate risk allele on 11q22.3. *J Med Genet* 2013; **50**: 725-732 [PMID: 24065354 DOI: 10.1136/jmedgenet-2013-101724]

86 **Tan W**, Xia J, Dan Y, Li M, Lin S, Pan X, Wang H, Tang Y, Liu N, Tan S, Liu M, He W, Zhang W, Mao Q, Wang Y, Deng G. Genome-wide association study identifies HLA-DR variants conferring risk of HBV-related acute-on-chronic liver failure. *Gut* 2018; **67**: 757-766 [PMID: 28130311 DOI: 10.1136/gutjnl-2016-313035]

87 **Han Y**, Jiang ZY, Jiao LX, Yao C, Lin QF, Ma N, Ju RQ, Yang F, Yu JH, Chen L. Association of human leukocyte antigen-DRB1 alleles with chronic hepatitis B virus infection in the Han Chinese of Northeast China. *Mol Med Rep* 2012; **5**: 1347-1351 [PMID: 22367481 DOI: 10.3892/mmr.2012.800]

88 **Zhang H**, Zhai Y, Hu Z, Wu C, Qian J, Jia W, Ma F, Huang W, Yu L, Yue W, Wang Z, Li P, Zhang Y, Liang R, Wei Z, Cui Y, Xie W, Cai M, Yu X, Yuan Y, Xia X, Zhang X, Yang H, Qiu W, Yang J, Gong F, Chen M, Shen H, Lin D, Zeng YX, He F, Zhou G. Genome-wide association study identifies 1p36.22 as a new susceptibility locus for hepatocellular carcinoma in chronic hepatitis B virus carriers. *Nat Genet* 2010; **42**: 755-758 [PMID: 20676096 DOI: 10.1038/ng.638]

89 **Li S**, Qian J, Yang Y, Zhao W, Dai J, Bei JX, Foo JN, McLaren PJ, Li Z, Yang J, Shen F, Liu L, Yang J, Li S, Pan S, Wang Y, Li W, Zhai X, Zhou B, Shi L, Chen X, Chu M, Yan Y, Wang J, Cheng S, Shen J, Jia W, Liu J, Yang J, Wen Z, Li A, Zhang Y, Zhang G, Luo X, Qin H, Chen M, Wang H, Jin L, Lin D, Shen H, He L, de Bakker PI, Wang H, Zeng YX, Wu M, Hu Z, Shi Y, Liu J, Zhou W. GWAS identifies novel susceptibility loci on 6p21.32 and 21q21.3 for hepatocellular carcinoma in chronic hepatitis B virus carriers. *PLoS Genet* 2012; **8**: e1002791 [PMID: 22807686 DOI: 10.1371/journal.pgen.1002791]

90 **Jiang DK**, Sun J, Cao G, Liu Y, Lin D, Gao YZ, Ren WH, Long XD, Zhang H, Ma XP, Wang Z, Jiang W, Chen TY, Gao Y, Sun LD, Long JR, Huang HX, Wang D, Yu H, Zhang P, Tang LS, Peng B, Cai H, Liu TT, Zhou P, Liu F, Lin X, Tao S, Wan B, Sai-Yin HX, Qin LX, Yin J, Liu L, Wu C, Pei Y, Zhou YF, Zhai Y, Lu PX, Tan A, Zuo XB, Fan J, Chang J, Gu X, Wang NJ, Li Y, Liu YK, Zhai K, Zhang H, Hu Z, Liu J, Yi Q, Xiang Y, Shi R, Ding Q, Zheng W, Shu XO, Mo Z, Shugart YY, Zhang XJ, Zhou G, Shen H, Zheng SL, Xu J, Yu L. Genetic variants in STAT4 and HLA-DQ genes confer risk of hepatitis B virus-related hepatocellular carcinoma. *Nat Genet* 2013; **45**: 72-75 [PMID: 23242368 DOI: 10.1038/ng.2483]

91 **Chan KY**, Wong CM, Kwan JS, Lee JM, Cheung KW, Yuen MF, Lai CL, Poon RT, Sham PC, Ng IO. Genome-wide association study of hepatocellular carcinoma in Southern Chinese patients with chronic hepatitis B virus infection. *PLoS One* 2011; **6**: e28798 [PMID: 22174901 DOI: 10.1371/journal.pone.0028798]

92 **Qu LS**, Jin F, Guo YM, Liu TT, Xue RY, Huang XW, Xu M, Chen

TY, Ni ZP, Shen XZ. Nine susceptibility loci for hepatitis B virus-related hepatocellular carcinoma identified by a pilot two-stage genome-wide association study. *Oncol Lett* 2016; **11**: 624-632 [PMID: 26870257 DOI: 10.3892/ol.2015.3958]

93 **Jemal A**, Bray F, Center MM, Ferlay J, Ward E, Forman D. Global cancer statistics. *CA Cancer J Clin* 2011; **61**: 69-90 [PMID: 21296855 DOI: 10.3322/caac.20107]

94 **Munirajan AK**, Ando K, Mukai A, Takahashi M, Suenaga Y, Ohira M, Koda T, Hirota T, Ozaki T, Nakagawara A. KIF1Bbeta functions as a haploinsufficient tumor suppressor gene mapped to chromosome 1p36.2 by inducing apoptotic cell death. *J Biol Chem* 2008; **283**: 24426-24434 [PMID: 18614535 DOI: 10.1074/jbc.M802316200]

95 **Nguyen KB**, Watford WT, Salomon R, Hofmann SR, Pien GC, Morinobu A, Gadina M, O'Shea JJ, Biron CA. Critical role for STAT4 activation by type 1 interferons in the interferon-gamma response to viral infection. *Science* 2002; **297**: 2063-2066 [PMID: 12242445 DOI: 10.1126/science.1074900]

96 **Chen K**, Shi W, Xin Z, Wang H, Zhu X, Wu X, Li Z, Li H, Liu Y. Replication of genome wide association studies on hepatocellular carcinoma susceptibility loci in a Chinese population. *PLoS One* 2013; **8**: e77315 [PMID: 24204805 DOI: 10.1371/journal.pone.0077315]

97 **Sawai H**, Nishida N, Mbarek H, Matsuda K, Mawatari Y, Yamaoka M, Hige S, Kang JH, Abe K, Mochida S, Watanabe M, Kurosaki M, Asahina Y, Izumi N, Honda M, Kaneko S, Tanaka E, Matsuura K, Itoh Y, Mita E, Korenaga M, Hino K, Murawaki Y, Hiasa Y, Ide T, Ito K, Sugiyama M, Ahn SH, Han KH, Park JY, Yuen MF, Nakamura Y, Tanaka Y, Mizokami M, Tokunaga K. No association for Chinese HBV-related hepatocellular carcinoma susceptibility SNP in other East Asian populations. *BMC Med Genet* 2012; **13**: 47 [PMID: 22712471 DOI: 10.1186/1471-2350-13-47]

98 **Sopipong W**, Tangkijvanich P, Payungporn S, Posuwan N, Poovorawan Y. The KIF1B (rs17401966) single nucleotide polymorphism is not associated with the development of HBV-related hepatocellular carcinoma in Thai patients. *Asian Pac J Cancer Prev* 2013; **14**: 2865-2869 [PMID: 23803045 DOI: 10.7314/APJCP.2013.14.5.2865]

99 **Zhong R**, Tian Y, Liu L, Qiu Q, Wang Y, Rui R, Yang BF, Duan SY, Shi JX, Miao XP, Wang L, Li H. HBV-related hepatocellular carcinoma susceptibility gene KIF1B is not associated with development of chronic hepatitis B. *PLoS One* 2012; **7**: e28839 [PMID: 22363396 DOI: 10.1371/journal.pone.0028839]

100 **Al-Qahtani A**, Al-Anazi M, Viswan NA, Khalaf N, Abdo AA, Sanai FM, Al-Ashgar H, Al-Ahdal M. Role of single nucleotide polymorphisms of KIF1B gene in HBV-associated viral hepatitis. *PLoS One* 2012; **7**: e45128 [PMID: 23028799 DOI: 10.1371/journal.pone.0045128]

101 **Jiang DK**, Ma XP, Wu X, Peng L, Yin J, Dan Y, Huang HX, Ding DL, Zhang LY, Shi Z, Zhang P, Yu H, Sun J, Lilly Zheng S, Deng G, Xu J, Liu Y, Guo J, Cao G, Yu L. Genetic variations in STAT4,C2,HLA-DRB1 and HLA-DQ associated with risk of hepatitis B virus-related liver cirrhosis. *Sci Rep* 2015; **5**: 16278 [PMID: 26538132 DOI: 10.1038/srep16278]

102 **Clark A**, Gerlach F, Tong Hv, Hoan NX, Song le H, Toan NL, Bock CT, Kremsner PG, Velavan TP. A trivial role of STAT4 variant in chronic hepatitis B induced hepatocellular carcinoma. *Infect Genet Evol* 2013; **18**: 257-261 [PMID: 23748017 DOI: 10.1016/j.meegid.2013.05.025]

103 **Kim LH**, Cheong HS, Namgoong S, Kim JO, Kim JH, Park BL, Cho SW, Park NH, Cheong JY, Koh I, Shin HD, Kim YJ. Replication of genome wide association studies on hepatocellular carcinoma susceptibility loci of STAT4 and HLA-DQ in a Korean population. *Infect Genet Evol* 2015; **33**: 72-76 [PMID: 25913043 DOI: 10.1016/j.meegid.2015.04.013]

104 **Lu Y**, Zhu Y, Peng J, Wang X, Wang F, Sun Z. STAT4 genetic polymorphisms association with spontaneous clearance of hepatitis B virus infection. *Immunol Res* 2015; **62**: 146-152 [PMID: 25829184 DOI: 10.1007/s12026-015-8645-1]

105 **Wen J**, Song C, Jiang D, Jin T, Dai J, Zhu L, An J, Liu Y, Ma S, Qin N, Liang C, Chen J, Jiang Y, Yang L, Liu J, Liu L, Geng T, Chen C, Jiang J, Chen J, Zhu F, Zhu Y, Yu L, Shen H, Zhai X, Xu J, Hu Z. Hepatitis B virus genotype, mutations, human leukocyte antigen polymorphisms and their interactions in hepatocellular carcinoma: a multi-centre case-control study. *Sci Rep* 2015; **5**: 16489 [PMID: 26568165 DOI: 10.1038/srep16489]

106 **Ji X**, Zhang Q, Li B, Du Y, Yin J, Liu W, Zhang H, Cao G. Impacts of human leukocyte antigen DQ genetic polymorphisms and their interactions with hepatitis B virus mutations on the risks of viral persistence, liver cirrhosis, and hepatocellular carcinoma. *Infect Genet Evol* 2014; **28**: 201-209 [PMID: 25281206 DOI: 10.1016/j.meegid.2014.09.032]

107 **Zhang X**, Zheng C, Zhou ZH, Li M, Gao YT, Jin SG, Sun XH, Gao YQ. Relationship between HLA-DP gene polymorphisms and the risk of hepatocellular carcinoma: a meta-analysis. *Genet Mol Res* 2015; **14**: 15553-15563 [PMID: 26634522 DOI: 10.4238/2015.December.1.6]

108 **Hai H**, Tamori A, Kawada N. Role of hepatitis B virus DNA integration in human hepatocarcinogenesis. *World J Gastroenterol* 2014; **20**: 6236-6243 [PMID: 24876744 DOI: 10.3748/wjg.v20.i20.6236]

109 **Katrinli S**, Ozdil K, Sahin A, Ozturk O, Kir G, Baykal AT, Akgun E, Sarac OS, Sokmen M, Doğanay HL, Dinler Doğanay G. Proteomic profiling of HBV infected liver biopsies with different fibrotic stages. *Proteome Sci* 2017; **15**: 7 [PMID: 28439208 DOI: 10.1186/s12953-017-0114-4]

110 **Casper M**, Grünhage F, Lammert F. Cancer risk in chronic hepatitis B: Do genome-wide association studies hit the mark? *Hepatology* 2011; **53**: 1390-1392 [PMID: 21480342 DOI: 10.1002/hep.24241]

111 **Budhu A**, Wang XW. Power play: scoring our goals for liver cancer with better GWAS study design. *J Hepatol* 2011; **54**: 823-824 [PMID: 21167853 DOI: 10.1016/j.jhep.2010.10.035]

112 **Zhu H**, Wu J, Shen X. Genome-wide association study: new genetic insights into HBV/HCV-related hepatocellular carcinoma genomes. *Scand J Gastroenterol* 2017; **52**: 209-215 [PMID: 27797287 DOI: 10.1080/00365521.2016.1245778]

113 **Tai DI**, Jeng WJ, Lin CY. A global perspective on hepatitis B-related single nucleotide polymorphisms and evolution during human migration. *Hepatol Commun* 2017; **1**: 1005-1013 [PMID: 29404438 DOI: 10.1002/hep4.1113]

P- Reviewer: Aghakhani A, Enomoto M, Gong ZG, Tai DI
S- Editor: Wang XJ **L- Editor**: A **E- Editor**: Yin SY

World Journal of Gastroenterology

Submit a Manuscript: http://www.f6publishing.com

World J Gastroenterol 2018 August 14; 24(30): 3361-3373

DOI: 10.3748/wjg.v24.i30.3361

ISSN 1007-9327 (print) ISSN 2219-2840 (online)

MINIREVIEWS

Current guidelines for the management of non-alcoholic fatty liver disease: A systematic review with comparative analysis

Simona Leoni, Francesco Tovoli, Lucia Napoli, Ilaria Serio, Silvia Ferri, Luigi Bolondi

Simona Leoni, Francesco Tovoli, Lucia Napoli, Ilaria Serio, Silvia Ferri, Luigi Bolondi, Department of Medical and Surgical Sciences (DIMEC), Division of Internal Medicine, University of Bologna, Bologna 40136, Italy

ORCID number: Simona Leoni (0000-0001-8825-9698); Francesco Tovoli (0000-0002-8350-1155); Lucia Napoli (0000-0002-5499-9310); Ilaria Serio (0000-0002-6676-4148); Silvia Ferri (0000-0002-6033-8594); Luigi Bolondi (0000-0002-1021-6388).

Author contributions: All authors equally contributed to this paper with conception and design of the study, literature review and analysis, drafting and critical revision, editing and approval of final version.

Conflict-of-interest statement: To the best of our knowledge, no conflict of interest exists.

Manuscript source: Invited manuscript

Correspondence to: Simona Leoni, MD, PhD, Doctor, Department of Medical and Surgical Sciences (DIMEC), Division of Internal Medicine, University of Bologna, via Massarenti 9, Bologna 40138, Italy. simona.leoni@aosp.bo.it
Telephone: +39-51-2142214
Fax:+39-51-2142725

Received: May 9, 2018
Peer-review started: May 10, 2018
First decision: May 24, 2018
Revised: May 31, 2018
Accepted: June 25, 2018

Article in press: June 25, 2018
Published online: August 14, 2018

Abstract

The current epidemic of non-alcoholic fatty liver disease (NAFLD) is reshaping the field of hepatology all around the world. The widespread diffusion of metabolic risk factors such as obesity, type2-diabetes mellitus, and dyslipidemia has led to a worldwide diffusion of NAFLD. In parallel to the increased availability of effective anti-viral agents, NAFLD is rapidly becoming the most common cause of chronic liver disease in Western Countries, and a similar trend is expected in Eastern Countries in the next years. This epidemic and its consequences have prompted experts from all over the word in identifying effective strategies for the diagnosis, management, and treatment of NAFLD. Different scientific societies from Europe, America, and Asia-Pacific regions have proposed guidelines based on the most recent evidence about NAFLD. These guidelines are consistent with the key elements in the management of NAFLD, but still, show significant difference about some critical points. We reviewed the current literature in English language to identify the most recent scientific guidelines about NAFLD with the aim to find and critically analyse the main differences. We distinguished guidelines from 5 different scientific societies whose reputation is worldwide recognised and who are representative of the clinical practice in different geographical regions. Differences were noted in: the definition of NAFLD, the opportunity of NAFLD screening in high-risk patients, the non-invasive test proposed for the diagnosis of NAFLD and the identification of NAFLD patients with advanced fibrosis, in the follow-up protocols and, finally, in the treatment strategy (especially in the proposed pharmacological management). These difference have been discussed in the light of the possible evolution of the scenario of

NAFLD in the next years.

Key words: Non-alcoholic fatty liver disease; Metformin; Liver steatosis; Liver biopsy; Non-invasive diagnosis; Pioglitazone; Clinical guidelines

Core tip: Non-alcoholic fatty liver disease (NAFLD) is becoming the most common cause of chronic liver disease. As such, an increasing number of scientific reports are investing this condition. To translate these evidence into clinical practice, international scientific societies have proposed guidelines for the management of NAFLD. In this review, we will critically analyse both the converging and diverging points in the current clinical guidelines of NAFLD, with a particular focus on the diagnostic and therapeutic aspects.

Leoni S, Tovoli F, Napoli L, Serio I, Ferri S, Bolondi L. Current guidelines for the management of non-alcoholic fatty liver disease: A systematic review with comparative analysis. *World J Gastroenterol* 2018; 24(30): 3361-3373 Available from: URL: http://www.wjgnet.com/1007-9327/full/v24/i30/3361.htm DOI: http://dx.doi.org/10.3748/wjg.v24.i30.3361

INTRODUCTION

Non-alcoholic fatty liver disease (NAFLD) includes a spectrum of disorders ranging from the simple fatty liver to non-alcoholic steatohepatitis, with increasing fibrosis leading to cirrhosis[1]. The prevalence of NAFLD is alarmingly growing worldwide in adult and children/adolescent populations, with a bidirectional association between NAFLD and metabolic syndrome[2]. Obesity, insulin resistance, type 2 diabetes mellitus, and dyslipidemia are the most relevant metabolic conditions related to this spectrum of diseases[1,2].

Clinicians and researchers from several scientific Associations worldwide put significant efforts into increasing knowledge and developing high-quality International Guidelines to improve the management of NAFLD patients in clinical practice. Multidisciplinary panels of experts in different continents have performed systematic analysis and review of the literature on specified topics in the last years. These efforts have led to the creation and publication of various Guidelines.

This paper aims to review and compare the most recently published International Guidelines for the diagnosis and the management of NAFLD in adult populations, to critically evaluate similarities and discrepancies. In particular, we tried to analyse some critical questions and challenges for clinicians in real life.

LITERATURE SEARCH

We performed a database search on PubMed selecting papers published between January 2016 and January 2018 in the English language. The following keywords and terms were considered: (1) Fatty liver disease (("fatty liver"[MeSH Terms] OR ("fatty"[All Fields] AND "liver"[All Fields]) OR "fatty liver"[All Fields]) AND ("disease"[MeSH Terms] OR "disease"[All Fields])) AND guideline ("guideline"[Publication Type] OR "guidelines as topic"[MeSH Terms] OR "guideline"[All Fields]) *AND management* ("organization and administration"[MeSH Terms] OR ("organization"[All Fields] AND "administration"[All Fields]) OR "organization and administration"[All Fields] OR "management"[All Fields] OR "disease management"[MeSH Terms] OR ("disease"[All Fields] AND "management"[All Fields]) OR "disease management"[All Fields]); (2) Fatty liver disease AND recommendation (("fatty liver"[MeSH Terms] OR ("fatty"[All Fields] AND "liver"[All Fields]) OR "fatty liver"[All Fields]) AND ("disease"[MeSH Terms] OR "disease"[All Fields])) AND recommendation[All Fields]; (3) Fatty liver disease and position paper (("fatty liver"[MeSH Terms] OR ("fatty"[All Fields] AND "liver"[All Fields]) OR "fatty liver"[All Fields]) AND ("disease"[MeSH Terms] OR "disease"[All Fields])) AND (position[All Fields] AND ("paper"[MeSH Terms] OR "paper"[All Fields])).

According to this criteria, 119 papers were identified. As a second step, we excluded papers which were not pertinent to any of the following criteria: (1) Clinical Guidelines related to diagnosis and management of NAFLD in the adult population; (2) clinical Guidelines published by Governmental agencies and Scientific Associations.

According to the selection criteria, out of 119 results of PubMed research, 5 Guidelines were finally included in this analysis. These guidelines are strictly focused on the topic of diagnosis and management of NAFLD in adult, excluding pediatric populations and special groups. In detail, the five selected papers included (from the oldest to the newest date of publication): (1) "EASL-EASD-EASO Clinical Practice Guidelines for the management of non-alcoholic fatty liver disease" by the European Association for the Study of The Liver (EASL), published in 2016[3]; (2) "Nonalcoholic fatty liver disease (NAFLD): Assessment and management" by the National Institute for Health and Care Excellence (NICE), published in 2016[4]; (3)"Asia-Pacific Working Party on Non-Alcoholic Fatty Liver Disease guidelines" published in 2017[5,6]; (4) Italian Association for the Study of the Liver (AISF). AISF position paper on nonalcoholic fatty liver disease (NAFLD): Updates and future directions, published in 2017[7]; (5) "The diagnosis and Management of Nonalcoholic Fatty Liver Disease: Practice Guidance From the American Association for the Study of Liver Diseases" published in 2018[8].

OPEN QUESTIONS

Definition, classification, and diagnostic criteria of NAFLD

Definition and classification: A definition of NAFLD

Table 1 Diagnostic criteria for non-alcoholic fatty liver disease according to the various guidelines

	EASL	NICE	Asia-Pacific	AISF	AASLD
Required criteria	Steatosis in > 5% of hepatocytes by either imaging or histology No other causes of steatosis Insulin resistance	Excessive fat in the liver No other causes of steatosis No significant alcohol consumption	Hepatic steatosis by either imaging or histology No other causes of steatosis No significant alcohol consumption	Hepatic steatosis on either imaging or histology No other causes of steatosis No significant alcohol consumption	Evidence of hepatic steatosis either by imaging or histology No other causes of steatosis No significant alcohol consumption No coexisting chronic liver disease
Alcohol consumption threshold (men)	30 g/d	30 g/d	2 standard drink/d 140 g/wk	30 g/d	21 standard drink/wk 294 g/wk
Alcohol consumption threshold (women)	20 g/d	20 g/d	1 standard drink/d 70 g/wk	20 g/d	14 standard drink/wk 196 g/wk

EASL: European Association for the Study of the Liver; NICE: National Institute for Health and Care Excellence; AISF: Italian Association for the study of the Liver; AASLD: American Association for the Study of Liver Diseases; MRI: Magnetic resonance imaging.

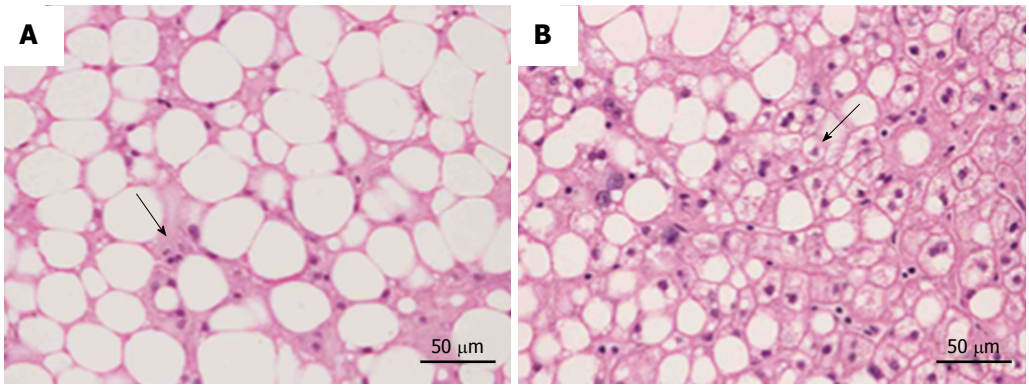

Figure 1 Main difference between non-alcoholic fatty liver and non-alcoholic steatohepatitis. A: Non-alcoholic fatty liver; B: Non-alcoholic steatohepatitis. NAFL is characterized by minimal inflammatory infiltrate without hepatocyte ballooning (arrow). Instead, NASH is associated with lobular inflammatory infiltrate and hepatocyte degeneration (arrow). NAFL: Non-alcoholic fatty liver; NASH: Non-alcoholic steatohepatitis.

is reported in all Guidelines (Table 1). The characteristic points of NAFLD definition include (1) the evidence of excessive hepatic fat accumulation in the liver parenchyma (detected by imaging techniques or histology); (2) the absence of other secondary causes of hepatic fat. Out of them, to strictly define NAFLD patients a significant ongoing or recent alcohol consumption have to be excluded in all recommendation[3-8].

All recommendations identify some different clinical-pathological entities, according to the progression of hepatic histological changes. Simple steatosis and non-alcoholic steatohepatitis (NASH) are defined in all guidelines[3-8]. In detail simple steatosis, also called non-alcoholic fatty liver (NAFL) includes all of the case characterized by steatosis with minimal or absent lobular inflammation. On the contrary, NASH is characterized by hepatocyte ballooning degeneration, diffused lobular inflammation and fibrosis (Figure 1)

Additionally, EASL Asia-Pacific Guidelines and AISF position paper also underline the problem of NAFLD-related HCC, potentially occurring in patients with NAFLD but without cirrhosis[9,10].

Diagnostic criteria: The role of alcohol: The agreement between the different guidelines is not complete when defining the threshold dose of alcohol consumption. As shown in Table 1, EASL[3], NICE, and AISF guidelines[3,4,7] consider as significant an alcohol consumption > 30 g/d in men and > 20 g/d in women. The AASLD guidance[8] indicate the reasonable threshold for significant alcohol consumption > 21 standard drink on average per week in men and > 14 in women. For Asia-Pacific Guidelines[5] a significant alcohol intake was considered > 7 standard alcoholic drinks/week (70 g ethanol) in women and > 14 (140 g) in men.

Who should be screened for NAFLD?

According to the screening programs adopted for other diseases, systematic screening has to be performed for significant health problem with available diagnostic facilities and accepted treatment. Also, there should be recognisable latent or early symptomatic stage, identifiable with sensitive tests. To adequately perform a screening program, the natural history of the disease should be understood, and the economic burden should

Table 2 Comparative analysis of the recommendations regarding the screening for non-alcoholic fatty liver disease

	EASL	NICE	Asia-Pacific	AISF	AASLD
Systematic screening	No	No	No	No	No
Screening in high-risk groups	Yes Obesity Metabolic syndrome Abnormal liver enzymes	Yes Obesity Type Ⅱ Diabetes	Yes Obesity Type Ⅱ Diabetes	Not mentioned	No[1]
Screening modality	Yes liver enzymes	No liver enzymes Yes ultrasonography	No liver enzymes Yes ultrasonography Yes transient elastography		

[1]"Active surveillance" (but not screening) suggested for patients with type Ⅱ diabetes mellitus. EASL: European Association for the Study of the Liver; NICE: National Institute for Health and Care Excellence; AISF: Italian Association for the Study of the Liver; AASLD: American Association for the Study of Liver Diseases.

be suitable.

The international guidelines partially diverge about this topic. This disagreement derives from essential considerations regarding natural history, special groups, diagnosis, and therapy: (1) NAFLD in a common cause of chronic liver disease in general population but cause severe liver disease in a small proportion of affected people[1]; (2)Type Ⅱ diabetes patients have higher prevalence of NAFLD, NASH and advanced fibrosis[11-13]; (3) There is a current lack of effective drug treatment; (4) Liver biopsy is a procedure with related risks; (6) Few cost-effective analysis are available[14].

All these considerations imply a different approach to screening in NAFLD by the Scientific Societies. Only EASL, NICE Asia-Pacific Guidelines[3-5] recommend screening respectively in particular, "high-risk" groups (Table 2). On the contrary, AASLD guidelines emphasise that, to date, there is no evidence of cost-effectiveness to support a NAFLD screening in adults even if they have several metabolic risk factors, instead suggesting a concept of "vigilance" in these populations[8].

Which noninvasive test(s) should be used to diagnose NAFLD?

Worldwide guidelines agree that, whenever NAFLD is suspected, the initial diagnostic workup should include a noninvasive imaging examination to confirm the presence of steatosis and general liver biochemistry[3-8]. Non-invasive assessment should aim first of all to identify NAFLD among patients with metabolic risk factors, and then to monitor disease progression and treatment response, identifying patients with the worst prognosis[3].

Imaging: There is a consensus for using abdominal ultrasound (US) as the first-line examination to identify liver steatosis in patients with increased liver blood exams or suspected NAFLD, in daily clinical practice (Figure 2). The main advantages of US derive from its broad availability and low cost. However, its sensitivity among morbidly obese patients (BMI > 40 kg/m^2) is low, and it may miss the diagnosis when the liver hepatic fat content is < 20%[15,16]. Despite these limitations, EASL and AISF underline how ultrasound can significantly assess moderate and severe steatosis, even if an observer dependency remains[15]. NICE guidelines propose to use liver ultrasound to detect hepatic steatosis for children with metabolic syndrome and type 2 diabetes and to retest it every three years if the first examination is negative[4].

On the other hand, magnetic resonance imaging (MRI), either by proton density fat fraction (^{1}H-MRS) or spectroscopy, remains the gold standard to assess and quantify hepatic steatosis, detecting the amount of liver fat as low as 5%-10%, its use in the clinical practice is still limited. In fact, despite its robust accuracy, its limited availability, high costs and a long time of execution, make the procedure not recommended in the daily clinical setting[17]. Asia-Pacific guidelines specify that ^{1}H-MRS is the best option to quantify even moderate changes in liver fat content in clinical trials, considering its high sensitivity compared to histological-proven liver fat reversal. Similarly, EASL guidelines highlight its role, primarily as screening imaging examination for clinical trials and experimental studies[3].

Another imaging technique used to quantify liver fat content is the ultrasonography-based transient elastography (TE) using continuous attenuation parameter (CAP). This promising tool has shown a good sensitivity, measuring simultaneously liver stiffness, potentially evaluating NAFLD severity at the same setting[13]. However, despite its low cost and rapidity of execution, its role in the clinical practice has still to be defined. In fact, EASL guidelines specify that TE has never been compared with hepatic steatosis measured by ^{1}H-MRS and there are limited data about its ability to discriminate different histological patterns[3]. On the other hand, Asia-Pacific guidelines propose CAP as a useful screening tool for NAFLD diagnosis, as well as for demonstrating improvement in hepatic steatosis after lifestyle intervention and body weight reduction[5].

Conventional liver biochemistry: Although NAFLD may present by standard laboratory liver tests, frequently a slight increase of aspartate aminotransferase (AST) or alanine aminotransferase (ALT) or gamma-glutamyl transpeptidase (GammaGT) is observed. However, all the guidelines agree that normal levels of liver enzymes may not exclude NAFLD, being a not sensitive screening

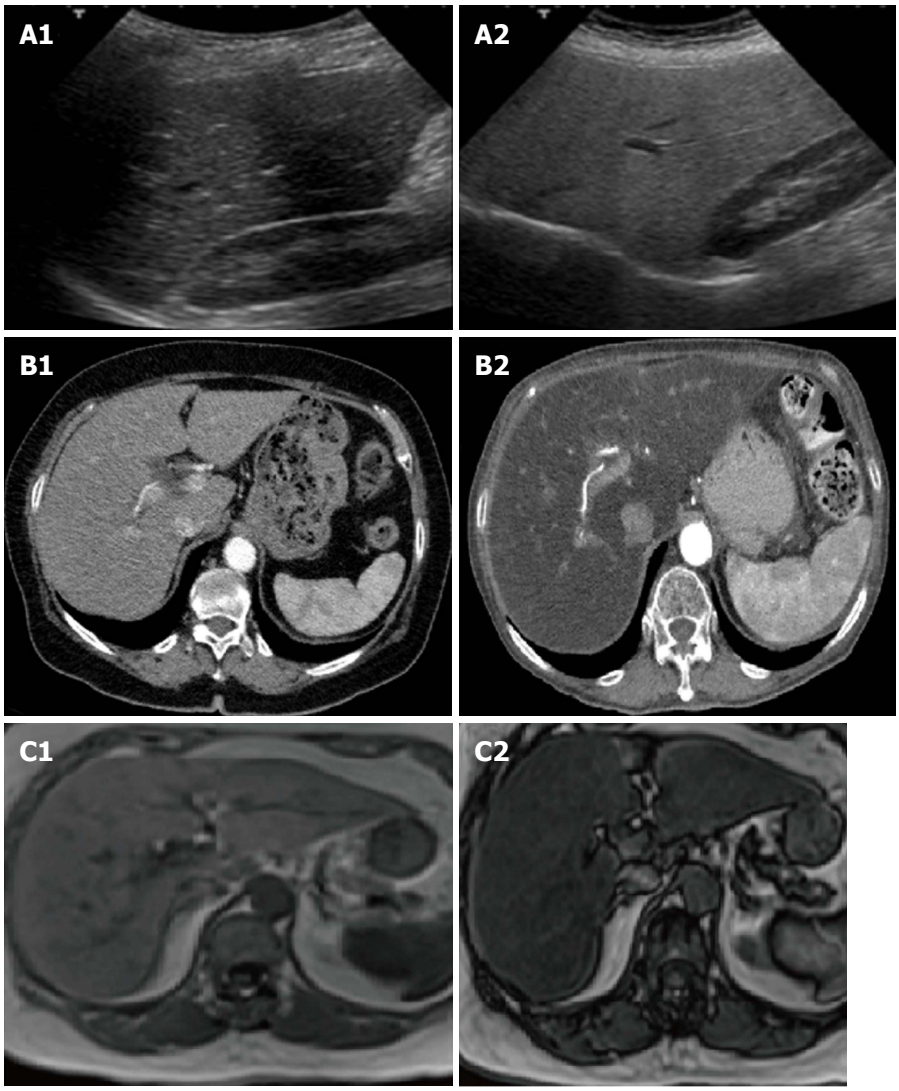

Figure 2 Aspects of liver steatosis according to the different imaging techniques. In normal ultrasound examination liver parenchyma is isoechoic to the renal parenchyma in normal conditions (A1), becoming hyperechoic in presence of liver steatosis (A2). In comparison to a normal liver (B1), a fatty liver appears hypodense compared to the spleen and to the hepatic veins (B2) in computed tomography scans. Finally, in the setting of a severe steatosis, the magnetic resonance signal has a clear fall from in phase (C1) to out phase sequencings (C2).

test[3-8].

Moreover, laboratory alterations may hide another cause of liver disease, in which steatosis is a coexisting condition. On the other hand, detection of abnormalities of laboratory exams (such as ferritin or autoantibodies) not always reflects the presence of another liver disease, but could be an epiphenomenon of NAFLD with no further clinical significance.

In particular, AASLD guidelines underline that elevate serum ferritin and low titers of autoimmune antibodies (especially antinuclear and anti-smooth muscle antibodies) are common features among NAFLD patients[18,19], and may not automatically indicate the presence of hemochromatosis or autoimmune liver disease[8].

Which is the role of diagnostic and prognostic scores?

Noninvasive predictor biomarkers and scores of steatosis and steatohepatitis: The current absence of a highly specific and sensitive noninvasive marker predicting inflammation and fibrosis is leading to a considerable interest in the identification of new markers of disease progression and to the development of clinical scores of disease severity.

To assess the presence of steatosis, EASL, Asia-Pacific, and Italian guidelines mention the Fatty Liver Index (FLI)[20] and the NAFLD liver fat score[21]. Both of these scores are easily calculated using common blood exams and simple clinical information. In detail, FLI is calculated from serum triglyceride, body mass index, waist circumference, and gamma-glutamyltransferase[20], while NAFLD liver fat score is calculated evaluating the presence/absence of metabolic syndrome and type 2 diabetes, fasting serum insulin, and aminotransferases[21]. They have been validated in a cohort of severely obese patients and the general population, reliably predicting the presence of steatosis, but not its severity[22]. On the contrary, the AASLD guidelines underline that only inflammation and fibrosis dictate the prognosis of NAFLD patients and, consequently, highlight the lack of evidence

of the usefulness of quantifying hepatic steatosis in the routine clinical setting. Instead, AASLD guidelines underline that the simultaneous presence of several metabolic diseases is the most potent predictor of hepatic inflammation and adverse outcome in patients with NAFLD.

The cytokeratin-18 fragment is currently the most studied biomarker to assess the presence of inflammation. Its circulating levels have been largely investigated as a signal of hepatocellular apoptotic activity and therefore as a characteristic feature of NASH[23]. Its role is addressed both by Asia-Pacific and EASL guidelines, which agree that the current evidence does not support its use in clinical practice and that more studies are needed[3,5]. In particular, Asia-Pacific guidelines highlight how increased levels of cytokeratin-18 have good predictive value for NASH *vs* normal livers but do not differentiate NASH *vs* simple steatosis[24,25]. On the other hand, EASL guidelines specify that has been demonstrated that cytokeratin-18 serum levels decrease parallel with histological improvement, but its predictive value is not better than ALT in identifying histological responders[26].

To conclude, guidelines agree that noninvasive tests for detecting NASH and distinguishing it from simple steatosis are not currently available and that liver biopsy remains necessary to detect hepatocyte ballooning and lobular inflammation[3-8].

Noninvasive assessment of advanced fibrosis: Liver fibrosis is considered the leading prognostic factor among patients with NAFLD because of its strong correlation with survival rate and liver-related outcomes[27]. Therefore, NAFLD patients with advanced fibrosis need a closer monitoring and a rigorous adherence to treatment. However, to date, no methods easily performed in daily clinical practice and with a high predictive value for differentiating grades of liver fibrosis have been identified.

Different tools have been investigated at this purpose, including noninvasive scores (NAFLD fibrosis score, Fibrosis 4 calculator, AST/ALT ratio index), serum biomarkers (ELF panel, Fibrometer, Fibrotest, Hepascore) and imaging techniques, such as transient elastography, magnetic resonance elastography (MRE) and shear wave elastography[28].

According to the NICE guideline, the enhanced liver fibrosis (ELF) blood test has shown the best cost-effectiveness in identifying patients with advanced fibrosis stages[29] and therefore should be offered to all patients with an incidental diagnosis of NAFLD[4]. On the other hand, EASL and Italian guidelines suggest the use of NAFLD fibrosis score (NFS) and Fibrosis 4 calculator (FIB-4) as noninvasive scores to identify patients with different risk of advanced fibrosis[3,7]. These two scores have been validated in various ethnically NAFLD patients, predicting liver and cardiovascular-related mortality[30]. Moreover AASLD guidelines highlight that in a recent study both NFS and FIB-4 have shown the best predictive value for advanced fibrosis among histological proven NAFLD patients in comparison with other scores[28]. EASL guidelines underline that NFS has a stronger negative predictive value for advanced fibrosis than the corresponding positive predictive value[30]. Hence, it should be used for excluding the presence of advanced fibrosis better than stratifying NAFLD patients on different fibrosis stages[3].

Transient elastography has been recently approved by US Food and Drug Administration to investigate adult and pediatric patients with liver disease. Its cut-off value for advanced fibrosis for adults with NAFLD has been established to 9.9 KpA with 95% sensitivity and 77% specificity[31]. In particular, elastography score has been shown to have good diagnostic accuracy for the presence of clinically significant fibrosis, with an AUROC of 0.93 (95%CI: 0.89-0.096) for advanced fibrosis ($\geqslant$ F3) and cirrhosis, and with a negative predictive value of 90% in ruling out cirrhosis when using a cut-off of 7.9 kPa. However, the ability in differentiating between F2 and F3 fibrosis seems less robust. Because of this high rate of false-positive results, EASL and Asia-Pacific guidelines point out that its low specificity limits its use in daily practice in diagnosing advanced grade of fibrosis and cirrhosis, as well as by a high failure rate[5]. Moreover considering the unreliable results among patients with high BMI and thoracic fold thickness, EASL guidelines highlight that it should not be used alone as first-line detection tool to identify advanced fibrosis or cirrhosis[3]. In this setting, its poor performance can be improved by using M or XL-probe, increasing the success rate[32,33].

American guidelines underline the vital role of magnetic resonance elastography (MRE) in identifying different degrees of fibrosis in patients with NAFLD, performing better than transient elastography for recognising intermediate stage of fibrosis, but showing a same predictive value for advanced fibrosis stages[34]. Therefore AASLD guidelines conclude that MRE and transient elastography are both useful tools for identifying NAFLD patients with advanced liver fibrosis.

On the other hand, shear wave elastography, in the same way as transient elastography, seems to be inappropriate to discriminate between intermediate stages of fibrosis and provide reliable results only in 73% of patients with BMI $\geqslant$ 30 kg/m^2[35].

Which are the best diagnostic algorithms and follow-up strategies?

The optimal strategy for stratifying NAFLD patients and follow disease progression has not been yet established. According to EASL and Italian guidelines, the combination of noninvasive scores (NFS and FIB-4) and transient elastography should be used to identify patients at low risk of advanced liver disease and for clinical decision-making. Moreover, this combination may instead identify patients who should undergo a liver biopsy to confirm advanced fibrosis, and in whom a more intensive approach is needed)[3,7]. Noninvasive serum scores should be calculated for every patient with

NAFLD to exclude the presence of significant fibrosis. If it cannot be ruled out, then transient elastography should be performed. Hence, if advanced fibrosis is suspected, liver biopsy should be performed for final diagnosis[3,7]. Moreover, a clinical, laboratory and instrumental follow-up for noninvasive monitoring of fibrosis, is suggested every two years for NAFLD patients with normal liver enzymes and low risk of advanced fibrosis. Patients with evidence of NASH or fibrosis should be screened annually and those with cirrhosis every six months, to perform HCC surveillance[3,7].

Similarly, the AASLD guidelines consider NFS, FIB-4, transient elastography, and MRE as the first-line examination to detect patients with advanced fibrosis[8]. Differently from the EASL guidance, however, no diagnostic algorithms or follow up strategies are provided.

The Asia-Pacific guidelines also agree that combined use of serum tests and imaging tools may offer more reliable information than using either method alone[6]. However, they do not specify which noninvasive test is best.

According to the NICE guidelines, every patient with an incidental finding of NAFLD should be screened for advanced fibrosis by ELF blood test. If negative, it should be repeated every three years for adults and two years for children. Moreover, children and young people with type 2 diabetes mellitus or metabolic syndrome, but without steatosis at ultrasound examination, should be reevaluated every three years[4].

Who should undergo liver biopsy?

To date, liver biopsy is the gold standard for diagnosing NASH and staging liver fibrosis, despite several limitations such as sampling error, variability in interpretation by pathologists, high cost and patient discomfort[36]. The "NAFLD Activity Score" (NAS)[37] and the "Steatosis Activity Fibrosis" (SAF) scoring system[38] are recommended to assess disease activity[8].

Except for the NICE guidelines (which do not provide specific indications about which patients should undergo liver biopsy), all of the remaining guidelines substantially agree that confirmatory liver biopsy should not be performed in every NAFLD patients. Instead, it should be reserved for the following two situations: (1) Uncertain diagnosis; (2) suspect of NAFLD-related advanced liver disease.

The AASLD guidelines suggest to perform liver biopsy in patients with metabolic syndrome who are at increased risk of liver inflammation, or when NFS, FIB-4 or liver stiffness measured by transient elastography or MRE suggest the presence of advanced liver fibrosis. In that case, patients would benefit the most from diagnosis, obtaining crucial prognostic information[8].

Similarly, EASL and Italian guidelines recommend performing a liver biopsy when both serum and imaging noninvasive tools show a medium/high risk of advanced liver disease, with the aim to confirm the presence of advanced liver fibrosis. Furthermore, they underline that in selected NAFLD patients at high risk of disease progression, the repetition of liver biopsy should be considered case-by-case every five years[3,7]. On the other hand, the Asia-Pacific guidelines recommend biopsy only when a competing aetiology of chronic liver disease cannot be excluded just by laboratory exams and personal anamnesis, or results of noninvasive tests are inconclusive[5,6].

How to treat NAFLD?

Lifestyle changes: Lifestyle modification consisting of diet, exercise, and weight loss has been advocated to treat patients with NAFLD in all guidelines (Tables 3 and 4). Indeed**,** weight loss has been reported as a keystone element in improving the histology features of NASH[39,40].

According to the AISF position paper[7], the best therapeutic approach is an adequate lifestyle change focused on weight loss and achieved by physical activity (aerobic activities and resistance training) and healthy diet. In particular, an energy restriction obtained with a low calorie (1200-1600 kcal/d), low fat (less than 10% of saturated fatty acid), low carbohydrate diet (< 50% of total kcal) is suggested. A Mediterranean diet is recommended as the most effective dietary option to induce a weight loss together with beneficial effects on all cardio-metabolic risk factors associated with NAFLD[7].

The Asia-Pacific guidelines agree with a lifestyle intervention strategy for the treatment of NAFLD, focusing the attention on the timing of weight loss that should be gradual because of the deleterious effect of crash diets on NASH. Very low-calorie diets are considered unsustainable, and any specific regimen is preferred over the others[6].

Also, the EASL[3], NICE[4], and AASLD[8] guidelines recommend structured programmes aimed at lifestyle changes towards a healthy diet and habitual physical activity. According to all of these guidelines, a 7%-10% weight loss is the target of most lifestyle interventions.

Pharmacological treatment: (1) Who to treat: According to the EASL guidelines[3], pharmacological therapy should be reserved for: Progressive NASH (bridging fibrosis and cirrhosis); early-stage NASH at high risk for disease progression (age > 50 years, metabolic syndrome, diabetes mellitus or increased ALT)[41]; active NASH with high necroinflammatory activities[42]. Similarly, in the AASLD and Asia-Pacific guidelines, a pharmacological approach is recommended only for patients with NASH and fibrosis[8]. In the NICE guidance, just people with an advanced liver fibrosis (ELF test > 10.51) are proposed for pharmacological treatment[4]. In the AISF position paper, drug therapy is suggested for patients who are at high risk for disease progression[7]. (2) Pharmacologic treatment: Currently, no drugs have been approved for the treatment of NASH by the US Food and Drug Administration or by the European Medicines Agency. All guidelines acknowledge that any medicines

Table 3 Comparison of recommendations about non-invasive evaluation of fibrosis and follow up strategies

	EASL	NICE	Asia-Pacific	AISF	AASLD
Non-invasive evaluation	NFS and FIB-4 upon diagnosis. If inconclusive, perform transient elastography	ELF blood test	Combination of serum tests and imaging tools (no specification about the preferred tests)	NFS + FIB-4 upon diagnosis. If inconclusive, perform transient elastography	NFS, FIB-4 and transient elastography (or MRE) upon diagnosis
Follow up	Negative markers > reassess every 2 yr; Fibrosis or abnormal liver enzymes > reassess every year; Cirrhosis-> surveillance every 6 mo	Negative ELF test, > reassess every 3 yr; Positive ELF test > liver biopsy	No information provided	Negative markers > reassess every 2 yr; Fibrosis or abnormal liver enzymes > reassess every year; Cirrhosis > surveillance every 6 mo	No information provided

EASL: European Association for the Study of the Liver; NICE: National Institute for Health and Care Excellence; AISF: Italian Association for the study of the Liver; AASLD: American Association for the Study of Liver Diseases; NFS: NAFLD fibrosis score; FIB-4: Fibrosis-4; ELF: Enhanced Liver Fibrosis; MRE: Magnetic resonance elastography.

Table 4 Guidance statements about lifestyle interventions

	EASL	NICE	Asia-Pacific	AISF	AASLD
Dietary restrictions	500-1000 kcal deficit; weight loss of 500-1000 g/wk with a 7%-10% total weight loss	Main recommendations on diet of NICE's obesity and preventing excess weight gain guidelines	500-1000 kcal deficit	1200-1600 kcal/d; fat-low (< 30% of total calories); carbohydrate-low (< 50% of total calories)	500-1000 kcal deficit
Physical activity	Aerobic and resistance training (150-200 min/wk in 3-5 sessions)	Main recommendation of on physical activity of NICE's obesity and preventing excess weight gain guidelines	Aerobic and resistance training	Aerobic and resistance training	Aerobic and resistance training (> 150 min/wk)
Gold standard diet	Low-to-moderate fat and moderate-to-high carbohydrate intake Low-carbohydrate ketogenic diets or high-protein Mediterranean diet	No specific suggestions	All, excluding very low-calorie diets	Mediterranean diet	No specific suggestions

EASL: European Association for the Study of the Liver; NICE: National Institute for Health and Care Excellence; AISF: Italian Association for the Study of the Liver; AASLD: American Association for the Study of Liver Diseases.

prescribed explicitly for NAFLD should be considered as an off-label treatment and that the decision should be discussed with the patient, carefully balancing the benefits and the safety. However, the guidelines are widely discordant about possibly helpful drugs (Table 5).

Metformin: Due to the evidence of its limited efficacy in improving the histological features of NAFLD[43-45], metformin is not recommended by any guidelines to specifically treat NAFLD[3-8].

Pioglitazone: Pioglitazone, a thiazolidinedione, is a peroxisome proliferator-activated receptor (PPAR) gamma agonist with insulin-sensitising effects. Treatment with pioglitazone improves insulin sensitivity, aminotransferases, steatosis, inflammation, and ballooning in patients with NASH and prediabetes or T2DM[46]. The PIVENS trial (a large multicenter RCT) compared low dose pioglitazone (30 mg/d) *vs* vitamin E (800 UI/d) *vs* placebo for two years in patients without overt diabetes. Pioglitazone improved all histological features (except for fibrosis) and achieved resolution of NASH more often than placebo[47]. The histological benefit occurred together with ALT improvement and partial correction of insulin resistance. The main side effects of glitazones are weight gain[48-51], and bone fractures in women[52]. The use of pioglitazone for the treatment of NAFLD is endorsed both by the NICE and AASLD guidelines, with significant limitations. In the first case, pioglitazone should be prescribed only in second and third level centres, after a careful evaluation[4]. In the latter case, pioglitazone is reserved for patients with biopsy-proven NASH[8]. The EASL guidelines are more cautious, generically suggesting to consider pioglitazone for the treatment of diabetes in patients with a concurrent NAFLD[3]. Even the Asia-Pacific and the Italian guidelines acknowledge the potential benefits of pioglitazone, however, suggest that more evidence should be available before a firm recommendation can be made[6,7].

Vitamin E: Vitamin E is an anti-oxidant and has been investigated to treat NASH. In the PIVENS trial, vitamin E at a dose of 800 IU/d of α-tocopherol for 96 wk was associated with a decrease in serum aminotransferases and histological improvement in steatosis, inflammation,

Table 5 Recommendations about pharmacological treatment of non-alcoholic fatty liver disease

	EASL	NICE	ASIA-PACIFIC	AISF	AASLD
Metformin	Insufficient evidence	Not beneficial	Not beneficial	Not mentioned	Not beneficial
Vitamin E	Insufficient evidence	Consider use regardless of diabetes	Not beneficial	Insufficient evidence	Consider use in non-diabetic, biopsy-proven NASH
PPAR-gamma agonists	Consider use in selected diabetic patients	Consider pioglitazone in adults regardless of diabetes	Insufficient evidence in Asian	Insufficient evidence, potentially useful	Pioglitazone indicated in biopsy-proven NASH (regardless of diabetes)
PUFA	Not beneficial	Insufficient evidence	Not beneficial	Not mentioned	Not beneficial
Pentoxifylline	Insufficient evidence	Not mentioned	Not beneficial	Not mentioned	Not mentioned
GLP-1 analogues	Insufficient evidence, potentially useful	Insufficient evidence	Insufficient evidence in Asian patients	Insufficient evidence, potentially useful	Insufficient evidence
UDCA	Not beneficial	Not beneficial	Not mentioned	Not mentioned	Not beneficial
Obetycolic acid	Scarce evidence	Not mentioned	waiting for ongoing RCT results	Waiting for ongoing RCT results	Insufficient evidence
Silymarin	Not mentioned	Not mentioned	insufficient evidence, potentially useful	Not mentioned	Not mentioned
Statins	Safe but not beneficial	Safe but not beneficial	Safe but not beneficial	Safe but not beneficial	Safe but not beneficial

EASL: European Association for the Study of the Liver; NICE: National Institute for Health and Care Excellence; AISF: Italian Association for the Study of the Liver; AASLD: American Association for the Study of Liver Diseases; PPAR: Peroxisome proliferator-activated receptors; PUFA: Poly-unsaturated fatty acids; GLP-1: Glucagon-like peptide-1.

and ballooning and resolution of steatohepatitis in adults with NASH[47]. Long-term safety of vitamin E is under dispute, with two different meta-analyses leading to conflicting results when analysing the all-cause mortality in patients treated with t doses of > 800 IU/d[51,52]. Similarly to pioglitazone, vitamin E is recommended by the NICE and AASLD guidelines (limited to biopsy-proven NASH in the latter case)[4,8]. EASL and AISF guidelines call for more evidence before any recommendation[3,7], while Asia-Pacific guidelines advice against the use of vitamin E which is described as not beneficial by the current evidence[6].

Glucagon-like peptide-1 (GLP-1) analogues: Incretin-mimetics, acting on the glucose-insulin interplay have shown favourable results in pre-marketing studies on liver enzymes[53]. Also, in a published randomised, placebo-controlled trial consisting of 52 patients with biopsy-proven NASH, liraglutide administered sub-cutaneously once-daily for 48 wk was associated with greater resolution of NASH and less progression of fibrosis[54]. Both the AASLD and NICE recommendations state that there is still too few evidence to support the use of GLP-1 analogues to specifically treat liver disease in patients with NAFLD[4,8]. The remaining guidelines also agree on this point, however also state that further evidence may prove the efficacy of these drugs. In particular, the APASL guidelines consider some more elements in their recommendations. On the one hand, GLP-1 agonists appeared to reduce glycated haemoglobin more efficiently in Asian patients with type 2 diabetes mellitus[55]. On the other hand, there has been no study on Asian NASH patients, even if the pharmacokinetics of GLP-1 agonists do not appear to differ between Asian and non-Asian patients according to preliminary evidence[56,57].

Statins: Historically, the use of statins in patients with chronic liver diseases has been considered as potentially troublesome due to the risk of hepatotoxicity. At the same time, a considerable portion of NAFLD patients usually receives statins because of their multiple cardiovascular risk factors. Consequently, the primary concern of the guidelines is the safety of statins. In this regard, a recent review underlined the safety of statin and their efficacy in reducing the associated cardiovascular morbidity in patients with NAFLD, including those with slightly elevated alanine transaminases (up to 3 × reference upper limit)[58]. All of the guidelines agree about the safety of prescribing statins (or continuing an ongoing statin therapy) in patients with NAFLD, even with compensated cirrhosis. However, routine prescription of a statin is not recommended in patients with decompensated cirrhosis and acute liver failure[59,60].

Silymarin: Silymarinis a complex mixture of six major flavonolignans (silybins A and B, isosilybins A and B, silychristin, and silydianin), as well as other minor poly-phenolic compounds[61].In a randomised, double-blinded, placebo-controlled study on patients with biopsy-proven NASH, silymarin dosage of 700 mg three times daily for 48 wk resulted in a significantly higher percentage of fibrosis reduction compared with placebo (22.4% *vs* 6.0%, $P = 0.023$)[62]. The dosage was safe and well tolerated[62]. Silymarin is mentioned as a potentially use-ful treatment for NASH in Asia-Pacific guidelines only. However, optimal dose and duration still require further studies before a full recommendation[6].

Bariatric surgery: In patients unresponsive to lifestyle changes and pharmacotherapy, bariatric surgery is an option for reducing weight and metabolic complications, with stable results in the long-term[63]. Bariatric surgery can also improve liver histology, both regarding steatosis and ballooning[64,65] and fibrosis[65]. However, the presence

of established cirrhosis is associated with peri-operative risks. In particular, in the analysis performed from the Nationwide Inpatient Sample (1998-2007), mortality was higher in patients with compensated cirrhosis (0.9%) and much higher in those with decompensated cirrhosis (16.3%)[66]. No robust data on the comparative effects of different bariatric procedures on liver fat are available in the literature.

Based on the evidence as mentioned earlier, the EASL guidelines consider bariatric surgery an option in patients unresponsive to lifestyle changes and pharmacotherapy, for reducing weight and metabolic complications[3]. Guidance statements by the AASLD also consider a role of foregut bariatric surgery in otherwise eligible obese individuals with NAFLD or NASH[8].

The Asia-Pacific recommendation limits the role of bariatric surgery only to patients with class Ⅱ obesity (BMI > 32.5 kg/m^2 in Asians and 35 kg/m^2 in Caucasians)[6]. AISF and NICE guidelines do not mention bariatric surgery.

Liver transplantation: NASH is becoming the most common indication to liver transplantation in Western Countries[67]. Because of the high prevalence of obesity, sarcopenia, cardiovascular disease and chronic kidney disease among patients with NASH, there is a higher frequency of post-transplant complications and increased graft loss[68,69]. Because of the risk of prolonged ventilation, poor wound healing, higher rate of primary graft non-function, and increased infectious complications, patients with severe obesity (BMI > 40 kg/m^2) may even be considered unfit for liver transplantation, unless efforts are made preoperatively to reduce body weight with individualized plans of lifestyle modifications[70].

AISF and NICE guidance do not mention liver transplantation. All of the remaining guidelines agree that liver transplantation is an acceptable procedure in NASH patients with an end-stage liver disease, with the same indications adopted for other etiologies of liver disease[3-8].

CONCLUSION

The comparative analysis of the most recent international guidelines for the management of NAFLD showed some common orientation between the different recommendations, as well as diverging points. The most notable differences involved: the identification of the alcohol threshold defining NAFLD, the screening strategies in high-risk populations, the preferred non-invasive biomarkers for the assessment of advanced fibrosis, and the pharmacological treatment. These differences should not be necessarily seen as a limitation, but rather an expression of the geographical differences in genetic predisposition to NAFLD, lifestyle habits, healthcare systems. Arguably, the similarity in the recommendations could greatly help in ensuring homogenous management of NALFD all over the world, with favourable repercussions both in clinical practice and in clinical trials. In the next years, we might see a trend toward more homogenous guidelines thanks to the increasing body of evidence. In particular, the advancements in the imaging technologies could lead to new and widely accepted noninvasive methods to assess advanced liver fibrosis. Moreover, some clinical trials are investigating potentially effective drugs. If positive, the currently diverging pharmacological recommendations may reach a higher concordance. NAFLD is becoming a leading field of research in hepatology: new evidence is destined to change the current landscape of knowledge, prompting greater benefits to the patients as well as changes in the recommendations for clinical practice.

REFERENCES

1 **De Minicis S**, Day C, Svegliati-Baroni G. From NAFLD to NASH and HCC: pathogenetic mechanisms and therapeutic insights. *Curr Pharm Des* 2013; **19**: 5239-5249 [PMID: 23394093 DOI: 10.2174/1381612811319290006]

2 **Schwimmer JB**, Deutsch R, Kahen T, Lavine JE, Stanley C, Behling C. Prevalence of fatty liver in children and adolescents. *Pediatrics* 2006; **118**: 1388-1393 [PMID: 17015527 DOI: 10.1542/peds.2006-1212]

3 **European Association for the Study of the Liver (EASL).** European Association for the Study of Diabetes (EASD); European Association for the Study of Obesity (EASO). EASL-EASD-EASO Clinical Practice Guidelines for the management of non-alcoholic fatty liver disease. *J Hepatol* 2016; **64**: 1388-1402 [PMID: 27062661 DOI: 10.1016/j.jhep.2015.11.004]

4 National Institute for Health and Care Excellence (UK). Non-Alcoholic Fatty Liver Disease: Assessment and Management. Available from: URL: http//www.niceorg.uk\guidance\ng49

5 **Wong VW**, Chan WK, Chitturi S, Chawla Y, Dan YY, Duseja A, Fan J, Goh KL, Hamaguchi M, Hashimoto E, Kim SU, Lesmana LA, Lin YC, Liu CJ, Ni YH, Sollano J, Wong SK, Wong GL, Chan HL, Farrell G. Asia-Pacific Working Party on Non-alcoholic Fatty Liver Disease guidelines 2017-Part 1: Definition, risk factors and assessment. *J Gastroenterol Hepatol* 2018; **33**: 70-85 [PMID: 28670712 DOI: 10.1111/jgh.13857]

6 **Chitturi S**, Wong VW, Chan WK, Wong GL, Wong SK, Sollano J, Ni YH, Liu CJ, Lin YC, Lesmana LA, Kim SU, Hashimoto E, Hamaguchi M, Goh KL, Fan J, Duseja A, Dan YY, Chawla Y, Farrell G, Chan HL. The Asia-Pacific Working Party on Non-alcoholic Fatty Liver Disease guidelines 2017-Part 2: Management and special groups. *J Gastroenterol Hepatol* 2018; **33**: 86-98 [PMID: 28692197 DOI: 10.1111/jgh.13856]

7 **Italian Association for the Study of the Liver (AISF)**. AISF position paper on nonalcoholic fatty liver disease (NAFLD): Updates and future directions. *Dig Liver Dis* 2017; **49**: 471-483 [PMID: 28215516 DOI: 10.1016/j.dld.2017.01.147]

8 **Chalasani N**, Younossi Z, Lavine JE, Charlton M, Cusi K, Rinella M, Harrison SA, Brunt EM, Sanyal AJ. The diagnosis and management of nonalcoholic fatty liver disease: Practice guidance from the American Association for the Study of Liver Diseases. *Hepatology* 2018; **67**: 328-357 [PMID: 28714183 DOI: 10.1002/hep.29367]

9 **Paradis V**, Zalinski S, Chelbi E, Guedj N, Degos F, Vilgrain V, Bedossa P, Belghiti J. Hepatocellular carcinomas in patients with metabolic syndrome often develop without significant liver fibrosis: a pathological analysis. *Hepatology* 2009; **49**: 851-859 [PMID: 19115377 DOI: 10.1002/hep.22734]

10 **Piscaglia F**, Svegliati-Baroni G, Barchetti A, Pecorelli A, Marinelli S, Tiribelli C, Bellentani S; HCC-NAFLD Italian Study Group. Clinical patterns of hepatocellular carcinoma in nonalcoholic fatty liver disease: A multicenter prospective study. *Hepatology* 2016; **63**: 827-838 [PMID: 26599351 DOI: 10.1002/hep.28368]

11 **Portillo-Sanchez P**, Bril F, Maximos M, Lomonaco R, Biernacki D,

Orsak B, Subbarayan S, Webb A, Hecht J, Cusi K. High Prevalence of Nonalcoholic Fatty Liver Disease in Patients With Type 2 Diabetes Mellitus and Normal Plasma Aminotransferase Levels. *J Clin Endocrinol Metab* 2015; **100**: 2231-2238 [PMID: 25885947 DOI: 10.1210/jc.2015-1966]

12 **Koehler EM**, Plompen EP, Schouten JN, Hansen BE, Darwish Murad S, Taimr P, Leebeek FW, Hofman A, Stricker BH, Castera L, Janssen HL. Presence of diabetes mellitus and steatosis is associated with liver stiffness in a general population: The Rotterdam study. *Hepatology* 2016; **63**: 138-147 [PMID: 26171685 DOI: 10.1002/hep.27981]

13 **Kwok R**, Choi KC, Wong GL, Zhang Y, Chan HL, Luk AO, Shu SS, Chan AW, Yeung MW, Chan JC, Kong AP, Wong VW. Screening diabetic patients for non-alcoholic fatty liver disease with controlled attenuation parameter and liver stiffness measurements: a prospective cohort study. *Gut* 2016; **65**: 1359-1368 [PMID: 25873639 DOI: 10.1136/gutjnl-2015-309265]

14 **Klebanoff MJ**, Corey KE, Chhatwal J, Kaplan LM, Chung RT, Hur C. Bariatric surgery for nonalcoholic steatohepatitis: A clinical and cost-effectiveness analysis. *Hepatology* 2017; **65**: 1156-1164 [PMID: 27880977 DOI: 10.1002/hep.28958]

15 **Saadeh S**, Younossi ZM, Remer EM, Gramlich T, Ong JP, Hurley M, Mullen KD, Cooper JN, Sheridan MJ. The utility of radiological imaging in nonalcoholic fatty liver disease. *Gastroenterology* 2002; **123**: 745-750 [PMID: 12198701 DOI: 10.1053/gast.2002.35354]

16 **Ryan CK**, Johnson LA, Germin BI, Marcos A. One hundred consecutive hepatic biopsies in the workup of living donors for right lobe liver transplantation. *Liver Transpl* 2002; **8**: 1114-1122 [PMID: 12474149 DOI: 10.1053/jlts.2002.36740]

17 **Szczepaniak LS**, Nurenberg P, Leonard D, Browning JD, Reingold JS, Grundy S, Hobbs HH, Dobbins RL. Magnetic resonance spectroscopy to measure hepatic triglyceride content: prevalence of hepatic steatosis in the general population. *Am J Physiol Endocrinol Metab* 2005; **288**: E462-E468 [PMID: 15339742 DOI: 10.1152/ajpendo.00064.2004]

18 **Valenti L**, Fracanzani AL, Bugianesi E, Dongiovanni P, Galmozzi E, Vanni E, Canavesi E, Lattuada E, Roviaro G, Marchesini G, Fargion S. HFE genotype, parenchymal iron accumulation, and liver fibrosis in patients with nonalcoholic fatty liver disease. *Gastroenterology* 2010; **138**: 905-912 [PMID: 19931264 DOI: 10.1053/j.gastro.2009.11.013]

19 **Vuppalanchi R**, Gould RJ, Wilson LA, Unalp-Arida A, Cummings OW, Chalasani N, Kowdley KV; Nonalcoholic Steatohepatitis Clinical Research Network (NASH CRN). Clinical significance of serum autoantibodies in patients with NAFLD: results from the nonalcoholic steatohepatitis clinical research network. *Hepatol Int* 2012; **6**: 379-385 [PMID: 21557024 DOI: 10.1007/s12072-011-9277-8]

20 **Bedogni G**, Bellentani S, Miglioli L, Masutti F, Passalacqua M, Castiglione A, Tiribelli C. The Fatty Liver Index: a simple and accurate predictor of hepatic steatosis in the general population. *BMC Gastroenterol* 2006; **6**: 33 [PMID: 17081293 DOI: 10.1186/1471-230X-6-33]

21 **Kotronen A**, Peltonen M, Hakkarainen A, Sevastianova K, Bergholm R, Johansson LM, Lundbom N, Rissanen A, Ridderstråle M, Groop L, Orho-Melander M, Yki-Järvinen H. Prediction of non-alcoholic fatty liver disease and liver fat using metabolic and genetic factors. *Gastroenterology* 2009; **137**: 865-872 [PMID: 19524579 DOI: 10.1053/j.gastro.2009.06.005]

22 **Fedchuk L**, Nascimbeni F, Pais R, Charlotte F, Housset C, Ratziu V; LIDO Study Group. Performance and limitations of steatosis biomarkers in patients with nonalcoholic fatty liver disease. *Aliment Pharmacol Ther* 2014; **40**: 1209-1222 [PMID: 25267215 DOI: 10.1111/apt.12963]

23 **Feldstein AE**, Wieckowska A, Lopez AR, Liu YC, Zein NN, McCullough AJ. Cytokeratin-18 fragment levels as noninvasive biomarkers for nonalcoholic steatohepatitis: a multicenter validation study. *Hepatology* 2009; **50**: 1072-1078 [PMID: 19585618 DOI: 10.1002/hep.23050]

24 **Shen J**, Chan HL, Wong GL, Chan AW, Choi PC, Chan HY, Chim AM, Yeung DK, Yu J, Chu WC, Wong VW. Assessment of non-alcoholic fatty liver disease using serum total cell death and apoptosis markers. *Aliment Pharmacol Ther* 2012; **36**: 1057-1066 [PMID: 23066946 DOI: 10.1111/apt.12091]

25 **Chan WK**, Sthaneshwar P, Nik Mustapha NR, Mahadeva S. Limited utility of plasma M30 in discriminating non-alcoholic steatohepatitis from steatosis--a comparison with routine biochemical markers. *PLoS One* 2014; **9**: e105903 [PMID: 25184298 DOI: 10.1371/journal.pone.0105903]

26 **Vuppalanchi R**, Jain AK, Deppe R, Yates K, Comerford M, Masuoka HC, Neuschwander-Tetri BA, Loomba R, Brunt EM, Kleiner DE, Molleston JP, Schwimmer JB, Lavine JE, Tonascia J, Chalasani N. Relationship between changes in serum levels of keratin 18 and changes in liver histology in children and adults with nonalcoholic fatty liver disease. *Clin Gastroenterol Hepatol* 2014; **12**: 2121-2130.e1-2 [PMID: 24846279 DOI: 10.1016/j.cgh.2014.05.010]

27 **Ekstedt M**, Hagström H, Nasr P, Fredrikson M, Stål P, Kechagias S, Hultcrantz R. Fibrosis stage is the strongest predictor for disease-specific mortality in NAFLD after up to 33 years of follow-up. *Hepatology* 2015; **61**: 1547-1554 [PMID: 25125077 DOI: 10.1002/hep.27368]

28 **Kaswala DH**, Lai M, Afdhal NH. Fibrosis Assessment in Nonalcoholic Fatty Liver Disease (NAFLD) in 2016. *Dig Dis Sci* 2016; **61**: 1356-1364 [PMID: 27017224 DOI: 10.1007/s10620-016-4079-4]

29 **Fagan KJ**, Pretorius CJ, Horsfall LU, Irvine KM, Wilgen U, Choi K, Fletcher LM, Tate J, Melino M, Nusrat S, Miller GC, Clouston AD, Ballard E, O'Rourke P, Lampe G, Ungerer JP, Powell EE. ELF score ⩾9.8 indicates advanced hepatic fibrosis and is influenced by age, steatosis and histological activity. *Liver Int* 2015; **35**: 1673-1681 [PMID: 25495373 DOI: 10.1111/liv.12760]

30 **Guha IN**, Parkes J, Roderick P, Chattopadhyay D, Cross R, Harris S, Kaye P, Burt AD, Ryder SD, Aithal GP, Day CP, Rosenberg WM. Noninvasive markers of fibrosis in nonalcoholic fatty liver disease: Validating the European Liver Fibrosis Panel and exploring simple markers. *Hepatology* 2008; **47**: 455-460 [PMID: 18038452 DOI: 10.1002/hep.21984]

31 **Tapper EB**, Challies T, Nasser I, Afdhal NH, Lai M. The Performance of Vibration Controlled Transient Elastography in a US Cohort of Patients With Nonalcoholic Fatty Liver Disease. *Am J Gastroenterol* 2016; **111**: 677-684 [PMID: 26977758 DOI: 10.1038/ajg.2016.49]

32 **Wong VW**, Vergniol J, Wong GL, Foucher J, Chan AW, Chermak F, Choi PC, Merrouche W, Chu SH, Pesque S, Chan HL, de Lédinghen V. Liver stiffness measurement using XL probe in patients with nonalcoholic fatty liver disease. *Am J Gastroenterol* 2012; **107**: 1862-1871 [PMID: 23032979 DOI: 10.1038/ajg.2012.331]

33 **Wong VW**, Vergniol J, Wong GL, Foucher J, Chan HL, Le Bail B, Choi PC, Kowo M, Chan AW, Merrouche W, Sung JJ, de Lédinghen V. Diagnosis of fibrosis and cirrhosis using liver stiffness measurement in nonalcoholic fatty liver disease. *Hepatology* 2010; **51**: 454-462 [PMID: 20101745 DOI: 10.1002/hep.23312]

34 **Imajo K**, Kessoku T, Honda Y, Tomeno W, Ogawa Y, Mawatari H, Fujita K, Yoneda M, Taguri M, Hyogo H, Sumida Y, Ono M, Eguchi Y, Inoue T, Yamanaka T, Wada K, Saito S, Nakajima A. Magnetic Resonance Imaging More Accurately Classifies Steatosis and Fibrosis in Patients With Nonalcoholic Fatty Liver Disease Than Transient Elastography. *Gastroenterology* 2016; **150**: 626-637.e7 [PMID: 26677985 DOI: 10.1053/j.gastro.2015.11.048]

35 **Cheah MC**, McCullough AJ, Goh GB. Current Modalities of Fibrosis Assessment in Non-alcoholic Fatty Liver Disease. *J Clin Transl Hepatol* 2017; **5**: 261-271 [PMID: 28936407 DOI: 10.14218/JCTH.2017.00009]

36 **Kleiner DE**, Brunt EM. Nonalcoholic fatty liver disease: pathologic patterns and biopsy evaluation in clinical research. *Semin Liver Dis* 2012; **32**: 3-13 [PMID: 22418883 DOI: 10.1055/s-0032-1306421]

37 **Bedossa P**, Poitou C, Veyrie N, Bouillot JL, Basdevant A, Paradis V, Tordjman J, Clement K. Histopathological algorithm and scoring system for evaluation of liver lesions in morbidly obese patients. *Hepatology* 2012; **56**: 1751-1759 [PMID: 22707395 DOI: 10.1002/hep.25889]

38 **Bedossa P**; FLIP Pathology Consortium. Utility and appropriateness of the fatty liver inhibition of progression (FLIP) algorithm and steatosis, activity, and fibrosis (SAF) score in the evaluation of biopsies of nonalcoholic fatty liver disease. *Hepatology* 2014; **60**: 565-575 [PMID: 24753132 DOI: 10.1002/hep.27173]

39 **Haufe S**, Engeli S, Kast P, Böhnke J, Utz W, Haas V, Hermsdorf M, Mähler A, Wiesner S, Birkenfeld AL, Sell H, Otto C, Mehling H, Luft FC, Eckel J, Schulz-Menger J, Boschmann M, Jordan J. Randomized comparison of reduced fat and reduced carbohydrate hypocaloric diets on intrahepatic fat in overweight and obese human subjects. *Hepatology* 2011; **53**: 1504-1514 [PMID: 21400557 DOI: 10.1002/hep.24242]

40 **Asrih M**, Jornayvaz FR. Diets and nonalcoholic fatty liver disease: the good and the bad. *Clin Nutr* 2014; **33**: 186-190 [PMID: 24262589 DOI: 10.1016/j.clnu.2013.11.003]

41 **Adams LA**, Sanderson S, Lindor KD, Angulo P. The histological course of nonalcoholic fatty liver disease: a longitudinal study of 103 patients with sequential liver biopsies. *J Hepatol* 2005; **42**: 132-138 [PMID: 15629518 DOI: 10.1016/j.jhep.2004.09.012]

42 **Sanyal AJ**, Friedman SL, McCullough AJ, Dimick-Santos L; American Association for the Study of Liver Diseases; United States Food and Drug Administration. Challenges and opportunities in drug and biomarker development for nonalcoholic steatohepatitis: findings and recommendations from an American Association for the Study of Liver Diseases-U.S. Food and Drug Administration Joint Workshop. *Hepatology* 2015; **61**: 1392-1405 [PMID: 25557690 DOI: 10.1002/hep.27678]

43 **Bugianesi E**, Gentilcore E, Manini R, Natale S, Vanni E, Villanova N, David E, Rizzetto M, Marchesini G. A randomized controlled trial of metformin versus vitamin E or prescriptive diet in nonalcoholic fatty liver disease. *Am J Gastroenterol* 2005; **100**: 1082-1090 [PMID: 15842582 DOI: 10.1111/j.1572-0241.2005.41583.x]

44 **Haukeland JW**, Konopski Z, Eggesbø HB, von Volkmann HL, Raschpichler G, Bjøro K, Haaland T, Løberg EM, Birkeland K. Metformin in patients with non-alcoholic fatty liver disease: a randomized, controlled trial. *Scand J Gastroenterol* 2009; **44**: 853-860 [PMID: 19811343 DOI: 10.1080/00365520902845268]

45 **Shields WW**, Thompson KE, Grice GA, Harrison SA, Coyle WJ. The Effect of Metformin and Standard Therapy versus Standard Therapy alone in Nondiabetic Patients with Insulin Resistance and Nonalcoholic Steatohepatitis (NASH): A Pilot Trial. *Therap Adv Gastroenterol* 2009; **2**: 157-163 [PMID: 21180541 DOI: 10.1177/1756283X09105462]

46 **Belfort R**, Harrison SA, Brown K, Darland C, Finch J, Hardies J, Balas B, Gastaldelli A, Tio F, Pulcini J, Berria R, Ma JZ, Dwivedi S, Havranek R, Fincke C, DeFronzo R, Bannayan GA, Schenker S, Cusi K. A placebo-controlled trial of pioglitazone in subjects with nonalcoholic steatohepatitis. *N Engl J Med* 2006; **355**: 2297-2307 [PMID: 17135584 DOI: 10.1056/NEJMoa060326]

47 **Sanyal AJ**, Chalasani N, Kowdley KV, McCullough A, Diehl AM, Bass NM, Neuschwander-Tetri BA, Lavine JE, Tonascia J, Unalp A, Van Natta M, Clark J, Brunt EM, Kleiner DE, Hoofnagle JH, Robuck PR; NASH CRN. Pioglitazone, vitamin E, or placebo for nonalcoholic steatohepatitis. *N Engl J Med* 2010; **362**: 1675-1685 [PMID: 20427778 DOI: 10.1056/NEJMoa0907929]

48 **Cusi K**, Orsak B, Bril F, Lomonaco R, Hecht J, Ortiz-Lopez C, Tio F, Hardies J, Darland C, Musi N, Webb A, Portillo-Sanchez P. Long-Term Pioglitazone Treatment for Patients With Nonalcoholic Steatohepatitis and Prediabetes or Type 2 Diabetes Mellitus: A Randomized Trial. *Ann Intern Med* 2016; **165**: 305-315 [PMID: 27322798 DOI: 10.7326/M15-1774]

49 **Aithal GP**, Thomas JA, Kaye PV, Lawson A, Ryder SD, Spendlove I, Austin AS, Freeman JG, Morgan L, Webber J. Randomized, placebo-controlled trial of pioglitazone in nondiabetic subjects with nonalcoholic steatohepatitis. *Gastroenterology* 2008; **135**: 1176-1184 [PMID: 18718471 DOI: 10.1053/j.gastro.2008.06.047]

50 **Yau H**, Rivera K, Lomonaco R, Cusi K. The future of thiazolidinedione therapy in the management of type 2 diabetes mellitus. *Curr Diab Rep* 2013; **13**: 329-341 [PMID: 23625197 DOI: 10.1007/s11892-013-0378-8]

51 **Miller ER 3rd**, Pastor-Barriuso R, Dalal D, Riemersma RA, Appel LJ, Guallar E. Meta-analysis: high-dosage vitamin E supplementation may increase all-cause mortality. *Ann Intern Med* 2005; **142**: 37-46 [PMID: 15537682 DOI: 10.7326/0003-4819-142-1-200501040-00110]

52 **Abner EL**, Schmitt FA, Mendiondo MS, Marcum JL, Kryscio RJ. Vitamin E and all-cause mortality: a meta-analysis. *Curr Aging Sci* 2011; **4**: 158-170 [PMID: 21235492 DOI: 10.2174/1874609811104020158]

53 **Vilsbøll T**, Christensen M, Junker AE, Knop FK, Gluud LL. Effects of glucagon-like peptide-1 receptor agonists on weight loss: systematic review and meta-analyses of randomised controlled trials. *BMJ* 2012; **344**: d7771 [PMID: 22236411 DOI: 10.1136/bmj.d7771]

54 **Armstrong MJ**, Gaunt P, Aithal GP, Barton D, Hull D, Parker R, Hazlehurst JM, Guo K; LEAN trial team, Abouda G, Aldersley MA, Stocken D, Gough SC, Tomlinson JW, Brown RM, Hübscher SG, Newsome PN. Liraglutide safety and efficacy in patients with non-alcoholic steatohepatitis (LEAN): a multicentre, double-blind, randomised, placebo-controlled phase 2 study. *Lancet* 2016; **387**: 679-690 [PMID: 26608256 DOI: 10.1016/S0140-6736(15)00803-X]

55 **Kim YG**, Hahn S, Oh TJ, Park KS, Cho YM. Differences in the HbA1c-lowering efficacy of glucagon-like peptide-1 analogues between Asians and non-Asians: a systematic review and meta-analysis. *Diabetes Obes Metab* 2014; **16**: 900-909 [PMID: 24655583 DOI: 10.1111/dom.12293]

56 **Cui YM**, Guo XH, Zhang DM, Tham LS, Tang CC, Mace K, Linnebjerg H. Pharmacokinetics, safety, and tolerability of single- and multiple-dose exenatide once weekly in Chinese patients with type 2 diabetes mellitus. *J Diabetes* 2013; **5**: 127-135 [PMID: 23332026 DOI: 10.1111/1753-0407.12020]

57 **Ingwersen SH**, Petri KC, Tandon N, Yoon KH, Chen L, Vora J, Yang W. Liraglutide pharmacokinetics and dose-exposure response in Asian subjects with Type 2 diabetes from China, India and South Korea. *Diabetes Res Clin Pract* 2015; **108**: 113-119 [PMID: 25684604 DOI: 10.1016/j.diabres.2015.01.001]

58 **Cohen DE**, Anania FA, Chalasani N; National Lipid Association Statin Safety Task Force Liver Expert Panel. An assessment of statin safety by hepatologists. *Am J Cardiol* 2006; **97**: 77C-81C [PMID: 16581333 DOI: 10.1016/j.amjcard.2005.12.014]

59 **Kumar S**, Grace ND, Qamar AA. Statin use in patients with cirrhosis: a retrospective cohort study. *Dig Dis Sci* 2014; **59**: 1958-1965 [PMID: 24838495 DOI: 10.1007/s10620-014-3179-2]

60 **Stone NJ**, Robinson JG, Lichtenstein AH, Bairey Merz CN, Blum CB, Eckel RH, Goldberg AC, Gordon D, Levy D, Lloyd-Jones DM, McBride P, Schwartz JS, Shero ST, Smith SC Jr, Watson K, Wilson PW, Eddleman KM, Jarrett NM, LaBresh K, Nevo L, Wnek J, Anderson JL, Halperin JL, Albert NM, Bozkurt B, Brindis RG, Curtis LH, DeMets D, Hochman JS, Kovacs RJ, Ohman EM, Pressler SJ, Sellke FW, Shen WK, Smith SC Jr, Tomaselli GF; American College of Cardiology/American Heart Association Task Force on Practice Guidelines. 2013 ACC/AHA guideline on the treatment of blood cholesterol to reduce atherosclerotic cardiovascular risk in adults: a report of the American College of Cardiology/American Heart Association Task Force on Practice Guidelines. *Circulation* 2014; **129**: S1-S45 [PMID: 24222016 DOI: 10.1161/01.cir.0000437738.63853.7a]

61 **Flora K**, Hahn M, Rosen H, Benner K. Milk thistle (Silybum marianum) for the therapy of liver disease. *Am J Gastroenterol* 1998; **93**: 139-143 [PMID: 9468229 DOI: 10.1111/j.1572-0241.1998.00139.x]

62 **Wah Kheong C**, Nik Mustapha NR, Mahadeva S. A Randomized Trial of Silymarin for the Treatment of Nonalcoholic Steatohepatitis. *Clin Gastroenterol Hepatol* 2017; **15**: 1940-1949 [PMID: 28419855 DOI: 10.1016/j.cgh.2017.04.016]

63 **Schauer PR**, Bhatt DL, Kirwan JP, Wolski K, Brethauer SA, Navaneethan SD, Aminian A, Pothier CE, Kim ES, Nissen SE, Kashyap SR; STAMPEDE Investigators. Bariatric surgery versus intensive medical therapy for diabetes--3-year outcomes. *N Engl J Med* 2014; **370**: 2002-2013 [PMID: 24679060 DOI: 10.1056/NEJMoa1401329]

64 **Mathurin P**, Hollebecque A, Arnalsteen L, Buob D, Leteurtre E, Caiazzo R, Pigeyre M, Verkindt H, Dharancy S, Louvet A, Romon M, Pattou F. Prospective study of the long-term effects of bariatric surgery on liver injury in patients without advanced disease. *Gastroenterology* 2009; **137**: 532-540 [PMID: 19409898 DOI: 10.1053/j.gastro.2009.04.052]

65 **Lassailly G**, Caiazzo R, Buob D, Pigeyre M, Verkindt H, Labreuche J, Raverdy V, Leteurtre E, Dharancy S, Louvet A, Romon M, Duhamel A, Pattou F, Mathurin P. Bariatric Surgery Reduces Features of Nonalcoholic Steatohepatitis in Morbidly Obese Patients. *Gastroenterology* 2015; **149**: 379-388; quiz e15-16 [PMID: 25917783 DOI: 10.1053/j.gastro.2015.04.014]

66 **Bower G**, Toma T, Harling L, Jiao LR, Efthimiou E, Darzi A, Athanasiou T, Ashrafian H. Bariatric Surgery and Non-Alcoholic Fatty Liver Disease: a Systematic Review of Liver Biochemistry and Histology. *Obes Surg* 2015; **25**: 2280-2289 [PMID: 25917981 DOI: 10.1007/s11695-015-1691-x]

67 **Charlton MR**, Burns JM, Pedersen RA, Watt KD, Heimbach JK, Dierkhising RA. Frequency and outcomes of liver transplantation for nonalcoholic steatohepatitis in the United States. *Gastroenterology* 2011; **141**: 1249-1253 [PMID: 21726509 DOI: 10.1053/j.gastro.2011.06.061]

68 **Nair S**, Verma S, Thuluvath PJ. Obesity and its effect on survival in patients undergoing orthotopic liver transplantation in the United States. *Hepatology* 2002; **35**: 105-109 [PMID: 11786965 DOI: 10.1053/jhep.2002.30318]

69 **Tandon P**, Ney M, Irwin I, Ma MM, Gramlich L, Bain VG, Esfandiari N, Baracos V, Montano-Loza AJ, Myers RP. Severe muscle depletion in patients on the liver transplant wait list: its prevalence and independent prognostic value. *Liver Transpl* 2012; **18**: 1209-1216 [PMID: 22740290 DOI: 10.1002/lt.23495]

70 **Hakeem AR**, Cockbain AJ, Raza SS, Pollard SG, Toogood GJ, Attia MA, Ahmad N, Hidalgo EL, Prasad KR, Menon KV. Increased morbidity in overweight and obese liver transplant recipients: a single-center experience of 1325 patients from the United Kingdom. *Liver Transpl* 2013; **19**: 551-562 [PMID: 23408499 DOI: 10.1002/lt.23618]

P- Reviewer: Jamali B, Lee HC, Jamali R, Yoshioka K
S- Editor: Wang XJ **L- Editor**: A **E- Editor**: Yin SY

World Journal of Gastroenterology

Submit a Manuscript: http://www.f6publishing.com

World J Gastroenterol 2018 August 14; 24(30): 3374-3383

DOI: 10.3748/wjg.v24.i30.3374

ISSN 1007-9327 (print) ISSN 2219-2840 (online)

MINIREVIEWS

Form confers function: Case of the 3'X region of the hepatitis C virus genome

Mariola Dutkiewicz, Jerzy Ciesiołka

Mariola Dutkiewicz, Jerzy Ciesiołka, Institute of Bioorganic Chemistry, Polish Academy of Sciences, Poznan 61-704, Poland

ORCID number: Mariola Dutkiewicz (0000-0003-1098-0308); Jerzy Ciesiołka (0000-0001-7274-0751).

Author contributions: All authors equally contributed to this paper with conception and design of the study, literature review and analysis, drafting and critical revision and editing, and final approval of the final version.

Supported by the Polish Ministry of Science and Higher Education under the KNOW program and Foundation for Polish Science, No. POMOST/2013-8/5.

Conflict-of-interest statement: No potential conflicts of interest. No financial support.

Manuscript source: Invited manuscript

Correspondence to: Mariola Dutkiewicz, PhD, Associate Professor, Institute of Bioorganic Chemistry, Polish Academy of Sciences, Noskowskiego 12/14, Poznan 61-704, Poland. mariolad@ibch.poznan.pl
Telephone: +48-61-8528503
Fax: +48-61-8528532

Received: April 28, 2018
Peer-review started: April 28, 2018
First decision: June 11, 2018
Revised: June 25, 2018
Accepted: June 30, 2018
Article in press: June 30, 2018
Published online: August 14, 2018

Abstract

At the 3' end of genomic hepatitis C virus (HCV) RNA there is a highly conserved untranslated region, the 3' X-tail, which forms part of the 3'UTR. This region plays key functions in regulation of critical processes of the viral life cycle. The 3'X region is essential for viral replication and infectivity. It is also responsible for regulation of switching between translation and transcription of the viral RNA. There is some evidence indicating the contribution of the 3'X region to the translation efficiency of the viral polyprotein and to the encapsidation process. Several different secondary structure models of the 3'X region, based on computer predictions and experimental structure probing, have been proposed. It is likely that the 3'X region adopts more than one structural form in infected cells and that a specific equilibrium between the various forms regulates several aspects of the viral life cycle. The most intriguing explanations of the structural heterogeneity problem of the 3'X region came with the discovery of its involvement in long-range RNA-RNA interactions and the potential for homodimer formation. This article summarizes current knowledge on the structure and function of the 3'X region of hepatitis C genomic RNA, reviews previous opinions, presents new hypotheses and summarizes the questions that still remain unanswered.

Key words: Hepatitis C virus; 3'UTR; 3'X-tail; 3'X region; 3'X RNA; RNA structure

Core tip: Several different secondary structure models of the 3'X region have been proposed. It is likely that the 3' X region adopts more than one structural form in infected cells and that a specific equilibrium between the various forms regulates several aspects of the viral life cycle. This article summarizes current knowledge of the structure and function of the 3'X region of hepatitis C genomic RNA,

reviews previous opinions, presents new hypotheses and summarizes the questions that still remain unanswered.

Dutkiewicz M, Ciesiołka J. Form confers function: Case of the 3' X region of the hepatitis C virus genome. *World J Gastroenterol* 2018; 24(30): 3374-3383 Available from: URL: http://www.wjgnet.com/1007-9327/full/v24/i30/3374.htm DOI: http://dx.doi.org/10.3748/wjg.v24.i30.3374

INTRODUCTION

Hepatitis C virus (HCV) belongs to the family *Flaviviridae*, a member of the genus *hepaciviruses*. HCV was identified in 1989 as one of the viruses capable of causing viral hepatitis, in addition to the previously known hepatitis A and B viruses (HAV, HBV)[1]. There are seven major HCV genotypes that differ in virulence and their geographic distribution[2]. Currently, it is estimated that worldwide more than 185 million people are infected with HCV, which represents 2.8% of the world's population[3]. Infection usually takes place in the absence of obvious clinical symptoms, and the resulting inflammation of the liver often progresses to become chronic, usually lasting for years. In time, the chronic inflammation can lead to cirrhosis of the liver and ultimately liver failure or to the development of primary liver cancer[4]. Although the virus replicates mainly in hepatocytes, it also occurs in peripheral blood mononuclear and central nervous system microglia[5,6]. In people with simultaneous infection with HIV (human immunodeficiency virus), HCV replication was also observed in other tissues[7]. Sometimes HCV enters cells of the immune system, leading to very long-lasting effects which are extremely difficult to treat effectively[8].

While progress has been made in the treatment of some other common viral infections, HCV infection remains an important health problem in the world. Current standard treatment methods have the desired therapeutic effect on 40%-60% of patients[4]. The new highly effective drug, grazoprevir, is able to cure patients with 93% effectivity[9], unfortunately, the treatment is still very expensive and out of reach for the majority of the infected individuals, many of whom live in Third World countries. So far, no HCV vaccine has been developed, which is due to the high genetic variability of the virus, comparable to the genetic variability of HIV. In the absence of widely accessible conventional drugs and vaccines, numerous attempts have been made to design inhibitors of viral proteins, inhibitory oligomers of the antisense and ribozyme type, and more recently also of RNA interference tools directed against viral RNA[4,10,11].

HCV is a small, enveloped virus with a diameter of 40-60 nm, whose genome is a single-stranded, positive-sense RNA of about 9.6 kb in length[6,10,12]. In the viral replication process, the positive-sense RNA strand is transcribed into negative-sense counterpart, the replication intermediate, which serves as the template for the RNA synthesis of progeny genomes. The HCV genome has one very long open reading frame (ORF). It encodes a precursor polyprotein, which is digested in a series of cleavage processes to finally produce proteins: C, E1, E2, p7, NS2, NS3, NS4A, NS4B, NS5A and NS5B[13]. The coding sequence of the HCV genome is flanked by two untranslated regions: the 5'UTR and the 3'UTR (5' and 3' untranslated regions). Both these regions play key functions in regulating HCV life cycle and determine its expression level. The 5'UTR contains a highly structured regulatory element, an IRES (internal ribosome entry site), that enables cap-independent translation. The 3' UTR is engaged in the replication process and in the regulation of translation. In addition, control of other processes as, for example, assembly of virions and switching between different developmental phases takes place with the participation of the structural RNA elements present at the very 3' end of the HCV genome.

This article presents the current state of knowledge about the structure and functions of the most terminal section of the 3'UTR of hepatitis C virus, the 3'X-tail.

STRUCTURE OF THE 3'UTR REGION

HCV 3'UTR has a variable length of 170 to 250 nucleotides (Figure 1). Three characteristic sections have been recognized in this region: immediately after the stop codon there is a variable region about 25-130 nucleotides in length, characterized by high sequence heterogeneity between various genotypes, but conserved within the same genotype of the virus. Next there is a poly-pyrimidine segment of varying length, independent of the type, or even a subtype of virus, ranging from about 30 to 130 nucleotides. At the very end of the genome, there is an 3'X region, discovered 6 years after cloning of the virus, which is 98 nucleotides long and is an almost absolutely conserved sequence[6].

Within the first, variable region of 3'UTR, two sequence motifs are present that are found in all genotypes of HCV. These are: the ACACUCC section, which represents a seed-region for miR-122[14], and the UG dinucleotide located at the very end of the region, directly upstream the poly (U/UC) section[6]. The stop codon is located in the apical loop of the stem-loop motif, named 5BSL3.4 or SL9360, which is created partly from the terminal nucleotides of the ORF encoding the NS5B protein and partly from non-coding nucleotides. The poly-pyrimidine section can be divided into a two poly (UC) parts uneven in length, which are separated by the one poly (U) region. The poly-pyrimidine segment is heterogeneous, not only in terms of length, but also in nucleotide sequence. In genotypes 2a, 3a, 3b there are several conserved adenosine residues in this region that are missing in genotypes 1b and 2b[6]. Individual guanosine residues are also observed on rare occasions.

3'X-tail

Initially, it was suspected that at the 3' terminus of the HCV genome a poly (U) or poly (A) sequence was

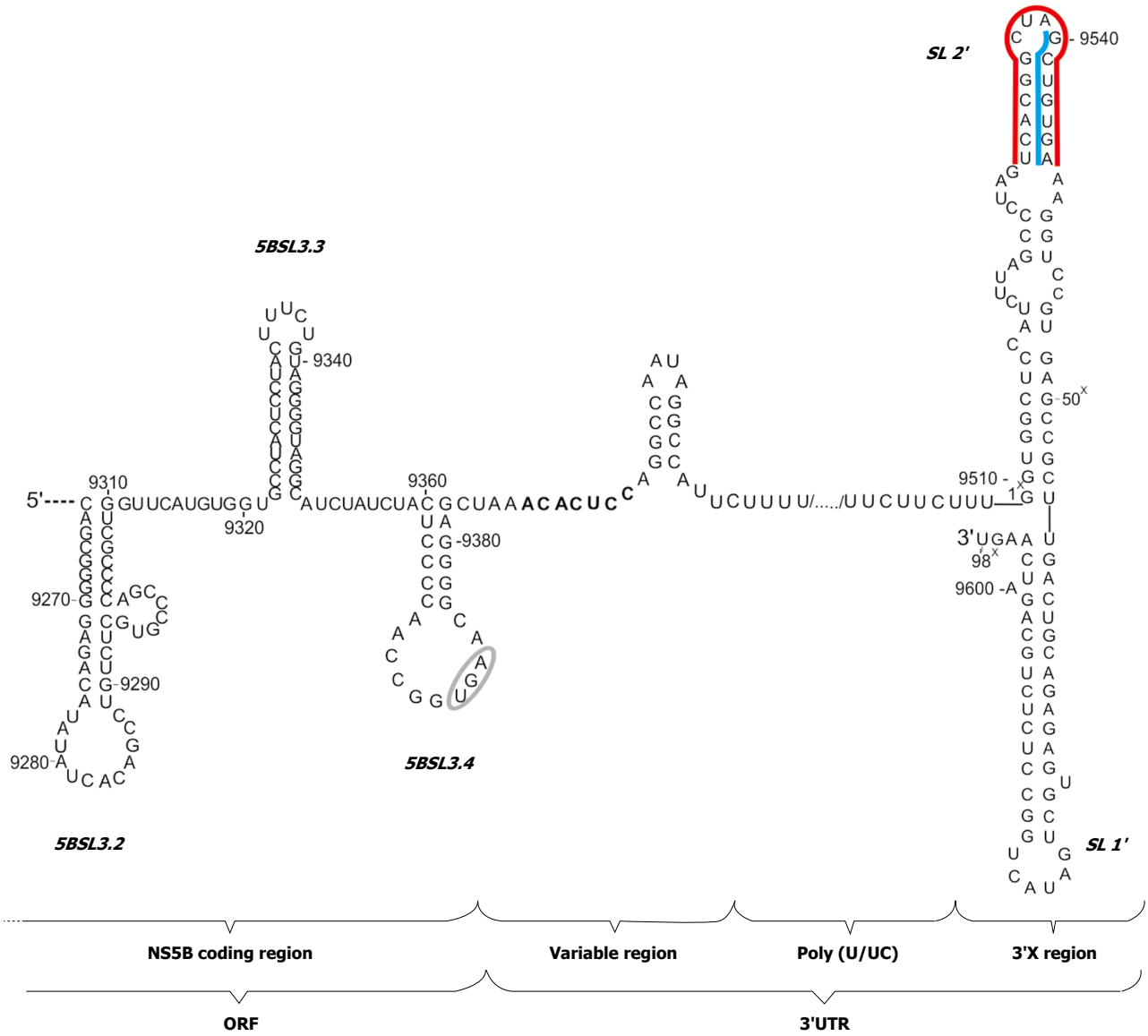

Figure 1 Secondary structure model of the 3'UTR of hepatitis C virus genome with adjacent 3' terminal sequence of the coding region. The stop codon is indicated by a gray ellipse. The regions involved in the kissing-interactions are marked with blue lines; the region involved in dimerization is indicated by a red line; the seed region for miR122 is highlighted in bold.

present. The existence of the 98-nt long 3'X region was discovered by Tanaka and colleagues in 1995[15]. Almost simultanously the presence of the 3'X at the end of the HCV genome identified Kolykhalov *et al*[16]. Comparison of the sequence of this RNA segment in different viral isolates indicated 96%-100% sequence conservation of the 3'X region, with only single substitutions in the 3' terminal 46-nt sequence[6]. This is an unusual feature for this dynamically changing virus, that suggests its extremely important function.

Several different secondary structure models of the 3'X region were proposed, based on computer predictions and experimental structure probing by chemical modification, enzyme digestion, RNA cleavage induced by Pb^{2+} ions, NMR (nuclear magnetic resonance) and SAXS (small angle X-ray scattering). A stable structure of the SL1 hairpin was proposed for the 3' part of the 3'X RNA, which is common to different structural models (Figure 2)[17-21]. The 52-nucleotide segment making up the 5' part of the 3'X region could not be assigned an unambiguous structure based on the experimental results obtained. The proposed models were only partially confirmed by the results of experimental studies[6,17,18]. Poor ordering of this fragment or formation of more than one structural form have been suggested[17,18,20].

One of the first structural models of the 3'X region suggested the presence of three hairpin motifs: SL1, SL2, and SL3 (Figure 2A)[17,18]. Another structural model suggested a set of four hairpins: SL1, SL2a, SL2b and SL3, where SL1 and SL3 did not differ from the first model, but two shorter hairpins replaced the SL2 motif[20]. The main reason for the proposed change was the observation of strong DMS modifications, as well as Pb^{2+} ion-induced cleavages, in the middle of the SL2 double-stranded stem (C44-C45), which indicated a single-stranded or highly flexible region there. In this four

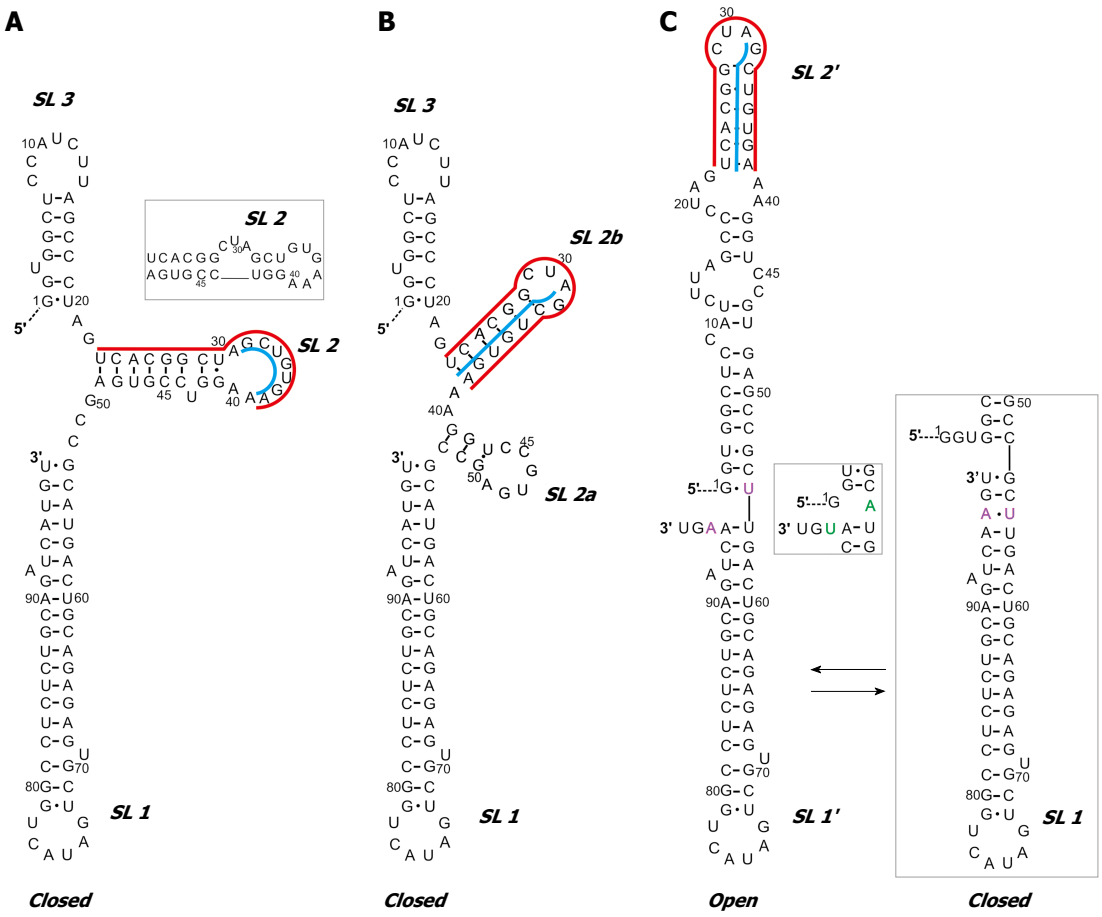

Figure 2 Diverse secondary structure models proposed for the 3'X region of hepatitis C virus genome. A: The 3xSL model[17,18]; B: The 4xSL model[20]; C: The 2xSL model[21]. The region involved in the kissing-interactions is indicated with blue line, the region involved in dimerization is marked with red line; possible alternative folding of separate fragments are displayed as gray rectangles.

stem-loop model (4xSL), the reactive cytidine residues are located in the apical loop of the short SL2b motif (Figure 2B). In addition, it was noted that the SL2a and SL2b hairpins have the potential to create a pseudoknot after rearrangement of their base pairing[20]. However, discovery of functionally important long-range kissing interactions between a sequence located in the apical loop of the SL2 hairpin and the upstream sequence in the region encoding NS5B[22] (see next section), seemed to support the three- (3xSL), but not the four- (4xSL) stem-loop model for the 3'X region. Thus, the 3xSL structure model of the 3'X-tail became the favored idea during the following decade.

Recently, based on NMR and SAXS studies, a two-hairpin model (2xSL) has been proposed for the 3'X region, consisting of the SL1 and SL2' (named elsewhere also SL2/3) (Figure 2C)[21,23,24]. In addition, in this model the SL1 hairpin may fold in two different ways: the closed structure - SL1 or the open one - SL1', differing by the three terminal base-pairs of the hairpin being paired or unpaired, respectively (Figure 2C)[21,23,25]. In the 2xSL model the previously identified flexible cytosine residues (C44-C45) are located within the internal loop of the SL2' motif. The closed conformation of SL1 is associated with long-range kissing interactions with another part of the genome, while the open conformation, SL1' with the 3' overhang is associated with dimerization (described in the next section).

The role of selected metal ions was investigated regarding its influence on the structure of the 3'X-tail but it seems that neither magnesium, nor sodium ion concentration determine its folding, within the range of normal physiological conditions[26]. However, at higher ionic strength, extended homodimers are preferentially formed over 2xSL monomers[24]. A chaperone role of the viral C protein (core protein), has also been suggested[23,27]. Long-range RNA-RNA interactions with 5' sequences in the genome or with a second genomic RNA molecule seems to influence the structure of the 3'X region more than the presence of specific metal ions.

It is very likely that the 3'X region can adopt more than one structural form in infected cells and that a specific equilibrium between these forms regulates several processes of the viral life cycle. These different structural forms may be favored by distinct viral genotypes what can help to explain their differential virulence and drug resistance[28,29].

Long range RNA-RNA interactions

Previous investigation of genomic HCV RNA and a con-

struct containing only 5'UTR and 3'UTR did not show any interaction of the X region with other regions of the molecules studied. This suggested the structural independence of these two regions of viral RNA from each other[17]. Later tertiary[30-32] interactions at the 3' end of the HCV genomic strand were proposed by Friebe *et al*[22]. The kissing interactions between the absolutely conserved "k" segment of the X region: 32^{X}-GCUGUGA-38^{X} and the "k'" segment of the NS5B coding sequence: 9281-UCACAGC-9287 do not require a protein chaperone. These sequence stretches are located within apical parts of SL elements called SL2 or SL2' and 5BSL3.2, which is one of the domains in the CRE (*cis*-acting replication element) (Figure 1)[22,28,31,33]. It is easy to imagine that kissing interactions could be initiated by any complementary stretch of nucleotides located within two apical loops of RNA hairpins. This scenario was previously suggested for the 3xSL model of the 3'X-tail[22,28,31,33]. However, recent studies with the use of mutagenesis, NMR and SAXS methods, indicate that before kissing-interactions are formed, the "k"- sequence in the X region is involved in base pairing within the SL2' element[21,24]. How the 5BSL3.2 element is able to induce the conformational transition from SL2' to SL2, or more globally: from 2xSL to 3xSL form of the 3'X, remains unclear. The next great challenge is to elucidate step by step how this transition occurs.

Two replicon systems, Con1b and JF-H1, have been investigated with a SHAPE method, which is based on a chemical modification of single-stranded RNA residues. The replicons are constructed on the basis of two different viral genotypes 1b and 2a, respectively. The experimental results showed that the proposed kissing interactions were detectable only for replicon JF-H1 (genotype 2a). The results obtained for replicon Con1b were in agreement with data obtained for the genotype 1a (strain H) of the virus and favors the open conformation of SL1'. In this open conformation the very 3' end of the SL' remains single-stranded, and that is associated with an increase in the efficiency of RNA synthesis initiation. In fact, subtype 1b is more virulent and resistant to interferon-based therapy than other genotypes, including subtype 2a[29,34]. This suggests how virus virulence and drug response is significantly influenced by the long-range kissing interactions, which likely cause changes in the base-pairing character of the very 3' terminal nucleotides.

Dimerization

Another intriguing set of tertiary interactions were proposed for the 3'X region of HCV genome by Ivanyi-Nagy *et al*[23]. Primarily *in vitro* investigations showed that the apical part of the SL2 hairpin in the 3xSL model, 29^{X}-CUAG-32^{X}, is able to interact with the respective palindromic sequence in the second 3'X RNA molecule thus inducing the formation of a homodimer[35]. The 16-nt palindromic sequence, called also DLS (dimerization leading stretch) is absolutely conserved among all HCV genotypes[36]. The homodimer, consisting of two isolated 3'X-RNA molecules, was characterized *in vitro* by NMR and SAXS. It was proposed that the resulting homoduplex could involve shorter (SL2) or extended (SL2') sequence fragments (Figure 3)[21,23-25,35]. The core protein supports the formation and stabilizes the extended homodimer[24].

The dimerization of the HCV genome still remains unproved *in vivo* and its function remains to be elucidated. It was suggested that the dimerization could be helpful in ensuring that only full-length progeny RNA molecules are encapsidated[24]. Moreover, the unwinding of the 3'-end of the genome, could greatly facilitate the minus RNA synthesis[37]. Masante *et al*[38] suggested that the homodimeric genome operates as a preferred template for the HCV polymerase (NS5B). Additionally, dimerization might enhance the rate of RNA recombination between two homologue RNA strands (resumed in[39]). The equilibrium between 2xSL monomers and dimers would likely also be tuned by the local concentration of RNA and the presence of core protein[24].

FUNCTIONS OF THE 3'UTR REGION

Hepatitis C virus can only infect humans and chimpanzees; there is no experimental model of its infectivity among small animals. For this reason, very few studies on the spread of the virus have been carried out *in vivo*. An experiment was carried out by Yanagi *et al*[40], in which a number of viral constructs containing deletions within the 3'UTR were injected into the liver of the chimpanzee at time intervals, and then the animal was examined for the presence of HCV RNA, anti-HCV antibodies and liver enzymes in its serum. Viral mutants lacking the entire 3'X region or parts thereof (nt: 1-50 and 57-98) were not able to replicate. Also viral infection was not observed when a mutant containing no poly (U/UC) segment was used. Only the construct devoid of 24 nucleotides within the variable region turned out to be infectious, indicating that this region is not essential for the viral life cycle under these conditions[40]. A similar experiment was carried out by Kolykhalov *et al*[41], and the obtained results were in line with previous observations of Yanagi *et al*[40].

One of the possible explanations of 3'X region function was its influence on genomic RNA stability. This has been shown *in vitro* but is not equally important for all genotypes of the virus[42].

Replication process

The information on the involvement of individual parts of the 3'UTR in the life cycle of the virus presented in the previous section was confirmed in research with the replicating Huh7 and HeLa cell systems[19,22,42,43]. Namely, constructs devoid of the entire poly (U/UC) section, were not able to replicate[42,43], and the minimum length of the polypyrimidine segment was 50 nt in one study[43], and only 26 nt in the other[42]. In contrast, the deletion of the

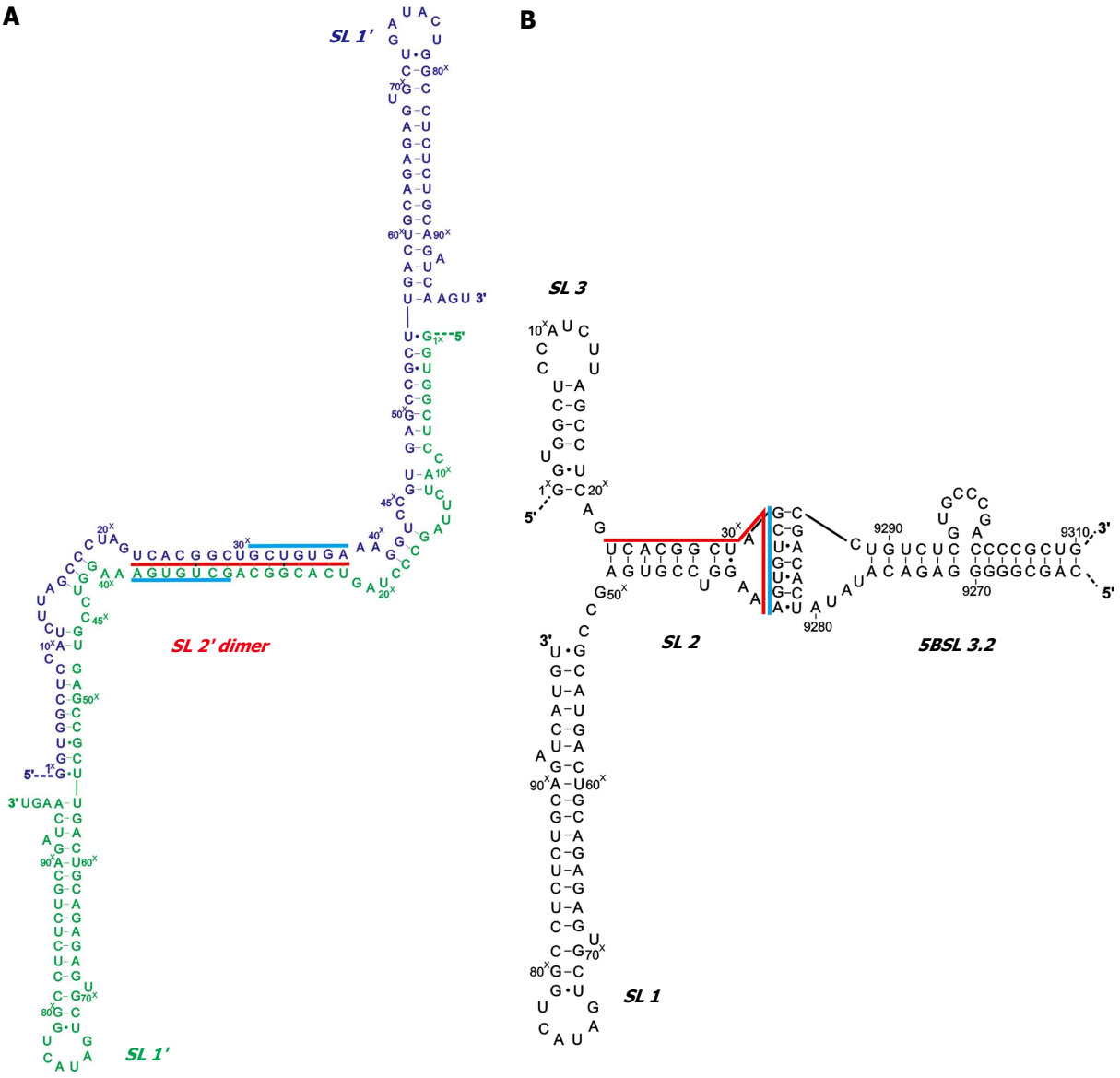

Figure 3 Long-range RNA-RNA interactions proposed for the 3'X region of hepatitis C virus genome. A: The homodimeric interactions between two 3'X regions embedded into two RNA molecules, model according to Cantero-Camacho *et al*[24]; B: The kissing-interactions with SL5B3.2[22,28,31,33]. Nucleotide sequence involved in dimerization is additionally indicated with red line, while those involved in the kissing-interactions are marked with blue lines.

3'X region or any one of its parts, SL1, SL2 or SL3, led to a complete failure to replicate[42,43] and only few point mutations in this region were tolerated[19,43]. In turn, the removal of the variable region from the 3'UTR of the viral genome only reduced the efficiency of the process leading to decrease in the rate of replication[22,42,43]. In addition, it has been shown that the region directly upstream the stop codon plays a key role in viral replication[22].

The site of the NS5B polymerase attachment within region 3'X has been mapped to be within the SL2 sequence and within the SL1[44]. They are protected against digestion with RNase T1 at guanosine residues at positions 41, 42, 50 and 53. The direct interaction of the 3'X RNA with the NS5B protein has been found in studies conducted *in vitro*[6,12,44-46]. The specificity of the viral polymerase to the model RNA template is relatively low and the presence of the 3'X region is not always necessary for RNA synthesis[6,12,37,45]. However, in the case of matrices containing genomic or subgenomic RNA, the presence of the 3'X region is necessary for the efficiency and the specificity of the process. It has been shown that the lack of this sequence, or a part thereof, almost completely inhibits replication, and in the case of deletion of nucleotides in positions 31-40, the product is too long[12,44].

The NS5B polymerase catalytic center probably only interacts with a single-stranded RNA fragment. The initiation of replication seems to take place in the SL1 loop, 21 nucleotides from the 3' end of the 3'X RNA[12]. However, another research group, Kim *et al*[46] indicates that the process begins near the 3' terminus, in a region rich in purines. However, in studies carried out in a cellular system, it has been shown that the presence

of the 3' terminal GU dinucleotide is preferred in the reaction[19]. Similar preferences of the replicase for the U at the 3'-end of the template RNA were observed by Shimm *et al*[47] in the *in vitro* system. Also, Kao *et al*[37] postulate that the enzyme requires a stable secondary template structure and at least one unpaired cytidine residue at its 3' end to initiate RNA synthesis. Butcher *et al*[48] proposed a replication initiation scenario, one common to various polymerases, in which the synthesis of a new strand of RNA begins with a nucleotide complementary to the penultimate of the 3' end of the nucleotide of the template molecule. Secondly, a complementary nucleotide is added to the remainder of the template at the 3' end, and only after the synthesis of this dinucleotide-primer is the complementary strand of viral RNA synthesized. Many observations suggest that NS5B is a non-specific enzyme, *i.e*. it can recognize more than one nucleotide sequence. The presence of specific Ⅰ-, Ⅱ- and tertiary structures at the 3'-end of the template RNA may allow modulation of the specificity of the enzyme for better yield and/or greater precision in the selection of the origin. In addition, both viral and host proteins can be involved in the replication process[6,49].

In summary, it should be noted that this replication phase of the life cycle of the virus has not yet been precisely understood. In addition to interacting with the viral polymerase, the 3'X region also interacts with other proteins one of them being the NS3 viral protein[49]. Acting as a helicase, it is probably a very important component of the replication complex, because the NS5B polymerase tends to detach from the RNA template when it encounters very stable RNA secondary structures[50]. The specific interaction between NS3 and the HCV 3'UTR probably involves a large part of this region containing the sequence 3'X and the poly (U/UC) section, since none of these elements alone is sufficient to form a stable complex with this protein[49].

Translation process

One of the earliest known cellular proteins interacting with HCV 3'UTR was the PTB protein. The interaction of PTB with the 3'X region may be related to the regulation of the translation process. The proposed site of PTB binding is 21 nucleotides from the 5' end of the 3'X region (SL3), containing a part of the consensus sequence recognized by this protein[18]. Similar results are presented by Tsuchihara *et al*[51] suggesting that the region involved in the interaction with PTB is 19 nucleotides from the 5' end of the 3'X region and extends 7 nucleotides upstream this sequence. The mutagenesis data showed that both secondary structure and the nucleotide sequence in the SL2 and SL3 regions are important for this interaction[18,51].

The 3'UTR has been ascribed as a translation enhancer[52-56]. One of mechanisms proposed by which enhancing the process is achieved, is the interaction between the 5' and 3' ends of the HCV genome, mediated by the PTB protein and another, hypothetical Y protein[57]. The effect of enhancing translation through genome cyclization is observed in many viruses[58]. However, not all results indicate PTB enhances HCV translation, sometimes the protein seems to be even inhibitory[59]. There is also no consensus on the impact of the 3'UTR on the efficiency of translation. For example, Murakami *et al*[59] observed that in an *in vitro* system, deletion of SL3 in the 3'X region and/or the poly (U/UC) section resulted in an increase in the amount of protein produced. A possible explanation for this observation would be that these sequence fragments, by interacting with other protein factors, inhibit the translation process. In other studies, however, it was observed that the presence of 3'UTR had no effect on the increase of the product amount and the efficiency of the polyprotein cleavage process[43,60]. It appears the choice of the experimental model plays a key role in this kind of research. For example, while in the lysate from rabbit reticulocytes no effect of 3'UTR on translation efficiency is observed[42,53], in HeLa cells, hepatocytes and in an *in vivo* mouse model the presence of the 3'UTR stimulates this process[53]. Recently, the role of 3'UTR in enhancing translational efficiency has been reported both in the rabbit reticulocyte lysate and in Huh7 cells[61].

Finally, it has been shown that the region X interacts with the ribosomal proteins L22, L3, S3 and mL3[62]. Similar viral RNA - L22 protein interactions have been observed for EBV (Epstein-Barr virus) and HPV-1 (human type 1 papilloma virus), showing a positive effect of L22 on translational efficiency[62]. Meanwhile, in the case of Qβ virus, ribosomal host proteins are involved in the formation of the viral replication complex[62]. It is unclear whether the interaction of ribosomal proteins with the HCV X region is related to the replication or translation process, or to both of these processes. The demonstrated ability of HCV protein NS5B to bind to the ribosome[63] is reminiscent of the strategy used by the Qβ virus, which uses ribosomal proteins to build its replication complex.

CONCLUSION

The most intriguing feature of the 3'X region is its extremely high sequence conservation. The maintenance of a 98-nt long stretch of RNA at over 95% conservation places severe constraints on such a fast-mutating RNA virus. Apparently almost any change to this stretch result in progeny incapable of reproducing which rapidly disappear from the population.

The high sequence conservation might be explained by existence of different structural forms of the 3'X region. Within one structure there is usually a way to neutralize point mutations by adaptive mutations in another structure, thus restoring important base-pairing. Simultaneous compensation of mutations in two (or more) different structures/forms is much less probable. However, instead of several different structural forms of the X-region, the long-range RNA-RNA interactions with the involvement of that region could explain its high

sequence conservation.

Evidence indicates the 3'X region is involved in a number of interactions including kissing 5BSL3.2 (required for replication), an interaction with the second RNA molecule carrying the X-region sequence (homodimerization), binding of the NS5B protein (for initiation of RNA synthesis), an interaction with NS3 helicase (for elongation of RNA synthesis), binding of PTB (for proposed translation regulation). Is it possible that one structural form of the 3'X region supports such different interactions? The answer is: yes, it is possible, but unlikely. On the other hand, it is easy to imagine that different structural forms of this region are responsible for different processes and interactions. For instance: 2xSL - structure for dimerization and enhanced RNA synthesis, 3xSL - structure for kissing interactions that supports translation.

Hopefully in-depth *in vivo* structure mapping of the 3'X-region at the various replication stages, in different cellular compartments will answer these questions to give us a better understanding of the virus and lead to additional means to control it.

ACKNOWLEDGMENTS

The authors thank Erik Wade for careful reading of the manuscript and valuable comments.

REFERENCES

1 **Choo KB**, Liew LN, Wang HC. Production of transgenic mice carrying the human hepatitis B virus or the human papillomavirus DNA sequences in Taiwan: analysis of physical structure and hereditary mode. *Proc Natl Sci Counc Repub China B* 1989; **13**: 314-318 [PMID: 2561574]

2 **Bartenshlager R**. Hepatitis C Virus: From Molecular Virology to Antiviral Therapy. *Current Topics in Microbiology and Immunology* 2013; **369**: V-VI [DOI: 10.1007/978-3-642-27340-7]

3 **Mohd Hanafiah K**, Groeger J, Flaxman AD, Wiersma ST. Global epidemiology of hepatitis C virus infection: new estimates of age-specific antibody to HCV seroprevalence. *Hepatology* 2013; **57**: 1333-1342 [PMID: 23172780 DOI: 10.1002/hep.26141]

4 **Dev A**, Patel K, McHutchison JG. New therapies for chronic hepatitis C virus infection. *Curr Gastroenterol Rep* 2004; **6**: 77-86 [PMID: 14720458 DOI: 10.1007/s11894-004-0030-5]

5 **Rijnbrand RC**, Lemon SM. Internal ribosome entry site-mediated translation in hepatitis C virus replication. *Curr Top Microbiol Immunol* 2000; **242**: 85-116 [PMID: 10592657 DOI: 10.1007/978-3-642-59605-6_5]

6 **Shi ST**, Lai MM. Hepatitis C viral RNA: challenges and promises. *Cell Mol Life Sci* 2001; **58**: 1276-1295 [PMID: 11577984 DOI: 10.1007/PL00000939]

7 **Laskus T**, Radkowski M, Wang LF, Vargas H, Rakela J. The presence of active hepatitis C virus replication in lymphoid tissue in patients coinfected with human immunodeficiency virus type 1. *J Infect Dis* 1998; **178**: 1189-1192 [PMID: 9806058 DOI: 10.1086/515682]

8 **Conca P**, Cafaro G, De Renzo A, Coppola A, Cimino E, Tarantino G. Successful and Safe Long-Term Standard Antiviral Therapy in a Patient with „Explosive" Immune Response in Course of HCV-Related Liver Cirrhosis. *Int J Mol Sci* 2015; **16**: 14075-14085 [PMID: 26101866 DOI: 10.3390/ijms160614075]

9 **Bell AM**, Wagner JL, Barber KE, Stover KR. Elbasvir/Grazoprevir: A Review of the Latest Agent in the Fight against Hepatitis C. *Int J Hepatol* 2016; **2016**: 3852126 [PMID: 27403342 DOI: 10.1155/2016/3852126]

10 **Gómez J**, Nadal A, Sabariegos R, Beguiristain N, Martell M, Piron M. Three properties of the hepatitis C virus RNA genome related to antiviral strategies based on RNA-therapeutics: variability, structural conformation and tRNA mimicry. *Curr Pharm Des* 2004; **10**: 3741-3756 [PMID: 15579068 DOI: 10.2174/1381612043382675]

11 **Randall G**, Rice CM. Interfering with hepatitis C virus RNA replication. *Virus Res* 2004; **102**: 19-25 [PMID: 15068876 DOI: 10.1016/j.virusres.2004.01.011]

12 **Oh JW**, Ito T, Lai MM. A recombinant hepatitis C virus RNA-dependent RNA polymerase capable of copying the full-length viral RNA. *J Virol* 1999; **73**: 7694-7702 [PMID: 10438859]

13 **Penin F**, Dubuisson J, Rey FA, Moradpour D, Pawlotsky JM. Structural biology of hepatitis C virus. *Hepatology* 2004; **39**: 5-19 [PMID: 14752815 DOI: 10.1002/hep.20032]

14 **Gerresheim GK**, Dünnes N, Nieder-Röhrmann A, Shalamova LA, Fricke M, Hofacker I, Höner Zu Siederdissen C, Marz M, Niepmann M. microRNA-122 target sites in the hepatitis C virus RNA NS5B coding region and 3' untranslated region: function in replication and influence of RNA secondary structure. *Cell Mol Life Sci* 2017; **74**: 747-760 [PMID: 27677491 DOI: 10.1007/s00018-016-2377-9]

15 **Tanaka T**, Kato N, Cho MJ, Shimotohno K. A novel sequence found at the 3' terminus of hepatitis C virus genome. *Biochem Biophys Res Commun* 1995; **215**: 744-749 [PMID: 7488017 DOI: 10.1006/bbrc.1995.2526]

16 **Kolykhalov AA**, Feinstone SM, Rice CM. Identification of a highly conserved sequence element at the 3' terminus of hepatitis C virus genome RNA. *J Virol* 1996; **70**: 3363-3371 [PMID: 8648666]

17 **Blight KJ**, Rice CM. Secondary structure determination of the conserved 98-base sequence at the 3' terminus of hepatitis C virus genome RNA. *J Virol* 1997; **71**: 7345-7352 [PMID: 9311812]

18 **Ito T**, Lai MM. Determination of the secondary structure of and cellular protein binding to the 3'-untranslated region of the hepatitis C virus RNA genome. *J Virol* 1997; **71**: 8698-8706 [PMID: 9343228]

19 **Yi M**, Lemon SM. Structure-function analysis of the 3' stem-loop of hepatitis C virus genomic RNA and its role in viral RNA replication. *RNA* 2003; **9**: 331-345 [PMID: 12592007 DOI: 10.1261/rna.2144203]

20 **Dutkiewicz M**, Ciesiolka J. Structural characterization of the highly conserved 98-base sequence at the 3' end of HCV RNA genome and the complementary sequence located at the 5' end of the replicative viral strand. *Nucleic Acids Res* 2005; **33**: 693-703 [PMID: 15681619 DOI: 10.1093/nar/gki218]

21 **Cantero-Camacho Á**, Gallego J. The conserved 3'X terminal domain of hepatitis C virus genomic RNA forms a two-stem structure that promotes viral RNA dimerization. *Nucleic Acids Res* 2015; **43**: 8529-8539 [PMID: 26240378 DOI: 10.1093/nar/gkv786]

22 **Friebe P**, Boudet J, Simorre JP, Bartenschlager R. Kissing-loop interaction in the 3' end of the hepatitis C virus genome essential for RNA replication. *J Virol* 2005; **79**: 380-392 [PMID: 15596831 DOI: 10.1128/jvi.79.1.380-392.2005]

23 **Ivanyi-Nagy R**, Kanevsky I, Gabus C, Lavergne JP, Ficheux D, Penin F, Fossé P, Darlix JL. Analysis of hepatitis C virus RNA dimerization and core-RNA interactions. *Nucleic Acids Res* 2006; **34**: 2618-2633 [PMID: 16707664 DOI: 10.1093/nar/gkl240]

24 **Cantero-Camacho Á**, Fan L, Wang YX, Gallego J. Three-dimensional structure of the 3'X-tail of hepatitis C virus RNA in monomeric and dimeric states. *RNA* 2017; **23**: 1465-1476 [PMID: 28630140 DOI: 10.1261/rna.060632.117]

25 **Cristofari G**, Ivanyi-Nagy R, Gabus C, Boulant S, Lavergne JP, Penin F, Darlix JL. The hepatitis C virus Core protein is a potent nucleic acid chaperone that directs dimerization of the viral (+) strand RNA in vitro. *Nucleic Acids Res* 2004; **32**: 2623-2631 [PMID: 15141033 DOI: 10.1093/nar/gkh579]

26 **Kranawetter C**, Brady S, Sun L, Schroeder M, Chen SJ, Heng X. Nuclear Magnetic Resonance Study of RNA Structures at the 3'-End of the Hepatitis C Virus Genome. *Biochemistry* 2017; **56**: 4972-4984 [PMID: 28829576 DOI: 10.1021/acs.biochem.7b00573]

27 **Sharma KK**, de Rocquigny H, Darlix JL, Lavergne JP, Pénin F,

Lessinger JM, Mély Y. Analysis of the RNA chaperoning activity of the hepatitis C virus core protein on the conserved 3'X region of the viral genome. *Nucleic Acids Res* 2012; **40**: 2540-2553 [PMID: 22127859 DOI: 10.1093/nar/gkr1140]

28 **Tuplin A**, Struthers M, Simmonds P, Evans DJ. A twist in the tail: SHAPE mapping of long-range interactions and structural rearrangements of RNA elements involved in HCV replication. *Nucleic Acids Res* 2012; **40**: 6908-6921 [PMID: 22561372 DOI: 10.1093/nar/gks370]

29 **Carter LDB**, Aronsohn A. Overcoming injustice: A roadmap to improve access to hepatitis C virus therapy for our medicaid patients. *Hepatology* 2017; **65**: 1735-1740 [PMID: 28160311 DOI: 10.1002/hep.29095]

30 **Diviney S**, Tuplin A, Struthers M, Armstrong V, Elliott RM, Simmonds P, Evans DJ. A hepatitis C virus cis-acting replication element forms a long-range RNA-RNA interaction with upstream RNA sequences in NS5B. *J Virol* 2008; **82**: 9008-9022 [PMID: 18614633 DOI: 10.1128/JVI.02326-07]

31 **You S**, Rice CM. 3' RNA elements in hepatitis C virus replication: kissing partners and long poly(U). *J Virol* 2008; **82**: 184-195 [PMID: 17942554 DOI: 10.1128/JVI.01796-07]

32 **You S**, Stump DD, Branch AD, Rice CM. A cis-acting replication element in the sequence encoding the NS5B RNA-dependent RNA polymerase is required for hepatitis C virus RNA replication. *J Virol* 2004; **78**: 1352-1366 [PMID: 14722290 DOI: 10.1128/jvi.78.3.1352-1366.2004]

33 **Tuplin A**, Struthers M, Cook J, Bentley K, Evans DJ. Inhibition of HCV translation by disrupting the structure and interactions of the viral CRE and 3' X-tail. *Nucleic Acids Res* 2015; **43**: 2914-2926 [PMID: 25712095 DOI: 10.1093/nar/gkv142]

34 **Irshad M**, Mankotia DS, Irshad K. An insight into the diagnosis and pathogenesis of hepatitis C virus infection. *World J Gastroenterol* 2013; **19**: 7896-7909 [PMID: 24307784 DOI: 10.3748/wjg.v19.i44.7896]

35 **Shetty S**, Kim S, Shimakami T, Lemon SM, Mihailescu MR. Hepatitis C virus genomic RNA dimerization is mediated via a kissing complex intermediate. *RNA* 2010; **16**: 913-925 [PMID: 20360391 DOI: 10.1261/rna.1960410]

36 **Yamada N**, Tanihara K, Takada A, Yorihuzi T, Tsutsumi M, Shimomura H, Tsuji T, Date T. Genetic organization and diversity of the 3' noncoding region of the hepatitis C virus genome. *Virology* 1996; **223**: 255-261 [PMID: 8806561 DOI: 10.1006/viro.1996.0476]

37 **Kao CC**, Yang X, Kline A, Wang QM, Barket D, Heinz BA. Template requirements for RNA synthesis by a recombinant hepatitis C virus RNA-dependent RNA polymerase. *J Virol* 2000; **74**: 11121-11128 [PMID: 11070008 DOI: 10.1128/JVI.74.23.11121-11128.2000]

38 **Masante C**, Jaubert C, Palau W, Plissonneau J, Besnard L, Ventura M, Di Primo C. Mutations of the SL2 dimerization sequence of the hepatitis C genome abrogate viral replication. *Cell Mol Life Sci* 2015; **72**: 3375-3385 [PMID: 25822205 DOI: 10.1007/s00018-015-1893-3]

39 **Romero-López C**, Barroso-delJesus A, Berzal-Herranz A. The chaperone-like activity of the hepatitis C virus IRES and CRE elements regulates genome dimerization. *Sci Rep* 2017; **7**: 43415 [PMID: 28233845 DOI: 10.1038/srep43415]

40 **Yanagi M**, St Claire M, Emerson SU, Purcell RH, Bukh J. In vivo analysis of the 3' untranslated region of the hepatitis C virus after in vitro mutagenesis of an infectious cDNA clone. *Proc Natl Acad Sci U S A* 1999; **96**: 2291-2295 [PMID: 10051634 DOI: 10.1073/pnas.96.5.2291]

41 **Kolykhalov AA**, Mihalik K, Feinstone SM, Rice CM. Hepatitis C virus-encoded enzymatic activities and conserved RNA elements in the 3' nontranslated region are essential for virus replication in vivo. *J Virol* 2000; **74**: 2046-2051 [PMID: 10644379 DOI: 10.1128/JVI.74.4.2046-2051.2000]

42 **Yi M**, Lemon SM. 3' nontranslated RNA signals required for replication of hepatitis C virus RNA. *J Virol* 2003; **77**: 3557-3568 [PMID: 12610131 DOI: 10.1128/JVI.77.6.3557-3568.2003]

43 **Friebe P**, Bartenschlager R. Genetic analysis of sequences in the 3' nontranslated region of hepatitis C virus that are important for RNA replication. *J Virol* 2002; **76**: 5326-5338 [PMID: 11991961 DOI: 10.1128/JVI.76.11.5326-5338.2002]

44 **Oh JW**, Sheu GT, Lai MM. Template requirement and initiation site selection by hepatitis C virus polymerase on a minimal viral RNA template. *J Biol Chem* 2000; **275**: 17710-17717 [PMID: 10749880 DOI: 10.1074/jbc.M908781199]

45 **Reigadas S**, Ventura M, Sarih-Cottin L, Castroviejo M, Litvak S, Astier-Gin T. HCV RNA-dependent RNA polymerase replicates in vitro the 3' terminal region of the minus-strand viral RNA more efficiently than the 3' terminal region of the plus RNA. *Eur J Biochem* 2001; **268**: 5857-5867 [PMID: 11722573 DOI: 10.1046/j.0014-2956.2001.02532.x]

46 **Kim M**, Kim H, Cho SP, Min MK. Template requirements for de novo RNA synthesis by hepatitis C virus nonstructural protein 5B polymerase on the viral X RNA. *J Virol* 2002; **76**: 6944-6956 [PMID: 12072495 DOI: 10.1128/JVI.76.14.6944-6956.2002]

47 **Shim JH**, Larson G, Wu JZ, Hong Z. Selection of 3'-template bases and initiating nucleotides by hepatitis C virus NS5B RNA-dependent RNA polymerase. *J Virol* 2002; **76**: 7030-7039 [PMID: 12072503 DOI: 10.1128/JVI.76.14.7030-7039.2002]

48 **Butcher SJ**, Grimes JM, Makeyev EV, Bamford DH, Stuart DI. A mechanism for initiating RNA-dependent RNA polymerization. *Nature* 2001; **410**: 235-240 [PMID: 11242087 DOI: 10.1038/35065653]

49 **Banerjee R**, Dasgupta A. Specific interaction of hepatitis C virus protease/helicase NS3 with the 3'-terminal sequences of viral positive- and negative-strand RNA. *J Virol* 2001; **75**: 1708-1721 [PMID: 11160669 DOI: 10.1128/jvi.75.4.1708-1721.2001]

50 **DeMarini DJ**, Johnston VK, Konduri M, Gutshall LL, Sarisky RT. Intracellular hepatitis C virus RNA-dependent RNA polymerase activity. *J Virol Methods* 2003; **113**: 65-68 [PMID: 14500128 DOI: 10.1016/S0166-0934(03)00226-X]

51 **Tsuchihara K**, Tanaka T, Hijikata M, Kuge S, Toyoda H, Nomoto A, Yamamoto N, Shimotohno K. Specific interaction of polypyrimidine tract-binding protein with the extreme 3'-terminal structure of the hepatitis C virus genome, the 3'X. *J Virol* 1997; **71**: 6720-6726 [PMID: 9261396]

52 **Ito T**, Tahara SM, Lai MM. The 3'-untranslated region of hepatitis C virus RNA enhances translation from an internal ribosomal entry site. *J Virol* 1998; **72**: 8789-8796 [PMID: 9765423]

53 **McCaffrey AP**, Ohashi K, Meuse L, Shen S, Lancaster AM, Lukavsky PJ, Sarnow P, Kay MA. Determinants of hepatitis C translational initiation in vitro, in cultured cells and mice. *Mol Ther* 2002; **5**: 676-684 [PMID: 12027551 DOI: 10.1006/mthe.2002.0600]

54 **Bradrick SS**, Walters RW, Gromeier M. The hepatitis C virus 3'-untranslated region or a poly(A) tract promote efficient translation subsequent to the initiation phase. *Nucleic Acids Res* 2006; **34**: 1293-1303 [PMID: 16510853 DOI: 10.1093/nar/gkl019]

55 **Song Y**, Friebe P, Tzima E, Jünemann C, Bartenschlager R, Niepmann M. The hepatitis C virus RNA 3'-untranslated region strongly enhances translation directed by the internal ribosome entry site. *J Virol* 2006; **80**: 11579-11588 [PMID: 16971433 DOI: 10.1128/jvi.00675-06]

56 **Bung C**, Bochkaeva Z, Terenin I, Zinovkin R, Shatsky IN, Niepmann M. Influence of the hepatitis C virus 3'-untranslated region on IRES-dependent and cap-dependent translation initiation. *FEBS Lett* 2010; **584**: 837-842 [PMID: 20079737 DOI: 10.1016/j.febslet.2010.01.015]

57 **Ito T**, Lai MM. An internal polypyrimidine-tract-binding protein-binding site in the hepatitis C virus RNA attenuates translation, which is relieved by the 3'-untranslated sequence. *Virology* 1999; **254**: 288-296 [PMID: 9986795 DOI: 10.1006/viro.1998.9541]

58 **Villordo SM**, Gamarnik AV. Genome cyclization as strategy for flavivirus RNA replication. *Virus Res* 2009; **139**: 230-239 [PMID: 18703097 DOI: 10.1016/j.virusres.2008.07.016]

59 **Murakami K**, Abe M, Kageyama T, Kamoshita N, Nomoto A. Down-regulation of translation driven by hepatitis C virus internal ribosomal entry site by the 3' untranslated region of RNA. *Arch Virol* 2001; **146**: 729-741 [PMID: 11402859 DOI: 10.1007/s007050170142]

60 **Imbert I**, Dimitrova M, Kien F, Kieny MP, Schuster C. Hepatitis C virus IRES efficiency is unaffected by the genomic RNA 3'NTR even in the presence of viral structural or non-structural proteins. *J Gen Virol* 2003; **84**: 1549-1557 [PMID: 12771425 DOI: 10.1099/vir.0.18907-0]

61 **Wang H**, Shen XT, Ye R, Lan SY, Xiang L, Yuan ZH. Roles of the polypyrimidine tract and 3' noncoding region of hepatitis C virus RNA in the internal ribosome entry site-mediated translation. *Arch Virol* 2005; **150**: 1085-1099 [PMID: 15747050 DOI: 10.1007/s00705-005-0491-3]

62 **Wood J**, Frederickson RM, Fields S, Patel AH. Hepatitis C virus 3' X region interacts with human ribosomal proteins. *J Virol* 2001; **75**: 1348-1358 [PMID: 11152508 DOI: 10.1128/jvi.75.3.1348-1358.2001]

63 **Tanaka T**, Sugiyama K, Ikeda M, Naganuma A, Nozaki A, Saito M, Shimotohno K, Kato N. Hepatitis C virus NS5B RNA replicase specifically binds ribosomes. *Microbiol Immunol* 2000; **44**: 543-550 [PMID: 10941940 DOI: 10.1111/j.1348-0421.2000.tb02532.x]

P- Reviewer: Lei YC, Tamori A, Tarantino G, Wang L
S- Editor: Wang XJ **L- Editor**: A **E- Editor**: Yin SY

World Journal of Gastroenterology

Submit a Manuscript: http://www.f6publishing.com

World J Gastroenterol 2018 August 14; 24(30): 3384-3397

DOI: 10.3748/wjg.v24.i30.3384

ISSN 1007-9327 (print) ISSN 2219-2840 (online)

ORIGINAL ARTICLE

Basic Study

Herb-partitioned moxibustion alleviates colon injuries in ulcerative colitis rats

Dan Zhang, Yan-Bo Ren, Kai Wei, Jue Hong, Yan-Ting Yang, Li-Jie Wu, Ji Zhang, Zheng Shi, Huan-Gan Wu, Xiao-Peng Ma

Dan Zhang, Jue Hong, Zheng Shi, Huan-Gan Wu, Xiao-Peng Ma, Laboratory of Acupuncture-moxibustion and Immunology, Shanghai Research Institute of Acupuncture and Meridian, Shanghai University of Traditional Chinese Medicine, Shanghai 200030, China

Yan-Bo Ren, Department of Integrated Traditional Chinese Medicine and Western Medicine, North Branch of Huashan Hospital, Fudan University, Shanghai 201907, China

Kai Wei, Key Laboratory of Systems Biomedicine (Ministry of Education), Shanghai Center for Systems Biomedicine, Shanghai Jiao Tong University, Shanghai 200240, China

Yan-Ting Yang, Li-Jie Wu, Ji Zhang, Xiao-Peng Ma, Yueyang Clinical Medicine School, Shanghai University of Traditional Chinese Medicine, Shanghai 201203, China

ORCID number: Dan Zhang (0000-0003-0747-8691); Yan-Bo Ren (0000-0003-0738-5591); Kai Wei (0000-0003-1102-1117); Jue Hong (0000-0002-9857-818X); Yan-Ting Yang (0000-0003-1388-4047); Li-Jie Wu (0000-0003-3349-0918); Ji Zhang (0000-0002-6016-1063); Zheng Shi (0000-0003-0726-954X); Huan-Gan Wu (0000-0003-0563-1560); Xiao-Peng Ma (0000-0002-0582-3562).

Author contributions: Zhang D, Ren YB, Wei K and Hong J contributed equally to this work; Ma XP designed and supervised this research; Zhang D and Ren YB performed the animal experiment; Ren YB, Wei K, Hong J, Yang YT and Zhang J contributed to detection of all indexes; Zhang D wrote this manuscript and Wu LJ analyzed the data; Zhang D, Ren YB, Wei K and Hong J revised this manuscript; Shi Z and Wu HG were devoted to the guidance; all authors approved the final version of this article, including the author list.

Supported by the National Natural Science Foundation of China, No. 81674073, 81202754, and 81273843; Training Project for Outstanding Discipline Leaders of Shanghai Municipal Commission of Health and Family Planning, No. 2017BR047; National Key Basic Research Program of China (973 Program), No. 2015CB554501 and 2009CB522900; Budgetary Project of Shanghai University of Traditional Chinese Medicine, No. 18LK050.

Institutional animal care and use committee statement: All procedures involving animals were reviewed and approved by the Institutional Animal Care and Use Committee of Shanghai University of Traditional Chinese Medicine.

Conflict-of-interest statement: The authors declare that there is no conflict of interest regarding the publication of this paper.

Data sharing statement: No additional data are available.

The ARRIVE guidelines statement: The ARRIVE Guidelines have been adopted.

Manuscript source: Unsolicited manuscript

Correspondence to: Xiao-Peng Ma, PhD, Professor, Laboratory of Acupuncture-moxibustion and Immunology, Shanghai Research Institute of Acupuncture and Meridian, Shanghai University of Traditional Chinese Medicine, No. 650 South Wanping Road, Xuhui District, Shanghai 200030, China. pengpengma@163.com
Telephone: +86-21-64690257
Fax: +86-21-64382181

Received: May 9, 2018
Peer-review started: May 9, 2018
First decision: June 15, 2018
Revised: June 22, 2018
Accepted: June 30, 2018
Article in press: June 30, 2018
Published online: August 14, 2018

Abstract

AIM

To observe the effect of herb-partitioned moxibustion (HPM) on expression of colonic cytokines in ulcerative colitis (UC) rats.

METHODS

A UC rat model was established by protein immunization in combination with topical chemical stimulation. Rats in the HPM group (n = 8) received HPM at bilateral Tianshu (ST25) points. The gross injury and pathological scores of the colon were recorded. The expression profile of colonic cytokines was assayed using the protein microarray technique. Specific differential cytokines were selected and verified by ELISA. The corresponding UniProt Accessions of the differentially expressed cytokines were retrieved in the UniProt database. The pathways involved were analyzed with the help of the KEGG PATHWAY database. The DAVID database was used for functional cluster and pathway analysis.

RESULTS

HPM improved colon injuries in UC rats, manifested by accelerated repair of ulcers and alleviation of inflammation, and the gross injury and pathological scores both significantly decreased (P < 0.01). Fold change > 1.3 or < 0.77 was taken as the screening standard. There were 77 down-regulated and 9 up-regulated differentially expressed colonic cytokines in the HPM group compared with the model group, and expression of 20 differed significantly (P < 0.05). Twelve of the 20 significantly differentially expressed cytokines [β-catenin, interleukin-1 receptor 6 (IL-1R6), IL-1β, B7-1, nerve growth factor receptor, AMP-activated protein kinase-α1, neuropilin-2, orexin A, adipocyte differentiation-related protein, IL-2, Fas and FasL] were up-regulated in the model group (n = 3, compared with the normal group) but down-regulated in the HPM group (n = 3, compared with the model group). Functional cluster analysis showed that the differentially expressed colonic cytokines in the HPM group regulated apoptosis and protein phosphorylation. KEGG pathway analysis showed that 52 down-regulated and 7 up-regulated differentially expressed colonic cytokines in the HPM group had pathways. The pathways that interacted between the cytokines and their receptors accounted for the largest proportion (28 of the down-regulated and 5 of the up-regulated cytokines).

CONCLUSION

HPM promotes the repair of colon injuries in UC rats, which is related to the regulation of several abnormally expressed cytokines.

Key words: Cytokine expression profile; Ulcerative colitis; Protein microarray; Rats; Herb-partitioned moxibustion

Core tip: Herb-partitioned moxibustion (HPM) has been shown to be effective in treating ulcerative colitis (UC) in recent years as a non-drug external therapy. In this study, we observed its effect on the expression profile of cytokines in UC rat colon. By protein functional cluster analysis and KEGG pathway analysis, we can conclude that the effect of HPM in promoting the repair of colon injuries of UC rats is plausibly related to the regulation of multiple abnormally-expressed cytokines, and the regulation of the signal pathways interacting between the cytokines and their receptors may be its significant immunological mechanism.

Zhang D, Ren YB, Wei K, Hong J, Yang YT, Wu LJ, Zhang J, Shi Z, Wu HG, Ma XP. Herb-partitioned moxibustion alleviates colon injuries in ulcerative colitis rats. *World J Gastroenterol* 2018; 24(30): 3384-3397 Available from: URL: http://www.wjgnet.com/1007-9327/full/v24/i30/3384.htm DOI: http://dx.doi.org/10.3748/wjg.v24.i30.3384

INTRODUCTION

As two major types of inflammatory bowel disease (IBD), ulcerative colitis (UC) and Crohn's disease (CD) are both mainly characterized by chronic nonspecific inflammation of the colon. The incidence of UC is higher than that of CD, and it is increasing annually, with an incidence of 24.3/100000 in Europe and America, and 2.22/100000 in Guangzhou, which is the highest in China[1-3]. As a commonly encountered digestive disorder, UC is often recurrent and persistent, manifested by abdominal pain, diarrhea and bloody or purulent stools, and has an adverse effect on quality of life. Long-term medical treatment may also incur a high cost[4-8]. Immune dysfunction in the intestinal lining is recognized as the biological mechanism in the development of UC. In patients with UC, a large number of immunocytes (T cells, B cells, macrophages and dendritic cells) and cytokines [proinflammatory cytokines such as tumor necrosis factor (TNF)-α, interferon (IFN)-γ, interleukin (IL)-6, IL-12, IL-17, IL-21, IL-23, and integrin; anti-inflammatory cytokines such as IL-10, transforming growth factor (TGF)-β and IL-35] are abnormally expressed in the colon[9]. The imbalance of cytokines modulated by activated immunocytes should be the initial factor that causes diffuse superficial inflammatory injuries in UC[10,11]. Regulation of the activity of immune cells and expression of cytokines is beneficial to healing the colonic lining and alleviation of inflammation in UC patients[12,13].

During recent years, acupuncture-moxibustion at Qihai (CV6) and bilateral Tianshu (ST25) has been shown to significantly improve symptoms, quality of life and immune homeostasis in the colon of UC patients[14-16]. Acupuncture-moxibustion is characterized by moderate therapeutic effect, content treatment perception and rapid action, and is especially effective in mitigating abdominal pain and diarrhea in UC patients[17]. Compared with oral medications, acupuncture-moxibustion, as a

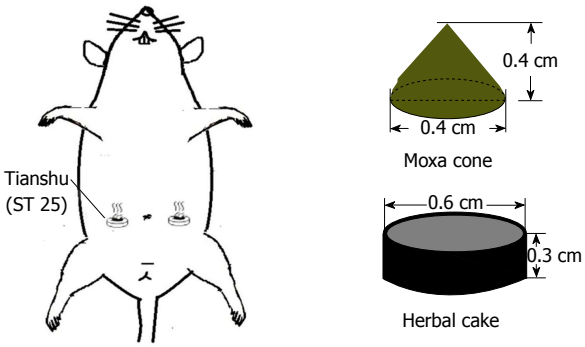

Figure 1 Illustration of herb-partitioned moxibustion. An herbal cake was placed on Tianshu (ST25) point with a moxa cone on the top to ignite. This point is located at the lower 1/3 between the xiphoid process and the midpoint of the pubic symphysis, 0.5 cm away.

nondrug external therapy, can also promote colonic blood circulation and intestinal peristalsis, heal damaged colonic lining, regulate colonic immune reactions, enhance self-healing and reduce relapse[18]. Although the efficacy of acupuncture-moxibustion in treating UC in both the short- and long-term is well recognized, their mechanism of action is still vague. Therefore, it is important to discover how acupuncture-moxibustion works in treating UC, and this will boost its application in the treatment of UC.

Protein microarray is an important tool in profiling the protein expression in IBD and screening new drugs. This technique is known for its high throughput, high sensitivity and high precision, and thoroughly and quantitatively analyzes the genre, number and correlation of proteins, by which complicated network and possible regulatory mechanisms are investigated[19-21]. Protein microarray has been gradually applied to research into traditional Chinese medicine (TCM), such as pharmacodynamics and toxicology of Chinese medications[22-24], yet it has rarely been used in the study of acupuncture-moxibustion therapy.

The present study established experimental UC rats and adopted the protein microarray technique to investigate the effect of herb-partitioned moxibustion (HPM) on the expression profile of colonic cytokines, to select those most associated with the therapeutic action of HPM. We used the UniProt and KEGG PATHWAY databases, as well as DAVID pathway and functional cluster analysis to study the immunopathogenesis of experimental UC and its treatment with HPM from the angle of cytokine expression profile.

MATERIALS AND METHODS

Experimental animals

Twenty-seven male Sprague-Dawley rats weighing 160 ± 20 g were provided by the Experimental Animal Center of Shanghai University of Traditional Chinese Medicine (SCXK (Hu) 2007-0005). The rats were housed for 3 d under controlled conditions (22 ± 2 ℃, relative humidity 64%) before the experiment started. All procedures for animal experiments were conducted in accordance with the International Guiding Principles for Biomedical Research Involving Animals recommended by the World Health Organization and were approved by the Animal Care and Use Committee of Shanghai University of Traditional Chinese Medicine. All rats were randomly divided into three groups as normal group, model group and HPM group, with nine rats per group.

Reagents and equipment

The following reagents and equipment were used: Freund's adjuvant (Sigma, St Louis, MO, United States), refined moxa wool (Nanyang Hanyi Moxa Co. Ltd., He' nan, China), Fugui formula 1 (Huaji Pharmaceutical Co. Ltd., Shanghai, China), hematoxylin and eosin (HE) staining kit (Nanjing Jiancheng Technology Co. Ltd., Nanjing, China), self-made cone-like copper moxa-cone mold, self-made columnar copper herbal cake mold, biotin label-based rat antibody array (90 rat proteins, RayBiotech, Norcross, GA, United States), ELISA kits for rat Fas/TNFRSF6, FasL/TNFSF6, IL-1R6 (IL-1Rrp2) and IL-1β (Bio-Techne, Minneapolis, MN, United States), phosphatase/protease inhibitor cocktail (Roche, Basel, Switzerland), RIPA lysis buffer, phenylmethanesulfonyl fluoride (PMSF) (Beyotime, Jiangsu, China), microplate reader (Thermo Fisher Scientific, Waltham, MA, United States), scanner (Qinghua Ziguang, Beijing, China), ScanAlyze image analysis software (Stanford University, CA, United States), pathological analysis system (Leica, Wetzlar, Germany), and light microscope and imaging system (Olympus, Tokyo, Japan).

Rat model of UC

The rat model of UC was established using immunization plus topical stimulation with formalin[25,26]. After modeling, each group contributed one rat for histopathological observation to verify the success of the UC model.

HPM

Rats in the HPM group were treated with HPM at bilateral Tianshu (ST25) points (Figure 1) by using a rat fixator. An herbal cake was placed on each point with a moxa cone on the top. The moxa cone was ignited, with two cones for each point as one session. The intervention was conducted once every other day, for four sessions and 8 d in total. Rats in the model group did not receive any interventions except the same grasping and fixing as in the HPM group. Rats in the normal group did not receive any modeling operation or interventions except for the same grasping and fixing.

Each moxa cone was made of 90 mg refined moxa wool by a copper mold, 0.4 cm in diameter and 0.4 cm in height. Guifu formula 1 was used to make herbal cakes, consisting of *Radix aconiti laterails preparata, Cortex cinnamon, Radix salvia miltiorrhizae, Flos carthami and Radix aucklandiae* (ratio: 10:2:3:3:1). The herbal powder was mixed with yellow rice wine immediately

before HPM treatment and then made into cakes of the same size using a specific mold (0.6 cm in diameter and 0.3 cm thickness).

Colon sample preparation

After the treatment, the rats were euthanized by an intraperitoneal injection of pentobarbital sodium (150 mg/kg). Colons (6-8 cm, cut at 2 cm away from the anus) were collected and opened longitudinally to observe and score gross injuries under a microscope. The scoring standard is shown in Supplementary Table 1. The colons were then cut into 2 pieces. The proximal part was stored at -80 ℃ and the distal part was fixed in 10% neutral-buffered formalin.

Morphological observation of the colon

After fixation in 10% neutral-buffered formalin overnight, colons were dehydrated, embedded in paraffin, sliced (3-5 μm) and baked (60 ℃) using the Leica pathological analysis system, followed by dewaxing and dehydration by dimethylbenzene and graded ethanol. The specimens were stained with hematoxylin for 10 min, differentiated by 1% HCl and ethanol, stained blue by 1% ammonia solution, stained by 0.5% eosin for 3 min, dehydrated through 70%, 85%, 95% and 100% ethanol, made transparent by dimethylbenzene, and sealed in neutral resin. Finally, the colon tissues were observed under a light microscope and scored. The scoring standard is shown in Supplementary Table 2.

Total protein extraction in the colon

Three colon samples were selected from each of the three groups to extract total protein. Lysis buffer containing protease inhibitor was added at 1 mL/250 mg (1 mL RIPA was mixed with 5 μL protease inhibitor solution, 5 μL PMSF and 5 μL phosphatase/protease inhibitor cocktail), and homogenized at a low speed (3000 rpm) for complete lysis of colon tissues. The colonic lysate was centrifuged at 14000 rpm for 15 min. The supernatant was collected to determine the concentration of total protein by bicinchoninic acid method.

Cytokine detection in colon

The protein chips were put into the reaction chamber of the chemiluminescent protein microarray kit from RayBiotech. A total of 2 mL blocking buffer was added into the reaction chamber, interacting for 30 min at room temperature. The protein chips were incubated with 1 mL sample supernatant (content of total proteins 50-500 μg), streptavidin antibody and horseradish-peroxidase-labeled anti-streptavidin antibody in sequence for 2 h at each step. After thorough washing, 500 μL chemiluminescent solution was added to the reaction chamber, which was incubated for 2 min at room temperature. The solution was then removed, and the protein chips were taken for imaging. Ninety kinds of cytokines are detailed in Supplementary Table 3.

Image and data analysis

The images were scanned and saved in .tiff format. ScanAlyze was used to transform the images into data that were then input into Microsoft Excel for normalization and analysis. Normalized result = [Original value - Blank (average)]/Positive (average). First, the protein abundance of rat colonic cytokines in each group was described. Second, intergroup fold change in normalized protein abundance was calculated. Fold change > 1.3 or < 0.77 were taken as the standard to define upregulation and downregulation of a cytokine, respectively.

UniProt accession and KEGG pathway analysis

Accessions of the differentially expressed cytokines were retrieved in the UniProt database to understand their protein structure and physicochemical properties. The corresponding pathways of the cytokines were sought in the KEGG PATHWAY database and then underwent functional cluster and pathway analysis with DAVID.

Validation of differentially expressed proteins in the colon

ELISA was used to verify the specific differentially expressed colonic cytokines. The appropriate amount of diluent samples, standard products and 10 μL avidin and 50 μL enzyme-labeled reagent were added to a 96-well dish and incubated at 37 ℃ for 30 min. When the above solutions were washed off, 50 μL chromogenic reagents A and B were added successively and mixed. The dish was kept at 37 ℃ for 15 min in the dark to allow developing. Finally, 50 μL stop solution was added to terminate the reaction. A microplate reader from Thermo Fisher was used to determine OD_{450}. The protein concentration was positively correlated with the OD value. The standard curve was drawn to reflect the cytokine concentration.

Statistical analysis

SPSS version 18.0 (IBM, Armonk, NY, United States) was used for statistical analysis. Measurement data including body weight, gross colon injury score, histopathological score, and expression of the 90 cytokines and differentially expressed cytokines, which completely or substantially conformed to a normal distribution and homogeneity of variance, were expressed as means ± SD. Body weight, gross colon injury score, histopathological score and expression of colonic differentially expressed cytokines were analyzed by one-way ANOVA followed by least significant difference test. An independent *t*-test was used for the between-group comparison of the expression of the 90 cytokines. $P < 0.05$ was considered to indicate statistical significance.

RESULTS

General condition

Rats in the normal group were vigorous and had normal intake of food, defecation, ruddy anus and steady increase of body weight. On the contrary, rats in the model group were weak and irritable, with reduced food intake, soft or loose stool sometimes with blood or pus, stained anus, and slower increase of body weight ($P < 0.01$). Compared with the model group, rats in the HPM

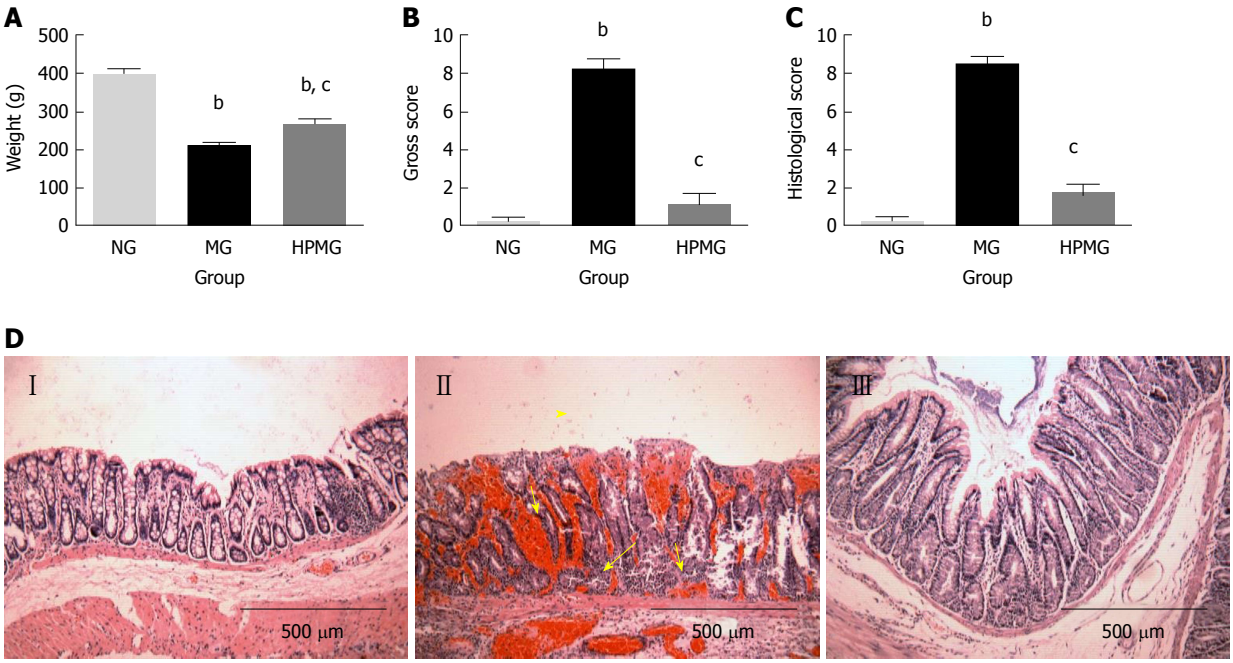

Figure 2 General condition, morphological observation and injury score of colon tissues in each group. A: Weight change of rats in each group; B: Gross injury score of rat colon in each group; C: Histological score of rat colon in each group; D: Histological and morphological structure under microscope by hematoxylin-eosin staining (Amplification × 100). NG (Ⅰ): Normal group, MG (Ⅱ): Model group; HPMG (Ⅲ): Herb-partitioned moxibustion group. Data are presented as the mean ± SD, n = 8 per group. $^{b}P < 0.01$ (*vs* normal group); $^{c}P < 0.01$ (*vs* model group).

group showed improvements in dieting, stool pattern and spiritual state, and body weight increased more significantly ($P < 0.01$) (Figure 2A).

Gross colon injury score

Compared with the normal group, colons in the model group were harder and darker, with thickened intestinal walls, less smooth lining with significant congestion and scattered ulcers covered by discharge, and the gross injury score was significantly higher ($P < 0.01$). Compared with the model group, colons in the HPM group showed notable improvement in colon injuries, presenting with soft pink intestines, slightly thickened intestinal walls, smooth and complete lining without visible ulcers, and the gross injury score was significantly lower ($P < 0.01$) (Figure 2B).

Morphological changes in the colon

Compared with the normal group, the model group had a significantly higher histopathological score for colon injuries ($P < 0.01$) and presented with disconnected colon lining, colonic gland necrosis or missing, disorganized crypts, atrophy in some colonic glands, and infiltration of the lamina propria and submucosa by many inflammatory cells such as neutrophils, eosinophils and mononuclear cells. Compared with the model group, rats in the HPM group showed significant improvements in colon injuries, manifested by substantially complete lining without noticeable ulcers but obvious growth of well-structured colonic glands, coupled with inflammatory polyps, alleviated inflammation in the lamina propria and submucosa, and a significantly lower histopathological score ($P < 0.01$), (Figure 2C and D).

Analysis of cytokine expression profiles

Compared with the normal group, 30 cytokines in colon tissues (n = 3) showed > 1.3 fold change in the model group (Table 1 and Figure 3A), among which 22 cytokines were significantly differentially expressed ($P < 0.05$); 34 cytokines showed < 0.77 fold change (Table 2, Figure 3A, and Figure 4), and 4 of them were significantly differentially expressed ($P < 0.05$).

Compared with the model group, 77 colonic cytokines showed < 0.77 fold change in the HPM group (Table 3, Figure 3B, and Figure 4), and 14 of them were significantly differentially expressed ($P < 0.05$); 9 cytokines showed > 1.3 fold change (Table 4 and Figure 3B), and 6 of them were significantly differentially expressed ($P < 0.05$).

Further analysis discovered that 12 cytokines that were upregulated (> 1.3 fold change) in the model group compared with those in the normal group were downregulated (< 0.77 fold change) after HPM intervention (Figure 5): *e.g.*, β-catenin, IL-1 receptor 6 (IL-1R6), B7-1, IL-1β, nerve growth factor receptor, AMP-activated protein kinase-α1, neuropilin-2, orexin A, adipocyte differentiation-related protein, IL-2, Fas and FasL. However, no cytokines that were downregulated (< 0.77 fold change) in the model group compared with those in the normal group were upregulated (> 1.3 fold change) after the intervention with HPM.

Functional cluster of the differentially expressed cytokines

Compared with the normal group, the differentially expressed cytokines in the model group regulated apoptosis, protein phosphorylation and modification,

Table 1 Cytokines associated with the development of ulcerative colitis (up-regulated)

Cytokine (up)	FC (M/N)	*P* value	Cytokine (up)	FC (M/N)	*P* value
FGF-BP	1.362082	0.02	FADD	2.012878	0.15
IL-5	1.383255	0.12	B7-1	2.121888	< 0.00
MIG-6	1.502947	0.01	Fas	2.133077	0.03
IL-10	1.538953	0.04	E-Selectin	2.193775	0.35
Fractalkine	1.562316	0.01	SPP1	2.286921	0.02
PDGF-AA	1.621171	0.05	IL-2	2.298734	0.01
β-Catenin	1.63583	< 0.000	Activin A	2.328823	0.01
FSL1	1.645565	0.004	IL-3	2.356267	0.08
AMPKα1	1.747397	0.001	ADFP	2.429592	< 0.00
RAGE	1.778351	0.02	Fas Ligand	2.476364	0.02
BDNF	1.800268	< 0.00	Neuropilin-2	2.742889	0.02
IC-1	1.812053	0.39	NGFR	3.519845	< 0.00
Insulin	1.917783	0.03	IL-1Rrp2/IL-1R6	3.668512	< 0.00
ACTH	1.919645	0.15	Orexin A	4.768017	0.01
PK1	1.956145	0.08	IL-1β	5.017418	< 0.000

FC: Fold change; M/N: Average of normalized result in the model group/average of normalized result in the normal group.

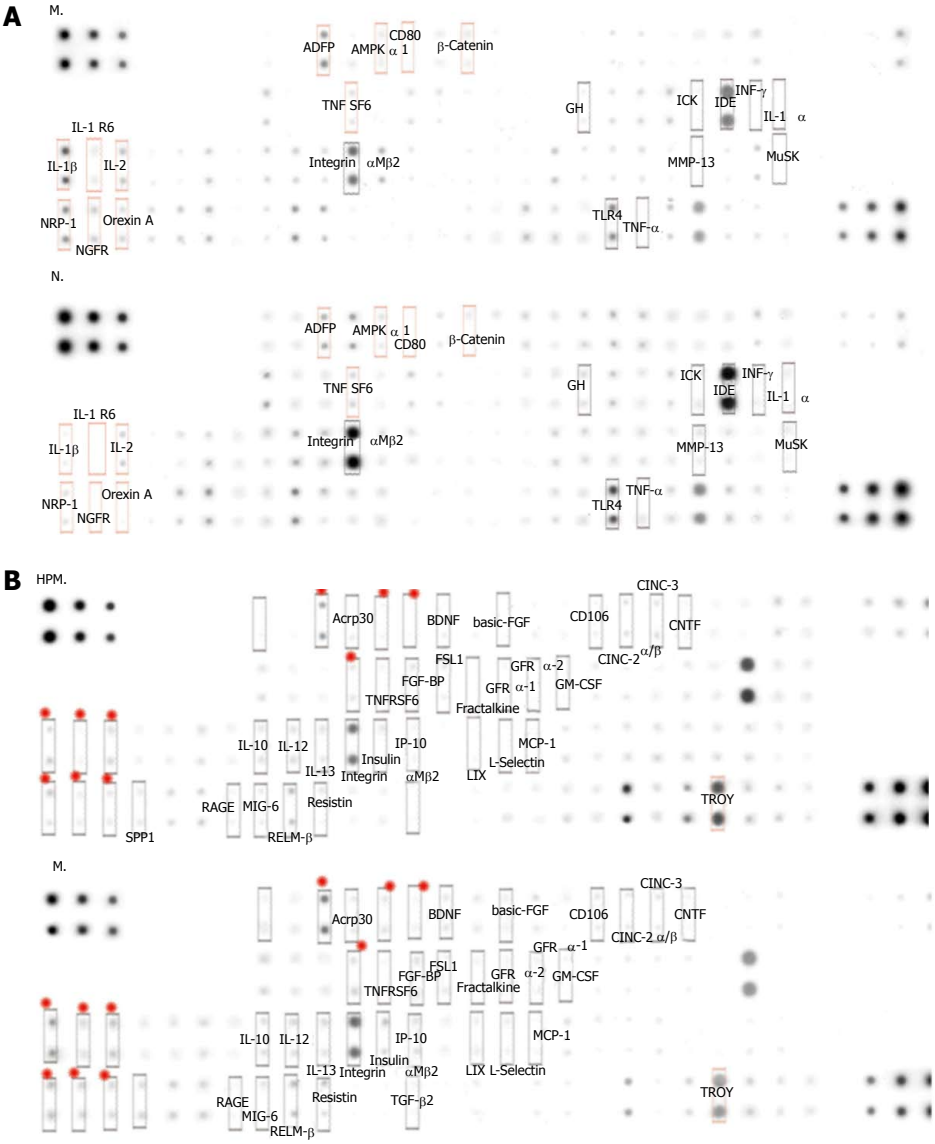

Figure 3 Protein abundances of colonic cytokines in each group. A: MG *vs* NG in comparing the change in mean protein abundance, and the cytokines with an obvious change are shown in the figure; B: HPMG *vs* MG in comparing the change in mean protein abundance, and the cytokines with an obvious change are shown in the figure. The significantly down-regulated proteins are marked in red (the focus of this study). NG: Normal group; MG: Model group; HPMG: Herb-partitioned moxibustion group.

Table 2 Cytokines associated with the development of ulcerative colitis (down-regulated)

Cytokine (down)	FC (M/N)	*P* value	Cytokine (down)	FC (M/N)	*P* value
MuSK	0.025485	0.26	GM-CSF	0.558641	0.01
MMP-13	0.191098	0.50	TRAIL	0.561294	0.73
ICK	0.206558	0.99	GH	0.583295	0.11
IFN-γ	0.210272	0.60	TLR4	0.605775	0.09
TNF-α	0.232403	0.54	CCR4	0.614899	0.15
IL-1α	0.283395	0.64	VEGF	0.630412	0.62
MIP-3α	0.297499	0.82	TIMP-2	0.636711	0.48
EGFR	0.362763	0.82	TGF-β1	0.644985	0.19
MMP-2	0.366125	0.94	CD106	0.6635	0.04
MIF	0.441963	0.52	ICAM-1	0.701176	0.3
MIP-1α	0.446228	0.69	Thrombospondin	0.708378	0.09
Ubiquitin	0.485159	0.59	IDE	0.711151	0.27
TIMP-3	0.489656	0.65	β-NGF	0.727731	0.13
MIP-2	0.513305	0.68	IC-3	0.748519	0.66
TIE-2	0.528072	0.81	MDC	0.749424	0.13
TGF-β3	0.550782	0.08	VEGF-C	0.768934	0.42
Growth hormone R	0.553239	0.50	CNTF	0.769193	0.02

FC: Fold change; M/N: Average of normalized result in the model group/average of normalized result in the normal group.

proliferation of white blood cells, lymphocytes and mononuclear cells, migration of white blood cells and vascular endothelial cells, activation of chemokines, and modulation of transcription factors of nuclear factor-κB and angiogenesis (Supplementary Tables 4 and 5). Compared with the model group, the differentially expressed cytokines in the HPM group regulated apoptosis, protein phosphorylation, cell migration, protein metabolism, activation and chemotaxis of neutrophils, activation of lymphocytes and transcription factors, migration of vascular endothelial cells, and secretion of cytokines (Supplementary Tables 6 and 7).

KEGG pathway analysis

Compared with the normal group, 18 of the up-regulated differentially expressed cytokines in the model group involved 18 signaling pathways. Eleven of them were pathways that interacted between cytokines and their receptors. The rest were pathways mainly involved in allotransplantation reactions, autoimmune thyroid disorders, type 1 diabetes, network of intestinal immunoglobulins, apoptosis, mitogen-activated protein kinase (MAPK) signaling pathway, graft *vs* host reaction, Janus kinase/signal transducer and activator of transcription (JAK/STAT) signaling pathway and Toll-like receptor (TLR) signaling pathway (Figure 6). Twenty-seven of the down-regulated differentially expressed cytokines in the model group involved 21 signaling pathways. Thirteen of them were pathways for the interaction between cytokines and their receptors. The rest were pathways mainly involved in the MAPK signaling pathway, TGF-β signaling pathway, natural killer (NK)-cell-mediated cytotoxicity, JAK/STAT signaling pathway, and apoptosis (Figure 6).

Compared with the model group, 52 of the 77 down-regulated differentially expressed cytokines in the HPM group were involved in 28 signaling pathways. The rest were involved in the JAK/STAT signaling pathway, cancer pathways, network of immunoglobulin A, MAPK signaling pathway, immunological rejection, TLR signaling pathway, chemokine signaling pathway, apoptosis, intercellular adhesion, graft *vs* host reaction, FcεRI and TGF-β signaling pathways, T-cell receptor pathways, mammalian target of rapamycin signaling pathway, NOD-like receptors and NK-cell-mediated cytotoxicity (Figure 7). There were ten pathways associated with the up-regulated cytokines that were differentially expressed in the HPM group compared with the model group (seven of the nine differentially expressed cytokines involved ten pathways). Five of them were for interactions between cytokines and receptors. The rest were mainly involved in the MAPK signaling pathway, graft *vs* host reaction, transplantation rejection, apoptosis, and TGF-β and TLR signaling pathways (Figure 7).

Verification of specific differential cytokines IL-1β, IL-1R6, Fas and FasL

Based on the protein microarray and functional cluster and pathway analysis, specific differential cytokines IL-1β, IL-1R6, Fas and FasL were selected for further verification by ELISA. Compared with the normal group, there were significant increases in expression of IL-1β, IL-1R6, Fas and FasL in the colon tissues of model group rats ($P < 0.01$, Figure 8). Compared with the model group, expression of IL-1β, IL-1R6, Fas and FasL decreased significantly in the HPM group ($P < 0.01$, Figure 8).

DISCUSSION

Although the development and application of oral medications or biological agents for UC have progressed, the treatment results have differed individually, not to mention that adverse effects have often been reported. Some research has proposed the use of more than two drugs together as a multitarget treatment to boost the efficacy, but more research is needed[27]. Conventional acupuncture-moxibustion therapy can produce a multi-

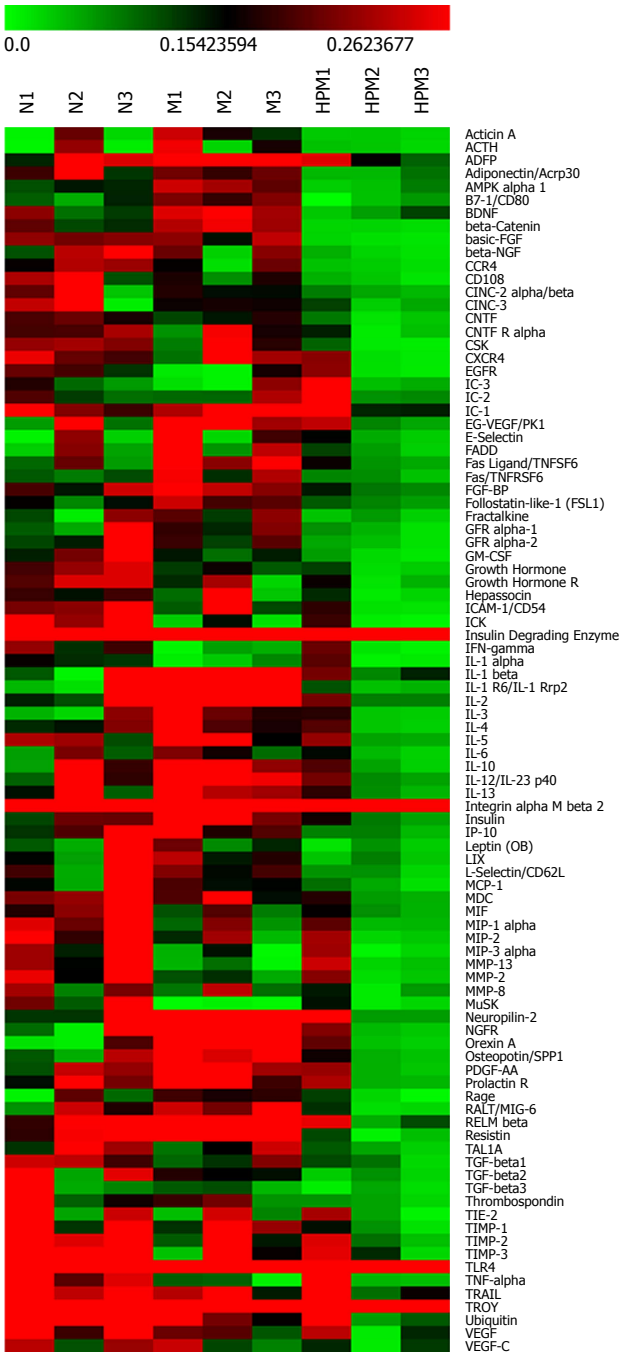

Figure 4 Clustering heatmap of colonic cytokines in each group. Red stands for those higher than the average density (marked in dark); green for those lower than the average density. *n* = 3 rats per group. N: Normal group; M: Model group; HPM: Herb-partitioned moxibustion group.

system, multitarget and multidirectional effect, without causing notable adverse reactions. For all these merits, it is recommended as an effective therapeutic approach for UC. Establishment of the mechanism of action of HPM in treating UC could provide important evidence to promote its application in treating IBD. The present study was a pilot study that used high-throughput protein microarray to elucidate the mechanism of action of HPM in the treatment of UC. Here, 86 differentially expressed cytokines in the colon were triggered by HPM. They mostly regulated apoptosis, protein phosphorylation, lymphocyte activation and chemotaxis, protein metabolism, and activation of transcription factors. This indicates that the effect of HPM in promoting the repair of colon injuries in UC rats is possibly linked to the effective regulation of several abnormal cytokines. According to KEGG pathway analysis, 38 pathways were related to these differentially expressed cytokines. The high number suggests a plausible relationship between the immunological action of HPM and the regulation of cytokines, their receptors and the involved pathways in treating UC.

Despite the unclear picture of the pathogenesis of UC, it is widely accepted that chronic nonspecific inflammation in the colon is its cardinal feature. A large number of immunocompetent cells presenting with excessive chemotaxis and abnormally expressed cytokines have been found in the colon of UC patients. Cytokines and their receptors, as well as the factors regulating signaling pathways, mainly serve to regulate the molecular network of colonic epithelial cells, immunocytes in lamina propria, and bacteria. Therefore, abnormal cytokines are possibly a crucial factor in causing immune disorders and colon injuries in UC[28,29]. Cytokines form a complicated network, interacting with immunocytes both as cause and effect, but their mechanism of action is still unclear. According to previous studies, the cytokines related to UC are comparatively precise, mainly focused on inflammatory factors, anti-inflammatory factors, chemokines and lymphocyte-activating factors, with a limited quantity for measurement. The present study has made up for the previous studies in genre and quantity of cytokines by examining important factors involved in apoptosis, cell proliferation, signaling pathway regulation, protein modification, tumor, and intestinal immune network. Besides the focus on inflammation, this study also used UniProt and KEGG pathway databases to further explore the possible pathogenesis of UC, providing new insights and foundations for UC and clinical intervention studies in the future.

HPM integrates moxibustion and Chinese herbal medicine and produces both pharmaceutical effects on the skin and physical thermal effects. It has been shown that HPM can exert definite effects in treating mild-to-moderate UC, by boosting colon healing and relief of inflammation; thus it is well accepted by patients[17]. Compared with oral medication and surgery, HPM is simple to operate, gentle in action, consistent in efficacy and extensive in regulation. It can significantly improve quality of life and restore intestinal function[30-32]. More and more cytokine antibodies have been approved for treatment of IBD, such as anti-TNF (*e.g.*, infliximab, etanercept and adalimumab) and anti-IL-12/23 p40 (*e.g.*, ustekinumab), indicating that regulation of cytokines is practical and essential in treating colitis[33]. How does HPM exert its effect on UC? Is it also related to the regulation of cytokines, and what else is involved? In this study, protein microarrays revealed that 12 cytokines

Table 3 Cytokines associated with the action of herb-partitioned moxibustion (down-regulated)

Cytokine (down)	FC (H/M)	*P* value	Cytokine (down)	FC (H/M)	*P* value
basic-FGF	0.0978	0.70	MCP-1	0.322376	0.71
β-Catenin	0.099918	0.03	PDGF-AA	0.329641	0.13
IL-1Rrp2/IL-1R6	0.157933	0.03	TGF-β3	0.335626	0.50
Resistin	0.165169	0.45	FADD	0.338264	0.33
B7-1/CD80	0.165526	0.02	Prolactin R	0.352073	0.57
Activin A	0.169884	0.23	IL-10	0.353484	0.23
IL-1β	0.181118	0.01	IL-3	0.354765	0.15
NGFR	0.205767	0.02	FSL1	0.374421	0.06
β-NGF	0.206263	0.52	PK1	0.374728	0.22
ACTH	0.206715	0.50	CINC-2 α/β	0.375162	0.76
AMPKα1	0.218363	0.01	FGF-BP	0.378172	0.21
CSK	0.220766	0.54	ICAM-1	0.379167	0.45
GFRα-2	0.222922	0.65	TAL1A	0.379464	0.52
CCR4	0.229987	0.26	CNTF Rα	0.380412	0.57
MIG-6	0.234297	0.22	IL-13	0.381048	0.52
Neuropilin-2	0.23433	0.04	IL-12	0.395678	0.55
Fractalkine	0.238117	0.39	CXCR4	0.397749	0.92
CD106	0.238859	0.32	IL-4	0.400025	0.30
GFRα-1	0.248202	0.66	CINC-3	0.404805	0.89
Orexin A	0.256555	0.01	MDC	0.417278	0.50
GM-CSF	0.259198	0.16	IL-5	0.41803	0.33
TGF-β2	0.261203	0.58	E-Selectin	0.424327	0.43
LIX	0.270135	0.91	Hepassocin	0.428314	0.61
BDNF	0.270917	0.06	GH	0.441903	0.02
RAGE	0.27422	0.24	Integrin αMβ2	0.458492	0.03
Leptin (OB)	0.276614	0.79	IL-6	0.47843	0.60
SPP1	0.278682	0.07	TGF-β1	0.511556	0.12
TIMP-1	0.280948	0.88	MMP-8	0.525606	0.65
L-Selectin	0.283725	0.91	GH R	0.581019	0.17
Fas	0.289612	0.06	TIMP-2	0.581976	0.31
RELMβ	0.290633	0.47	VEGF-C	0.610166	0.54
ADFP	0.290674	0.01	IC-1	0.639561	0.12
Acrp30	0.291541	0.81	IDE	0.678174	0.01
IP-10	0.295663	0.88	TIMP-3	0.69365	0.16
IL-2	0.298121	0.03	MIP-2	0.713848	0.13
Insulin	0.305481	0.09	MIF	0.725496	0.18
CNTF	0.310717	0.10	Ubiquitin	0.73656	0.09
Fas Ligand	0.319733	< 0.05	MIP-1α	0.761068	0.09
Thrombospondin	0.322261	0.55	VEGF	0.765926	0.13

FC: Fold change; H/M: Average of normalized result in the herb-partitioned moxibustion group/average of normalized result in the model group.

Table 4 Cytokines associated with the action of herb-partitioned moxibustion (up-regulated)

Cytokine (up)	FC (H/M)	*P* value	Cytokine (up)	FC (H/M)	*P* value
EGFR	1.335106	0.13	TNF-α	1.937065	0.04
TROY	1.34044	0.31	IFN-γ	2.000647	0.01
TLR4	1.511846	0.04	MMP-13	2.19335	0.04
IC-3	1.664604	0.74	MuSK	12.24563	0.02
IL-1α	1.845212	0.01			

FC: Fold change; H/M: Average of normalized result in the herb-partitioned moxibustion group/average of normalized result in the model group.

upregulated (fold change > 1.3) in the model group compared with the normal group were downregulated (fold change < 0.77) after HPM intervention. These cytokines are involved in the modulation of inflammation, apoptosis, adhesion, activation of co-stimulatory signals, metabolism, and nervous regulation. The pathway analysis also suggested an association between the effect of HPM in healing colon injuries of UC and the down-regulation of several abnormally expressed cytokines. Hence, regulation of signaling pathways of cytokines and their receptors is possibly an important immunological mechanism. So far, we have seen that HPM has several regulatory effects on colonic cytokines. However, it remains a question whether this non-drug therapy can compare with oral or venous application of antibodies, immunosuppressive agents, steroidal and anti-inflammatory drugs.

We showed that HPM significantly downregulated

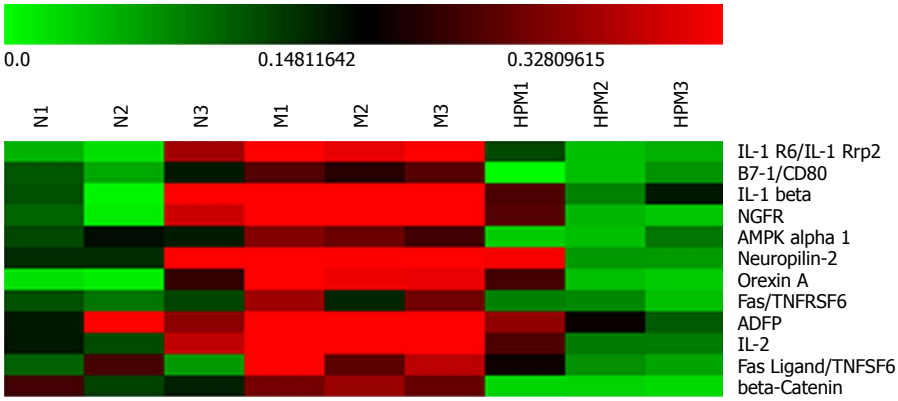

Figure 5 Clustering heatmap of the specific differential cytokines in each group. Red stands for those higher than the average density (marked in dark); green for those lower than the average density. *n* = 3 rats per group. N: Normal group; M: Model group; HPM: Herb-partitioned moxibustion group.

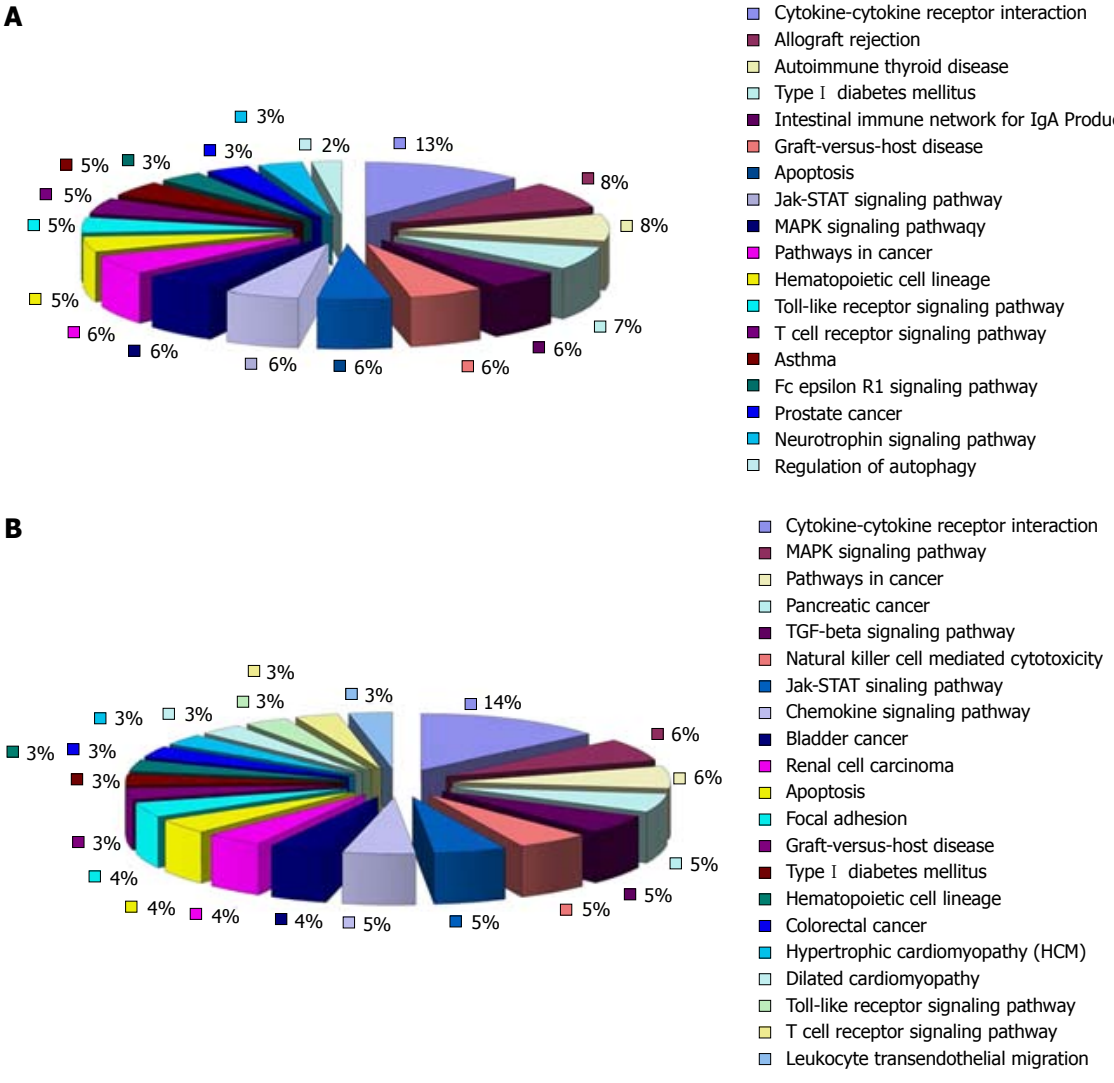

Figure 6 KEGG pathway analysis of the cytokines related to the development of ulcerative colitis. A: Eleven of all the major signaling pathways of the up-regulated cytokines in the model group (compared with the normal group) are involved in the interaction between cytokines and their receptors (36.7%); B: Of the major signaling pathways of the down-regulated cytokines in the model group (compared with the normal group), 13 pathways regulate the interaction between cytokines and their receptors (39.4%) (Supplementary Tables 4 and 5).

the expression of IL-1β, IL-1R6, Fas and FasL, which agreed with previous studies[16,34-40]. We demonstrated that inflammatory infiltration and apoptosis in the colonic epithelium, controlled by cytokines and their network,

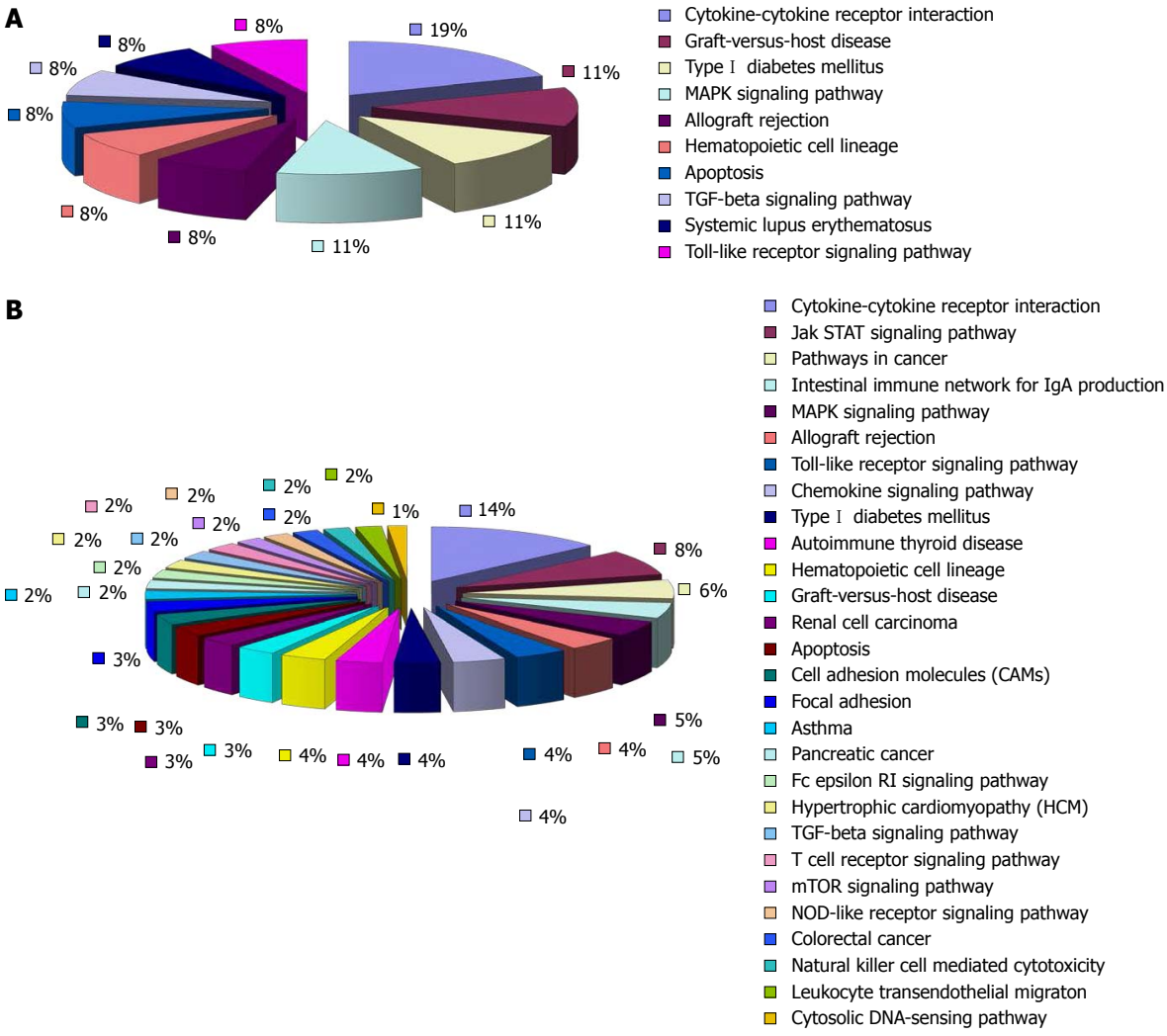

Figure 7 KEGG pathway analysis of the cytokines related to the action of herb-partitioned moxibustion. A: Among the major signaling pathways related to the up-regulated cytokines in the herb-partitioned moxibustion group (compared with the model group), five pathways were involved in the interaction between cytokines and their receptors (55.6%); B: Of the major signaling pathways related to the down-regulated cytokines in the herb-partitioned moxibustion group (compared with the model group), 27 pathways were involved in the interaction between cytokines and their receptors (38%) (Supplementary Tables 6 and 7).

are crucial factors in the pathogenesis of UC. We also discovered that the proinflammatory factor IL-1β was significantly upregulated, while the immunoregulatory factor TGF-β was down-regulated in UC. This caused an imbalance between proinflammatory and anti-inflammatory factors, which also agreed with previous studies. However, in our study, the proinflammatory factors TNF-α and IFN-γ were downregulated, although without significance, which differed from the previous results. The UC modeling method could have accounted for this difference. IL-1β originates from the innate intestinal immune system, while TNF-α and IFN-γ are produced by T helper cells of the acquired immune system. Our study used immunological and chemical stimulation to establish the UC model, which may have a different mechanism of injury from that induced by bacteria[41,42]. By using protein microarray, we systematically discussed the pathogenesis of UC and possible action mechanism of HPM and hope to inspire more studies to further verify the findings.

ARTICLE HIGHLIGHTS

Research background

The imbalance of cytokines modulated by activated immunocytes has been verified as an initial factor inducing inflammatory injuries in ulcerative colitis (UC). Herb-partitioned moxibustion (HPM), a non-drug external therapy, produces valid efficacy in treating UC, but its potential mechanism is still unclear.

Research motivation

The action mechanism of HPM was explored by using high throughout analysis of cytokine expression profiles in the colon and their network effects in our research.

Research objectives

By identifying the key cytokines in the action of HPM and analyzing their signal pathways, our research aimed to provide research ideas and crucial targets for further elaboration of the anti-inflammation mechanism of HPM in treating UC.

Research methods

A UC rat model was established by protein immunization in combination with topical chemical stimulation. Rats in the HPM group received HPM at bilateral Tianshu (ST25) points. The expression profile of colonic cytokines was assayed

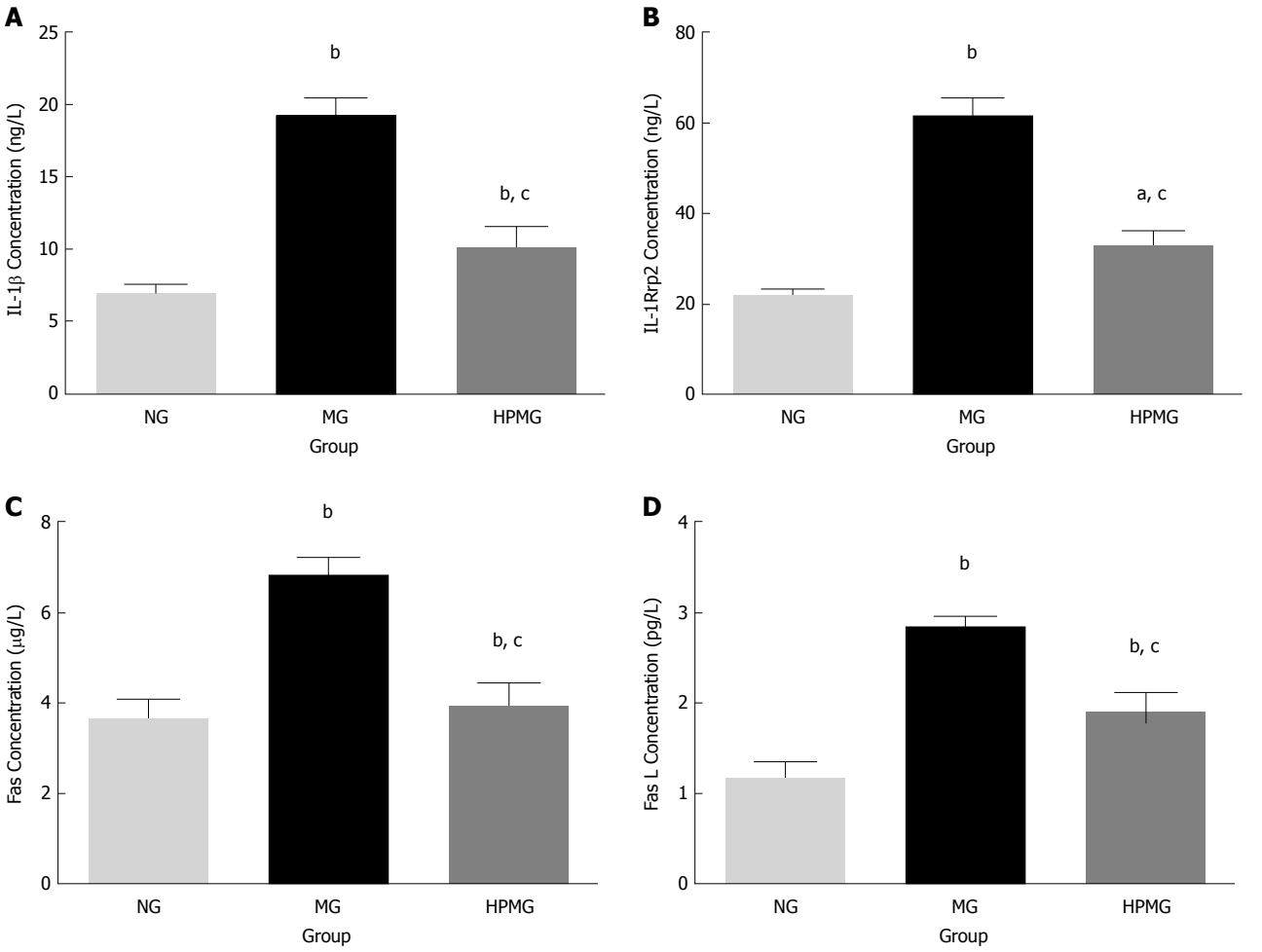

Figure 8 Validation of the specific differential cytokines. A: Expression of IL-1β protein in colon; B: Expression of IL-1Rrp2/IL-1R6 protein in colon; C: Expression of Fas protein in colon; D: Expression of FasL protein in colon. Data are presented as the mean ± SD, $n = 8$ rats per group. $^{b}P < 0.01$, $^{a}P < 0.05$, (*vs* normal group); $^{c}P < 0.01$ (*vs* model group). NG: Normal group; MG: Model group; HPMG: Herb-partitioned moxibustion group.

using the protein microarray technique.

Research results

Seventy-seven down-regulated and nine up-regulated differentially-expressed colonic cytokines were found in the HPM group. Functional cluster analysis showed that the differentially-expressed colonic cytokines in the HPM group regulated apoptosis and protein phosphorylation. KEGG pathway analysis showed that the pathways interacting between the cytokines and their receptors accounted for the largest proportion (28 of 52 down-regulated cytokines and 5 of 7 up-regulated cytokines).

Research conclusions

HPM promotes the repair of colon injuries in UC rats, which is related to the regulation of several abnormally-expressed cytokines.

Research perspectives

By functional cluster and KEGG pathway analyses, this study selected specific differential cytokines in HPM treatment of UC, which can provide potential targets for targeted therapy in the future and also research ideas for further elaboration of signal pathways in the action of HPM for UC. The results showed that the signal pathways interacting between cytokines and their receptors were closely related to the action of HPM, and the MAPK signaling pathway and JAK/STAT signaling pathway were possibly involved in the anti-inflammation process of HPM for colitis. A focus on this field may help better understand the mechanism of moxibustion in treating UC.

REFERENCES

1 **Molodecky NA**, Soon IS, Rabi DM, Ghali WA, Ferris M, Chernoff G, Benchimol EI, Panaccione R, Ghosh S, Barkema HW, Kaplan GG. Increasing incidence and prevalence of the inflammatory bowel diseases with time, based on systematic review. *Gastroenterology* 2012; **142**: 46-54.e42; quiz e30 [PMID: 22001864 DOI: 10.1053/j.gastro.2011.10.001]

2 **Cosnes J**, Gower-Rousseau C, Seksik P, Cortot A. Epidemiology and natural history of inflammatory bowel diseases. *Gastroenterology* 2011; **140**: 1785-1794 [PMID: 21530745 DOI: 10.1053/j.gastro.2011.01.055]

3 **Ng WK**, Wong SH, Ng SC. Changing epidemiological trends of inflammatory bowel disease in Asia. *Intest Res* 2016; **14**: 111-119 [PMID: 27175111 DOI: 10.5217/ir.2016.14.2.111]

4 **Włodarczyk M**, Sobolewska-Włodarczyk A, Stec-Michalska K, Fichna J, Wiśniewska-Jarosińska M. The influence of family pattern abnormalities in the early stages of life on the course of inflammatory bowel diseases. *Pharmacol Rep* 2016; **68**: 852-858 [PMID: 27199029 DOI: 10.1016/j.pharep.2016.04.008]

5 **Bernklev T**, Jahnsen J, Schulz T, Sauar J, Lygren I, Henriksen M, Stray N, Kjellevold Ø, Aadland E, Vatn M, Moum B. Course of disease, drug treatment and health-related quality of life in patients with inflammatory bowel disease 5 years after initial diagnosis. *Eur J Gastroenterol Hepatol* 2005; **17**: 1037-1045 [PMID: 16148548 DOI: 10.1097/00042737-200510000-00006]

6 **Zeitz J**, Ak M, Müller-Mottet S, Scharl S, Biedermann L, Fournier N, Frei P, Pittet V, Scharl M, Fried M, Rogler G, Vavricka S; Swiss IBD Cohort Study Group. Pain in IBD Patients: Very Frequent and Frequently Insufficiently Taken into Account. *PLoS One* 2016; **11**: e0156666 [PMID: 27332879 DOI: 10.1371/journal.pone.0156666]

7 **Casellas F**, López-Vivancos J, Casado A, Malagelada JR. Factors affecting health related quality of life of patients with inflammatory bowel disease. *Qual Life Res* 2002; **11**: 775-781 [PMID: 12482161 DOI: 10.1023/A:1020841601110]

8 **Burkhalter H**, Stucki-Thür P, David B, Lorenz S, Biotti B, Rogler G, Pittet V. Assessment of inflammatory bowel disease patient's needs and problems from a nursing perspective. *Digestion* 2015; **91**: 128-141 [PMID: 25677558 DOI: 10.1159/000371654]

9 **Ince MN**, Elliott DE. Immunologic and molecular mechanisms in inflammatory bowel disease. *Surg Clin North Am* 2007; **87**: 681-696 [PMID: 17560420 DOI: 10.1016/j.suc.2007.03.005]

10 **de Souza HS**, Fiocchi C. Immunopathogenesis of IBD: current state of the art. *Nat Rev Gastroenterol Hepatol* 2016; **13**: 13-27 [PMID: 26627550 DOI: 10.1038/nrgastro.2015.186]

11 **Loddo I**, Romano C. Inflammatory Bowel Disease: Genetics, Epigenetics, and Pathogenesis. *Front Immunol* 2015; **6**: 551 [PMID: 26579126 DOI: 10.3389/fimmu.2015.00551]

12 **Fiorino G**, Bonovas S, Cicerone C, Allocca M, Furfaro F, Correale C, Danese S. The safety of biological pharmacotherapy for the treatment of ulcerative colitis. *Expert Opin Drug Saf* 2017; **16**: 437-443 [PMID: 28279079 DOI: 10.1080/14740338.2017.1298743]

13 **Katsanos KH**, Papadakis KA. Inflammatory Bowel Disease: Updates on Molecular Targets for Biologics. *Gut Liver* 2017; **11**: 455-463 [PMID: 28486793 DOI: 10.5009/gnl16308]

14 **Joos S**, Wildau N, Kohnen R, Szecsenyi J, Schuppan D, Willich SN, Hahn EG, Brinkhaus B. Acupuncture and moxibustion in the treatment of ulcerative colitis: a randomized controlled study. *Scand J Gastroenterol* 2006; **41**: 1056-1063 [PMID: 16938719 DOI: 10.1080/00365520600580688]

15 **Wu H**, Chen H, Hua X, Shi Z, Zhang L, Chen J. Clinical therapeutic effect of drug-separated moxibustion on chronic diarrhea and its immunologic mechanisms. *J Tradit Chin Med* 1997; **17**: 253-258 [PMID: 10437206]

16 **Zhou EH**, Liu HR, Wu HG, Shi Z, Zhang W, Zhu Y, Shi DR, Zhou S. Down-regulation of protein and mRNA expression of IL-8 and ICAM-1 in colon tissue of ulcerative colitis patients by partition-herb moxibustion. *Dig Dis Sci* 2009; **54**: 2198-2206 [PMID: 19083096 DOI: 10.1007/s10620-008-0620-4]

17 **Ji J**, Huang Y, Wang XF, Ma Z, Wu HG, Im H, Liu HR, Wu LY, Li J. Review of Clinical Studies of the Treatment of Ulcerative Colitis Using Acupuncture and Moxibustion. *Gastroenterol Res Pract* 2016; **2016**: 9248589 [PMID: 27885326 DOI: 10.1155/2016/9248589]

18 **Ji J**, Lu Y, Liu H, Feng H, Zhang F, Wu L, Cui Y, Wu H. Acupuncture and moxibustion for inflammatory bowel diseases: a systematic review and meta-analysis of randomized controlled trials. *Evid Based Complement Alternat Med* 2013; **2013**: 158352 [PMID: 24204388 DOI: 10.1155/2013/158352]

19 **Mourad FH**, Yau Y, Wasinger VC, Leong RW. Proteomics in Inflammatory Bowel Disease: Approach Using Animal Models. *Dig Dis Sci* 2017; **62**: 2266-2276 [PMID: 28717845 DOI: 10.1007/s10620-017-4673-0]

20 **Chan PP**, Wasinger VC, Leong RW. Current application of proteomics in biomarker discovery for inflammatory bowel disease. *World J Gastrointest Pathophysiol* 2016; **7**: 27-37 [PMID: 26909226 DOI: 10.4291/wjgp.v7.i1.27]

21 **Yau Y**, Leong RW, Zeng M, Wasinger VC. Proteomics and metabolomics in inflammatory bowel disease. *J Gastroenterol Hepatol* 2013; **28**: 1076-1086 [PMID: 23489082 DOI: 10.1111/jgh.12193]

22 **Chen L**, Hou Q, Zhou ZZ, Li MR, Zhong LZ, Deng XD, Zhu ZY, Cheng ZY, Zhu J, Xiang CL, He WJ, Fu XB. Comparative Proteomic Analysis of the Effect of the Four-Herb Chinese Medicine ANBP on Promoting Mouse Skin Wound Healing. *Int J Low Extrem Wounds* 2017; **16**: 154-162 [PMID: 28741388 DOI: 10.1177/1534734617720623]

23 **Teschke R**, Eickhoff A. Herbal hepatotoxicity in traditional and modern medicine: actual key issues and new encouraging steps. *Front Pharmacol* 2015; **6**: 72 [PMID: 25954198 DOI: 10.3389/fphar.2015.00072]

24 **Fang H**, Wang K, Zhang J. Transcriptome and proteome analyses of drug interactions with natural products. *Curr Drug Metab* 2008; **9**: 1038-1048 [PMID: 19075620 DOI: 10.2174/138920008786927802]

25 **Xu SY**, Bian RL, Chen X. Pharmacology Experiment Methodology. Beijing, China: People's Medical Publishing House 2002: 1335

26 **Wang X**, Liu Y, Dong H, Wu L, Feng X, Zhou Z, Zhao C, Liu H, Wu H. Herb-Partitioned Moxibustion Regulates the TLR2/NF-κB Signaling Pathway in a Rat Model of Ulcerative Colitis. *Evid Based Complement Alternat Med* 2015; **2015**: 949065 [PMID: 26339273 DOI: 10.1155/2015/949065]

27 **Di Sario A**, Bendia E, Schiadà L, Sassaroli P, Benedetti A. Biologic Drugs in Crohn's Disease and Ulcerative Colitis: Safety Profile. *Curr Drug Saf* 2016; **11**: 55-61 [PMID: 26882354 DOI: 10.2174/1574886311011602121717 57]

28 **Kunkel EJ**, Campbell DJ, Butcher EC. Chemokines in lymphocyte trafficking and intestinal immunity. *Microcirculation* 2003; **10**: 313-323 [PMID: 12851648 DOI: 10.1038/sj.mn.7800196]

29 **Beck PL**, Wallace JL. Cytokines in inflammatory bowel disease. *Mediat of Inflammat* 1997; **6**: 95-103 [PMID: 18472842 DOI: 10.1080/09629359791785]

30 **Li H**, He T, Xu Q, Li Z, Liu Y, Li F, Yang BF, Liu CZ. Acupuncture and regulation of gastrointestinal function. *World J Gastroenterol* 2015; **21**: 8304-8313 [PMID: 26217082 DOI: 10.3748/wjg.v21.i27.8304]

31 **Takahashi T**. Effect and mechanism of acupuncture on gastrointestinal diseases. *Int Rev Neurobiol* 2013; **111**: 273-294 [PMID: 24215928 DOI: 10.1016/B978-0-12-411545-3.00014-6]

32 **Cheifetz AS**, Gianotti R, Luber R, Gibson PR. Complementary and Alternative Medicines Used by Patients With Inflammatory Bowel Diseases. *Gastroenterology* 2017; **152**: 415-429.e15 [PMID: 27743873 DOI: 10.1053/j.gastro.2016.10.004]

33 **Danese S**, Vuitton L, Peyrin-Biroulet L. Biologic agents for IBD: practical insights. *Nat Rev Gastroenterol Hepatol* 2015; **12**: 537-545 [PMID: 26284562 DOI: 10.1038/nrgastro.2015.135]

34 **De Santis S**, Kunde D, Galleggiante V, Liso M, Scandiffio L, Serino G, Pinto A, Campiglia P, Sorrentino R, Cavalcanti E, Santino A, Caruso ML, Eri R, Chieppa M. TNFα deficiency results in increased IL-1β in an early onset of spontaneous murine colitis. *Cell Death Dis* 2017; **8**: e2993 [PMID: 28796256 DOI: 10.1038/cddis.2017.397]

35 **Fonseca-Camarillo G**, Yamamoto-Furusho JK. Immunoregulatory Pathways Involved in Inflammatory Bowel Disease. *Inflamm Bowel Dis* 2015; **21**: 2188-2193 [PMID: 26111210 DOI: 10.1097/MIB.0000000000000477]

36 **Yao J**, Cao X, Zhang R, Li YX, Xu ZL, Zhang DG, Wang LS, Wang JY. Protective Effect of Baicalin Against Experimental Colitis via Suppression of Oxidant Stress and Apoptosis. *Pharmacogn Mag* 2016; **12**: 225-234 [PMID: 27601854 DOI: 10.4103/0973-1296.186342]

37 **Iwamoto M**, Koji T, Makiyama K, Kobayashi N, Nakane PK. Apoptosis of crypt epithelial cells in ulcerative colitis. *J Pathol* 1996; **180**: 152-159 [PMID: 8976873 DOI: 10.1002/(SICI)1096-9896(199610)180:2<152::AID-PATH649>3.0.CO;2-Y]

38 **O'Neill LA**. The interleukin-1 receptor/Toll-like receptor superfamily: 10 years of progress. *Immunol Rev* 2008; **226**: 10-18 [PMID: 19161412 DOI: 10.1111/j.1600-065X.2008.00701.x]

39 **Wu HG**, Liu HR, Tan LY, Gong YJ, Shi Y, Zhao TP, Yi Y, Yang Y. Electroacupuncture and moxibustion promote neutrophil apoptosis and improve ulcerative colitis in rats. *Dig Dis Sci* 2007; **52**: 379-384 [PMID: 17211698 DOI: 10.1007/s10620-006-9561-y]

40 **Ma TM**, Xu N, Ma XD, Bai ZH, Tao X, Yan HC. Moxibustion regulates inflammatory mediators and colonic mucosal barrier in ulcerative colitis rats. *World J Gastroenterol* 2016; **22**: 2566-2575 [PMID: 26937144 DOI: 10.3748/wjg.v22.i8.2566]

41 **Singh UP**, Singh NP, Murphy EA, Price RL, Fayad R, Nagarkatti

M, Nagarkatti PS. Chemokine and cytokine levels in inflammatory bowel disease patients. *Cytokine* 2016; **77**: 44-49 [PMID: 26520877 DOI: 10.1016/j.cyto.2015.10.008]

42 **Guan Q**, Zhang J. Recent Advances: The Imbalance of Cytokines in the Pathogenesis of Inflammatory Bowel Disease. *Mediators Inflamm* 2017; **2017**: 4810258 [PMID: 28420941 DOI: 10.1155/2017/4810258]

P- Reviewer: Kukongviriyapan V, Weinhausel A **S- Editor**: Wang XJ
L- Editor: Filipodia **E- Editor**: Yin SY

World Journal of Gastroenterology

Submit a Manuscript: http://www.f6publishing.com

World J Gastroenterol 2018 August 14; 24(30): 3398-3413

DOI: 10.3748/wjg.v24.i30.3398

ISSN 1007-9327 (print) ISSN 2219-2840 (online)

ORIGINAL ARTICLE

Basic Study

Novel sericin-based hepatocyte serum-free medium and sericin's effect on hepatocyte transcriptome

Yun Huang, Qing Peng, Hai-Yan Li, Zhi-Dong Jia, Yang Li, Yi Gao

Yun Huang, Qing Peng, Hai-Yan Li, Zhi-Dong Jia, Yang Li, Department of Hepatobiliary Surgery Ⅱ, Guangdong Provincial Research Center for Artificial Organ and Tissue Engineering, Guangzhou Clinical Research and Transformation Center for Artificial Liver, Institute of Regenerative Medicine, Zhujiang Hospital, Southern Medical University, Guangzhou 510280, Guangdong Province, China

Yi Gao, Department of Hepatobiliary Surgery Ⅱ, Guangdong Provincial Research Center for Artificial Organ and Tissue Engineering, Guangzhou Clinical Research and Transformation Center for Artificial Liver, Institute of Regenerative Medicine, Zhujiang Hospital, Southern Medical University, Guangzhou 510280, Guangdong Province, China

Yi Gao, State Key Laboratory of Organ Failure Research, Southern Medical University, Guangzhou 510515, Guangdong Province, China

ORCID number: Yun Huang (0000-0002-4247-8964); Qing Peng (0000-0002-7790-6455); Hai-Yan Li (0000-0002-3842-8964); Zhi-Dong Jia (0000-0001-5362-5205); Yang Li (0000-0003-4718-1825); Yi Gao (0000-0003-3525-0133).

Author contributions: Huang Y performed the whole process of this study, including the concept, study design, operation of the experiments, data analysis, statistics and article drafting; Peng Q assisted with study design and critical revision of the article; Li HY, Jia ZD and Li Y assisted with the operation of the experiments; Gao Y laid out the concept and performed the critical revision and final approval of the article.

Supported by the National Natural Science Foundation of China, No. 81470875; the Natural Science Foundation of Guangdong Province, No. 2014A030312013; Science and Technology Planning Project of Guangdong Province, No. 2014B020227002, No. 2015B090903069, and No. 2015B020229002; and Science and Technology Program of Guangzhou, No. 201604020002.

Conflict-of-interest statement: All authors declare no conflicts-of-interest related to this article.

Data sharing statement: No additional data are available.

Manuscript source: Unsolicited manuscript

Correspondence to: Yi Gao, MD, PhD, Chief Doctor, Professor, Surgeon, Department of Hepatobiliary Surgery Ⅱ, Guangdong Provincial Research Center for Artificial Organ and Tissue Engineering, Guangzhou Clinical Research and Transformation Center for Artificial Liver, Institute of Regenerative Medicine, Zhujiang Hospital of Southern Medical University, 253 Middle Industrial Avenue, Guangzhou 510515, Guangdong Province, China. gaoyi6146@163.com
Telephone: +86-18922345399
Fax: +86-20-61643207

Received: May 11, 2018
Peer-review started: May 11, 2018
First decision: June 11, 2018
Revised: June 17, 2018
Accepted: June 28, 2018
Article in press: June 28, 2018
Published online: August 14, 2018

Abstract

AIM

To develop a novel hepatocyte serum-free medium based on sericin, and to explore the effect of sericin on the hepatocyte transcriptome.

METHODS

A controlled trial comparing novel serum-free medium and other media: C3A cells were cultured in our novel serum-free medium, HepatoZYME, complete medium (DMEM/F12 with 100 mL/L FBS), and DMEM/F12, and

then cell attachment, proliferation, and function as well as the biocompatibility of the media were assessed. A comparative study of serum-free media with or without 2 mg/mL sericin: the effect of sericin on C3A growth was assessed by cell viability and proliferation, the effect of sericin on C3A cell cycle distribution was determined by flow cytometry, and the effect of sericin on the C3A transcriptome was assessed by gene-chip array and RT-qPCR.

RESULTS

More C3A cells attached to the plate containing our serum-free medium than to those containing HepatoZYME and DMEM/F12 at 24 h post-seeding. Both the viability and proliferation rate of C3A cells in sericin-based serum-free medium were superior to those of cells in HepatoZYME and DMEM/F12 ($P < 0.001$). The content of albumin and urea in our serum-free medium was significantly higher than that in HepatoZYME and DMEM/F12 throughout the whole culture period ($P < 0.001$) and was similar to that in complete medium at day 3, 4, and 5. In part 2, cell viability and proliferation were greater in the presence of 2 mg/mL sericin ($P < 0.001$), as was the proportion of cells in S phase (16.21% ± 0.98% *vs* 12.61% ± 0.90%, $P < 0.01$). Gene-chip array analysis indicated that the expression of *CCR6*, *EGFR*, and *FOS* were up-regulated by 2 mg/mL sericin, and RT-qPCR revealed that the expression of *CCR6*, *EGFR*, *FOS*, *AKT1*, *JNK1*, *NFkB1*, *MMP-9*, *MEK2*, *ERK1/2* and *MYC* was up-regulated by 2 mg/mL sericin ($P < 0.05$).

CONCLUSION

We developed a novel hepatocyte serum-free medium. Sericin probably enhances cell attachment through the CCR6-Akt-JNK-NF-κB pathway and promotes cell proliferation through CCR6-mediated activation of the ERK1/2-MAPK pathway.

Key words: Sericin; Serum-free medium; MAPK pathway; Bioartificial liver support system; *CCR6*

Core tip: In recent decades, few studies have focused on the development of hepatocyte serum-free medium. In this study, we developed a novel hepatocyte serum-free medium suitable for *in vitro* culture of C3A cells and applied an advanced method, gene-chip array, to explore the effect of sericin on the hepatocyte transcriptome. We found that sericin probably enhanced cell attachment through the CCR6-Akt-JNK-NF-κB pathway and promoted cell proliferation through CCR6-mediated activation of the ERK1/2-MAPK pathway. These findings inspired the following study on the mechanism by which sericin promotes cell attachment and proliferation.

Huang Y, Peng Q, Li HY, Jia ZD, Li Y, Gao Y. Novel sericin-based hepatocyte serum-free medium and sericin's effect on hepatocyte transcriptome. *World J Gastroenterol* 2018; 24(30): 3398-3413 Available from: URL: http://www.wjgnet.com/1007-9327/full/v24/i30/3398.htm DOI: http://dx.doi.org/10.3748/wjg.v24.i30.3398

INTRODUCTION

The bioartificial liver support system (BALSS) is a novel and ideal therapy for hepatic insufficiency, which can provide additional liver function for patients with acute liver injury and end-stage liver failure[1]. During the BALSS operation, hepatocytes in the bioreactor perform various functions such as albumin synthesis, ammonia elimination, and bilirubin metabolism, which can decrease the symptoms of liver failure[2].

The BALSS is mainly composed of a hepatocyte culture module and an extracorporeal circulation device[3]. At the present time, the cells used in BALSS are mainly primary porcine hepatocytes[4] and immortalized cells, such as HepG2 and C3A[5]. C3A is a human hepatocellular carcinoma cell line, with high albumin production and excellent ability of ammonia elimination. Therefore, C3A is selected as the hepatocyte in the extracorporeal liver assist device (ELAD), which has proven to be effective in liver support and biocompatible in patients in clinical trials[6].

Normally, *in vitro* culture of hepatocytes requires serum of animal-origin. However, the serum possesses several shortcomings, including immunogenicity, allergenicity and exposure to microorganisms[7]. During the operation of the BALSS, the hepatocyte culture medium is in contact with the patient's plasma in the bioreactor, resulting in the potential for a variety of adverse reactions such as anaphylaxis and bacteremia. Therefore, serum-free medium suitable for hepatocyte culture in the BALSS has been needed within recent decades. However, few studies have focused on this topic.

HepatoZYME-SFM, the most popular of all hepatocyte serum-free media, is a serum-free medium for the long-term maintenance of hepatocyte phenotypic expression including the active and inducible forms of cytochrome P450 and active phase Ⅱ enzymes[8]. However, it is mainly used for serum-free primary hepatocyte culture, and serum is required for the adherence of hepatocytes at the early stage of serum-free culture with HepatoZYME.

Generally, serum-free medium comprises nutrients, growth factors, adherence-promoting factors, hormones, and trace elements. Advanced DMEM/F-12 (Dulbecco's Modified Eagle Medium/Ham's F-12) is a widely used basal medium that allows the culture of mammalian cells with reduced (10-50 mL/L) fetal bovine serum (FBS) supplementation, so it is often selected as the basal medium of the serum-free medium. Growth factor is the key component of serum-free culture medium, as it promotes cell growth. Hepatocyte growth factor (HGF) is a key ligand that elicits G1/S progression of epithelial cells, including hepatocytes, by up-regulating cyclin-E1 *via* the proline-mTOR pathway[9]. Epidermal growth factor (EGF) is not only a promoter of the growth of epithelial cells but also an important regulator that promotes

CYP3A4 expression in hepatocytes[10]. Dexamethasone affects the growth of hepatocytes in a dose-dependent manner. HGF-induced DNA synthesis and proliferation in primary cultures of adult rat hepatocytes are promoted by dexamethasone at the concentration of 10^{-10} mol/L, but are inhibited at the concentration of 10^{-8} mol/L[11]. Furthermore, dexamethasone effectively induces gluconeogenesis in malignant hepatocytes both *in vitro* and *in vivo* by up-regulating PEPCK and G6Pase expression[12].

Sericin, a silk-derived protein that constitutes 20%-30% of silk, is soluble in the water and envelops the fibroin fibers on the surface of silk. Sericin is widely used in the garment industry, cosmetics, pharmaceuticals, and biomedical engineering because of its moisture-regulating ability, ultraviolet (UV) resistance, and antibacterial, anticancer, and anticoagulant properties[13-15]. It is well known that sericin has the ability to promote the attachment and proliferation of several mammalian cells[16], and as a consequence, sericin has been widely used in cell cultures. In DMEM containing 100 mL/L FBS, cell viability and proliferation of normal animal cells, tumor cells, hybridoma cells and normal mouse fibroblast L929 cells were improved by adding sericin at a certain concentration[17].

Along with the development of culture technology, sericin has also been used for 3D cell culture. Mandal *et al*[18] reported that a novel biopolymeric matrix fabricated by chemically cross-linking polyvinyl alcohol (PVA) with silk sericin was superior to PVA with respect to swellability, mechanical strength and flexibility, and cell attachment and viability. In another study, a silk sericin/gelatin 3-D scaffold showed enhanced mechanical strength, and higher compressibility, swellability, and porosity than a 2-D film. Moreover, improved cell attachment and viability, and low immunogenicity have suggested that a sericin/gelatin 3-D scaffold may be an ideal biomedical material[19]. Sericin has also been used for hepatocyte culture and cryopreservation, the glucose consumption, urea secretion rate, and intracellular albumin content of HepG2 cells were increased in sericin-alginate-chitosan microcapsules[20]. Miyamoto *et al*[21] demonstrated that a serum-free solution containing sericin and maltose improved the attachment capability of cryopreserved primary hepatocytes.

Although sericin has been shown to promote cell attachment, viability, and proliferation, the mechanism has been clarified. It is probably that the promotion of viability and proliferation is based on enhanced cell attachment. Aramwit *et al*[22] showed that sericin had the capability to improve the production of type-Ⅰ collagen in the mouse fibroblast cell line L929 and that sericin increased the production of collagen in a dose-dependent manner within the range of 0.2-1.0 mg/mL.

Despite the advantages of sericin, it has not been used in the development of serum-free medium. The purpose of this study was to develop a novel serum-free medium suitable for *in vitro* hepatocyte culture based on sericin, growth factors, and other additives. In addition, the effects of sericin on the gene expression of hepatocytes were also investigated using a gene-chip array in order to explore the mechanism by which sericin promotes cell viability and proliferation.

MATERIALS AND METHODS

There were two parts to this study. Part 1 was a controlled trial comparing the novel serum-free medium to other media. Part 2 was a comparative study between serum-free medium with or without sericin.

Materials

Sericin, insulin-transferrin-sodium selenite liquid media supplement (ITS), and 3-(4,5-dimethylthiazol-2)-2,5-diphenyltetrazolium bromide (MTT) were purchased from Sigma-Aldrich. Advanced DMEM/F12, HepatoZYME, L-glutamine, FBS, and phosphate-buffered saline (PBS) were purchased from Thermo Fisher Scientific. Penicillin-streptomycin and 2.5 g/L trypsin-EDTA solution were purchased from Leagene. HGF, EGF, and dexamethasone were purchased from R&D Systems. Dimethyl sulfoxide (DMSO) was purchased from MP Biomedicals. A Live/Dead kit (calcein AM/PI) was purchased from Dojindo. SYBR Green qPCR SuperMix (a qPCR kit) was purchased from Invitrogen. TRIzol reagent and the RNeasy Plus Mini kit (reagents for extracting RNA from cells) were purchased from Ambion and Qiagen, respectively. An Olympus phase-contrast microscope and fluorescence microscope were used for cell observation. A Bio-Tek ELx800 absorbance reader was used for the MTT assay. An Aeroset automated biochemistry analyzer was used for the measurement of albumin and urea. A BioPhotometer plus (Eppendorf) and an ABI PRISM®7500 Sequence Detection System (Thermo Fisher Scientific) were used for RT-qPCR. A BD FACSVerse was used for flow cytometry.

Preparation of medium

Sericin, HGF, and EGF were dissolved into PBS, and dexamethasone (Dex) was dissolved into DMSO at a certain concentration to create stock solutions, respectively. DMEM/F12 and HepatoZYME were employed as the basal medium for their corresponding group. The medium for each group in part 1 of the study was prepared by adding the supplements into the basal medium as shown in Table 1. In part 2, the medium used for group A was the same medium used for group A in part 1, while the medium used for group B was sericin knock-out (Table 2).

Cell lines and culture

The human hepatocellular carcinoma cell line C3A was obtained from ATCC (ATCC® CRL-10741). C3A cells were inoculated into 25 cm^2 flasks after thawing and cultured in DMEM containing FBS (100 mL/L) and penicillin-streptomycin (100 U/mL) under 50 mL/L CO_2 at 37 ℃. The medium was changed every two days. Once the cells reached confluence, they were harvested using 2.5 g/L trypsin-EDTA, followed by the addition of fresh culture medium to create a new single-cell suspension for further

Table 1 Medium formula of each group in part 1

Group A	Group B	Group C	Group D
DMEM/F12	HepatoZYME	DMEM/F12	DMEM/F12
ITS 10 mL/L	L-Glutamine 2 μmol/mL	FBS 100 mL/L	PEN-SM 100 U/mL
HGF 20 ng/mL	PEN-SM 100 U/mL	PEN-SM 100 U/mL	
EGF 10 ng/mL			
Dex 1 nmol/mL			
Sericin 2 mg/mL			
PEN-SM 100 U/mL			

ITS: Insulin-transferrin-sodium; HGF: Hepatocyte growth factor; EGF: Epidermal growth factor; Dex: Dexamethasone; PEN-SM: Penicillin-streptomycin; FBS: Fetal bovine serum.

Table 2 Medium formula of each group in part 2

Group A (sericin)	Group B (control)
DMEM/F12	DMEM/F12
ITS 10 mL/L	ITS 10 mL/L
HGF 20 ng/mL	HGF 20 ng/mL
EGF 10 ng/mL	EGF 10 ng/mL
Dex 1 nmol/mL	Dex 1 nmol/mL
Sericin 2 mg/mL	PEN-SM 100 U/mL
PEN-SM 100 U/mL	

ITS: Insulin-transferrin-sodium; HGF: Hepatocyte growth factor; EGF: Epidermal growth factor; Dex: Dexamethasone; PEN-SM: Penicillin-streptomycin; FBS: Fetal bovine serum.

incubation. The concentration of FBS was gradually reduced from 100 mL/L to 50 mL/L, then to 20 mL/L, and finally to 10 mL/L. After stable growth was achieved in DMEM containing 10 mL/L FBS, the cells were cultured in the corresponding medium for each group.

Live/dead fluorescence microscopy assay

Cell attachment after inoculation was evaluated by fluorescence microscopy using a Live/Dead kit. This method allows the simultaneous detection of both live and dead cells with calcein acetoxymethyl (calcein AM) and propidium iodide (PI) dyes. Calcein AM is a nonfluorescent and permeable reagent, which is converted by intracellular esterases to the intensely green fluorescent calcein. Propidium iodide enters dead cells through damaged membranes and produces a bright red fluorescence when bound to nucleic acids.

The cells were inoculated into 24-well plates at a density of 1×10^5 cells/well, and then cultured in the respective medium. Twenty-four hours later, the medium was discarded, and the cells were washed three times with PBS and incubated with calcein AM and PI under 50 mL/L CO_2 at 37 ℃ for 15 min. The morphology and quantity of the cells were observed using a fluorescence microscope at the wavelengths of 490 nm and 545 nm, respectively. The number of live cells in each photo was counted using the ImageJ software.

Cell growth curves

Cell growth was investigated every 24 h for seven days. Briefly, the cells were inoculated into 12-well plates at a density of 1×10^5 cells/well, and cultured in the respective medium under 50 mL/L CO_2 at 37 ℃. Every 24 h, the medium was changed, and the cells in each group were counted using a phase-contrast microscope in triplicate.

Cell viability and proliferation assessment

The viability and the proliferation capacity of the cells were quantitatively assessed by MTT assay. This assay is based on the reduction of MTT (a tetrazolium salt solution) to purple formazan by metabolically active cells. For this analysis, 5×10^3 cells were inoculated into each well of 96-well plates, and subsequently cultured in the respective medium under 50 mL/L CO_2 at 37 ℃ for seven days. Every 24 h, the cells were incubated with 1 mg/mL MTT for 4 h. After solubilization in DMSO for 10 min, the concentration of the formazan produced by the metabolically active cells was quantified at 490 nm with a Bio-Tek ELx800 absorbance reader in quintuplicate.

Cell function assessment

Cell function was assessed by the amount of albumin and urea produced by metabolically active cells. The cells were inoculated into 24-well plates at a density of 1×10^5 cells/well and cultured in the respective medium under 50 mL/L CO_2 at 37 ℃ for seven days. The supernatant was collected every 24 h for quantitative testing of albumin and urea using an Aeroset automated biochemistry analyzer in triplicate.

Biocompatibility assessment for mediums

The biocompatibility of the media was evaluated by aspartate transaminase (AST) and lactate dehydrogenase (LDH), which were released into the culture medium by the cells through damaged membranes after suffering an acute injury. Their concentrations in the culture media are correlated with membrane damage and the biocompatibility of the medium.

Every 24 h post-seeding, the supernatant was harvested for quantitative testing of AST and LDH using an Aeroset automated biochemistry analyzer in triplicate for seven days.

Cell cycle analysis

Cells were inoculated into 6-well plates at a density of 5×10^5 cells/well, and cultured in the respective medium

under 50 mL/L CO_2 at 37 ℃. Seventy-two hours later, the cells were detached by trypsinization, centrifuged, and the pellet of cells was immediately fixed with ice-cold 700 mL/L ethanol. Afterwards, cells were washed three times with cold PBS to remove the ethanol, and finally stained with PI using a standard method[23]. Cells were analyzed by flow cytometry using BD FACSVerse.

Gene chip array

The differences in the transcriptomes of the cells cultured in the presence of sericin were quantitatively assessed using the GeneChip® PrimeView™ Human Gene Expression Array. The cells were inoculated into 6-well plates at a density of 1.5×10^6 cells/well, and subsequently cultured in the respective medium under 50 mL/L CO_2 at 37 ℃. Seventy-two hours post seeding, the cells were harvested and total RNA was extracted using a Qiagen RNeasy Plus Mini kit. After the quality was verified using a Thermo Nanodrop 2000 and Agilent 2100 Bioanalyzer, the RNA was analyzed using GeneChip® PrimeView™ to reveal the differentially expressed genes related to proliferation. The expression differences of up-regulated genes were presented as fold-change (group A/group B ratio), and differences between samples were considered statistically significant at a value of fold-change > 1.5.

Real time quantification of gene expression

RT-qPCR was used to distinguish the differences of genes related to hepatocyte function in each group of part 1, and to verify the differentially expressed genes in the gene chip array of part 2. The cells were inoculated into 6-well plates at a density of 1.5×10^6 cells/well, and subsequently cultured in the respective medium under 50 mL/L CO_2 at 37 ℃. At each set time point, the cells were harvested and total RNA was extracted using a Qiagen RNeasy Plus Mini kit. After RNA quality verification, RT-qPCR was performed using an ABI PRISM®7500 Sequence Detection System and SYBR Green qPCR SuperMix. The genes related to hepatocyte function were assessed two, four, and six days after seeding, and included uridinediphosphate-glucuronosyl transferase (UGT: The enzyme catalyzing the conversion of unconjugated bilirubin into conjugated bilirubin), glutathione S-transferase (GST: The enzyme catalyzing the conjugation of the reduced form of glutathione to xenobiotic substrates for the purpose of detoxification), glutamate-ammonia ligase (GLUL: The key enzyme in glutamine synthesis), glucose-6-phosphatase (G6P: The key enzyme in gluconeogenesis and glycogenolysis), albumin, carbamoyl phosphate synthetase Ⅰ (CPS1: The key enzyme in the production of urea), and cytochrome P-450 (CYP3A4, CYP2D6: the oxidizing enzymes in drug metabolism). The genes screened by the gene chip array were assessed one, two, three, and four days after seeding. The relative expression of each gene was presented as the value of $2^{-\Delta\Delta Ct}$.

Statistical analysis

The statistical analyses of the data in parts 1 and 2 were performed using one-way ANOVA and a *t*-test, respectively, with SPSS version 20.0 software. The results were expressed as the mean ± standard deviation (SD) using GraphPad Prism Software. Differences between samples were considered statistically significant at a value of $P < 0.05$.

RESULTS

Part 1

In part 1, group A is our novel serum-free medium, group B is HepatoZYME, group C is the complete medium (DMEM/F12 with 100 mL/L FBS), and group D is DMEM/F12 (Table 1).

Live/dead fluorescence microscopy assay: Cell behavior in terms of attachment and viability was qualitatively investigated after 24 h of culture under standard conditions by fluorescence microscopy, based on the simultaneous staining of live (green-labeled) and dead (red-labeled) cells (Figure 1).

The density of attached living cells in group A was obviously higher than those in group B and group D, and almost approached that of group C. C3A cells in group A possessed a greater attachment capability than those in group B and group D ($P < 0.01$).

Cell growth curves: Cell growth was directly measured by counting the cell number in each group with standard hemocytometry every 24 h. During the seven days post-seeding, the cell number in each group increased gradually at different rates (Figure 2A). Within three days post-seeding, the difference in the cell numbers among groups A, B and C were not significant. Beginning on the fourth day post-seeding, the cell number in group A was significantly higher than those in group B and group D at each time point ($P < 0.001$). Although the daily cell number in group A was lower than that in group C starting on the fifth day post-seeding ($P < 0.001$), they were close in number during the first four days of culture.

Cell viability and proliferation assessment: To examine cell viability and the proliferation rate, the MTT assay was employed in which the number of metabolically active cells is linearly associated with the absorbance at 490 nm within a certain range. During the whole culture period, the curve of each group rose gradually at different rates (Figure 2B). Within three days post-seeding, the cell viability and proliferation of group A were similar to group C. Afterwards, the number of metabolically active cells in group A was less than that in group C ($P < 0.001$), and reached the maximum at day 5. The viabilities of groups A, B and D declined after day 5. Nevertheless, the daily number of metabolically active cells in group A was significantly greater than those in group B and group D during the whole culture period ($P < 0.001$).

Cell function assessment: Cell function was assessed by the quantity of albumin and urea produced by C3A

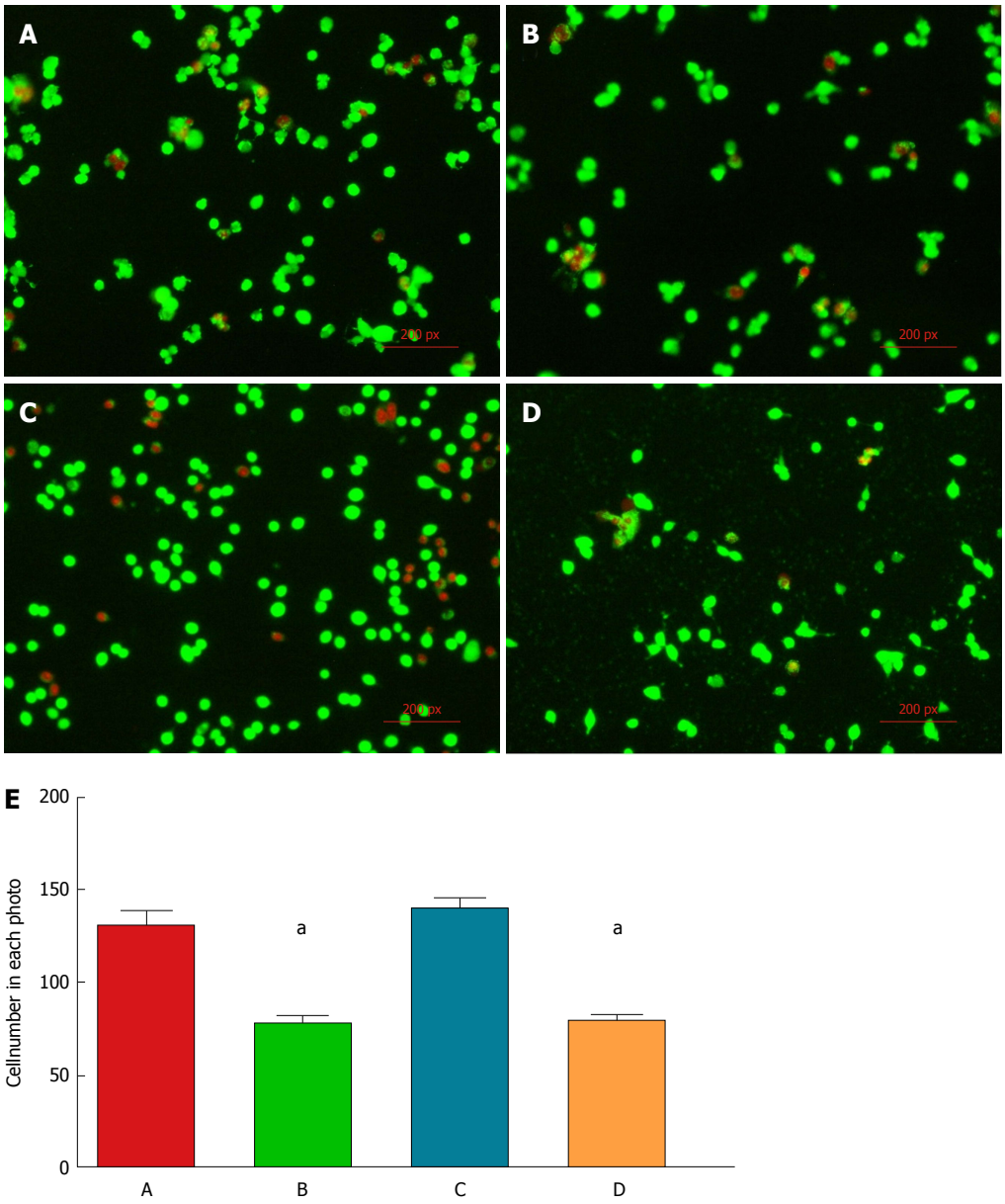

Figure 1 Fluorescence microscopy assessment of live (green-labeled) and dead (red-labeled) C3A cells at 24 h post-seeding in each group. A: Serum-free medium; B: HepatoZYME; C: DMEM/F12 with 100 mL/L FBS; D: DMEM/F12; and E: comparison of cell number from photos in each group: (group A) serum-free medium, (group B) HepatoZYME, (group C) DMEM/F12 with 100 mL/L FBS, and (group D) DMEM/F12. Data are expressed as mean ± SD (n = 3). $^{a}P < 0.05$. FBS: Fetal bovine serum.

cells. With respect to albumin (Figure 2C), the curves of group A and group C showed a slightly declining trend throughout the whole culture period. On days 1, 2, 6, and 7, the albumin in the supernatant of group A was lower than that in group C ($P < 0.001$), but there was no significant difference on days 3, 4, and 5. Throughout the culture process, the quantity of albumin secreted by C3A cells in group A was greater than that in group B and group D at each time point ($P < 0.001$). With respect to urea (Figure 2D), the content of urea in the supernatant of each group decreased gradually during the culture period. At each time point, the urea synthesized by the C3A cells in group A was lower than that in group C ($P < 0.001$), but it was significantly greater than that in group B and group D ($P < 0.001$).

Biocompatibility assessment for media: As they reflect hepatocyte injury, AST and LDH were selected to assess the biocompatibility of each medium with C3A cells. With respect to AST leakage (Figure 2E), there were no differences among the groups during the first 24 h. Beginning on day 2, AST leakage in groups A, C, and D was similar until day 6, and significantly lower than that in group B at each time point ($P < 0.001$). AST leakage in group A was lower than that in all the other groups on day 7 ($P < 0.001$). With respect to LDH leakage (Figure 2F), on days 1, 2, 5, and 6, LDH leakage in group A was greater than that in group C, but they shared a similar level at the other time points. During the whole culture period, LDH leakage in group B was significantly greater than that in group A and group C (P

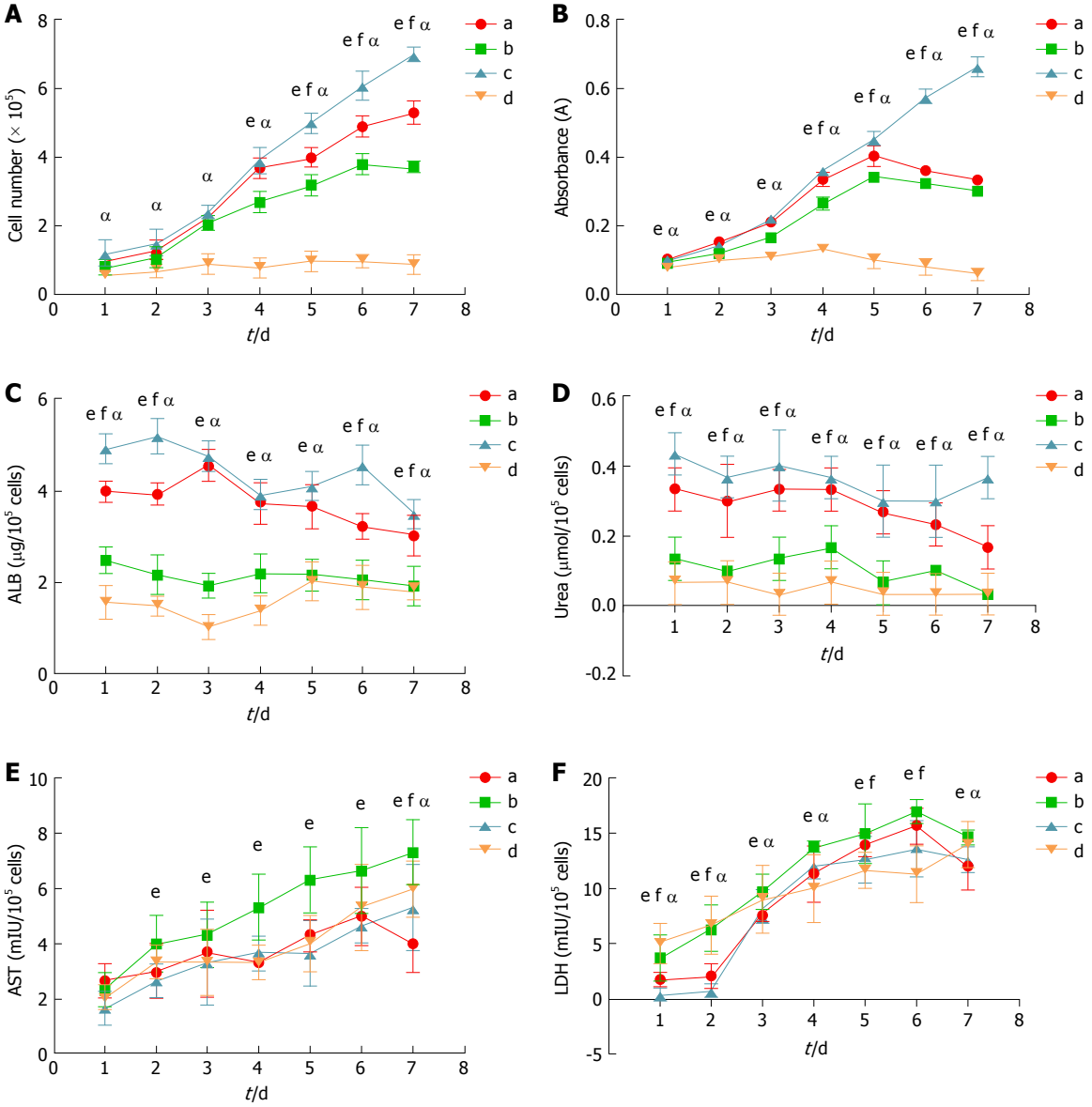

Figure 2 Comparison on (A) cell growth, (B) cell viability, (C) ALB secretion, (D) urea production, (E) AST leakage and (F) LDH leakage in each group. (group a) Serum-free medium, (group b) HepatoZYME, (group c) DMEM/F12 with 100 mL/L FBS, (group d) DMEM/F12. Data are expressed as mean ± SD (n = 5 in B and 3 in the others). e: Significant difference between group A and group B at the same incubation time. f: Significant difference between group A and group C at the same incubation time. α: Significant difference between group A and group D at the same incubation time. P < 0.05. AST: Aspartate transaminase; LDH: Lactate dehydrogenase; FBS: Fetal bovine serum.

< 0.001). In the early stage of culture, the LDH content in the supernatant of group D was greater than that in group A and group C, and unexpectedly, LDH levels in group D was the lowest from day 4 to day 6 (P < 0.001).

Expression of genes related to hepatocyte functions: The differences in gene expression related to hepatocyte functions were estimated by using RT-qPCR, a highly sensitive and effective method to detect the expression of specific genes. Uridinediphosphate-glucuronosyl transferase (*UGT*) (Figure 3A): On day 2 and day 6, the relative expression in group A was lower than that in group C, but higher than that in group B and group D (P < 0.001). On day 4, the relative expression in group A was slightly lower than that in group B and group C, but still higher than that of group D (P < 0.001). Glutathione S-transferase (*GST*) (Figure 3B): At each time point, the relative expression of group A was lower than that of group B and group C, but greater than that of group D (P < 0.001). Glutamate-ammonia ligase (*GLUL*) (Figure 3C): The relative expression in group C was higher than that in the other groups at all time points. The relative expression in group A was lower than that in group B at day 2 and 4, but significantly higher at day 6 (P < 0.002). Glucose-6-Phosphatase (*G6P*) (Figure 3D): At each time point, the expression in group A was lower than that in group B and group C, but higher than that in group D (P < 0.001). Albumin (Figure 3E): The relative expression in group A was lower than that in group C, but significantly higher than that in the other

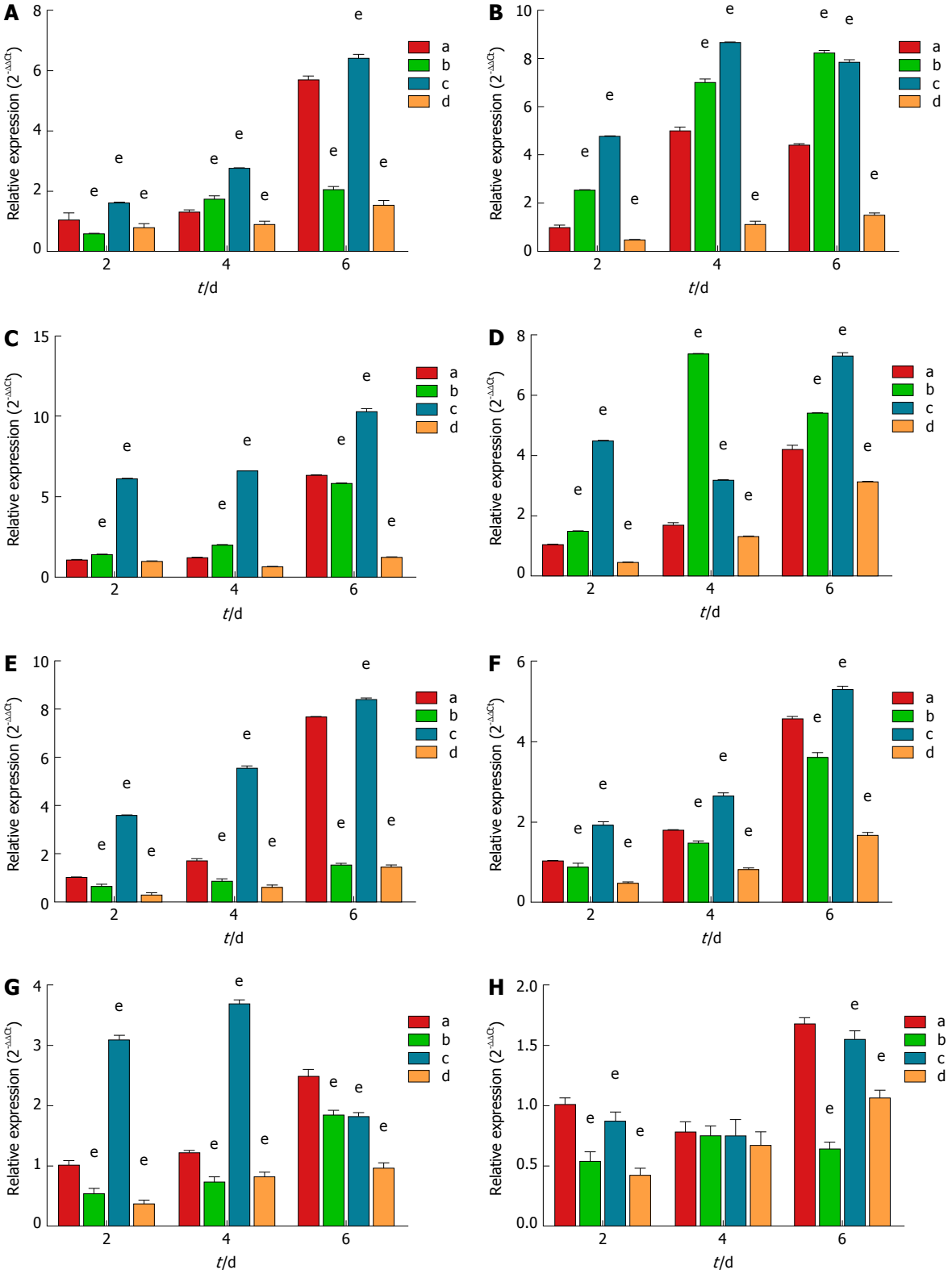

Figure 3 Relative expression of genes related to hepatocyte function. A: *UGT*; B: *GST*; C: *GLUL*; D: *G6P*; E: *albumin*; F: *CPS1*; G: *CYP3A4*; and H: *CYP2D6* in each group. (group a) Serum-free medium, (group b) HepatoZYME, (group c) DMEM/F12 with 100 mL/L FBS, (group d) DMEM/F12. Data are expressed as mean ± SD (n = 3). $^{e}P < 0.05$, significant difference from group a at the same incubation time. *UGT*: Uridinediphosphate-glucuronosyl transferase; *GLUL*: Glutamate-ammonia ligase; *CPS1*: Carbamoyl phosphate synthetase I; *G6P*: Glucose-6-phosphatase; *CYP3A4*: Cytochrome P3A4; *CYP2D*: Cytochrome P2D6; FBS: Fetal bovine serum.

groups ($P < 0.001$). Carbamoyl phosphate synthetase 1 (*CPS1*) (Figure 3F): The expression in group A was greater than that in group B and group D, although lower than that in group C ($P < 0.001$). Cytochrome P 3A4 (*CYP3A4*) (Figure 3G): At each time point, the expression in group A was greater than that in group B and group D (*P*

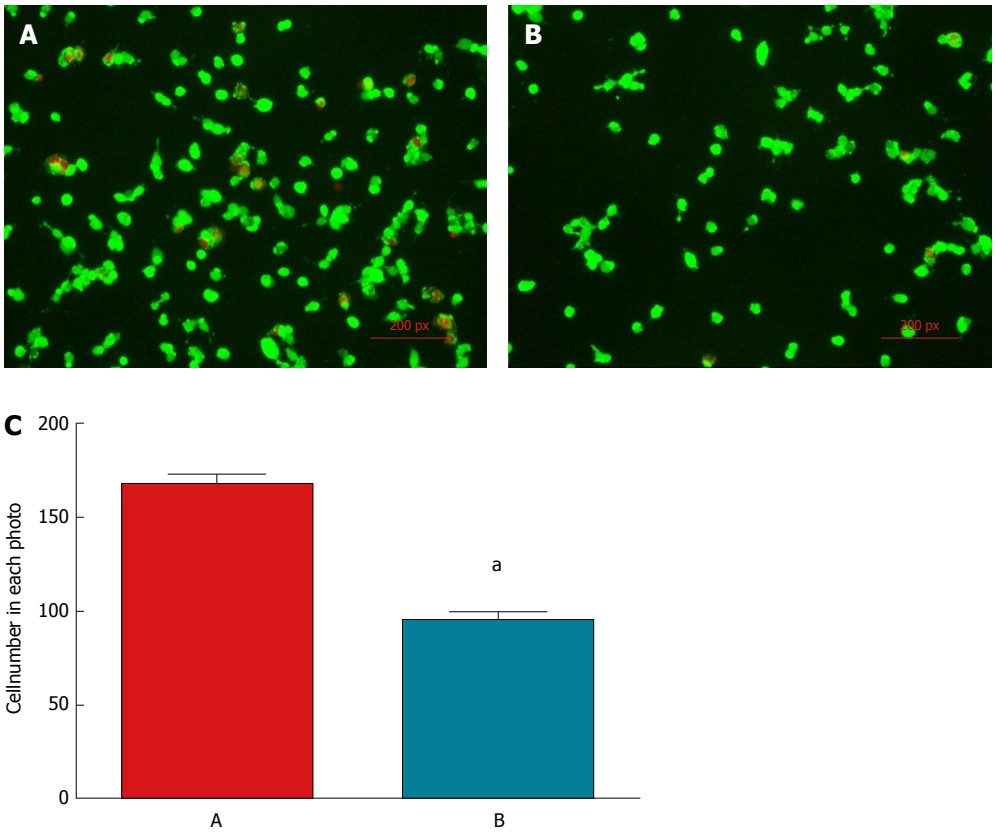

Figure 4 Fluorescence microscopy assessment of live (green-labeled) and dead (red-labeled) C3A cells 24 h post-seeding in each group. (A) serum-free medium containing 2 mg/mL sericin, (B) serum-free medium without sericin, (C) Comparison of cell number from photos in each group: (group A) Serum-free medium containing 2 mg/mL sericin, (group B) serum-free medium without sericin. Data are expressed as mean ± SD (n = 3). $^{a}P < 0.05$, significant difference between group A and group B at the same incubation time.

< 0.001). The expression in group A was lower than that in group C on days 2 and 4, but higher than that in the other groups on day 6 ($P < 0.001$). Cytochrome P 2D6 (*CYP2D6*) (Figure 3H): On day 2 and 6, the expression in group A was significantly higher than that in the other groups ($P < 0.001$); however, there were no significant differences on day 4.

Part 2

Live/dead fluorescence microscopy assay: The attachment capability of C3A cells was evaluated by the amount of live cells adhering to the plate (green-labeled) 24 h post-seeding. In the presence of sericin, a larger number of cells adhered to the surface ($P < 0.01$), and afterwards proceeded with proliferation as well as normal physiological functions (Figure 4).

Cell growth curves: Daily cell counting revealed that the cell growth curves of both groups rose gradually in the early stage of culture, then reached a plateau at day 5 (Figure 5A). At every time point, the cell growth in group A was superior to that in group B ($P < 0.001$).

Cell viability and proliferation assessment: The absorbance curves in both groups rose gradually within four days post-seeding (Figure 5B). On day 5, the viability of group A reached a peak value and then declined slightly, while that of group B reached a plateau. Over the whole culture period, there were more metabolically active cells in group A than in group B ($P < 0.001$).

Cell cycle analysis: The cell cycle was divided as G0/G1, S, and G2/M phase, and S phase was the DNA synthesis period. Therefore, the percentage of cells in S phase of the whole cell population was used to evaluate cell proliferation. The cell cycle analysis indicated that the proportion of cells in S phase in group A was 16.21% ± 0.98%, while that in group B was 12.61% ± 0.90% ($P = 0.009$) (Figure 6). These results indicated that the cells in group A possessed a stronger proliferative capability than those in group B.

Gene chip array: Since the previous experiments verified that the attachment and proliferative capabilities of C3A cells were significantly enhanced by 2 mg/mL sericin, we decided to proceed with exploring the impact of sericin on the C3A transcriptome. The differential gene expression profile between the two groups was analyzed by gene chip array, and the expression differences in up-regulated genes were presented as fold-change (group A/group B ratio). A cut-off of > 1.5-fold increase was applied, and the results revealed that a total of 250 genes were significantly up-regulated by sericin.

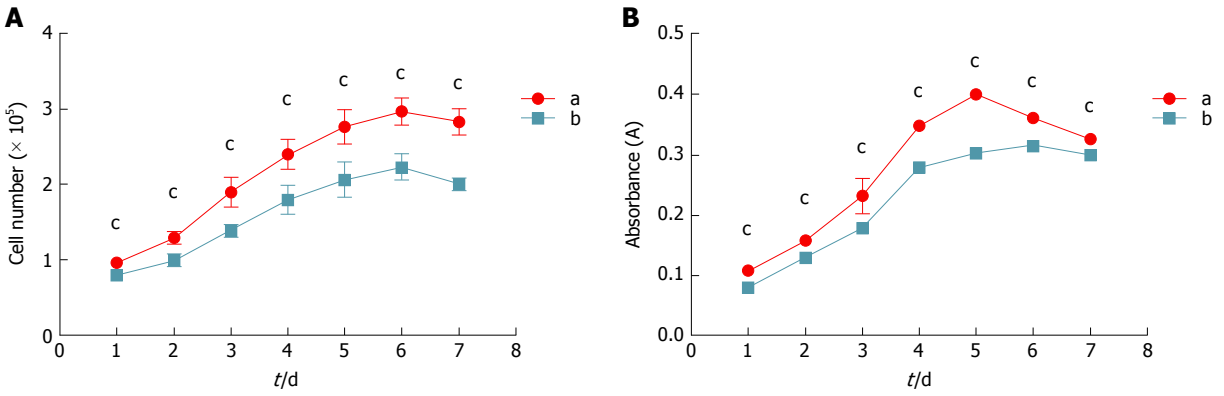

Figure 5 Comparison of (A) cell growth curve and (B) cell viability curve of each group. (group a) Serum-free medium containing 2 mg/mL sericin, (group b) serum-free medium without sericin. Data are expressed as mean ± SD (n = 3 and 5, respectively). °P < 0.05, significant difference between group a and group b at the same incubation time.

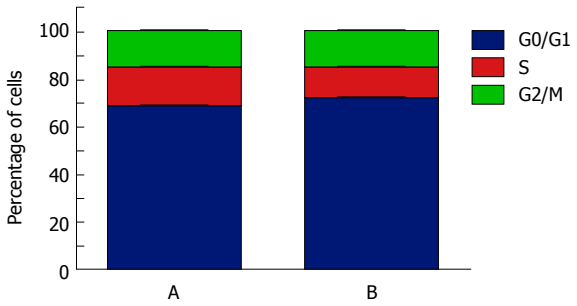

Figure 6 Cell cycle distribution of each group. (group A) Serum-free medium containing 2 mg/mL sericin and (group B) serum-free medium without sericin. Data are expressed as mean ± SD (n = 3). The portion of cells in S phase in group A (16.21% ± 0.98%) was significantly higher than that in group B (12.61% ± 0.90%) (P = 0.009).

To characterize the signaling pathways modulated by sericin in C3A cells, a pathway enrichment analysis was conducted using Ingenuity Pathway Analysis (IPA) according to the KEGG and BIOCARTA databases. The top significantly enriched pathways modulated by sericin were determined (Figure 7), among which KEGG-pathways in cancer and the MAPK signaling pathway were associated with cell proliferation. The genes related to cell proliferation were *COL4A6*, *MAX*, *EGFR*, *FOS*, *CDC42*, *FGF12*, and *SLC2A1* within the pathways in cancer, and *EGFR*, *FOS*, and *MAPK13* within the MAPK signaling pathway. The classic MAPK signaling pathway is included in the pathways in cancer, so the genes included in both pathways, *EGFR* and *FOS* (Table 3), were considered to be the genes affecting the proliferation of C3A cells with the most potential.

Subsequently, the other significantly up-regulated genes in group A in comparison with group B were screened by literature review to determine the genes related to proliferation. It has been demonstrated that *CCR6* and the MAPK pathway are associated with the migration and proliferation of breast epithelial cells. Thus, RT-qPCR was used to verify the gene expressions of *CCR6*, *EGFR*, and *c-FOS*, as well as the molecules in the MAPK pathway, including *Src*, *PI3K*, *AKT1*, *JNK1*, *NFkB1*, *MMP-9*, *GRB2*, *SHC2*, *K-RAS*, *RAF1*, *MEK2*, *ERK1/2*, *c-myc* and *cyclinE1*.

mRNA expression of CCR6 and the MAPK pathway: The early stage is the key period for attachment and proliferation, so RT-qPCR was performed on the samples at days 1, 2, 3, and 4 post-seeding. The expression difference at each time point was presented as fold-change [fold-change = $2^{-(\Delta Ct\ groupA\ -\ \Delta Ct\ groupB)}$] in Table 4. *CCR6*: The expression of *CCR6* in group A was greater than that in group B from inoculation until day 3 (P < 0.02), and *CCR6* showed a 2.36-fold increase in group A compared to group B on day 3. *EGFR*: The expression in group A was greater at all time points (P < 0.01), and the increases of *EGFR* in group A were 7.71- and 2.34-fold compared to group B on days 2 and 4, respectively. *FOS*: On day 1 and day 3, the expression in group A was higher than that in group B (P < 0.001). *Src*: Beginning on day 2, the mRNA expression in group A was significantly higher than that in group B (P < 0.001), and the increases of *Src* in group A were 2.44- and 3.67-fold compared to group B on days 2 and 4, respectively. *PI3K*: The significant increases in expression in group A ranged from 3.00- to 3.10-fold compared to group B on days 1, 2 and 4 (P < 0.001). *AKT1*: At each time point, the expression in group A was greater than that in group B (P < 0.01), and the increase of *AKT1* in group A was 2.04-fold compared to group B on day 3. *JNK1*: In the early stage of culture, the expression of the two groups was similar, but the expression in group A significantly increased 2.69- and 2.09-fold compared to group B on days 3 and 4 (P < 0.001). *NFkB1*: The expression in group A was greater than that in group B on days 2 and 3 (P < 0.001). *MMP-9*: The expression was greater in group A at all time points except on day 2 (P < 0.006). *GRB2*: On days 2 and day 3 the expression was significantly greater in the presence of sericin (P < 0.001). *SHC2*: Beginning on day 3, the expression was greater in group A (P < 0.001). *K-RAS*: The expression in group A was higher than that in group B at each time point except on day 1 (P < 0.01). *RAF1*: Beginning on day 2, the expression in group A was greater than that

Table 3 Up-regulated genes associated with cell proliferation

Up-regulated genes	Pathways involved	Fold change
CCR6	Cytokine-cytokine receptor interaction	1.99
EGFR	Pathways in cancer, MAPK signaling pathway	1.55
FOS	Pathways in cancer, MAPK signaling pathway	1.59

Table 4 Comparison of *CCR6* expression and genes in the MAPK pathway

Genes	FC in gene chip	FC1	FC2	FC3	FC4
CCR6	1.99	1.36 ± 0.09[1]	1.40 ± 0.01	2.36 ± 0.04[1]	0.75 ± 0.01
EGFR	1.55	1.76 ± 0.04[1]	7.71 ± 0.49[1]	1.46 ± 0.13[1]	2.34 ± 0.24[1]
FOS	1.59	1.22 ± 0.09[1]	0.96 ± 0.07	1.77 ± 0.05[1]	0.96 ± 0.01
Src	1.15	0.84 ± 0.16[1]	2.44 ± 0.08[1]	1.93 ± 0.70[1]	3.67 ± 0.40[1]
PI3K	1.24	3.00 ± 0.27[1]	3.01 ± 0.39[1]	1.43 ± 0.15	3.10 ± 0.14[1]
AKT1	1.13	1.22 ± 0.04[1]	1.21 ± 0.05[1]	2.04 ± 0.10[1]	1.59 ± 0.06[1]
JNK1	1.09	0.98 ± 0.07	1.07 ± 0.11	2.69 ± 0.09[1]	2.09 ± 0.04[1]
NFκB1	1.03	0.97 ± 0.07	1.51 ± 0.02[1]	1.77 ± 0.04[1]	0.84 ± 0.02
MMP-9	1.22	1.38 ± 0.15[1]	1.10 ± 0.06	1.51 ± 0.04[1]	1.56 ± 0.04[1]
GRB2	1.05	1.04 ± 0.10	1.48 ± 0.03[1]	1.34 ± 0.01[1]	1.06 ± 0.05
SHC2	1.30	0.98 ± 0.03	1.13 ± 0.06	1.39 ± 0.21[1]	1.47 ± 0.17[1]
K-RAS	1.09	1.16 ± 0.05	1.21 ± 0.08[1]	1.42 ± 0.04[1]	1.53 ± 0.01[1]
RAF1	1.01	1.09 ± 0.10	1.24 ± 0.02[1]	1.48 ± 0.02[1]	1.22 ± 0.03[1]
MEK2	1.02	5.86 ± 1.22[1]	4.61 ± 1.11[1]	2.38 ± 1.05[1]	8.45 ± 1.00[1]
ERK1	1.07	1.80 ± 0.62[1]	1.29 ± 0.03[1]	1.02 ± 0.26	1.19 ± 0.02
ERK2	1.18	2.58 ± 0.21[1]	2.52 ± 0.62[1]	5.15 ± 0.26[1]	1.63 ± 0.06[1]
c-myc	1.17	2.32 ± 0.21[1]	1.67 ± 0.27[1]	1.41 ± 0.30[1]	0.06 ± 0.01[1]
cyclinE1	1.04	1.04 ± 0.13	1.52 ± 0.03[1]	2.21 ± 0.02[1]	1.48 ± 0.01[1]

[1]Significant difference between group A and group B at the same incubation time ($P < 0.05$). FC1, FC2, FC3, FC4 was the fold change (group A/group B) of gene expression measured by RT-qPCR on days 1, 2, 3, 4, respectively. Data are expressed as mean ± SD ($n = 3$).

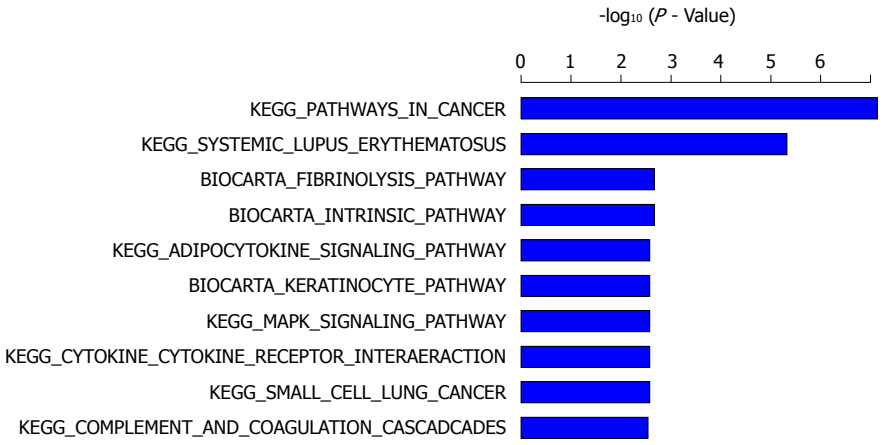

Figure 7 Pathway enrichment in the gene chip array.

in group B ($P < 0.001$). *MEK2*: The significant increase in expression in group A ranged from 2.38- to 8.45-fold compared to group B ($P < 0.001$). *ERK1*: The expression of *ERK1* in group A was greater than that in group B on the first two days ($P < 0.001$). *ERK2*: The expression was greater in group A at every time point ($P < 0.001$), and the fold change ranged from 1.63 to 5.15. *c-myc*: In the first three days, the mRNA expression of *c-myc* was higher in the presence of sericin ($P < 0.001$), and the fold change on day 1 was 2.32. *cyclinE1*: The expression in group A was greater except on day 1 ($P < 0.001$), and the fold change on day 3 was 2.21.

DISCUSSION

Serum is a necessary supplement for the *in vitro* culture of mammalian cells, because of its capability to simulate a suitable microenvironment similar to that of *in vivo* culture. However, serum is always removed from the culture for certain purposes, such as avoiding the impacts of serum on the experiment results and immunological rejection in heterogeneous animal *in vivo* experiments. To maintain normal attachment, proliferation, synthesis, and other cellular physiological processes, serum-free medium needs to contain a number of essential factors

including basic nutrients, attachment promoters, growth factors, trace elements, and hormones[24,25].

In previous experiments, we selected several biomaterials including sericin, HGF, EGF, and dexamethasone as supplements in serum-free medium, followed by exploring their optimal concentrations in the serum-free medium. Finally, the most suitable serum-free medium was successfully prepared for subsequent controlled trials, and included HepatoZYME, DMEM/F12 and DMEM/F12 supplemented with 100 mL/L FBS (complete medium).

Sericin, the "glue" on the surface of the silk fibers, has been proven to be one of the perfect substitutes for serum[26]. Sericin has the ability to promote the attachment and proliferation of mammalian cells[27]. Our experiment exploring the best concentration of sericin in serum-free culture medium indicated that C3A cells proliferated at the highest rate in the medium containing 2 mg/mL sericin. In contrast, the C3A cells in the medium containing 5 mg/mL sericin exhibited growth arrest. This result corresponded to that reported by Terada *et al*[16], which demonstrated that an overload of sericin was harmful to the cells.

In this study, cell attachment, cell viability and proliferation, hepatocyte function, biocompatibility of the medium with the cells, and the expression of genes related to hepatocyte functions were examined in the different media. For hepatocytes, attachment to a carrier is necessary for biological processes. During the first 24 h after inoculation, a larger number of C3A cells adhered to the surface of the plate in our serum-free medium compared with HepatoZYME and DMEM/F12. In addition, the adherence approached that observed for a complete medium. The excellent adherence of C3A cells in our serum-free medium can be mostly attributed to the attachment-promoting capability of sericin, which has been shown in a number of other studies. Akturk *et al*[28] demonstrated that a sericin/collagen membrane had the ability to enhance the initial attachment of keratinocytes 24 h post-seeding, and adhesion proteins such as collagen, laminin, and fibronectin were also present in their sericin/collagen membrane, which even contained the arginine-glycine-aspartic (RGD) acid sequence recognized by the cell surface receptors integrins.

During the culture period, the daily cell number in our serum-free medium was similar to that in the complete medium in the early period, and greater than that in HepatoZYME and DMEM/F12 during the whole culture period. Furthermore, this result was consistent with the cell viability and proliferation assessment. As previously mentioned, sericin promotes cell proliferation, making our serum-free medium superior to other media with respect to cell growth. Although HGF and EGF are also mitogens for hepatocytes, the results of the experiments in part 2 indicated that sericin was the dominant growth promoter in our serum-free medium. However, in the later stage of culture, the viability of hepatocytes in the serum-free medium declined slightly, indicating that the promotion of proliferation by the serum-free medium on hepatocytes was a short-term (within the first four-five days of culture) effect.

Biocompatibility with the cells, tissues, and organs is an important evaluation standard for biomaterials. Sericin has been proven to be a biocompatible material for a variety of cells, as it does not cause cell cycle arrest and it releases few inflammatory mediators[19,29]. AST and LDH concentrations in the supernatant are commonly employed as indicators of acute hepatocyte damage because of their leakage from hepatocytes after injury. In this study, the AST concentration in our serum-free medium and the complete medium were similar during almost the whole culture period, and significantly lower than that in HepatoZYME at each time point. Similarly, LDH leakage in the serum-free medium was less than that in HepatoZYME. These results indicated that there was excellent biocompatibility of our serum-free medium with hepatocytes. However, low AST leakage should be attributed to not only the excellent biocompatibility of sericin but also the protection of HGF. Glanemann *et al*[30] demonstrated that pretreatment with HGF significantly reduced AST leakage in rat hepatocytes and reactive oxygen intermediate formation by increasing glutathione synthesis during inflammation.

As the core of the BALSS, the hepatocyte functions attract the most attention. In this study, biochemical assays and RT-qPCR were employed to evaluate hepatocyte functions. The albumin synthesis in the serum-free medium was similar to that in the complete medium in the middle of the culture period, and greater than that in HepatoZYME and DMEM/F12 at every time point. This result was consistent with the mRNA expression of albumin assessed by RT-qPCR. However, during long-term culture, the albumin synthesized by C3A cells was on a downward trend. In other words, the hepatocytes used in BALSS should be replaced every four-five days in order to ensure persistent albumin synthesis. The eximious ALB synthesis was associated with HGF in our serum-free medium, as shown by Hou *et al*[31]. Hou *et al*[31] manufactured a HGF/heparin-immobilized collagen system as a synthetic extracellular matrix for hepatocyte culture, in which albumin synthesis was greater than that in heparin-immobilized collagen, revealing that HGF promotes albumin synthesis in hepatocytes.

Though lower than that in complete medium, urea production in our serum-free medium was significantly greater than that in HepatoZYME and DMEM/F12, as indicated by both the quantitative detection of urea and the mRNA expression of *CPS1*.

UGT is the primary phase Ⅱ enzyme catalyzing the conjugation of glucuronic acid to the xenobiotics, with polar groups facilitating their clearance[32]. The *UGT* expression in our serum-free medium was greater than that in HepatoZYME and DMEM/F12, and approached that in complete medium. CYP450 are phase Ⅰ enzymes responsible for the metabolism of at least 90% of drugs[33], among which CYP3A4 and CYP2D6 are the most important. Our study showed excellent CYP450 expression in the serum-free medium, close to

and even sometimes superior to that in the complete medium. Dexamethasone is considered an inducer of CYP3A4[34]. In sheep small intestine, dexamethasone caused a significant enhancement of CYP3A apoprotein level in the duodenal mucosa[35]. Thus, we suggest that dexamethasone played an important role in the excellent CYP450 expression in the serum-free medium. Although it was shown that dexamethasone could effectively up-regulate G6Pase expression[12], the result in our study was the opposite, probably because of the different concentration of dexamethasone used in the studies.

Compared with HepatoZYME and DMEM/F12, our serum-free medium exhibited advantages in C3A cell attachment, proliferation, functions, and biocompatibility, making it a perfect medium for serum-free hepatocyte culture.

Since the C3A cells exhibited excellent proliferation in our serum-free medium, the key factor, sericin, became the focus of the study. In part 2, we designed a controlled trial with two groups: the serum-free medium with or without sericin. Twenty-four hours after inoculation, more C3A cells were attached to the surface of the plate in the presence of 2 mg/mL sericin, followed by better proliferation and viability during the whole culture period, which corroborated the conclusions of other studies[19,20,36]. Based on its positive effects on cell proliferation, sericin has been added to antimicrobial creams and wound dressings to ameliorate wound healing[28,37].

Considering that sericin promotes cell proliferation, the experiments in part 2 were designed to explore the underlying mechanisms. As a key cyclin for liver regeneration[38], cyclinE1 is an important regulator of G1/S progression in hepatocytes. Up-regulated cyclinE1 could prompt cells to proceed from G1 phase to S phase, when DNA is synthesized in a large amount for the subsequent mitosis[9]. Our study clarified that the percentage of S phase cells was elevated in the presence of sericin, while that of cells in G0/G1 phase was reduced accordingly. In addition, the expression of *cyclinE1* was significantly higher in the presence of sericin, indicating that the promotion of sericin for cell proliferation might result from active G1/S progression mediated by cyclinE1.

To explore the mechanism by which sericin promotes cell proliferation, we performed gene chip array analysis to distinguish the differences in the transcriptome between the two groups. Among the most significantly up-regulated genes, *CCR6*, *EGFR*, and *FOS* were implicated in cell proliferation.

Chemokine receptor 6 (CCR6) is the unique receptor of chemokine (C-C motif) ligand 20 (CCL20), which has been proven to promote the proliferation of malignant cells[39]. The up-regulation of *CCR6* promotes spontaneous intestinal tumorigenesis[40]. Brand *et al*[41] demonstrated that *CCR6* mediated the activation of *Akt*, *ERK-1/2*, and *SAPK/JNK* MAP kinases, resulting in increased intestinal epithelial cell migration and proliferation. In breast epithelial cells, CCL20/CCR6 binding promotes cell migration and proliferation by activating the MAPK pathway[42]. Fujii *et al*[43] also reported that CCL20 enhanced the growth of HuH7 cells *via* phosphorylation of p44/42 MAPK *in vitro*. As signaling molecules in the MAPK pathway, up-regulated *EGFR* and *c-FOS* have been demonstrated to be promotors of proliferation. EGFR is the receptor for EGF, the phosphorylation and activation of which induces proliferation of several cells[44,45]. Mitogenic effects of many substances are mediated by *c-FOS*[46], and its overexpression could increase the proliferation of human hepatocytes by stabilizing nuclear Cyclin D1[47], while its blockage inhibits the proliferation and invasion of cancer cells[48].

Based on the gene chip array results and conclusion of the other studies, we assessed *CCR6* and molecules in the MAPK pathway by RT-qPCR to identify differential expression between the two groups. As a transmembrane receptor, the expression of *CCR6* was up-regulated in the early post-seeding period, resulting in increased expression of molecules in the MAPK pathway at different time points. At the transcription level, it was speculated that sericin promoted attachment and proliferation by two pathways: CCR6 on the C3A cell membrane was activated in the presence of sericin; subsequently the signal was transduced through the activation of *Src*, *PI3K*, *AKT1*, *JNK1* and *NFkB1*, and finally *MMP-9* was up-regulated. *MMP-9* is associated with cell migration because of its capability to remodel the extracellular matrix[49]. *MMP-9* up-regulation through a *Src*-dependent pathway is consistent with previous studies showing that oleic acid and denatured type-IV collagen induced *MMP-9* secretion and invasion in breast cancer cells[50,51]. The enhanced attachment of C3A cells by sericin was supposed to result from the increased migration. On the other hand, the CCL20/CCR6 binding transactivated the EGFR on the membrane, leading to a chain up-regulation of *GRB2*, *SHC2*, *K-RAS*, *RAF1*, *MEK2* and *ERK1/2*. Furthermore, ERK1/2 translocates into the nucleus and enhances transcription of early-response genes including *c-myc* and *c-FOS*[52]. Subsequently, the up-regulation of *c-myc* and *c-FOS* increased the expression of *cyclinE1*, promoting the G1/S progression and proliferation of C3A cells. However, this inference has not been proven by protein expression, so more effort should be made to clarify the mitogenic mechanism of sericin.

There are some limitations in this study. Although it is proven that our serum-free medium is suitable for *in vitro* culture of C3A cells, and sericin promotes the attachment and proliferation of C3A cells, it is still not clear whether the results obtained are restricted to C3A cells. In the further study, we are going to verify whether this serum-free medium is suitable for other hepatocytes, and determine the effect of sericin on other hepatocytes, such as HepG2, HuH7 and primary porcine hepatocytes. Hyperammonemia and hyperbilirubinemia are the clinical features of patients with liver failure. However, the urea production under an overload of $NH4^+$ and the ability to convert non-conjugated bilirubin into conjugated bilirubin of hepatocytes were not assessed in this study. These functions of hepatocytes will be assessed in the further

study.

In summary, a novel serum-free medium for hepatocytes was developed in this study, and it exhibits excellent biocompatibility, and an enhanced capability of promoting cell attachment and proliferation, and provides a suitable microenvironment for hepatocyte functioning. It raises the possibility of large-scale serum-free culture of hepatocytes in the BALSS. In addition, the mechanism by which sericin promotes cell proliferation was explored, and it is speculated that sericin enhances cell attachment through the CCR6-Akt-JNK-NF-κB pathway, and promotes cell proliferation through CCR6-mediated activation of the ERK1/2-MAPK pathway.

ARTICLE HIGHLIGHTS

Research background

A serum-free medium suitable for hepatocyte culture in the bioartificial liver support system (BALSS) has been needed within recent decades, but few studies have focused on the development of hepatocyte serum-free medium. Sericin was proven to promote cell attachment and proliferation, but the mechanism is not clarified.

Research motivation

Poor adherence and proliferation were often observed in the serum-free culture. Sericin has the ability to promote the attachment and proliferation of several mammalian cells, so it was selected as a key supplement in our serum-free medium. The mechanism how sericin promotes the attachment and proliferation of hepatocytes was not clarified. So, the effect of sericin on the hepatocyte transcriptome was explored in this study.

Research objectives

To develop a novel serum-free hepatocyte medium and to clarify the effect of sericin on the hepatocyte transcriptome.

Research methods

Part 1 is a controlled trial comparing the novel serum-free medium and other media: C3A cells were cultured in our novel serum-free medium, HepatoZYME, complete medium (DMEM/F12 with 100 mL/L FBS), and DMEM/F12, then cell attachment, proliferation, and function as well as the biocompatibility of the media were assessed. Part 2 is a comparative study of serum-free media with or without 2 mg/mL sericin: The effect of sericin on C3A growth was assessed by cell viability and proliferation, the effect of sericin on C3A cell cycle distribution was determined by flow cytometry, and the effect of sericin on the C3A transcriptome was assessed by gene-chip array and RT-qPCR.

Research results

More C3A cells attached to the plate containing our serum-free medium than to those containing HepatoZYME and DMEM/F12 at 24 h post-seeding. Both the viability and proliferation rate of C3A cells in sericin-based serum-free medium were superior to those of cells in HepatoZYME and DMEM/F12. The content of albumin and urea in our serum-free medium was significantly higher than that in HepatoZYME and DMEM/F12 throughout the whole culture period, and was similar to that in complete medium at day 3, 4, and 5. In part 2, cell viability and proliferation were greater in the presence of 2 mg/mL sericin, as was the proportion of cells in S phase. Gene-chip array analysis indicated that the expression of *CCR6*, *EGFR*, and *FOS* were up-regulated by 2 mg/mL sericin, and RT-qPCR revealed that the expression of *CCR6*, *EGFR*, *FOS*, *AKT1*, *JNK1*, *NFkB1*, *MMP-9*, *MEK2*, *ERK1/2* and *C-MYC* was up-regulated by 2 mg/mL sericin.

Research conclusions

We developed a novel serum-free hepatocyte medium in this research and demonstrated that sericin probably enhances cell attachment through the CCR6-Akt-JNK-NF-kB pathway and promotes cell proliferation through CCR6-mediated activation of the ERK1/2-MAPK pathway.

Research perspectives

In future studies, we will use the novel serum-free hepatocyte medium in large scale hepatocyte culture in the BALSS and assess the biocompatibility, immunogenicity and allergenicity in animal and clinical experiments. To clarify the mechanism of promotion of sericin on cell attachment and proliferation, we are going to study the protein level expression of CCR6-Akt-JNK-NF-kB pathway and ERK1/2-MAPK pathway components.

ACKNOWLEDGMENTS

Our thanks are due to the staff of the Department of Hepatobiliary Surgery Ⅱ and Institute of Regenerative Medicine in Zhujiang Hospital, Southern Medical University.

REFERENCES

1 **You S**, Zhu B, Liu H, Rong Y, Liu W, Zang H, Zhang A, Wan Z, Xin S. Safety of Human Hepatoma Cell-Line Constructing Bioartificial Liver Supporting System Treating Patients with Liver Failure. *Hepatogastroenterology* 2014; **61**: 933-936 [PMID: 26158144]

2 **Zhang Z**, Zhao YC, Cheng Y, Jian GD, Pan MX, Gao Y. Hybrid bioartificial liver support in cynomolgus monkeys with D-galactosamine-induced acute liver failure. *World J Gastroenterol* 2014; **20**: 17399-17406 [PMID: 25516651 DOI: 10.3748/wjg.v20.i46.17399]

3 **Lee JH**, Lee DH, Park JK, Kim SK, Kwon CH, Lee SK. Potentiality of immobilized pig hepatocyte spheroids in bioartificial liver system. *Transplant Proc* 2012; **44**: 1012-1014 [PMID: 22564612 DOI: 10.1016/j.transproceed.2012.03.010]

4 **Sheil AG**, Sun J, Mears DC, Waring M, Woodman K, Johnston B, Horvat M, Watson J, Koutalistras N, Wang L. Positive biochemical effects of a bioartificial liver support system (BALSS) in a porcine fulminant hepatic failure (FHF) model. *Int J Artif Organs* 1998; **21**: 43-48 [PMID: 9554825]

5 **Tsiaoussis J**, Newsome PN, Nelson LJ, Hayes PC, Plevris JN. Which hepatocyte will it be? Hepatocyte choice for bioartificial liver support systems. *Liver Transpl* 2001; **7**: 2-10 [PMID: 11150414 DOI: 10.1053/jlts.2001.20845]

6 **Thompson J**, Jones N, Al-Khafaji A, Malik S, Reich D, Munoz S, MacNicholas R, Hassanein T, Teperman L, Stein L, Duarte-Rojo A, Malik R, Adhami T, Asrani S, Shah N, Gaglio P, Duddempudi A, Borg B, Jalan R, Brown R, Patton H, Satoskar R, Rossi S, Parikh A, ElSharkawy A, Mantry P, Sher L, Wolf D, Hart M, Landis C, Wigg A, Habib S, McCaughan G, Colquhoun S, Henry A, Bedard P, Landeen L, Millis M, Ashley R, Frank W, Henry A, Stange J, Subramanian R; VTI-208 Study Group. Extracorporeal cellular therapy (ELAD) in severe alcoholic hepatitis: A multinational, prospective, controlled, randomized trial. *Liver Transpl* 2018; **24**: 380-393 [PMID: 29171941 DOI: 10.1002/lt.24986]

7 **van der Valk J**, Brunner D, De Smet K, Fex Svenningsen A, Honegger P, Knudsen LE, Lindl T, Noraberg J, Price A, Scarino ML, Gstraunthaler G. Optimization of chemically defined cell culture media--replacing fetal bovine serum in mammalian in vitro methods. *Toxicol In Vitro* 2010; **24**: 1053-1063 [PMID: 20362047 DOI: 10.1016/j.tiv.2010.03.016]

8 **Catania JR**, McGarrigle BP, Rittenhouse-Olson K, Olson JR. Induction of CYP2B and CYP2E1 in precision-cut rat liver slices cultured in defined medium. *Toxicol In Vitro* 2007; **21**: 109-115 [PMID: 17011741 DOI: 10.1016/j.tiv.2006.08.001]

9 **Oka K**, Ohya-Shimada W, Mizuno S, Nakamura T. Up-regulation of cyclin-E(1) via proline-mTOR pathway is responsible for HGF-mediated G(1)/S progression in the primary culture of rat hepatocytes. *Biochem Biophys Res Commun* 2013; **435**: 120-125 [PMID: 23618858 DOI: 10.1016/j.bbrc.2013.04.052]

10 **Yin M**, Yang H, Su X, Li Z, Yue Z, Zhang X, Sun D, Shi Y, Li D. Identification of EGF as an important regulator for promoting CYP3A4 expression in human embryonic stem cell-derived hepatocytes using TALEN-based gene targeting. *J Genet Genomics* 2014; **41**: 349-352 [PMID: 24976124 DOI: 10.1016/j.jgg.2014.03.008]

11 **Kimura M**, Moteki H, Ogihara M. Inhibitory effects of dexamethasone on hepatocyte growth factor-induced DNA synthesis and proliferation in primary cultures of adult rat hepatocytes. *J Pharmacol Sci* 2011; **115**: 390-398 [PMID: 21350311 DOI: 10.1254/jphs.10302FP]

12 **Ma R**, Zhang W, Tang K, Zhang H, Zhang Y, Li D, Li Y, Xu P, Luo S, Cai W, Ji T, Katirai F, Ye D, Huang B. Switch of glycolysis to gluconeogenesis by dexamethasone for treatment of hepatocarcinoma. *Nat Commun* 2013; **4**: 2508 [PMID: 24149070 DOI: 10.1038/ncomms3508]

13 **Zhaorigetu S**, Yanaka N, Sasaki M, Watanabe H, Kato N. Inhibitory effects of silk protein, sericin on UVB-induced acute damage and tumor promotion by reducing oxidative stress in the skin of hairless mouse. *J Photochem Photobiol B* 2003; **71**: 11-17 [PMID: 14705634 DOI: 10.1016/S1011-1344(03)00092-7]

14 **Kurioka A**, Kurioka F, Yamazaki M. Characterization of sericin powder prepared from citric acid-degraded sericin polypeptides of the silkworm, Bombyx Mori. *Biosci Biotechnol Biochem* 2004; **68**: 774-780 [PMID: 15118302 DOI: 10.1271/bbb.68.774]

15 **Sano M**, Tamada Y, Niwa K, Morita T, Yoshino G. Sulfated sericin is a novel anticoagulant influencing the blood coagulation cascade. *J Biomater Sci Polym Ed* 2009; **20**: 773-783 [PMID: 19323889 DOI: 10.1163/156856209X426853]

16 **Terada S**, Nishimura T, Sasaki M, Yamada H, Miki M. Sericin, a protein derived from silkworms, accelerates the proliferation of several mammalian cell lines including a hybridoma. *Cytotechnology* 2002; **40**: 3-12 [PMID: 19003099 DOI: 10.1023/a:1023993400608]

17 **Cao TT**, Zhang YQ. Viability and proliferation of L929, tumour and hybridoma cells in the culture media containing sericin protein as a supplement or serum substitute. *Appl Microbiol Biotechnol* 2015; **99**: 7219-7228 [PMID: 25895088 DOI: 10.1007/s00253-015-6576-3]

18 **Mandal BB**, Ghosh B, Kundu SC. Non-mulberry silk sericin/poly (vinyl alcohol) hydrogel matrices for potential biotechnological applications. *Int J Biol Macromol* 2011; **49**: 125-133 [PMID: 21549749 DOI: 10.1016/j.ijbiomac.2011.03.015]

19 **Mandal BB**, Priya AS, Kundu SC. Novel silk sericin/gelatin 3-D scaffolds and 2-D films: fabrication and characterization for potential tissue engineering applications. *Acta Biomater* 2009; **5**: 3007-3020 [PMID: 19398392 DOI: 10.1016/j.actbio.2009.03.026]

20 **Nayak S**, Dey S, Kundu SC. Silk sericin-alginate-chitosan microcapsules: hepatocytes encapsulation for enhanced cellular functions. *Int J Biol Macromol* 2014; **65**: 258-266 [PMID: 24486492 DOI: 10.1016/j.ijbiomac.2014.01.042]

21 **Miyamoto Y**, Teramoto N, Hayashi S, Enosawa S. An improvement in the attaching capability of cryopreserved human hepatocytes by a proteinaceous high molecule, sericin, in the serum-free solution. *Cell Transplant* 2010; **19**: 701-706 [PMID: 20525438 DOI: 10.3727/096368910X508799]

22 **Aramwit P**, Kanokpanont S, De-Eknamkul W, Kamei K, Srichana T. The effect of sericin with variable amino-acid content from different silk strains on the production of collagen and nitric oxide. *J Biomater Sci Polym Ed* 2009; **20**: 1295-1306 [PMID: 19520013 DOI: 10.1163/156856209X453006]

23 **Darzynkiewicz Z**, Halicka HD, Zhao H. Analysis of cellular DNA content by flow and laser scanning cytometry. *Adv Exp Med Biol* 2010; **676**: 137-147 [PMID: 20687474 DOI: 10.1007/978-1-4419-6199-0_9]

24 **Bowen WC**, Michalopoulos AW, Orr A, Ding MQ, Stolz DB, Michalopoulos GK. Development of a chemically defined medium and discovery of new mitogenic growth factors for mouse hepatocytes: mitogenic effects of FGF1/2 and PDGF. *PLoS One* 2014; **9**: e95487 [PMID: 24743506 DOI: 10.1371/journal.pone.0095487]

25 **Fernández-Fígares I**, Shannon AE, Wray-Cahen D, Caperna TJ. The role of insulin, glucagon, dexamethasone, and leptin in the regulation of ketogenesis and glycogen storage in primary cultures of porcine hepatocytes prepared from 60 kg pigs. *Domest Anim Endocrinol* 2004; **27**: 125-140 [PMID: 15219932 DOI: 10.1016/j.domaniend.2004.02.003]

26 **Sahu N**, Pal S, Sapru S, Kundu J, Talukdar S, Singh NI, Yao J, Kundu SC. Non-Mulberry and Mulberry Silk Protein Sericins as Potential Media Supplement for Animal Cell Culture. *Biomed Res Int* 2016; **2016**: 7461041 [PMID: 27517047 DOI: 10.1155/2016/7461041]

27 **Dinescu S**, Gălăţeanu B, Albu M, Lungu A, Radu E, Hermenean A, Costache M. Biocompatibility assessment of novel collagen-sericin scaffolds improved with hyaluronic Acid and chondroitin sulfate for cartilage regeneration. *Biomed Res Int* 2013; **2013**: 598056 [PMID: 24308001 DOI: 10.1155/2013/598056]

28 **Akturk O**, Tezcaner A, Bilgili H, Deveci MS, Gecit MR, Keskin D. Evaluation of sericin/collagen membranes as prospective wound dressing biomaterial. *J Biosci Bioeng* 2011; **112**: 279-288 [PMID: 21697006 DOI: 10.1016/j.jbiosc.2011.05.014]

29 **Aramwit P**, Kanokpanont S, De-Eknamkul W, Srichana T. Monitoring of inflammatory mediators induced by silk sericin. *J Biosci Bioeng* 2009; **107**: 556-561 [PMID: 19393558 DOI: 10.1016/j.jbiosc.2008.12.012]

30 **Glanemann M**, Knobeloch D, Ehnert S, Culmes M, Seeliger C, Seehofer D, Nussler AK. Hepatotropic growth factors protect hepatocytes during inflammation by upregulation of antioxidative systems. *World J Gastroenterol* 2011; **17**: 2199-2205 [PMID: 21633529 DOI: 10.3748/wjg.v17.i17.2199]

31 **Hou YT**, Ijima H, Matsumoto S, Kubo T, Takei T, Sakai S, Kawakami K. Effect of a hepatocyte growth factor/heparin-immobilized collagen system on albumin synthesis and spheroid formation by hepatocytes. *J Biosci Bioeng* 2010; **110**: 208-216 [PMID: 20547342 DOI: 10.1016/j.jbiosc.2010.01.016]

32 **Yang N**, Sun R, Liao X, Aa J, Wang G. UDP-glucuronosyltransferases (UGTs) and their related metabolic cross-talk with internal homeostasis: A systematic review of UGT isoforms for precision medicine. *Pharmacol Res* 2017; **121**: 169-183 [PMID: 28479371 DOI: 10.1016/j.phrs.2017.05.001]

33 **Shimada T**. Inhibition of Carcinogen-Activating Cytochrome P450 Enzymes by Xenobiotic Chemicals in Relation to Antimutagenicity and Anticarcinogenicity. *Toxicol Res* 2017; **33**: 79-96 [PMID: 28443179 DOI: 10.5487/TR.2017.33.2.079]

34 **Teo YL**, Saetaew M, Chanthawong S, Yap YS, Chan EC, Ho HK, Chan A. Effect of CYP3A4 inducer dexamethasone on hepatotoxicity of lapatinib: clinical and in vitro evidence. *Breast Cancer Res Treat* 2012; **133**: 703-711 [PMID: 22370628 DOI: 10.1007/s10549-012-1995-7]

35 **Maté ML**, Lifschitz A, Sallovitz J, Ballent M, Muscher AS, Wilkens MR, Schröder B, Lanusse C, Virkel G. Cytochrome P450 3A expression and function in liver and intestinal mucosa from dexamethasone-treated sheep. *J Vet Pharmacol Ther* 2012; **35**: 319-328 [PMID: 21906085 DOI: 10.1111/j.1365-2885.2011.01334.x]

36 **Terada S**, Sasaki M, Yanagihara K, Yamada H. Preparation of silk protein sericin as mitogenic factor for better mammalian cell culture. *J Biosci Bioeng* 2005; **100**: 667-671 [PMID: 16473778 DOI: 10.1263/jbb.100.667]

37 **Aramwit P**, Palapinyo S, Srichana T, Chottanapund S, Muangman P. Silk sericin ameliorates wound healing and its clinical efficacy in burn wounds. *Arch Dermatol Res* 2013; **305**: 585-594 [PMID: 23748948 DOI: 10.1007/s00403-013-1371-4]

38 **Nevzorova YA**, Tschaharganeh D, Gassler N, Geng Y, Weiskirchen R, Sicinski P, Trautwein C, Liedtke C. Aberrant cell cycle progression and endoreplication in regenerating livers of mice that lack a single E-type cyclin. *Gastroenterology* 2009; **137**: 691-703, 703.e1-703.e6 [PMID: 19445941 DOI: 10.1053/j.gastro.2009.05.003]

39 **Wallace AE**, Catalano RD, Anderson RA, Jabbour HN. Chemokine (C-C) motif ligand 20 is regulated by PGF(2α)-F-prostanoid receptor signalling in endometrial adenocarcinoma and promotes cell proliferation. *Mol Cell Endocrinol* 2011; **331**: 129-135 [PMID: 20816914 DOI: 10.1016/j.mce.2010.08.018]

40 **Nandi B**, Pai C, Huang Q, Prabhala RH, Munshi NC, Gold JS. CCR6, the sole receptor for the chemokine CCL20, promotes

spontaneous intestinal tumorigenesis. *PLoS One* 2014; **9**: e97566 [PMID: 24866282 DOI: 10.1371/journal.pone.0097566]

41 **Brand S**, Olszak T, Beigel F, Diebold J, Otte JM, Eichhorst ST, Göke B, Dambacher J. Cell differentiation dependent expressed CCR6 mediates ERK-1/2, SAPK/JNK, and Akt signaling resulting in proliferation and migration of colorectal cancer cells. *J Cell Biochem* 2006; **97**: 709-723 [PMID: 16215992 DOI: 10.1002/jcb.20672]

42 **Marsigliante S**, Vetrugno C, Muscella A. CCL20 induces migration and proliferation on breast epithelial cells. *J Cell Physiol* 2013; **228**: 1873-1883 [PMID: 23460117 DOI: 10.1002/jcp.24349]

43 **Fujii H**, Itoh Y, Yamaguchi K, Yamauchi N, Harano Y, Nakajima T, Minami M, Okanoue T. Chemokine CCL20 enhances the growth of HuH7 cells via phosphorylation of p44/42 MAPK in vitro. *Biochem Biophys Res Commun* 2004; **322**: 1052-1058 [PMID: 15336571 DOI: 10.1016/j.bbrc.2004.07.207]

44 **Gao M**, Zhan YQ, Yu M, Ge CH, Li CY, Zhang JH, Wang XH, Ge ZQ, Yang XM. Hepassocin activates the EGFR/ERK cascade and induces proliferation of L02 cells through the Src-dependent pathway. *Cell Signal* 2014; **26**: 2161-2166 [PMID: 24768768 DOI: 10.1016/j.cellsig.2014.04.013]

45 **Lanaya H**, Natarajan A, Komposch K, Li L, Amberg N, Chen L, Wculek SK, Hammer M, Zenz R, Peck-Radosavljevic M, Sieghart W, Trauner M, Wang H, Sibilia M. EGFR has a tumour-promoting role in liver macrophages during hepatocellular carcinoma formation. *Nat Cell Biol* 2014; **16**: 972-977 [PMID: 25173978 DOI: 10.1038/ncb3031]

46 **Biasin V**, Chwalek K, Wilhelm J, Best J, Marsh LM, Ghanim B, Klepetko W, Fink L, Schermuly RT, Weissmann N, Olschewski A, Kwapiszewska G. Endothelin-1 driven proliferation of pulmonary arterial smooth muscle cells is c-fos dependent. *Int J Biochem Cell Biol* 2014; **54**: 137-148 [PMID: 25016214 DOI: 10.1016/j.biocel.2014.06.020]

47 **Güller M**, Toualbi-Abed K, Legrand A, Michel L, Mauviel A, Bernuau D, Daniel F. c-Fos overexpression increases the proliferation of human hepatocytes by stabilizing nuclear Cyclin D1. *World J Gastroenterol* 2008; **14**: 6339-6346 [PMID: 19009649 DOI: 10.3748/wjg.14.6339]

48 **Long Y**, Wu Z, Yang X, Chen L, Han Z, Zhang Y, Liu J, Liu W, Liu X. MicroRNA-101 inhibits the proliferation and invasion of bladder cancer cells via targeting c-FOS. *Mol Med Rep* 2016; **14**: 2651-2656 [PMID: 27485165 DOI: 10.3892/mmr.2016.5534]

49 **Cheng X**, Yang Y, Fan Z, Yu L, Bai H, Zhou B, Wu X, Xu H, Fang M, Shen A, Chen Q, Xu Y. MKL1 potentiates lung cancer cell migration and invasion by epigenetically activating MMP9 transcription. *Oncogene* 2015; **34**: 5570-5581 [PMID: 25746000 DOI: 10.1038/onc.2015.14]

50 **Cortes-Reynosa P**, Robledo T, Macias-Silva M, Wu SV, Salazar EP. Src kinase regulates metalloproteinase-9 secretion induced by type IV collagen in MCF-7 human breast cancer cells. *Matrix Biol* 2008; **27**: 220-231 [PMID: 18061419 DOI: 10.1016/j.matbio.2007.11.003]

51 **Soto-Guzman A**, Navarro-Tito N, Castro-Sanchez L, Martinez-Orozco R, Salazar EP. Oleic acid promotes MMP-9 secretion and invasion in breast cancer cells. *Clin Exp Metastasis* 2010; **27**: 505-515 [PMID: 20617371 DOI: 10.1007/s10585-010-9340-1]

52 **Ebisuya M**, Kondoh K, Nishida E. The duration, magnitude and compartmentalization of ERK MAP kinase activity: mechanisms for providing signaling specificity. *J Cell Sci* 2005; **118**: 2997-3002 [PMID: 16014377 DOI: 10.1242/jcs.02505]

P- Reviewer: Chmiela M, Grassi G, Jung Y **S- Editor**: Wang XJ
L- Editor: Filipodia **E- Editor**: Yin SY

World Journal of Gastroenterology

Submit a Manuscript: http://www.f6publishing.com

World J Gastroenterol 2018 August 14; 24(30): 3414-3425

DOI: 10.3748/wjg.v24.i30.3414

ISSN 1007-9327 (print) ISSN 2219-2840 (online)

ORIGINAL ARTICLE

Basic Study

Total flavone of *Abelmoschus manihot* suppresses epithelial-mesenchymal transition *via* interfering transforming growth factor-β1 signaling in Crohn's disease intestinal fibrosis

Bo-Lin Yang, Ping Zhu, You-Ran Li, Min-Min Xu, Hao Wang, Li-Chao Qiao, Hai-Xia Xu, Hong-Jin Chen

Bo-Lin Yang, Ping Zhu, You-Ran Li, Min-Min Xu, Hao Wang, Li-Chao Qiao, Hai-Xia Xu, Hong-Jin Chen, Department of Colorectal Surgery, The Affiliated Hospital of Nanjing University of Chinese Medicine, Nanjing 210029, Jiangsu Province, China

ORCID number: Bo-Lin Yang (0000-0002-2474-4085); Ping Zhu (0000-0003-2583-7822); You-Ran Li (0000-0002-3179-6692); Min-Min Xu (0000-0001-6272-4643); Hao Wang (0000-0002-4058-2717); Li-Chao Qiao (0000-0292-2936); Hai-Xia Xu (0000-0002-2583-7822), Hong-Jin Chen (0000-0003-2222-3582).

Author contributions: Yang BL and Chen HJ contributed to the conception and design of the study, acquisition, analysis and interpretation of data; all authors drafted the article and made critical revisions, and approved the final version of the article to be published.

Supported by the Natural Science Foundation of Jiangsu Province, China, No. BK2016157; the National Natural Science Foundation of China, No. 81673973; Phase II Project Funded by the Priority Academic Program Development of Jiangsu Higher Education Institutions, No. 035062002003; and Developing Program for High-level Academic Talent in Jiangsu Hospital of TCM, No. y2018rc16.

Conflict-of-interest statement: To the best of our knowledge, no conflict of interest exists.

Data sharing statement: No additional data are available.

Manuscript source: Unsolicited manuscript

Correspondence to: Hong-Jin Chen, MD, Chief Doctor, Department of Colorectal Surgery, The Affiliated Hospital of Nanjing University of Chinese Medicine, Hanzhong 155 Rd, Nanjing 210029, Jiangsu Province, China. 260789@njucm.edu.cn
Telephone: +86-13851887158

Received: May 10, 2018
Peer-review started: May 10, 2018
First decision: June 11, 2018
Revised: June 27, 2018
Accepted: June 28, 2018
Article in press: June 28, 2018
Published online: August 14, 2018

Abstract

AIM

To explore the role and mechanism of total flavone of *Abelmoschus manihot* (TFA) on epithelial-mesenchymal transition (EMT) progress of Crohn's disease (CD) intestinal fibrosis.

METHODS

First, CCK-8 assay was performed to assess TFA on the viability of intestinal epithelial (IEC-6) cells and select the optimal concentrations of TFA for our further studies. Then cell morphology, wound healing and transwell assays were performed to examine the effect of TFA on morphology, migration and invasion of IEC-6 cells treated with TGF-β1. In addition, immunofluorescence, real-time PCR analysis (qRT-PCR) and western blotting assays were carried out to detect the impact of TFA on EMT progress. Moreover, western blotting assay was performed to evaluate the function of TFA on the Smad and MAPK signaling pathways. Further, the role of co-treatment of TFA and si-Smad or MAPK inhibitors has been examined by qRT-PCR, western blotting, morphology, wound healing and

transwell assays.

RESULTS

In this study, TFA promoted transforming growth factor-β1 (TGF-β1)-induced (IEC-6) morphological change, migration and invasion, and increased the expression of epithelial markers and reduced the levels of mesenchymal markers, along with the inactivation of Smad and MAPK signaling pathways. Moreover, we revealed that si-Smad and MAPK inhibitors effectively attenuated TGF-β1-induced EMT in IEC-6 cells. Importantly, co-treatment of TFA and si-Smad or MAPK inhibitors had better inhibitory effects on TGF-β1-induced EMT in IEC-6 cells than either one of them.

CONCLUSION

These findings could provide new insight into the molecular mechanisms of TFA on TGF-β1-induced EMT in IEC-6 cells and TFA is expected to advance as a new therapy to treat CD intestinal fibrosis.

Key words: Crohn's disease; Intestinal fibrosis; Epithelial-to-mesenchymal transition; Total flavone of *Abelmoschus manihot*; Transforming growth factor-β1/Smad signaling; Transforming growth factor-β1/non-Smad signaling

Core tip: Regulating transforming growth factor-β (TGF-β) and its downstream signaling pathways, mediating the epithelial-mesenchymal transition (EMT) process and restoring the biological function of abnormally activated intestinal fibroblasts, may be an important way to seek drug therapy for Crohn's disease (CD) intestinal fibrosis. Total flavone of *Abelmoschus manihot* (TFA) can inhibit TGF-β1-induced morphological change, migration, invasion of rat intestinal epithelial cells, and promote induction of EMT partially by inhibiting TGF-β1-activated Smad and non-Smad signaling pathways. Therefore, TFA is expected to advance as a new therapy to treat CD intestinal fibrosis, and its continued advancement may open the door to a new class of treatment for CD intestinal fibrosis.

Yang BL, Zhu P, Li YR, Xu MM, Wang H, Qiao LC, Xu HX, Chen HJ. Total flavone of *Abelmoschus manihot* suppresses epithelial-mesenchymal transition *via* interfering transforming growth factor-β1 signaling in Crohn's disease intestinal fibrosis. *World J Gastroenterol* 2018; 24(30): 3414-3425 Available from: URL: http://www.wjgnet.com/1007-9327/full/v24/i30/3414.htm DOI: http://dx.doi.org/10.3748/wjg.v24.i30.3414

INTRODUCTION

Crohn's disease (CD) is a chronic relapsing inflammation of the gut, which causes significant impairment of quality of life with a rising incidence and prevalence during recent decades[1,2]. Although the clinical manifestations and pathologic progress of CD are different, fibrosis of intestinal organization and strictures induced by transmural inflammation will eventually cause intestinal obstruction, which is the characteristic clinical manifestation[3-5]. In addition, more than 1/3 of CD patients need at least one intestinal operation in their lives, while 70% of the CD patients with fibrosis strictures need partial resection of the intestinal tract within 10 years of disease progression, and 70%-90% patients will have a recurrence of anastomotic strictures and over 50% patients will form new strictures[6,7]. Moreover, a large number of clinical and experimental results have confirmed that the main drugs for treatment of CD, such as glucocorticoids, immune agents and biological agents, can effectively inhibit intestinal inflammation, but do not have positive activity in preventing the further progress of intestinal fibrosis[8,9]. Thus, there is still a lack of drugs that can effectively inhibit or reverse CD intestinal fibrosis.

The process of intestinal fibrosis in CD patients involves a variety of cells and multiple molecular signaling pathways[10,11]. Due to the continuous role of chronic intestinal inflammation, activated T and B cells will produce large amounts of pro-inflammatory cytokines and pro-fibrogenic factors, and induce fibroblast, epithelial cells, endothelial cells and stellate cells to migrate, proliferate, activate and differentiate into myofibroblasts, which finally results in excessive proliferation of myofibroblasts and excessive deposition of extracellular matrix (ECM), leading to the formation of intestinal fibrosis[12-14]. Studies have shown that even if inflammation of the intestinal tract is effectively controlled, the process of fibrosis will continue and eventually lead to intestinal stenosis[15]. Epithelial to mesenchymal transition (EMT) plays an important role in the activation of fibroblasts[16]. Epithelial cells will lose epithelial polarity and epithelial phenotype contacted with basement membrane and produce fibroblasts to repair tissue injury caused by trauma and inflammatory reactions through the EMT progress[17]. In physiological states, when the inflammatory reaction is relieved, the transformation process stops spontaneously. However, in the case of continuous activation of the inflammatory reaction, the EMT process will also continue to exist, and eventually cause organ fibrosis. Under pathophysiologic conditions, when the inflammatory reaction is relieved, the transformation process will stop spontaneously. However, in the case of continuous activation of inflammatory response, the EMT process will also exist continuously, and eventually cause organ fibrosis[18,19]. Nowadays, although the role and regulation mechanism of EMT in CD intestinal fibrosis has not been fully understood, the transforming growth factor-β (TGF-β)/Smad/MAPK signaling pathway has been confirmed to play an important role in regulating EMT in organs such as lung, liver, kidney and so on[20-22]. Therefore, studying the role of EMT in the formation of intestinal fibrosis based on the TGF-β/Smad/MAPK signaling pathway, may provide a new target for the treatment of CD intestinal fibrosis.

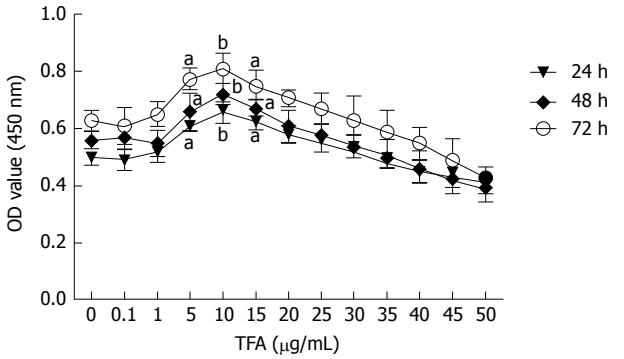

Figure 1 Effect of total flavone of *Abelmoschus manihot* at different concentrations on IEC-6 cell viability. IEC-6 cell viability after treatment with TFA at increasing concentrations was examined by CCK-8 at 24, 48 and 72 h. The results were expressed as the mean ± SD of three independent experiments, and each was performed in triplicate. $^{a}P < 0.05$, $^{b}P < 0.01$ compared with that of non-TFA treated group. TFA: Total flavone of *Abelmoschus manihot*.

Total flavone of *Abelmoschus manihot* L. Medic (TFA), as the main components of the water extract of traditional Chinese medicine *Abelmoschus manihot (L.)*, has been reported to play an important role in the improvement of renal inflammation, nephrotic syndrome, purpura nephritis, IgA nephropathy, membranous nephropathy and diabetic nephropathy (DN) effectively in the clinical trial[23-26]. Further, our previous research has shown that TFA could significantly inhibit the release of the intestinal inflammatory cytokines tumor necrosis factor (TNF)-α and interferon (IFN)-γ in a CD rat model induced by 2,4,6-trinitrobenzene sulfonic acid (TNBS), improve the model animal survival rate, and effectively improve intestinal inflammation. Moreover, immunohistochemical staining showed that the expression of TGF-β, alpha-smooth muscle actin (α-SMA) and matrix metalloproteinase-2 (MMP-2) were obviously reduced after intervention of TFA. Further, Masson staining confirmed that collagen fibrils of the mucosa and lamina propria of the colon were markedly decreased, indicating that TFA had positive inhibitory effects on CD intestinal fibrosis, which may be related to the EMT mechanism mediated by TGF-β. Thus, we hypothesized that TFA could inhibit or reverse the CD intestinal fibrosis *via* regulation of EMT based on TGF-β and its downstream Smad and MAPK signaling pathways. Therefore, this study was designed to focus on the influence of EMT on CD intestinal fibrosis and to further explore the role and mechanism of TFA on the progress of CD intestinal fibrosis.

MATERIALS AND METHODS

Preparation of TFA

Abelmoschus Manihot L. Medic was collected from Jiangyan of Jiangsu province, China. TFA was extracted from the flowers of *Abelmoschus Manihot* by the Jiangsu Province Hospital of TCM, Nanjing, China. A total of 500 g of *Abelmoschus Manihot* flowers was immersed in 8000 mL 75% ethanol for 1 h. The mixture was refluxed for 1 h at 90 ℃ and filtered by analytical filter paper. The extracts were evaporated by rotary evaporation under vacuum at 60 ℃[27]. For cell experiments, TFA was dissolved in dimethyl sulfoxide.

Cell culture

Rat intestinal epithelial (IEC-6) cells were obtained from the American Type Culture Collection (Manassas, VA, United States). Cells were cultured in Dulbecco's modified eagle's medium (DMEM, Gibco, United States) supplemented with 10% fetal bovine serum (FBS, Invitrogen, CA, United States), 2 mmol/L GlutaMAX-I (Invitrogen, CA, United States), 100 U/mL penicillin, and 100 μg/mL streptomycin (Invitrogen) in 5% CO_2 atmosphere at 37 ℃.

TFA working concentration

The concentration of TFA for further study was evaluated based on cell viability. Cell viability was determined by Cell Counting Kit-8 assay (CCK-8, Sigma Chemical Co, St Louis, MO, United States). Briefly, IEC-6 cells with a density of 1×10^4 cells/well in 100 μL of complete culture medium were seeded in 96-well plates. After culturing for 24 h, the medium was replaced with serum-free media or serum-free media containing TFA at concentrations ranging from 0.1 μg/mL to 50 μg/mL, and incubated in a humidified incubator at 37 ℃ for 24, 48 or 72 h. After incubation, 10 μL CCK-8 was added to each well for 2 h at 37 ℃. The optical density (OD) was recorded at 450 nm using a microplate reader (Dojindo Molecular Technology, Rockville, MD, United States).

Based on the results in Figure 1A, 5, 10, and 15 μg/mL TFA represented the optimal working concentrations and were used in our subsequent experiments.

Gene silencing with siRNAs

Cells were transfected with non-targeting negative control siRNA (Dharmacon, Lafayette, CO, United States) or Smad2/3 (Dharmacon, Lafayette, CO, United States) using LipoRNAiMax according to the manufacturer's protocol. The cells were maintained for 72 h and then subjected to protein extraction. The antisense and sense oligo template sequences for these siRNAs were: Smad2 siRNA antisense: AAGAGGAGTGCGCTTATATTACCTGTCTC, sense: AATAATATAAGCGCACTCCTCCCTGTCTC; Smad3 siRNA antisense: AATATTCCAGAAACCCCACCCCCTGTCTC, sense: AAGGGTGGGGTT TCTGGAATACCTGTCTC.

Wound healing assay

IEC-6 cells were seeded into 6-well plates at a density of 6×10^5 cells per well, and were cultured in fresh culture media to full confluence. After that, we created a wound using a plastic scraper. After being washed with PBS, the medium was replaced with 10 ng/mL TGF-β1[14] and TFA, and incubated at 37 ℃ for 48 h. The cell migration images were photographed at 0 and 48 h following scraping. Three to four different fields were visualized and photographed under a microscope (Nikon, Tokyo,

Japan).

Trans-well invasion assay

The cell invasion assay was performed using Trans-well chambers (8 μm pore-size, Corning, United States). Matrigel was purchased from BD Biosciences and stored at -20 ℃. After thawing at 4 ℃ overnight, the matrigel was diluted in serum-free medium, and 30 μL of the diluted matrigel were evenly inoculated into the upper chamber to form a gel at 37 ℃. Cells (1×10^5) suspended in 300 μL of serum-free medium were seeded into the upper compartments and treated with 10 ng/mL TGF-β1 and TFA for 48 h, and the lower compartments were filled with 600 μL of medium with 20% FBS. After incubation, the non-invasive cells were removed from the upper surface of the membrane by scrubbing. The cells that invaded to the lower surface of the membrane were fixed with 4% paraformaldehyde and stained in 10% crystal violet. Cells were counted under a microscope (Olympus, Tokyo, Japan).

Real-time PCR analysis (qRT-PCR)

IEC-6 cells were incubated in a 6-well plate with a density of 6×10^5 cell per well. When cells reached 60% confluence, 10 ng/mL TGF-β1 and TFA (0, 5, 10 and 15 μg/mL) were added to the plates and incubated for 48 h. Total RNA was extracted from the cultured cells using Trizol reagent (Invitrogen) according to the manufacturer's instructions and reversed transcribed into cDNA using the TaqMan microRNA Reverse Transcription Kit (Applied Biosystems, United States). The qRT-PCR reactions were performed using the Fast Start Universal SYBR Green Master (Rox) (Roche Applied Science) on a 7500 Real-time system (Applied Biosystems, United States) according to the manufacturer's protocols. Primer sequences used were designed as follows: E-cadherin forward, 5′-GAGGTCTACATTCCTGGTG-3′, E-cadherin reverse, 5′-TCTGTAGACATTTGAATCGG-3′, ZO-1 forward, 5′-CCATCTTGGACCGATTGCTG-3′, ZO-1 reverse, TAATGCCCGAGCTCCGATG-3′, Vimentin forward, 5′-CCGACACTCCT ACAAGATTTAGA-3′, Vimentin reverse, 5′-CAAAGATTTATTGAAGCAGAACC-3′, N-cadherin forward, 5′-ATCCTACTGGACGGTTCG-3′, N-cadherin reverse, 5′-TTGGCTAATGGCACTTGA-3′, GAPDH forward, 5′ -GGACCTGACCTGCCGTCTAG-3′, GAPDH reverse, 5′-GTAGCCCAGGATG CCCTTGA-3′. GAPDH was used as an internal standard.

Western blotting assay

IEC-6 cells were plated into 6-well plates at a density of 3×10^5 cells/mL. When cells reached 60% confluence, 10 ng/mL TGF-β1 and TFA (0, 5, 10 and 15 μg/mL) were added to the plates and incubated for 48 h. Each concentration group was performed in triplicate. Protein lysates were prepared using RIPA lysis buffer. Lysates were then subjected to SDS-polyacrylamide gel electrophoresis and transferred to PVDF membranes. After blocking with non-fat milk, blots were incubated overnight at 4 ℃ with the indicated antibodies. After incubation for 24 h, membranes were washed and incubated for 2 h at room temperature with corresponding secondary antibodies. For protein detection, membranes were developed with SuperSignal west femto maximum sensitivity substrate (Pierce, Rockford, IL, United States) and the Gel-Pro Analyzer 6.0 software was applied for image analysis. E-cadherin (1:500), ZO-1 (1:500), Vimentin (1:500), N-cadherin (1:500), p-ERK (1:500), ERK (1:500), p-p38 (1:500), p38 (1:500), p-JNK (1:500), JNK (1:500) and GAPDH (1:1000) antibodies were purchased from Sigma-Aldrich, and anti-mouse secondary antibodies were obtained from Proteintech (Chicago, IL, United States).

Immunofluorescence assay

IEC-6 cells were plated into 6-well plates at a density of 3×10^5 cells/mL. When cells reached 60% confluence, 10 ng/mL TGF-β1 and TFA (0, 5, 10 and 15 μg/mL) were added to the plates and incubated for 48 h. After that, IEC-6 cells were fixed with 4% paraformaldehyde. After blocking cells with 3% BSA for 2 h at room temperature, the cells were incubated with the anti-E-cadherin (1:50) antibody or anti-Vimentin (1:50) antibody at room temperature for 2 h. After washing three times with PBS, the second antibody conjugated with FITC was incubated on these cells for 1 h at room temperature. The nuclei were counterstained with DAPI for 5 min. Cells were imaged using a Nikon Eclipse TE2000-U fluorescence microscope.

Statistical analysis

Graph Pad Prism 5.0 statistical software was utilized to analyze the above experimental data. Measurement data were represented as X ± SD (n = 3); One-way analysis of variance was applied to compare differences between multiple groups. When only two groups were compared, Student's t-test was conducted. A value of $P < 0.05$ indicated that the difference was statistically significant.

RESULTS

Effect of TFA on IEC-6 cell viability

In order to observe the effect of TFA on the EMT progress of IEC-6 cells mediated by TGF-β1, a CCK-8 assay was performed to assess the effect of TFA on the viability of IEC-6 cells and to select the optimal concentrations of TFA for our further studies. IEC-6 cells were treated with increasing concentrations of TFA ranging from 0.1 to 50 μg/mL at different time points (24, 48 and 72 h). From the results of Figure 1, we found that TFA had the positive activities on viability of IEC-6 cells with the concentrations of 5, 10 and 15 μg/mL compared to the control group (TFA 0 μg/mL). Further, the TFA-treated group at 10 μg/mL displayed the maximum proliferative rate at 24, 48 and 72 h. Therefore, 5, 10 and 15 μg/mL TFA were chosen to be the optimal concentrations for our further studies.

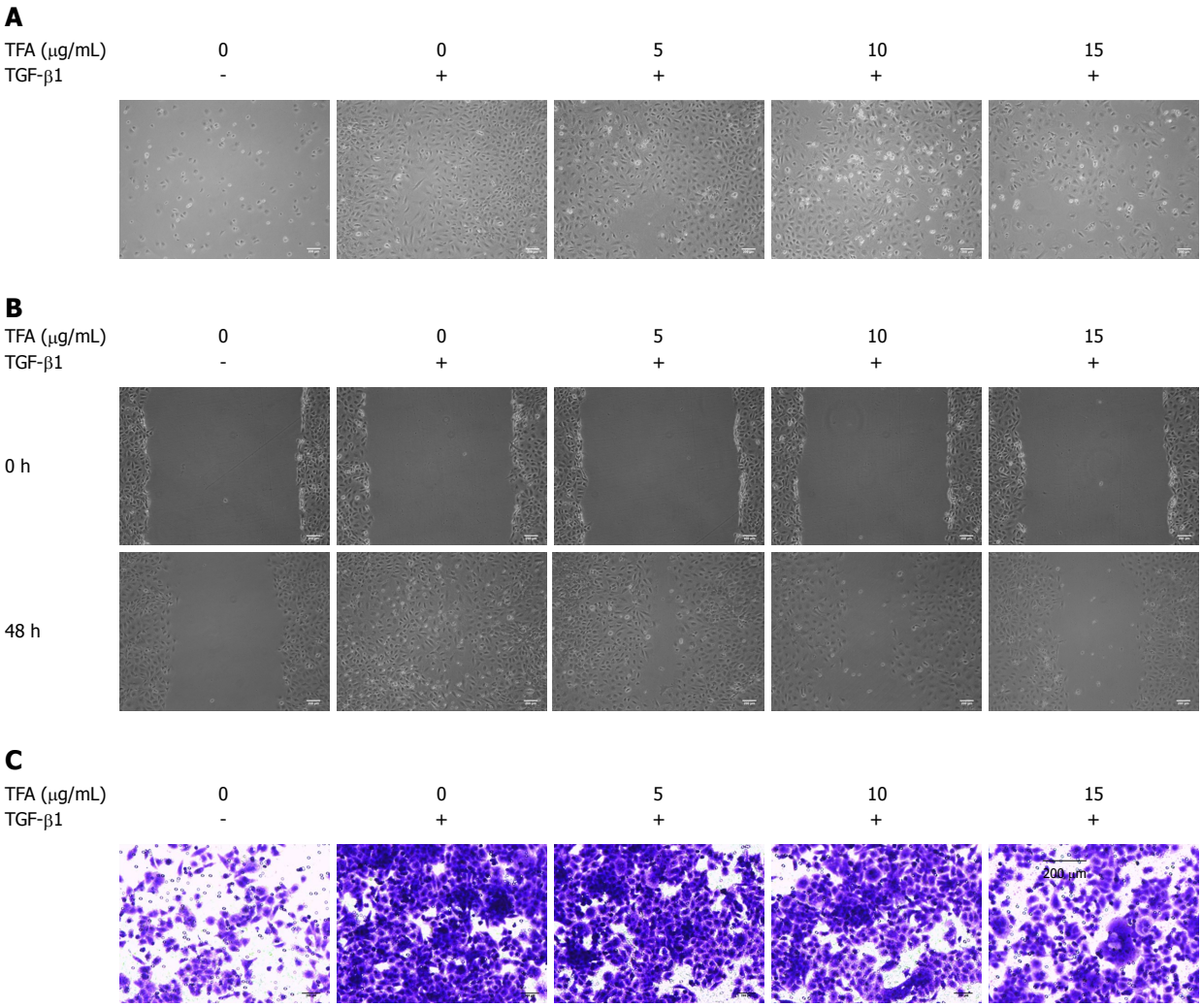

Figure 2 Total flavone of *Abelmoschus manihot* inhibited transforming growth factor-β1 induced migration and invasion of IEC-6 cells. A: The inhibitory effect of TFA (5, 10 and 15 μg/mL) on TGF-β1-induced morphological changes at 48 h was observed by phase contrast microscopy; B: The representative image of the wound healing assay; C: The representative image of transwell assay. The tendency is concomitant with the wound healing assay. TGF-β1 induced the migration and invasion of IEC-6 cells, whereas TFA suppressed this phenomenon. TFA: Total flavone of *Abelmoschus manihot*; TGF: Transforming growth factor.

TFA inhibited TGF-β1 induced migration and invasion of IEC-6 cells

The EMT process is characterized by alteration of cell morphology, migration and invasion capacity, as well as epithelial and mesenchymal markers expression. In the morphology assay, 10 ng/mL TGF-β1 in the medium for 48 h led to significant morphological changes from cuboidal epithelial cells to fibroblast-like spindle-shaped cells when compared with the control group. Interestingly, TFA effectively suppressed TGF-β1-induced morphological changes of IEC-6 cells in a dose dependent manner (Figure 2A). Moreover, for wound healing assays, 10 ng/ml TGF-β1 could promote the migration of IEC-6 cells compared with the control group, while TFA obviously reduced the TGF-β1-induced migration of IEC-6 cells in a dose dependent manner (Figure 2B). In addition, we examined the effects of TFA on TGF-β1-induced invasion, and we found that 10 ng/mL TGF-β1 in the medium for 48 h induced IEC-6 cells across the membrane, and addition of 5, 10 and 15 μg/mL TFA decreased the number of IEC-6 cells that passed though the Matrigel (Figure 2C). The results indicated that TFA could significantly suppress the morphological change, migration and invasion of IEC-6 cells induced by TGF-β1.

TFA inhibited TGF-β1-induced EMT

To examine the alterations of EMT markers, as shown in Figure 3A, the expression of epithelial marker E-cadherin was decreased along with the increasing expression of the mesenchymal marker Vimentin after treatment with 10 ng/mL TGF-β1. However, TFA effectively inhibited this induction, especially at higher concentrations. Besides, western blotting and qRT-PCR were carried out to examine the alterations of EMT markers, and we found that the protein levels of epithelial markers, including E-cadherin and ZO-1, were markedly increased by TFA treatment. On the contrary, TFA treatment obviously decreased the expression levels of mesenchymal proteins, including Vimentin and N-cadherin (Figure 3B). Likewise, similar changes were observed for mRNA

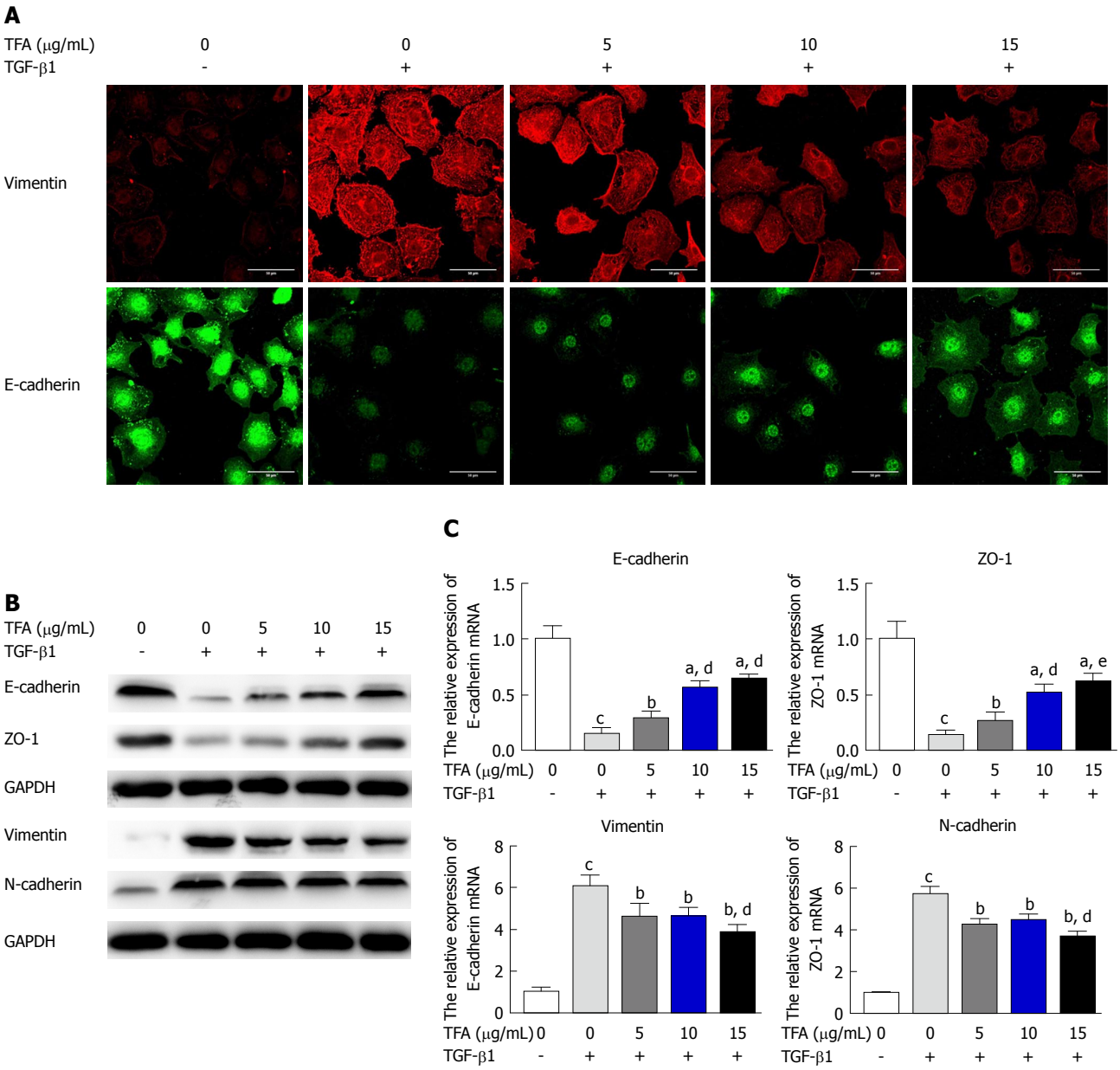

Figure 3 Total flavone of *Abelmoschus manihot* inhibited transforming growth factor-β1-induced epithelial-mesenchymal transition. A and B: The EMT-related label proteins were measured by immunocytochemistry (A) and western blotting (B) assays when IEC-6 cells were treated with TGF-β1 (10 ng/mL) alone or in combination with TFA (5, 10 and 15 μg/mL) for 48 h; C: The inhibitory effect of TFA (5, 10 and 15 μg/mL) on TGF-β1-induced EMT-related mRNAs was detected by qRT-PCR assay. [a]*P* < 0.05, [b]*P* < 0.01, [c]*P* < 0.001 compared with thef non-TFA treated group, [d]*P* < 0.05, [e]*P* < 0.01 compared with the TGF-β1 (10 ng/mL) treated group. EMT: Epithelial-mesenchymal transition; TFA: Total flavone of *Abelmoschus manihot*; TGF: Transforming growth factor.

expression of epithelial and mesenchymal markers in TFA-treated TGF-β1-induced IEC-6 cells (Figure 3C). Together, these results demonstrated that TFA could attenuate TGF-β1-induced EMT of IEC-6 cells.

TFA inhibited TGF-β1-induced activation of the Smad signaling pathway

The activation of phosphorylated Smad2/3 plays an important role in the TGF-β1-mediated EMT progress[28]. The status of the Smad pathways was determined in TGF-β1-treated IEC-6 cells following TFA treatment with the concentrations of 5, 10 and 15 μg/mL for 48 h, and the results have shown that TFA remarkably inhibited the level of phosphorylated Smad 2/3 in a dose dependent manner (Figure 4A). Next, we examined the role of Smad in TGF-β1-mediated IEC-6 cells. In IEC-6 cells, western blotting analysis demonstrated that Smad2/3 expression was inhibited after transfection of si-Smad2/3 (Figure 4B). Moreover, our results revealed that si-Smad2/3 could diminish TGF-β1-triggered EMT in IEC-6 cells and inhibit the TGF-β1-elicited changes in the expression of EMT markers, as measured by western blotting and qRT-PCR assays (Figure 4B and C). Besides, si-Smad2/3 suppressed TGF-β1-mediated mensenchymal-like morphological changes in IEC-6 cells as shown in Figure 5A. Wound healing and trans-well

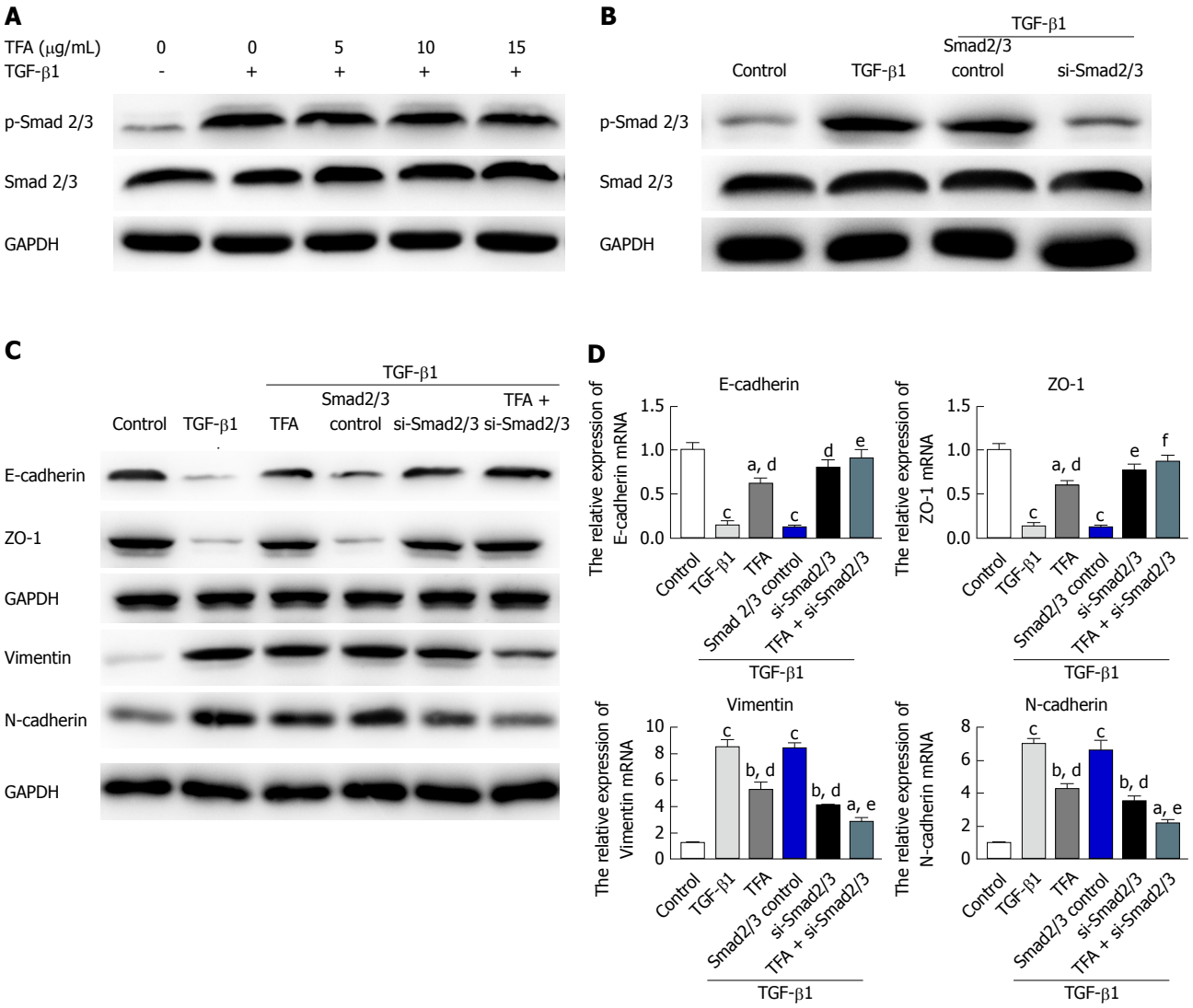

Figure 4 Total flavone of *Abelmoschus manihot* inhibited transforming growth factor-β1-induced activation of the Smad signaling pathway. A: The effects of TFA on TGF-β1-induced activation of Smad signaling were evaluated by western blotting; B: The expression of Smad signaling was examined by western blotting after transfection of si-Smad2/3; C and D: The effect of si-Smad or TFA combined with si-Smad2/3 on TGF-β1-induced activation of Smad signaling was evaluated by western blotting (C) and qRT-PCR (D) assays. $^{a}P < 0.05$, $^{b}P < 0.01$, $^{c}P < 0.001$ compared with that of non-TFA treated group, $^{e}P < 0.01$, $^{f}P < 0.001$ compared with that of TGF-β1 (10 ng/mL) treated group. TFA: Total flavone of *Abelmoschus manihot*; TGF: Transforming growth factor.

assays also showed that si-Smad2/3 suppressed the migration and invasion capacities of IEC-6 cells triggered by TGF-β1 (Figure 5B and C). Furthermore, 15 μg/mL TFA combined with si-Smad2/3 could further restrain TGF-β1-mediated EMT progress in IEC-6 cells. These results suggested that TFA might reverse EMT induced by TGF-β1 *via* Smad inactivation in IEC-6 cells.

TFA inhibited TGF-β1-induced activation of the non-Smad signaling pathway

In addition to the Smad2/3 signaling pathway, TGF-β has been reported to activate other signaling molecules, such as MAPKs, which include extracellular signal-regulated kinase (ERK) 1/2, c-Jun NH2-terminal kinase (JNK), and p38 mitogen-activated protein kinase (p38 MAPK)[29]. To explore the involvement of non-Smad signaling in the anti TGF-β1-induced EMT activity of TFA, we tested whether TFA could inhibit the TGF-β1-induced activation of p38, JNK and ERK1/2 by western blotting, and we found that TGF-β1 could significantly activate the expressions of p-p38, p-JNK and p-ERK1/2, while TFA at the concentrations of 5, 10 and 15 μg/mL obviously suppressed the TGF-β1-induced increase in p-p38, p-JNK and p-ERK1/2 levels in IEC-6 cells in a dose dependent manner (Figure 6A). Thus, in order to further explore the role of MAPKs in TGF-β1-treated IEC-6 cells, ERK1/2 inhibitor (PD98059, 5 μmol/L), p38 inhibitor (SB203580, 5 μmol/L) and JNK inhibitor (SP600125, 2 μmol/L) were used to treat IEC-6 cells mediated by TGF-β1. From the results in Figure 6A, we found that PD98059, SB203580 and SP600125 could significantly inhibit the activation of p-p38, p-JNK and p-ERK, respectively. Besides, PD98059, SB203580 and SP600125 could promote the changes in EMT markers by western blotting and qRT-PCR assays (Figure 6B and C). In addition, PD98059, SB203580 and SP600125 treatment inhibited TGF-β1-induced men-

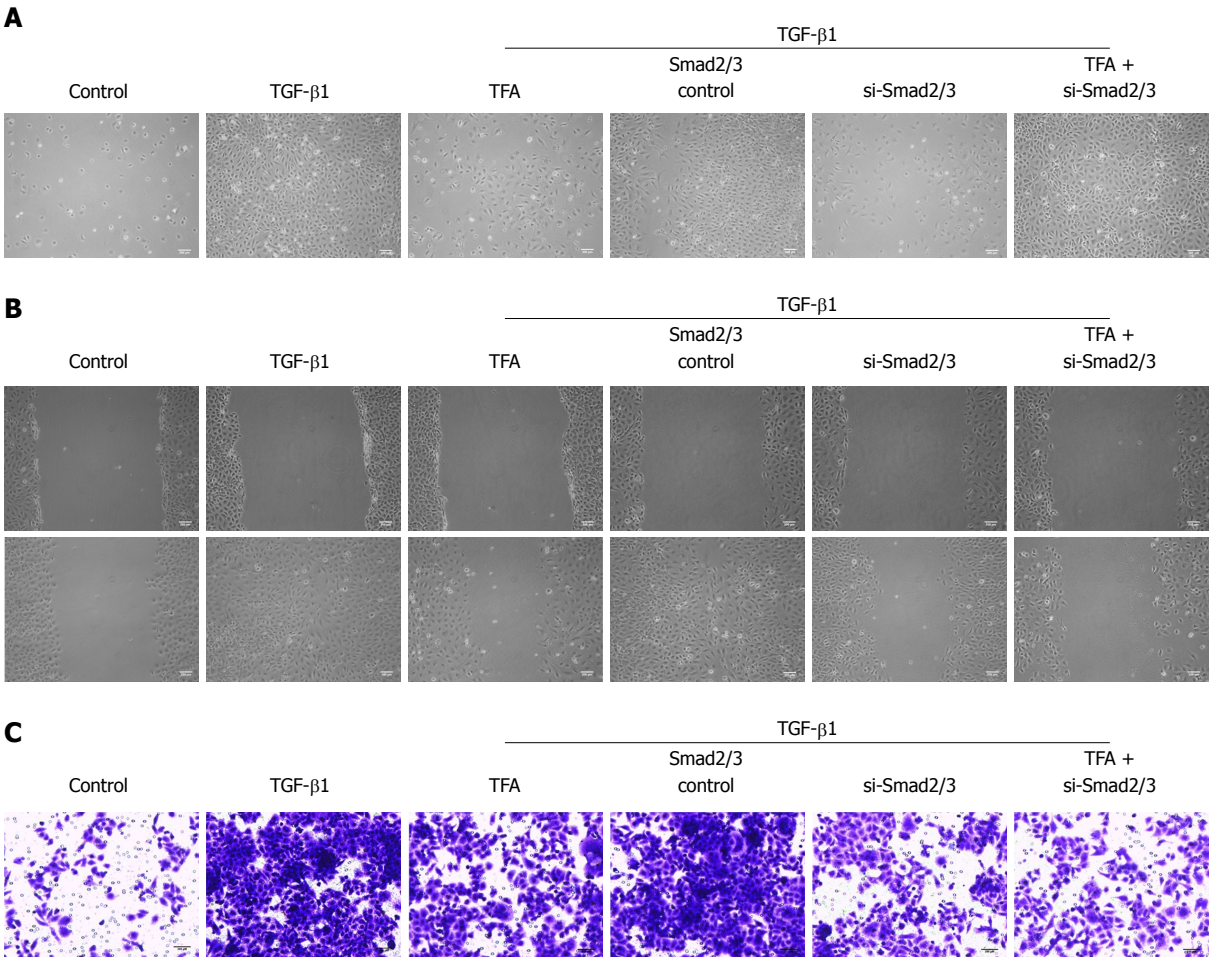

Figure 5 Total flavone of *Abelmoschus manihot* (TFA) combined with si-Smad2/3 had synergistic role in inhibiting transforming growth factor-β1-induced migration and invasion of IEC-6 cells. A: The inhibitory effect of si-Smad or TFA (15 μg/mL) combined with si-Smad2/3 on TGF-β1-induced morphological changes at 48 h was observed by phase contrast microscopy; B and C: The migration and invasion abilities of si-Smad or TFA (15 μg/mL) combined with si-Smad2/3 were examined by wound healing (B) and transwell (C) assays. TFA: Total flavone of *Abelmoschus manihot*; TGF: Transforming growth factor.a

senchymal-like morphological changes in IEC-6 cells, as shown in Figure 7A. Moreover, PD98059, SB203580 and SP600125 inhibited the migration and invasion of IEC-6 cells mediated by TGF-β1 *via* wound healing and transwell assays (Figure 7B and C). Importantly, co-treatment of TFA with PD98059, SB203580 or SP600125 had better inhibitory effects on TGF-β1-induced EMT in IEC-6 cells than either one of them. Taken together, these results indicated that TFA might exert its role in reversing TGF-β1-mediated EMT *via* non-Smad inactivation in IEC-6 cells.

DISCUSSION

CD intestinal fibrosis is characterized by activation of myofibroblasts, resulting in abnormal ECM deposition, which eventually leads to tissue stiffness and progressive intestinal dysfunction[30]. In addition to interstitial cells such as fibroblasts and smooth muscle cells, the differentiation of epithelial cells through EMT is a major source of intestinal fibrotic cells[18]. EMT refers to the transformation of epithelial cells with polar cells to the interstitial cells under a specific physiological and pathological condition. The most important features of EMT are the loss of epithelial cell phenotype and the acquisition of interstitial properties, as reflected in the down-regulation of E-cadherin and ZO-1, resulting in loss of adhesion between cells or between cells and matrix, over-expression of N-cadherin and vimentin, leading to the acquisition of migration and invasion, and over-expression of EMT transcription factors[31,32]. Moreover, EMT plays a key role in tissue formation, organ fibrosis and so on. Through EMT, epithelial cells lose cell polarity and epithelial phenotypes, such as connection to the basement membrane, while acquiring interstitial cell phenotypes with the functions of fibroblasts and myofibroblasts[33-35]. Moreover, in the case of continuous activation of inflammatory response, the EMT process will also continuously exist and eventually cause organ fibrosis. Therefore, it will have a positive significance to search for a method for the treatment of CD intestinal fibrosis.

Our previous studies have found that TFA, a main component of the water extract of traditional Chinese medicine, could reduce the expression of TGF-β, α-SMA and MMP-2 and decrease collagen fibrils, which indi-

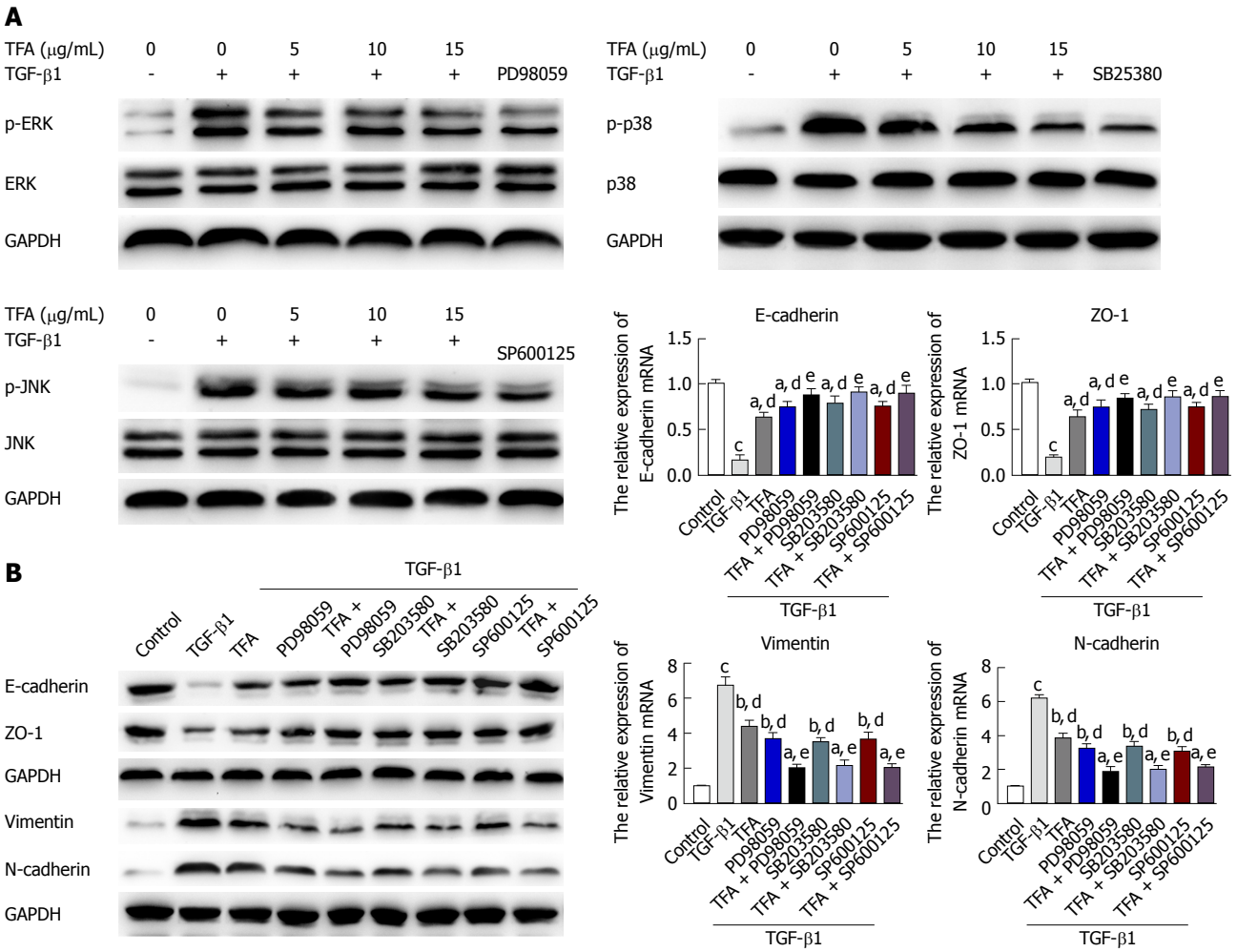

Figure 6 Total flavone of *Abelmoschus manihot* inhibited transforming growth factor-β1-induced activation of MAPK signaling pathway. A: The effect of TFA on TGF-β1-induced activation of MAPK signaling was evaluated by western blotting; B: The expression of MAPK signaling was examined by western blotting after transfection with MAPK inhibitors; B and C: The effects of MAPK inhibitors or TFA combined with MAPK inhibitors on TGF-β1-induced activation of Smad signaling were evaluated by western blotting (B) and qRT-PCR (C) assays. $^{a}P < 0.05$, $^{b}P < 0.01$, $^{c}P < 0.001$ compared with that of non-TFA treated group, $^{d}P < 0.05$, $^{e}P < 0.01$ compared with that of TGF-β1 (10 ng/mL) treated group. TFA: Total flavone of *Abelmoschus manihot*; TGF: Transforming growth factor.

cated that TFA may inhibit or reverse EMT during CD intestinal fibrosis. Firstly, we used TGF-β1 to induce EMT of IEC-6 cells and chose the optimal concentrations of TFA to disrupt TGF-β1 activity in IEC-6 cells. From the results, we knew that TGF-β1 could obviously promote the progression of EMT, such as changing morphology from cuboidal epithelial cells to fibroblast-like spindle-shaped cells, and enhancing the abilities of migration and invasion. Despite this, TFA treatment could restrain the changes caused by TGF-β1 in a dose dependent manner.

Effective inhibition of CD intestinal inflammation does not play a positive role in preventing intestinal fibrosis and inhibiting the pro-fibrosis signaling pathway, resulting in persistence of the process of tissue fibrosis[36,37]. Therefore, it is necessary to further study how to block the fibrotic signaling pathway and promote ECM decomposition to inhibit or reverse the process of fibrosis. TGF-β is the strongest inducer, playing an important role in EMT[38]. The Smad signaling pathway induced by TGF-β can promote the expression of ECM and inhibit the transcriptional activity of matrix degradation genes, resulting in ECM deposition in interstitial cells and leading to fibrosis[39]. Actually, in our experiments, we found that 10 ng/mL TGF-β1 could significantly inhibit the expression of p-Smad2/3, while TFA remarkably reversed the phenomenon in a dose dependent manner in TGF-β1-treated IEC-6 cells. Blocking TGF-β/Smad signaling has become a hot spot to inhibit or even reverse fibrosis. It has been reported that silencing Smad 2/3 could block Smad signaling and reduce collagen synthesis and proliferation of fibroblasts[40,41]. We silenced the expression of p-Smad2/3 and explored the role of Smad2/3 in TGF-β1-treated IEC-6 cells. We found that silencing Smad2/3 could effectively improve the EMT progression of IEC-6 cells induced by TGF-β1 no matter morphology, migration, invasion or EMT markers. Interestingly, when TFA was combined with si-Smad2/3, it had better inhibitory activities on EMT progression than either one of them alone, which suggested that TFA might exert its effects in reversing TGF-β1-mediated EMT *via* Smad inactivation in IEC-6 cells.

Recent researches have shown that the MAPK path-

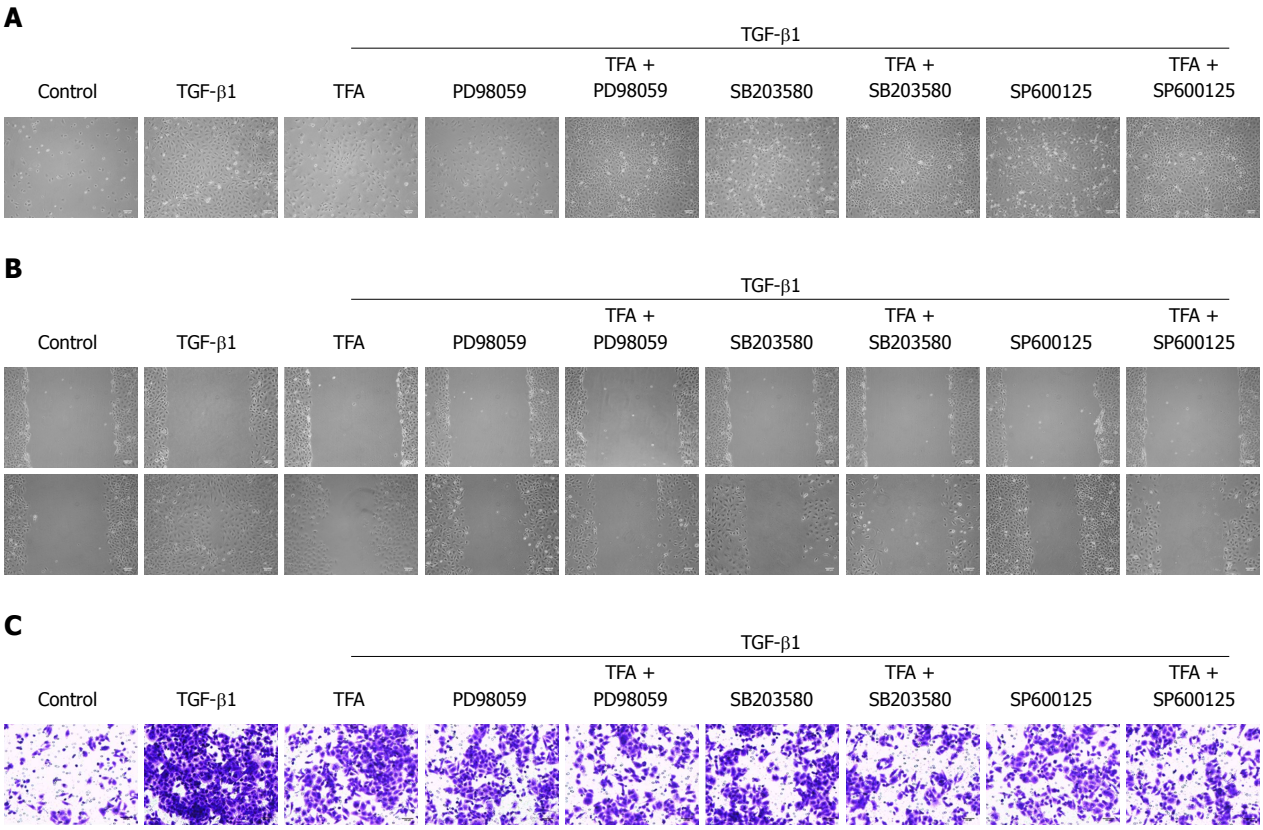

Figure 7 Total flavone of *Abelmoschus manihot* combined with MAPK inhibitors had synergistic role in inhibiting transforming growth factor-β1 -induced migration and invasion of IEC-6 cells. A: The inhibitory effect of MAPK inhibitors or TFA (15 μg/mL) combined with MAPK inhibitors on TGF-β1-induced morphological changes at 48 h was observed by phase contrast microscopy; B and C: The migration and invasion abilities of MAPK inhibitors or TFA (15 μg/mL) combined with MAPK inhibitors were examined by wound healing (B) and transwell (C) assays. TFA: Total flavone of *Abelmoschus manihot*; TGF: Transforming growth factor.

way, including p38, JNK and ERK1/2, is closely related to the regulation of TGF-β signaling pathway and fibrosis[42]. TGF-β can not only carry out signal transduction through TGF-β/Smad, but can also activate p38, JNK and ERK signaling pathways, which indicates that regulation of MAPK signaling pathways can affect the TGF-β/Smad signal transduction pathway and play a role in inhibiting fibrosis[43,44]. In this experiment, we found that 10 ng/mL TGF-β1 could significantly inhibit the expression of p-p38, p-JNK and p-ERK1/2, while TFA obviously suppressed the levels in a dose dependent manner in TGF-β1-treated IEC-6 cells. In addition, we also investigated the role of MAPK in TGF-β1-mediated EMT of IEC-6 cells. We used an ERK1/2 inhibitor (PD98059), p38 inhibitor (SB203580) and JNK inhibitor (SP600125) to inhibit the expression of p-p38, p-JNK and p-ERK1/2 in IEC-6 cells, respectively. We found that PD98059, SB203580 and SP600125 treatment could have positive inhibitory effects on EMT progress, similar to the si-Smad. Moreover, co-treatment of TFA combined with PD98059, SB203580 or SP600125 had better positive activities on inhibiting EMT progress in TGF-β1-mediated IEC-6 cells than either one of them alone, indicating that TFA might exert its role in reversing EMT induced by TGF-β1 *via* MAPK inactivation in IEC-6 cells.

Stated thus, regulating TGF-β and its downstream Smad and MAPK signaling pathways, mediating the EMT process and restoring the biological function of abnormally activated intestinal fibroblasts, may be an important way to seek drug therapy for CD intestinal fibrosis. TFA is able to inhibit TGF-β1-induced morphological change, migration, invasion of IEC-6 cells. TFA promoted the induction of EMT partly by inhibiting TGF-β1-activated Smad signaling pathway and non-Smad signaling pathway. To conclude, TFA is expected to advance as a new therapy to treat CD intestinal fibrosis, and its continued advancement may open the door to a new class of treatment for CD intestinal fibrosis.

ARTICLE HIGHLIGHTS

Research background

Epithelial-mesenchymal transition (EMT) is a crucial process in Crohn's disease (CD) intestinal fibrosis. Total flavone of *Abelmoschus manihot* (TFA) has been found as an effective component to reduce CD intestinal fibrosis *in vivo*. However, the role and mechanism of TFA on EMT progress of CD intestinal fibrosis have not been understood yet.

Research motivation

EMT is a crucial process in CD intestinal fibrosis. TFA has been found as an effective component to reduce CD intestinal fibrosis *in vivo*. However, the role and mechanism of TFA on EMT progress of CD intestinal fibrosis have not been understood yet. In the present study, we performed CCK-8, morphology, wound

healing, transwell, qRT-PCR, western blotting and immunofluorescence assays to explore the role and the underlying mechanisms of TFA on CD intestinal fibrosis, and the results indicated that TFA was expected to advance as a new therapy to treat CD intestinal fibrosis.

Research objectives

To explore the role and mechanism of TFA on EMT progress of CD intestinal fibrosis.

Research methods

First, a CCK-8 assay was performed to assess the effect of TFA on the viability of IEC-6 cells and to select the optimal concentrations of TFA for our further studies. Then cell morphology, wound healing and transwell assays were performed to examine the effect of TFA on morphology, migration and invasion of IEC-6 cells treated with transforming growth factor-β1 (TGF-β1). In addition, immunofluorescence, qRT-PCR and western blotting assays were carried out to detect the impact of TFA on EMT progress. Moreover, western blotting assay was performed to evaluate the function of TFA on the Smad and MAPK signaling pathways. Further, the role of co-treatment of TFA and si-Smad or MAPK inhibitors was examined by qRT-PCR, western blotting, morphology, wound healing and transwell assays.

Research results

In this study, TFA promoted TGF-β1-induced IEC-6 cell morphological change, migration and invasion, and increased the expression of epithelial markers and reduced the levels of mesenchymal markers, along with the inactivation of Smad and MAPK signaling pathways. Moreover, we revealed that si-Smad and MAPK inhibitors effectively attenuated TGF-β1-induced EMT in TEC-6 cells. Importantly, co-treatment of TFA and si-Smad or MAPK inhibitors had better inhibitory effects on TGF-β1-induced EMT in IEC-6 cells than either one of them alone.

Research conclusions

These findings could provide new insight into the molecular mechanisms of TFA on TGF-β1-induced EMT in IEC-6 cells, and TFA is expected to advance as a new therapy to treat CD intestinal fibrosis.

Research perspectives

TFA promoted the induction of EMT partly by inhibiting TGF-β1-activated Smad signaling pathway and non-Smad signaling pathway. TFA is expected to advance as a new therapy to treat CD intestinal fibrosis, and its continued advancement may open the door to a new class of treatment for CD intestinal fibrosis.

REFERENCES

1 **Hirten RP,** Shah S, Sachar DB, Colombel JF. The Management of Intestinal Penetrating Crohn's Disease. *Inflamm Bowel Dis* 2018; **24**: 752-765 [PMID: 29528400 DOI: 10.1093/ibd/izx108]

2 **Stidham RW**, Wu J, Shi J, Lubman DM, Higgins PD. Serum Glycoproteome Profiles for Distinguishing Intestinal Fibrosis from Inflammation in Crohn's Disease. *PLoS One* 2017; **12**: e0170506 [PMID: 28114331 DOI: 10.1371/journal.pone.0170506]

3 **Wilkens R**, Hagemann-Madsen RH, Peters DA, Nielsen AH, Nørager CB, Glerup H, Krogh K. Validity of Contrast-enhanced Ultrasonography and Dynamic Contrast-enhanced MR Enterography in the Assessment of Transmural Activity and Fibrosis in Crohn's Disease. *J Crohns Colitis* 2018; **12**: 48-56 [PMID: 28981627 DOI: 10.1093/ecco-jcc/jjx111]

4 **Rogler G**, Hausmann M. Factors Promoting Development of Fibrosis in Crohn's Disease. *Front Med* (Lausanne) 2017; **4**: 96 [PMID: 28736729 DOI: 10.3389/fmed.2017.00096]

5 **Hui CK**, Hui NK. Collagenous colitis presenting with skip lesions mimicking Crohn's disease and complicated by intestinal obstruction. *J Dig Dis* 2017; **18**: 487-491 [PMID: 28682012 DOI: 10.1111/1751-2980.12507]

6 **Ma C**, Moran GW, Benchimol EI, Targownik LE, Heitman SJ, Hubbard JN, Seow CH, Novak KL, Ghosh S, Panaccione R, Kaplan GG. Surgical Rates for Crohn's Disease are Decreasing: A Population-Based Time Trend Analysis and Validation Study. *Am J Gastroenterol* 2017; **112**: 1840-1848 [PMID: 29087396 DOI: 10.1038/ajg.2017.394]

7 **Ha FJ**, Thong L, Khalil H. Quality of Life after Intestinal Resection in Patients with Crohn Disease: A Systematic Review. *Dig Surg* 2017; **34**: 355-363 [PMID: 28099962 DOI: 10.1159/000453590]

8 **Sobrado CW**, Leal RF, Sobrado LF. THERAPIES FOR CROHN' S DISEASE: a clinical update. *Arq Gastroenterol* 2016; **53**: 206-211 [PMID: 27438429 DOI: 10.1590/S0004-28032016000300016]

9 **Deepak P**, Loftus EV Jr. Ustekinumab in treatment of Crohn's disease: design, development, and potential place in therapy. *Drug Des Devel Ther* 2016; **10**: 3685-3698 [PMID: 27956825 DOI: 10.2147/DDDT.S102141]

10 **Wang X**, Lu Y, Wu L, Zhao C, Song C, Yu S, Zhao B, Zhao T, Liu H, Dou C, Zhang Y, Wu H. Moxibustion Inhibits the ERK Signaling Pathway and Intestinal Fibrosis in Rats with Crohn's Disease. *Evid Based Complement Alternat Med* 2013; **2013**: 198282 [PMID: 23970928 DOI: 10.1155/2013/198282]

11 **Abreu MT**, Taylor KD, Lin YC, Hang T, Gaiennie J, Landers CJ, Vasiliauskas EA, Kam LY, Rojany M, Papadakis KA, Rotter JI, Targan SR, Yang H. Mutations in NOD2 are associated with fibrostenosing disease in patients with Crohn's disease. *Gastroenterology* 2002; **123**: 679-688 [PMID: 12198692 DOI: 10.1053/gast.2002.35393]

12 **Hassan-Zahraee M**, Banerjee A, Cheng JB, Zhang W, Ahmad A, Page K, von Schack D, Zhang B, Martin SW, Nayak S, Reddy P, Xi L, Neubert H, Fernandez Ocana M, Gorelick K, Clare R, Vincent M, Cataldi F, Hung K. Anti-MAdCAM Antibody Increases ß7+ T Cells and CCR9 Gene Expression in the Peripheral Blood of Patients With Crohn's Disease. *J Crohns Colitis* 2018; **12**: 77-86 [PMID: 28961803 DOI: 10.1093/ecco-jcc/jjx121]

13 **Zheng Y**, Ge W, Ma Y, Xie G, Wang W, Han L, Bian B, Li L, Shen L. miR-155 Regulates IL-10-Producing $CD24^{hi}CD27B^{+}$ Cells and Impairs Their Function in Patients with Crohn's Disease. *Front Immunol* 2017; **8**: 914 [PMID: 28824639 DOI: 10.3389/fimmu.2017.00914]

14 **Mortensen JH**, Godskesen LE, Jensen MD, Van Haaften WT, Klinge LG, Olinga P, Dijkstra G, Kjeldsen J, Karsdal MA, Bay-Jensen AC, Krag A. Fragments of Citrullinated and MMP-degraded Vimentin and MMP-degraded Type III Collagen Are Novel Serological Biomarkers to Differentiate Crohn's Disease from Ulcerative Colitis. *J Crohns Colitis* 2015; **9**: 863-872 [PMID: 26188349 DOI: 10.1093/ecco-jcc/jjv123]

15 **Kurahara LH**, Hiraishi K, Sumiyoshi M, Doi M, Hu Y, Aoyagi K, Jian Y, Inoue R. Significant contribution of TRPC6 channel-mediated Ca^{2+} influx to the pathogenesis of Crohn's disease fibrotic stenosis. *J Smooth Muscle Res* 2016; **52**: 78-92 [PMID: 27818466 DOI: 10.1540/jsmr.52.78]

16 **Jiang H**, Shen J, Ran Z. Epithelial-mesenchymal transition in Crohn' s disease. *Mucosal Immunol* 2018; **11**: 294-303 [PMID: 29346350 DOI: 10.1038/mi.2017.107]

17 **Scharl M**, Frei P, Frei SM, Biedermann L, Weber A, Rogler G. Epithelial-to-mesenchymal transition in a fistula-associated anal adenocarcinoma in a patient with long-standing Crohn's disease. *Eur J Gastroenterol Hepatol* 2014; **26**: 114-118 [PMID: 24284372 DOI: 10.1097/MEG.0b013e32836371a2]

18 **Scharl M**, Huber N, Lang S, Fürst A, Jehle E, Rogler G. Hallmarks of epithelial to mesenchymal transition are detectable in Crohn' s disease associated intestinal fibrosis. *Clin Transl Med* 2015; **4**: 1 [PMID: 25852817 DOI: 10.1186/s40169-015-0046-5]

19 **Chen Y**, Xiao Y, Ge W, Zhou K, Wen J, Yan W, Wang Y, Wang B, Qu C, Wu J, Xu L, Cai W. miR-200b inhibits TGF-β1-induced epithelial-mesenchymal transition and promotes growth of intestinal epithelial cells. *Cell Death Dis* 2013; **4**: e541 [PMID: 23492772 DOI: 10.1038/cddis.2013.22]

20 **Liu TJ**, Guo JL, Wang HK, Xu X. Semaphorin-7A contributes to growth, migration and invasion of oral tongue squamous cell carcinoma through TGF-β-mediated EMT signaling pathway. *Eur*

Rev Med Pharmacol Sci 2018; **22**: 1035-1043 [PMID: 29509252]
21 **Sommerova L**, Ondrouskova E, Vojtesek B, Hrstka R. Suppression of AGR2 in a TGF-β-induced Smad regulatory pathway mediates epithelial-mesenchymal transition. *BMC Cancer* 2017; **17**: 546 [PMID: 28810836 DOI: 10.1186/s12885-017-3537-5]
22 **Sun S**, Xie F, Zhang Q, Cui Z, Cheng X, Zhong F, He K, Zhou J. Advanced oxidation protein products induce hepatocyte epithelial-mesenchymal transition via a ROS-dependent, TGF-β/Smad signaling pathway. *Cell Biol Int* 2017; **41**: 842-853 [PMID: 28500745 DOI: 10.1002/cbin.10792]
23 **Liu Z**, Liu S, Zhou L, Gao X, Ju W, Tan H, Yang C. Effects of HuangKui capsules on glibenclamide pharmacokinetics in rats. *J Ethnopharmacol* 2012; **139**: 1-5 [PMID: 21527329 DOI: 10.1016/j.jep.2011.03.043]
24 **Tu Y**, Sun W, Wan YG, Che XY, Pu HP, Yin XJ, Chen HL, Meng XJ, Huang YR, Shi XM. Huangkui capsule, an extract from Abelmoschus manihot (L.) medic, ameliorates adriamycin-induced renal inflammation and glomerular injury via inhibiting p38MAPK signaling pathway activity in rats. *J Ethnopharmacol* 2013; **147**: 311-320 [PMID: 23518420 DOI: 10.1016/j.jep.2013.03.006]
25 **Ge J**, Miao JJ, Sun XY, Yu JY. Huangkui capsule, an extract from Abelmoschus manihot (L.) medic, improves diabetic nephropathy via activating peroxisome proliferator-activated receptor (PPAR)-α/γ and attenuating endoplasmic reticulum stress in rats. *J Ethnopharmacol* 2016; **189**: 238-249 [PMID: 27224243 DOI: 10.1016/j.jep.2016.05.033]
26 **Liu S**, Ye L, Tao J, Ge C, Huang L, Yu J. Total flavones of Abelmoschus manihot improve diabetic nephropathy by inhibiting the iRhom2/TACE signalling pathway activity in rats. *Pharm Biol* 2017; **56**: 1-11 [PMID: 29221422 DOI: 10.1080/13880209.2017.1412467]
27 **Guo J**, Xue C, Duan JA, Qian D, Tang Y, You Y. Anticonvulsant, antidepressant-like activity of Abelmoschus manihot ethanol extract and its potential active components in vivo. *Phytomedicine* 2011; **18**: 1250-1254 [PMID: 21784623 DOI: 10.1016/j.phymed.2011.06.012]
28 **Chen Q**, Yang W, Wang X, Li X, Qi S, Zhang Y, Gao MQ. TGF-β1 Induces EMT in Bovine Mammary Epithelial Cells Through the TGFβ1/Smad Signaling Pathway. *Cell Physiol Biochem* 2017; **43**: 82-93 [PMID: 28848180 DOI: 10.1159/000480321]
29 **Ling G**, Ji Q, Ye W, Ma D, Wang Y. Epithelial-mesenchymal transition regulated by p38/MAPK signaling pathways participates in vasculogenic mimicry formation in SHG44 cells transfected with TGF-β cDNA loaded lentivirus in vitro and in vivo. *Int J Oncol* 2016; **49**: 2387-2398 [PMID: 27748800 DOI: 10.3892/ijo.2016.3724]
30 **Cayci M**, Bostanci EB, Turhan N, Karaman K, Dalgic T, Ozer I, Ercan M, Ulas M, Akoglu M. The analysis of clinico-pathologic characteristics in patients who underwent surgery due to stricturing and non-perineal fistulizing forms of Crohn's disease: a retrospective cohort study. *Int J Surg* 2015; **15**: 49-54 [PMID: 25647540 DOI: 10.1016/j.ijsu.2015.01.029]
31 **Conway J**, Al-Zahrani KN, Pryce BR, Abou-Hamad J, Sabourin LA. Transforming growth factor β-induced epithelial to mesenchymal transition requires the Ste20-like kinase SLK independently of its catalytic activity. *Oncotarget* 2017; **8**: 98745-98756 [PMID: 29228724 DOI: 10.18632/oncotarget.21928]
32 **Ma F**, Li W, Liu C, Li W, Yu H, Lei B, Ren Y, Li Z, Pang D, Qian C. MiR-23a promotes TGF-β1-induced EMT and tumor metastasis in breast cancer cells by directly targeting CDH1 and activating Wnt/β-catenin signaling. *Oncotarget* 2017; **8**: 69538-69550 [PMID: 29050223]
33 **You J**, Li M, Tan Y, Cao L, Gu Q, Yang H, Hu C. Snail1-expressing cancer-associated fibroblasts induce lung cancer cell epithelial-mesenchymal transition through miR-33b. *Oncotarget* 2017; **8**: 114769-114786 [PMID: 29383119 DOI: 10.18632/oncotarget.23082]
34 **Ke X**, Yang D, Liang J, Wang X, Wu S, Wang X, Hu C. Human Endothelial Progenitor Cell-Derived Exosomes Increase Proliferation and Angiogenesis in Cardiac Fibroblasts by Promoting the Mesenchymal-Endothelial Transition and Reducing High Mobility Group Box 1 Protein B1 Expression. *DNA Cell Biol* 2017; **36**: 1018-1028 [PMID: 28920705 DOI: 10.1089/dna.2017.3836]
35 **Guan R**, Wang X, Zhao X, Song N, Zhu J, Wang J, Wang J, Xia C, Chen Y, Zhu D, Shen L. Emodin ameliorates bleomycin-induced pulmonary fibrosis in rats by suppressing epithelial-mesenchymal transition and fibroblast activation. *Sci Rep* 2016; **6**: 35696 [PMID: 27774992 DOI: 10.1038/srep35696]
36 **Boland BS**, Vermeire S. Janus Kinase Antagonists and Other Novel Small Molecules for the Treatment of Crohn's Disease. *Gastroenterol Clin North Am* 2017; **46**: 627-644 [PMID: 28838419 DOI: 10.1016/j.gtc.2017.05.015]
37 **Ramos GP**, Faubion WA, Papadakis KA. Targeting Specific Immunologic Pathways in Crohn's Disease. *Gastroenterol Clin North Am* 2017; **46**: 577-588 [PMID: 28838416 DOI: 10.1016/j.gtc.2017.05.009]
38 **Chen H**, Chen Q, Jiang CM, Shi GY, Sui BW, Zhang W, Yang LZ, Li ZY, Liu L, Su YM, Zhao WC, Sun HQ, Li ZZ, Fu Z. Triptolide suppresses paraquat induced idiopathic pulmonary fibrosis by inhibiting TGFB1-dependent epithelial mesenchymal transition. *Toxicol Lett* 2018; **284**: 1-9 [PMID: 29195901 DOI: 10.1016/j.toxlet.2017.11.030]
39 **Perumal N**, Perumal M, Halagowder D, Sivasithamparam N. Morin attenuates diethylnitrosamine-induced rat liver fibrosis and hepatic stellate cell activation by co-ordinated regulation of Hippo/Yap and TGF-β1/Smad signaling. *Biochimie* 2017; **140**: 10-19 [PMID: 28552397 DOI: 10.1016/j.biochi.2017.05.017]
40 **Luong VH**, Chino T, Oyama N, Matsushita T, Sasaki Y, Ogura D, Niwa SI, Biswas T, Hamasaki A, Fujita M, Okamoto Y, Otsuka M, Ihn H, Hasegawa M. Blockade of TGF-β/Smad signaling by the small compound HPH-15 ameliorates experimental skin fibrosis. *Arthritis Res Ther* 2018; **20**: 46 [PMID: 29544542 DOI: 10.1186/s13075-018-1534-y]
41 **Ma YL**, Chen F, Yang SX, Chen BP, Shi J. MicroRNA-21 promotes the progression of peritoneal fibrosis through the activation of the TGF-β/Smad signaling pathway: An in vitro and in vivo study. *Int J Mol Med* 2018; **41**: 1030-1038 [PMID: 29207016]
42 **Cao Y**, Liu Y, Ping F, Yi L, Zeng Z, Li Y. miR-200b/c attenuates lipopolysaccharide-induced early pulmonary fibrosis by targeting ZEB1/2 via p38 MAPK and TGF-β/smad3 signaling pathways. *Lab Invest* 2018; **98**: 339-359 [PMID: 29200203 DOI: 10.1038/labinvest.2017.123]
43 **Bansal T**, Chatterjee E, Singh J, Ray A, Kundu B, Thankamani V, Sengupta S, Sarkar S. Arjunolic acid, a peroxisome proliferator-activated receptor α agonist, regresses cardiac fibrosis by inhibiting non-canonical TGF-β signaling. *J Biol Chem* 2017; **292**: 16440-16462 [PMID: 28821620 DOI: 10.1074/jbc.M117.788299]
44 **Che X**, Wang Q, Xie Y, Xu W, Shao X, Mou S, Ni Z. Astragaloside IV suppresses transforming growth factor-β1 induced fibrosis of cultured mouse renal fibroblasts via inhibition of the MAPK and NF-κB signaling pathways. *Biochem Biophys Res Commun* 2015; **464**: 1260-1266 [PMID: 26220342 DOI: 10.1016/j.bbrc.2015.07.116]

P- Reviewer: Sipahi AM, Sultan K, Smith SM **S- Editor**: Wang XJ
L- Editor: Filipodia **E- Editor**: Yin SY

World Journal of Gastroenterology

Submit a Manuscript: http://www.f6publishing.com

World J Gastroenterol 2018 August 14; 24(30): 3426-3439

DOI: 10.3748/wjg.v24.i30.3426

ISSN 1007-9327 (print) ISSN 2219-2840 (online)

ORIGINAL ARTICLE

Basic Study

Identification of a five-long non-coding RNA signature to improve the prognosis prediction for patients with hepatocellular carcinoma

Qiu-Jie Zhao, Jiao Zhang, Lin Xu, Fang-Feng Liu

Qiu-Jie Zhao, Jiao Zhang, Lin Xu, Department of Gastroenterology, Shandong Provincial Hospital affiliated to Shandong University, Jinan 250021, Shandong Province, China

Fang-Feng Liu, Department of Hepatobiliary Surgery, Shandong Provincial Hospital affiliated to Shandong University, Jinan 250021, Shandong Province, China

ORCID number: Qiu-Jie Zhao (0000-0003-4053-8406); Jiao Zhang (0000-0002-9178-1003); Lin Xu (0000-0003-0253-608X); Fang-Feng Liu (0000-0002-3745-5012).

Author contributions: Zhao QJ conceived the study, drafted and revised the manuscript; Zhang J and Xu L helped with the statistical analysis; Liu FF helped participated in data mining; all authors read and approved the final manuscript.

Supported by the National Nature Science Foundation of China, No. 81702816 (to Zhao QJ); and Shandong Provincial Natural Science Foundation, No. ZR2017PH030 (to Zhao QJ).

Institutional review board statement: This studied mined the TCGA database and doesn't involve any experiments with animals or human beings. Because the TCGA data are a community resource project, additional ethical approval was not acquired.

Conflict-of-interest statement: The authors declare that there is no conflict of interest related to this study.

Data sharing statement: The datasets supporting the conclusions of this article are included within the article.

Manuscript source: Unsolicited manuscript

Correspondence to: Qiu-Jie Zhao, PhD, Chief Doctor, Department of Gastroenterology, Shandong Provincial Hospital affiliated to Shandong University, No. 324, Jingwuwei 7th Road, Jinan 250021, Shandong Province, China. zhaoqiujiesdu@126.com
Telephone: +86-531-68772952

Received: March 27, 2018
Peer-review started: March 28, 2018
First decision: May 9, 2018
Revised: May 24, 2018
Accepted: June 22, 2018
Article in press: June 22, 2018
Published online: August 14, 2018

Abstract

AIM

To construct a long non-coding RNA (lncRNA) signature for predicting hepatocellular carcinoma (HCC) prognosis with high efficiency.

METHODS

Differentially expressed lncRNAs (DELs) between HCC specimens and peritumor liver specimens were identified using the edgeR package to analyze The Cancer Genome Atlas (TCGA) LIHC dataset. Univariate Cox proportional hazards regression was performed to obtain the DELs significantly associated with overall survival (OS) in a training set. These OS-related DELs were further analyzed using a stepwise multivariate Cox regression model. Those lncRNAs fitted in the multivariate Cox regression model and independently associated with overall survival were chosen to build a prognostic risk formula. The prognostic value of

this formula was then validated in the test group and the entire cohort and further compared with two previously identified prognostic signatures for HCC. Gene ontology and Kyoto Encyclopedia of Genes and Genomes pathway analyses were performed to explore the potential biological functions of the lncRNAs in the signature.

RESULTS

Based on lncRNA expression profiling of 370 HCC patients from the TCGA database, we constructed a 5-lncRNA signature (AC015908.3, AC091057.3, TMCC1-AS1, DCST1-AS1 and FOXD2-AS1) that was significantly associated with prognosis. HCC patients with high-risk scores based on the expression of the 5 lncRNAs had significantly shorter survival times compared to patients with low-risk scores in both the training and test groups. Multivariate Cox regression analysis demonstrated that the prognostic value of the 5 lncRNAs was independent of clinicopathological parameters. A comparison study involving two previously identified prognostic signatures for HCC demonstrated that this 5-lncRNA signature showed improved prognostic power compared with the other two signatures. Functional enrichment analysis indicated that the 5 lncRNAs were potentially involved in metabolic processes, fibrinolysis and complement activation.

CONCLUSION

Our present study constructed a 5-lncRNA signature that improves survival prediction and can be used as a prognostic biomarker for HCC patients.

Key words: Long non-coding RNA; Hepatocellular carcinoma; Prognosis; Survival prediction; Prognostic biomarker

Core tip: In the present study, we developed a 5-long non-coding RNA (lncRNA) signature for predicting the prognosis of hepatocellular carcinoma (HCC) patients based on The Cancer Genome Atlas database. The signature was reproducible and robust in another independent large-scale HCC cohort, supporting its utility and effectiveness. In addition, the prognostic value of the 5-lncRNA signature was independent of clinicopathological variables. When compared with two previously identified signatures for HCC survival prediction, this 5-lncRNA signature showed superior prognostic power. Our study indicates that the 5-lncRNA signature could improve survival prediction and could be used as a prognostic biomarker for HCC patients.

Zhao QJ, Zhang J, Xu L, Liu FF. Identification of a five-long non-coding RNA signature to improve the prognosis prediction for patients with hepatocellular carcinoma. *World J Gastroenterol* 2018; 24(30): 3426-3439 Available from: URL: http://www.wjgnet.com/1007-9327/full/v24/i30/3426.htm DOI: http://dx.doi.org/10.3748/wjg.v24.i30.3426

INTRODUCTION

Hepatocellular carcinoma (HCC) is the sixth most commonly diagnosed cancer in the world[1]. According to previous epidemiologic studies, the incidence of HCC varies strikingly worldwide and is particularly high in eastern Asian countries, including China, and sub-Saharan Africa[2,3]. The 5-year overall survival rate for HCC is lower than 20%[4], and the ratio of its mortality to morbidity is 0.95[1]. Because of its poor prognosis, HCC ranks as the second leading cause of cancer-related deaths worldwide[1]. An estimated 782500 new liver cancer cases and 745500 deaths occurred worldwide in 2012, among which 50% occurred in China[3]. There are multiple risk factors related to HCC, including hepatitis B or C viral infection, chronic alcohol abuse, nonalcoholic fatty liver disease and smoking[5,6]. Although treatment for HCC, including surgical resection, has improved over the past decades, the overall survival rate for this disease remains devastatingly high due to its high recurrence rate (50%-70% at 5 years)[7-9]. Because HCC is a heterogeneous disease with substantially variable clinical outcomes, the search for effective biomarkers to predict recurrence and prognosis is indispensable. To date, no widely accepted molecular biomarkers for HCC aggressiveness are available. In the past 40 years, serum alpha fetoprotein (AFP) levels have been utilized for the diagnosis of HCC and for predicting its response to therapy. However, AFP levels can be influenced by tumor size and cancer stage, and they are not reliable in clinical applications[10]. In addition, the American Association for the Study of Liver Diseases concluded that the use of AFP levels lacks sufficient sensitivity and specificity to effectively monitor or diagnose HCC[11].

With the development of high-throughput sequencing technologies, it has become easy to acquire whole genome profiles for specific cancers and develop more reliable prognostic signatures. Long non-coding RNAs (lncRNAs) are mRNA-like transcripts of more than 200 nucleotides (nt) with little or no protein-coding capacity[12,13]. In the past, they were previously thought to be redundant segments of the genome, but in recent decades, emerging studies have indicated the importance of lncRNAs in cellular physiological and pathological processes[14,15]. Increasing evidence suggests that dysregulated lncRNAs are associated with various human diseases, particularly the initiation and progression of various human cancers[16,17]. Prognostic lncRNA signatures have been examined in many cancer types, including renal cancer, glioblastoma, colorectal cancer, lymphoma, and others[18-21]. For HCC, most of the published gene signatures associated with prognosis have focused on mRNAs and microRNAs[22-25]. To the

Table 1 Clinicopathological parameters of hepatocellular carcinoma patients in each cohort

Variables		Training group (n = 184)	Test group (n = 186)	Entire group (n = 370)
Age, yr	< 60	84	85	169
	⩾ 60	100	101	201
Sex	Male	129	120	24
	Female	55	66	121
Weight, kg	< 70	92	85	177
	⩾ 70	78	89	167
	NA	14	12	26
Child-Pugh grade	A	109	107	216
	B	9	12	21
	C	0	1	1
	NA	66	66	132
Fibrosis ishak score	0	32	42	74
	1-5	38	31	69
	6	36	33	69
	NA	78	80	158
Vascular tumor invasion	None	100	106	206
	Micro	45	46	91
	Macro	8	9	17
	NA	31	25	56
Serum FAP level, ng/mL	< 100	102	90	192
	⩾ 100	37	48	85
	NA	45	48	93
Tumor grade	1	37	18	55
	2	82	95	177
	3 + 4	61	72	133
	NA	4	1	5
Pathologic stage	I	92	79	171
	II	43	42	85
	III + IV	37	53	90
	NA	12	12	24

best of our knowledge, very few lncRNA signatures have been developed for HCC prognosis prediction[26]. Thus, it is necessary to identify a more effective lncRNA signature for HCC prognosis. In the present study, we aimed to construct a lncRNA signature capable of predicting HCC prognosis with high efficiency.

In this work, we analyzed a cohort of 370 HCC patients from The Cancer Genome Atlas (TCGA) to identify a potential lncRNA signature for predicting the survival of HCC patients. We identified a five-lncRNA prognostic signature from the TCGA dataset and determined that its prognostic value was independent from clinical factors. The identification of prognostic lncRNAs suggests the potential roles of lncRNAs in HCC pathogenesis and progression.

MATERIALS AND METHODS

Data and patients

Level 3 RNA-seq data (HTSeq-counts) from 374 HCC tumor specimens and 50 peritumoral liver specimens and their corresponding clinicopathological information were downloaded from the TCGA project (https://cancergenome.nih.gov/) on June 2, 2017. Because TCGA data are a community resource project, additional ethical approval was not acquired, and the present study adhered to TCGA publication guidelines and data access policies. After excluding the data without complete survival information, a total of 370 HCC patients with complete follow up data were enrolled in our study and then randomly divided into a training set (n = 184) and test set (n = 186) using SPSS software (version 24.0). The clinicopathological parameters of the HCC patients in each group are listed in Table 1.

LncRNA expression profile in the TCGA LIHC cohort

Only lncRNAs with a description in NCBI or Ensemble were selected for further study in this paper. We obtained the expression profiles of 6929 lncRNAs from the RNA-seq data of the TCGA LIHC cohort. Differentially expressed lncRNAs (DELs) between the HCC specimens and peritumor liver specimens were identified with the edgeR package, using an adjusted $P < 0.05$ and $\log_2$ |fold change| > 1. The expression level of each lncRNA was $\log_2$ transformed for the downstream analyses.

Identification of prognostic lncRNAs and construction of the risk formula for overall survival prediction

Univariate Cox proportional hazards regression was performed to obtain the DELs that were significantly associated with the overall survival (OS) of HCC patients in the training group. After acquiring survival-related lncRNAs ($P < 0.01$), we excluded those not expressed in at least 10% of the samples. The remaining OS-related lncRNAs were then adjusted sing the stepwise multivariate Cox regression model. Finally, those lncRNAs fitted in the multivariate Cox regression model and independently associated with OS were chosen. A

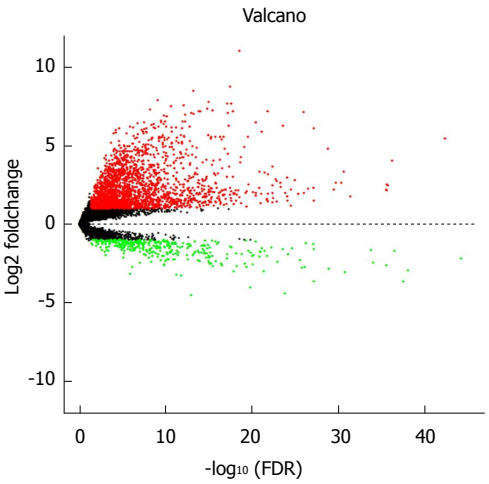

Figure 1 Volcano plot of the differentially expressed long non-coding RNAs between hepatocellular carcinoma tumor specimens and peritumoral liver specimens. The X-axis represents the adjusted FDR, and the Y-axis represents the value of the $\log_2$ fold change. Aberrantly expressed long non-coding RNAs (lncRNAs) were calculated using the EdgeR package. Red dots represent upregulated lncRNAs in the hepatocellular carcinoma (HCC) tumor specimens, while green dots indicate downregulated lncRNAs compared with the peritumoral liver specimens. Black dots show the lncRNAs without significant differences between the HCC tumor and peritumoral liver specimens. Altogether, 2240 upregulated and 353 downregulated lncRNAs were found. This volcano plot was conducted using the ggplot2 package of R language.

prognostic risk formula was established based on a linear combination of the expression level of these lncRNAs multiplied by the regression coefficient derived from the multivariate Cox regression model as previously described[18-21].The subjects in each dataset were classified into a high-risk group and low-risk group according to the median risk score of the risk formula derived from the training set.

Statistical analysis

Univariate Cox proportional hazards regression was performed to obtain survival-related DELs, and the stepwise multivariate Cox regression model was performed for further selection. Overall survival analyses in the high-risk and low-risk groups were performed using Kaplan-Meier survival curves and a log-rank test. Receiver operating curve analyses were performed to assess the specificity and sensitivity of the prognosis prediction. The above analyses were performed using R (version 3.3.1). To verify the independence of the prognostic value of the 5-lncRNA signature and clinicopathological parameters, univariate and multivariate Cox regression analyses were performed using SPSS software (version 24.0). In the comparison study, Kaplan-Meier survival analysis and receiver operating curve (ROC) analysis were also performed using SPSS (version 24.0).

Functional enrichment analyses

To identify co-expressed lncRNA-mRNA pairs, we performed Person correlation analyses with R (version 3.3.1) for each of the five lncRNAs with protein-coding genes based on the RNA-seq data of the TCGA LIHC cohort. The protein-coding genes with a correlation coefficient > 0.5 and a $P < 0.01$ were considered to be significantly correlated genes. For functional enrichment analysis, the correlated protein-coding genes were subjected to gene ontology (GO) and Kyoto Encyclopediaof Genes and Genomes (KEGG) pathway analyses using DAVID Bioinformatics Resources (version 6.8)[27,28]. Significant functional categories were identified and limited to GO terms in the "Biological Process" (GOTERM-BP-DIRECT) and KEGG pathway categories, using the human whole genome as the background. Significantly enriched GO terms with similar functions were visualized using the EnrichmentMap plugin in Cytoscape (version 3.5.1)[29].

RESULTS

Determining prognostic lncRNAs from the training set

Using the edgeR package, we identified a total of 2593 lncRNAs differentially expressed ($\log_2$|fold change| > 1 and adjusted $P < 0.05$) between 374 HCC tumor specimens and 50 peritumor liver specimens, including 2240 upregulated and 353 downregulated lncRNAs (Figure 1). A total of 370 HCC samples with complete survival information were subjected to further analyses. For the training set, univariate Cox proportional hazards regression analyses revealed 82 lncRNAs significantly correlated with OS ($P < 0.01$) among the 2593 differentially expressed lncRNAs. Among the 82 OS-related lncRNAs, we further excluded those expressed in less than 10% of the HCC specimens, and the remaining 30 lncRNAs were subjected to further selection.

Construction of a lncRNA-based prognostic signature and validation in the training group

Stepwise multivariable Cox proportional hazards regression analyses were performed to identify the optimal prognostic lncRNAs among the 30 candidate lncRNAs. Based on this model, a final 5 lncRNAs were found to be significantly and independently related to prognosis. We then constructed a prognostic signature based on the expression levels of these 5 lncRNAs and their coefficients derived from the multivariable Cox model. The formula is as follows: risk score = (-0.1900 × the expression level of AC015908.3) + (0.1764 × the expression level of FOXD2-AS1) + (0.3588 × the expression level of AC091057.3) + (0.5615 × the expression level of TMCC1-AS1) + (0.4877 × the expression level of DCST1-AS1). Detailed information for the 5 lncRNAs is listed in Table 2. The risk score for each patient in the training group was calculated using the formula. The training set was then divided into a high-risk group (n = 92) and a low-risk group (n = 92) according to the median risk score. Kaplan-Meier analysis revealed that the high-risk group had a significantly poorer prognosis than that of the low-

Table 2 The 5 long non-coding RNAs significantly associated with overall survival of hepatocellular carcinoma patients

Gene ID	Gene symbol	Coefficient	Hazard ratio	*P* value
ENSG00000264016	AC015908.3	-0.1900	0.7792	0.000305
ENSG00000237424	FOXD2-AS1	0.1764	1.2865	0.007317
ENSG00000269974	AC091057.3	0.3588	1.4682	0.000375
ENSG00000271270	TMCC1-AS1	0.5615	1.5417	0.000287
ENSG00000232093	DCST1-AS1	0.4877	1.3909	0.001632

risk group (*P* = 1.3e-09, log-rank test, Figure 2A). The median survival time for the high-risk group and the low-risk group was 2.096 and 6.811 years, respectively. Additionally, the 3- and 5-year survival rates of the high-risk group were 40% and 23.5%, whereas the corresponding survival rates were 90% and 71.8%, respectively, in the low-risk group. To evaluate the performance of the 5-lncRNA signature for predicting the prognosis of HCC patients, a time-dependent ROC analysis was conducted. The area under the ROC curve (AUC) for the 5-lncRNA signature was 0.857, which indicated good performance (Figure 2B). The risk scores of patients in the training group were also ranked, and survival status was plotted for each patient on a dot plot (Figure 2C). The mortality for patients in the high-risk group was much higher than that in the low-risk group. A heat map displays the expression profiles of these five lncRNAs in the samples from the training group; the expression profiles are ranked according to risk score (Figure 2D). Among the 5 lncRNAs, AC015908.3 showed a negative coefficient derived for the multivariate Cox regression model and seemed to be a protective factor, as its high expression predicts a low risk. The other 4 lncRNAs with positive coefficients, including FOXD2-AS1, AC091057.3, TMCC1-AS1 and DCST1-AS1, seemed to be risk factors and all were upregulated in the high-risk group compared to the low-risk group within the training set.

Validation of the prognostic value of the 5-lncRNA signature for the test set and the entire cohort

To further verify the prognostic value of the 5-lncRNA signature for HCC patients, risk scores for patients in the test group were calculated according to the constructed formula based on the expression of the 5 lncRNAs. The test group was also divided into high-risk (*n* = 97) and low-risk (*n* = 89) groups using the same cutoff as for the training group. Kaplan-Meier analysis revealed that the survival rate of the high-risk subgroup was much lower than that of the low-risk subgroup in the test set (median OS: 2.293 years *vs* 8.562 years; log-rank *P* = 1.64e-05) (Figure 3A). For the entire set, a similar result was obtained by Kaplan-Meier analysis. Among the entire cohort, the median survival of the high-risk group (*n* = 189) was 2.197 years, which was significantly lower than the median OS of 6.937 years for the low-risk group (*n* = 181) (*P* = 2.69e-13, Figure 4A). The AUC for the 5-lncRNA-based risk score of overall survival was 0.709 and 0.769 for the test group (Figure 3B) and the entire group (Figure 4B), respectively, with both showing robust utility. In addition, ranked risk scores and survival status for each subject were plotted for the test group (Figure 3C) and the entire set (Figure 4C). Heatmaps display the expression profiles of the five lncRNAs for each subject in the test group (Figure 3D) and the entire cohort (Figure 4D), which were ranked according to risk score.

The prognostic value of the 5-lncRNA signature was independent of clinical characteristics

Univariate and multivariate Cox regression analyses were performed with the 5-lncRNA-based risk score and clinicopathological factors, including age, gender, weight, Child-Pugh grading, fibrosis extent, vascular tumor invasion, serum FAP levels, tumor grade and pathological stage as explanatory variables and overall survival as the dependent variable. The univariate Cox regression demonstrated that the 5-lncRNA signature-based risk score and pathologic stage were able to effectively predict the prognosis of HCC patients. In addition, in the training set and the entire set, patient age seemed to be related to survival, although this did not reach significance (Table 3). In contrast, none of the other clinicopathological parameters were associated with prognosis in either set. Multivariate Cox regression analysis revealed that after adjusting for other factors, age (only for the entire set), pathologic stage and the 5-lncRNAsignature were the only factors significantly associated with overall survival (Table 2). Patients from the entire cohort were then stratified by age (Figure 5A) and pathological stage (Figure 5B). Each subgroup was then divided into a high-risk and low-risk group based on the 5-lncRNA risk score median derived from the training group. Kaplan-Meier analysis revealed that for all of the subgroups, the high-risk group had significantly poorer survival than the low-risk group. All of these results strongly suggest that the prognostic value of the 5-lncRNA-based risk score is independent of clinicopathological factors.

Comparison of the 5-lncRNA signature with existing prognostic signatures for HCC

Two HCC-related prognostic signatures have recently been developed and reported, including a 3-gene signature by Binghua Li and a 4-lncRNA signature by Zhonghao Wang that were both derived from the TCGA dataset[25,26]. To compare the prognostic value of the 5-lncRNA signature developed in our present study

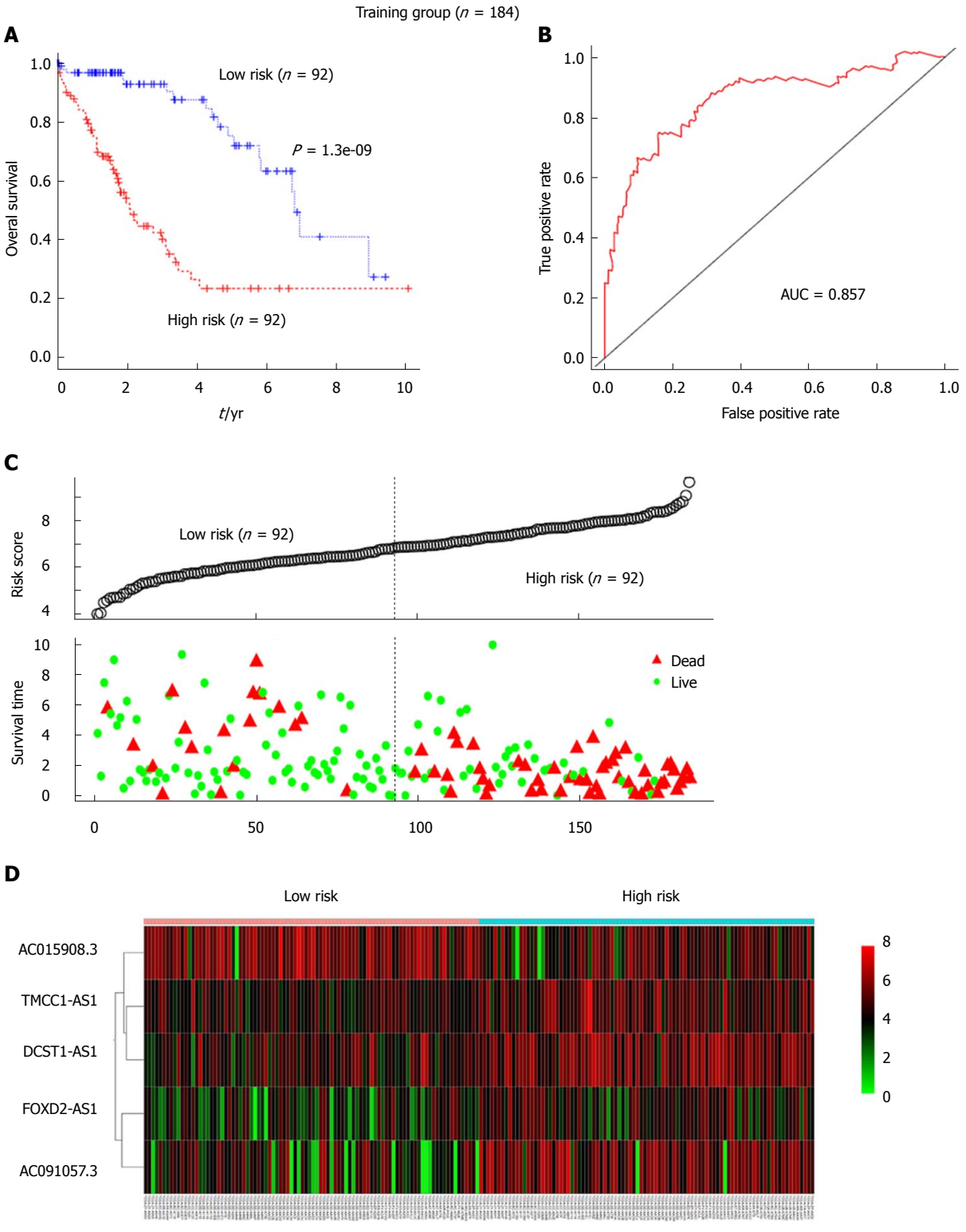

Figure 2 The 5-long non-coding RNA signature-based risk score predicted the overall survival of patients with hepatocellular carcinoma in the training set (*n* = 184). A: Kaplan-Meier analysis of patients' overall survival in the high-risk (*n* = 92) and low-risk (*n* = 92) subgroups of the training set; B: The receiver operating characteristic (ROC) analysis of the risk score for prediction the overall survival of the training set. The area under the curve was calculated for ROC curves; C: The 5-lncRNA-based risk score distribution, patient survival status; D: Heatmap of the 5-lncRNA expression profiles in the high-risk and low-risk subgroups for the training set.

(hereafter referred to as 5LncSig) with the existing 3-gene signature by Binghua Li (hereafter referred to as 3GeneSig) and the 4-lncRNA signature by Zhonghao Wang (hereafter referred to as ZhongSig), we calculated the risk scores of each patient in the entire cohort based on formulae derived from each of these signatures. The 3GeneSig and ZhongSig both successfully and significantly predicted prognosis in the entire TCGA LIHC cohort (Figure 6A and B). Furthermore, comparison of the Kaplan-Meier curves revealed that patients in the high-risk group predicted by 5LncSig showed a dramatically poorer prognosis than those in the low-

Table 3 Univariate and multivariate Cox regression analysis of overall survival

Variables	Univariate analysis			Multivariate analysis		
	HR	95%CI of HR	*P* value	HR	95%CI of HR	*P* value
Training set (*n* = 184)						
Risk score	2.718	2.093-3.530	< 0.0001	2.830	2.091-3.831	< 0.0001
Age	1.018	0.998-1.038	0.073			
Sex (Male/Female)	1.022	0.619-1.690	0.931			
Weight	1.006	0.993-1.108	0.397			
Child-Pugh grade	0.845	0.253-2.827	0.195			
Fibrosis ishak score	0.685	0.756-1.283	0.910			
Vascular invasion (yes/no)	0.834	0.480-1.449	0.519			
FAP	0.805	0.932-1.056	0.805			
Tumor grade (G1 + G2/G3 + G4)	1.133	0.680-1.887	0.632			
Pathologic stage				1.900	1.098-3.288	0.022
Ⅰ / Ⅱ	0.604	0.303-1.203	0.152			
Ⅰ / Ⅲ + Ⅳ	0.298	0.163-0.543	< 0.0001			
Test set (*n* = 186)						
Risk score	1.603	1.270-2.024	< 0.0001	1.568	1.196-2.055	**0.001**
Age	1.006	0.987-1.026	0.522			
Sex (Male/Female)	1.420	0.856-2.356	0.174			
Weight	1.000	0.984-1.105	0.960			
Child-Pugh grade	0.475	0.195-1.157	0.101			
Fibrosis ishak score	1.640	0.706-3.813	0.250			
Vascular invasion (yes/no)	1.069	0.613-1.866	0.614			
FAP	1.035	0.981-1.093	0.210			
Tumor grade (G1 + G2/G3 + G4)	1.092	0.655-1.818	0.736			
Pathologic stage				2.103	1.193-3.707	0.010
Ⅰ / Ⅱ	0.865	0.426-1.757	0.688			
Ⅰ / Ⅲ + Ⅳ	0.445	0.250-0.793	0.006			
Entire set (*n* = 370)						
Risk score	1.957	1.646-2.327	< 0.0001	2.011	1.638-2.469	< 0.0001
Age	1.013	0.999-1.027	0.068	1.016	1.000-1.032	0.048
Sex (Male/Female)	1.166	0.817-1.664	0.396			
Weight	0.998	0.988-1.007	0.615			
Child-Pugh grade (A/B + C)	0.620	0.306-1.256	0.184			
Fibrosis ishak score	1.232	0.742-2.045	0.365			
Vascular invasion (yes/no)	0.962	0.650-1.424	0.846			
Serum AFP level	1.023	0.980-1.068	0.306			
Tumor grade (G1 + G2/G3 + G4)	1.119	0.780-1.604	0.542			
Pathologic stage				2.017	1.359-2.993	0.027
Ⅰ / Ⅱ	0.648	0.398-1.056	0.082			
Ⅰ / Ⅲ + Ⅳ	0.351	0.236-0.524	< 0.0001			

risk groups predicted by the 3GeneSig and ZhongSig (Figure 6A and B), and patients in the low-risk group predicted by 5LncSig had a much better prognosis than those in the high-risk group predicted by the other two signatures (Figure 6A and B). To compare the sensitivity and specificity of the 5LncSig for prognosis prediction with the other two existing signatures, we performed time-dependent ROC analysis. The AUC of overall survival for the 3GeneSig and the ZhongSig was 0.701 and 0.721, respectively (Figure 6C), both lower than that of the 5LncSig (0.769). Thus, the prognostic power of 5LncSig, developed in the present study, was superior to that of the previously developed 3-gene and 4-lncRNA signatures.

Functional characteristics of the five prognostic lncRNAs

To explore the functional implications of these 5 lncRNAs, we performed Pearson correlation analyses between the 5 lncRNAs and protein-coding genes based on their expression levels in the TCGA LIHC cohort. The protein-coding genes that correlated with at least 1 of the 5 lncRNAs (Pearson coefficient > 0.5, $P < 0.01$) were considered to be correlated genes. We chose the 200 correlated genes with the highest Pearson coefficients for further analysis. Functional enrichment analysis revealed that these genes were primarily enriched in 32 GO terms (Benjamin *P* value < 0.1, Figure 7A) and 23 KEGG pathways ($P < 0.001$, Figure 7B). Further analysis revealed that these enriched GO functional terms are mostly involved in metabolic processes, fibrinolysis and complement activation (Figure 7A).

DISCUSSION

HCC is a heterogeneous disease with differential

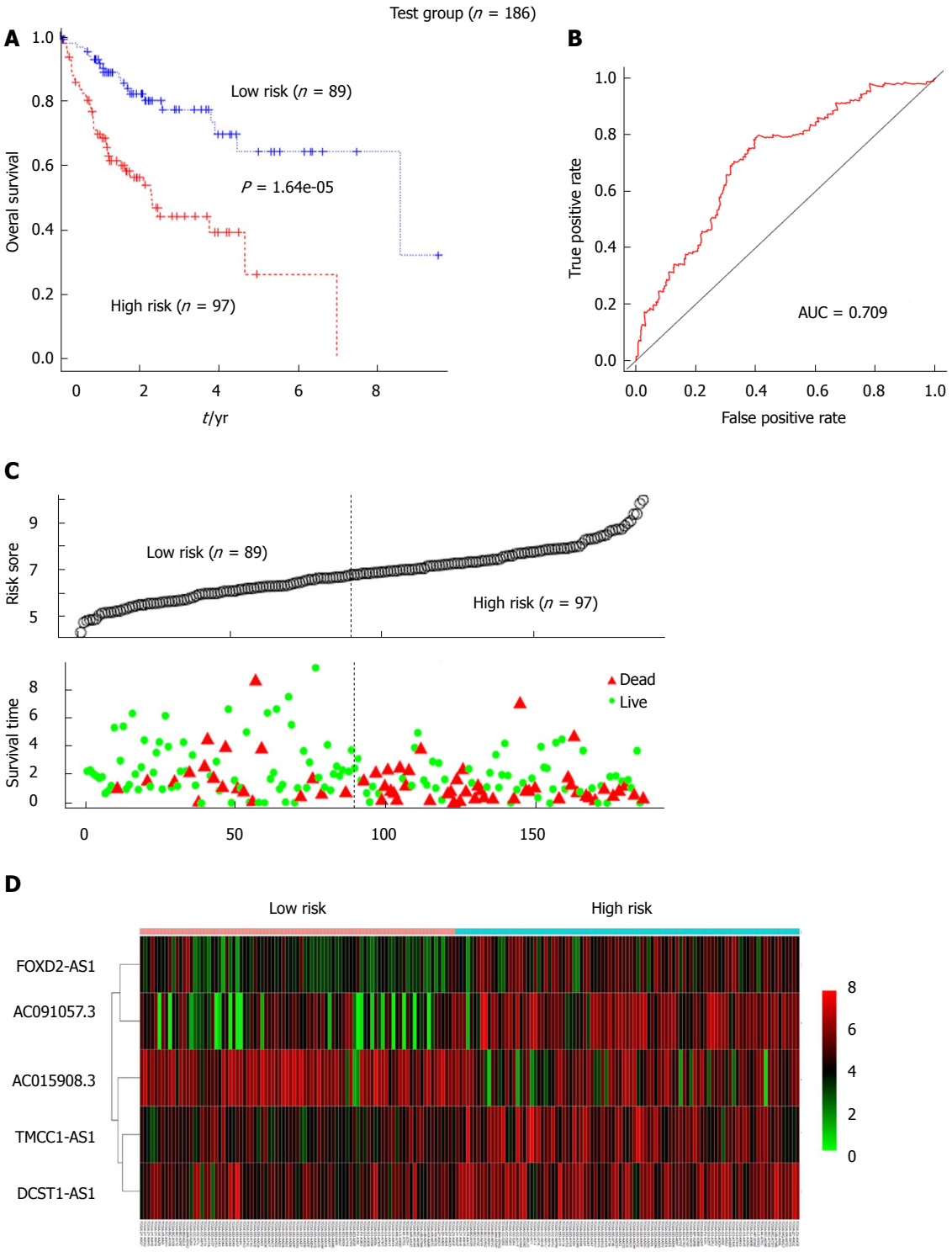

Figure 3 Validation of the prognostic value of the 5-long non-coding RNA signature for the hepatocellular carcinoma patients in the test group. A: Kaplan-Meier analysis indicated that patients in the high-risk (*n* = 97) subgroup exhibited significantly poorer survival than the low-risk subgroup (*n* = 89) in the test group; B: The receiver operating characteristic analysis of the risk score for predicting the overall survival of the test set; C: The 5-long non-coding RNA (lncRNA)-based risk score distribution, patient survival status; D: Heatmap of the 5-lncRNA expression profiles in the high-risk and low-risk subgroups of the test set.

prognoses and a high mortality. Until now, no biomarkers have been shown to effectively predict the survival of HCC patients, and thus, finding effective biomarkers for HCC is crucial.

Previous investigations of gene regulation and disease pathogenesis have mainly focused on protein-coding genes, which account for only a very small proportion (2%) of transcribed genes in eukaryotic species[13]. Recent developments in genome and transcriptome sequencing technologies have profoundly expanded our knowledge of non-coding RNAs, which are much more abundant than canonical protein-coding mRNAs[30,31]. Multiple studies indicate that lncRNAs act not only as intermediaries between DNA and protein but also

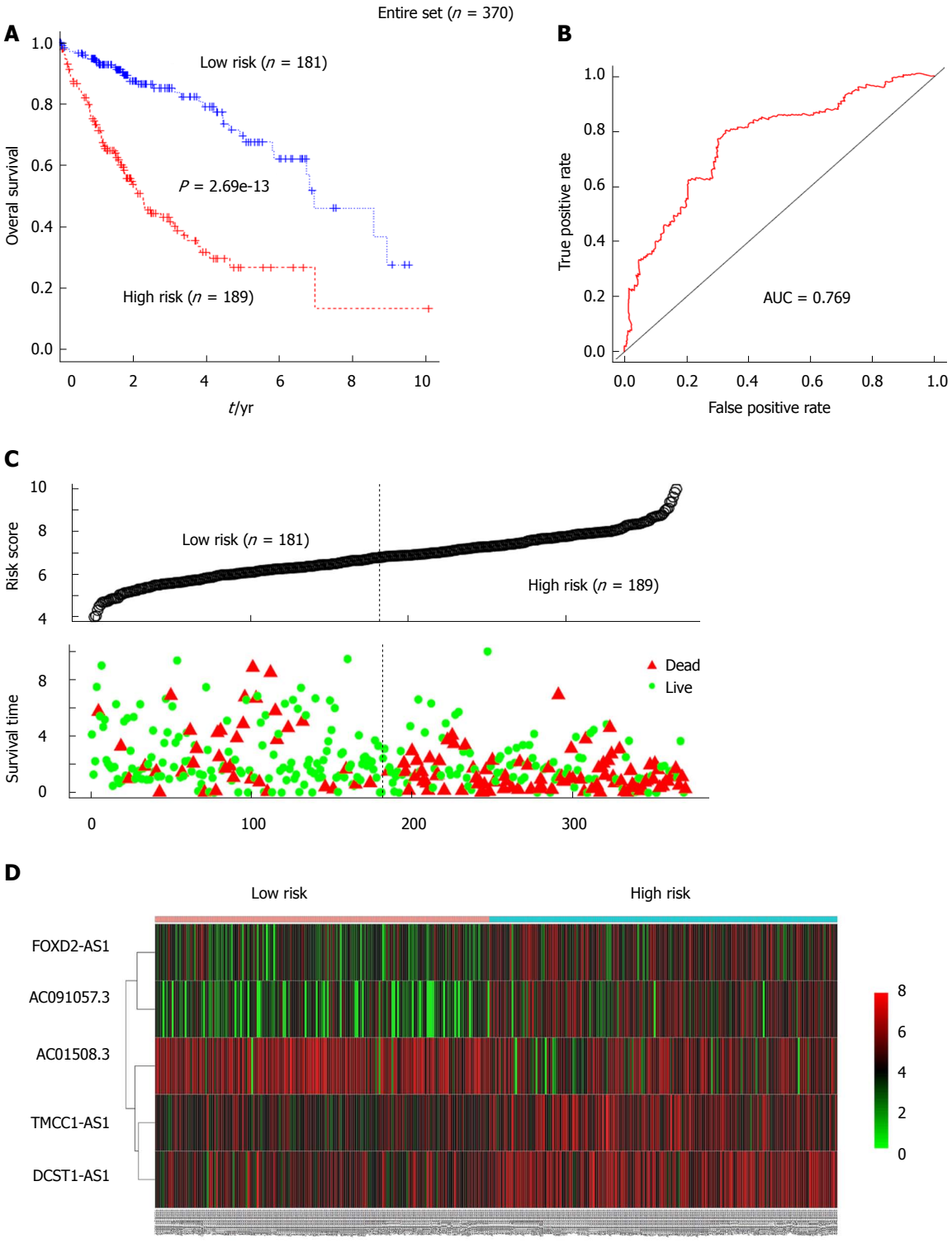

Figure 4 The prognostic value of the 5-long non-coding RNA signature for the hepatocellular carcinoma patients in the entire set (*n* = 370). A: Kaplan-Meier analysis of patients' overall survival in the high-risk (*n* = 189) and low-risk subgroups (*n* = 181) for the entire set; B: The receiver operating characteristic analysis of the risk score for predicting the overall survival of the test set; C: The 5-long non-coding RNA (5-lncRNA)-based risk score distribution, patient survival status; D: Heatmap of the 5-lncRNA expression profiles in the high-risk and low-risk subgroups for the entire set.

as important regulators of diverse cellular functions. lncRNAs have been shown to regulate the expression and function of protein-coding genes at the chromatin, transcriptional and post-transcriptional levels[31]. Many studies have revealed the contribution of lncRNAs in cancer development, indicating their potential as novel biomarkers for cancer diagnosis and prognosis[32-35].

LncRNA signatures for prognostic prediction prognoses have been developed for many cancers including renal cancer, glioblastoma, and colorectal cancer, among others[18-21]. Regarding HCC, the existing gene signatures for survival prediction have focused mostly on mRNAs and microRNAs. Several potential lncRNA biomarkers associated with the progression and

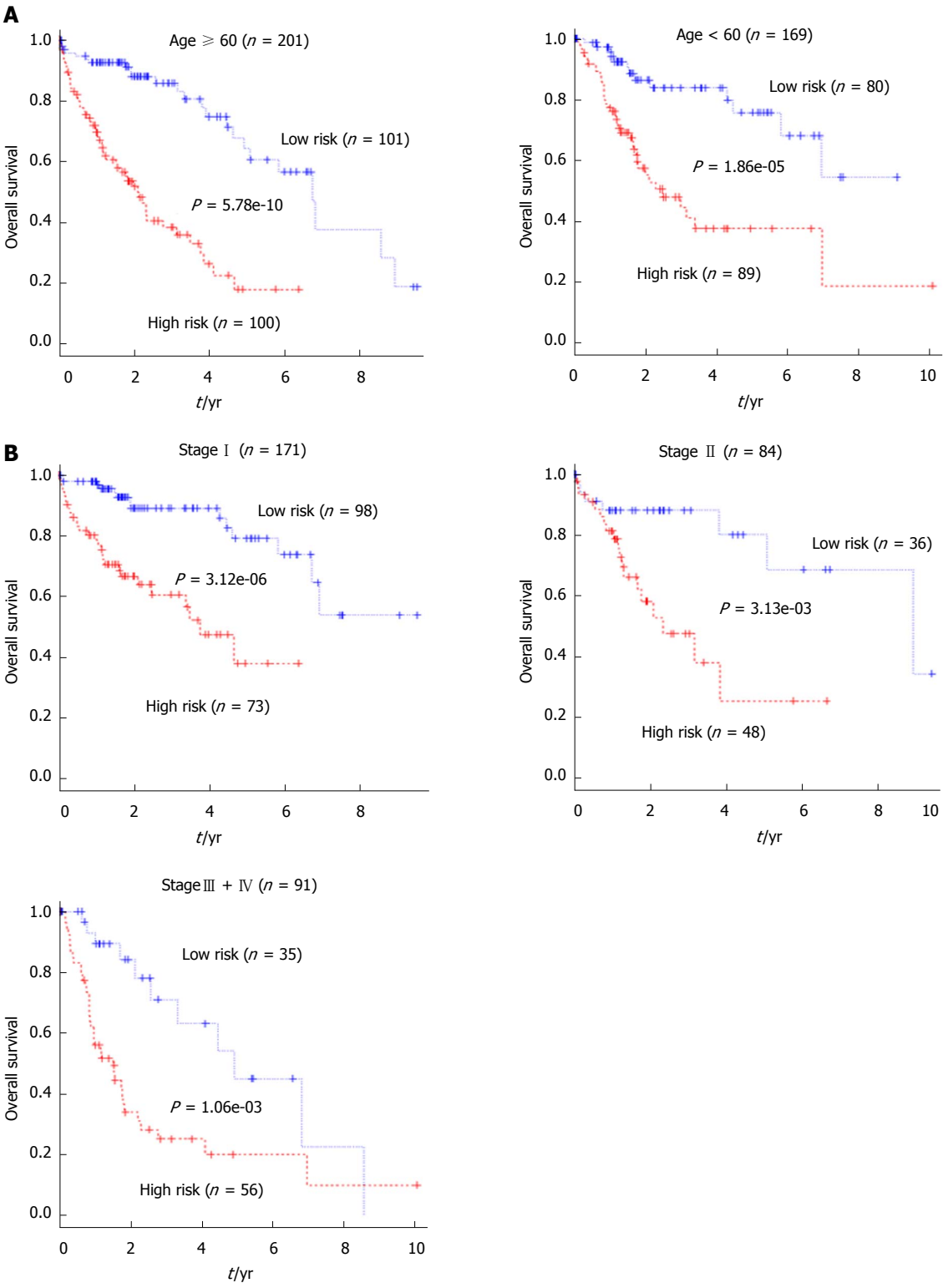

Figure 5 Stratification analyses of the prognostic value of the 5-long non-coding RNA signature-based risk score for all 370 hepatocellular carcinoma patients in the entire set. A: Kaplan-Meier analysis of the overall survival of hepatocellular carcinoma patients < 60 or ⩾ 60 years old; B: Kaplan-Meier analysis of the overall survival of patients with different pathological stages.

prognosis of HCC have been identified, such as TSLNC8, HOXD-AS1 and CACS2[36-38]. These lncRNAs are thought to impact HCC progression through their regulation of tumor cell proliferation, EMT, apoptosis and migration. Although many of these lncRNAs are closely associated with the prognosis and survival of HCC patients, their prognostic value has been tested only in small-scale studies; they have not yet been validated in a large clinical cohort. Until now, relatively few comprehensive lncRNA signatures for the prediction of HCC survival

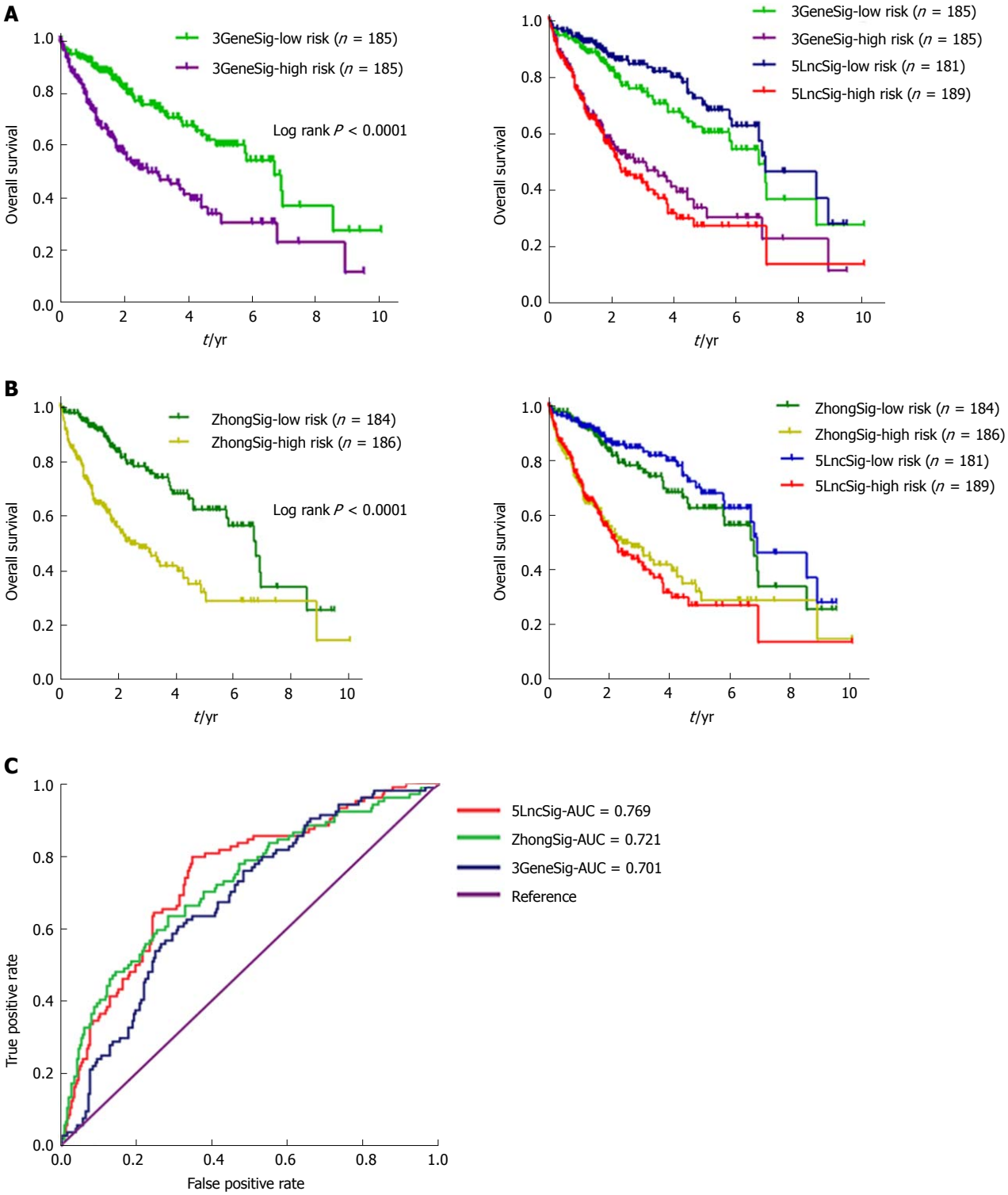

Figure 6 Comparison of the sensitivity and specificity for hepatocellular carcinoma survival prediction by the 5-long non-coding RNA signature and two existing signatures in the entire set. A: Kaplan-Meier analysis of patients' overall survival in the high-risk (*n* = 185) and low-risk (*n* = 185) subgroups based on the 3GeneSig in the entire set (left panel) and comparison of the survival difference based on the 5 long non-coding RNA (lncRNA) signature and the 3GeneSig by Kaplan-Meier analysis (right panel); B: Kaplan-Meier analysis of patients' overall survival in the high-risk (*n* = 186) and low-risk (*n* = 184) subgroups based on the ZhongSig in the entire set (left panel) and comparison of the survival difference based on the 5 lncRNA signature and the ZhongSig (right panel); C: The ROC analysis of overall survival for the 5-lncRNA signature, ZhongSig and 3GeneSig.

have been constructed[26]. TCGA is an open-access database including samples from hundreds of patients with various malignancies. In the present study, we downloaded the RNA sequencing data of the TCGA LIHC cohort and acquired lncRNA expression profiles for HCC patients in the dataset. Using univariate and stepwise multivariate Cox regression analyses, we developed a prognostic formula for HCC based on the expression

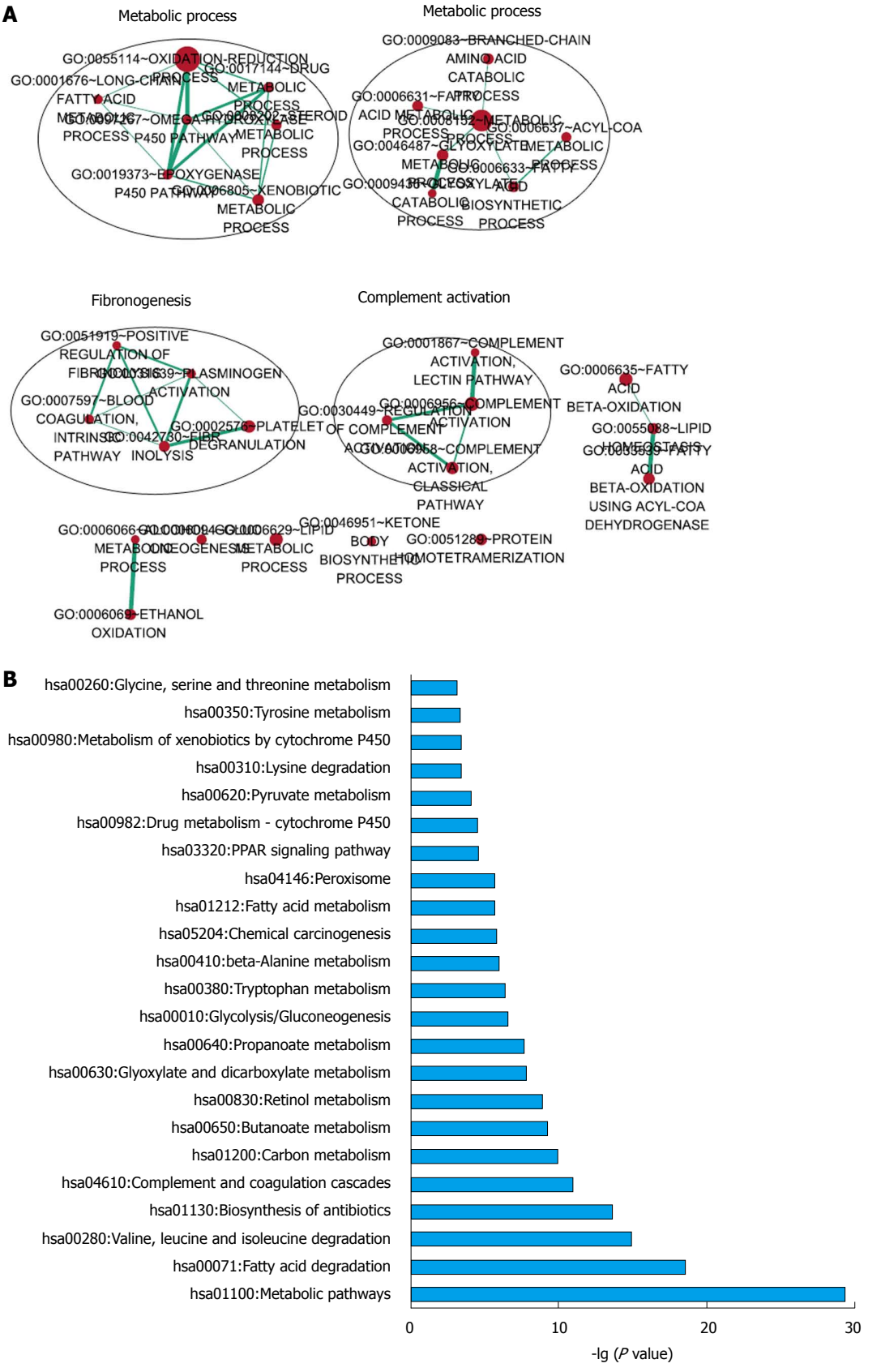

Figure 7 Functional enrichment analysis of the 5-long non-coding RNA based on their correlated protein-coding genes. A: Functional enrichment map of significantly enriched gene ontology terms; B: KEGG pathways significantly associated with the correlated protein-coding genes.

of 5 lncRNAs including AC015908.3, AC091057.3, TMCC1-AS1, DCST1-AS1 and FOXD2-AS1. In the training set, HCC patients with high-risk scores based on the 5-lncRNA signature had a significantly reduced

survival time compared to those with low-risk scores. The prognostic value of the 5-lncRNA signature for HCC patients was further validated in the test group and the entire group, with robust and reproducible predictive indices. The results of these analyses suggest that the prognostic value of the 5-lncRNA-based risk model is robust and reliable for predicting survival in HCC patients.

In the present study, when adjusted using multivariate Cox regression analyses, age (only for the entire set), pathological stage and the 5-lncRNA signature were shown to independently predict the survival of HCC patients. The results of stratification analyses demonstrated that the prognostic value of the 5-lncRNA signature remained significant and robust in HCC subgroups stratified by age and pathological stage. In an attempt to further validate its prognostic value in other HCC cohorts, we downloaded data from several GEO datasets. Unfortunately, most of the 5 lncRNA probes could not be found. There are many existing prognostic signatures for HCC, and we therefore compared our 5-lncRNA signature with two recently developed signatures: a 3-gene signature and a 4-lncRNA signature. The results indicate that the predictive performance of the 5-lncRNA signature was superior to that of the other two signatures for HCC overall survival.

To the best of our knowledge, the functions of these 5 lncRNAs have not been reported. Functional enrichment analysis revealed that the protein-coding genes that were significantly correlated with these 5lncRNAs are enriched for metabolic processes, fibrinolysis and complement activation. KEGG pathway analysis revealed that these genes are enriched in pathways related to metabolism. These results suggest that the 5 lncRNAs may participate in the initiation and progression of HCC through these pathways. However, further studies are needed to investigate and validate the functions of these 5 lncRNAs.

In conclusion, our present study developed a 5-lncRNA signature for predicting the prognosis of HCC patients. The signature was reproducible and robust in a second independent large-scale HCC cohort, supporting its value and effectiveness. In addition, the prognostic value of the 5-lncRNA signature was independent of clinicopathological variables. Our study indicates that the 5-lncRNA signature could improve survival prediction and could be used as a prognostic biomarker for HCC patients.

ARTICLE HIGHLIGHTS

Research background

Hepatocellular carcinoma (HCC) is the sixth most commonly diagnosed cancer in the world. Although treatment for HCC, including surgical resection, has improved over the past decades, its overall survival rate remains devastatingly high due to its high rate of recurrence. Because HCC is a heterogeneous disease with substantially variable clinical outcomes, the search for effective biomarkers to predict recurrence and prognosis is crucial.

Research motivation

Recent studies have demonstrated the importance of long non-coding RNAs (lncRNAs) in physiological and pathological cellular processes. Increasing evidence suggests that lncRNA dysregulation is associated with various human diseases, particularly the initiation and progression of various human cancers. For patients with HCC, most of the existing prognostic signatures have focused on mRNAs or microRNAs, and only a few lncRNA signatures have been developed. In the present study, we aimed to construct a lncRNA signature for the prediction of HCC prognosis with high efficiency.

Research objectives

To construct a lncRNA signature for the prediction of HCC prognosis with high efficiency.

Research methods

Differentially expressed lncRNAs (DELs) between HCC specimens and peritumor liver specimens were acquired from the The Cancer Genome Atlas (TCGA) LIHC dataset using the edgeR package. Univariate Cox proportional hazards regression was performed to identify the DELs that were significantly associated with overall survival for the training set. The stepwise multivariate Cox regression model was applied. Those lncRNAs fitted in the multivariate Cox regression model and independently associated with overall survival were chosen to build a prognostic risk formula. The prognostic value of this formula was validated in the test group and the full cohort and further compared with two previously developed prognostic signatures for HCC.

Research results

We identified a five-lncRNA prognostic signature from the TCGA dataset and determined that its prognostic value was independent from clinicopathological factors. The signature was reproducible and robust in another independent large-scale HCC cohort, supporting its utility and effectiveness.

Research conclusions

This study constructed a 5-lncRNA signature that improves survival prediction, and can be used as a prognostic biomarker for HCC patients.

REFERENCES

1 **Ferlay J**, Soerjomataram I, Dikshit R, Eser S, Mathers C, Rebelo M, Parkin DM, Forman D, Bray F. Cancer incidence and mortality worldwide: sources, methods and major patterns in GLOBOCAN 2012. *Int J Cancer* 2015; **136**: E359-E386 [PMID: 25220842 DOI: 10.1002/ijc.29210]

2 **Torre LA**, Bray F, Siegel RL, Ferlay J, Lortet-Tieulent J, Jemal A. Global cancer statistics, 2012. *CA Cancer J Clin* 2015; **65**: 87-108 [PMID: 25651787 DOI: 10.3322/caac.21262]

3 **Venook AP**, Papandreou C, Furuse J, de Guevara LL. The incidence and epidemiology of hepatocellular carcinoma: a global and regional perspective. *Oncologist* 2010; **15** Suppl 4: 5-13 [PMID: 21115576 DOI: 10.1634/theoncologist.2010-S4-05]

4 **Allemani C**, Weir HK, Carreira H, Harewood R, Spika D, Wang XS, Bannon F, Ahn JV, Johnson CJ, Bonaventure A, Marcos-Gragera R, Stiller C, Azevedo e Silva G, Chen WQ, Ogunbiyi OJ, Rachet B, Soeberg MJ, You H, Matsuda T, Bielska-Lasota M, Storm H, Tucker TC, Coleman MP; CONCORD Working Group. Global surveillance of cancer survival 1995-2009: analysis of individual data for 25,676,887 patients from 279 population-based registries in 67 countries (CONCORD-2). *Lancet* 2015; **385**: 977-1010 [PMID: 25467588 DOI: 10.1016/S0140-6736(14)62038-9]

5 **Mittal S**, El-Serag HB. Epidemiology of hepatocellular carcinoma: consider the population. *J Clin Gastroenterol* 2013; **47** Suppl: S2-S6 [PMID: 23632345 DOI: 10.1097/MCG.0b013e3182872f29]

6 **El-Serag HB**, Rudolph KL. Hepatocellular carcinoma: epidemiology and molecular carcinogenesis. *Gastroenterology* 2007; **132**: 2557-2576 [PMID: 17570226 DOI: 10.1053/j.gastro.2007.04.061]

7 **Joliat GR**, Allemann P, Labgaa I, Demartines N, Halkic N.

Treatment and outcomes of recurrent hepatocellular carcinomas. *Langenbecks Arch Surg* 2017; **402**: 737-744 [PMID: 28497194 DOI: 10.1007/s00423-017-1582-9]
8 **Bruix J**, Gores GJ, Mazzaferro V. Hepatocellular carcinoma: clinical frontiers and perspectives. *Gut* 2014; **63**: 844-855 [PMID: 24531850 DOI: 10.1136/gutjnl-2013-306627]
9 **Zheng J**, Kuk D, Gönen M, Balachandran VP, Kingham TP, Allen PJ, D'Angelica MI, Jarnagin WR, DeMatteo RP. Actual 10-Year Survivors After Resection of Hepatocellular Carcinoma. *Ann Surg Oncol* 2017; **24**: 1358-1366 [PMID: 27921192 DOI: 10.1245/s10434-016-5713-2]
10 **Kudo M**. Surveillance, diagnosis, treatment, and outcome of liver cancer in Japan. *Liver Cancer* 2015; **4**: 39-50 [PMID: 26020028 DOI: 10.1159/000367727]
11 **Bruix J**, Sherman M; American Association for the Study of Liver Diseases. Management of hepatocellular carcinoma: an update. *Hepatology* 2011; **53**: 1020-1022 [PMID: 21374666 DOI: 10.1002/hep.24199]
12 **Schmitt AM**, Chang HY. Long Noncoding RNAs: At the Intersection of Cancer and Chromatin Biology. *Cold Spring Harb Perspect Med* 2017; **7**: [PMID: 28193769 DOI: 10.1101/cshperspect.a026492]
13 **Hangauer MJ**, Vaughn IW, McManus MT. Pervasive transcription of the human genome produces thousands of previously unidentified long intergenic noncoding RNAs. *PLoS Genet* 2013; **9**: e1003569 [PMID: 23818866 DOI: 10.1371/journal.pgen.1003569]
14 **Mercer TR**, Dinger ME, Mattick JS. Long non-coding RNAs: insights into functions. *Nat Rev Genet* 2009; **10**: 155-159 [PMID: 19188922 DOI: 10.1038/nrg2521]
15 **Moran VA**, Perera RJ, Khalil AM. Emerging functional and mechanistic paradigms of mammalian long non-coding RNAs. *Nucleic Acids Res* 2012; **40**: 6391-6400 [PMID: 22492512 DOI: 10.1093/nar/gks296]
16 **Hauptman N**, Glavač D. Long non-coding RNA in cancer. *Int J Mol Sci* 2013; **14**: 4655-4669 [PMID: 23443164 DOI: 10.3390/ijms14034655]
17 **Gibb EA**, Brown CJ, Lam WL. The functional role of long non-coding RNA in human carcinomas. *Mol Cancer* 2011; **10**: 38 [PMID: 21489289 DOI: 10.1186/1476-4598-10-38]
18 **Shi D**, Qu Q, Chang Q, Wang Y, Gui Y, Dong D. A five-long non-coding RNA signature to improve prognosis prediction of clear cell renal cell carcinoma. *Oncotarget* 2017; **8**: 58699-58708 [PMID: 28938589 DOI: 10.18632/oncotarget.17506]
19 **Zhou M**, Zhang Z, Zhao H, Bao S, Cheng L, Sun J. An Immune-Related Six-lncRNA Signature to Improve Prognosis Prediction of Glioblastoma Multiforme. *Mol Neurobiol* 2018; **55**: 3684-3697 [PMID: 28527107 DOI: 10.1007/s12035-017-0572-9]
20 **Zeng JH**, Liang L, He RQ, Tang RX, Cai XY, Chen JQ, Luo DZ, Chen G. Comprehensive investigation of a novel differentially expressed lncRNA expression profile signature to assess the survival of patients with colorectal adenocarcinoma. *Oncotarget* 2017; **8**: 16811-16828 [PMID: 28187432 DOI: 10.18632/oncotarget.15161]
21 **Sun J**, Cheng L, Shi H, Zhang Z, Zhao H, Wang Z, Zhou M. A potential panel of six-long non-coding RNA signature to improve survival prediction of diffuse large-B-cell lymphoma. *Sci Rep* 2016; **6**: 27842 [PMID: 27292966 DOI: 10.1038/srep27842]
22 **Lin Z**, Xu SH, Wang HQ, Cai YJ, Ying L, Song M, Wang YQ, Du SJ, Shi KQ, Zhou MT. Prognostic value of DNA repair based stratification of hepatocellular carcinoma. *Sci Rep* 2016; **6**: 25999 [PMID: 27174663 DOI: 10.1038/srep25999]
23 **Lu M**, Kong X, Wang H, Huang G, Ye C, He Z. A novel microRNAs expression signature for hepatocellular carcinoma diagnosis and prognosis. *Oncotarget* 2017; **8**: 8775-8784 [PMID: 28060739 DOI: 10.18632/oncotarget.14452]
24 **Borel F**, Konstantinova P, Jansen PL. Diagnostic and therapeutic potential of miRNA signatures in patients with hepatocellular carcinoma. *J Hepatol* 2012; **56**: 1371-1383 [PMID: 22314424 DOI: 10.1016/j.jhep.2011.11.026]
25 **Li B**, Feng W, Luo O, Xu T, Cao Y, Wu H, Yu D, Ding Y. Development and Validation of a Three-gene Prognostic Signature for Patients with Hepatocellular Carcinoma. *Sci Rep* 2017; **7**: 5517 [PMID: 28717245 DOI: 10.1038/s41598-017-04811-5]
26 **Wang Z**, Wu Q, Feng S, Zhao Y, Tao C. Identification of four prognostic LncRNAs for survival prediction of patients with hepatocellular carcinoma. *PeerJ* 2017; **5**: e3575 [PMID: 28729955 DOI: 10.7717/peerj.3575]
27 **Huang da W**, Sherman BT, Lempicki RA. Bioinformatics enrichment tools: paths toward the comprehensive functional analysis of large gene lists. *Nucleic Acids Res* 2009; **37**: 1-13 [PMID: 19033363 DOI: 10.1093/nar/gkn923]
28 **Huang da W**, Sherman BT, Lempicki RA. Systematic and integrative analysis of large gene lists using DAVID bioinformatics resources. *Nat Protoc* 2009; **4**: 44-57 [PMID: 19131956 DOI: 10.1038/nprot.2008.211]
29 **Merico D**, Isserlin R, Stueker O, Emili A, Bader GD. Enrichment map: a network-based method for gene-set enrichment visualization and interpretation. *PLoS One* 2010; **5**: e13984 [PMID: 21085593 DOI: 10.1371/journal.pone.0013984]
30 **Chen JA**, Conn S. Canonical mRNA is the exception, rather than the rule. *Genome Biol* 2017; **18**: 133 [PMID: 28687088 DOI: 10.1186/s13059-017-1268-1]
31 **Shi X**, Sun M, Liu H, Yao Y, Song Y. Long non-coding RNAs: a new frontier in the study of human diseases. *Cancer Lett* 2013; **339**: 159-166 [PMID: 23791884 DOI: 10.1016/j.canlet.2013.06.013]
32 **Bi M**, Yu H, Huang B, Tang C. Long non-coding RNA PCAT-1 over-expression promotes proliferation and metastasis in gastric cancer cells through regulating CDKN1A. *Gene* 2017; **626**: 337-343 [PMID: 28571676 DOI: 10.1016/j.gene.2017.05.049]
33 **Hua F**, Liu S, Zhu L, Ma N, Jiang S, Yang J. Highly expressed long non-coding RNA NNT-AS1 promotes cell proliferation and invasion through Wnt/β-catenin signaling pathway in cervical cancer. *Biomed Pharmacother* 2017; **92**: 1128-1134 [PMID: 28628975 DOI: 10.1016/j.biopha.2017.03.057]
34 **Xu S**, Kong D, Chen Q, Ping Y, Pang D. Oncogenic long noncoding RNA landscape in breast cancer. *Mol Cancer* 2017; **16**: 129 [PMID: 28738804 DOI: 10.1186/s12943-017-0696-6]
35 **Spurlock CF 3rd**, Shaginurova G, Tossberg JT, Hester JD, Chapman N, Guo Y, Crooke PS 3rd, Aune TM. Profiles of Long Noncoding RNAs in Human Naive and Memory T Cells. *J Immunol* 2017; **199**: 547-558 [PMID: 28600289 DOI: 10.4049/jimmunol.1700232]
36 **Zhang J**, Li Z, Liu L, Wang Q, Li S, Chen D, Hu Z, Yu T, Ding J, Li J, Yao M, Huang S, Zhao Y, He X. Long noncoding RNA TSLNC8 is a tumor suppressor that inactivates the interleukin-6/STAT3 signaling pathway. *Hepatology* 2018; **67**: 171-187 [PMID: 28746790 DOI: 10.1002/hep.29405]
37 **Lu S**, Zhou J, Sun Y, Li N, Miao M, Jiao B, Chen H. The noncoding RNA HOXD-AS1 is a critical regulator of the metastasis and apoptosis phenotype in human hepatocellular carcinoma. *Mol Cancer* 2017; **16**: 125 [PMID: 28724429 DOI: 10.1186/s12943-017-0676-x]
38 **Wang Y**, Liu Z, Yao B, Li Q, Wang L, Wang C, Dou C, Xu M, Liu Q, Tu K. Long non-coding RNA CASC2 suppresses epithelial-mesenchymal transition of hepatocellular carcinoma cells through CASC2/miR-367/FBXW7 axis. *Mol Cancer* 2017; **16**: 123 [PMID: 28716020 DOI: 10.1186/s12943-017-0702-z]

P- Reviewer: Namisaki T, Tsui SK **S- Editor**: Wang JL
L- Editor: Filipodia **E- Editor**: Huang Y

World Journal of Gastroenterology

Submit a Manuscript: http://www.f6publishing.com

World J Gastroenterol 2018 August 14; 24(30): 3440-3447

DOI: 10.3748/wjg.v24.i30.3440

ISSN 1007-9327 (print) ISSN 2219-2840 (online)

ORIGINAL ARTICLE

Retrospective Study

Application of modified primary closure of the pelvic floor in laparoscopic extralevator abdominal perineal excision for low rectal cancer

Yan-Lei Wang, Xiang Zhang, Jia-Jia Mao, Wen-Qiang Zhang, Hao Dong, Fan-Pei Zhang, Shuo-Hui Dong, Wen-Jie Zhang, Yong Dai

Yan-Lei Wang, Xiang Zhang, Jia-Jia Mao, Wen-Qiang Zhang, Hao Dong, Fan-Pei Zhang, Shuo-Hui Dong, Wen-Jie Zhang, Yong Dai, Department of Colorectal and Anal Surgery, Qilu Hospital of Shandong University, Jinan 250012, Shandong Province, China

ORCID number: Yan-Lei Wang (0000-0003-1420-9529); Xiang Zhang (0000-0001-7417-6082); Jia-Jia Mao (0000-0002-2210-8456); Wen-Qiang Zhang (0000-0003-1162-2350); Hao Dong (0000-0002-7185-9002); Fan-Pei Zhang (0000-0001-9276-8436); Shuo-Hui Dong (0000-0002-2912-8046); Wen-Jie Zhang (0000-0003-1976-1523); Yong Dai (0000-0001-6163-8022).

Author contributions: Wang YL and Dai Y designed the study; Wang YL, Zhang X and Dai Y performed the surgery; Mao JJ performed subject follow up and control subject data collection; Zhang WQ and Dong SH performed the statistical analysis; Zhang X, Zhang FP, Dong H and Zhang WJ wrote the manuscript; Wang YL, Zhang X, Mao JJ, Zhang WQ, Dong H, Zhang FP, Dong SH, Zhang WJ, Dai Y revised the manuscript for final submission.

Supported by the National Key and Development Program of China, No. 2016YFC0106003; the National Natural Science Foundation of China, No. 81700708/H0712; and the Key and Development Program of Shandong Province, No. 2016GSF201125.

Institutional review board statement: This study was approved by the Ethics Committee of Scientific Research of Shandong University Qilu Hospital.

Conflict-of-interest statement: The authors declare that there are no conflicts of interest related to this study.

Data sharing statement: No additional data are available.

Manuscript source: Unsolicited manuscript

Correspondence to: Yong Dai, MD, PhD, Attending Doctor, Chief Doctor, Surgeon, Department of Colorectal and Anal Surgery, Qilu Hospital of Shandong University, No. 107 West Wenhua Road, Jinan 250012, Shandong Province, China. yongdai@hotmail.com
Telephone: +86-531-82166391

Received: May 31, 2018
Peer-review started: May 31, 2018
First decision: June 15, 2018
Revised: June 18, 2018
Accepted: June 30, 2018
Article in press: June 30, 2018
Published online: August 14, 2018

Abstract

AIM

To introduce a novel, modified primary closure technique of laparoscopic extralevator abdominal perineal excision (LELAPE) for low rectal cancer.

METHODS

We retrospectively analyzed data from 76 patients with rectal cancer who underwent LELAPE from March 2013 to May 2016. Patients were classified into the modified primary closure group (32 patients) and the biological mesh closure group (44 patients). The total operating time, reconstruction time, postoperative stay duration, total cost, postoperative complications and tumor recur-

rence were compared.

RESULTS

All surgery was successfully performed. The pelvic reconstruction time was 14.6 ± 3.7 min for the modified primary closure group, which was significantly longer than that of the biological mesh closure group (7.2 ± 1.9 min, $P < 0.001$). The total operating time was not different between the two groups (236 ± 20 min *vs* 248 ± 43 min, $P = 0.143$). The postoperative hospital stay duration was 8.1 ± 1.9 d, and the total cost was 9297 ± 1260 USD for the modified primary closure group. Notably, both of these categories were significantly lower in this group than those of the biological mesh closure group ($P = 0.001$ and $P = 0.003$, respectively). There were no differences observed between groups when comparing other perioperative data, long-term complications or oncological outcomes.

CONCLUSION

The modified primary closure method for reconstruction of the pelvic floor in LELAPE for low rectal cancer is technically feasible, safe and cost-effective.

Key words: Extralevator abdominoperineal excision; Rectal cancer; Pelvic floor; Laparoscopy

Core tip: The modified primary closure approach requires laparoscopic closure of the pelvic peritoneum and layered closure of the perineal defect. By using this modified approach, the length of hospital stay and the total cost were decreased significantly, while other clinical outcomes did not differ, except for a relatively longer time for pelvic reconstruction (14.6 ± 3.7 min *vs* 7.2 ± 1.9 min). We conclude that the modified primary closure method for reconstruction of the pelvic floor in laparoscopic extralevator abdominal perineal excision for low rectal cancer is technically feasible, safe and cost-effective.

Wang YL, Zhang X, Mao JJ, Zhang WQ, Dong H, Zhang FP, Dong SH, Zhang WJ, Dai Y. Application of modified primary closure of the pelvic floor in laparoscopic extralevator abdominal perineal excision for low rectal cancer. *World J Gastroenterol* 2018; 24(30): 3440-3447 Available from: URL: http://www.wjgnet.com/1007-9327/full/v24/i30/3440.htm DOI: http://dx.doi.org/10.3748/wjg.v24.i30.3440

INTRODUCTION

To improve the oncological outcome of patients with low rectal cancer, extralevator abdominal perineal excision (ELAPE) has been introduced to reduce the rate of positive circumferential margin and intraoperative perforation[1-4]. Assisted by laparoscopy, ELAPE can minimize physical invasion while ensuring oncological benefits[5,6]. However, the extended resection of ELAPE may increase the risk of severe perineal wound complications, including perineal hernia, with a reported incidence of 20%-26%[7]. Thus, how to reconstruct the pelvic floor and close the perineum after massive resection has become a major concern and challenge in laparoscopic ELAPE (LELAPE). The established reconstruction methods include: primary perineal closure, omentoplasty, biological or synthetic mesh placement, myocutaneous flaps, and negative wound pressure therapy[8-12]. These methods all have their own advantages as well as restrictions, and no consensus has been reached so far. In traditional abdominoperineal resection (APR), the pelvic peritoneum is usually closed prior to reconstruction of the pelvic floor, in order to separate the small intestine from the presacral operating field, which is technically challenging in LELAPE. We have recently modified the primary closure technique by adding the laparoscopic pelvic peritoneum suture procedure, and applied it to LELAPE. In the present study, we compare this method with biological mesh closure in the reconstruction of the pelvic floor after LELAPE, and evaluate its feasibility, safety and cost-effectiveness.

MATERIALS AND METHODS

Study design

We retrospectively analyzed the data from 76 patients with rectal cancer undergoing LELAPE from March 2013 to May 2016. Patients were classified into the modified primary closure group (32 patients) and the biological mesh closure group (44 patients). Total operating time, reconstruction time, postoperative stay duration, total cost, postoperative complications and tumor recurrence were compared. The protocol was approved by the Ethics Committee of Qilu Hospital, Shandong University, Jinan, China.

General procedure

We have described the LELAPE procedure in a previous report[13]. The abdominal procedure was performed with the patient being placed in the Trendelenburg position, and the port placement was set up as shown in Figure 1A. After laparoscopic exploration, dissection and division of the pedicle of the inferior mesenteric vessels were performed. The sigmoid colon was mobilized from medial to lateral, and the rectum was mobilized following the total mesorectal excision principle. The sigmoid mesentery was trimmed at the rectosigmoid junction, where the rectum was transected with an endoscopic linear stapler (Figure 1B). The distal rectum and mesorectum were pushed down to the pelvic cavity (Figure 1C).

Modified primary closure

For modified primary closure, the pelvic peritoneum was closed with continuous suturing using a barbed suture (Covidien, Shanghai, China) (Figure 1D and E) before

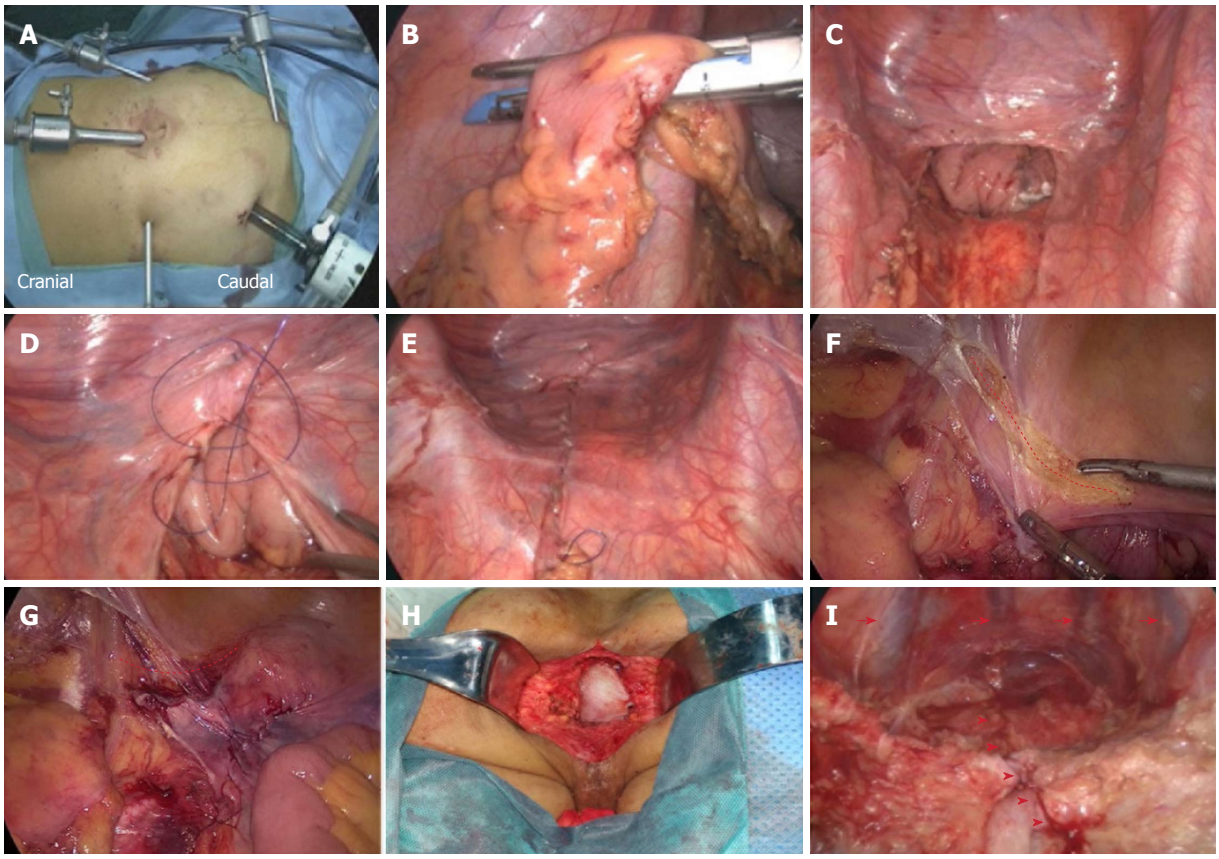

Figure 1 Surgical procedures. A: Port placement; B: Transection of the rectum at the rectosigmoid junction with an ENDO-GIA; C: Distal rectum pushed down to the pelvis; D: Closure of the pelvic peritoneum with a continuous suture using a barbed thread; E: Closure of the pelvic peritoneum; F: Tension reduction of the adjacent peritoneum (the dotted line shows the incised peritoneum); G: Closure of the peritoneum after tension reduction (the dotted line shows the incised peritoneum); H: Reconstruction of the pelvic floor with biological mesh; I: View of the closed peritoneum from the perineal wound in the prone position (the arrows show the presacral veins, and the arrowheads show the closed peritoneum).

creation of a colostomy. For tension-free suturing, the adjacent pelvic peritoneum was dissected to reduce tension if necessary (Figure 1F and G). The patient was turned over to the prone jackknife position. The levator ani was transected at its origin, and a cylindrical specimen was removed. The procedure was completed with both the placement of one negative-pressure drainage tube in the presacral space, and the layered closure of the ischiorectal fat and skin. The drainage tube was removed when the drainage fluid was clear and < 10 mL in volume. The coccyx was not routinely removed.

Biological mesh closure

For biological mesh closure, the patient was changed into a prone position for perineal dissection after creation of a colostomy. The levator ani was transected at its origin, and a cylindrical specimen was removed. A human acellular dermal matrix mesh (Ruinuo, Qingyuanweiye Bio-Tissue Engineering Ltd., Beijing, China) was implanted and fixed to the tendinous arch by continuous prolene sutures (Covidien) for reconstruction of the pelvic floor (Figure 1H). The procedure was completed with both the placement of one negative-pressure drainage tube below the mesh, and the layered closure of the ischiorectal fat and skin. All the operations were finished by the same surgical group.

Statistical analysis

Numerical data were expressed as mean ± SD and analyzed with Student's *t* tests. Categorical data were analyzed with the χ test or Fisher's exact test. Repeated measures analysis of variance was performed for postoperative drainage and temperature change. All analyses were performed using SPSS 19.0 (SPSS Inc., Chicago, IL, United States). $P < 0.05$ was considered to be statistically significant.

RESULTS

The baseline characteristics, including male/female ratio, age, body mass index, neoadjuvant therapy, distance to anal verge, and postoperative TNM staging, were comparable between the two groups ($P > 0.05$ each, Table 1). All patients were successfully followed up postoperatively for one year.

All operations were successfully performed without serious intraoperative complications. The pelvic reconstruction time was 14.6 ± 3.7 min for the modified primary closure group, which was significantly longer than that of the biological mesh closure group (7.2 ±

Table 1 Baseline characteristics.

	Modified primary closure (n = 32)	Biological mesh closure (n = 44)	P value
Male/female	24/8	31/13	0.662
Age (yr)	52.8 ± 12.2	58.2 ± 12.5	0.137
BMI	26.8 ± 3.2	25.7 ± 2.7	0.097
Neoadjuvant therapy	8	7	0.326
Tumor location, Distance to anal verge (cm)	2.6 ± 0.8	2.8 ± 0.9	0.278
Postoperative TNM staging			
Ⅱ	23	29	0.581
Ⅲ	9	15	

BMI: Body mass index.

Table 2 Perioperative data.

	Modified primary closure (n = 32)	Biological mesh closure (n = 44)	P value
Reconstruction time (min)	14.6 ± 3.7	7.2 ± 1.9	< 0.001
Total operative time (min)	236 ± 20	248 ± 43	0.143
Intraoperative blood loss (mL)	165 ± 57	149 ± 52	0.242
Positive CRM	0	0	N/A
Bowel perforation	0	1	1.000
Recovery of bowel function (h)	22.8 ± 4.7	23.6 ± 5.0	0.475
Intestinal obstruction	0	1	1.000
Drainage removal (days after surgery)	6.6± 1.1	7.3 ± 2.0	0.094
Postoperative hospital stay (d)	8.1 ± 1.9	10.1 ± 2.8	0.001
Cost (USD)	9297 ± 1260	10719 ± 2360	0.003

CRM: Circumferential margin; USD: United States Dollar.

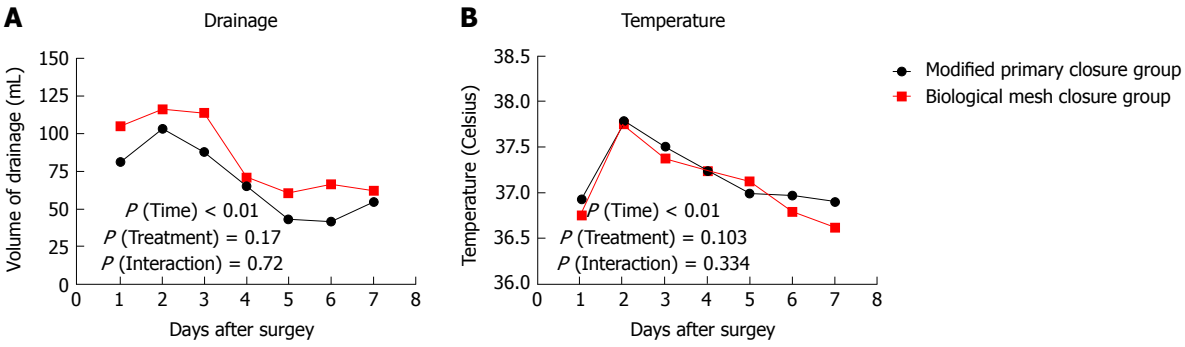

Figure 2 Drainage and temperature changes. A: Postoperative drainage volumes in the two groups; B: Postoperative temperature changes in the two groups.

1.9 min, P < 0.001). The total operating time did not differ between the two groups (236 ± 20 min *vs* 248 ± 43 min, P = 0.143). One patient in the biological mesh closure group developed bowel perforation due to a large tumor within the anterior wall of the rectum. No positive circumferential margin was observed in either group. Intraoperative blood loss and recovery of bowel function were comparable between the two groups (both P > 0.05) (Table 2). The drainage tube was removed postoperatively at 6.6 ± 1.1 d in the modified primary closure group, which was earlier than in the biological mesh closure group (7.3 ± 2.0 d, P = 0.094). The volume of drainage fluid peaked at 2 d postoperatively and then decreased gradually, without any difference between the two groups (P treatment > 0.05, P interaction > 0.05) (Figure 2A). The temperature changes after operation showed a similar pattern to drainage volume, with no difference between the groups (P treatment > 0.05, P interaction > 0.05) (Figure 2B). Postoperative hospital stay was 8.1 ± 1.9 d, and the total cost was 9297 ± 1260 USD for the modified primary closure group. Both of these categories in this group were significantly less than those of the biological mesh closure group (P = 0.001 and P = 0.003, respectively) (Table 2). One patient in the biological mesh closure group developed postoperative intestinal obstruction at 40 d. Conservative therapy did not work, and a laparoscopic exploration was performed at 42 d. The middle part of the ileum, approximately 100 cm to the ileocecal junction, adhered to the pelvic floor, leading to dilation of the proximal small intestine

Table 3 Follow-up data

	Modified primary closure (n = 32)	Biological mesh closure (n = 44)	P value
Normal perineal wound healing[1]			
10 d postoperatively	29	39	0.546
30 d postoperatively	27	41	0.270
60 d postoperatively	32	44	1.000
Perineal wound infection	5	5	0.734
Clear or haemoserous discharge	3	1	0.304
Pus/purulent discharge	1	2	1.000
Deep infection with or without tissue breakdown	1	2	1.000
Postoperative perineal hernia (12 mo)	0	0	N/A
Postoperative feeling of bulge (12 mo)	4	2	0.233
Postoperative chemotherapy	23	28	0.330
Postoperative radiotherapy	7	14	0.339
Postoperative local recurrence (12 mo)	0	1	1
Postoperative liver/lung metastasis (12 mo)	2	3	1
Postoperative death (12 mo)	0	0	N/A

[1]Grade 0 or Grade I by the Southampton Wound Scoring System.

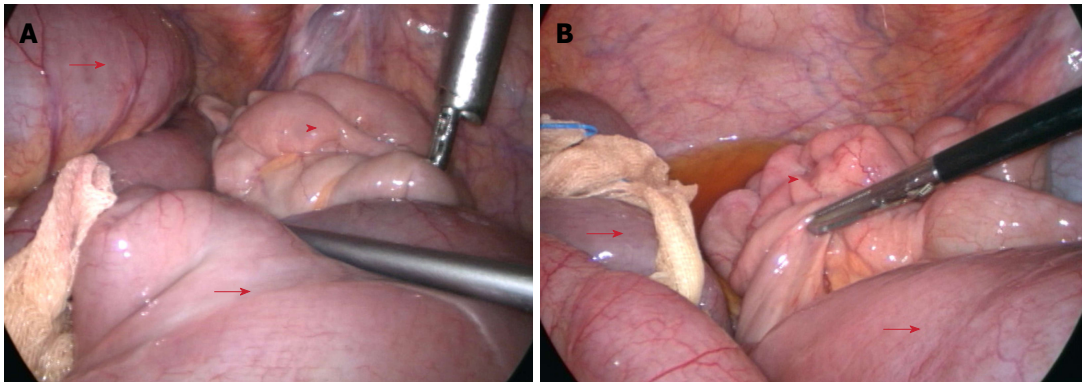

Figure 3 Laparoscopy. Laparoscopic exploration of the abdominal cavity in the patient with intestinal obstruction (the arrow shows the proximal dilated small intestine, and the arrowhead shows the distal normal small intestine).

(Figure 3). The patient was healed by decompression of the small intestine and intestinal rearrangement under laparotomy.

In the modified primary closure group, five patients had perineal wound infection. Within the first 10 d postoperatively, three patients had haemoserous discharge from the perineal wound, and were healed following potassium permanganate hip bath after 1 mo. At 12 d, one patient showed purulent discharge, which was solved after daily dressing change and thermal therapy. At 15 d, the perineal wound broke down in one female patient with type 2 diabetes. Debridement and secondary suturing were performed at 33 d after daily dressing change. Likewise, in the biological mesh closure group, five patients had perineal wound infection within the first 10 d (Table 3), and recovered within 60 d after appropriate treatment. No difference in infection rate or grade was found between the two groups (P > 0.05 each). Perineal hernia is theoretically expected to be more frequent without the placement of meshes. However, at 12 mo postoperatively, no perineal hernia occurred in either of the groups. Notably, four patients in the modified primary closure group and two in the biological mesh group experienced the feeling of bulging. Computed tomography at 12 mo showed that in the modified primary closure group, the small intestine was kept in the pelvic cavity with a clear descent of the pelvic peritoneum. In the biological mesh group, without suturing the pelvic peritoneum, the small intestine was also kept in the presacral space. No obvious postoperative differences were detected in the computed tomography scans between the two groups at 12 mo (Figure 4).

Postoperative chemotherapy (the XELOX or FOLFOX regimen) and radiotherapy were given to 23 and seven patients in the modified primary closure group, as well as 28 and 14 patients in the biological mesh closure group, respectively (P = 0.330 and P = 0.339). In the biological mesh closure group, local recurrence occurred in one patient, who received only postoperative chemotherapy with the XELOX regimen, and the patient was subsequently treated with radiotherapy. Three patients had minor liver metastases and were cured with local ablative treatment. In the modified primary closure group, minor lung metastasis and minor liver metastases were found in two patients, respectively. Both of these

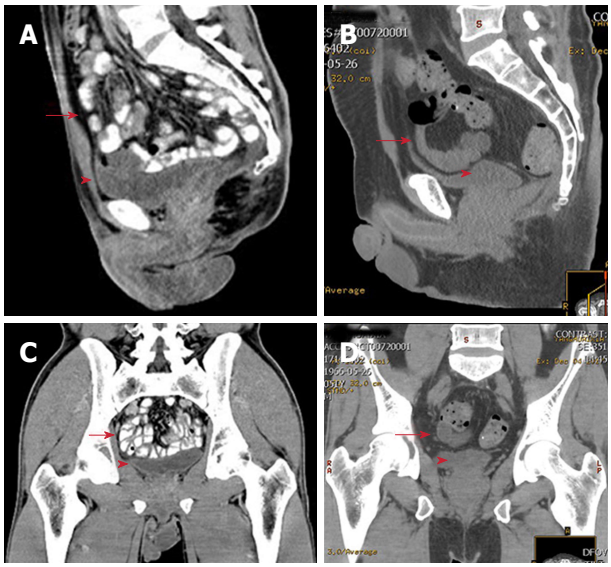

Figure 4 Postoperative magnetic resonance imaging. A: Twelve-month postoperative Sagittal CT scan in the modified primary closure group; B: Twelve-month postoperative Sagittal CT scan in the biological mesh closure group; C: Twelve-month postoperative Coronal CT scan in the modified primary closure group; D: Twelve-month postoperative Coronal CT scan in the biological mesh closure group (the arrow shows the small intestine, and the arrowhead shows the bladder). CT: Computed tomography.

patients received local ablative treatment. No patients died in either of the two groups.

DISCUSSION

The necessity of reconstruction of the pelvic floor after ELAPE has been widely accepted in order to avoid postoperative perineal complications[14,15]. However, the feasibility and superiority of various methods proposed for this reconstruction remain to be investigated. In the present study, we compared two methods, modified primary closure and biological mesh closure, in 76 patients with lower rectal cancer undergoing LELAPE. The major findings were that modified primary closure required longer reconstruction time, shorter postoperative hospital stay and was more cost-effective when compared to biological mesh closure. No difference in other perioperative data, long-term complications or oncological outcomes was observed.

Various methods have been developed for perineal wound healing after ELAPE. Of these, perineal closure with myocutaneous flaps, biological or synthetic mesh placement, and omentoplasty with perineal closure are currently the most widely performed[8-12]. Myocutaneous flaps can be obtained by various approaches, including gluteal rotation/advancement flaps[16], inferior gluteal artery myocutaneous island transposition flaps (IGAM)[17], transverse rectus/vertical rectus abdominis (TRAM/VRAM)[18,19], and gracilis[20]. Myocutaneous flaps have the benefit of delivering good perfusion and oxygenation, thus facilitating the healing process of large perineal defects. However, this approach requires plastic surgeons and may cause additional complications (*e.g.*, a donor site hernia)[14]. Mesh repair has the advantage of reducing operative duration, and is therefore more cost-effective compared to myocutaneous flaps[21]. However, it should be noted that the inertness of biomesh might be a reason for small bowel obstruction[22], and synthetic mesh carries the potential for fistula formation[23]. By contrast, omentoplasty with perineal closure represents a safer approach for the reconstruction of the pelvic floor. Owing to its rich lymphovascular supply, the mobilized omentum in the pelvic cavity inhibits regional fluid collection, and hence prevents small intestine adhesion to the pelvic floor, thus dramatically reducing related complications[24]. For some patients, this technique may not apply when it is not technically feasible to mobilize the omentum to reach the pelvic cavity, or when the omentum has been resected previously.

The major strength of the modified primary closure method is the reconstruction of the pelvic peritoneum, which keeps the small intestine in the abdominal and pelvic cavities, thus avoiding adhesion to extraperitoneal tissues. In the present study, one case of intestinal obstruction in the biological mesh closure group appeared, which was caused by adhesion of the small intestine to the pelvic floor. However, the rate of postoperative intestinal obstruction did not show any difference between the two groups, which is likely due to insufficient study power. Compared with biological mesh closure, modified primary closure reduced postoperative hospital stay duration and total cost.

The pelvic floor is usually left open after APR due to the concern that incomplete closure of the pelvic floor may cause pelvic floor hernias and intestinal obstruction. However, APR is associated with clinically significant perineal hernias, albeit < 1% of the incidence[23]. ELAPE requires extensive resection of the pelvic floor, and thus contributes to the development of perineal hernias, with an incidence of 2.8% *vs* 0.8% compared to traditional APR[1]. As to LELAPE, perineal hernias could occur in nearly half of the patients without reconstruction of the pelvic floor[25]. In LELAPE, closure of the pelvic peritoneum is more challenging because the distal rectum has not been removed at that time. When mobilizing the sigmoid and rectum, the peritoneum on both sides should be intentionally preserved for re-approximation of the pelvic peritoneum. One possible concern is that the intentionally preserved peritoneum may lead to compromised oncological outcomes. However, in the present study, the oncological outcomes did not show any difference between the two groups. The rectum should be transected at the sigmoidorectal junction area, or even lower if possible. A continuous suture with barbed thread is recommended to facilitate the procedure. In obese patients, the peripheral peritoneum should be dissected to reduce tension. The perineal wound was directly sutured in layers. No pelvic floor hernias and perineal hernias occurred in all of our patients, with a mean followup of 12 mo. With regard to patients with rigid peritoneums after neoadjuvant radiotherapy or large pelvic peritoneum defects, this procedure may not

be eligible and other reconstructive methods should be applied.

In conclusion, based on our preliminary experience, the modified primary closure method for reconstruction of the pelvic floor is technically feasible, safe and cost-effective. However, as the present study was retrospective, the safety and feasibility of this method still warrants high evidence-level research.

ARTICLE HIGHLIGHTS

Research background

Laparoscopic extralevator abdominal perineal excision (LELAPE) was introduced to reduce the rate of positive circumferential margins and intraoperative perforation, however its extensive dissection requires reconstruction of the pelvic floor.

Research motivation

To introduce a novel modified primary closure technique of LELAPE for low rectal cancer.

Research objectives

To assess the feasibility, safety and cost-effectiveness of the newly introduced technique by comparing it with the traditional method.

Research methods

Data from 76 patients with rectal cancer undergoing LELAPE from March 2013 to May 2016 were retrospectively analyzed. Patients were classified into the modified primary closure group (32 patients) and the biological mesh closure group (44 patients). Total operating time, reconstruction time, postoperative stay duration, total cost, postoperative complications and tumor recurrence were compared.

Research results

The modified primary closure of the pelvic floor requires longer reconstruction time, but total operating time was not different compared with the biological mesh closure group. The postoperative length of hospital stay and the total cost were both less in the modified primary closure group. No differences in other perioperative data, long-term complications or oncological outcomes were observed.

Research conclusions

The modified primary closure method for reconstruction of the pelvic floor in LELAPE for low rectal cancer is technically feasible, safe and cost-effective.

Research perspectives

Future multicentered randomized controlled trials should be performed to confirm the conclusions made in the present study.

REFERENCES

1 **West NP**, Anderin C, Smith KJ, Holm T, Quirke P; European Extralevator Abdominoperineal Excision Study Group. Multicentre experience with extralevator abdominoperineal excision for low rectal cancer. *Br J Surg* 2010; **97**: 588-599 [PMID: 20186891 DOI: 10.1002/bjs.6916]

2 **Yu HC**, Peng H, He XS, Zhao RS. Comparison of short- and long-term outcomes after extralevator abdominoperineal excision and standard abdominoperineal excision for rectal cancer: a systematic review and meta-analysis. *Int J Colorectal Dis* 2014; **29**: 183-191 [PMID: 24271080 DOI: 10.1007/s00384-013-1793-7]

3 **Yang Y**, Xu H, Shang Z, Chen S, Chen F, Deng Q, Luo L, Zhu L, Shi B. Outcome of extralevator abdominoperineal excision over conventional abdominoperineal excision for low rectal tumor: a meta-analysis. *Int J Clin Exp Med* 2015; **8**: 14855-14862 [PMID: 26628967]

4 **Stelzner S**, Hellmich G, Sims A, Kittner T, Puffer E, Zimmer J, Bleyl D, Witzigmann H. Long-term outcome of extralevator abdominoperineal excision (ELAPE) for low rectal cancer. *Int J Colorectal Dis* 2016; **31**: 1729-1737 [PMID: 27631643 DOI: 10.1007/s00384-016-2637-z]

5 **Chi P**, Chen ZF, Lin HM, Lu XR, Huang Y. Laparoscopic extralevator abdominoperineal resection for rectal carcinoma with transabdominal levator transection. *Ann Surg Oncol* 2013; **20**: 1560-1566 [PMID: 23054115 DOI: 10.1245/s10434-012-2675-x]

6 **Kipling SL**, Young K, Foster JD, Smart NJ, Hunter AE, Cooper E, Francis NK. Laparoscopic extralevator abdominoperineal excision of the rectum: short-term outcomes of a prospective case series. *Tech Coloproctol* 2014; **18**: 445-451 [PMID: 24081545 DOI: 10.1007/s10151-013-1071-2]

7 **Christensen HK**, Nerstrøm P, Tei T, Laurberg S. Perineal repair after extralevator abdominoperineal excision for low rectal cancer. *Dis Colon Rectum* 2011; **54**: 711-717 [PMID: 21552056 DOI: 10.1007/DCR.0b013e3182163c89]

8 **Musters GD**, Buskens CJ, Bemelman WA, Tanis PJ. Perineal wound healing after abdominoperineal resection for rectal cancer: a systematic review and meta-analysis. *Dis Colon Rectum* 2014; **57**: 1129-1139 [PMID: 25101610 DOI: 10.1097/DCR.0000000000000182]

9 **Peirce C**, Martin S. Management of the Perineal Defect after Abdominoperineal Excision. *Clin Colon Rectal Surg* 2016; **29**: 160-167 [PMID: 27247542 DOI: 10.1055/s-0036-1580627]

10 **Sumrien H**, Newman P, Burt C, McCarthy K, Dixon A, Pullyblank A, Lyons A. The use of a negative pressure wound management system in perineal wound closure after extralevator abdominoperineal excision (ELAPE) for low rectal cancer. *Tech Coloproctol* 2016; **20**: 627-631 [PMID: 27380256 DOI: 10.1007/s10151-016-1495-6]

11 **Alam NN**, Narang SK, Köckerling F, Daniels IR, Smart NJ. Biologic Mesh Reconstruction of the Pelvic Floor after Extralevator Abdominoperineal Excision: A Systematic Review. *Front Surg* 2016; **3**: 9 [PMID: 26909352 DOI: 10.3389/fsurg.2016.00009]

12 **Ge W**, Jiang SS, Qi W, Chen H, Zheng LM, Chen G. Extralevator abdominoperineal excision for rectal cancer with biological mesh for pelvic floor reconstruction. *Oncotarget* 2017; **8**: 8818-8824 [PMID: 27732566 DOI: 10.18632/oncotarget.12502]

13 **Wang YL**, Dai Y, Jiang JB, Yuan HY, Hu SY. Application of laparoscopic extralevator abdominoperineal excision in locally advanced low rectal cancer. *Chin Med J* (Engl) 2015; **128**: 1340-1345 [PMID: 25963355 DOI: 10.4103/0366-6999.156779]

14 **Butt HZ**, Salem MK, Vijaynagar B, Chaudhri S, Singh B. Perineal reconstruction after extra-levator abdominoperineal excision (eLAPE): a systematic review. *Int J Colorectal Dis* 2013; **28**: 1459-1468 [PMID: 23440362 DOI: 10.1007/s00384-013-1660-6]

15 **Jensen KK**, Rashid L, Pilsgaard B, Møller P, Wille-Jørgensen P. Pelvic floor reconstruction with a biological mesh after extralevator abdominoperineal excision leads to few perineal hernias and acceptable wound complication rates with minor movement limitations: single-centre experience including clinical examination and interview. *Colorectal Dis* 2014; **16**: 192-197 [PMID: 24251666 DOI: 10.1111/codi.12492]

16 **Anderin C**, Martling A, Lagergren J, Ljung A, Holm T. Short-term outcome after gluteus maximus myocutaneous flap reconstruction of the pelvic floor following extra-levator abdominoperineal excision of the rectum. *Colorectal Dis* 2012; **14**: 1060-1064 [PMID: 21981319 DOI: 10.1111/j.1463-1318.2011.02848.x]

17 **Boccola MA**, Rozen WM, Ek EW, Grinsell D, Croxford MA. Reconstruction of the irradiated extended abdominoperineal excision (APE) defect for locally advanced colorectal cancer. *J Gastrointest Cancer* 2011; **42**: 26-33 [PMID: 20972664 DOI: 10.1007/s12029-010-9224-2]

18 **Petrie N**, Branagan G, McGuiness C, McGee S, Fuller C, Chave H. Reconstruction of the perineum following anorectal cancer excision. *Int J Colorectal Dis* 2009; **24**: 97-104 [PMID: 18688618 DOI: 10.1007/s00384-008-0557-2]

19 **McMenamin DM**, Clements D, Edwards TJ, Fitton AR, Douie WJ. Rectus abdominis myocutaneous flaps for perineal reconstruction:

modifications to the technique based on a large single-centre experience. *Ann R Coll Surg Engl* 2011; **93**: 375-381 [PMID: 21943461 DOI: 10.1308/003588411X572268]

20 **Shibata D**, Hyland W, Busse P, Kim HK, Sentovich SM, Steele G Jr, Bleday R. Immediate reconstruction of the perineal wound with gracilis muscle flaps following abdominoperineal resection and intraoperative radiation therapy for recurrent carcinoma of the rectum. *Ann Surg Oncol* 1999; **6**: 33-37 [PMID: 10030413 DOI: 10.1007/s10434-999-0033-4]

21 **Peacock O**, Pandya H, Sharp T, Hurst NG, Speake WJ, Tierney GM, Lund JN. Biological mesh reconstruction of perineal wounds following enhanced abdominoperineal excision of rectum (APER). *Int J Colorectal Dis* 2012; **27**: 475-482 [PMID: 22006494 DOI: 10.1007/s00384-011-1325-2]

22 **Jess P**, Bulut O. Small bowel obstruction after reconstruction of the pelvic floor with porcine dermal collagen (Permacol) after extended abdominoperineal extirpation for rectal cancer: report of two cases. *Colorectal Dis* 2010; **12**: e178-e179 [PMID: 19832869 DOI: 10.1111/j.1463-1318.2009.02060.x]

23 **Mjoli M**, Sloothaak DA, Buskens CJ, Bemelman WA, Tanis PJ. Perineal hernia repair after abdominoperineal resection: a pooled analysis. *Colorectal Dis* 2012; **14**: e400-e406 [PMID: 22308975 DOI: 10.1111/j.1463-1318.2012.02970.x]

24 **Hultman CS**, Sherrill MA, Halvorson EG, Lee CN, Boggess JF, Meyers MO, Calvo BA, Kim HJ. Utility of the omentum in pelvic floor reconstruction following resection of anorectal malignancy: patient selection, technical caveats, and clinical outcomes. *Ann Plast Surg* 2010; **64**: 559-562 [PMID: 20395804 DOI: 10.1097/SAP.0b013e3181ce3947]

25 **Sayers AE**, Patel RK, Hunter IA. Perineal hernia formation following extralevator abdominoperineal excision. *Colorectal Dis* 2015; **17**: 351-355 [PMID: 25413255 DOI: 10.1111/codi.12843]

P- Reviewer: Higgins PD, Knittel T, Michael HJ, Tomiyasu A
S- Editor: Wang XJ **L- Editor**: Filipodia **E- Editor**: Yin SY

World Journal of Gastroenterology

Submit a Manuscript: http://www.f6publishing.com

World J Gastroenterol 2018 August 14; 24(30): 3448-3461

DOI: 10.3748/wjg.v24.i30.3448

ISSN 1007-9327 (print) ISSN 2219-2840 (online)

ORIGINAL ARTICLE

Observational Study

Altered oral microbiota in chronic hepatitis B patients with different tongue coatings

Yu Zhao, Yu-Feng Mao, Yi-Shuang Tang, Ming-Zhu Ni, Qiao-Hong Liu, Yan Wang, Qin Feng, Jing-Hua Peng, Yi-Yang Hu

Yu Zhao, Yu-Feng Mao, Yi-Shuang Tang, Ming-Zhu Ni, Qiao-Hong Liu, Yan Wang, Qin Feng, Jing-Hua Peng, Institute of Liver Diseases, Shuguang Hospital Affiliated to Shanghai University of Traditional Chinese Medicine, Shanghai 201203, China

Yi-Yang Hu, Institute of Liver Diseases, Key Laboratory of Liver and Kidney Diseases (Ministry of Education), Shuguang Hospital Affiliated to Shanghai University of Traditional Chinese Medicine, Shanghai 201203, China

ORCID number: Yu Zhao (0000-0002-2208-2882); Yu-Feng Mao (0000-0002-8604-9096); Yi-Shuang Tang (0000-0001-5125-8376); Ming-Zhu Ni (0000-0002-5675-953X); Qiao-Hong Liu (0000-0001-9887-8126); Yan Wang (0000-0002-6710-8695); Qin Feng (0000-0002-4641-1636); Jing-Hua Peng (0000-0002-0665-7666); Yi-Yang Hu (0000-0001-9127-7002).

Author contributions: Hu YY designed the study; Zhao Y and Tang YS performed the tongue coating microbial experiments; Tang YS, Liu QH and Wang Y performed the tongue coating metabolic experiments; Tang YS, Feng Q and Peng JH performed the clinical trial; Mao YF and Ni MZ performed the statistical analyses; Zhao Y wrote the paper.

Supported by the Shanghai Educational Development Foundation, No. 14CG41; the National Natural Science Foundation of China, No. 81403298 and No. 81373857; and the National Key New Drug Creation Project, No. 2017ZX09304002.

Institutional review board statement: The study was reviewed and approved by the IRB of Shuguang Hospital affiliated with the Shanghai University of TCM Institutional Review Board.

Informed consent statement: All study participants, or their legal guardian, provided informed written consent prior to study enrollment.

Conflict-of-interest statement: There are no conflicts of interest to report.

STROBE statement: The authors have read the STROBE Statement checklist of items, and the manuscript was prepared and revised according to the STROBE Statement checklist of items.

Manuscript source: Unsolicited manuscript

Correspondence to: Yi-Yang Hu, MD, PhD, Doctor, Senior Researcher, Institute of Liver Diseases, Key Laboratory of Liver and Kidney Diseases (Ministry of Education), Shuguang Hospital affiliated to Shanghai University of Traditional Chinese Medicine, No.528 Zhangheng Road, Pudong New Area, Shanghai 201203, China. yyhuliver@163.com
Telephone: +86-21-20256526
Fax: +86-21-20256521

Received: May 4, 2018
Peer-review started: May 4, 2018
First decision: May 23, 2018
Revised: June 8, 2018
Accepted: June 25, 2018
Article in press: June 25, 2018
Published online: August 14, 2018

Abstract

AIM

To elucidate tongue coating microbiota and metabolic differences in chronic hepatitis B (CHB) patients with yellow or white tongue coatings.

METHODS

Tongue coating samples were collected from 53 CHB

patients (28 CHB yellow tongue coating patients and 25 CHB white tongue coating patients) and 22 healthy controls. Microbial DNA was extracted from the tongue samples, and the bacterial 16S ribosomal RNA gene V3 region was amplified from all samples and sequenced with the Ion Torrent PGM™ sequencing platform according to the standard protocols. The metabolites in the tongue coatings were evaluated using a liquid chromatography-mass spectrometry (LC-MS) platform. Statistical analyses were then performed.

RESULTS

The relative compositions of the tongue coating microbiotas and metabolites in the CHB patients were significantly different from those of the healthy controls, but the tongue coating microbiota abundances and diversity levels were not significantly different. Compared with the CHB white tongue coating patients, the CHB yellow tongue coating patients had higher hepatitis B viral DNA (HBV-DNA) titers (median 21210 *vs* 500, respectively, $P = 0.03$) and a significantly lower level of Bacteroidetes (20.14% *vs* 27.93%, respectively, $P = 0.013$) and higher level of Proteobacteria (25.99% *vs* 18.17%, respectively, $P = 0.045$) in the microbial compositions at the phylum level. The inferred metagenomic pathways enriched in the CHB yellow tongue coating patients were mainly those involved in amino acid metabolism, which was consistent with the metabolic disorder. The abundances of bacteria from Bacteroidales at the order level were higher in the CHB white tongue coating patients (19.2% *vs* 27.22%, respectively, $P = 0.011$), whereas Neisseriales were enriched in the yellow tongue coating patients (21.85% *vs* 13.83%, respectively, $P = 0.029$). At the family level, the abundance of Neisseriaceae in the yellow tongue patients was positively correlated with the HBV-DNA level but negatively correlated with the S-adenosyl-L-methionine level.

CONCLUSION

This research illustrates specific clinical features and bacterial structures in CHB patients with different tongue coatings, which facilitates understanding of the traditional tongue diagnosis.

Key words: 16S rRNA gene sequencing; Metabolomics; Chronic hepatitis B; Tongue diagnosis; Microbiota

Core tip: Tongue diagnosis has important guiding significance for clinical syndrome differentiation and drug use in traditional Chinese medicine (TCM), but lacks scientific explanations. This study illustrates the existence of specific clinical features and bacterial structure in chronic hepatitis B (CHB) patients with different tongue coatings. Compared with the CHB white tongue coating patients, the yellow tongue coating patients had higher viral titers and a significantly lower level of Bacteroidetes and higher level of Proteobacteria in their microbial compositions at the phylum level. This study explores the micro-features between different tongue coatings, which will promote our understanding of the TCM tongue diagnosis and facilitate therapeutic strategies for individualized treatment.

Zhao Y, Mao YF, Tang YS, Ni MZ, Liu QH, Wang Y, Feng Q, Peng JH, Hu YY. Altered oral microbiota in chronic hepatitis B patients with different tongue coatings. *World J Gastroenterol* 2018; 24(30): 3448-3461 Available from: URL: http://www.wjgnet.com/1007-9327/full/v24/i30/3448.htm DOI: http://dx.doi.org/10.3748/wjg.v24.i30.3448

INTRODUCTION

Tongue diagnosis is a characteristic diagnostic method of traditional Chinese medicine (TCM) with a long history. TCM believes that the tongue is an important window for changes in the body, which are closely related to the *zang* and *fu* (internal organs), meridians, *qi* and *xue* (blood) and *body fluids*. Therefore, changes of the tongue can help doctors distinguish syndromes and guide diagnoses, which has great significance for clinical treatment *via* TCM. Different tongue coating colors in TCM have different treatment principles. Tongue diagnosis has the advantages of convenience and intuitiveness and represents first-hand information for TCM doctors that should not neglected. However, the physiological and pathological changes that contribute to the TCM tongue diagnosis have not been elucidated. According to TCM theory, the formation of tongue coating is closely related to *wei-qi* (spleen and stomach). Reports have noted that micro-ecological changes in the local flora are important manifestations of pathological tongue images[1]. As part of the human microbiome, the oral microbiota can interfere with the gut microbiota and is associated with multiple diseases[2]. The microbiota can produce metabolites and active ingredients that participate in the regulation of host metabolism and immunity and is closely related to the pathological processes of many diseases. Some reports have found abnormalities in the microbiota or metabolites in pathological tongue coatings[3,4]. However, integrated analyses of the pathological tongue coating microbiotas and metabolites have rarely been reported. As an important diagnostic factor, elucidating the "intension" of the material basis of tongue coatings and providing the scientific basis for individualized treatment and clinical syndrome differentiation have great significance in TCM.

Chronic hepatitis B (CHB) is a major infectious disease that may lead to liver cirrhosis and hepatocellular carcinoma (HCC). In China, CHB is a huge health burden, and 60% and 80% of China's liver cirrhosis and HCC patients, respectively, are infected with hepatitis B virus (HBV)[5]. Intestinal bacteria are widely involved in the pathogenesis of chronic liver diseases, which can affect liver homeostasis based on energy absorption and storage, interfere with bile metabolism, participate in immune regulation and affect other processes[6].

Some studies have shown that dysbiosis of the oral microbiota may be involved in the development of HBV-induced chronic liver disease. Moreover, key oral-derived phylotypes may invade the gut as opportunistic pathogens and alter the composition of the gut microbiota, and cirrhotic patients have a more limited salivary defenses and worse inflammation than healthy patients[7]. In China, many patients with chronic liver disease are treated with TCM, which has been reported to decrease the incidence of liver cancer in a recent 15-year follow-up study of 21020 newly diagnosed CHB patients[8]. Changes in the tongue are important for TCM diagnoses[9,10], and CHB patients have different tongue coating phenotypes, which most commonly manifested as a yellow or a white tongue coating. These tongue coatings lead to different treatment strategies in TCM. Therefore, we speculate that microbiota differences may exist between CHB patients with different tongue coatings.

In this study, we characterize the microbiota and metabolic compositions of CHB patients with yellow or white tongue coatings and investigate the association between the tongue coating microbiotas, metabolites and host physiological indices to elucidate the differences between CHB patients with yellow and white tongue coatings. These results will contribute to our understanding of the relationship between the tongue coating appearance and the microbiota and metabolic microfeatures differences.

MATERIALS AND METHODS

Patients

All samples from this study were collected at the Shanghai University of TCM-affiliated Shuguang Hospital in Shanghai, the Nanjing Second Hospital and the Huai'an Fourth People's Hospital in Jiangsu province, People's Republic of China, from 2013 to 2014. The criteria used for the diagnosis of CHB were from the "The Guidelines for the Prevention and Treatment of Chronic Hepatitis B (2010 version)" issued by the Chinese Society of Liver Diseases and the Chinese Society of Infectious Diseases. Healthy age- and gender-matched control subjects were recruited from the Shanghai University of TCM-affiliated Shuguang Hospital Medical Center. We excluded patients who had been on absorbable antibiotics within the past 3 mo; were undergoing periodontal disease treatment; had other viral liver hepatitises, liver cirrhosis, or HCC; were pregnant or lactating women; or had other severe primary diseases. Informed written consent was obtained before the participants' enrollment. This project was approved by the IRB of Shuguang Hospital, which was affiliated with the Shanghai University of TCM (Permit Number: 2012-206-22-01) and conformed to the ethical guidelines of the Declaration of Helsinki (2008).

Sample collection

Each subject underwent serum and tongue coating collection on the same day in the morning before breakfast. For tongue coating collection, all participants were required to rinse their mouth with physiological saline and then were photographed with the tongue diagnostic information acquisition system in a stable light source (Daosh Co., Shanghai, China). Sterile spoons scraped the fixed parts of the tongue surface twice to collect tongue coating samples, which were dissolved in sanitized Eppendorf tubes filled with 2 mL of physiological saline[4]. Spare samples were stored in a -80 ℃ freezer. Blood samples were taken for clinical analyses after an overnight fast of at least 10 h.

Biochemical measurements

Clinical and biochemical indices were determined for each patient, including the following: (1) liver and kidney function, including serum alanine aminotransferase (ALT), aspartate aminotransferase (AST), alkaline phosphatase (ALP), γ-glutamyl transpeptidase (GGT), total bilirubin (TBIL), direct bilirubin (DBIL), albumin (ALB), globulin (GLB), creatinine (Cr), blood urea nitrogen (BUN) and uric acid (UA); (2) lipid profiles, including triglycerides (TG), total cholesterol (TC), high-density lipoprotein (HDL) and low-density lipoprotein (LDL); (3) clotting function, including the prothrombin time (PT); and (4) virological indicators, including hepatitis B surface antigen (HBsAg), hepatitis B surface antibody (HBsAb), hepatitis Be antigen (HBeAg), hepatitis Be antibody (HBeAb), hepatitis B core antibody (HBcAb) and the HBV-DNA titers were determined for each patient.

Tongue coating microbial diversity analysis

DNA extraction and PCR amplification: Microbial DNA was extracted from the tongue samples using a QIAGEN QIAamp DNA Stool Mini Kit (50) according to manufacturer's protocols. The V3 region of the bacterial 16S ribosomal RNA (rRNA) gene was amplified by PCR (95 ℃ for 2 min, followed by 25 cycles at 95 ℃ for 30 s, 55 ℃ for 30 s and 72 ℃ for 30 s and a final extension at 72 ℃ for 5 min) using the primers 341F (5'-CCTACGGGAGGCAGCAG-3') and 518R (5'-ATTACCGCGGCTGCTGG-3'), which included a barcode that was an eight-base sequence unique to each sample. The PCR reactions were performed in triplicate with a 20 μL mixture containing 4 μL of 5 × FastPfu buffer, 2 μL of 2.5 mmol/L dNTPs, 0.8 μL of each primer (5 μmol/L), 0.4 μL of KAPA HiFi Polymerase, and 10 ng of template DNA.

Ion Torrent PGM™ sequencing: Amplicons were extracted from 2% agarose gels, purified using the AxyPrep DNA Gel Extraction Kit (Axygen Biosciences, Union City, CA, United States) according to the manufacturer's instructions and then quantified using the Qubit 2.0 Fluorometer (Invitrogen, United States). Purified amplicons were pooled at equimolar concentrations and sequenced on an Ion Torrent PGM™ platform according to standard protocols. The raw reads were deposited

into the NCBI Sequence Read Archive (SRA) database (Accession Number: SRP127002).

Processing of sequencing data: Raw FASTQ files were demultiplexed and quality-filtered using the fastx_Toolkit (version 0.0.13.2) with the following criteria. The 200 bp reads were truncated at any site receiving an average quality score < 20, and truncated reads that were shorter than 50 bp were discarded. Operational taxonomic units (OTUs) were clustered with 97% similarity cutoff using UCHIME (version 7.1 http://drive5.com/uparse/), with also identified and removed chimeric sequences. The taxonomy of each 16S rRNA gene sequence was analyzed using the RDP Classifier (http://rdp.cme.msu.edu/) against the SILVA (SSU123)16S rRNA database with a confidence threshold of 70%[11].

Metabolomic profiling of human tongue coating samples

Sample preparations: The tongue coating samples were thawed on ice, and quality control (QC) samples were made by mixing and blending equal volumes (20 μL) of each sample. A 100 μL aliquot of the samples was added to 500 μL of 100% methanol, which was vibrated for 30 s and centrifuged at 15000 *g* for 10 min. The supernatant was dried in a vacuum centrifuge at 30 ℃. The dried samples were dissolved in 300 μL of water/methanol (1:1, 4 ℃) and filtered through a 0.22 μm membrane. A 3 μL aliquot of tongue coating was injected for LC-MS analysis, and another 100 μL was sampled for subsequent MS/MS identification.

LC-MS experiments: A Waters ACQUITY UPLC system analysis was performed on an ACQUITY UPLC® HSS T3 column (150 mm × 2.1 mm, 1.8 μm particle size; Waters Corporation, Milford, MA, United States) for separation of samples using a binary gradient mode. The sample was eluted with a gradient mobile phase composed of 0.1% (v/v) formic acid/water (A) and 0.1% (v/v) formic acid/acetonitrile (B) as follows: 0-1 min, 2% B; 1-11 min, linear increase from 2 to 50% B; 11-17 min, linear increase from 50 to 98% B; 17-18 min, 98% B; 18-19 min, linear decrease from 98 to 2% B and 19-20 min, 2% B. The flow rate was set to 0.3 mL/min. The column and sample-tray temperatures were maintained at 35 and 8 ℃, respectively.

A Thermo Scientific™ LTQ XL™ mass spectrometer (Thermo Scientific, San Jose, CA, United States) was combined with electrospray ionization (ESI) operating in both the negative and positive ion modes. The positive ionization mode was operated using a spray voltage of 4.8 kV, and the negative ionization mode used a spray voltage of 4.50 kV. The capillary temperature was 325 ℃, and the sheath gas and auxiliary gas were set at flow rates of 45 and 10 L/min, respectively. The mass scanning range was set at 89-1000 m/z in positive ionization mode and 87-1000 m/z in negative ionization mode.

Data processing and metabolite identification: The raw LC-MS data files were converted into the mzXML format and then analyzed by the XCMS program in the R statistical language (v3.1.1) for peak identification, filtering and alignment. For the subsequent multivariate linear regression analysis, the XCMS results were ultimately converted into two-dimensional data matrices that consisted of retention time (Rt)-m/z pairs and their peak area. The data were normalized by their sum peak areas, and 1043 positive ion mode variables and 540 negative ion mode variables were finally obtained for the subsequent analysis.

Metabolites driving the differences among the 3 groups were filtered with a variable importance (VIP) > 1, a correlation P(corr) > 0.4, and a threshold of 1 using the 7-fold cross-validated partial least squares-discriminant analysis (PLS-DA) model. By using retention time-m/z pairs as the identifiers for each ion, we examined and optimized the parameters individually. The possible identities of the metabolites were first confirmed based on their exact molecular weights (molecular weight error < 15 ppm), followed by the comparison of their exact molecular weight and MS/MS fragmentation patterns to entries in the Human Metabolome Database (HMDB) (http://www.hmdb.ca) and the METLIN (https://metlin.scripps.edu), MassBank (http://www.massbank.jp) and mzCloud (https://www.mzcloud.org) databases.

Statistical analysis

We compared the clinical difference among the 3 groups using the Kruskal-Wallis test and the Nemenyi test was used for post-pairwise comparisons. The HBV-DNA titers between the CHB yellow and white tongue coating patients and the metabolites differences between the CHB and the healthy controls were compared using the standard non-parametric Mann-Whitney *U* test. Unsupervised principal component analysis (PCA) and supervised PLS-DA analysis were performed using the Simca-P software (version 13.0, Umetrics, Umea, Sweden). The microbiota results were analyzed using Metastats analysis, the Kruskal-Wallis test and the linear discriminant analysis (LDA) effect size (LEfSe) method was implemented in LEfSe v1.0[12]. The functionality of the microbiota was assessed using PiCRUST[13] and compared among the groups. The metabolomics enrichment analysis was performed using MetaboAnalyst 3.0[14] (http://www.metaboanalyst.ca). We correlated the microbiota with clinical index and metabolites and visualized the results with a Spearman's correlation coefficient> 0.3 and $P < 0.05$ in Cytoscape (version 3.6.0).

RESULTS

Physiological characteristics

A total of 75 subjects, including 22 healthy subjects and 53 CHB patients, were enrolled in this study. Twenty-eight of the 53 CHB patients exhibited a yellow tongue coating, and 25 CHB patients exhibited a white tongue coating; their physiological characteristics are shown in Table 1. The ages, genders and body mass indices (BMIs) did not significantly differ among the groups. The CHB group had a significantly higher level of liver function,

Table 1 Physiological characteristics of the subjects

	Healthy	CHB patients		*P* value
		White tongue coating	Yellow tongue coating	
Age	34.09 ± 7.16	34.46 ± 9.92	38.08 ± 9.89	0.255
Gender, male/female	13/9	21/7	17/8	0.488
BMI (kg/m^2)	21.22 (16.61-25.56)	23.44 (18.42-31.64)	23.30 (18.37-45.67)	0.077
Antiviral drugs (%)	/	78.60%	64%	0.24
Chinese herbs (%)	/	17.90%	28%	0.378
TBIL (μmol/L)	14.87 (8.29-31.62)	12.85 (7.9-27.7)	17.27 (6.4-45.6)	0.27
DBIL (μmol/L)	3.065 (1.7-6.76)	3.9 (1.64-9.2)	4.8 (2.05-34.7)[b]	0.006
IDBIL (μmol/L)	11.6 (6.3-25.7)	8.95 (5-18.7)	10.2 (4.2-19.6)	0.282
ALT (IU/L)	15 (10-34)	28.75 (8.5-170)[b]	47 (11.1-533)[c]	< 0.001
AST (IU/L)	17.5 (11-31)	27 (12-133)[b]	38 (14.8-543)[c]	< 0.001
ALP(IU/L)	15.28 (9-52)	25.8 (10.01-98)	38 (8.6-274)[c]	< 0.001
GGT (IU/L)	70.5 (35-119)	72.7 (37.1-131)	76.3 (41.7-202)	0.62
ALB (g/L)	44.97 (40.89-50.77)	48.7 (43.1-56.3)[ad]	46 (36.6-50.1)	0.003
PT (s)	12.55 (11.3-13.9)	12.7 (11.1-16.4)	13.3 (11.3-16)	0.032
HBV-DNA (IU/mL)	/	500 (500-44830000)[d]	21210 (500-324100000)	0.03
BUN (mmol/L)	4.39 (2.97-6.39)	4.96 (2.96-8.9)	4.2 (2.4-7.28)	0.074
Gr (μmol/L)	72.355 (45.1-106.67)	70 (27.4-96.7)	69 (35.9-83)	0.449
UN (μmol/L)	305.5 (201-406)	325 (207-550)	294 (154-429)	0.204
FPG (mmol/L)	5.2 (3.96-5.63)	5.2 (4.29-7.09)	5.215 (4.07-15.54)	0.532
TC (mmol/L)	4.04 (0.37-6.34)	4.55 (3.15-6.52)	4.36 (3.1-6.74)	0.102
TG (mmol/L)	0.84 (0.37-1.91)	1.17 (0.58-3.31)[a]	1.11 (0.68-2.62)[a]	0.008
HDL (mmol/L)	1.14 (0.74-1.76)	1.145 (0.72-1.86)	1.07 (0.58-2.02)	0.779
LDL (mmol/L)	2.205 (1.38-5.04)	2.27 (1.47-3.8)	2.44 (1.12-3.73)	0.647
APOA-A (g/L)	1.175 (0.85-1.62)	1.08 (0.76-1.91)[c]	1.02 (0.71-1.42)[c]	0.013

Quantitative results are expressed as median with minimum and maximum into brackets. The *P* values indicate the significance of difference among groups, and the Kruskal-Wallis test for 3 groups and Nemenyi test were used for post pairwise comparisons. The HBV-DNA titers between the chronic hepatitis B (CHB) yellow and white tongue coating patients were compared using the standard non-parametric Mann-Whitney *U* test. The antiviral drugs usage and the Chinese herbs usage were compared between CHB yellow and white tongue coating patients using the Chi-square test. [a]$P < 0.05$ *vs* healthy controls, [b]$P < 0.01$ *vs* healthy controls, [c]$P < 0.001$ *vs* healthy controls, [d]$P < 0.05$ *vs* CHB yellow tongue coating patients.

including ALT, AST and GGT activity. The CHB yellow tongue coating patients had a trend toward higher TBIL, DBIL, ALT, AST, ALP, GGT and PT levels. Additionally, the HBV viral titer was significantly higher in yellow tongue coating patients than in the white coating patients ($P = 0.03$), whereas the ALB level was lower in the yellow tongue coating patients ($P = 0.003$).

Overview of tongue coating microbial differences among the patients

In this study, the qualified sequences were rarefied to 9300 sequences per sample for downstream analysis. A summary is shown in Supplementary Table 1, Good's coverage values were high in the three groups, indicating that the sequencing depth was sufficient for investigation. As shown in Figure 1A show, the oral microbiota abundance and diversity level did not significantly differ between the CHB patients and the healthy controls. A PCA plot based on the OTU distributions showed that the overall compositions of the tongue coating microbiota were not significantly shifted by age, gender, BMI and antiviral treatment (Supplementary Figure 1). However, the PLS-DA plot showed a clear separation between the CHB patients and the healthy groups, and the CHB yellow tongue coating and white tongue coating patients were also well separated (Figure 1B). A Venn diagram showed that 1569 OTUs were common in all samples and that 705 and 741 OTUs were unique to the CHB yellow tongue coating and white tongue coating patients, respectively (Figure 1C). Most of the tongue coating microbiota were assigned to the Firmicutes, Bacteroidetes, Proteobacteria, Actinobacteria and Fusobacteria phyla (relative abundance > 1% of the total DNA sequences, Figure 2A). In total, 112 genera were classified, and most of the genera were present in low abundance in the oral microbiota samples.

A Metastats analysis was used to detect differentially abundant features at different taxon levels. Compared with the white tongue patients, the relative abundance of Bacteroidetes was decreased in the CHB yellow tongue coating patients, whereas the abundance of Proteobacteria and Gracilibacteria were increased (Figure 2B). At the family level, Neisseriaceae and Gracilibacteria_bacterium_oral_taxon_873 were dominant in the CHB yellow tongue coating and had prevalent differences compared with the abundances in the healthy controls and CHB white tongue coating patients, whereas SR1_bacterium_canine_oral_taxon_380 was decreased. At the genus level, *Neisseria* and *Gracilibacteria_bacterium_oral_taxon_873* were enriched in the CHB yellow tongue coating samples compared with the healthy controls and the CHB white tongue coating patients. The relative abundance of *Actinomyces, Porphyromonas*, *Bergeyella*, *Centipeda, Alysiella, Bulleidia, Candidatus_Saccharibacteria_bacterium_UB2523* and *Pseudoramibacter* in the CHB white tongue coating samples were significantly different

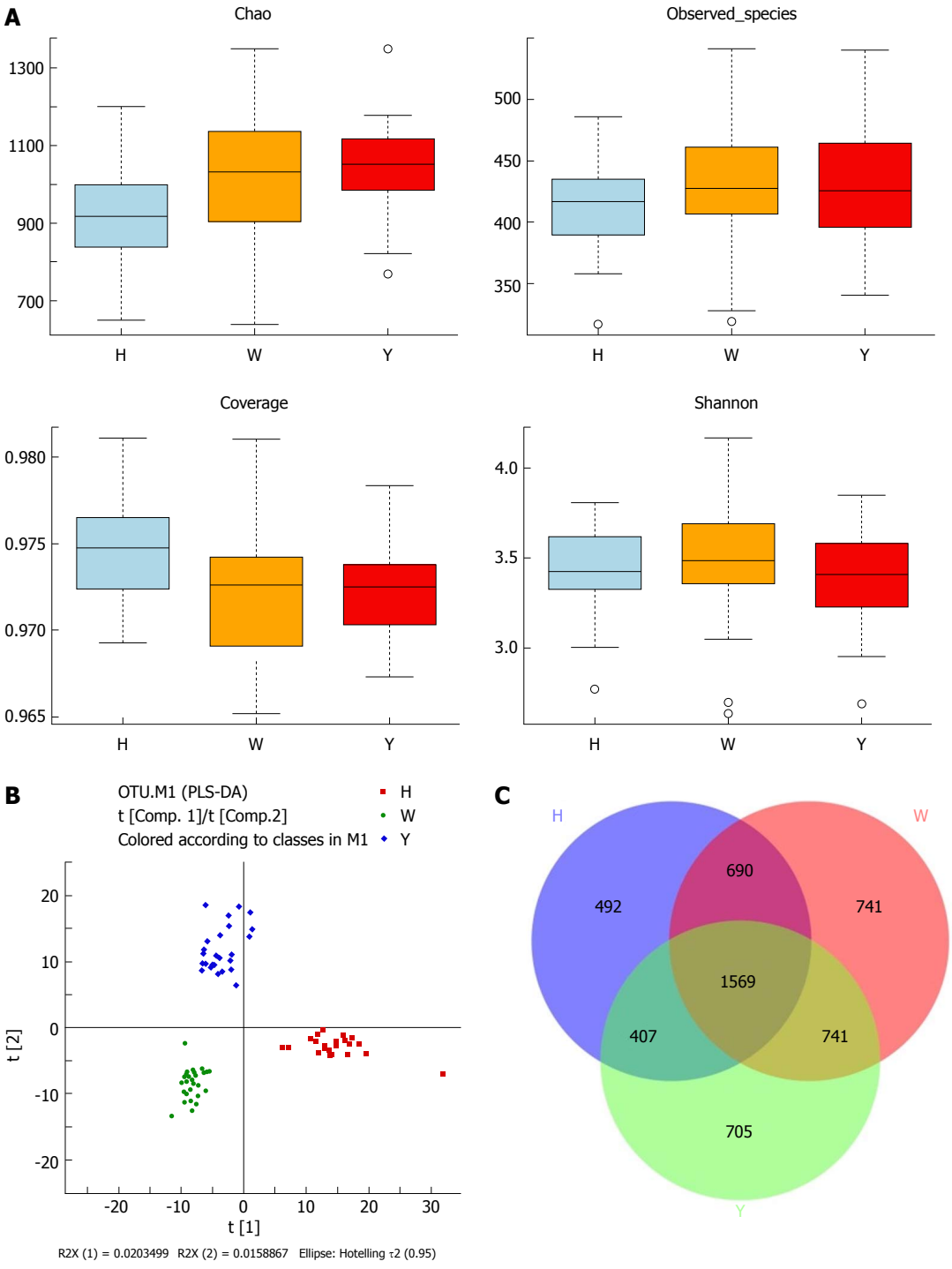

Figure 1 Overview of the tongue coating microbiota among groups. A: Detailed characteristics of alpha diversity; B: PLS-DA discriminant analysis plot; C: Venn diagram based on OTUs. PLS-DA: Partial least squares-discriminant analysis; OTUs: Operational taxonomic units.

from those of the healthy controls, but no differences were found compared to the abundances of the CHB yellow tongue coating patients (Figure 3A). We used LEfSe to identify the specific OTUs associated with each group. A cladogram representative of the structure of the tongue coating microbiotas in the CHB yellow tongue coating and CHB white tongue coating patients and the healthy controls is shown in Figure 3B. According to the LDA values ($\log_{10}^{\text{LDA score}} > 4$), the tongue coating bacteria with advantages in the CHB yellow tongue coating were Betaproteobacteria, Neisseriales, Neisseriaceae, Proteobacteria and *Neisseria*, the CHB white tongue coating samples were dominated by Bacteroidia and Bacteroidales, and the healthy controls were dominated by Actinomycetaceae, Actinomycetales and *Actinomyces* (Figure 3C).

Predicted microbial function

The gene functions in the tongue coating microbiotas were predicted by PICRUSt, and the results were com-

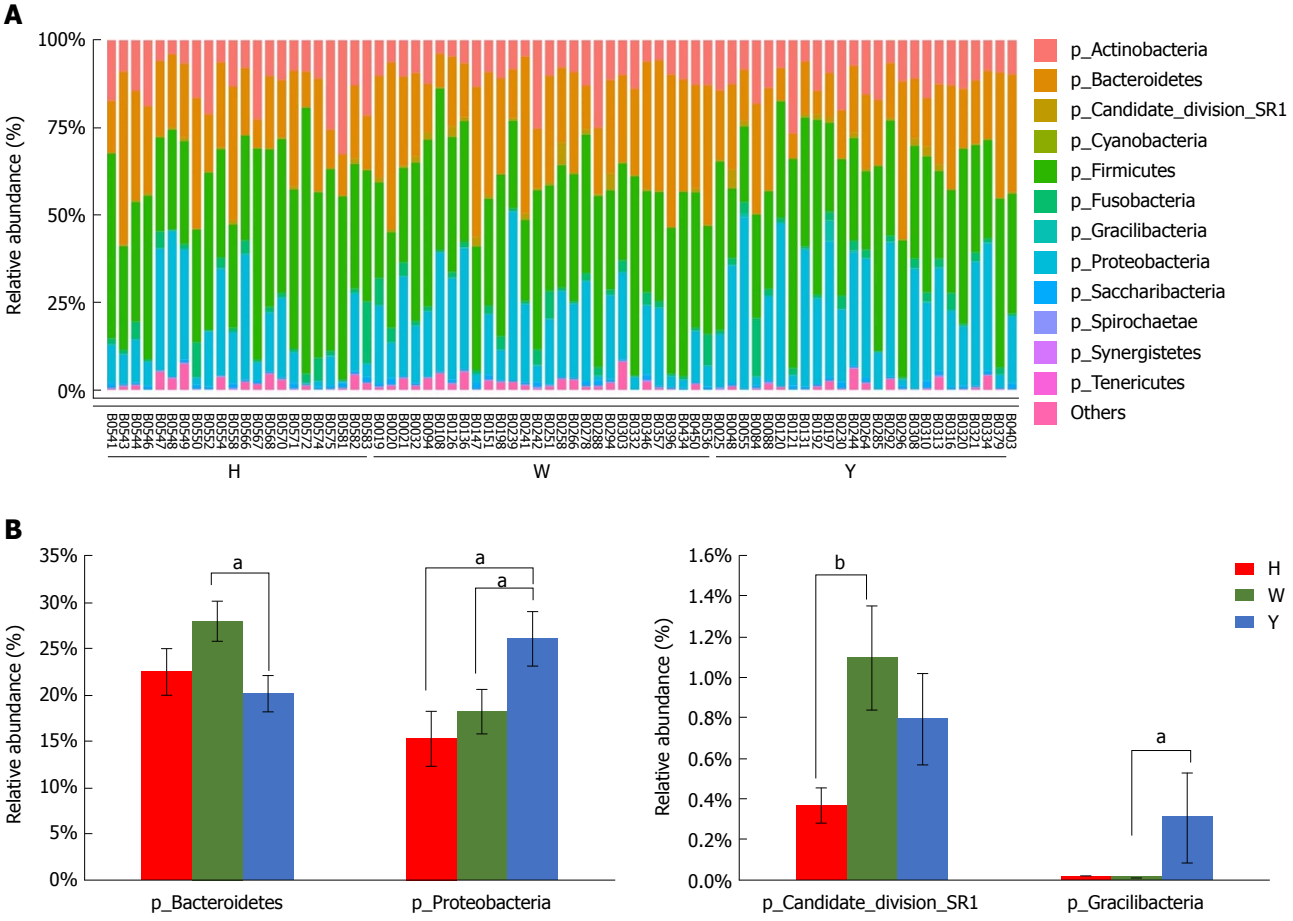

Figure 2 Taxonomic classification of the tongue coating microbiota at the phylum level. A: Taxonomic classification of the tongue-coating microbiota at the phylum level; B: Metastats analysis of differences in the relative proportions difference at the phylum level. $^{a}P < 0.05$, $^{b}P < 0.01$.

pared between groups (Figure 4). Microbes with greater relative abundances in the healthy controls had functions that were most related to carbohydrate metabolism (fructose and mannose metabolism). The microbiotas in the white tongue coatings were more likely than those in the yellow tongue coatings and healthy controls to have functionality related to renetic information processing, including the level-2 functionality of replication and repair (DNA replication proteins, homologous recombination and mismatch repair) and transcription (transcription machinery, ribosome and translation factors). In contrast, the microbiotas in the yellow tongue coatings were probably related to amino acid metabolism (alanine aspartate and glutamate metabolism, arginine and proline metabolism, cysteine and methionine metabolism, lysine biosynthesis, phenylalanine tyrosine and tryptophan biosynthesis, phenylalanine metabolism, tyrosine metabolism and valine leucine and isoleucine biosynthesis), membrane transport (bacterial secretion system and secretion system) and cell motility (bacterial motility proteins).

Metabolites in the tongue coatings

The typical total ion chromatograms (TICs) of the samples run in positive ion modes are shown in supplementary Figure 2A. Because the PCA did not distinguish the groups well, the supervised PLS-DA model was used for further analysis and resulted in good separation of the CHB patients and healthy volunteers, however, the CHB yellow tongue coating and the white tongue coating patients were not completely distinguished (Supplementary Figure 2B). A total of 21 endogenous compounds were obtained with a VIP > 1 and *P*(corr) > 0.4 in the PLS-DA model (Table 2). The presence of 6 compounds differed between the CHB patients and healthy subjects ($P < 0.05$), and these compounds were mainly involved in histidine metabolism and methylhistidine metabolism ($P < 0.05$, Supplementary Figure 3). The metabolites were not significantly different between the CHB yellow and white tongue coating patients, but the number of amino acid metabolites was greater in the CHB yellow tongue coating patients than in the white tongue coating patients.

Associations of the tongue coating microbiotas with metabolites and clinical indices

To better understand the relationships among the tongue coating microbiota, metabolites and clinical indicators, we performed a correlation analysis of the differential microbiota at the family level with the metabolites and clinical indicators and constructed the related network (|correlation r| > 0.3, $P < 0.05$). The abundance of

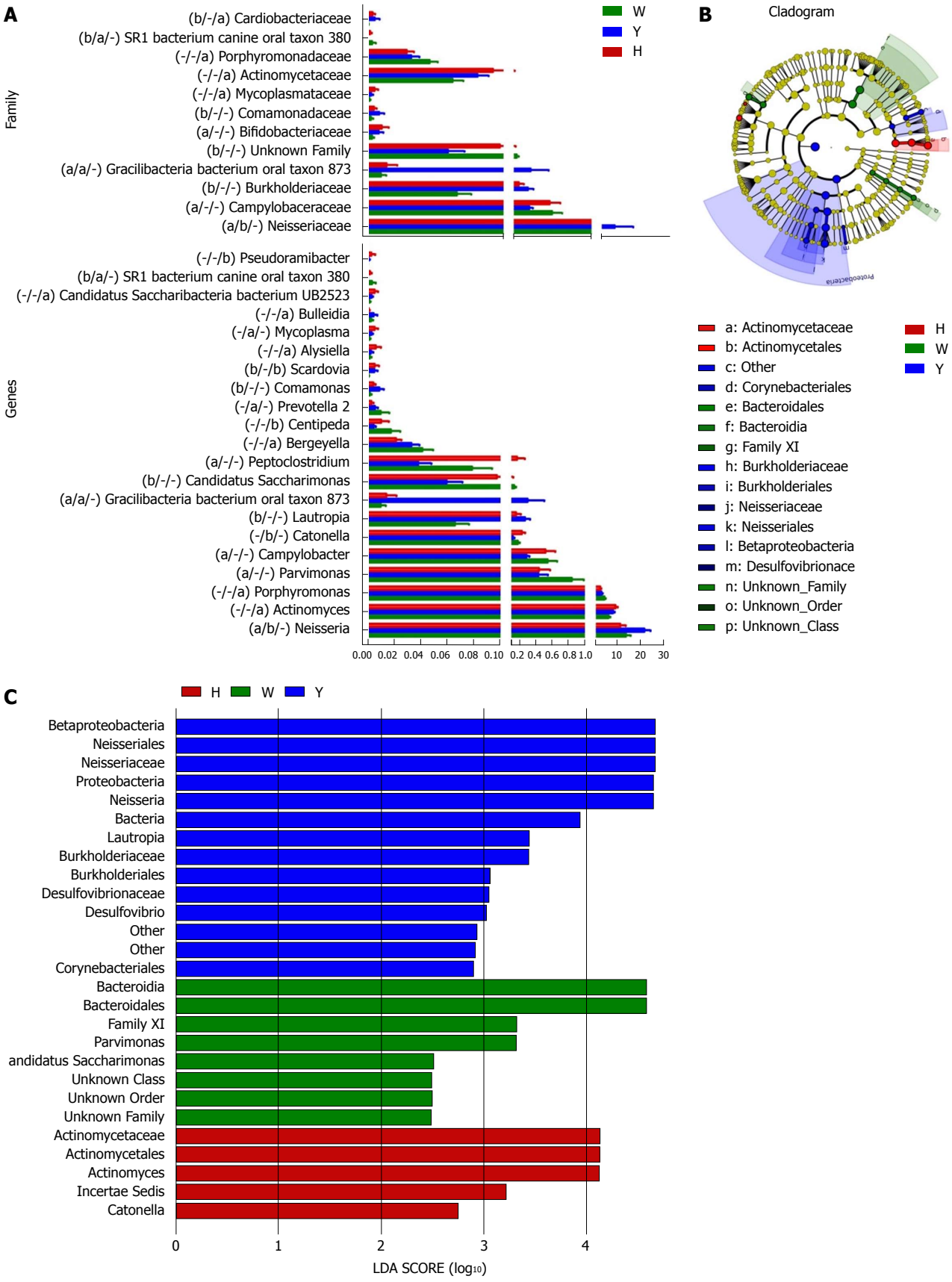

Figure 3 The most differentially abundant taxa in the chronic hepatitis B yellow and white tongue coating patients. A: Comparison of the relative abundance at the bacterial family and genus levels, the marks of significance from left to right in parentheses are the CHB yellow tongue coating patients *vs* the healthy controls, the CHB yellow tongue coating patients *vs* the CHB white tongue coating patients and the CHB white tongue coating patients *vs* the healthy controls. $^{a}P < 0.05$, $^{b}P < 0.01$, "–" indicates no significant difference based on the Metastats analysis; B: Taxonomic cladogram of the LEfSe analysis of the 16S sequences. (Red) healthy-control enriched taxa; (Green) CHB white tongue coating patients-enriched taxa; and (Blue) CHB yellow tongue coating patients-enriched taxa. C: LDA scores of enriched taxa in the healthy controls (Red), CHB white tongue coating patients (Green) and CHB yellow tongue coating patients (Blue). LDA: Linear discriminant analysis.

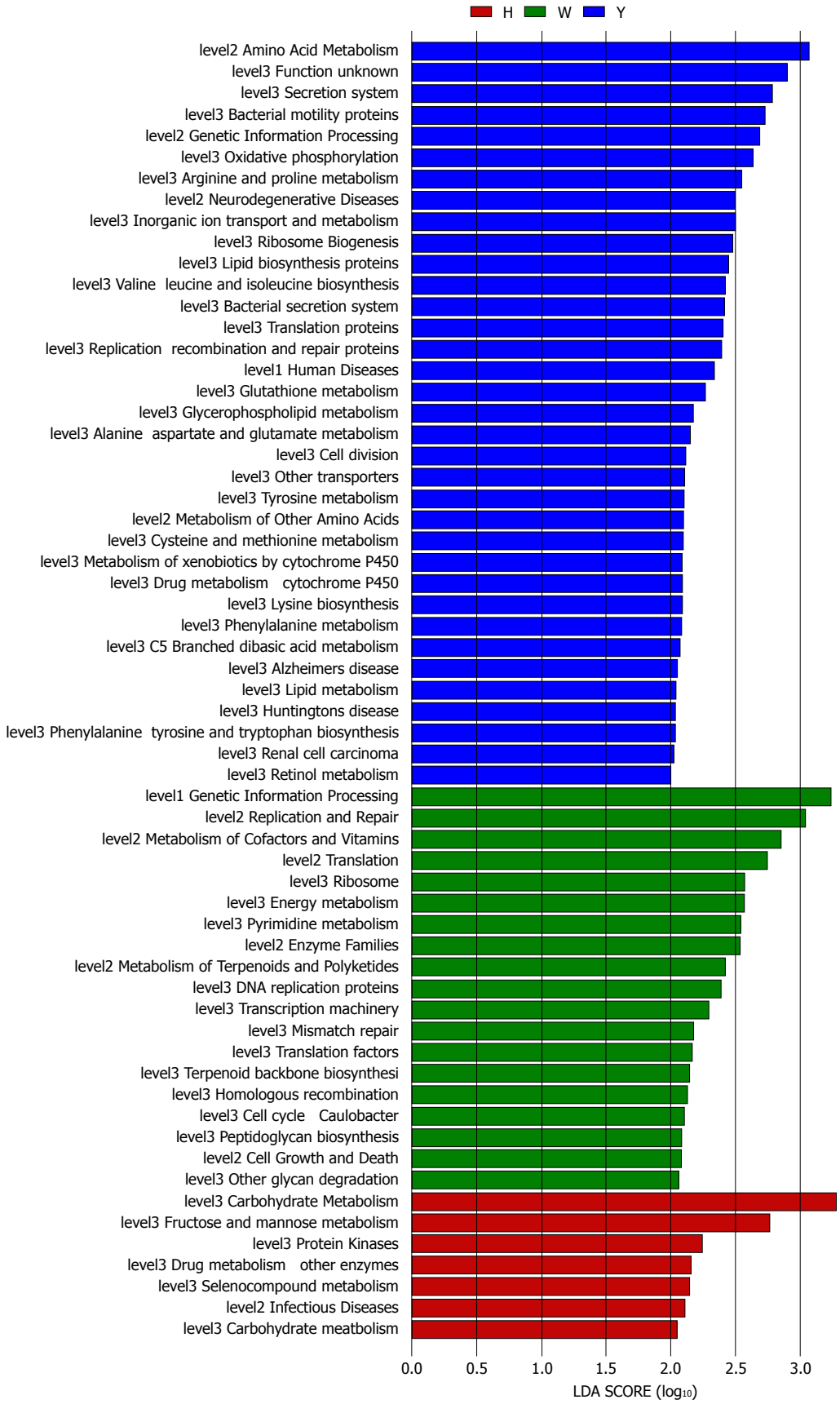

Figure 4 Linear discriminant analysis scores of the enriched microbial functions in the healthy-controls (Red), chronic hepatitis B white tongue coating patients (Green) and chronic hepatitis B yellow tongue coating patients (Blue). LDA: Linear discriminant analysis.

Table 2 Metabolites detected in the tongue coatings

Metabolites	Formula	Rt (min)	Type	KEGG compounds	VIP	*P* (corr)	CHB *VS* H		Healthy	CHB White tongue coating	CHB Yellow tongue coating
							P value	FC			
L-Proline	$C_5H_9NO_2$	83.3392	$[M+H]^+$	C00148	1.04	-0.68	0.134	1.473	1.01 (0.13-12)	3 (0.16-20.14)	3.88 (0.09-15.28)
L-Valine	$C_5H_{11}NO_2$	120.7915	$[M+H]^+$	C00183	1.07	-0.76	0.081	1.608	2.92 (0.82-17.97)	3.98 (1.13-38.65)	7.44 (1.08-31.3)
L-Isoleucine	$C_6H_{13}NO_2$	194.3545	$[M+H]^+$	C00123	1.15	-0.81	0.069	1.641	5.55 (0.43-30.81)	7.23 (1.23-58.36)	13.28 (0.22-45.18)
L-Leucine	$C_6H_{13}NO_2$	212.576	$[M+H]^+$	C00123	1.07	-0.81	0.029	1.715	8.9 (0.02-44.58)	14.65 (2.89-84.8)	21.6 (0.44-61.98)
Hypoxanthine	$C_5H_4N_4O$	154.305	$[M+H]^+$	C00262	1.07	-0.80	0.039	2.218	0.42 (0.01-6.93)	1.31 (0.05-17.87)	2.46 (0.01-14.33)
Urocanic acid	$C_6H_6N_2O_2$	132.3225	$[M+H]^+$	C00785	1.00	-0.78	0.044	2.587	0.62 (0.07-4.46)	0.93 (0.08-12.84)	1.93 (0.08-13.92)
L-Lysine	$C_6H_{14}N_2O_2$	64.124	$[M+H]^+$	C00047	1.01	-0.72	0.683	1.510	0.08 (0.05-0.28)	0.08 (0.03-0.81)	0.08 (0.03-0.65)
Glutamate	$C_5H_9NO_4$	76.6581	$[M+H]^+$	C00025	1.04	-0.75	0.159	1.955	0.14 (0.02-1.17)	0.2 (0-2.99)	0.39 (0-2.52)
Methionine	$C_5H_{11}NO_2S$	131.208	$[M+H]^+$	C00073	1.16	-0.80	0.144	1.543	1.08 (0.01-7.21)	1.74 (0.13-10.21)	2.26 (0-9.75)
Xanthine	$C_5H_4N_4O_2$	183.102	$[M+H]^+$	C00385	1.01	-0.73	0.151	2.058	0.09 (0-2.91)	0.24 (0-4.93)	0.47 (0-4.75)
L-Phenylalanine	$C_9H_{11}NO_2$	277.369	$[M+H]^+$	C00079	1.17	-0.82	0.069	1.534	6.72 (0.83-24.15)	11.07 (1.84-51.35)	13.1 (0.31-36.18)
Glycyl-Valine	$C_7H_{14}N_2O_3$	205.364	$[M+H]^+$		1.07	-0.70	0.078	1.548	0.07 (0-1.1)	0.15 (0-0.84)	0.19 (0-1.38)
Citrulline	$C_6H_{13}N_3O_3$	77.3246	$[M+H]^+$	C00327	1.16	-0.74	0.216	1.486	0.12 (0-1.28)	0.14 (0.01-1.7)	0.3 (0-1.38)
L-Tyrosine	C_9H11NO_3	204.441	$[M+H]^+$	C00082	1.17	-0.81	0.095	1.512	2.63 (0.33-11.35)	4.36 (0.71-22.15)	5.67 (0.1-16.28)
Benzophenone	$C_{13}H_{10}O$	882.111	$[M+H]^+$	C06354	1.19	0.81	< 0.001	0.752	0.25 (0.16-0.3)	0.19 (0.1-0.3)	0.18 (0.07-0.25)
L-Tryptophan	$C_{11}H_{12}N_2O_2$	338.856	$[M+H]^+$	C00078	1.03	-0.74	0.23	1.940	0.57 (0.09-3.63)	0.74 (0.07-12.67)	1.11 (0.1-9.81)
12-Hydroxylauric acid	$C_{12}H_{24}O_3$	906.316	$[M+H]^+$	C08317	1.12	0.72	< 0.001	0.697	10.81 (8.25-16.18)	7.3 (0.08-12.49)	7.61 (0.08-14.08)
N-Acetyl-D-glucosamine	$C_8H_{15}NO_6$	82.3978	$[M+H]^+$	C03878	1.02	-0.39	0.936	0.942	0.04 (0-0.46)	0.07 (0-0.34)	0.07 (0-0.44)
L-cystathionine	$C_7H_{14}N_2O_4S$	836.2685	$[M+H]^+$	C02291	1.10	0.67	0.24	0.919	0.48 (0.31-0.79)	0.48 (0.2-0.81)	0.43 (0.22-0.66)
S-adenosyl-L-methionine	$C_{15}H_{22}N_6O_5S$	66.1963	$[M+H]^+$	C00019	1.02	0.79	0.029	0.888	9.98 (8.09-12.77)	9.2 (4.71-12.09)	8.58 (4.98-14.58)
Guanosine	$C_{10}H_{13}N_5O_5$	230.687	$[M+H]^-$	C00387	1.01	0.02	0.824	0.763	3.02 (0.55-14.19)	2.98 (0-10.27)	3.52 (0-10.89)

Neisseriaceae, which was the dominant bacterial family in the CHB yellow tongue coating, was positively correlated with the serum HBV-DNA, TC, L-leucine, hypoxanthine, urocanic acid and methionine levels but negatively correlated with thebenzophenone and S-adenosyl-L-methionine levels. Another relatively abundant member of the microbiota in the CHB yellow tongue coating (Gracilibacteria_bacterium_oral_taxon_873) was positively correlated with the guanosine and BUN levels but negatively correlated with the S-adenosyl-L-methionine level (Figure 5).

DISCUSSION

Chinese medicine theory believes that tongue demonstration is a window of body change and that the oral microbiome is an integral part of the whole body's microbiome. Indeed, an increasing number of studies have found that many diseases, including atherosclerosis[15], rheumatoid arthritis[16], diabetes[17] and liver cirrhosis[18], are accompanied by disorder of the oral and intestinal microbiotas. Although the oral and gut communities share little taxonomic resemblance, the oral and intestinal microflora have general dynamic characteristics[19], the oral bacterial populations seed the gut[20], and the observed bacterial structures in the oral cavity or intestine can predict each other[21]. Because tongue diagnosis has the advantages of intuition and simplicity, some scholars have recently discovered the importance of the tongue image for the diagnosis and prognostic prediction of diseases[22,23]. The oral microbiota varies according to the different sampling sites with a high diversity[24], but as the tongue texture and tongue color form an important basis for diagnosis and treatment in TCM[25]. The treatments adopted for patients with white and yellow tongue coatings are different, thus, the tongue coating oral microbiotas were selected for analysis in our study, and the samples were grouped by the color of the tongue coating.

The complex and dynamic interactions between microbes and hosts are very important for maintaining homeostasis because microbiome dysbiosis may interact with the host's immune system and influence the degree of hepatic steatosis, inflammation and fibrosis[26]. Our recent study found that the gut microbiota was significantly altered in

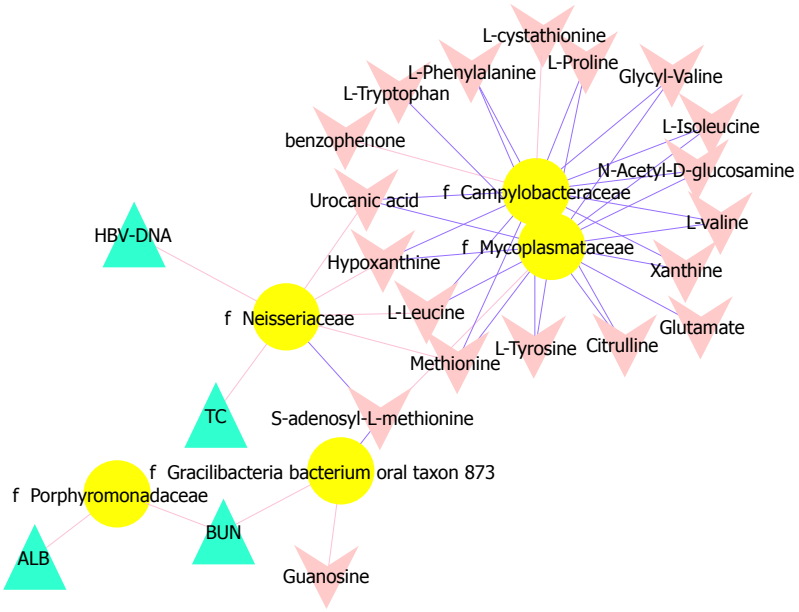

Figure 5 Associations of the tongue coating microbiotas with metabolites and clinical indices. Correlations were detected, and the indices with Spearman's correlation coefficients > 0.3 were visualized in Cytoscape. Triangles represent clinical indicators, arrows represent metabolites and dots represent oral microbial families. If the correlations are negative, the connecting line is blue; if the correlation is positive, the connecting line is red. The line thickness represents the size of the correlation coefficient.

CHB patients with low Child-Pugh scores[27]. Evidence is accumulating that the intestinal microbiome has good clinical prospects as a target for the treatment of chronic liver disease. Chinese scholars transplanted the intestinal flora of healthy volunteers into HBeAg-positive CHB patients with long-term antiviral treatment, and this approach showed a good effect on HBeAg seroclearance[28]. However, few studies have been performed on the oral microbiotas in CHB patients. In one of the limited reports, Ling *et al*[29] noted the decreased diversity of the oral microbiotas in supragingival plaque samples from patients with HBV-induced chronic liver disease. However, in this study, the richness and diversity of the tongue coating did not differ between the CHB patients and healthy controls. Ren *et al*[30] used 16S rRNA gene pyrosequencing and metagenomic sequencing to examine oral microbial compositions and their functional variations in children with halitosis. They found that the tongue coatings of the subjects with halitosis had greater bacterial richness than those of the healthy subjects, but the number of OTUs and the Chao levels were slightly lower in the saliva samples from the subjects with halitosis than in the healthy subjects. The microbiotas among individuals and habitats are highly personalized in the oral cavity[31]. Therefore, we concluded that the data differences in data might be due to the use of different sampling sites.

Taxonomic and predicted function differences were found between the CHB yellow and white tongue coating patients in the LEfSe analysis. The CHB yellow tongue coating patients had specific clinical and microbiota characteristics that were distinct from those of the white coating patients. First, the CHB patients with yellow tongue coatings had significantly higher viral titers but lower ALB levels than the white coating patients ($P <$ 0.05). The remaining indicators of liver function, including TBIL, DBIL, ALT, AST, ALP, GGT and PT, exhibited elevated trend in the CHB yellow tongue coating patients. Because a yellow tongue is an important indicator for the diagnosis of CHB *damp heat* syndrome, the results are consistent with studies showing that the CHB *damp-heat* syndrome patients have higher ALT and AST levels[32], which indicats that these patients have greater liver damage. The correlation analysis between bacteria and metabolites also confirmed this outcome. The relatively dominant bacterial families in the CHB yellow tongue coating (Neisseriaceae and Gracilibacteria_bacterium _oral_taxon_873) were negatively correlated with the S-adenosyl-L-methionine level. S-adenosyl-L-methionine, which is also known as SAM or AdoMet, is a donor in the methylation reactions of all mammalian cells but is found most abundantly in the liver. Patients with chronic liver disease have reduced AdoMet levels, and reduced hepatic AdoMet levels can contribute to the development of oxidative stress, steatohepatitis, and hepatocellular carcinoma (HCC)[33]. In addition, according to TCM, a yellow tongue coating is a manifestation of TCM *hot* Syndrome, which has been reported to be involved in inflammation or an immune regulation imbalance in the host[34,35]. Jiang *et al*[3] compared the yellow and white tongue coating microbiomes with those of gastritis patients and found that yellow dense tongue coating bacteria were associated with TCM *hot* syndrome-related inflammation such as halitosis, tonsil infection and periodontal inflammation. Therefore, we therefore hypothesized that the patients with CHB yellow tongue coatings might have had more inflammation, although this speculation requires further confirmation. Second, the yellow tongue coating subjects showed similarities at the phylum level with a gut disorder in patients

with cirrhosis, which was manifested as a reduced abundance of Bacteroidetes and increased Proteobacteria content[18,26,36]. The LEfSe analysis suggested that Neisseriaceae was enriched in the yellow tongue coating patients and was positively correlated with the serum HBV-DNA level. Ling's research reported that members of Neisseriaceae were significantly more abundant in the oral microbiota of liver cirrhosis patients than in those of CHB patients[29]. Lv *et al*[37] found that Neisseriaceae, which are opportunistic pathogens, were enriched in primary biliary cirrhosis (PBC) patients. Third, according to the LDA score, the inferred metagenomic pathways that were enriched in the CHB yellow tongue coating patients were mainly those involved in amino acid metabolism, and the detected metabolites were mainly essential amino acids, including L-proline, L-valine, L-isoleucine, L-leucine, L-lysine, glutamate and L-tryptophan, and were generally present in larger amounts trend in the yellow tongue coatings. The relationship between amino acid metabolism and the CHB patients with yellow tongue coatings is unclear, and relevant literature reports are limited. However, one report noted that people with the TCM *damp-heat* syndrome people with HBV-related chronic liver diseases, whom mainly manifested yellow greasy tongue coatings, had increased leucine, phenylalanine and valine expression in urinary metabolomic studies[38], which indirectly explained the severe disordered amino acid metabolism in CHB patients with the yellow coating. Finally, this study found that membrane transport (secretion system) and cell motility (bacterial motility proteins) were enriched in the yellow coatings, which indicated that the CHB yellow coating patients might be more susceptible to bacterial colonization. The functional analysis of tongue coating flora and metabolites in CHB white tongue coating patients lacked correspondence, the underlying reason might be the microbiotas functionality in the CHB white tongue coating patients were most likely related to genetic information processing, which association with metabolites is relatively little.

Tongue diagnosis is a simple, non-invasive and valuable procedure that has been repeatedly verified by TCM clinical practitioners. We found that the yellow and white tongue coatings of CHB patients had microbiota compositional and functional differences in this study, but the sample sizes were small. In the future, we will expand the sample size to verify the results of this study. In addition, we will focus on the relationship between changes in the oral and intestinal microbiota in different tongue coating patients and explore the effects of oral microbiota variance on immunity and metabolic alterations in the body to further explain the modern theoretical mechanism of TCM tongue diagnosis. These studies will facilitate the development of therapeutic strategies for individualized treatment.

ARTICLE HIGHLIGHTS

Research background

Chronic hepatitis B is a major infectious disease in China and Chinese medicine has a wide range of applications in the treatment of CHB. Tongue diagnosis has important guiding significance for clinical syndrome differentiation and drug use in TCM, but lacks scientific explanations. Some reports have found abnormalities in the microbiota or metabolites in pathological tongue coatings. However, integrated analyses of the pathological tongue coating microbiotas and metabolites have rarely been reported. Elucidating the tongue coatings micro-features differences will promote our understanding of the TCM tongue diagnosis and facilitate therapeutic strategies for individualized treatment.

Research motivation

The motivation of this study was to explore the microfeatures of different tongue coatings, which could promote our understanding of the TCM tongue diagnosis from a modern perspective.

Research objectives

The objective of this research was to elucidate tongue coating microbiota and metabolic differences in CHB patients with yellow or white tongue coatings.

Research methods

We collected tongue coating samples from 28 CHB yellow tongue coating patients and 25 CHB white tongue coating patients, and an additional 22 samples were collected from healthy controls. The tongue coating bacterial 16S ribosomal RNA gene V3 region was amplified and sequenced with the Ion Torrent PGM™ sequencing platform. The metabolites in the tongue coatings were examined using a LC-MS platform. The microbiota results were analyzed using Metastats analysis, the Kruskal-Wallis test and LEfSe analysis. The functionality of the microbiota was assessed using PiCRUST and compared among groups. The metabolomics enrichment analysis was performed with MetaboAnalyst 3.0 (http://www.metaboanalyst.ca). We correlated the microbiota with the clinical indices and metabolites and visualized the results with Spearman's correlation coefficients > 0.3 and $P < 0.05$ in Cytoscape.

Research results

This study found taxonomic and predicted function differences between the CHB yellow and white tongue coating patients. Distinct from those of the white coating patients, the CHB yellow tongue coating patients had specific clinical and microbiota characteristics. The microbiota of the CHB patients with yellow tongue coatings had similarities with a gut disorder in patients with cirrhosis at the phylum level, which manifested as a reduced abundance of Bacteroidetes and increased Proteobacteria content. Neisseriaceae, which is a dominant bacterial family enriched in yellow tongue coating patients, was positively correlated with the serum HBV-DNA level. The inferred metagenomic pathways enriched in the CHB yellow tongue coating patients were mainly those involved in amino acid metabolism, whereas the detected metabolites were mainly essential amino acids and generally were present in larger amounts than in the white tongue coatings.

Research conclusions

We found that the yellow and white tongue coatings of CHB patients had microbiota compositional and functional differences in this study.

Research perspectives

The sample size in this study was small. In the future, we will expand the sample size to further verify the results and focus on the relationship between changes in the oral and intestinal microbiotas to explore the effects of oral microbiota variance on immunity and metabolic alterations in the body. These studies will further explain the modern theoretical mechanism of TCM tongue diagnosis.

ACKNOWLEDGMENTS

The authors thank the doctors from the Shanghai University of TCM-affiliated Shuguang Hospital, the Nanjing Second Hospital and the Huai'an Fourth People's Hospital for the support with clinical information and samples collection.

REFERENCES

1 **Ye J**, Cai X, Cao P. Problems and prospects of current studies on the microecology of tongue coating. *Chin Med* 2014; **9**: 9 [PMID: 24597827 DOI: 10.1186/1749-8546-9-9]

2 **Lira-Junior R**, Boström EA. Oral-gut connection: one step closer to an integrated view of the gastrointestinal tract? *Mucosal Immunol* 2018; **11**: 316-318 [PMID: 29297500 DOI: 10.1038/mi.2017.116]

3 **Jiang B**, Liang X, Chen Y, Ma T, Liu L, Li J, Jiang R, Chen T, Zhang X, Li S. Integrating next-generation sequencing and traditional tongue diagnosis to determine tongue coating microbiome. *Sci Rep* 2012; **2**: 936 [PMID: 23226834 DOI: 10.1038/srep00936]

4 **Sun ZM**, Zhao J, Qian P, Wang YQ, Zhang WF, Guo CR, Pang XY, Wang SC, Li FF, Li Q. Metabolic markers and microecological characteristics of tongue coating in patients with chronic gastritis. *BMC Complement Altern Med* 2013; **13**: 227 [PMID: 24041039 DOI: 10.1186/1472-6882-13-227]

5 **Wang FS**, Fan JG, Zhang Z, Gao B, Wang HY. The global burden of liver disease: the major impact of China. *Hepatology* 2014; **60**: 2099-2108 [PMID: 25164003 DOI: 10.1002/hep.27406]

6 **Chassaing B**, Etienne-Mesmin L, Gewirtz AT. Microbiota-liver axis in hepatic disease. *Hepatology* 2014; **59**: 328-339 [PMID: 23703735 DOI: 10.1002/hep.26494]

7 **Bajaj JS**, Betrapally NS, Hylemon PB, Heuman DM, Daita K, White MB, Unser A, Thacker LR, Sanyal AJ, Kang DJ, Sikaroodi M, Gillevet PM. Salivary microbiota reflects changes in gut microbiota in cirrhosis with hepatic encephalopathy. *Hepatology* 2015; **62**: 1260-1271 [PMID: 25820757 DOI: 10.1002/hep.27819]

8 **Tsai TY**, Livneh H, Hung TH, Lin IH, Lu MC, Yeh CC. Associations between prescribed Chinese herbal medicine and risk of hepatocellular carcinoma in patients with chronic hepatitis B: a nationwide population-based cohort study. *BMJ Open* 2017; **7**: e014571 [PMID: 28122837 DOI: 10.1136/bmjopen-2016-014571]

9 **Kang H**, Zhao Y, Li C, Chen Y, Tang K, Yang L, Ma C, Peng J, Zhu R, Liu Q, Hu Y, Cao Z. Integrating clinical indexes into four-diagnostic information contributes to the Traditional Chinese Medicine (TCM) syndrome diagnosis of chronic hepatitis B. *Sci Rep* 2015; **5**: 9395 [PMID: 25797918 DOI: 10.1038/srep09395]

10 **Zhao Y**, Kang H, Peng JH, Xu L, Cao ZW, Hu YY. Key symptoms selection for two major syndromes diagnosis of Chinese medicine in chronic hepatitis B. *Chin J Integr Med* 2017; **23**: 253-260 [PMID: 27225292 DOI: 10.1007/s11655-016-2253-3]

11 **Amato KR**, Yeoman CJ, Kent A, Righini N, Carbonero F, Estrada A, Gaskins HR, Stumpf RM, Yildirim S, Torralba M, Gillis M, Wilson BA, Nelson KE, White BA, Leigh SR. Habitat degradation impacts black howler monkey (Alouatta pigra) gastrointestinal microbiomes. *ISME J* 2013; **7**: 1344-1353 [PMID: 23486247 DOI: 10.1038/ismej.2013.16]

12 **Segata N**, Izard J, Waldron L, Gevers D, Miropolsky L, Garrett WS, Huttenhower C. Metagenomic biomarker discovery and explanation. *Genome Biol* 2011; **12**: R60 [PMID: 21702898 DOI: 10.1186/gb-2011-12-6-r60]

13 **Langille MG**, Zaneveld J, Caporaso JG, McDonald D, Knights D, Reyes JA, Clemente JC, Burkepile DE, Vega Thurber RL, Knight R, Beiko RG, Huttenhower C. Predictive functional profiling of microbial communities using 16S rRNA marker gene sequences. *Nat Biotechnol* 2013; **31**: 814-821 [PMID: 23975157 DOI: 10.1038/nbt.2676]

14 **Xia J**, Sinelnikov IV, Han B, Wishart DS. MetaboAnalyst 3.0--making metabolomics more meaningful. *Nucleic Acids Res* 2015; **43**: W251-W257 [PMID: 25897128 DOI: 10.1093/nar/gkv380]

15 **Koren O**, Spor A, Felin J, Fåk F, Stombaugh J, Tremaroli V, Behre CJ, Knight R, Fagerberg B, Ley RE, Bäckhed F. Human oral, gut, and plaque microbiota in patients with atherosclerosis. *Proc Natl Acad Sci U S A* 2011; **108 Suppl 1**: 4592-4598 [PMID: 20937873 DOI: 10.1073/pnas.1011383107]

16 **Zhang X**, Zhang D, Jia H, Feng Q, Wang D, Liang D, Wu X, Li J, Tang L, Li Y, Lan Z, Chen B, Li Y, Zhong H, Xie H, Jie Z, Chen W, Tang S, Xu X, Wang X, Cai X, Liu S, Xia Y, Li J, Qiao X, Al-Aama JY, Chen H, Wang L, Wu QJ, Zhang F, Zheng W, Li Y, Zhang M, Luo G, Xue W, Xiao L, Li J, Chen W, Xu X, Yin Y, Yang H, Wang J, Kristiansen K, Liu L, Li T, Huang Q, Li Y, Wang J. The oral and gut microbiomes are perturbed in rheumatoid arthritis and partly normalized after treatment. *Nat Med* 2015; **21**: 895-905 [PMID: 26214836 DOI: 10.1038/nm.3914]

17 **Xiao E**, Mattos M, Vieira GHA, Chen S, Corrêa JD, Wu Y, Albiero ML, Bittinger K, Graves DT. Diabetes Enhances IL-17 Expression and Alters the Oral Microbiome to Increase Its Pathogenicity. *Cell Host Microbe* 2017; **22**: 120-128.e4 [PMID: 28704648 DOI: 10.1016/j.chom.2017.06.014]

18 **Qin N**, Yang F, Li A, Prifti E, Chen Y, Shao L, Guo J, Le Chatelier E, Yao J, Wu L, Zhou J, Ni S, Liu L, Pons N, Batto JM, Kennedy SP, Leonard P, Yuan C, Ding W, Chen Y, Hu X, Zheng B, Qian G, Xu W, Ehrlich SD, Zheng S, Li L. Alterations of the human gut microbiome in liver cirrhosis. *Nature* 2014; **513**: 59-64 [PMID: 25079328 DOI: 10.1038/nature13568]

19 **Bashan A**, Gibson TE, Friedman J, Carey VJ, Weiss ST, Hohmann EL, Liu YY. Universality of human microbial dynamics. *Nature* 2016; **534**: 259-262 [PMID: 27279224 DOI: 10.1038/nature18301]

20 **Atarashi K**, Suda W, Luo C, Kawaguchi T, Motoo I, Narushima S, Kiguchi Y, Yasuma K, Watanabe E, Tanoue T, Thaiss CA, Sato M, Toyooka K, Said HS, Yamagami H, Rice SA, Gevers D, Johnson RC, Segre JA, Chen K, Kolls JK, Elinav E, Morita H, Xavier RJ, Hattori M, Honda K. Ectopic colonization of oral bacteria in the intestine drives TH1 cell induction and inflammation. *Science* 2017; **358**: 359-365 [PMID: 29051379 DOI: 10.1126/science.aan4526]

21 **Ding T**, Schloss PD. Dynamics and associations of microbial community types across the human body. *Nature* 2014; **509**: 357-360 [PMID: 24739969 DOI: 10.1038/nature13178]

22 **Han S**, Yang X, Qi Q, Pan Y, Chen Y, Shen J, Liao H, Ji Z. Potential screening and early diagnosis method for cancer: Tongue diagnosis. *Int J Oncol* 2016; **48**: 2257-2264 [PMID: 27035407 DOI: 10.3892/ijo.2016.3466]

23 **RiYang L**, HangYing Y, JunYan Q, YaYu L, YuHui W, YaZhen Y, JiaZhen Y, Jin Y, Jun N, DongRong Y. Association between tongue coating thickness and clinical characteristics among idiopathic membranous nephropathy patients. *J Ethnopharmacol* 2015; **171**: 125-130 [PMID: 25997785 DOI: 10.1016/j.jep.2015.05.008]

24 **Human Microbiome Project Consortium**. Structure, function and diversity of the healthy human microbiome. *Nature* 2012; **486**: 207-214 [PMID: 22699609 DOI: 10.1038/nature11234]

25 **Lee TC**, Lo LC, Wu FC. Traditional Chinese Medicine for Metabolic Syndrome via TCM Pattern Differentiation: Tongue Diagnosis for Predictor. *Evid Based Complement Alternat Med* 2016; **2016**: 1971295 [PMID: 27313640 DOI: 10.1155/2016/1971295]

26 **Tilg H**, Cani PD, Mayer EA. Gut microbiome and liver diseases. *Gut* 2016; **65**: 2035-2044 [PMID: 27802157 DOI: 10.1136/gutjnl-2016-312729]

27 **Wang J**, Wang Y, Zhang X, Liu J, Zhang Q, Zhao Y, Peng J, Feng Q, Dai J, Sun S, Zhao Y, Zhao L, Zhang Y, Hu Y, Zhang M. Gut Microbial Dysbiosis Is Associated with Altered Hepatic Functions and Serum Metabolites in Chronic Hepatitis B Patients. *Front Microbiol* 2017; **8**: 2222 [PMID: 29180991 DOI: 10.3389/fmicb.2017.02222]

28 **Ren YD**, Ye ZS, Yang LZ, Jin LX, Wei WJ, Deng YY, Chen XX, Xiao CX, Yu XF, Xu HZ, Xu LZ, Tang YN, Zhou F, Wang XL, Chen MY, Chen LG, Hong MZ, Ren JL, Pan JS. Fecal microbiota transplantation induces hepatitis B virus e-antigen (HBeAg) clearance in patients with positive HBeAg after long-term antiviral therapy. *Hepatology* 2017; **65**: 1765-1768 [PMID: 28027582 DOI: 10.1002/hep.29008]

29 **Ling Z**, Liu X, Cheng Y, Jiang X, Jiang H, Wang Y, Li L. Decreased Diversity of the Oral Microbiota of Patients with Hepatitis B Virus-Induced Chronic Liver Disease: A Pilot Project. *Sci Rep* 2015; **5**: 17098 [PMID: 26606973 DOI: 10.1038/srep17098]

30 **Ren W**, Xun Z, Wang Z, Zhang Q, Liu X, Zheng H, Zhang Q, Zhang Y, Zhang L, Wu C, Zheng S, Qin N, Ehrlich SD, Li Y, He X, Xu T, Chen T, Chen F. Tongue Coating and the Salivary Microbial Communities Vary in Children with Halitosis. *Sci Rep* 2016; **6**: 24481 [PMID: 27080513 DOI: 10.1038/srep24481]

31 **Aas JA**, Paster BJ, Stokes LN, Olsen I, Dewhirst FE. Defining the normal bacterial flora of the oral cavity. *J Clin Microbiol* 2005; **43**: 5721-5732 [PMID: 16272510 DOI: 10.1128/JCM.43.11.5721-5732.2005]

32 **Sun YG**, Sun YL. Progress of the study on the relationship between TCM Syndromes of chronic hepatitis B and objective indicators. *Zhongyiyao Daobao* 2011; **17**: 76-78 [DOI: 10.13862/j.cnki.cn43-1446/r.2011.12.027]

33 **Lu SC**, Mato JM. S-adenosylmethionine in liver health, injury, and cancer. *Physiol Rev* 2012; **92**: 1515-1542 [PMID: 23073625 DOI: 10.1152/physrev.00047.2011]

34 **Li R**, Ma T, Gu J, Liang X, Li S. Imbalanced network biomarkers for traditional Chinese medicine Syndrome in gastritis patients. *Sci Rep* 2013; **3**: 1543 [PMID: 23529020 DOI: 10.1038/srep01543]

35 **Lu YY**, Zhao Y, Song YN, Dong S, Wei B, Chen QL, Hu YY, Su SB. Serum cytokine profiling analysis for zheng differentiation in chronic hepatitis B. *Chin Med* 2015; **10**: 24 [PMID: 26312063 DOI: 10.1186/s13020-015-0055-8]

36 **Chen Y**, Yang F, Lu H, Wang B, Chen Y, Lei D, Wang Y, Zhu B, Li L. Characterization of fecal microbial communities in patients with liver cirrhosis. *Hepatology* 2011; **54**: 562-572 [PMID: 21574172 DOI: 10.1002/hep.24423]

37 **Lv LX**, Fang DQ, Shi D, Chen DY, Yan R, Zhu YX, Chen YF, Shao L, Guo FF, Wu WR, Li A, Shi HY, Jiang XW, Jiang HY, Xiao YH, Zheng SS, Li LJ. Alterations and correlations of the gut microbiome, metabolism and immunity in patients with primary biliary cirrhosis. *Environ Microbiol* 2016; **18**: 2272-2286 [PMID: 27243236 DOI: 10.1111/1462-2920.13401]

38 **Guo Z**, Wang WY, Dai JY, Fan ZQ, Cao HJ, Sun SJ, Zhang YY, Xu LM, Hu YY, Su SB. Investigation on Urinary Metabolomic in Syndrome Types of Cirrhosis Caused by Hepatitis B. *Shijie Kexue Jishu-Zhongyiyao Xiandaihua* 2012; **14**: 1282-1287

P- Reviewer: Jafari SA, Liu Y, Su SB **S- Editor**: Gong ZM
L- Editor: A **E- Editor**: Yin SY

World Journal of Gastroenterology

Submit a Manuscript: http://www.f6publishing.com

World J Gastroenterol 2018 August 14; 24(30): 3462-3468

DOI: 10.3748/wjg.v24.i30.3462

ISSN 1007-9327 (print) ISSN 2219-2840 (online)

CASE REPORT

Large heterotopic gastric mucosa and a concomitant diverticulum in the rectum: Clinical experience and endoscopic management

Wen-Guo Chen, Hua-Tuo Zhu, Ming Yang, Guo-Qiang Xu, Li-Hua Chen, Hong-Tan Chen

Wen-Guo Chen, Hua-Tuo Zhu, Ming Yang, Guo-Qiang Xu, Li-Hua Chen, Hong-Tan Chen, Department of Gastroenterology, The First Affiliated Hospital, College of Medicine, Zhejiang University, Hangzhou 310003, Zhejiang Province, China

ORCID number: Wen-Guo Chen (0000-0001-6286-1808); Hua-Tuo Zhu (0000-0002-5098-7734); Ming Yang (0000-0001-6417-9669); Guo-Qiang Xu (0000-0002-7553-415X); Li-Hua Chen (0000-0003-0498-4361); Hong-Tan Chen (0000-0002-0633-2343).

Author contributions: Chen WG wrote the paper; Zhu HT collected and analyzed the data; Yang M performed the research; Xu GQ and Chen LH were study supervisors; Chen HT conceived and designed the study; all the authors approved the final version of the article to be published.

Supported by the National Natural Science Foundation of China, No. 81600413 and No. 81600414.

Informed consent statement: Written informed consent was provided by the patient prior to study inclusion. All details that might disclose the identity of the subject were omitted or anonymized.

Conflict-of-interest statement: The authors of this manuscript have no conflicts of interest to disclose.

CARE Checklist (2013) statement: The authors have read the CARE Checklist (2013), and the manuscript was prepared and revised according to the CARE Checklist (2013).

Manuscript source: Unsolicited manuscript

Correspondence to: Hong-Tan Chen, MD, Chief Doctor, Department of Gastroenterology, The First Affiliated Hospital, College of Medicine, Zhejiang University, Qingchun road, Hangzhou 310003, Zhejiang Province, China. 1510026@zju.edu.cn.
Telephone: +86-571-87236729
Fax: +86-571-87236611

Received: May 25, 2018
Peer-review started: May 26, 2018
First decision: July 6, 2018
Revised: July 9, 2018
Accepted: July 16, 2018
Article in press: July 16, 2018
Published online: August 14, 2018

Abstract

Heterotopic gastric mucosa (HGM) in the rectum is an extremely rare clinical entity which may be missed or misdiagnosed due to a lack of knowledge. In the present study, a 14-year-old girl visited our hospital due to a 5-year history of repeated hematochezia. Colonoscopy showed a solitary superficial depressed lesion approximately 5 cm in size and a concomitant 1.5 cm deep diverticulum in the rectum. Histological examination of the endoscopic biopsy showed typical ectopic gastric mucosa in the depressed lesion and inside the diverticulum. Narrow band imaging further confirmed the histological results. Endoscopic ultrasound indicated that the lesion originated from the mucosal layer, and partially involved the submucosal layer. Endoscopic submucosal dissection was performed in this patient due to the large size and shape of the lesion. No bleeding, perforation or other adverse events were observed. The presence of HGM in the diverticular cavity greatly increased the surgical difficulty. A literature review was also carried out in our study.

Key words: Endoscopic submucosal dissection; Rectum;

Helicobacter pylori; Endoscopy; Heterotopic gastric mucosa

Core tip: Heterotopic gastric mucosa (HGM) in the rectum is an extremely rare clinical entity with unclear pathogenesis and no standard guidelines regarding optimal treatment. We present a patient with HGM and a concomitant diverticulum in the rectum, indicated its endoscopic ultrasound and narrow band imaging characteristics. Endoscopic submucosal dissection (ESD) was performed in this patient due to the large size and shape of the lesion. This is the first report of the resection of HGM and a concomitant diverticulum by ESD. A literature review was also carried out to investigate the clinical characteristics, diagnosis and management of HGM in the rectum.

Chen WG, Zhu HT, Yang M , Xu GQ, Chen LH, Chen HT. Large heterotopic gastric mucosa and a concomitant diverticulum in the rectum: Clinical experience and endoscopic management. *World J Gastroenterol* 2018; 24(30): 3462-3468 Available from: URL: http://www.wjgnet.com/1007-9327/full/v24/i30/3462.htm DOI: http://dx.doi.org/10.3748/wjg.v24.i30.3462

INTRODUCTION

Heterotopic gastric mucosa (HGM) is the most commonly reported epithelial heterotopia and has been described as heteroplasia in organogenesis or metaplasia during the repair of damaged epithelium[1]. Although HGM may be congenital or acquired, the true pathogenesis of this condition remains unclear. HGM has been reported to be ubiquitous throughout the gastrointestinal (GI) tract from the oral cavity to the anorectum and can also involve the pancreas, biliary tract, gallbladder, scrotum, and mediastinum[2]. In the GI tract, HGM is predominantly observed in the esophagus, duodenum, Meckel's diverticulum, and in gastrointestinal duplication[3]. HGM in the rectum is an extremely rare clinical entity, which may be missed or misdiagnosed due to a lack of knowledge. To the best of our knowledge, only 50-100 cases of HGM in the rectum have been reported in the literature since the first description by Ewell and Jackson in 1939[4]. The majority of these patients were from Europe and North America.

In this report, we present the case of a young girl with a large 5 cm HGM in the rectum. Interestingly, a diverticular cavity 1.5 cm deep was found which was also lined with HGM. We report our clinical experience of this patient followed by a review of the recent literature on this entity. The clinical characteristics, endoscopic findings, diagnosis, treatment, and the relationship with Helicobacter pylori (*H. pylori*) infection and neoplastic transformation were analyzed to enhance physician awareness. In addition, our therapeutic approach using endoscopic submucosal dissection (ESD) which, to our knowledge, has been rarely reported.

CASE REPORT

A 14-year-old girl visited our hospital due to a 5-year history of repeated hematochezia. The bleeding episodes occurred intermittently without abdominal pain, mucous, pus or other symptoms. Her medical and family history was unremarkable. Carbohydrate antigen (CA) 19-9 was 61.2 U/mL (normal range 0-37 U/mL), hemoglobin was 116 g/L (normal range 113-151 g/L) and stool occult blood examination was weakly positive. Other laboratory examinations were normal. Abdominal computed tomography (CT), gastroscopy, and capsule endoscopy (CE) revealed no obvious GI lesions. A technetium-99m (Tc-99m) pertechnetate scan for Meckel's diverticulum and other sites of ectopic gastric mucosa was normal. On rectal examination, the patient had no anal fissures, hemorrhoids or fistulae.

At colonoscopy, a solitary superficial depressed lesion, approximately 5 cm in size, with a diverticular cavity was identified in the posterior wall of the lower part of the rectum proximal to the dentate line of the anal canal. The lesion was well-circumscribed, covering 1/3 of the circumference of the enteric cavity. Mucosa in the lesion appeared hyperemia and erythematous, with nodule changes. The tissue in the border of the lesion was slightly raised. The diverticulum was located in the anal side of the lesion, and was 1.5 cm deep and 2 cm in diameter. The mucosa was similar to the surrounding tissue. Histological examination of the endoscopic biopsy showed typical ectopic gastric mucosa in the depressed lesion and inside the diverticulum. Intestinal metaplasia, dysplasia, malignancy and colonization by *H. pylori* were not observed. Thus, the diagnosis of this rare entity was made on the basis of histological findings. Narrow band imaging (NBI) examination further confirmed the histological results. By means of NBI-magnifying endoscopy examination, it could visualize the microsurface and microvascular architecture immediately.

In this case, the NBI result showed the major gastric fundic-type mucosa (honey comb microvascular, small round microsurface) and focal pyloric-type mucosa (coiled microvascular, polygon microsurface) which lined the rectal mucosa. Endoscopic ultrasound (EUS) showed that the lesion originated from the mucosal layer, and partially involved the submucosal layer. Thickening of the mucosal layer with hypoechoic changes was observed in the intestinal wall of the lesion.

Although treatment with proton pump inhibitors or H2 receptor blockers may ameliorate the symptoms, we decided to remove the lesion by endoscopic resection due to repeated bleeding. As a result of its endoscopic features, ESD was performed in order to ensure complete resection. Unlike the routine ESD procedure used in a lateral spreading tumor (LST), the presence of the diver-

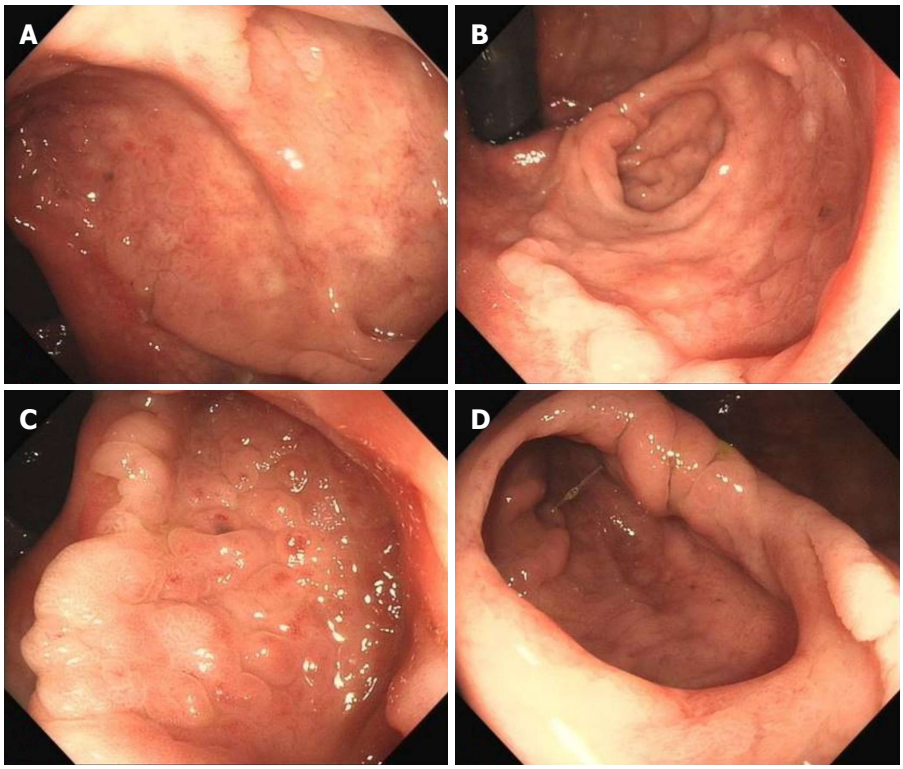

Figure 1 Endoscopic imaging. A and B: The lesion was observed by colonoscopy in the normal/reverse position; C: The slightly raised border, hyperemia and erythematous, nodule changed mucosa in the depressed lesion; D: Diverticulum in the heterotopic gastric mucosa lesion.

ticulum greatly increased the technical difficulties. After the lesion was marked with a dual knife, a mixture of glycerol fructose solution, indigo carmine and epinephrine were injected into the submucosal layer. The lifting sign was positive in this lesion which indicated that the muscularis propria was not involved. A circumferential incision was then performed. The submucosal dissection was started from the peripheral margin to the base of the diverticulum. When the dissection reached the anal side of the lesion near the anal canal, lidocaine was injected into the submucosal layer to relieve anal pain. Due to the narrow space in the diverticular cavity, ESD could not be accomplished. At the base of the diverticulum, piecemeal resection with snare was performed. In order to reduce residual HGM in the diverticulum, argon plasma coagulation (APC) was carried out in the interior of the diverticulum. Due to the hypervascular characteristics of the rectum, the full extent of the wound was carefully inspected, and a hemostatic clamp was used to manage the remnants of vessels. Finally, the lesion was resected without bleeding, perforation or other adverse events. Histological evaluation of the resected specimen revealed ectopic gastric mucosa of the fundic-type.

This study was approved by the Ethics Committee and Institutional Review Board of the First Affiliated Hospital, College of Medicine, Zhejiang University, Hangzhou, China. Informed consent was obtained from the patient, and the record/information of the patient was anonymized and de-identified prior to analysis (Figures 1-5).

DISCUSSION

HGM has been reported to occur throughout the alimentary tract, but is mainly detected in the upper esophageal sphincter and is easily ignored by endoscopists if the gastroscope is withdrawn quickly without care. The incidence of HGM in the esophagus varies widely from 0.1% to 13.8% and HGM in the duodenum varies from 0.5% to 8.9% in published series[5]. HGM of the large bowel is infrequent, and is mostly reported in the rectum. Due to the limited number of patients, there is a lack of epidemiological studies and published data on HGM of the rectum. In a review of published reports, males were more commonly affected, and patients were predominantly children and adolescents[6,7]. Several hypotheses have been proposed to explain the origin of HGM, and false differentiation of pluripotent primitive endoderm stem cells is the most plausible and accepted hypothesis. Errors during embryonic development or metaplasia of rectal mucosa following mucosal injury are other mechanisms for the development of HGM[8].

The clinical presentation of HGM varies and depends on lesion size and location, and most are secondary to hydrochloric acid secretion. More than 90% of reported cases in the rectum were symptomatic[9]. The most common symptom was rectal bleeding, which also occurred in our case. Bleeding is usually painless, slight, intermittent and of varying duration. Other common symptoms include abdominal pain, diarrhea, tenesmus, perianal ulceration, anal pruritus, fistula, and bowel

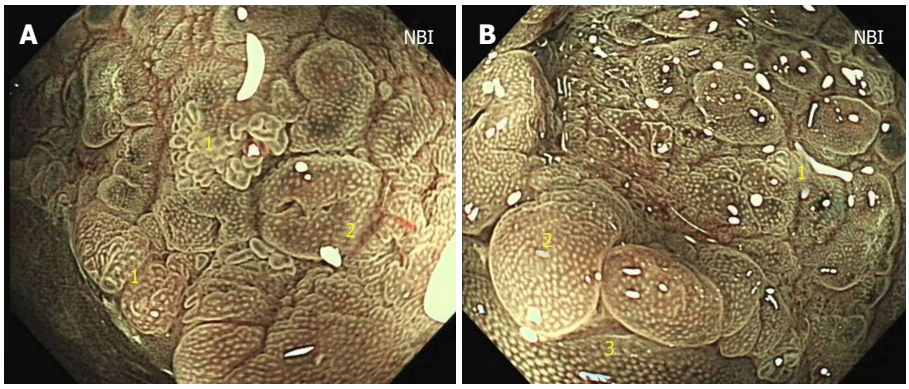

Figure 2 Narrow band imaging examinations. NBI showed that the lesion mainly consisted of gastric fundic-type mucosa with focal pyloric-type mucosa (1: Pyloric-type mucosa; 2: Fundic-type mucosa; 3: Rectal mucosa). NBI: Narrow band imaging.

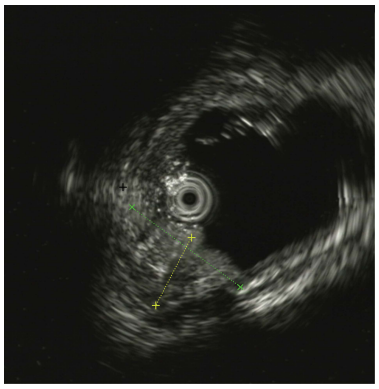

Figure 3 Endoscopic ultrasound examinations. Endoscopic ultrasound indicated that the lesion originated from the mucosal layer and partially involved the submucosal layer.

perforation. The report by Federico Iacopini showed that patients with specific anorectal symptoms were significantly younger than asymptomatic patients or patients with nonspecific abdominal symptoms and were frequently pediatrics (≤ 18 years)[10].

Endoscopically, HGM usually appears as an inlet patch in the proximal esophagus, a nodular mass in the duodenum, or a line in the interior of Meckel's diverticulum[11]. In the rectum, HGM lesions may be identified as ulcers, polyps, diverticula, and flat or depression lesions with a reddish-appearance. HGM mimicking a rectal submucosal tumor has also been reported[12]. Our patient, who had a 5 cm superficial depressed lesion and a concomitant 1.5 cm deep diverticulum, is the first reported case with this condition. The lesion was well-circumscribed with a slightly raised border and hyperemia, erythematous, and nodule altered mucosa. In most reported cases, the HGM lesion in the large intestine was solitary. Murray described a girl with repeated episodes of rectal bleeding due to HGM in the rectum, sigmoid colon, ascending colon, and cecum[13]. HGM is generally localized in the right posterior wall of the rectum and more than 5 cm above the anal verge[14]. EUS can provide valuable information for the diagnosis of HGM and can indicate the appropriate management. In general, most lesions are found within the mucosal layer, and may involve the submucosal layer. EUS images have indicated a hypoechoic pattern change, and several small anechoic areas may be detected due to dilated gastric-type glands, which are characteristic of HGM[15]. Thickening of the mucosal layer can also be seen in EUS images. NBI and NBI-magnifying endoscopy are useful tools for the diagnosis of HGM and can differentiate gastric-type glands from the intestinal mucosa. To our knowledge, this case is also the first report of the use of NBI in HGM of the rectum. NBI clearly showed gastric fundic-type and pyloric-type mucosa lining the rectum and helped us to make a definitive diagnosis.

For the diagnosis of HGM in the rectum, histopathological examination is the gold standard and provides fragments of rectal mucosa coexisting with gastric mucosa. In a literature report, fundic-type mucosa was the most common histologic type of HGM, and was characterized by oxyntic features other than antral- or transitional-type[16]. Histopathology in our case also mainly showed fundic-type mucosa. Tc-99m pertechnetate abdominal scintigraphy is important in the diagnosis and localization of ectopic gastric mucosa, especially in Meckel's diverticulum. In the study by Sciarra *et al*[17], the sensitivity of Tc-99m scintigraphy ranged from 50% to 91%, which may have depended on the location and size of the heterotopic tissue. Our patient had a negative result with no increased uptake of foci in the GI tract. In addition to NBI, confocal laser endomicroscopy (CLE) is a new endoscopic tool that allows magnification of 1000 times with the aid of a miniaturized confocal microscope inserted into the biopsy canal of a conventional endoscope. Through high-resolution and high-magnification assessment, it can provide images that can reliably predict histology without the need for biopsies[18]. Thus, HGM in the rectum may be correctly detected using CLE.

No current guidelines regarding the optimal treatment of HGM in the rectum are available due to reported sporadic cases. By the inhibition of gastric acid secretion, H2 receptor blockers or proton pump inhibitors may ameliorate or eliminate symptoms caused by HGM in

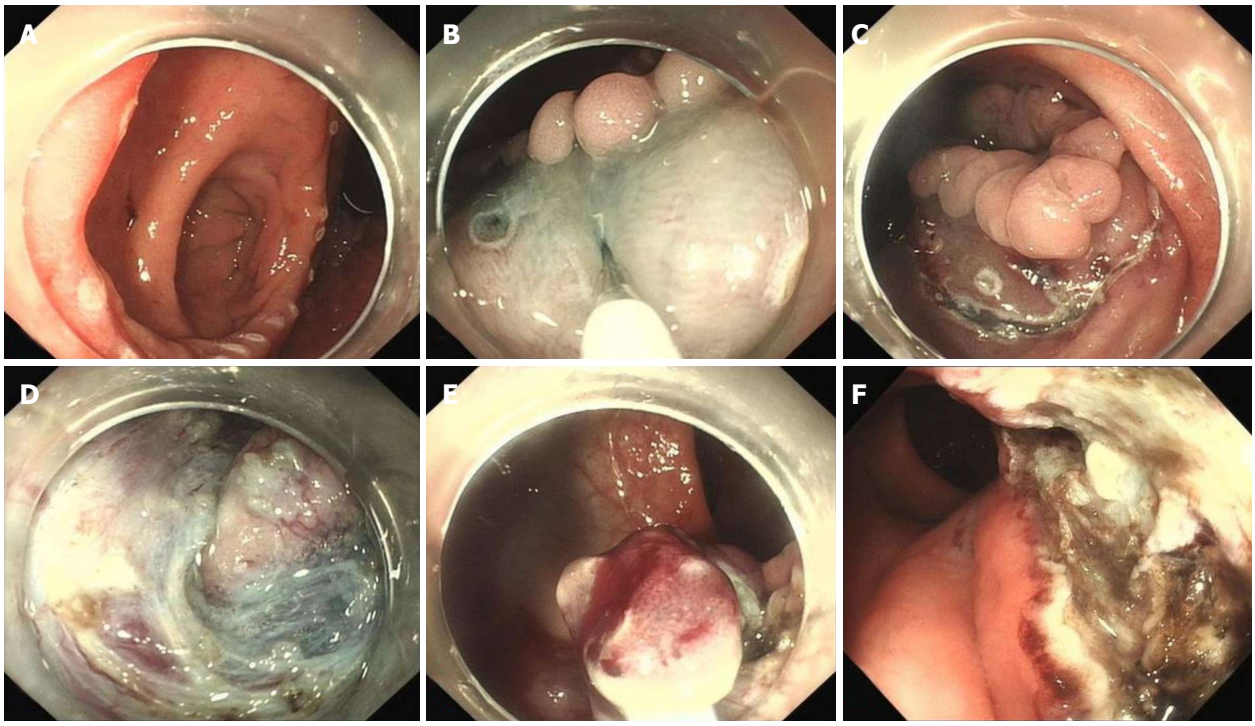

Figure 4 Endoscopic submucosal dissection of heterotopic gastric mucosa. A: Lesion marker; B: Submucosal layer injection; C: Circumferential incision; D: Dissection in the diverticular cavity; E: Piecemeal resection with a snare; F: Wound management.

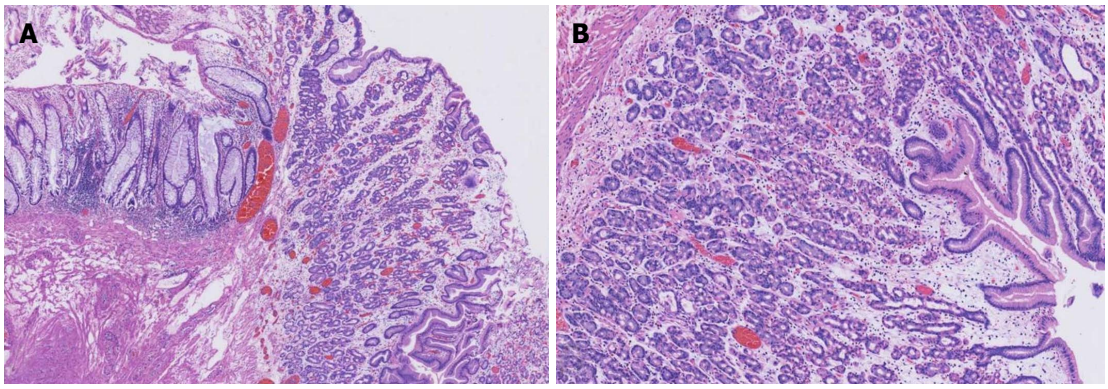

Figure 5 Histological examinations. Histologically, the specimen resected by endoscopic submucosal dissection showed ectopic gastric mucosa of the fundic-type.

the rectum. In most reported cases, rectal bleeding was successfully treated with proton pump inhibitor therapy and ulcer healing was achieved. However, recurrence can develop following the cessation of therapy and medication has failed to resolve heterotopic mucosa. In the surveillance report by Sauer *et al*[19], macroscopically the size of the lesion was unchanged after 4 mo of acid inhibition. Therefore, medical therapy relieves symptoms only in the short-term and could be used, to some extent, before definitive HGM excision. Endoscopic resection or surgical excision is generally considered the treatment of choice and has resulted in complete relief following removal of the HGM. Conventional endoscopic interventions such as endoscopic snare resection (polypectomy or endoscopic mucosal resection[20]) and ablation with APC are indicated in HGM patients mimicking polyps and small superficial lesions. ESD, enables *en bloc* resection of superficial lesions especially in early GI cancer and LST, and could also be used in the treatment of HGM. To date, HGM in the rectum treated with ESD has been reported in only 2 cases[10,12]. Surgery is another definitive treatment and can achieve complete resection of the lesion. However, given the concerns related to this benign entity, excessive surgery should be viewed with great caution, and would be the preferred approach in HGM with rectal duplication or serious complications such as major gastrointestinal bleeding, perforation, abscess or fistula, and for lesions following failed endoscopic resection.

In the present study, ESD was performed in our patient due to the large size and shape of the lesion. The presence of HGM in the diverticular cavity greatly increased the surgical difficulty. In addition, gastric acid secreted by HGM can induce chronic gastritis and

ulcerative complications that may lead to submucosal fibrosis and further influence the submucosal dissection. Lesion marker and submucosal layer injection were performed used a dual knife as in conventional ESD. We attempted dissection from the oral side and anal side separately to the base of the diverticulum to the best of our ability. Based on our previous experience, lidocaine was injected into the submucosal layer in order to relieve anal pain during dissection of the rectum near the anal canal due to its rich nerve supply. *En bloc* resection could not be completed due to the narrow space in the diverticulum, and piecemeal resection with a snare was feasible. Finally, endoscopic ablation of the lesion with low wattage APC was performed to manage possible residual HGM in the interior of the diverticulum. The lesion should be resected completely if possible as residual HGM can produce gastric acid and induce repeated delayed hemorrhage of the wound. This is the first reported case of the resection of a large HGM lesion and a concomitant diverticulum in the rectum treated by ESD. Histological result revealed ectopic gastric mucosa of the fundic-type. No pyloric-type gastric mucosa was detected which was not in accordance with the results of NBI. This may have been due to less focal tissue of pyloric-type gastric mucosa in comparison with fundic-type gastric mucosa in the piecemeal resected lesion, the sampling or cutting site of the histological biopsy.

Recently, more and more new issues related to HGM in the rectum have been addressed. Many studies have reported the potential progression to malignancy in the esophagus and gallbladder. The risk and possibility of intestinal metaplasia, dysplasia and malignant progression to adenocarcinoma in the rectum have been incompletely evaluated. The study by Ko *et al*[21] examined a case of colonic adenocarcinoma arising from gastric heterotopia, which was the first case report in the literature. The colonization of *H. pylori* in rectal gastric heterotopic mucosa has been noted. In the review by Jarosław Swatek of 50 rectal gastric heterotopic mucosa patients, *H. pylori* was present in six patients[22]. It is of interest to note that *H. pylori* passed through the whole GI tract to the rectum. *H. pylori* infection may have resulted in chronic active gastritis, ulceration or bleeding in the rectum. Thus, in cases associated with *H. pylori*, eradication treatment should be prescribed as the first therapeutic option[23].

In summary, heterotopic gastric mucosa of the rectum is a very rare clinical entity which mainly presents as chronic painless rectal bleeding. The pathogenesis of this condition is unclear. The definitive diagnosis of HGM relies on histopathological examination. Endoscopy techniques such as NBI and CLE could help in the diagnosis of HGM without the need for biopsies. Endoscopic resection is thought to be the first-line treatment and surgical excision may be preferred in some patients. Further investigations on the pathogenesis, malignant transformation, *H. pylori* infection, and optimal treatment are necessary.

ARTICLE HIGHLIGHTS

Case characteristics

A 14-year-old girl visited our hospital due to a 5-year history of repeated hematochezia.

Clinical diagnosis

Heterotopic gastric mucosa (HGM) and a concomitant diverticulum in the rectum found through colonoscopy examination.

Differential diagnosis

Ulcerative colitis.

Laboratory diagnosis

CA 19-9 was 61.2 U/mL, hemoglobin was 116 g/L, and stool occult blood examination was weakly positive. Other laboratory results were close to normal.

Imaging diagnosis

At colonoscopy, a solitary superficial depressed lesion, approximately 5 cm in size, with a diverticular cavity was identified in the rectum. Abdominal computed tomography revealed no obvious gastrointestinal lesions.

Pathological diagnosis

The pathology test confirmed the diagnosis of HGM.

Treatment

Endoscopic submucosal dissection.

Related reports

To the best of our knowledge, this is the first report of large HGM lesion and a concomitant diverticulum in the rectum treated by endoscopic submucosal dissection (ESD).

Term explanation

HGM is the most commonly reported epithelial heterotopia and has been described as heteroplasia in organogenesis or metaplasia during the repair of damaged epithelium.

Experiences and lessons

ESD is thought to be the safe and efficient treatment for HGM.

REFERENCES

1 **Dinarvand P**, Vareedayah AA, Phillips NJ, Hachem C, Lai J. Gastric heterotopia in rectum: A literature review and its diagnostic pitfall. *SAGE Open Med Case Rep* 2017; **5**: 2050313X17693968 [PMID: 28321304 DOI: 10.1177/2050313X17693968]

2 **Salem GA**, Fazili J, Ali T. Gastric heterotopia in the rectum. A rare cause of ectopic gastric tissue. *Arab J Gastroenterol* 2017; **18**: 42-43 [PMID: 28223104 DOI: 10.1016/j.ajg.2017.01.005]

3 **Cai J**, Yu H. Giant polypoid gastric heterotopia in the small intestine in a boy: A case report and literature review. *Medicine* (Baltimore) 2017; **96**: e5854 [PMID: 28072748 DOI: 10.1097/MD.0000000000005854]

4 **Ewell GH**, Jackson RH. Aberrant gastric mucosa in the rectum with ulceration and hemorrhage. *Wis Med J* 1939; **38**: 641-643

5 **Yu L**, Yang Y, Cui L, Peng L, Sun G. Heterotopic gastric mucosa of the gastrointestinal tract: prevalence, histological features, and clinical characteristics. *Scand J Gastroenterol* 2014; **49**: 138-144 [PMID: 24279774 DOI: 10.3109/00365521.2013.860558]

6 **Huelsen A**, Falvey J, Whitehead M, Ding S. Education and Imaging. Gastrointestinal: large heterotopic gastric mucosa in the rectum. *J Gastroenterol Hepatol* 2012; **27**: 1641 [PMID: 22994433 DOI: 10.1111/j.1440-1746.2012.07224.x]

7 **Al-Hussaini A**, Lone K, Al-Sofyani M, El Bagir A. Gastric

heterotopia of rectum in a child: a mimicker of solitary rectal ulcer syndrome. *Ann Saudi Med* 2014; **34**: 245-249 [PMID: 25266186 DOI: 10.5144/0256-4947.2014.245]
8 **Wolff M**. Heterotopic gastric epithelium in the rectum: a report of three new cases with a review of 87 cases of gastric heterotopia in the alimentary canal. *Am J Clin Pathol* 1971; **55**: 604-616 [PMID: 5090217 DOI: 10.1093/ajcp/55.5.604]
9 **Ikematsu H**, Fu KI, Saito Y, Matsuda T, Shimoda T, Fujii T. Ectopic gastric mucosa in the rectum mimicking an early depressed cancer treated by endoscopic mucosal resection. *Endoscopy* 2007; **39** Suppl 1: E171-E172 [PMID: 17614073 DOI: 10.1055/s-2007-966581]
10 **Iacopini F**, Gotoda T, Elisei W, Rigato P, Montagnese F, Saito Y, Costamagna G, Iacopini G. Heterotopic gastric mucosa in the anus and rectum: first case report of endoscopic submucosal dissection and systematic review. *Gastroenterol Rep* (Oxf) 2016; **4**: 196-205 [PMID: 27103738 DOI: 10.1093/gastro/gow006]
11 **Tai CM**, Chang IW, Wang HP. Heterotopic gastric mucosa of the ileum. *Endoscopy* 2015; **47** Suppl 1: E423 [PMID: 26397851 DOI: 10.1055/s-0034-1392666]
12 **Tan Y**, Wang Y, Liu D. Heterotopic gastric mucosa mimicking a rectal submucosal tumor. *Endoscopy* 2015; **47** Suppl 1: E329-E330 [PMID: 26115400 DOI: 10.1055/s-0034-1392323]
13 **Murray FE**, Lombard M, Dervan P, Fitzgerald RJ, Crowe J. Bleeding from multifocal heterotopic gastric mucosa in the colon controlled by an H2 antagonist. *Gut* 1988; **29**: 848-851 [PMID: 3290067 DOI: 10.1136/gut.29.6.848]
14 **Limdi JK**, Sapundzieski M, Chakravarthy R, George R. Gastric heterotopia in the rectum. *Gastrointest Endosc* 2010; **72**: 190-191; discussion 191 [PMID: 20620280 DOI: 10.1016/j.gie.2010.01.045]
15 **Eguchi K**, Aoyagi K, Nimura S, Sakisaka S. Diagnostic value of endoscopic and endoscopic ultrasound characteristics of duodenal submucosal tumour-like heterotopic gastric mucosa. *Can J Gastroenterol* 2011; **25**: 365-367 [PMID: 21876857 DOI: 10.1155/2011/104815]
16 **Fang Y**, Chen L, Chen DF, Ren WY, Shen CF, Xu Y, Xia YJ, Li JW, Wang P, Zhang AR, Shao SZ, Yu XN, Peng GY, Fang DC. Prevalence, histologic and clinical characteristics of heterotopic gastric mucosa in Chinese patients. *World J Gastroenterol* 2014; **20**: 17588-17594 [PMID: 25516674 DOI: 10.3748/wjg.v20.i46.17588]
17 **Sciarra A**, Hessler R, Godat S, Fraga M, Dromain C, Duran R, Halkic N, Sempoux C. Heterotopic Gastric Mucosa in a Duplication Cyst of the Common Hepatic Duct Mimicking Cholangiocarcinoma. *Int J Surg Pathol* 2018; **26**: 84-88 [PMID: 28830294 DOI: 10.1177/1066896917727101]
18 **López-Cerón Pinilla M**, Jimeno Ramiro M, Rodríguez de Miguel C, Pellisé Urquiza M. Heterotopic gastric mucosa diagnosed by confocal endomicroscopy. *Rev Esp Enferm Dig* 2011; **103**: 40-41 [PMID: 21341938 DOI: 10.4321/S1130-01082011000100009]
19 **Sauer CG**, Bickston SJ, Borowitz SM. Gastric heterotopia of the rectum. *J Pediatr Gastroenterol Nutr* 2010; **50**: 329-333 [PMID: 19668007 DOI: 10.1097/MPG.0b013e3181a1c476]
20 **Soares J**, Ferreira C, Marques M, Corujeira S, Tavares M, Lopes J, Carneiro F, Amil Dias J, Trindade E. Endoscopic Mucosectomy in a Child Presenting with Gastric Heterotopia of the Rectum. *GE Port J Gastroenterol* 2017; **24**: 288-291 [PMID: 29255771 DOI: 10.1159/000478939]
21 **Ko H**, Park SY, Cha EJ, Sohn JS. Colonic adenocarcinoma arising from gastric heterotopia: a case study. *Korean J Pathol* 2013; **47**: 289-292 [PMID: 23837024 DOI: 10.4132/KoreanJPathol.2013.47.3.289]
22 **Swatek J**, Wronecki L, Ciechanek R, Szumiło J. Asymptomatic gastric heterotopia in the rectum with Helicobacter pylori infection. *Pol J Pathol* 2015; **66**: 426-429 [PMID: 27003777 DOI: 10.5114/pjp.2015.57258]
23 **Colsa-Gutiérrez P**, Kharazmi-Taghavi M, Sosa-Medina RD, Berrío-Obregón JI, Ingelmo-Setién A. [Heterotopic gastric mucosa in the rectum: Report of a case]. *Cir Cir* 2016; **84**: 160-163 [PMID: 26242819 DOI: 10.1016/j.circir.2015.06.013]

P- Reviewer: Ikematsu H, Ishida T **S- Editor**: Wang XJ
L- Editor: A **E- Editor**: Yin SY

Published by **Baishideng Publishing Group Inc**
7901 Stoneridge Drive, Suite 501, Pleasanton, CA 94588, USA
Telephone: +1-925-223-8242
Fax: +1-925-223-8243
E-mail: bpgoffice@wjgnet.com
Help Desk: http://www.f6publishing.com/helpdesk
http://www.wjgnet.com

ISSN 1007-9327